Journal of Diabetes Research

Diabetes Mellitus and its Cardiovascular Complications: New Insights into an Old Disease 2020

Lead Guest Editor: Celestino Sardu
Guest Editors: Gaetano Santulli, Markus Wallner, and Claudio De Lucia

Diabetes Mellitus and its Cardiovascular Complications: New Insights into an Old Disease 2020

Journal of Diabetes Research

Diabetes Mellitus and its Cardiovascular Complications: New Insights into an Old Disease 2020

Lead Guest Editor: Celestino Sardu
Guest Editors: Gaetano Santulli, Markus Wallner, and Claudio De Lucia

Contents

A Role of Glucose Overload in Diabetic Cardiomyopathy in Nonhuman Primates
Xiu Wang, Shi Jin, and Weina Hu
Research Article (9 pages), Article ID 9676754, Volume 2021 (2021)

Early Diabetic Nephropathy and Retinopathy in Patients with Type 1 Diabetes Mellitus Attending Sudan Childhood Diabetes Centre
Hana Ahmed, Tayseer Elshaikh, and Mohamed Abdullah
Research Article (8 pages), Article ID 7181383, Volume 2020 (2020)

Calcium Homeostasis in Ventricular Myocytes of Diabetic Cardiomyopathy
Lina T. Al Kury
Review Article (12 pages), Article ID 1942086, Volume 2020 (2020)

Type 2 Diabetes Mellitus and Chronic Heart Failure with Midrange and Preserved Ejection Fraction: A Focus on Serum Biomarkers of Fibrosis
D. A. Lebedev, E. A. Lyasnikova, E. Yu Vasilyeva, A. Yu Babenko, and E. V. Shlyakhto
Research Article (9 pages), Article ID 6976153, Volume 2020 (2020)

Combination of Composite Autonomic Symptom Score 31 and Heart Rate Variability for Diagnosis of Cardiovascular Autonomic Neuropathy in People with Type 2 Diabetes
Zhiyin Zhang, Yujin Ma, Liujun Fu, Liping Li, Jie Liu, Huifang Peng, and Hongwei Jiang
Research Article (8 pages), Article ID 5316769, Volume 2020 (2020)

Association of Glycemic Indices (Hyperglycemia, Glucose Variability, and Hypoglycemia) with Oxidative Stress and Diabetic Complications
Eleftheria Papachristoforou, Vaia Lambadiari, Eirini Maratou, and Konstantinos Makrilakis
Review Article (17 pages), Article ID 7489795, Volume 2020 (2020)

Association of Maternal Diabetes Mellitus and Polymorphisms of the *NKX2.5* Gene in Children with Congenital Heart Disease: A Single Centre-Based Case-Control Study
Mingyi Zhao, Jingyi Diao, Peng Huang, Jinqi Li, Yihuan Li, Yang Yang, Liu Luo, Senmao Zhang, Letao Chen, Tingting Wang, Ping Zhu, and Jiabi Qin
Research Article (12 pages), Article ID 3854630, Volume 2020 (2020)

Prevalence of Cardiovascular Disease in Patients with Type 2 Diabetes Mellitus in Iran: A Systematic Review and Meta-Analysis
Mohsen Kazeminia, Nader Salari, and Masoud Mohammadi
Review Article (9 pages), Article ID 3069867, Volume 2020 (2020)

Protective Role of Tangshen Formula on the Progression of Renal Damage in *db/db* Mice by TRPC6/Talin1 Pathway in Podocytes
Qian Wang, Xuefei Tian, Wei'e Zhou, Yan Wang, Hailing Zhao, Jialin Li, Xuefeng Zhou, Haojun Zhang, Tingting Zhao, and Ping Li
Research Article (19 pages), Article ID 3634974, Volume 2020 (2020)

The Alteration of Carnitine Metabolism in Second Trimester in GDM and a Nomogram for Predicting Macrosomia
Man Sun, Baihui Zhao, Sainan He, Ruopeng Weng, Binqiao Wang, Yunping Ding, Xinwen Huang, and Qiong Luo
Research Article (12 pages), Article ID 4085757, Volume 2020 (2020)

Geranylgeranyl Transferase-I Knockout Inhibits Oxidative Injury of Vascular Smooth Muscle Cells and Attenuates Diabetes-Accelerated Atherosclerosis
Guo-Ping Chen, Jian Yang, Guo-Feng Qian, Wei-Wei Xu, and Xiao-Qin Zhang
Research Article (14 pages), Article ID 7574245, Volume 2020 (2020)

Evaluation of Foveal and Parafoveal Microvascular Changes Using Optical Coherence Tomography Angiography in Type 2 Diabetes Patients without Clinical Diabetic Retinopathy in South Korea
Young Gun Park, Minhee Kim, and Young Jung Roh
Research Article (7 pages), Article ID 6210865, Volume 2020 (2020)

Atherogenic Index of Plasma (AIP) a Tool to Assess Changes in Cardiovascular Disease Risk Post Laparoscopic Sleeve Gastrectomy
Eman Al Shawaf, Ebaa Al-Ozairi, Fahad Al-Asfar, Anwar Mohammad, Shaima Al-Beloushi, Sriraman Devarajan, Fahd Al-Mulla, Jehad Abubaker, and Hossein Arefanian
Research Article (9 pages), Article ID 2091341, Volume 2020 (2020)

Research Progress on the Pathological Mechanisms of Podocytes in Diabetic Nephropathy
Lili Zhang, Zhige Wen, Lin Han, Yujiao Zheng, Yu Wei, Xinmiao Wang, Qing Wang, Xinyi Fang, Linhua Zhao, and Xiaolin Tong
Review Article (15 pages), Article ID 7504798, Volume 2020 (2020)

Genetic and Biological Effects of ICAM-1 E469K Polymorphism in Diabetic Kidney Disease
Xiuli Zhang, Norhashimah Abu Seman, Henrik Falhammar, Kerstin Brismar, and Harvest F. Gu
Review Article (7 pages), Article ID 8305460, Volume 2020 (2020)

The 7-Year Change in the Prevalence of Insulin Resistance, Inflammatory Biomarkers, and Their Determinants in an Urban South African Population
Saarah Fatoma Gadija Davids, Tandi Edith Matsha, Nasheeta Peer, Rajiv Timothy Erasmus, and Andre Pascal Kengne
Research Article (11 pages), Article ID 3781214, Volume 2020 (2020)

Hindawi
Journal of Diabetes Research
Volume 2021, Article ID 9676754, 9 pages
https://doi.org/10.1155/2021/9676754

Research Article

A Role of Glucose Overload in Diabetic Cardiomyopathy in Nonhuman Primates

Xiu Wang,[1] **Shi Jin**,[2] **and Weina Hu**[3]

[1]*Department of Anesthesiology, The Fourth Affiliated Hospital of China Medical University, Shenyang 110034, China*
[2]*Department of Endocrinology, The Fourth Affiliated Hospital of China Medical University, Shenyang 110034, China*
[3]*Department of Cardiology, The Fourth Affiliated Hospital of China Medical University, Shenyang 110034, China*

Correspondence should be addressed to Shi Jin; jinshi_1981@163.com and Weina Hu; cmu4h_huweina@163.com

Received 26 March 2020; Revised 19 January 2021; Accepted 23 March 2021; Published 31 March 2021

Academic Editor: Gaetano Santulli

Type 2 diabetes (T2D) plays a major role in the development of heart failure. Patients with T2D have an increased risk to develop HF than healthy subjects, and they always have very poor outcomes and survival rates. However, the underlying mechanisms for this are still unclear. To help develop new therapeutic interventions, well-characterized animal models for preclinical and translational investigations in T2D and HF are urgently needed. Although studies in rodents are more often used, the research findings in rodents have often failed to be translated into humans due to the significant metabolic differences between rodents and humans. Nonhuman primates (NHPs) serve as valuable translational models between basic studies in rodent models and clinical studies in humans. NHPs can recapitulate the natural progress of these diseases in humans and study the underlying mechanism due to their genetic similarity and comparable spontaneous T2D rates to humans. In this review, we discuss the importance of using NHPs models in understanding diabetic cardiomyopathy (DCM) in humans with aspects of correlations between hyperglycemia and cardiac dysfunction progression, glucose overload, and altered glucose metabolism promoting cardiac oxidative stress and mitochondria dysfunction, glucose, and its effect on cardiac resynchronization therapy with defibrillator (CRT-d), the currently available diabetic NHPs models and the limitations involved in the use of NHP models.

1. Introduction

The prevalence of worldwide type 2 diabetes (T2D) is increasing exponentially across age and gender. It is estimated that the number of global T2D patients has reached 425 million in 2017 [1]. T2D, one of the main cardiovascular (CV) risk factors, contributes to the yearly increased CV morbidity and mortality [2, 3]. Heart failure and T2D are always accompanied by each other in clinical practice. Around 20%-40% of HF patients are having T2D [4, 5]. Patients with T2D have more than twice folds of risk developing HF than people without diabetes [6–9]. The increased prevalence of HF and the poor outcomes and survival rate of HF patients make it the most worrying diabetes complications over several decades [10]. Diabetic cardiomyopathy (DCM) is now recognized as a separate myocardial disease manifested as impaired cardiac functions independent of coronary artery disease, atherosclerosis, and hypertension [11–13]. Cardiac magnetic resonance imaging (cardiac MRI or CMR) [14] and echocardiography [15] have been used as the gold standards to evaluate the cardiac structure, ventricular function, and tissue characterization noninvasively. There are 2 distinct phenotypes of DCM: one is heart failure with preserved left ventricular (LV) ejection fraction (HFpEF), or diastolic dysfunction, often characterized by a normal ejection fraction (EF), abnormal ratio of the peak velocities at early (E), and late (A) diastole (E/A), a slow LV relaxation, thick LV walls, and elevated LV filling pressures [13]. This phenotype may precede the development of systolic dysfunction [16, 17], named heart failure with reduced left ventricular ejection fraction (HFrEF), which is characterized as a reduced EF, enlarged LV cavity, and impaired contractility. T2D is closely associated with those 2 phenotypes of cardiomyopathy in humans [18]. Recent studies have shown that poor glycemic control correlates with increased risk of HF in diabetic patients, and the myocardial changes

in those patients are believed to be induced by hyperglycemia [19, 20]. T2D was known to be one of the main risk factors and determinants of HFrEF. A recent study has reported the detrimental epigenetic effects of T2D on the cardiac pump and cardiac remodeling process in HF patients. MicroRNAs (miRs), a family of small regulatory noncoding RNAs, are implicated in epigenetic regulation of different aspects of cardiac structure and function such as cardiac fibrosis, apoptosis, and hypertrophy. Therefore, miRs were served as biomarkers for patients with both HF and T2D [21, 22]. T2D is also a heterogeneous disease, and the association between T2D and type 2 ryanodine receptor/Ca^{2+} release channel (RyR2), a key regulator for excitation-contraction coupling in the heart, has been identified by GWAS. It was reported that mutant leaky RyR2 channels were found in HF patients, and leaky RyR2 played a critical role in the pathogenesis of cardiac arrhythmias and impaired glucose metabolism [23]. Although significant progress has been achieved, the precise mechanism of DCM remains unclear. The foundation of these researches has been the use of small animals to uncover mechanisms of DCM and develop novel treatments. This review briefly discussed the common NHP models of T2D and HF and summarized the contributions of our understanding of glucose overload in DCM and drug discovery.

2. Finding an Ideal Animal Model

Ideally, the human-relevant T2D and HF research would be performed in humans but this is impossible due to technical and ethical considerations. Therefore, it is necessary to have an ideal model to recapitulate the human T2D and HF process in nonhuman systems. Although some of this can be done without the use of animals but through computer models or in vitro systems, these systems are incapable of reproducing the complex and multifactorial in vivo pathophysiology of T2D and HF.

Rodents are the most widely used animal species for various reasons. Practically, they are inexpensive, small in size, easy to breed, and genetically modifiable and have a short generation time and an accelerated lifespan. Furthermore, rodents are biologically similar to humans in many diseases and conditions and are well-established experimental models for studying the pathogenesis of diabetes-related cardiac dysfunction. However, several crucial differences between humans and rodents limit their potential as an ideal model [24, 25]. Among these disadvantages are the fact that rodents are only distantly related to humans, they do not naturally develop T2D, and are also resistant to diet-induced obesity, T2D, and cardiac dysfunction [26]. Rodent models have small size limitations, nocturnal activities, and they do not have menstrual cycles. These issues ultimately led to the use of animal models that more closely mimic humans.

3. Studies in Cardiac Mediated Cellular Pathways in Diabetes Nonhuman Primates (NHPs)

Although rodent models exhibit distinct advantages [27, 28], essential differences in the cardiometabolic process between rodents and humans have impeded direct translation of discoveries in rodents to humans. NHPs served as an ideal translational bridge between basic research and clinical application due to the findings from NHP studies are highly translatable to humans. Spontaneously, T2D and DCM develop in nonhuman primates (NHPs) just as it does in humans. NHPs exhibit clinical features of obesity, insulin resistance, diabetes, cardiac dysfunction, and pancreatic pathology that are observed the same in humans [29–33]. The cytoarchitecture and function of NHPs pancreatic islets that produce insulin are very similar to humans [34], making NHPs a critical model for T2D and DCM. Cardiac MRI and echocardiography have also been used to characterize cardiac functions in NHPs with T2D and DCM [31, 35, 36]. NHPs and humans have very similar systems in regulating blood glucose. Some researchers have shown that the incidence of low EF and abnormal E/A ratio in hyperglycemic NHPs was significantly higher than those in normal glycemic ones [31]. Consistently, there were also significant differences in the incidence of LV dysfunction between normal and high glycated hemoglobin (HbA1C) in NHPs [31]. Besides, NHPs have patterns of comorbidity that mirror humans and also exhibit long average life spans [37]. NHP studies also allow for complete control of the experimental environment including housing, experimental diet, and social interactions [28]. Furthermore, the use of NHPs studies meets the U.S. Food and Drug Administration (FDA) drug development requirement that toxicology testing should be conducted in a pharmacologically relevant species. Therefore, the NHP models are believed to be greatly suitable for preclinical drug development studies.

Cardiac metabolism and metabolic flexibility are impaired in the diabetic heart as evidenced by impaired glucose utilization and fatty acid oxidation both in humans and NHPs [33, 38]. This alteration leads to glucotoxicity and lipotoxicity, thus, further contribute to cellular dysfunction in all forms of obesity and diabetes, progression to DCM [39–41]. What is more, diabetes and dyslipidemia commonly occur together, with lipid abnormalities affecting two-thirds of T2D patients. High glucose accelerates atherosclerosis formation in the setting of diabetic dyslipidemia and eventually contribute to heart dysfunction [42]. Although the underlying pathogenesis and mechanisms of DCM are complex and multifactorial, here, we summarize some of the mechanisms involved in the glucose overload of DCM in NHPs.

3.1. Cardiac Glucose Metabolism Alteration and the Role of Glucose in Cardiac Dysfunction in Diabetic NHPs. Free fatty acids and glucose are two major substrates as the source of energy in the heart and glucose generates 10% to 20% of the energy. Diabetic hyperglycemia seems to be an important cause of the pathogenesis of DCM [33, 43], and reduced glucose oxidation and increased fatty acid oxidation are observed in the diabetic heart [40, 44]. This results in a high consumption of mitochondrial oxygen and contributes to cardiac dysfunction [45, 46]. Insulin plays an important role in maintaining cardiovascular homeostasis and glucose utilization [47]. Insulin resistance is another characteristic of T2D. NHPs with the onset of T2D characterized as impaired

pancreatic insulin secretion ability have some abnormal glycemic parameters, including increased fasting glucose level, increased glycated plasma proteins and hemoglobin, delayed/decreased glucose clearance rate, and deteriorated carbohydrate metabolism [26, 48, 49].

One of the limiting steps in cardiac glucose metabolism is glucose uptake by glucose transporters GLUT1 and GLUT4. GLUT1 is responsible for maintaining a basal rate of glucose uptake. GLUT4 is a major mediator of glucose removal from circulation in the adult heart and plays a key role in maintaining whole-body glucose homeostasis. Its translocation to the cell membrane requires insulin, which is impaired in insulin-resistant humans and NHPs [50, 51]. This reduced insulin-stimulated glucose transport is partially compensated by the elevations in plasma glucose-enhanced glucose uptake through mass action [52]. Therefore, although the GLUT4 activity is impaired in the diabetic myocardium, the glycolytic influx is not limited based on enough amount of glucose for hexokinase reaction.

Glycolysis is one of the most important routes of glucose metabolism in cardiomyocytes. Once transported into cardiomyocytes, glucose is broken down to produce pyruvate by glycolysis. In the diabetic heart, the ability of glycolysis and pyruvate oxidation is reduced in different animal models, including NHPs [53–55]. The activity of pyruvate dehydrogenase (PDH), a regulatory enzyme for the balance between cardiac carbohydrate and fat metabolism, is also decreased in T2D, thus, limits pyruvate oxidation. The uncoupling of pyruvate oxidation from glycolysis in diabetic hearts results in accumulated glycolytic intermediates, which further contribute to the development of cardiac dysfunction in diabetes [56, 57].

The previous study has shown that hyperglycemia (glucose overload) can independently regulate diabetic heart glucose metabolism [44]. A study of LV function in NHPs model of dysmetabolism and diabetes has demonstrated that hyperglycemia is strongly associated with the incidence of LV systolic dysfunction (low EF) but insulin treatment has no significant effects in improving the LV systolic dysfunction in T2D NHPs [31]. Another study showed that mechanical dysfunction of cardiomyocytes is correlated with mitochondrial dysfunction in patients with T2D but not with insulin-sensitive obesities. They also demonstrated that mitochondrial dysfunction correlated with HbA1c, not with insulin resistance [58]. This suggests that hyperglycemia, not insulin resistance, is the crucial component of cardiac dysfunction associated with T2D. Moreover, mechanistic and cellular studies have also shown that glucose per se can alter cardiomyocyte and heart contact and contractile properties [59], and that high-glucose exposure induces cardiomyocyte apoptosis [60] and endoplasmic reticulum (ER) stress [61].

Further, there was a relative risk reduction in cardiovascular mortality and hospitalization for HF patients with T2D under the treatment of sodium-glucose cotransporter-2 inhibitors (SGLT2i) [38]. SGLT2i is a class of antidiabetic drugs that reduces glucotoxicity by promoting glycosuria in humans and NHPs [62]. The effect of SGLT2i in cardiac function improvement was also observed in several T2D rodent models [63, 64], thereby supporting the central role of glucose overload in cardiomyopathy development.

3.2. High Glucose Increases Oxidative Stress and Mitochondrial Dysfunction in Diabetic NHPs. Excess glucose can increase the production of nicotinamide adenine dinucleotide phosphate hydrogen (NADPH) through the pentose phosphate pathway generated from glucose-6-phosphate (G6P). NADPH is the substrate of cytosolic NADPH oxidase which is known to generate reactive oxygen species (ROS) and served as the principal source of glucose-induced ROS formation in the cells and tissues of diabetic models [65]. Therefore, glucose excess contributes to ROS production and eventually can affect cardiac function. Oxidative stress plays a pivotal role in the pathophysiology of DCM and HF [52, 66]. Mitochondria serve a critical role in energy transduction and intracellular signaling. Interestingly, all the underlying mechanisms of cardiac dysfunction in diabetes are related to mitochondrial injury [67, 68].

Mitochondria disarrangement and impaired mitochondria function were often observed in the diabetic NHP hearts. Mitochondria are the major source of ROS production, and the altered glucose metabolism in diabetic hearts causes mitochondrial oxidative stress evidenced as the excess amount of pyruvate and acetyl-CoA was produced during glycolysis, thus, elevating the production of NADH, an electron carrier. The elevated level of NADH will cause an electron pressure on the mitochondrial electron transport chain, leading to mitochondria dysfunction. The direct role of hyperglycemia in mitochondria dysfunction has been well established in NHPs. A recent study has shown that short-term (1 month) hyperglycemia in cynomolgus monkeys increases mitochondria oxidative stress, and superoxide production, the major form of ROS released from mitochondria, contributes to mitochondria dysfunction [69]. By using cultured NHPs vascular smooth muscle cells with high glucose, Ungvari et al. [70] have shown significantly elevated cellular peroxide levels and mitochondria ROS production.

3.3. Accumulation of Advanced Glycation End Products (AGEs) and Activation of Hexosamine Biosynthesis in Diabetic NHPs. Accumulation of advanced glycation end products (AGEs) and increased hexosamine biosynthesis pathway (HBP) has also been found to play major roles in mediating high glucose-induced mitochondria impairment. AGEs, as a group of irreversible adducts from nonenzymatic glucose reactions with proteins (glycation), participate in the pathogenesis of DCM [71]. Previous studies have shown that chronic hyperglycemia alters mitochondrial function through glycation of mitochondria proteins in diabetic rats and mice [72, 73]. Treatment with an AGEs cross-link breaker, ALT-711, significantly improved ventricular function in diabetic rats [74] and reversed the impaired coupling between the vasculature and heart which is common in aging NHPs [75]. Recently, HBP flux has also been involved in the regulation of mitochondrial dysfunction in DCM. O-linked β-N-acetylglucosamine moiety (O-GlcNAc), supplied by HBP flux, is O-linked on the serine and threonine residues of numerous proteins by O-GlcNAc transferase (OGT). Previous studies have shown that the O-GlcNAcylation process is highly activated in diabetic hyperglycemia in rodents [76] and stressed NHPs [77]. Hu et al. have found that increased

O-GlcNAcylation of mitochondrial proteins impairs mitochondrial function in cardiomyocytes exposed to high glucose [78]. A recent study has demonstrated that dysregulation of O-GlcNAcylation in diabetic cardiac mitochondria plays a key role in mitochondrial dysfunction [79]. Taken together, these results highlight the important role of cardiac O-GlcNAcylation in regulating mitochondrial function in the diabetic heart.

3.4. High Glucose Affects the Response to Cardiac Resynchronization Therapy with Defibrillator (CRT-d) in Diabetic NHPs. Cardiac resynchronization therapy with defibrillator (CRT-d) was often used in HF patients to improve cardiac contractile function, clinical outcomes, and quality of life and to reverse ventricular remodeling [80]. CRT-d was also found to be beneficial for the HF NHPs with the fibrotic myocardial disease based on clinical signs [81]. However, as reported previously, high glucose and T2D are related to an increased percentage of cardiovascular disease (CVD) progression towards HF, which is closely correlated to the proinflammatory and prothrombotic state. Several studies reported that insulin-dependent T2D patients showed a worse prognosis after CRT-d. The researcher believed these were attributed to the alterations in the mitogenic and metabolic pathways in those patients, leading to a poor CVD pathogenesis progression [22]. Recently, authors showed that T2D and other risk factors (hypertension, overweight) influenced the CRT-d's functionality in HFrEF patients by a proarrhythmic status, then can result in a reduced survival rate and higher hospital admissions rate in these patients [80, 82].

Recent findings demonstrated that the ameliorative effects of CRT-d treatment such as improved myocardial ventricular geometry and functional capacity in humans with T2D are determinants of reduced hospitalizations and arrhythmias [83]. Moreover, Sardu et al. found that the multipolar CRT-d pacing was much better than the bipolar CRT-d pacing with a significant reduction of hospitalizations for HF worsening, PNS (phrenic nerve stimulation), LV catheter dislodgment, and atrial fibrillation events, and multipolar CRT-d pacing could be an independent predictor of above events [84]. Furthermore, a recent new technique, an automatic-optimized CRT-d with SensoR technology was found to be superior to the echo-guided CRT-d with respect to the significant increase of CRT-d responder rate and the significant reduction of hospital admissions for HF worsening and cardiac deaths. Therefore, this could be used to reduce the worse prognosis in HF patients with T2D [85]. However, the loss of CRT-d effects was often observed in patients with T2D, which may be due to multiple molecular, electrical, and metabolic cardiac changes. In this setting, the new incretin drugs such as glucagon-like peptide 1 receptor agonists (GLP-1 RA) have been used in HF patients with T2D, and interestingly, the risk of hospitalization for those patients was not increased. Therefore, GLP-1 RA in addition to conventional hypoglycemic therapy was also introduced to HF patients with T2D to improve the CRT-d responder rate. It was confirmed that GLP-1 RA therapy in addition to standard hypoglycemic drugs significantly reduced inflammation, B type natriuretic peptide values (linked to the improvement of LVEF), hemodynamic effects, arrhythmic burden, and hospitalization for HF worsening in failing heart patients with T2D treated by CRT-d [86]. Thus, this describes the glycemic control necessary to successfully manage these HF patients in conjunction with CRT-d therapy.

3.5. Experimental Diabetic NHP Models

3.5.1. Spontaneous Diabetic NHP Models. Several NHP species develop obesity and diabetes spontaneously, and these NHPs exhibit clinical characteristics of obesity and diabetes including insulin resistance, hyperinsulinemia, dyslipidemia, progressive hyperglycemia, and pancreas pathology are similar to humans [87]. This makes these NHPs valuable resources for studying therapeutic interventions and molecular and cellular mechanisms of human T2D as well as related cardiovascular disease (CVD). Macaques, including cynomolgus macaques and rhesus macaques, are the most widely studied spontaneous diabetic NHP models [88].

Previous studies have shown that approximately 30% of middle-aged cynomolgus monkeys (>15 years-old) exhibit impaired glucose tolerance (IGT) with moderate hyperinsulinemia before becoming overt hyperglycemia [48]. Like humans, cynomolgus monkeys progress from IGT to T2DM with a decrease in pancreatic insulin secretion. T2D monkeys always exhibit increased glycated hemoglobin (HbA1c), hyperglycaemic, dyslipidemic with severe insulin resistance, and decreased glucose clearance rate for years before clinical intervention is needed [89]. A recent study in spontaneous obese, dysmetabolic, and diabetic cynomolgus monkeys has demonstrated LV systolic and diastolic dysfunctions in these NHPs, similarly to that in diabetic patients [31].

The increased baseline of insulin secretion and impaired insulin response to glucose challenge are the earliest characteristics in T2D rhesus monkeys. Wang et al. previously screened 3 middle and elderly aged rhesus monkeys from 100 rhesus monkeys by glucose tolerance test and glycosuria test [90]. This indicated the morbidity rate of spontaneous diabetes in rhesus monkeys is consistent with that observed in humans. Rhesus monkeys also exhibit age-related clinical diabetes features including decreased insulin sensitivity and decreased insulin response to glucose challenge [91, 92]. By echocardiography and magnetic resonance imaging, 6 out of 15 T2D rhesus monkeys were diagnosed with diastolic dysfunction [93]. Importantly, female NHPs have menstrual cycles that closely approximate that of humans and gestational diabetes (GD) has been demonstrated in cynomolgus [94] and rhesus monkeys [95]. GD monkeys exhibit elevated glucose and insulin and deliver macrosomic infants, similar to women with GD [94], and there is a risk of developing T2D following GD in monkeys as in humans [48].

3.5.2. Inducing Diabetic NHP Models. Given that the disease progression is relatively slow and the percentage of NHPs progressing to overt diabetes is small, researchers successfully induced T2D monkey models by diet regimens. These T2D monkey models are more closely resemble human T2D

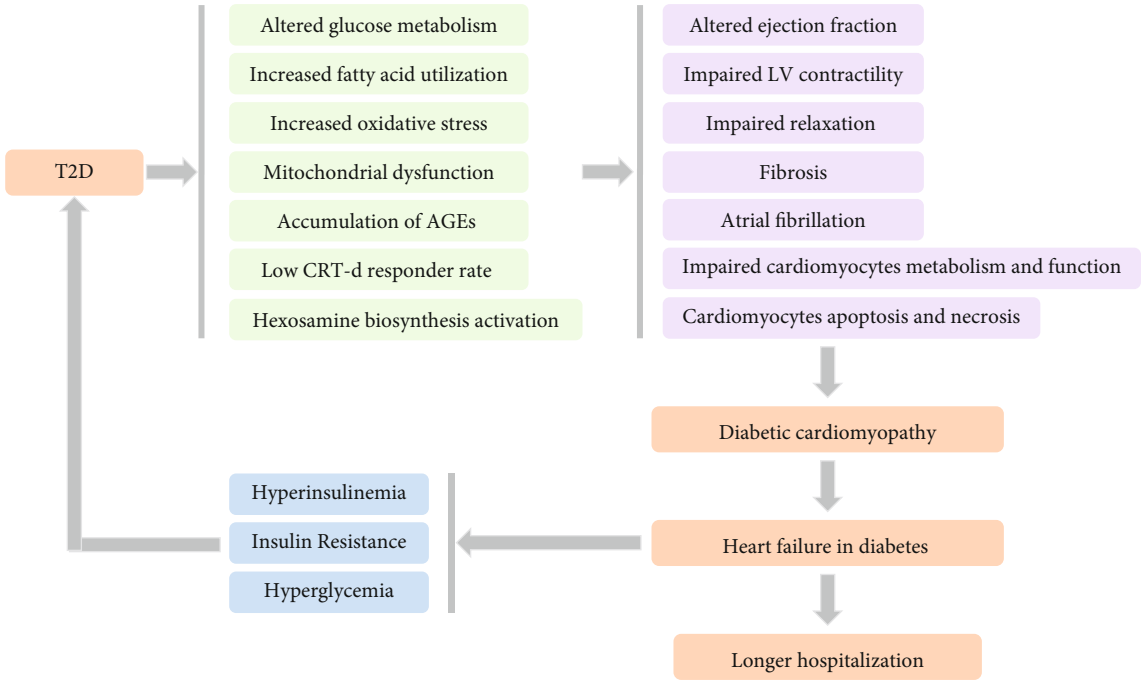

Figure 1: The effects of type 2 diabetes (T2D) in patients with heart failure (HF). Patients with T2D can lead to altered glucose metabolism, increased fatty acid utilization and oxidative stress, mitochondrial dysfunction, accumulation of advanced glycation end products (AGEs), lower cardiac resynchronization therapy with defibrillator (CRT-d) responder rate, and hexosamine biosynthesis activation. These effects cause altered ejection fraction, impaired left ventricular (LV) contractility, impaired relaxation, heart fibrosis, atrial fibrillation, impaired cardiomyocytes metabolism and function, cardiomyocytes apoptosis, and necrosis, all of which contribute to diabetic cardiomyopathy, leading to increased heart failure in diabetes. T2D patients with HF present longer hospitalization and a higher rate of hyperinsulinemia, insulin resistance, and hyperglycemia, which can further exacerbate T2D progression.

pathogenesis as compared with models induced by streptozotocin, a specific β-cell toxin. Streptozotocin-induced diabetic monkeys, presenting different extent of islet damage, are usually not insulin resistant but require exogenous insulin treatment [96].

Many NHPs fed with high fat and/or high sugar diet progressively developed from insulin resistance and impaired glucose tolerance to T2D, as in humans [97]. Bremer et al. demonstrated that a high fructose dietary additive was able to induce metabolic syndrome features including central obesity and T2D in rhesus monkeys [98]. Kavanagh et al. have shown that long-term administration of trans fatty acids in monkeys leads to significant weight gain and insulin resistance in this NHP model [99]. Taken together, the above findings also provided data on further optimizing dietary strategies to establish more effective animal models for studying human T2D.

As discussed above, glucose overload plays a central role in the development of DCM, therefore, glucose control is the primary objective for the treatment of DCM. Caloric restriction is a successful intervention for the management of T2-related metabolic abnormalities both for humans and NHPs [99, 100]. A caloric restriction study in cynomolgus and rhesus monkeys successfully decreased plasma glucose and insulin level and increased insulin sensitivity [101, 102]. Other treatments including SGLT2i, which is a new class of antidiabetic drugs that reduces glucotoxicity by promoting glycosuria, have been conducted in NHPs [62] and used to treat HF patients with T2D [38].

Metformin and thiazolidinedione are used to improve insulin resistance and glucose uptake. Sulfonylureas, glucagon-like peptide-1 (GLP-1) agonists, and dipeptidyl peptidase-4 (DPP-4) inhibitors are also used in both humans and NHPs to stimulate insulin secretion to lower blood glucose [103].

4. Advantages and Limitations of NHP Models

The most important advantages of NHP models are the genetic and physiological similarities to humans, and the genomes of some NHP species have been sequenced [104, 105]. The second advantage in NHP studies is the complete control of diet, drug treatment regimens, which are quite difficult to be controlled in human subjects. Additionally, the biopsies of different organs can be sequentially acquired through minimally invasive approaches in the studies of NHPs, which is not possible in humans. Nevertheless, there are very few studies using nonhuman primate aging models likely because of their limited existing numbers, high cost, and potential ethical concerns. There are also very limited facilities that can provide support for NHP research due to the challenges of limited resources and required technical expertise.

5. Conclusions of the Importance of NHPs in DCM Research

Given the fact that T2D is a major risk factor for HF and hyperglycemia is strongly associated with diastolic dysfunction in diabetes patients, summarized in Figure 1, and the investment in T2D and HF research by the whole society, reliable preclinical models of human disease are urgently needed. NHPs are such an invaluable translational model in the study of human DCM pathology. First, NHPs show the greatest similarities to the disease of humans. Second, the genomes of the commonly used NHPs in biomedical research have been sequenced. Third, NHP models served as unique models for establishing the safety and efficacy of novel drug development in humans.

Data Availability

The data supporting this review are from previously reported studies and datasets, which have been cited.

Conflicts of Interest

The authors declare that they have no conflicts of interest.

Acknowledgments

This work was supported partly by the Science and Technology Program in Liao Ning Province (2019-ZD-0774).

References

[1] N. H. Cho, J. E. Shaw, S. Karuranga et al., "IDF Diabetes Atlas: Global estimates of diabetes prevalence for 2017 and projections for 2045," *Diabetes Research and Clinical Practice*, vol. 138, pp. 271–281, 2018.

[2] G. Danaei, Y. Lu, G. M. Singh et al., "Cardiovascular disease, chronic kidney disease, and diabetes mortality burden of cardiometabolic risk factors from 1980 to 2010: a comparative risk assessment," *The Lancet Diabetes & Endocrinology*, vol. 2, pp. 634–647, 2014.

[3] I. Martín-Timón, C. Sevillano-Collantes, A. Segura-Galindo, and F. J. del Cañizo-Gómez, "Type 2 diabetes and cardiovascular disease: have all risk factors the same strength?," *World Journal of Diabetes*, vol. 5, no. 4, pp. 444–470, 2014.

[4] F. A. McAlister, K. K. Teo, M. Taher et al., "Insights into the contemporary epidemiology and outpatient management of congestive heart failure," *American Heart Journal*, vol. 138, no. 1, pp. 87–94, 1999.

[5] M. C. Thomas, "Type 2 diabetes and heart failure: challenges and solutions," *Current Cardiology Reviews*, vol. 12, no. 3, pp. 249–255, 2016.

[6] M. Tate, D. J. Grieve, and R. H. Ritchie, "Are targeted therapies for diabetic cardiomyopathy on the horizon?," *Clinical Science (London, England)*, vol. 131, no. 10, pp. 897–915, 2017.

[7] W. B. Kannel and D. L. McGee, "Diabetes and glucose tolerance as risk factors for cardiovascular disease: the Framingham study," *Diabetes Care*, vol. 2, no. 2, pp. 120–126, 1979.

[8] T. H. Marwick, "Diabetic heart disease," *Heart*, vol. 92, pp. 296–300, 2008.

[9] S. A. Hayat, B. Patel, R. S. Khattar, and R. A. Malik, "Diabetic cardiomyopathy: mechanisms, diagnosis and treatment," *Clinical Science*, vol. 107, no. 6, pp. 539–557, 2004.

[10] A. Norhammar, J. Bodegard, T. Nystrom, M. Thuresson, J. W. Eriksson, and D. Nathanson, "Incidence, prevalence and mortality of type 2 diabetes requiring glucose-lowering treatment, and associated risks of cardiovascular complications: a nationwide study in Sweden, 2006-2013," *Diabetologia*, vol. 59, no. 8, pp. 1692–1701, 2016.

[11] J. D. Schilling and D. L. Mann, "Diabetic cardiomyopathy: bench to bedside," *Heart Failure Clinics*, vol. 8, no. 4, pp. 619–631, 2012.

[12] E. Picano, "Diabetic cardiomyopathy. The importance of being earliest," *Journal of the American College of Cardiology*, vol. 42, no. 3, pp. 454–457, 2003.

[13] S. Boudina and E. D. Abel, "Diabetic cardiomyopathy revisited," *Circulation*, vol. 115, no. 25, pp. 3213–3223, 2007.

[14] J. Webb, L. Fovargue, K. Tøndel et al., "The emerging role of cardiac magnetic resonance imaging in the evaluation of patients with HFpEF," *Current Heart Failure Reports*, vol. 15, no. 1, pp. 1–9, 2018.

[15] A. Lorenzo-Almoros, J. Tunon, M. Orejas, M. Cortes, J. Egido, and O. Lorenzo, "Diagnostic approaches for diabetic cardiomyopathy," *Cardiovascular Diabetology*, vol. 16, no. 1, p. 28, 2017.

[16] D. C. Raev, "Which left ventricular function is impaired earlier in the evolution of diabetic cardiomyopathy? An echocardiographic study of young type I diabetic patients," *Diabetes Care*, vol. 17, no. 7, pp. 633–639, 1994.

[17] D. S. H. Bell, "Diabetic cardiomyopathy," *Diabetes Care*, vol. 26, no. 10, pp. 2949–2951, 2003.

[18] L. Zhang, J. J. Liebelt, N. Madan, J. Shan, and C. C. Taub, "Comparison of predictors of heart failure with preserved versus reduced ejection fraction in a multiracial cohort of preclinical left ventricular diastolic dysfunction," *The American Journal of Cardiology*, vol. 119, no. 11, pp. 1815–1820, 2017.

[19] C. Iribarren, A. J. Karter, A. S. Go et al., "Glycemic control and heart failure among adult patients with diabetes," *Circulation*, vol. 103, no. 22, pp. 2668–2673, 2001.

[20] J. Y. Cho, K. H. Kim, S. E. Lee et al., "Admission hyperglycemia as a predictor of mortality in acute heart failure: comparison between the diabetics and non-diabetics," *Journal of Clinical Medicine*, vol. 9, no. 1, p. 149, 2020.

[21] R. Marfella, C. Di Filippo, N. Potenza et al., "Circulating microRNA changes in heart failure patients treated with cardiac resynchronization therapy: responders vs. non-responders," *European Journal of Heart Failure*, vol. 15, no. 11, pp. 1277–1288, 2013.

[22] C. Sardu, M. Barbieri, M. R. Rizzo, P. Paolisso, G. Paolisso, and R. Marfella, "Cardiac resynchronization therapy outcomes in type 2 diabetic patients: role of microRNA changes," *Journal Diabetes Research*, vol. 2016, article 7292564, pp. 1–8, 2016.

[23] G. Santulli, G. Pagano, C. Sardu et al., "Calcium release channel RyR2 regulates insulin release and glucose homeostasis," *The Journal of Clinical Investigation*, vol. 125, no. 5, pp. 1968–1978, 2015.

[24] R. Wichi, C. Malfitano, K. Rosa et al., "Noninvasive and invasive evaluation of cardiac dysfunction in experimental diabetes in rodents," *Cardiovascular Diabetology*, vol. 6, no. 1, p. 14, 2007.

[25] J. Fuentes-Antras, B. Picatoste, A. Gomez-Hernandez, J. Egido, J. Tunon, and O. Lorenzo, "Updating experimental models of diabetic cardiomyopathy," *Journal Diabetes Research*, vol. 2015, article 656795, pp. 1–15, 2015.

[26] H. J. Harwood Jr., P. Listrani, and J. D. Wagner, "Nonhuman primates and other animal models in diabetes research," *Journal of Diabetes Science and Technology*, vol. 6, no. 3, pp. 503–514, 2012.

[27] T. A. Lutz, "An overview of rodent models of obesity and type 2 diabetes," *Methods in Molecular Biology*, vol. 2128, pp. 11–24, 2020.

[28] B. Ludwig, E. Wolf, U. Schonmann, and S. Ludwig, "Large animal models of diabetes," *Methods in Molecular Biology*, vol. 2128, pp. 115–134, 2020.

[29] J. D. Harding, "Nonhuman primates and translational research: progress, opportunities, and challenges," *ILAR Journal*, vol. 58, no. 2, pp. 141–150, 2017.

[30] J. E. Wagner, K. Kavanagh, G. M. Ward, B. J. Auerbach, H. J. Harwood Jr., and J. R. Kaplan, "Old world nonhuman primate models of type 2 diabetes mellitus," *ILAR Journal*, vol. 47, no. 3, pp. 259–271, 2006.

[31] H. Gu, Y. Liu, S. Mei et al., "Left ventricular diastolic dysfunction in nonhuman primate model of dysmetabolism and diabetes," *BMC Cardiovascular Disorders*, vol. 15, no. 1, p. 141, 2015.

[32] A. Clark, E. J. de Koning, A. T. Hattersley, B. C. Hansen, C. S. Yajnik, and J. Poulton, "Pancreatic pathology in non-insulin dependent diabetes (NIDDM)," *Diabetes Research and Clinical Practice*, vol. 28, pp. S39–S47, 1995.

[33] S. Krog, T. P. Ludvigsen, O. L. Nielsen et al., "Myocardial changes in diabetic and nondiabetic nonhuman primates," *Veterinary Pathology*, vol. 57, no. 2, pp. 332–343, 2020.

[34] O. Cabrera, D. M. Berman, N. S. Kenyon, C. Ricordi, P. O. Berggren, and A. Caicedo, "The unique cytoarchitecture of human pancreatic islets has implications for islet cell function," *Proceedings of the National Academy of Sciences of the United States of America*, vol. 103, no. 7, pp. 2334–2339, 2006.

[35] S. Sampath, M. Klimas, D. Feng et al., "Characterization of regional left ventricular function in nonhuman primates using magnetic resonance imaging biomarkers: a test-retest repeatability and inter-subject variability study," *PLoS One*, vol. 10, no. 5, article e0127947, 2015.

[36] B. S. Chung, C. Y. Jeon, J. W. Huh et al., "Rise of the visible monkey: sectioned images of rhesus monkey," *Journal of Korean Medical Science*, vol. 34, no. 8, article e66, 2019.

[37] R. J. Colman, "Non-human primates as a model for aging," *Biochimica et Biophysica Acta - Molecular Basis of Disease*, vol. 1864, no. 9, pp. 2733–2741, 2018.

[38] L. Athithan, G. S. Gulsin, G. P. McCann, and E. Levelt, "Diabetic cardiomyopathy: pathophysiology, theories and evidence to date," *World Journal of Diabetes*, vol. 10, no. 10, pp. 490–510, 2019.

[39] I. Ungar, M. Gilbert, A. Siegel, J. M. Blain, and R. J. Bing, "Studies on myocardial metabolism: IV. Myocardial metabolism in diabetes," *The American Journal of Medicine*, vol. 18, no. 3, pp. 385–396, 1955.

[40] H. Taegtmeyer, C. Beauloye, R. Harmancey, and L. Hue, "Insulin resistance protects the heart from fuel overload in dysregulated metabolic states," *American Journal of Physiology. Heart and Circulatory Physiology*, vol. 305, no. 12, pp. H1693–H1697, 2013.

[41] A. R. Wende and E. D. Abel, "Lipotoxicity in the heart," *Biochimica et Biophysica Acta*, vol. 1801, no. 3, pp. 311–319, 2010.

[42] C. C. Low Wang, C. N. Hess, W. R. Hiatt, and A. B. Goldfine, "Clinical update: cardiovascular disease in diabetes mellitus: atherosclerotic cardiovascular disease and heart failure in type 2 diabetes mellitus-mechanisms, management, and clinical considerations," *Circulation*, vol. 133, no. 24, pp. 2459–2502, 2016.

[43] B. Stratmann and D. Tschoepe, "The diabetic heart: sweet, fatty and stressed," *Expert Review of Cardiovascular Therapy*, vol. 9, no. 9, pp. 1093–1096, 2014.

[44] H. Taegtmeyer, P. McNulty, and M. E. Young, "Adaptation and maladaptation of the heart in diabetes: part I: general concepts," *Circulation*, vol. 105, no. 14, pp. 1727–1733, 2002.

[45] S. K. Verma, V. N. S. Garikipati, and R. Kishore, "Mitochondrial dysfunction and its impact on diabetic heart," *Biochimica et Biophysica Acta - Molecular Basis of Disease*, vol. 1863, no. 5, pp. 1098–1105, 2017.

[46] J. Gollmer, A. Zirlik, and H. Bugger, "Mitochondrial mechanisms in diabetic cardiomyopathy," *Diabetes and Metabolism Journal*, vol. 44, no. 1, pp. 33–53, 2020.

[47] C. Riehle and E. D. Abel, "Insulin signaling and heart failure," *Circulation Research*, vol. 118, no. 7, pp. 1151–1169, 2016.

[48] J. D. Wagner, J. M. Cline, M. K. Shadoan, B. C. Bullock, S. E. Rankin, and W. T. Cefalu, "Naturally occurring and experimental diabetes in cynomolgus monkeys: a comparison of carbohydrate and lipid metabolism and islet pathology," *Toxicologic Pathology*, vol. 29, pp. 142–148, 2001.

[49] B. Wang, X. Wang, G. Sun et al., "Dysglycemia and dyslipidemia models in nonhuman primates: part I. Model of naturally occurring diabetes," *Journal of Diabetes & Metabolism*, vol. s13, 2015.

[50] M. S. Byers, C. Howard, and X. Wang, "Avian and mammalian facilitative glucose transporters," *Microarrays*, vol. 6, no. 2, p. 7, 2017.

[51] M. K. Shadoan, L. Zhang, and J. D. Wagner, "Effects of hormone therapy on insulin signaling proteins in skeletal muscle of cynomolgus monkeys," *Steroids*, vol. 69, no. 5, pp. 313–318, 2004.

[52] M. Isfort, S. C. Stevens, S. Schaffer, C. J. Jong, and L. E. Wold, "Metabolic dysfunction in diabetic cardiomyopathy," *Heart Failure Reviews*, vol. 19, no. 1, pp. 35–48, 2014.

[53] L. S. Mansor, E. R. Gonzalez, M. A. Cole et al., "Cardiac metabolism in a new rat model of type 2 diabetes using high-fat diet with low dose streptozotocin," *Cardiovascular Diabetology*, vol. 12, no. 1, p. 136, 2013.

[54] W. C. Stanley, G. D. Lopaschuk, and J. G. McCormack, "Regulation of energy substrate metabolism in the diabetic heart," *Cardiovascular Research*, vol. 34, no. 1, pp. 25–33, 1997.

[55] H. Yan, W. Gu, J. Yang et al., "Fully human monoclonal antibodies antagonizing the glucagon receptor improve glucose homeostasis in mice and monkeys," *The Journal of Pharmacology and Experimental Therapeutics*, vol. 329, no. 1, pp. 102–111, 2009.

[56] M. E. Young, P. McNulty, and H. Taegtmeyer, "Adaptation and maladaptation of the heart in diabetes: part II: potential mechanisms," *Circulation*, vol. 105, no. 15, pp. 1861–1870, 2002.

[57] Y. Zhong, S. Ahmed, I. L. Grupp, and M. A. Matlib, "Altered SR protein expression associated with contractile dysfunction

in diabetic rat hearts," *American Journal of Physiology. Heart and Circulatory Physiology*, vol. 281, no. 3, pp. H1137–H1147, 2001.

[58] D. Montaigne, X. Marechal, A. Coisne et al., "Myocardial contractile dysfunction is associated with impaired mitochondrial function and dynamics in type 2 diabetic but not in obese patients," *Circulation*, vol. 130, no. 7, pp. 554–564, 2014.

[59] D. Dyntar, P. Sergeev, J. Klisic, P. Ambuhl, M. C. Schaub, and M. Y. Donath, "High glucose alters cardiomyocyte contacts and inhibits myofibrillar formation," *The Journal of Clinical Endocrinology and Metabolism*, vol. 91, no. 5, pp. 1961–1967, 2006.

[60] L. Cai, W. Li, G. Wang, L. Guo, Y. Jiang, and Y. J. Kang, "Hyperglycemia-induced apoptosis in mouse myocardium: mitochondrial cytochrome C-mediated caspase-3 activation pathway," *Diabetes*, vol. 51, no. 6, pp. 1938–1948, 2002.

[61] S. Sen, B. K. Kundu, H. C. Wu et al., "Glucose regulation of load-induced mTOR signaling and ER stress in mammalian heart," *Journal of the American Heart Association*, vol. 2, no. 3, article e004796, 2013.

[62] W. Zhang, X. Li, H. Ding et al., "Metabolism and disposition of the SGLT2 inhibitor bexagliflozin in rats, monkeys and humans," *Xenobiotica*, vol. 50, no. 5, pp. 559–569, 2020.

[63] M. Joubert, B. Jagu, D. Montaigne et al., "The sodium-glucose cotransporter 2 inhibitor dapagliflozin prevents cardiomyopathy in a diabetic lipodystrophic mouse model," *Diabetes*, vol. 66, no. 4, pp. 1030–1040, 2017.

[64] J. Habibi, A. R. Aroor, J. R. Sowers et al., "Sodium glucose transporter 2 (SGLT2) inhibition with empagliflozin improves cardiac diastolic function in a female rodent model of diabetes," *Cardiovascular Diabetology*, vol. 16, no. 1, p. 9, 2017.

[65] O. O. Oguntibeju, "Type 2 diabetes mellitus, oxidative stress and inflammation: examining the links," *International Journal of Physiology, Pathophysiology and Pharmacology*, vol. 11, no. 3, pp. 45–63, 2019.

[66] N. Kaludercic and F. Di Lisa, "Mitochondrial ROS formation in the pathogenesis of diabetic cardiomyopathy," *Frontiers in Cardiovascular Medicine*, vol. 7, p. 12, 2020.

[67] J. D. Schilling, "The mitochondria in diabetic heart failure: from pathogenesis to therapeutic promise," *Antioxidants & Redox Signaling*, vol. 22, no. 17, pp. 1515–1526, 2015.

[68] W. I. Sivitz and M. A. Yorek, "Mitochondrial dysfunction in diabetes: from molecular mechanisms to functional significance and therapeutic opportunities," *Antioxidants & Redox Signaling*, vol. 12, no. 4, pp. 537–577, 2010.

[69] P. A. Rowe, K. Kavanagh, L. Zhang, H. J. Harwood, and J. D. Wagner, "Short-term hyperglycemia increases arterial superoxide production and iron dysregulation in atherosclerotic monkeys," *Metabolism*, vol. 60, no. 8, pp. 1070–1080, 2011.

[70] Z. Ungvari, L. Bailey-Downs, T. Gautam et al., "Age-associated vascular oxidative stress, Nrf2 dysfunction, and NF-κB activation in the nonhuman primate Macaca mulatta," *The Journals of Gerontology. Series A, Biological Sciences and Medical Sciences*, vol. 66, pp. 866–875, 2011.

[71] H. Ma, S. Y. Li, P. Xu et al., "Advanced glycation endproduct (AGE) accumulation and AGE receptor (RAGE) up-regulation contribute to the onset of diabetic cardiomyopathy," *Journal of Cellular and Molecular Medicine*, vol. 13, no. 8b, pp. 1751–1764, 2009.

[72] M. G. Rosca, T. G. Mustata, M. T. Kinter et al., "Glycation of mitochondrial proteins from diabetic rat kidney is associated with excess superoxide formation," *American Journal of Physiology. Renal Physiology*, vol. 289, no. 2, pp. F420–F430, 2005.

[73] H. Bugger, D. Chen, C. Riehle et al., "Tissue-specific remodeling of the mitochondrial proteome in type 1 diabetic akita mice," *Diabetes*, vol. 58, no. 9, pp. 1986–1997, 2009.

[74] B. H. Wolffenbuttel, C. M. Boulanger, F. R. Crijns et al., "Breakers of advanced glycation end products restore large artery properties in experimental diabetes," *Proceedings of the National Academy of Sciences of the United States of America*, vol. 95, no. 8, pp. 4630–4634, 1998.

[75] P. V. Vaitkevicius, M. Lane, H. Spurgeon et al., "A cross-link breaker has sustained effects on arterial and ventricular properties in older rhesus monkeys," *Proceedings of the National Academy of Sciences of the United States of America*, vol. 98, no. 3, pp. 1171–1175, 2001.

[76] K. A. Robinson, M. L. Weinstein, G. E. Lindenmayer, and M. G. Buse, "Effects of diabetes and hyperglycemia on the hexosamine synthesis pathway in rat muscle and liver," *Diabetes*, vol. 44, no. 12, pp. 1438–1446, 1995.

[77] N. E. Zachara, N. O'Donnell, W. D. Cheung, J. J. Mercer, J. D. Marth, and G. W. Hart, "Dynamic *O*-GlcNAc Modification of Nucleocytoplasmic Proteins in Response to Stress:," *Journal of Biological Chemistry*, vol. 279, no. 29, pp. 30133–30142, 2004.

[78] Y. Hu, J. Suarez, E. Fricovsky et al., "Increased enzymatic O-GlcNAcylation of mitochondrial proteins impairs mitochondrial function in cardiac myocytes exposed to high glucose∗," *The Journal of Biological Chemistry*, vol. 284, no. 1, pp. 547–555, 2009.

[79] P. S. Banerjee, J. Ma, and G. W. Hart, "Diabetes-associated dysregulation of O-GlcNAcylation in rat cardiac mitochondria," *Proceedings of the National Academy of Sciences of the United States of America*, vol. 112, no. 19, pp. 6050–6055, 2015.

[80] C. Sardu, M. Santamaria, S. Funaro et al., "Cardiac electrophysiological alterations and clinical response in cardiac resynchronization therapy with a defibrillator treated patients affected by metabolic syndrome," *Medicine (Baltimore)*, vol. 96, no. 14, article e6558, 2017.

[81] E. M. Rush, A. L. Ogburn, and D. Monroe, "Clinical management of a western lowland gorilla (Gorilla gorilla gorilla) with a cardiac resynchronization therapy device," *Journal of Zoo and Wildlife Medicine*, vol. 42, no. 2, pp. 263–276, 2011.

[82] C. Sardu, R. Marfella, M. Santamaria et al., "Stretch, injury and inflammation markers evaluation to predict clinical outcomes after implantable cardioverter defibrillator therapy in heart failure patients with metabolic syndrome," *Frontiers in Physiology*, vol. 9, p. 758, 2018.

[83] C. Sardu, R. Marfella, and G. Santulli, "Impact of diabetes mellitus on the clinical response to cardiac resynchronization therapy in elderly people," *Journal of Cardiovascular Translational Research*, vol. 7, no. 3, pp. 362–368, 2014.

[84] C. Sardu, M. Barbieri, M. Santamaria et al., "Multipolar pacing by cardiac resynchronization therapy with a defibrillators treatment in type 2 diabetes mellitus failing heart patients: impact on responders rate, and clinical outcomes," *Cardiovascular Diabetology*, vol. 16, no. 1, p. 75, 2017.

[85] C. Sardu, P. Paolisso, V. Ducceschi et al., "Cardiac resynchronization therapy and its effects in patients with type 2 DIAbetes mellitus OPTimized in automatic vs. echo guided

approach. Data from the DIA-OPTA investigators," *Cardiovascular Diabetology*, vol. 19, no. 1, p. 202, 2020.

[86] C. Sardu, P. Paolisso, C. Sacra et al., "Cardiac resynchronization therapy with a defibrillator (CRTd) in failing heart patients with type 2 diabetes mellitus and treated by glucagon-like peptide 1 receptor agonists (GLP-1 RA) therapy vs. conventional hypoglycemic drugs: arrhythmic burden, hospitalizations for heart failure, and CRTd responders rate," *Cardiovascular Diabetology*, vol. 17, p. 137, 2018.

[87] W. T. Cefalu, "Animal models of type 2 diabetes: clinical presentation and pathophysiological relevance to the human condition," *ILAR Journal*, vol. 47, no. 3, pp. 186–198, 2006.

[88] J. Wagner, J. Cann, L. Zhang, and H. Harwood Jr., "Diabetes and obesity research using nonhuman primates," in *Nonhuman primates in biomedical research Volume 2: Diseases*, pp. 699–732, Elsevier, 2012.

[89] J. D. Wagner, C. S. Carlson, T. D. O'Brien, M. S. Anthony, B. C. Bullock, and W. T. Cefalu, "Diabetes mellitus and islet amyloidosis in cynomolgus monkeys," *Laboratory Animal Science*, vol. 46, no. 1, pp. 36–41, 1996.

[90] Y. Wang, H. Ye, and J. Shao, "Discussion of rhesus monkey model of the spontaneous diabetes," *Chinese Journal of Laboratory Animal Science*, vol. 14, pp. 13–15, 2004.

[91] J. J. Ramsey, J. L. Laatsch, and J. W. Kemnitz, "Age and gender differences in body composition, energy expenditure, and glucoregulation of adult rhesus monkeys," *Journal of Medical Primatology*, vol. 29, no. 1, pp. 11–19, 2000.

[92] X. T. Tigno, G. Gerzanich, and B. C. Hansen, "Age-related changes in metabolic parameters of nonhuman primates," *The Journals of Gerontology. Series A, Biological Sciences and Medical Sciences*, vol. 59, no. 11, pp. 1081–1088, 2004.

[93] C. Qian, L. Gong, Z. Yang et al., "Diastolic dysfunction in spontaneous type 2 diabetes rhesus monkeys: a study using echocardiography and magnetic resonance imaging," *BMC Cardiovascular Disorders*, vol. 15, no. 1, p. 59, 2015.

[94] J. D. Wagner, M. J. Jayo, B. C. Bullock, and S. A. Washburn, "Gestational diabetes mellitus in a cynomolgus monkey with group A streptococcal metritis and hemolytic uremic syndrome," *Journal of Medical Primatology*, vol. 21, no. 7-8, pp. 371–374, 1992.

[95] M. J. Kessler, C. F. Howard Jr., and W. T. London, "Gestational diabetes mellitus and impaired glucose tolerance in an aged Macaca mulatta," *Journal of Medical Primatology*, vol. 14, no. 5, pp. 237–244, 1985.

[96] Y. Saisho, A. E. Butler, E. Manesso et al., "Relationship between fractional pancreatic beta cell area and fasting plasma glucose concentration in monkeys," *Diabetologia*, vol. 53, no. 1, pp. 111–114, 2010.

[97] S. D. Tardif, M. L. Power, C. N. Ross, J. N. Rutherford, D. G. Layne-Colon, and M. A. Paulik, "Characterization of obese phenotypes in a small nonhuman primate, the common marmoset (Callithrix jacchus)," *Obesity (Silver Spring)*, vol. 17, no. 8, pp. 1499–1505, 2009.

[98] A. A. Bremer, K. L. Stanhope, J. L. Graham et al., "Fructose-fed rhesus monkeys: a nonhuman primate model of insulin resistance, metabolic syndrome, and type 2 diabetes," *Clinical and Translational Science*, vol. 4, no. 4, pp. 243–252, 2011.

[99] K. Kavanagh, K. L. Jones, J. Sawyer et al., "Trans fat diet induces abdominal obesity and changes in insulin sensitivity in monkeys," *Obesity (Silver Spring)*, vol. 15, no. 7, pp. 1675–1684, 2007.

[100] B. C. Hansen, N. L. Bodkin, and H. K. Ortmeyer, "Calorie restriction in nonhuman primates: mechanisms of reduced morbidity and mortality," *Toxicological Sciences*, vol. 52, no. 90001, pp. 56–60, 1999.

[101] N. L. Bodkin, H. K. Ortmeyer, and B. C. Hansen, "Long-term dietary restriction in older-aged rhesus monkeys: effects on insulin resistance," *The Journals of Gerontology. Series A, Biological Sciences and Medical Sciences*, vol. 50, pp. B142–B147, 1995.

[102] Z. Q. Wang, Z. E. Floyd, J. Qin et al., "Modulation of skeletal muscle insulin signaling with chronic caloric restriction in cynomolgus monkeys," *Diabetes*, vol. 58, no. 7, pp. 1488–1498, 2009.

[103] J. M. Forbes and M. E. Cooper, "Mechanisms of diabetic complications," *Physiological Reviews*, vol. 93, no. 1, pp. 137–188, 2013.

[104] T. Tan, L. Xia, K. Tu et al., "Improved Macaca fascicularis gene annotation reveals evolution of gene expression profiles in multiple tissues," *BMC Genomics*, vol. 19, no. 1, p. 787, 2018.

[105] C. Xue, M. Raveendran, R. A. Harris et al., "The population genomics of rhesus macaques (Macaca mulatta) based on whole-genome sequences," *Genome Research*, vol. 26, no. 12, pp. 1651–1662, 2016.

Hindawi
Journal of Diabetes Research
Volume 2020, Article ID 7181383, 8 pages
https://doi.org/10.1155/2020/7181383

Research Article

Early Diabetic Nephropathy and Retinopathy in Patients with Type 1 Diabetes Mellitus Attending Sudan Childhood Diabetes Centre

Hana Ahmed,[1] **Tayseer Elshaikh**,[2] **and Mohamed Abdullah**[1]

[1]*Department of Paediatric and Child Health, Faculty of Medicine, University of Khartoum, Khartoum, Sudan*
[2]*Department of Ophthalmology, Jabir Abu Eliz Diabetes Centre, Khartoum, Sudan*

Correspondence should be addressed to Hana Ahmed; hanahassanahmed2017@gmail.com

Received 17 April 2020; Revised 8 November 2020; Accepted 15 November 2020; Published 24 November 2020

Academic Editor: Markus Wallner

Objective. Data on microvascular complications in children and adolescents with type 1 diabetes mellitus (T1DM) in Sudan are scarce. This study was aimed at determining the prevalence of diabetic nephropathy (DN) and retinopathy (DR) and their relationship to certain risk factors in children with T1DM attending the Sudan Childhood Diabetes Centre. *Design and Methods*. A clinic-based cross-sectional study of 100 patients with T1DM aged 10-18 years. Patients with disease duration exceeding 5 years if the onset of diabetes was prepubertal and 2 years if it was postpubertal were included. Relevant sociodemographic, clinical, and biochemical information was obtained. Blood pressure was measured. The patients were screened for DN and DR using urinary microalbumin estimation and fundus photography, respectively. *Results*. The frequency of microalbuminuria and diabetic retinopathy was 36% and 33%, respectively. Eleven percent had both retinopathy and microalbuminuria. Seven percent of the patients were found to be hypertensive. Patients with diabetic retinopathy had significantly higher HbA1c levels ($p = 0.009$) and longer diabetes duration ($p = 0.02$) than patients without retinopathy. Logistic regression showed that high HbA1c (odds ratio (OR) 0.83, confidence interval (CI) 0.68-1.00, $p = 0.04$), but not age, duration, ethnic group, BMI, blood pressure, and presence of nephropathy, was an independent risk factor for retinopathy. Likewise, high blood pressure (OR 6.89, CI 1.17-40.52, $p = 0.03$), but not age, duration, ethnic group, BMI, HbA1c, and presence of retinopathy, was a predictor for nephropathy. *Conclusion*. High prevalence of incipient DN and early stages of DR were observed in this study. Longer diabetes duration and higher HbA1c were associated with the presence of diabetic retinopathy. High blood pressure was a risk factor for DN. So regular screening for these complications and optimization of glycemic control are needed.

1. Introduction

Type 1 diabetes mellitus (T1DM) can lead to microvascular complications including nephropathy, retinopathy, and neuropathy. These chronic complications lower the quality of life and cause premature death in patients with diabetes [1–3]. Clinically evident diabetes-related microvascular complications are rare in childhood and adolescence. However, early functional and structural abnormalities may be present a few years after the onset of the disease [2]. So screening for these complications is important to identify their occurrence at an early stage.

These microvascular complications of T1DM are associated with certain risk factors like age, ethnicity [4–6], age at onset, diabetes duration, height, BMI, and puberty [1, 2, 7–11].

Other modifiable risk factors include high blood pressure (BP) [2, 12, 13] and long-term glycemic control [8, 9, 14]. The latter was found by many studies to be the most important risk factor for the development of diabetic microangiopathies [8, 14]. Based on the results of the DCCT (Diabetes Control and Complications Trial) and its follow-up study EDIC (Epidemiology of Diabetes Interventions and Complications), it was recommended to optimize glycemic control as early and close to normal as possible in all patients with

T1DM to prevent the development and progression of microvascular complications [3].

There is a paucity of studies on microvascular complications in children and adolescents with T1DM in sub-Saharan Africa. However, all the African published studies showed high prevalence rates in patients with relatively short duration and at a young age [15–17]. Whether this is due to the expected suboptimal glycemic control in developing economies or genetic elements remains a question for further studies. In Sudan, one unpublished study, from 2012, examined young patients with diabetes aged 11-19 years. It reported microalbuminuria in 25% and macroalbuminuria in 15% of the participants [18].

This study was aimed at determining the prevalence and risk factors for diabetic nephropathy and retinopathy among patients with T1DM attending the Sudan Childhood Diabetes Centre.

2. Research Design and Methods

This is a cross-sectional study of consecutively enrolled 100 children with T1DM aged 10-18 years attending the Sudan Childhood Diabetes Centre. The study lasted from February to September 2018. The Sudan Childhood Diabetes Centre is a specialized centre with a comprehensive multidisciplinary team that includes trained endocrinologists, dentists, ophthalmologists, diabetes nurses, diabetes educators, psychologists, dieticians, and social workers. The centre provides free insulin and glucometers either free or at a low cost. Ethical approval was obtained from the Sudan Childhood Diabetes Centre. Informed consent was obtained from the patient and/or his parents.

The diagnosis of T1DM was mostly made by the treating paediatric endocrinologist in the centre clinically, as routine testing for autoantibodies or c-peptide is expensive.

Patients aged ≥10 years with diabetes duration≥5 years if the onset was prepubertal and ≥2 years if it was postpubertal were included [2]. The assessment was performed during the clinic visit, using a validated structured questionnaire. Sociodemographic data include age, sex, residence, and the tribe of the patient using the most accepted ethnic classification of the Sudanese population [19]. Additionally, data on age at onset, duration of diabetes, state of home blood glucose monitoring, dose, and regimen of insulin were collected. A conventional insulin regimen was defined as twice per day premixed insulin plus prelunch regular insulin, while an intensive insulin regimen (MDI = multi-insulin injection regimen) as insulin glargine once/day or NPH twice a day as basal plus regular or rapid-acting insulin before each meal.

Anthropometric measurements, pubertal staging, and blood pressure measurement were done during the interview.

2.1. Blood Pressure Measurement. To assess blood pressure (BP), the patient sat down for a few minutes for rest before two measurements with a 5-10-minute interval, using an aneroid sphygmomanometer, were done. The Korotkoff phases I and V were the systolic and diastolic readings, respectively. Blood pressure was categorized according to BP tables from the fourth report of the national high blood pressure education program working group on the diagnosis, evaluation, and treatment of high blood pressure in children and adolescents, using age and height percentiles, with normotension defined as blood pressure under the 90th percentile, prehypertension systolic blood pressure (SBP) and/or diastolic blood pressure (DBP) 90th to 95th percentile, and hypertension greater than the 95th percentile [20].

2.2. Anthropometric Measurements. Weight was measured using weighing scales to the nearest 0.1 kg. Height was measured using a stadiometer and was expressed in centimeters with no decimal. BMI was categorized according to the Centers for Disease Control and Prevention (CDC) age- and sex-specific growth charts. The following categories were used: underweight: <5th percentile, normal weight: 5th to 85th percentile, overweight: 85th to 95th percentile, and obese: >95th percentile [21]. The sexual maturity rating of the children was determined using the Tanner scale [22].

2.3. Laboratory Evaluation. The most recent HbA1c was obtained from the patients' record. HbA1c was performed in the centre's laboratory with a point-of-care ichromȁ analyzer (company). Then, the patients were classified according to ISPAD 2018 (International Society for Pediatric and Adolescent Diabetes) guidelines which consider HbA1c < 7.5% to be the level for optimal control in resource-limited environments [23].

Urine was examined for the presence of microalbumin in a spot random urine sample, using quantitative immunoturbidimetry of the HemoCue brand (company). Any reading less than 20 mg/l, between 20 mg/l and 200 mg/l, and more than 200 mg/l was considered negative, microalbuminuria, and macroalbuminuria, respectively. Testing on any febrile child, a child with a urinary tract infection, or menstruating female patients was postponed till the next visit. As per ISPAD Clinical Practice Consensus Guidelines 2018 [24], a patient was considered to have persistent microalbuminuria if he had two out of three positive results in the 3-6-month period.

2.4. Retinopathy Diagnosis. Retinopathy was assessed by nonmydriatic two-field digital fundus photography using a fundus camera of the DRS brand (Digital Retinography System) manufactured by CenterVue. The photography was carried out by an experienced optician, and the comments on the photos were made by an ophthalmologist experienced in diabetic retinopathy. Both the optician and the ophthalmologist were masked to the clinical status of the patient.

The classification of diabetic retinopathy was based on the Early Treatment Diabetic Retinopathy Study (ETDRS) classification [25], which regards any diabetes-related retinal lesion, commonly microaneurysms, as the onset of diabetic retinopathy. This is following the latest ISPAD recommendation for retinopathy screening [24].

2.5. Statistical Analysis. Descriptive statistics were reported as mean ± standard deviation when normally distributed and as median (interquartile range) for nonparametric data. Clinical characteristics and complication rates were compared using chi-square tests or Fisher's exact test for categorical variables,

Table 1: Characteristics of the total participants and patients with and without nephropathy and retinopathy.

Risk factor	Total subjects	No DN	DN	p value	No DR	DR	p value
N (%)	100 (100%)	64 (64%)	36 (36%)	—	67 (67%)	33 (33%)	—
Median age (years)	15.6 (14.1-17)	15.4 (13.9-16.9)	15.9 (14.4-17.2)	0.33	15.3 (14-16.9)	15.7 (14.7-17.3)	0.33
Male/female (%)	39/61 (39%/61%)	22/42 (34.4%/65.6%)	17/19 (47.2%/52.8%)	0.21	26/41 (38.8%/61.2%)	13/20 (39.4%/60.6%)	0.95
Residence: urban/rural	57/43 (57%/43%)	38/26 (59.4%/40.6%)	19/17 (52.8%/47.2%)	0.52	36/31 (53.7%/46.3%)	21/12 (63.6%/36.4%)	0.35
Ethnic group							
Afro-Asiatic	79 (79%)	48/64 (75%)	31/36 (86.1%)		50/67 (74.7%)	29/33 (87.8%)	
Nilo-Saharan	12 (12%)	9/64 (14%)	3/36 (8.3%)	0.40	10/67 (14.9%)	2/33 (6.1%)	0.3
Niger-Congo	9 (9%)	7/64 (11%)	2/36 (5.6%)		7/67 (10.4%)	2/33 (6.1%)	
Median age at diabetes diagnosis (years)	9 (7-11.4)	9.1 (5.5-11.5)	9 (7-11.3)	0.94	9 (7-12)	8.7 (5.3-11)	0.15
Median diabetes duration (years)	6 (4-9)	6 (4-8.7)	6.6 (4-9)	0.76	5.3 (4-8)	7 (5.1-10.2)	0.02
BMI (overweight+obese/total)	9/100 (9%)	6/64 (9.4%)	3/36 (8.3%)	0.43	6/67 (9%)	3/33 (9%)	0.45
Puberty (pubertal/total)	94/100 (94%)	59/64 (92.2%)	35/36 (97.2%)	0.18	63/67 (94%)	31/33 (94%)	0.47
Blood pressure							
Normal	85/100 (85%)	58/64 (90.6%)	27/36 (75%)		57/67 (85%)	28/33 (85%)	
Prehypertension	8/100 (8%)	4/64 (6.3%)	4/36 (11.1%)	0.07	6/67 (9%)	2/33 (6%)	0.76
Hypertension	7/100 (7%)	2/64 (3.1%)	5/36 (13.9%)		4/67 (6%)	3/33 (9%)	
Median HbA1c (%)	11.8% (9-14)	11.7 (9-13.3)	12 (9-14)	0.75	10.2 (8.6-12)	12.4 (9.1-14)	0.009

t -tests for normally distributed continuous data, and Mann-Whitney U tests for skewed data. Comparison between more than two groups was performed using the Kruskal-Wallis test. The distribution of continuous data was tested for normality by the Kolmogorov-Smirnov test. Logistic regression was performed with the presence of DR and DN as dependent variables. The independent variables were age, diabetes duration, ethnic group, BMI, blood pressure, HbA1c, and the presence of the other complication (DR for DN and vice versa). Because of the significant collinearity between duration and age at onset and age and Tanner stage, age at onset and Tanner stage were omitted from the final model. Results are reported as odds ratio (OR) and 95% CI. All statistical tests were two-tailed with a p value < 0.05 considered significant. Data were analyzed using the Statistical Package for the Social Sciences program (IBM-SPSS) version 23.

3. Results

3.1. Sociodemographic and Clinical Characteristics of the Participants. A total of one hundred patients with T1DM constituted the study population; their sociodemographic, ethnic, and clinical characteristics are shown in Table 1. As shown, the majority were Afro-Asiatic (79%). Regarding the growth and pubertal status of the study population, the majority had normal BMI (71%) and were pubertal (94%). Only 2% were obese. Seven percent had hypertension, and 8% had prehypertension. The youngest patient with hypertension was 12 years old. Fifty-seven percent of the patients with hypertension and 50% of those with prehypertension had microalbuminuria.

Most patients (95%) had a glucometer for home blood glucose monitoring, yet only 10% were checking daily and 39% check only when symptomatic. The rest do 2-3 readings per day in fixed 2 days per week.

Regarding the glycemic control of the study population, the median HbA1c was 11.8% (IQR = 9-14), and only 10% had HbA1c < 7.5%. The analysis showed that there was a significant correlation between regular home blood glucose monitoring and glycemic control ($p \leq 0.001$). However, there was no statistically significant correlation between glycemic control and insulin regimen ($p = 0.73$), as well as insulin dose ($p = 0.74$).

Regarding insulin treatment, most of the participants (95%) were on a conventional insulin regimen, 5% were on an intensive regimen, none of the patients were using an insulin pump. The median (IQR) insulin dose in unit/kg was 0.9 (IQR = 0.8-1.1).

3.2. Microvascular Complications. The presence of incipient diabetic nephropathy (persistent microalbuminuria) was observed in 36% of the participants. The youngest patient with microalbuminuria aged 11 years. Two patients had persistent macroalbuminuria (albuminuria more than 200 mg/l). Diabetic retinopathy was observed in 33% of the patients. The youngest patient with diabetic retinopathy aged 10 years and 7 months. Most of the patients with diabetic retinopathy had very mild nonproliferative diabetic retinopathy (66.7%). 30% had mild nonproliferative diabetic retinopathy. Only one patient (0.3%) had moderate nonproliferative retinopathy. Eleven percent of the patients were found to have

Table 2: Results of logistic regression analysis for risk factors of microvascular complications.

Predictor	Diabetic nephropathy		Diabetic retinopathy	
	Odds ratio (95% CI)	p value	Odds ratio (95% CI)	p value
Age	1.16 (0.91-1.48)	0.23	1.14 (0.88-0.88)	1.49
Ethnic group	0.40 (0.08-1.99)	0.26	0.57 (0.10-3.16)	0.52
Diabetes duration	1.02 (0.88-1.18)	0.81	1.12 (0.97-1.30)	0.13
BMI class	0.43 (0.13-1.43)	0.17	2.05 (0.57-7.41)	0.27
BP class	6.89 (1.17-40.52)	0.03	0.65 (0.10-4.36)	0.66
The most recent HbA1c	1.07 (0.89-1.29)	0.47	0.83 (0.68-1.00)	0.04
Presence of the other complication (DN/DR)	0.75 (0.28-2.05)	0.58	0.72 (0.26-2.01)	0.53

both diabetic nephropathy and retinopathy. The youngest of them was 11 years old.

Out of the total study participants, only six patients were prepubertal. All of them had normal blood pressure. However, one of them had both microalbuminuria and bilateral very mild diabetic retinopathy. This patient whose age was 11 years had diabetes duration of only 3 years. Another patient whose age was 10 and a half with diabetes for 2 years had unilateral very mild diabetic retinopathy. This last patient had hypothyroidism, was overweight, and had a family history of T1DM and essential hypertension.

Characteristics of patients with and without any of the two microangiopathies are described in Table 1. As shown, patients with diabetic retinopathy had significantly longer duration of diabetes ($p = 0.02$) and higher HbA1c ($p = 0.009$) compared to patients without retinopathy. However, these two factors were not significantly different between groups with and without DN. There was no statistically significant difference between patients with and without any of the two microangiopathies regarding age, ethnic group, age at diabetes onset, BMI, puberty, and blood pressure.

3.3. Logistic Regression Analysis of Risk Factors. In a logistic regression analysis, considering the presence of DN to be the dependent variable, blood pressure (OR = 6.89, 95%CI = 1.17-40.52, $p = 0.03$) was a predictor for the presence of DN, while the only variable that predicts DR was HbA1c level (OR = 0.83, 95%CI = 0.68-1.00, $p = 0.04$). Age, duration, ethnic group, BMI, and the presence of the other microangiopathy were not associated with any of the complications (Table 2).

4. Discussion

This study was the first of its type, to the authors' knowledge, to be carried out in Sudan examining the frequency of diabetic nephropathy and retinopathy and their associated risk factors in this age group. As estimated, the incidence of T1DM in Sudan is rising from 9.5/100,000 in 1991 [26] to 10.1/100,000 in 2015 [27]. Diabetes has a profound impact on children and families, both emotionally and economically, particularly in the developing world. Poor control leads to future microvascular complications. Most mortality in a cohort of South African patients with T1DM was as a result of diabetic nephropathy [28].

This cross-sectional study involved both rural and urban populations who belong to the three main Sudanese ethnic groups: Nilo-Saharan, Afro-Asiatic, and Niger-Congo [19]. Most of the participants in the present study were Afro-Asiatic (79%), so the three ethnic groups were not equally represented in this study.

Regarding metabolic control, most of the participants (90%) were not achieving the target control (HbA1c less than 7.5%) [23]. This finding is common in African studies that involved old children and adolescents with T1DM [15, 16, 29, 30]. However, diabetes control is universally found to be worse in adolescent patients compared to younger children [29].

In the current study, the poor glycemic control as measured by HbA1c was statistically strongly related to the lack of regular home blood glucose monitoring, caused by the unavailability of sustained glucometer's strip supply ($p \leq 0.001$). Although most of the patients are supplied with glucometers for free by the Sudan Childhood Diabetes Association (95% of the study group had a glucometer), most of the families could not afford to purchase the test strips as prices have increased tremendously over the last few years. In African cohort studies on children with diabetes, better metabolic control was achieved by frequent self-monitoring of blood glucose [17, 31]. However, poor glycemic control in the current study was associated with neither the insulin dose per kilogram nor the insulin regimen. This might be explained by the homogeneity of our participants regarding the insulin regimen since the vast majority (95%) were on conventional insulin. All types of insulin are provided for free funded by the Sudan Childhood Diabetes Association except insulin glargine. As insulin analogs are expensive and there is limited supply of NPH, most patients are put on premixed insulin alone or plus short-acting human insulin. This explains why most of our patients are on a conventional regimen. The trend in the last decade toward better diabetes control has been associated with the availability of frequent self-monitoring of blood glucose (SMBG), the use of insulin analogs, and more intensive management of diabetes including insulin pumps [29], things that are hard to afford in developing economics. The situation in this study is not different from that in other sub-Saharan countries where neither analog insulin nor multiple daily test strips are currently affordable [16, 29, 30, 32, 33].

One of the most noteworthy findings of this study is the high prevalence of microvascular chronic complications at

a young age. Diabetic nephropathy was present in 36%, and diabetic retinopathy in 33% of the patients. Altogether, 22% had isolated diabetic retinopathy, 25% had isolated diabetic nephropathy, and 11% had both diabetic retinopathy and nephropathy. Thus, almost half of the patients (58 patients, 58%) had either one or both of the complications, and only 42 (42%) had neither of these complications. These findings concur with other African reports [15–17]. Among studies done in sub-Saharan Africa for instance, the observed prevalence of incipient diabetic nephropathy in this study is close to that in a Tanzanian study with comparable sample size and diabetes duration [16]. The DN frequency in this study is also comparable to the results of a recent Nigerian study carried out on a smaller number of patients with T1DM in the same age range as in this study [15]. Regarding the prevalence of DR in the current study (33%), it is slightly higher than the prevalence obtained by these two above-mentioned studies, which reported prevalence rates of 22.7% [16] and 16.7% [15] in their participants, respectively. This could be attributed to the inclusion of younger patients with shorter duration in the Tanzanian study [16] or to the use of fundoscopy to diagnose DR in both of the studies. It is known that fundoscopy is less sensitive than fundus photography in detecting the early stages of DR [34]. Therefore, securing fundus cameras if possible is recommended to detect more cases of early retinopathy as what happened in our study. Provision of fundus cameras for the screening of a common preventable cause of blindness like DR is cost-effective, especially in a poor country like Sudan. DN prevalence in the current study is also not far from that obtained by a Rwandan study [17].

The prevalence of microalbuminuria in the current study is much higher than that in a study carried out in Egypt which included wide age range participants with better glycemic control than ours [35]. These two factors in plus the use of fundoscopy could also explain the lower DR prevalence than that of our study.

The frequency of both of the microvascular complications in our study is higher than those reported from the developed world mostly due to better diabetes control and possibly genetic or ethnic variation [1, 9, 34, 36–38].

In line with previous similar studies [15, 16, 35], almost all the patients with DR in this study were at the stage of mild or very mild nonproliferative diabetic retinopathy, except one patient who had moderate nonproliferative DR.

In this study, 11 (11%) had combined diabetic retinopathy and nephropathy. No statistically significant relationship between the presence of diabetic nephropathy and retinopathy was found, a finding that contradicts many studies [9, 13, 39]. To explain this, further studies are needed as it may be due to different risk factors for these two microvascular complications in our population.

Out of the total study participants, seven percent of patients had hypertension and 8% had prehypertension, a prevalence that is not very different from the prevalence of hypertension in healthy Sudanese school children [40]. Compared to the previously reported prevalence of hypertension among adolescents with T1DM, it is not far from those in some previous studies [1, 41], but higher than others [42, 43] and lower than that obtained by one study [37]. This variation in the prevalence of hypertension among young patients with T1DM might be explained by other confounding factors like difference in the prevalence of obesity, lifestyle, genetics, or another unknown factor. In this study, 57% of the patients with hypertension and 50% of the patients with prehypertension had microalbuminuria. There was no statistically significant difference regarding the blood pressure status between the groups with and without DN. However, when logistic regression was done, high blood pressure was found to be a predictor of microalbuminuria ($p = 0.03$). High blood pressure association with DN was found by many studies [1, 8, 10, 13, 37, 38, 42]. However, it is not yet known which parameter of the blood pressure heralds the occurrence of microalbuminuria. Perhaps, it is the elevation from the baseline blood pressure, not the high blood pressure itself [44, 45]. Therefore, it is important to check and follow the blood pressure of young patients with T1DM to pick up the early elevation of blood pressure. In places with limited resources like Sudan, this can be an easy and early predictor of diabetic nephropathy. Since this is a cross-sectional study, it is hard to know whether high blood pressure had developed concomitantly, after or before microalbuminuria. Whatever the case, these groups of patients need close control of their blood pressure to halt the progress of nephropathy, as it is well known that monitoring and early treatment of hypertension prevent the progression of nephropathy [6, 46]. No significant relationship between high blood pressure and DR was found in this study, a finding that is in concordance with a previous study [9], but in contradistinction to others [8, 12, 13, 42, 47]. The role of BP in the development of early retinopathy in adolescents with T1DM was studied by Gallego et al. who concluded that both systolic and diastolic blood pressure are predictors of DR independently of incipient nephropathy [12]. However, there may be different pathogenic mechanisms for DR in our population.

No relationship between the presence of any of the two microangiopathies and ethnicity was found in this study; this might be attributed to the fact that the participants were homogeneous regarding ethnic groups, as the majority (79%) belong to the Afro-Asiatic group. The role of ethnicity and genetics in the development of diabetic microvascular complications had been suggested by many studies that showed geographic as well as ethnic variation in the susceptibility to these complications [5, 6, 14, 48]. Other studies suggested that these observed differences may be linked primarily to the unfavourable social and economic conditions that worsen the risk of poor blood glucose and blood pressure control [49, 50]. Another study attributed this difference to a mixture of genetic and socioeconomic factors that delay access to care [4]. Nevertheless, the role of genetics in susceptibility to nephropathy, retinopathy, and other diabetic complications largely remains to be explored.

Moreover, no relation between age at onset and DN or DR was found, a finding that is in agreement with some studies [6, 9], but in contradiction to other studies [8–10, 38]. This could be due to the interaction with other factors like length of prepubertal duration, age at puberty, or other unknown factors.

This study was relatively small and cross-sectional in design, yet it was able to show that patients with DR had significantly longer duration than patients without DR. However, the duration was not a predictor for DR when logistic regression was made. Many studies concluded that diabetes duration is a risk factor for DR development [10, 15, 47]. Moreover, some studies found that long diabetes duration is the major risk factor for the development of diabetic retinopathy in T1DM [9, 13, 36, 42, 47]. An association between duration of diabetes and diabetic nephropathy was not found in this study in keeping with other studies [6, 15, 16, 39, 51, 52]. However, contradictory results were found by others [1, 9, 38, 42, 53]. In fact, one study concluded that given sufficient diabetes duration, retinopathy is almost universal, but not all patients develop nephropathy [54].

Lastly, regarding glycemic control, patients with DR had significantly higher HbA1c than those without DR, and high HbA1c is a predictor for DR in the logistic regression, an observation that was also demonstrated by the landmark DCCT/EDIC [55] and numerous previous studies [5, 8, 9, 15, 42, 56]. Lack of appropriate glycemic control especially in the peripubertal years was found to be a significant risk factor for the onset and progression of DR by one recent African study [15].

This study did not demonstrate any significant difference in glycemic control between groups with and without nephropathy so do most other available studies from sub-Saharan Africa [4, 6, 15, 44, 57]. In a longitudinal study done in the Rwandan youth, the microalbuminuria rate did not significantly change even after a significant improvement in glycemic control [17]. This might be explained by the hypothesis that other factors such as high blood pressure or genetic predisposition may contribute more to the development of diabetic nephropathy [9]. An additional explanation could be that the relationship between hyperglycemia and the development of DN is not straightforward. Some studies found that it is the earlier poor glycemic control during the first few years of the disease course that is associated with the development of microalbuminuria [9]. Other studies hypothesized that hyperglycemia is a necessary but not sufficient factor for the development of diabetic nephropathy [39]. Nevertheless, the relationship between glycemic control and the development of DN in our population has to be fully elucidated by further studies.

It is known that the risk factors involved in the development and progression of different diabetic microangiopathies in T1DM are overlapping but not identical [58]. Additionally, it is hypothesized that genetic factors modulate the effects of different risk factors [5]. This might explain why some risk factors were found to be significant for one microangiopathy but not for the other. However, the root cause of this discrepancy needs further large prospective studies.

In conclusion, in the present study, a high prevalence of early signs of diabetic nephropathy and retinopathy was demonstrated among children and adolescents at a relatively young age and short duration of T1DM, since more than half of the individuals included in this study suffered from at least one of these two chronic complications attributable to diabetes. The fact that the majority of our participants had poor glycemic control could partially explain this high prevalence. High blood pressure was found to be a predictor for diabetic nephropathy. Associations of diabetic retinopathy with longer disease duration and poor glycemic control were verified. However, no such association was found for diabetic nephropathy.

This is the first exploratory study of diabetes-related microvascular complications in Sudanese children and adolescents. The rates we had found are high and suggest that health policymakers should prioritize diabetes care as a major component of health provision in Sudan to minimize the development of such costly and life-threatening complications, since the early stages of microvascular complications such as nephropathy and retinopathy are often asymptomatic. The primary clinical care emphasis on the prevention of vision loss or renal impairment must be appropriately directed at good glycemic control, early identification, accurate classification, and timely treatment of these complications. In this study, the proportion of patients with poor glycemic control was high, and therefore, focusing on glycemic control would be of great benefit. Large prospective studies are also necessary to validate the current findings.

Abbreviations

BP: Blood pressure
CDC: Centers for Disease Control and Prevention
DCCT: Diabetes Control and Complications Trial
DM: Diabetes mellitus
DN: Diabetic nephropathy
DR: Diabetic retinopathy
EDIC: Epidemiology of Diabetes Interventions and Complications
IQR: Interquartile range
ISPAD: International Society for Pediatric and Adolescent Diabetes
NPDR: Nonproliferative diabetic retinopathy
T1DM: Type 1 diabetes mellitus.

Data Availability

The data of this research will be available on request.

Conflicts of Interest

The authors declare that there is no conflict of interest regarding the publication of this paper.

Acknowledgments

The authors acknowledge the laboratory team at the Sudan Childhood Diabetes Centre for doing all the laboratory investigations of this study. Also, we would like to thank the team of ophthalmologists at the Jabir Abu Eliz Centre for doing and interpreting the fundus photos.

References

[1] F. Demirel, D. Tepe, Ö. Kara, and İ. Esen, "Microvascular complications in adolescents with type 1 diabetes mellitus," *Journal*

of Clinical Research in Pediatric Endocrinology, vol. 5, no. 3, pp. 145–149, 2013.

[2] K. C. Donaghue, R. P. Wadwa, L. A. Dimeglio et al., "Microvascular and macrovascular complications in children and adolescents," *Pediatric Diabetes*, vol. 15, Suppl 20, pp. 257–269, 2014.

[3] The Diabetes Control and Complications Trial Research Group, "The effect of intensive treatment of diabetes on the development and progression of long-term complications in insulin-dependent diabetes mellitus," *The New England Journal of Medicine*, vol. 329, no. 14, pp. 977–986, 1993.

[4] M. G. Goldschmid, W. S. Domin, D. C. Ziemer, D. L. Gallina, and L. S. Phillips, "Diabetes in urban African-Americans: II. High prevalence of microalbuminuria and nephropathy in African-Americans with diabetes," *Diabetes Care*, vol. 18, no. 7, pp. 955–961, 1995.

[5] and the WHO Multinational Study Group, H. Keen, E. T. Lee et al., "The appearance of retinopathy and progression to proliferative retinopathy: the WHO Multinational Study of Vascular Disease in Diabetes," *Diabetologia*, vol. 44, no. S2, pp. S22–S30, 2001.

[6] J. J. K. Lutale, H. Thordarson, Z. G. Abbas, and K. Vetvik, "Microalbuminuria among type 1 and type 2 diabetic patients of African origin in Dar Es Salaam, Tanzania," *BMC Nephrology*, vol. 8, no. 1, 2007.

[7] M. Vladu, D. Clenciu, I. C. Efrem et al., "Insulin resistance and chronic kidney disease in patients with type 1 diabetes mellitus," *Journal of Nutrition and Metabolism*, vol. 2017, Article ID 6425359, 5 pages, 2017.

[8] E. Downie, M. E. Craig, S. Hing, J. Cusumano, A. K. Chan, and K. C. Donaghue, "Continued reduction in the prevalence of retinopathy in adolescents with type 1 diabetes: role of insulin therapy and glycemic control," *Diabetes Care*, vol. 34, no. 11, pp. 2368–2373, 2011.

[9] M. Svensson, J. W. Eriksson, and G. Dahlquist, "Early glycemic control, age at onset, and development of microvascular complications in childhood-onset type 1 diabetes: a population-based study in northern Sweden," *Diabetes Care*, vol. 27, no. 4, pp. 955–962, 2004.

[10] F. Mohsin, M. E. Craig, J. Cusumano et al., "Discordant trends in microvascular complications in adolescents with type 1 diabetes from 1990 to 2002," *Diabetes Care*, vol. 28, no. 8, pp. 1974–1980, 2005.

[11] K. Donaghue, M. Craig, A. Chan et al., "Prevalence of diabetes complications 6 years after diagnosis in an incident cohort of childhood diabetes," *Diabetic Medicine*, vol. 22, no. 6, pp. 711–718, 2005.

[12] P. H. Gallego, M. E. Craig, S. Hing, and K. C. Donaghue, "Role of blood pressure in development of early retinopathy in adolescents with type 1 diabetes: prospective cohort study," *BMJ*, vol. 337, no. aug26 1, p. a918, 2008.

[13] T. C. Rodrigues, M. Pecis, L. H. Canani et al., "Characterization of patients with type 1 diabetes mellitus in southern Brazil: chronic complications and associated factors," *Revista da Associação Médica Brasileira*, vol. 56, no. 1, pp. 67–73, 2010.

[14] A. T. Borchers, R. Uibo, and M. Gershwin, "The geoepidemiology of type 1 diabetes," *Autoimmunity Reviews*, vol. 9, no. 5, pp. A355–A365, 2010.

[15] C. F. Ogugua, U. N. Chikani, M. U. Ibekwe, T. Ngwieri, and H. Allen, "Early signs of microvascular complications in pediatric patients with short duration of type 1 diabetes mellitus seen in Southeast Nigeria," *Annals of African Medicine*, vol. 18, no. 4, pp. 200–205, 2019.

[16] E. S. Majaliwa, E. Munubhi, K. Ramaiya et al., "Survey on acute and chronic complications in children and adolescents with type 1 diabetes at Muhimbili National Hospital in Dar es Salaam, Tanzania," *Diabetes Care*, vol. 30, no. 9, pp. 2187–2192, 2007.

[17] S. L. Marshall, D. V. Edidin, V. C. Arena et al., "Glucose control in Rwandan youth with type 1 diabetes following establishment of systematic, HbA1c based, care and education," *Diabetes Research and Clinical Practice*, vol. 107, no. 1, pp. 113–122, 2015.

[18] K. J. R. Sahar Mohammed Mirgani and M. A. Abdullah, *Prevalence and Predictors for Development of Microalbuminuria in a Subset of Sudanese Children with Type 1 Diabetes Mellitus*, 2012.

[19] H. Y. Hassan, P. A. Underhill, L. L. Cavalli-Sforza, and M. E. Ibrahim, "Y-chromosome variation among Sudanese: restricted gene flow, concordance with language, geography, and history," *American Journal of Physical Anthropology*, vol. 137, no. 3, pp. 316–323, 2008.

[20] National High Blood Pressure Education Program, "The fourth report on the diagnosis, evaluation, and treatment of high blood pressure in children and adolescents," *Pediatrics*, vol. 114, no. 2, pp. 555–576, 2004.

[21] C. L. Ogden, "Defining overweight in children using growth charts," *Maryland medicine: MM: a publication of MEDCHI, the Maryland State Medical Society*, vol. 5, no. 3, pp. 19–21, 2004.

[22] W. A. Marshall and J. M. Tanner, "Variations in pattern of pubertal changes in girls," *Archives of Disease in Childhood*, vol. 44, no. 235, pp. 291–303, 1969.

[23] L. A. DiMeglio, C. L. Acerini, E. Codner et al., "ISPAD Clinical Practice Consensus Guidelines 2018: glycemic control targets and glucose monitoring for children, adolescents, and young adults with diabetes," *Pediatric Diabetes*, vol. 19, no. S27, pp. 105–114, 2018.

[24] K. C. Donaghue, L. Marcovecchio, R. P. Wadwa et al., "ISPAD Clinical Practice Consensus Guidelines 2018 microvascular and macrovascular complications in children and adolescents," *Pediatric Diabetes*, vol. 19, pp. 262–274, 2018.

[25] Early Treatment Diabetic Retinopathy Study Research Group, "Early Treatment Diabetic Retinopathy Study design and baseline patient characteristics," *Ophthalmology*, vol. 98, no. 5, pp. 741–756, 1991.

[26] A. Elamin, M. Ghalib, B. Eltayeb, and T. Tuvemo, "High incidence of type I diabetes mellitus in Sudanese children, 1991-1995," *Annals of Saudi Medicine*, vol. 17, no. 4, pp. 478–480, 1997.

[27] F. M. Mohammed Abdullah, "Incidence and prevalence of type 1 diabetes mellitus in children and adolescents aged 0-19 years in Khartoum state," Sudan, 2015.

[28] S. Tesfaye and G. Gill, "Chronic diabetic complications in Africa," *African Journal of Diabetes Medicine*, vol. 19, no. 1, pp. 4–8, 2011.

[29] L. J. Mukama, A. Moran, M. Nyindo, R. Philemon, and L. Msuya, "Improved glycemic control and acute complications among children with type 1 diabetes mellitus in Moshi, Tanzania," *Pediatric Diabetes*, vol. 14, no. 3, pp. 211–216, 2013.

[30] T. Ngwiri, F. Were, B. Predieri, P. Ngugi, and L. Iughetti, "Glycemic control in Kenyan children and adolescents with type 1

diabetes mellitus," *International Journal of Endocrinology*, vol. 2015, Article ID 761759, 7 pages, 2015.

[31] B. Davey and D. G. Segal, "Self-monitoring of blood glucose measurements and glycaemic control in a managed care paediatric type 1 diabetes practice," *South African Medical Journal*, vol. 105, no. 5, pp. 405–407, 2015.

[32] G. D. Ogle, A. C. Middlehurst, and M. Silink, "The IDF Life for a Child Program Index of diabetes care for children and youth," *Pediatric Diabetes*, vol. 17, no. 5, pp. 374–384, 2016.

[33] A. O. Ogbera and S. F. Kuku, "Insulin use, prescription patterns, regimens and costs-a narrative from a developing country," *Diabetology & Metabolic Syndrome*, vol. 4, no. 1, 2012.

[34] V. Viswanathan, "Preventing microvascular complications in type 1 diabetes mellitus," *Indian Journal of Endocrinology and Metabolism*, vol. 19, no. 7, p. 36, 2015.

[35] M. H. El Samahy, N. S. Elbarbary, and H. M. Elmorsi, "Current status of diabetes management, glycemic control and complications in children and adolescents with diabetes in Egypt. Where do we stand now? And where do we go from here?," *Diabetes Research and Clinical Practice*, vol. 107, no. 3, pp. 370–376, 2015.

[36] Y. H. Cho, M. E. Craig, S. Hing et al., "Microvascular complications assessment in adolescents with 2- to 5-yr duration of type 1 diabetes from 1990 to 2006," *Pediatric Diabetes*, vol. 12, no. 8, pp. 682–689, 2011.

[37] M. C. Eppens, M. E. Craig, J. Cusumano et al., "Prevalence of diabetes complications in adolescents with type 2 compared with type 1 diabetes," *Diabetes Care*, vol. 29, no. 6, pp. 1300–1306, 2006.

[38] K. Raile, A. Galler, S. Hofer et al., "Diabetic nephropathy in 27,805 children, adolescents, and adults with type 1 diabetes: effect of diabetes duration, A1C, hypertension, dyslipidemia, diabetes onset, and sex," *Diabetes Care*, vol. 30, no. 10, pp. 2523–2528, 2007.

[39] P. Rossing, P. Hougaard, and H.-H. Parving, "Risk factors for development of incipient and overt diabetic nephropathy in type 1 diabetic patients: a 10-year prospective observational study," *Diabetes Care*, vol. 25, no. 5, pp. 859–864, 2002.

[40] Z. Salman, G. D. Kirk, and M. D. DeBoer, "High rate of obesity-associated hypertension among primary schoolchildren in Sudan," *International Journal of Hypertension*, vol. 2011, Article ID 629492, 5 pages, 2011.

[41] K. O. Schwab, J. Doerfer, W. Hecker et al., "Spectrum and prevalence of atherogenic risk factors in 27, 358 children, adolescents, and young adults with type 1 diabetes: cross-sectional data from the German diabetes documentation and quality management system (DPV)," *Diabetes Care*, vol. 29, no. 2, pp. 218–225, 2006.

[42] P. Kumar, P. Krishna, S. C. Reddy, M. Gurappa, S. Aravind, and C. Munichoodappa, "Incidence of type 1 diabetes mellitus and associated complications among children and young adults: results from Karnataka Diabetes Registry 1995-2008," *Journal of the Indian Medical Association*, vol. 106, no. 11, pp. 708–711, 2008.

[43] R. Cobas, B. Santos, L. Braga, E. F. Cunha, and M. B. Gomes, "Evolução para hipertensão arterial em pacientes com diabetes tipo 1," *Arquivos Brasileiros de Endocrinologia e Metabologia*, vol. 52, no. 4, pp. 628–634, 2008.

[44] E. Sobngwi, J.-C. Mbanya, E. Nyolo Moukouri, and K. Blackett Ngu, "Microalbuminuria and retinopathy in a diabetic population of Cameroon," *Diabetes Research and Clinical Practice*, vol. 44, no. 3, pp. 191–196, 1999.

[45] J. L. Gross, M. J. De Azevedo, S. P. Silveiro, L. H. Canani, M. L. Caramori, and T. Zelmanovitz, "Diabetic nephropathy: diagnosis, prevention, and treatment," *Diabetes Care*, vol. 28, no. 1, pp. 164–176, 2004.

[46] D. W. Cooke and L. Plotnick, "Type 1 diabetes mellitus in pediatrics," *Pediatrics in Review*, vol. 29, no. 11, pp. 374–385, 2008.

[47] C. E. M. de Block, I. H. de Leeuw, and L. F. van Gaal, "Impact of overweight on chronic microvascular complications in type 1 diabetic patients," *Diabetes Care*, vol. 28, no. 7, pp. 1649–1655, 2005.

[48] A. A. Motala, F. J. Pirie, E. Gouws, A. Amod, and M. A. Omar, "Microvascular complications in South African patients with long-duration diabetes mellitus," *South African Medical Journal*, vol. 91, no. 11, pp. 987–992, 2001.

[49] E. Sidibe, Ed., "Main complications of diabetes mellitus in Africa," *Annales de Medecine Interne*, vol. 151, no. 8, pp. 624–628, 2000.

[50] W. J. Kalk, J. Joannou, S. Ntsepo, I. Mahomed, P. Mahanlal, and P. J. Becker, "Ethnic differences in the clinical and laboratory associations with retinopathy in adult onset diabetes: studies in patients of African, European and Indian origins," *Journal of Internal Medicine*, vol. 241, no. 1, pp. 31–37, 2003.

[51] C. J. Schultz, T. Konopelska-Bahu, R. N. Dalton et al., "Microalbuminuria prevalence varies with age, sex, and puberty in children with type 1 diabetes followed from diagnosis in a longitudinal study. Oxford Regional Prospective Study Group," *Diabetes Care*, vol. 22, no. 3, pp. 495–502, 1999.

[52] R. W. Holl, M. Grabert, A. Thon, and E. Heinze, "Urinary excretion of albumin in adolescents with type 1 diabetes: persistent versus intermittent microalbuminuria and relationship to duration of diabetes, sex, and metabolic control," *Diabetes Care*, vol. 22, no. 9, pp. 1555–1560, 1999.

[53] M. E. Craig, T. W. Jones, M. Silink, and Y. J. Ping, "Diabetes care, glycemic control, and complications in children with type 1 diabetes from Asia and the Western Pacific Region," *Journal of Diabetes and its Complications*, vol. 21, no. 5, pp. 280–287, 2007.

[54] A. Kofoed-Enevoldsen, K. Borch-Johnsen, S. Kreiner, J. Nerup, and T. Deckert, "Declining incidence of persistent proteinuria in type I (insulin-dependent) diabetic patients in Denmark," *Diabetes*, vol. 36, no. 2, pp. 205–209, 1987.

[55] The Diabetes Control and Complications Trial Research Group, "The relationship of glycemic exposure (HbA1c) to the risk of development and progression of retinopathy in the diabetes control and complications trial," *Diabetes*, vol. 44, no. 8, pp. 968–983, 1995.

[56] J.-C. Mbanya and E. Sobngwi, "Diabetes in Africa. Diabetes microvascular and macrovascular disease in Africa," *Journal of Cardiovascular Risk*, vol. 10, no. 2, pp. 97–102, 2003.

[57] F. Wanjohi, F. Otieno, E. Ogola, and E. Amayo, "Nephropathy in patients with recently diagnosed type 2 diabetes mellitus in black Africans," *East African Medical Journal*, vol. 79, no. 8, pp. 399–404, 2002.

[58] O. Kordonouri, T. Danne, W. Hopfenmüller, I. Enders, G. Hövener, and B. Weber, "Lipid profiles and blood pressure: are they risk factors for the development of early background retinopathy and incipient nephropathy in children with insulin-dependent diabetes mellitus?," *Acta Paediatrica*, vol. 85, no. 1, pp. 43–48, 1996.

Hindawi
Journal of Diabetes Research
Volume 2020, Article ID 1942086, 12 pages
https://doi.org/10.1155/2020/1942086

Review Article

Calcium Homeostasis in Ventricular Myocytes of Diabetic Cardiomyopathy

Lina T. Al Kury

Department of Health Sciences, College of Natural and Health Sciences, Zayed University, Abu Dhabi 144534, UAE

Correspondence should be addressed to Lina T. Al Kury; lina.alkury@zu.ac.ae

Received 8 July 2020; Revised 24 October 2020; Accepted 29 October 2020; Published 16 November 2020

Academic Editor: Celestino Sardu

Diabetes mellitus (DM) is a chronic metabolic disorder commonly characterized by high blood glucose levels, resulting from defects in insulin production or insulin resistance, or both. DM is a leading cause of mortality and morbidity worldwide, with diabetic cardiomyopathy as one of its main complications. It is well established that cardiovascular complications are common in both types of diabetes. Electrical and mechanical problems, resulting in cardiac contractile dysfunction, are considered as the major complications present in diabetic hearts. Inevitably, disturbances in the mechanism(s) of Ca^{2+} signaling in diabetes have implications for cardiac myocyte contraction. Over the last decade, significant progress has been made in outlining the mechanisms responsible for the diminished cardiac contractile function in diabetes using different animal models of type I diabetes mellitus (TIDM) and type II diabetes mellitus (TIIDM). The aim of this review is to evaluate our current understanding of the disturbances of Ca^{2+} transport and the role of main cardiac proteins involved in Ca^{2+} homeostasis in the diabetic rat ventricular cardiomyocytes. Exploring the molecular mechanism(s) of altered Ca^{2+} signaling in diabetes will provide an insight for the identification of novel therapeutic approaches to improve the heart function in diabetic patients.

1. Introduction

Diabetes mellitus (DM) is a chronic metabolic disorder commonly characterized by abnormally high blood glucose levels, resulting from defects in insulin production or insulin resistance, or both. Over the years, prevalence of diabetes has increased globally, and it is classified as one of the leading causes of mortality and morbidity. TIDM is characterized by decreased insulin secretion due to the damage in β cells of the pancreas [1, 2]. In contrast, TIIDM is characterized by decreased peripheral resistance to insulin, resulting in reduced insulin sensitivity to the skeletal muscles, adipose tissues, and liver [1, 3]. Hyperglycemia plays an important role in the onset and development of diabetes complications, mainly by generating reactive oxygen species (ROS) which causes lipid peroxidation and membrane damage. Furthermore, hyperglycemia results in excessive nonenzymatic glycation of proteins and formation of advanced glycation end products (AGE). The glycation modifications can further deteriorate the pathology of diabetes [4, 5].

Diabetic cardiomyopathy is one of the complications in DM. Electrical and mechanical problems, resulting in cardiac contractile dysfunction, are the major complications present in diabetic hearts. Clinical and preclinical studies have demonstrated a variety of diastolic and systolic dysfunctions in diabetic patients with the severity of abnormalities depending on the patients' age and duration of diabetes. Cardiac contractility is controlled through the precise interplay between several cellular Ca^{2+} transport protein complexes. During the excitation-contraction coupling process, the arrival of an action potential (AP) at a cardiac myocyte depolarizes the cell membrane leading to the opening of L-type Ca^{2+} channels and the influx of small amounts of Ca^{2+}. This influx of Ca^{2+} triggers a much larger Ca^{2+} release from the sarcoplasmic reticulum (SR) via the ryanodine receptors (RyRs) and a transient increase in intracellular Ca^{2+} (Ca^{2+} transient). Ca^{2+} binds to troponin C and initiates and regulates the process of myocyte contraction. Myocyte relaxation takes place by the Ca^{2+} removal from the cytosol via main pathways including the uptake of Ca^{2+} into the SR through

the SR Ca^{2+}-ATPase (SERCA pump), transport outside the cell mainly via the Na^+/Ca^{2+} exchanger (NCX), in addition to the plasma membrane Ca^{2+}-ATPase (PMCA) [6]. A fourth pathway of the Ca^{2+} extrusion potentially involves mitochondria which are equipped with an efficient machinery for Ca^{2+} transport and are capable of storing large amounts of Ca^{2+} [7–10].

Disturbances in the mechanism(s) of Ca^{2+} signaling predictably have implications for cardiac myocyte contraction. It is well established that cardiovascular complications are common in both types of diabetes. Over the last decade, significant progress has been made in outlining the mechanisms responsible for the diminished cardiac contractile function in diabetes using different animal models of TIDM and TIIDM. The aim of this review is to evaluate our current understanding of the disturbances of Ca^{2+} transport and the role of main cardiac proteins involved in Ca^{2+} homeostasis in the diabetic rat ventricular cardiomyocytes. Exploring the molecular mechanism(s) of altered Ca^{2+} signaling in diabetes will provide an insight for the identification of novel therapeutic approaches to improve heart function in diabetic patients.

2. L-Type Ca^{2+} Channel

The cardiac voltage-gated L-type Ca^{2+} channel, $Ca_v1.2$, is the main pathway for the Ca^{2+} entry into the cardiac cell. The fully functional $Ca_v1.2$ channel is a heterotetrameric polypeptide complex containing the pore-forming $Ca_v\alpha1c$ subunit, in addition to the accessory subunits $Ca_v\beta$, $Ca_v\alpha2\delta$, and $Ca_v\gamma$ [11]. The pore-forming $Ca_v\alpha1c$ subunit contains the main biophysical and pharmacological properties of the channel and plays a critical role in excitation–contraction coupling. Entry of Ca^{2+} through $Ca_v1.2$ channels shapes the plateau phase of the ventricular action potential and determines the action potential duration. In addition to the ion channel pore, the $Ca_v\alpha1c$ subunit also consists of the voltage sensor, selectivity filter, and the determinants for the binding of drugs and toxins. The current through the $Ca_v\alpha1c$ subunit is modulated by the interactions with the accessory subunits that are tightly bound to the $Ca_v\alpha1c$ subunit. All of these accessory subunits play important roles in the regulation of both the biophysical properties and trafficking of L-type Ca^{2+} channels [11–13].

Compared to the surface sarcolemma, L-type Ca^{2+} channels are more localized in the T-tubule [13]. Within the T-tubule, most of L-type Ca^{2+} channels are concentrated in a specific region called dyad. Each dyad consists of clusters of L-Type Ca^{2+} channels on the sarcolemma closely opposed to clusters of RyRs on the SR membrane [6]. The two molecules are separated by a very limited space (10–15 nm) that enables a few Ca^{2+} ions to pass through the L-type Ca^{2+} channels and activate the RyRs. Such distribution forms the structural basis of excitation–contraction coupling [6, 13].

The L-type Ca^{2+}channel activity is positively regulated by protein kinase A (PKA) phosphorylation. β-Adrenergic stimulation and the resulting PKA-mediated phosphorylation of key residues cause an approximately threefold surge in the L-type Ca^{2+} channel activity as a result of an increase in the channel open probability (P_o) [14, 15]. The L-type current inactivates via two distinct mechanisms: a voltage-dependent inactivation, that is regulated by $Ca_V\beta$, and a Ca^{2+}-dependent inactivation, that is regulated by calmodulin (CaM). Both processes are thought to limit the amount of Ca^{2+} influx during the AP [16].

2.1. L-Type Ca^{2+} Channel in Type I Diabetes Mellitus. Various animal models are used to study TIDM. Deficiency in insulin production is achieved by a variety of mechanisms, ranging from chemical induction of beta cell damage (STZ-induced and alloxan-induced diabetes) [17] to genetic induction (e.g., AKITA mice) [18]. Previous studies in TIDM animal models have variously reported either no change [19–22] or reduction in the L-type Ca^{2+} current [20, 23–28] in ventricular myocytes isolated from the STZ-induced diabetic rat. For example, Chattou et al. 1999 found that, in rat diabetic myocytes, the density of the Ca^{2+} current was significantly reduced by TIDM in the range of test potentials between -10 and +50 mV. In addition, the fast time constant of the Ca^{2+} current inactivation was significantly higher in diabetic compared to normal myocytes which indicates that SR Ca^{2+} release-induced inactivation is delayed in TIDM. The decrease in the L-type Ca^{2+} current, which is the trigger for Ca^{2+}-induced Ca^{2+} release (CICR) from SR, may explain the significantly lowered peak systolic intracellular Ca^{2+} in diabetic ventricular myocytes [20, 23–26]. Supporting this finding, Bracken et al. (2006) have shown that TIDM induced voltage-dependent decrease in contraction that was associated with the reduced L-type Ca^{2+} channel activity [28]. In cardiac myocytes of type 1 diabetic Akita Mice, decreased contractility was associated with reduced PI 3-kinase signaling and reduced cell surface expression of L-type Ca^{2+} channels. This change results in the decrease of the L-type Ca^{2+} current density that was reversed to control levels by insulin treatment and intracellular infusion of PI 3,4,5-trisphosphate [PI(3,4,5)P3] [27].

In contrast to the above findings, a recent study conducted by Smail et al. (2016) has shown that the L-type Ca^{2+} channel activation, inactivation, and recovery from inactivation were not significantly altered in epicardial and endocardial myocytes from STZ-treated rats [19].

2.2. L-Type Ca^{2+} Channel in Type II Diabetes Mellitus. In db/db obese type II diabetic mice, the depressed cardiac function was associated with reduction in the membrane permeability to Ca^{2+}. Although the macroscopic L-type Ca^{2+} current was reduced in db/db cardiomyocytes, the single Ca^{2+} channel activity was similar, suggesting that diabetic myocytes express fewer functional Ca^{2+} channels [29]. The diminished T-tubular density was also observed in db/db mice in cardiomyocytes from mice with type II diabetes (db/db) [30]. Zucker diabetic fatty rat is a genetic model in which the male homozygous (FA/FA) animals develop obesity and TIIDM. In this model, earlier study has shown that the L-type Ca^{2+} current was reduced, and inactivation was prolonged over a range of test potentials in diabetic ventricular myocytes. Upregulation of the gene encoding the $\alpha1$ subunit of the Cav1.2 ion channel (Cacna1c) may provide an early compensatory mechanism for the reduced density and

prolonged inactivation of the L-type Ca^{2+} current demonstrated in myocytes from Zucker diabetic fatty rat compared to their respective controls [31]. In contrast to these findings, recent studies on the Goto–Kakizaki (GK) rat, a nonobese genetic model of TIIDM, have shown no change in the L-type Ca^{2+} channel activity in ventricular myocytes [32, 33]. Effects of TIDM and TIIDM on the L-type Ca^{2+} channel are summarized in Table 1.

3. The Ryanodine Receptor Type 2

Ryanodine receptor type 2 (RyR2) is a member of the RyR family. It is a macromolecular homotetrameric protein complex that regulates Ca^{2+} release from the SR during the process of excitation-contraction coupling in the heart. Sarcolemmal depolarization results in the entry of a small amount of Ca^{2+} to the cardiac cell. This influx of Ca^{2+} stimulates a large release of Ca^{2+} from the SR via RyR2 resulting in a transient rise of cytosolic Ca^{2+}. In fact, activation of single RyR2 cluster (8–100 channels) results in an increase in the concentration of cytosolic Ca^{2+}, known as a Ca^{2+} spark [34]. The summation of all Ca^{2+} sparks produced by activated RyR2 clusters throughout the cardiomyocyte leads to a Ca^{2+} transient that causes cardiac muscle contraction [35]. Recently, super-resolution imaging methods have provided an estimate for the number of RyRs in each cluster (dyad) from ≈14 in peripheral couplings to ≈100 in intracellular sites [34, 36]. A number of accessory proteins are associated with RyR2 and modulate its function including (1) the Ca^{2+} binding protein calmodulin which directly binds with and regulates RyR2 channels; (2) auxilliary proteins, calsequestrin, triadin, and junctin, which form the luminal Ca^{2+} sensor of RyR2 within the SR [37–39]; and (3) FK506 binding proteins (FKBP12 and FKBP12.6), which are believed to interact with RyR2 and stabilize the channel, preventing spontaneous Ca^{2+} release and SR Ca^{2+} leak [40]. In addition, the protein complex interacts with a number of enzymes including PKA, Ca^{2+}/calmodulin-dependent protein kinase II (CaMK II), and phosphatases 1, 2A, and 2B that reversibly modulate the receptor phosphorylation state [41, 42].

3.1. The Ryanodine Receptor in Type I Diabetes Mellitus. To date, the molecular mechanism underlying RyR2 dysregulation during chronic diabetes is incompletely understood. Alteration in the sensitivity of RyR2 to the Ca^{2+} activation, oxidation of RyR2 by ROS and/or reactive carbonyl species [43–46], and functional uncoupling of RyR2 from L-type Ca^{2+} channels on the T-tubule membranes could be partly responsible for the dyssynchronous Ca^{2+} release from SR in diabetes [47].

In STZ-injected rats, earlier study conducted by Yu et al. (1994) reported a decrease in ^{3}H-labeled ryanodine binding sites in diabetic myocardium, suggesting decreased density of the RyR protein [48]. Supporting this finding, Teshima et al. (2000) reported a decrease in the expression of RyR2 mRNA, 12 weeks after the STZ injection in the diabetic rat heart [22]. A more recent study also showed a significant decrease in the expression of RyR2 in 4-, 8-, and 12-week STZ-treated diabetic groups [49]. Together, the decreased density of RyR2 in the STZ rat heart can be explained by corresponding decrease in the mRNA expression.

It is well known that metabolic changes associated with diabetes increase the production of ROS. As the RyR structure is rich in free thiol groups, it is highly subject to oxidative stress, changing its tertiary structure and altering its sensitivity to Ca^{2+} [2, 50]. In an earlier study in 7-week sedentary type-1 diabetic rats, Ca^{2+} spark frequency was threefold higher, and evoked Ca^{2+} release was dyssynchronous with diastolic Ca^{2+} release. Although the steady state of the RyR2 protein (the state under which there is a continuous presence of critical Ca^{2+} to maintain the channel in its open state) was not altered, its response to Ca^{2+} was changed [51]. Yaras et al. (2005), however, found that in STZ-treated diabetic rats, Ca^{2+} transients exhibit significantly reduced amplitude and prolonged time courses, as well as depressed Ca^{2+} loading of SR. Spatiotemporal properties of the Ca^{2+} sparks were also significantly altered. Furthermore, protein levels of RyR2 were depleted [52]. Supporting these findings, the decreased expression of RyR2 receptors was reported earlier using the quantitative immunoblot technique. As a result, the decreased RyR function was responsible for the slow release of Ca^{2+} from SR and prolonged time to peak Ca^{2+} transients observed in diabetic rat myocytes [21]. Similar findings were also reported by other groups [51, 53, 54].

Alterations in the sensitivity of RyR2 to the Ca^{2+} activation could result from increased phosphorylation by PKA and CaMKII [43, 55, 56]. PKA was found to phosphorylate two sites of RyR2, primarily Ser2808 (in human and rodents) or Ser2809 (in rabbit) and Ser2030 (or Ser2031 in rabbit). CAMKII also phosphorylates the Ser2808 site, in addition to the Ser2814 (Ser2815 in rabbit) site [57]. The functional role of PKA and CaMKII-mediated phosphorylation of RyR2 has been implicated in many heart diseases, including heart failure [51, 53, 58]. For example, Marx et al. (2000) showed that PKA phosphorylation regulates the binding of FKBP12.6 to RyR2. PKA phosphorylation dissociates the regulatory subunit FKBP12.6 from the channel, resulting in the altered channel function which is manifested as increased probability of open state (P_o), increased sensitivity to the Ca^{2+}-induced activation, and destabilization of the channel [58].

In diabetic rat ventricular cardiomyocytes, Shao et al. (2009) showed that the RyR displayed about 1.5-fold increase in phosphorylation at Ser 2808 and Ser 2814 residues 7 weeks after STZ injection [51]. Interestingly, the PKA activity was reduced by 75%, but the CaMKII activity was increased by 50% [51]. Conversely, Yaras et al. (2005) reported that PKA-dependent phosphorylation of RyR2 was partly responsible for impaired intracellular Ca^{2+} signaling, as well as decreased SR Ca^{2+} load [52]. However, the role of CaMKII in phosphorylation of RyR2 and disturbance of Ca^{2+} signaling has been reported in STZ-diabetic rats [59] and *db*/*db* mice [30]. Interestingly, Tian et al. (2011) stated that the change in the RyR2 function observed in single channel recordings was independent of phosphorylation at either S2808 or S2814 sites. Instead, the increase in open channel probability (P_o) and reduction in conductance were attributed to the increased responsiveness to cytoplasmic activators including Ca^{2+} [60].

Table 1: Effect of DM on the L-type Ca^{2+} channel.

TIDM	Effect	References
	Reduced L-type Ca^{2+} current in STZ-treated rat ventricular myocytes	Hamouda et al. 2015 [23]; Wang et al. 1995 [24]; Chattou et al. 1999 [26]; Bracken et al. 2006 [28]; Woodall et al. 2004 [25]
	Reduced L-type Ca^{2+} current in Akita(ins2) mice	Lu et al. 2007 [27]
	No significant change in the L-type Ca^{2+} current in STZ-treated rat ventricular myocytes	Smail et al. 2016 [19]; Lacombe et al. 2007 [20]; Choi et al. 2002 [21]; Teshima et al. 2000 [22]
TIIDM	Effect	References
	Reduced number of L-type Ca^{2+} channels in sarcolemma in db/db mice	Pereira et al. 2006 [29]
	Reduced density of T-tubular in *db*/*db* mice	Stølen et al. 2009 [30]
	No change in L-type Ca^{2+} channels in Goto-Kakizaki rats	Salem et al. 2013 [32]; Al Kury et al. 2018 [33]
	Upregulation of the gene encoding $Ca_v1.2$ ion channel (Cacna1c)	Howarth et al. 2011 [31]

3.2. The Ryanodine Receptor in Type II Diabetes Mellitus. In the prediabetic animal model of metabolic syndrome, the integrity of RyR2 was assessed by Ser 2809 phosphorylation, in addition to the receptor's ability to bind [^{3}H]ryanodine. RyR2 phosphorylation at Ser 2809 was significantly elevated in the right and left ventricles from high-fat-fed dogs compared to normal controls. This hyperphosphorylation was associated with a decrease in RyR2 binding affinity in the right and left ventricles. However, there was no change in the level of expression of RyR2 [61]. In a more recent study on rats with metabolic syndrome, induced by a 16-week high-sucrose diet, cardiomyocytes exhibited altered Ca^{2+} signaling that was partly attributed to increased phosphorylation and altered RyR2 function [62]. Gaber et al. (2014) found that, in the GK rat model, changes in ventricular cardiomyocyte shortening and Ca^{2+} signaling were associated with a decrease in RyR2 mRNA levels [63]. Supporting this finding, prolonged SR Ca^{2+} release and associated reduced RyR2 expression and increased phosphorylation were reported in the right atrial myocardium of TIIDM patients [64].

Diabetes and obesity are associated with an increased risk of arrhythmia and sudden cardiac death that could be partly attributed to abnormal lipid accumulation. Recently, the transgenic mouse model of cardiac lipid overload, with the cardiac-specific overexpression of peroxisome proliferator-activated receptor gamma (PPAR-γ), was used to study the change in Ca^{2+} handling [65, 66]. The PPAR-γ overexpression was found to perturb the intracellular Ca^{2+} homeostasis in cardiomyocytes leading to ventricular arrhythmias and cardiac sudden death in animals. The results of a recent study conducted by Joseph et al. (2016) showed that PPAR-γ cardiomyocytes had more frequent triggered activity, increased sparks, and SR Ca^{2+} leak. This was attributed to the significant increase in RyR2 oxidation [65]. Other studies have also reported that in vitro oxidation of RyR2 increases the channel response to cytoplasmic Ca^{2+} concentration and favors Ca^{2+} release in isolated cardiomyocytes, generating Ca^{2+} waves and arrhythmias [67, 68].

In mice fed with a high-fat diet (HFD), more frequent occurrence of arrhythmic episodes was associated with an enhanced response of single RyR2 channels to cytoplasmic Ca^{2+}. At the molecular level, RyR2 channels from HFD-fed mice had substantially fewer free thiol residues, suggesting that redox modifications were responsible for the higher activity of RyR2 [69]. Effects of TIDM and TIIDM on RyR2 are summarized in Table 2.

4. The Sarcoplasmic Reticulum Ca^{2+}-ATPase

SERCA pump plays a predominant role in cardiac excitation–contraction coupling and cardiac contractility. This pump is encoded by a family of three genes, SERCA1, 2, and 3, which are spliced in several isoforms. To date, more than 10 different SERCA isoforms have been identified at the protein level. In the cardiac tissue, SERCA2a is the predominant form which is responsible for facilitating the storage of Ca^{2+} in the SR. The function of the SERCA2a pump is modulated by the endogenous molecules phospholamban (PLB), sarcolipin (SLN), and by direct phosphorylation through CaMK II. In the dephosphorylated form, PLB inhibits SERCA2a, while PKA-dependent phosphorylation of the phosphoresidue serine-16 or Ca^{2+}/calmodulin-dependent phosphorylation of threonine-17 reverses this inhibition [70, 71]. SERCA2a is also under the control of CaMK II, which has been shown to phosphorylate SERCA2a on residue serine-38 and enhance and Ca^{2+}-reuptake into the SR [72]. These effects that are mediated through phosphorylation result in an overall increased SR Ca^{2+}-load and enhanced contractility.

4.1. The Sarcoplasmic Reticulum Ca^{2+}-ATPase in Type I Diabetes Mellitus. Because SERCA2 plays a major role in muscle contraction, various investigations have focused on understanding its role in cardiac disease. Many studies have reported that the SERCA2a expression and activity were decreased in a number of pathophysiological conditions including diabetes [73]. In TIDM, decreased activity of SERCA2a was associated with decreased level of mRNA levels or expression of protein, increased formation of ROS, change in the expression of PLB, and increased posttranslational modification such as increased carbonylation, glycation, and O-GlcNAcylation (Table 3). For example, in the STZ-induced diabetic rat heart, the expression of SERCA2a mRNA was

Table 2: Effect of DM on ryanodine receptor type 2.

TIDM	Effect	References
	Decrease in ^{3}H-labeled ryanodine binding sites, decrease in the mRNA expression	Yu et al. 1994 [48]; Teshima et al. 2000 [22]; Choi et al. 2002 [21]; Zhao et al. 2014 [49]
	Hyperphosphorylation of RyR2	Yaras et al. 2005 [52]; Shao et al. 2007 [54]; Shao et al. 2009 [51]
	Hyperphosphorylation of RyR2 due to both high phosphorylation levels of both PKA and CaMKII	Tuncay et al. 2014 [53]; Netticadan et al. 2001 [59]
	AGEs on RyR2, disulfide bond formation on RyR2, oxidation of RyR2 by reactive oxygen species (ROS), and/or reactive carbonyl species	Bidasee et al. 2003a [2]; Bidasee et al. 2003b [102]; Shao et al. 2012 [46]
	Slow release of Ca^{2+} from SR and prolonged time to peak Ca^{2+} transients	Choi et al. 2002 [21]
TIIDM	Effect	References
	Decrease in RyR2 mRNA levels in the GK model	Gaber et al. 2014 [62]
	Decrease in [^{3}H]ryanodine binding affinity in the right and left ventricle	Dincer et al. 2006 [60]
	Increase in RyR2 phosphorylation at Ser 2808/Ser 2809	Dincer et al. 2006 [60]; Okatan et al. 2016 [61]
	Increased oxidation of RyR2, decreased *S*-nitrosylation, and diastolic Ca^{2+} leak; increased activity in PPAR-γ overexpressed mice with high lipid; and increased RyR2 activity due to redox modification in HFD-fed mice	Oda et al. 2015 [66]; Gonzalez et al. 2007 [67]; Joseph et al. 2016 [64]; Xie et al. 2016 [65]; Sánchez et al. 2018 [68]

significantly reduced 3 weeks after the STZ injection [22]. Kim et al. (2001) found that the maximal Ca^{2+} uptake and the affinity of SERCA2a for Ca^{2+} were decreased while the exogenous phosphorylation level of PLB was increased in STZ-induced diabetic rat SR. Levels of both mRNA and protein of PLB were significantly increased in the diabetic hearts, whereas those of SERCA2a were significantly decreased. Consequently, the relative PLB/Ca^{2+}-ATPase ratio was 1.88 in the diabetic hearts, and these changes were correlated with changes in the rates of SR Ca^{2+} uptake [74]. Choi et al. (2002) also found that the depression in the SR function was associated with decreased SERCA2a and increased nonphosphorylated PLB proteins [21]. Supporting these findings, Bidasee et al. (2004) found that the hearts of 8-week STZ-treated animals expressed lower levels of the SERCA2a protein and higher levels of monomeric unphosphorylated PLB [75]. Decreased function of SERCA2a was also reported in other studies including studies on the alloxan model of TIDM [20, 76, 77].

Oxygen-derived free radicals have been reported to damage SERCA, leading to cellular Ca^{2+} overload. For example, earlier study by Okabe et al. (1983) showed that a decrease in Ca^{2+} uptake occurs in isolated SR after exposure to xanthine/xanthine oxidase, an enzymatic system capable of generating superoxide radicals [78]. Zu et al. (1997) found that hydroxyl radical inhibits the SERCA2a function by directly attacking the ATP binding site [79]. A more recent study by Ying et al. (2008) showed that exposure of cardiac SR membranes directly to peroxynitrite reduces the SERCA2a activity by oxidizing Cysteine 674, as well as interfering with the ATP binding site [80].

4.2. The Sarcoplasmic Reticulum Ca^{2+}-ATPase in Type II Diabetes Mellitus. Previous studies in TIIDM animal models have variously reported either no change, decreased or increased expression of SERCA2a. Although Støle et al. (2009) reported no change in the SERCA2a expression in the *db*/*db* mouse, the decreased activity of SERCA2a was attributed to the increased PLB expression [30]. Similarly, in ventricular myocytes isolated from adult rats fed on sucrose for 9-12 weeks, shortening/relengthening were significantly shorter compared to starch- (ST-) fed controls. Although the SERCA2a expression was unaltered, the inhibition was associated with decreased SR Ca^{2+} uptake and increased PLB phosphorylation [81].

In contrast to the above findings, both a decrease and an increase in the SERCA2a expression were observed in *Zucker Diabetic Fatty* rat, an early TIIDM model. While Young et al. (2002) reported a decrease in the SERCA2a expression and cardiac contractility [82], a more recent study conducted by Fredersdorf et al. (2012) showed that the SERCA2a expression is upregulated, whereas the expression of PLB mRNA was reduced. The changes were associated with a significant increase in SR Ca^{2+} uptake. Interestingly, the SERCA2a expression and SERCA/PLB ratio in diabetic animals were further increased by insulin treatment. From a pathophysiological point of view, insulin-induced upregulation of SERCA2a could be regarded as a feedback mechanism in handling the volume overload caused by high glucose levels in the early phase of TIIDM, when insulin levels are high [83]. Effects of TIDM and TIIDM on SERCA2a are summarized in Table 3.

5. The Sodium-Calcium Exchanger

The NCX is an electrogenic transporter located at the plasma membrane that catalyses the countertransport of Na^+ and Ca^{2+}. To date, 4 isoforms have been identified for NCX, namely, NCX1, NCX2, NCX3, and NCX4 [84]. The cardiac isoform, NCX1, is organized into ten transmembrane segments (TMSs) with a large cytoplasmic loop between TMSs 5 and 6 that plays a regulatory role. Ion transport is associated with two regions of intramolecular similarity named α repeats. They consist of TMSs 2–3 and TMSs 7–8 and their connecting links [85]. NCX1 plays an important role in Ca^{2+} homeostasis, typically by operating in forward mode

Table 3: Effect of DM on sarcoplasmic reticulum Ca^{2+}-ATPase.

TIDM	Effect	References
	Decrease in mRNA level/protein expression of SERCA2a in STZ-treated diabetic rats	Teshima et al. 2000 [22]; Choi et al. 2002 [21]; Kim et al. 2001 [73]; Bidasee et al. 2004 [74]; Lacombe et al. 2007 [20]
	Increase in mRNA level/protein expression of non-phosphorylated PLB in STZ-treated diabetic rats	Choi et al. 2002 [21]; Kim et al. 2001 [73]; Bidasee et al. 2004 [74]
	Decrease in the SERCA2a function in alloxan/STZ-treated diabetic rats	Lopaschuk et al. 1983 [75]; Allo et al. 1991 [76]; Zhao et al. 2014 [49]; Lacombe et al. 2007 [20]
	Inhibition of SERCA2 by free radicals through the direct attack of ATP-binding site	Xu et al. 1997 [78]; Ying et al. 2008 [79]
	Downregulation through posttranslational modifications (glycation, carbonylation, and O-GlcNAcylation)	Bidasee et al. 2004 [74]
TIIDM	Effect	References
	Decreased SR Ca^{2+} uptake, increased PLB phosphorylation, unaltered SERCA2a expression in db/db mouse, and adult rats fed on sucrose	Wold et al. 2005 [80]
	Decreased SERCA2a function, enhanced CaMKII-mediated phosphorylation of PLB in Ob/Ob mice.	Stølen et al. 2009 [30]
	Decreased SERCA2a expression in Zucker Diabetic Fatty rat	Young et al. 2002 [81]
	Increased SERCA2a expression in Zucker Diabetic Fatty rat	Fredersdorf et al. 2012 [82]

to extrude one Ca^{2+} ion for 3 Na^+ ions. The direction of Ca^{2+} transport reverses at membrane potentials near that of the AP plateau, generating an influx of Ca^{2+} into the cell [86]. NCX1 is regulated by intracellular Ca^{2+} [87], signaling lipid phosphatidylinositol-4,5-bisphosphate (PIP_2) [86], and free radicals, as well as PKA and PKC [88, 89]. Alterations in the ionic and electrical conditions that accompany cardiac diseases promote reverse-mode of the NCX1 activity, leading to Ca^{2+} overload and electrical dysfunction [86].

5.1. The Sodium-Calcium Exchanger in Type I Diabetes Mellitus. Earlier studies have shown that the NCX current density was reduced [20, 26, 90, 91], and current inactivation was prolonged [26] in ventricular myocytes from STZ-induced diabetic rat. These variations in amplitude and kinetics of the current were accompanied with reduced NCX mRNA [90] and reduced or unaltered NCX protein in the STZ-induced diabetic rat heart [21, 92, 93]. In alloxan-injected rats, the NCX function was depressed 2 weeks after diabetes induction [94]. Most recent data from our lab has shown that the NCX current was significantly smaller in endocardial and epicardial ventricular cardiomyocytes compared to controls, 5-6 months after the induction of diabetes with STZ [95].

Despite the fact that all of the abov-mentioned studies have supported the decrease in NCX function in TIDM, results from the Akita(ins2) TIDM model showed an increase in the NCX expression as a compensatory mechanism in response to reduced contractility in the heart. Such increase was protective against systolic failure [96].

5.2. The Sodium-Calcium Exchanger in Type II Diabetes Mellitus. In mice with TIIDM (db/db), either no change or increased activity of NCX1 was observed. For example, in insulin-resistant sucrose-fed rats, the normal expression of NCX1 was observed [81]. Similarly, Ricci et al. (2006) found no change in the NCX current density in HFD mice [97]. However, Stølen et al. (2009) found an increased activity of NCX1in TIIDM (db/db) [30]. An increased NCX1 gene expression was observed in human with TIIDM and was associated with comparable left ventricular hypertrophy [98]. Effects of TIDM and TIIDM on NCX1 are summarized in Table 4.

6. Effect of Advanced Glycation Products on Ca^{2+} Handling Proteins in Diabetes

Chronic hyperglycemia results in excessive formation of advanced glycation end products (AGE). The glycation modifications can further deteriorate the pathology of diabetes [4, 5]. AGEs are a heterogenous group of molecules resulting from the nonenzymatic glycation and oxidation of proteins and lipids in the presence of reducing sugars. AGEs may alter cellular function through crosslinking of cellular proteins or by activating the AGE receptor (RAGE). In cardiomyocytes, AGEs were shown to crosslink the domains of both the RyR and SERCA2a [99]. Yan et al. (2014) showed that the AGE/RAGE signal enhanced Ca^{2+} spark-mediated SR Ca^{2+} leak, which resulted in partial depletion of the SR Ca^{2+} content and consequently, decreased systolic Ca^{2+} transient. Altogether, these effects have contributed to contractile dysfunction reported in diabetic cardiomyopathy [100, 101].

As mentioned earlier, the RyR2 structure is rich in free thiol groups and therefore, it is highly susceptible to oxidative stress. Hegab et al. (2017) found that the AGE-induced activation of RAGE enhanced the activity of NADPH oxidase and hence the production of ROS. This was accompanied with activation of p38 kinase, nuclear translocation of NF-κB, and subsequently induction of inducible nitric oxide synthase (iNOS) expression, leading to increased NO production. Elevation of ROS and NO was found to alter Ca^{2+} handling through *S*-nitrosylation of key proteins such as SERCA2a, RyR2, and L-type Ca^{2+} channel [100, 102].

Table 4: Effect of DM on sodium-calcium exchanger.

TIDM	Effect	References
	Reduction NCX current density	Chattou et al. (1999) [26]; Hattori et al. 2000 [89]; Lacombe et al. 2007 [20]; Sheikh et al. 2012 [90]; Zhao et al. 2014 [49]
	Reduced in NCX mRNA	Hattori et al. 2000 [89]
	Reduced or unaltered NCX protein	Choi et al. 2002 [21]; Lee et al. 2013 [91], Zhang et al. 2013 [92]
	Decreased NCX activity in alloxan-treated rats	Golfman et al. 1998 [93]; Allo et al. 1991 [76]
	Increased NCX expression in Akita(ins2) TIDM	LaRocca et al. 2012 [94]
TIIDM	Effect	References
	No change in the NCX expression and current density in insulin-resistant sucrose-fed rats and HFD mice	Wold et al. 2005 [80]; Ricci et al. 2006 [96]
	Increased activity in the TIIDM model (db/db)	Stølen et al. 2009 [30]
	Increased NCX1 gene expression	Ashrafi et al. 2017 [97]

The relationship between diabetes-induced decrease in the RyR2 activity and the formation of AGE during chronic diabetes was also shown in other studies. Bidasee et al. (2003) have shown that AGEs are formed on RyR2 during diabetes. RyR2 from 8-week STZ-induced diabetic rat hearts contained several noncrosslinking AGEs. Noticeably, decreased ability to bind [^{3}H]ryanodine and altered sensitivity to Ca^{2+} indicated the loss of functional integrity of RyR2 from these hearts [2]. In fact, formation of AGEs on RyR2 was not the only contributor to RyR2 dysfunction. In a previous study conducted by the same group on 6-week STZ-diabetic rat hearts, it was shown that the dysfunction of RyR2 stems in part from diabetes-induced increase in its disulfide bond content [103]. Furthermore, glycation of RyR2 was found to alter its gating properties and was associated with increased SR Ca^{2+} leak, elevated mitochondrial Ca^{2+} content, and concomitant mitochondrial Ca^{2+} overload and damage [104] .

SERCA2a is susceptible to posttranslational modifications during diabetes. It has been identified as a prominent target of glycative damage. Hearts from 8-week-old diabetic rats treated with STZ showed several cytosolic SERCA2a peptides, modified by single noncrosslinked and crosslinked AGEs. Lysine residues within the actuator domain (*A*, cytoplasmic) and phosphorylation domain (*P*, cytoplasmic) were crosslinked to arginine residues within the nucleotide binding domain (*N*, cytoplasmic) via pentosidine AGEs. 2 weeks of insulin treatment initiated after 6 weeks of diabetes significantly improved the cardiac function and also prevented the formation of crosslinking AGEs on SERCA2a. It is suggested that the disruption in the tertiary structure by AGE complexes prevented the structural movements required for translocating Ca^{2+} from the cytosol to the lumen of the SR and resulted in a decrease in the SERCA2a activity [75]. Other studies have identified carbonylation and O-GlcNAcylation as important mechanisms that contribute to the loss of the SERCA2a activity and diastolic dysfunction in a rat model of TIDM [46, 105].

7. Targeting Ca^{2+} Handling in Diabetes

Taken together, studies strongly suggest that several facets related to Ca^{2+} handling are dysregulated in diabetic cardiomyopathy, including altered expression and/or activity levels of the L-type Ca^{2+} channel activity, RyR2, SERCA2a, and NCX. Therefore, targeting these proteins provide potential therapeutic approaches to improve cardiac cell function in diabetes. Many studies have shown that the L-type Ca^{2+} channel activity is either unaltered or reduced in diabetes. The diminished Ca^{2+} entry through the L-type Ca^{2+} channel is a critical contributor to the negative effect on cardiac contractility observed in diabetic cardiomyopathy, and therefore, an increase of the trigger produced by the L-type Ca^{2+} current will increase the amplitude of Ca^{2+} transients and contraction. Gain-of-function mutations in the channel's α1-subunit or other proteins favoring cellular depolarization might be beneficial in diabetic cardiomyopathy. For example, mutations that increase the window current and maximal conductance for Ca^{2+} will augment the trigger for RyR2-mediated Ca^{2+} release, thereby improving the systolic function in the diabetic heart. Although the increased Ca^{2+} entry into the myocytes substantially contributes to the positive inotropic effect, it is worth noting that excess Ca^{2+} influx through the L-type Ca^{2+} channel is likely to contribute to intracellular Ca^{2+} overload.

The NCX function is also reduced according to many diabetic models. In fact, inhibition of NCX in the forward mode will further increase the cellular Ca^{2+} content. This could be an advantage in conditions of low inotropy but could also lead to relaxation abnormalities and adverse accumulation of Ca^{2+} in cytosol and cell death [106]. On the contrary, the inhibition of NCX in the reverse mode could be of pharmacological importance in limiting the cellular Ca^{2+} content and Ca^{2+} overload in ventricular cardiomyocytes where the NCX activity is increased.

It is evident that remodeling the activity of SERCA2a and RyR2 favors the improvement of Ca^{2+} handling in diabetes. Majority of studies in both models of diabetes have shown that the activity of RyR2 is increased, while the activity of SERCA2a is diminished in diabetic ventricular cardiomyocytes. Suppressing RyR2-mediated SR Ca^{2+} leak by directly modifying RyR2 gating represents an effective strategy for preventing spontaneous Ca^{2+} waves. In this regard, several drugs with unique inhibitory action on Ca^{2+} waves have been tested in earlier studies [107, 108]. These drugs have been

shown to possess antiarrhythmic effects and could probably have cardioprotective properties. However, their mechanisms of action are both complex and controversial. Modulation of the RyR2 activity can also be achieved by targeting CaMK II, which inhibits RyR2 phosphorylation and results in an overall decreased SR Ca^{2+} overload [109].

Although the role of RyR2 in excitation-contraction coupling in cardiomyocytes is well established, a functional role for RyR2 in β cell insulin secretion is not well understood. Missense mutations in RYR2 were shown to be associated with catecholaminergic polymorphic ventricular tachycardia (CPVT), which is characterized by exercise-induced arrhythmias and sudden cardiac death. CPVT patients were found to have leaky RyR2, present with glucose intolerance. In mice, the transgenic expression of CPVT-associated RyR2 resulted in impaired glucose homeostasis. Furthermore, β cells from these animals revealed intracellular Ca^{2+} leak via oxidized and nitrosylated RyR2 channels [110]. It is important to mention that chronic intracellular Ca^{2+} leak via RyR2 channels in the pancreatic β cell causes store depletion, triggers ER stress, and results in mitochondrial dysfunction. Consequently, these effects lead to the reduction in ATP synthesis and eventually decreased glucose-stimulated insulin secretion by β cells. Impaired mitochondrial function also leads to increased production of ROS, which triggers redox modifications of RyR2, thereby aggravating the Ca^{2+} leak [111]. Therefore, pharmacological inhibition of intracellular Ca^{2+} leak via RyR2 channels in diabetic patients would be critically important.

Many studies in both models of diabetes have shown that the activity of SERCA2a is diminished in diabetic ventricular cardiomyocytes. Therefore, remodeling the activity of SERCA2a would play an important role in improving the process of Ca^{2+} handling in diabetes. The overexpression of SERCA2a and modulation of the inhibitory action of the regulatory protein PLB provide potentially important therapeutic approaches in improving ventricular contractile function in diabetes [12]; however, such approaches will need further extensive studies and testing in relevant animal and preclinical models.

It is worth mentioning that the levels of SERCA can be assayed in peripheral blood lymphocytes, and their levels correlate with SERCA levels obtained in the cardiac tissue [112]. Mechanistically, the decreased SERCA activity results in Ca^{2+} overload in the cytoplasm which is known to be arrhythmogenic. For this reason, assay of SERCA levels could provide valuable information on proarrhythmogenesis. This aspect might help clinicians to identify patients with higher rate of arrhythmic events and worse prognosis. Additionally, SERCA may become a therapeutic target of tailored therapies and interventional approaches to reduce the arrhythmic burden in patients. A recent study was conducted to evaluate atrial fibrillation (AF) recurrence and SERCA levels in patients treated by epicardial thoracoscopic ablation for persistent AF [113]. After a successful epicardial ablation procedure, there was significant increase in the SERCA expression in responders compared to baseline and to nonresponders. Responders also displayed a marked reduction of inflammatory cytokines. The findings of this study indicated that SERCA may represent an effective therapeutic target to reduce postablative recurrences in patients with persistent AF.

8. Conclusion

Over the last decade, significant progress has been made in outlining the mechanisms responsible for the altered cardiac contractile function in diabetes using different animal models of TIDM and TIIDM. Exploring the molecular mechanism(s) involved in the disturbances of Ca^{2+} transport and the role of main cardiac proteins responsible for Ca^{2+} homeostasis in the diabetic rat ventricular cardiomyocytes will provide an insight for the identification of novel therapeutic approaches to improve heart function in diabetic patients.

Conflicts of Interest

The author declares that there is no competing interest regarding the publication of this review.

References

[1] J. M. Forbes and M. E. Cooper, "Mechanisms of diabetic complications," *Physiological Reviews*, vol. 93, no. 1, pp. 137–188, 2013.

[2] K. R. Bidasee, K. Nallani, Y. Yu et al., "Chronic diabetes increases advanced glycation end products on cardiac ryanodine receptors/calcium-release channels," *Diabetes*, vol. 52, no. 7, pp. 1825–1836, 2003.

[3] D. K. Patel, R. Kumar, D. Laloo, and S. Hemalatha, "Diabetes mellitus: an overview on its pharmacological aspects and reported medicinal plants having antidiabetic activity," *Asian Pacific Journal of Tropical Biomedicine*, vol. 2, no. 5, pp. 411–420, 2012.

[4] S. Sekhon-Loodu and H. P. V. Rupasinghe, "Evaluation of antioxidant, Antidiabetic and Antiobesity Potential of Selected Traditional Medicinal Plants," *Frontiers in Nutrition*, vol. 6, p. 53, 2019.

[5] H. Choudhury, M. Pandey, C. K. Hua et al., "An update on natural compounds in the remedy of diabetes mellitus: a systematic review," *Journal of Traditional and Complementary Medicine*, vol. 8, no. 3, pp. 361–376, 2018.

[6] D. A. Eisner, J. L. Caldwell, K. Kistamás, and A. W. Trafford, "Calcium and excitation-contraction coupling in the heart," *Circulation Research*, vol. 121, no. 2, pp. 181–195, 2017.

[7] I. Bodi, G. Mikala, S. E. Koch, S. A. Akhter, and A. Schwartz, "The L-type calcium channel in the heart: the beat goes on," *The Journal of Clinical Investigation*, vol. 115, no. 12, pp. 3306–3317, 2005.

[8] F. Brette, J. Leroy, J. Y. le Guennec, and L. Sallé, "Ca2+ currents in cardiac myocytes: old story, new insights," *Progress in Biophysics and Molecular Biology*, vol. 91, no. 1-2, pp. 1–82, 2006.

[9] D. M. Bers, "Cardiac excitation-contraction coupling," *Nature*, vol. 415, no. 6868, pp. 198–205, 2002.

[10] C. Walsh, S. Barrow, S. Voronina, M. Chvanov, O. H. Petersen, and A. Tepikin, "Modulation of calcium signalling by mitochondria," *Biochimica et Biophysica Acta*, vol. 1787, no. 11, pp. 1374–1382, 2009.

[11] R. M. Shaw and H. M. Colecraft, "L-type calcium channel targeting and local signalling in cardiac myocytes," *Cardiovascular Research*, vol. 98, no. 2, pp. 177–186, 2013.

[12] S. Hamilton and D. Terentyev, "Proarrhythmic remodeling of calcium homeostasis in cardiac disease; Implications for Diabetes and Obesity," *Frontiers in Physiology*, vol. 9, article 1517, 2018.

[13] J. S. Rougier and H. Abriel, "Cardiac voltage-gated calcium channel macromolecular complexes," *Biochimica et Biophysica Acta (BBA) - Molecular Cell Research*, vol. 1863, no. 7, pp. 1806–1812, 2016.

[14] A. Y. H. Woo and R. P. Xiao, "β-Adrenergic receptor subtype signaling in heart: from bench to bedside," *Acta Pharmacologica Sinica*, vol. 33, no. 3, pp. 335–341, 2012.

[15] D. T. Yue, S. Herzig, and E. Marban, "Beta-adrenergic stimulation of calcium channels occurs by potentiation of high-activity gating modes," *Proceedings of the National Academy of Sciences of the United States of America*, vol. 87, no. 2, pp. 753–757, 1990.

[16] B. Z. Peterson, C. DeMaria, J. P. Adelman, and D. T. Yue, "Calmodulin is the Ca2+ sensor for Ca2+ -dependent inactivation of L-type calcium channels," *Neuron*, vol. 22, no. 3, pp. 549–558, 1999.

[17] R. Bansal, N. Ahmad, and J. R. Kidwai, "Alloxan-glucose interaction: effect on incorporation of 14C-leucine into pancreatic islets of rat," *Acta Diabetologica Latina*, vol. 17, no. 2, pp. 135–143, 1980.

[18] C. E. Mathews, S. H. Langley, and E. H. Leiter, "New mouse model to study islet transplantation in insulin-dependent diabetes mellitus," *Transplantation*, vol. 73, no. 8, pp. 1333–1336, 2002.

[19] M. M. A. Smail, M. A. Qureshi, A. Shmygol et al., "Regional effects of streptozotocin-induced diabetes on shortening and calcium transport in epicardial and endocardial myocytes from rat left ventricle," *Physiological Reports*, vol. 4, no. 22, article e13034, 2016.

[20] V. A. Lacombe, S. Viatchenko-Karpinski, D. Terentyev et al., "Mechanisms of impaired calcium handling underlying subclinical diastolic dysfunction in diabetes," *American Journal of Physiology. Regulatory, Integrative and Comparative Physiology*, vol. 293, no. 5, pp. R1787–R1797, 2007.

[21] K. M. Choi, Y. Zhong, B. D. Hoit et al., "Defective intracellular Ca(2+) signaling contributes to cardiomyopathy in type 1 diabetic rats," *American Journal of Physiology. Heart and Circulatory Physiology*, vol. 283, no. 4, pp. H1398–H1408, 2002.

[22] Y. Teshima, N. Takahashi, T. Saikawa et al., "Diminished expression of sarcoplasmic reticulum Ca(2+)-ATPase and ryanodine sensitive Ca(2+)channel mRNA in streptozotocin-induced diabetic rat heart," *Journal of Molecular and Cellular Cardiology*, vol. 32, no. 4, pp. 655–664, 2000.

[23] N. N. Hamouda, V. Sydorenko, M. A. Qureshi, J. M. Alkaabi, M. Oz, and F. C. Howarth, "Dapagliflozin reduces the amplitude of shortening and Ca(2+) transient in ventricular myocytes from streptozotocin-induced diabetic rats," *Molecular and Cellular Biochemistry*, vol. 400, no. 1-2, pp. 57–68, 2015.

[24] D. W. Wang, T. Kiyosue, S. Shigematsu, and M. Arita, "Abnormalities of K+ and Ca2+ currents in ventricular myocytes from rats with chronic diabetes," *The American Journal of Physiology*, vol. 269, 4 Part 2, pp. H1288–H1296, 1995.

[25] A. Woodall, N. Bracken, A. Qureshi, F. C. Howarth, and J. Singh, "Halothane alters contractility and Ca2+ transport in ventricular myocytes from streptozotocin-induced diabetic rats," *Molecular and Cellular Biochemistry*, vol. 261, no. 1, pp. 251–261, 2004.

[26] S. Chattou, J. Diacono, and D. Feuvray, "Decrease in sodium-calcium exchange and calcium currents in diabetic rat ventricular myocytes," *Acta Physiologica Scandinavica*, vol. 166, no. 2, pp. 137–144, 1999.

[27] Z. Lu, Y. P. Jiang, X. H. Xu, L. M. Ballou, I. S. Cohen, and R. Z. Lin, "Decreased L-type Ca2+ current in cardiac myocytes of type 1 diabetic Akita mice due to reduced phosphatidylinositol 3-kinase signaling," *Diabetes*, vol. 56, no. 11, pp. 2780–2789, 2007.

[28] N. Bracken, F. C. Howarth, and J. Singh, "Effects of streptozotocin-induced diabetes on contraction and calcium transport in rat ventricular cardiomyocytes," *Annals of the New York Academy of Sciences*, vol. 1084, no. 1, pp. 208–222, 2006.

[29] L. Pereira, J. Matthes, I. Schuster et al., "Mechanisms of [Ca2+]i transient decrease in cardiomyopathy of db/db type 2 diabetic mice," *Diabetes*, vol. 55, no. 3, pp. 608–615, 2006.

[30] T. O. Stølen, M. A. Høydal, O. J. Kemi et al., "Interval training normalizes cardiomyocyte function, diastolic Ca2+ control, and SR Ca2+ release synchronicity in a mouse model of diabetic cardiomyopathy," *Circulation Research*, vol. 105, no. 6, pp. 527–536, 2009.

[31] F. C. Howarth, M. A. Qureshi, Z. Hassan et al., "Changing pattern of gene expression is associated with ventricular myocyte dysfunction and altered mechanisms of Ca2+ signalling in young type 2 Zucker diabetic fatty rat heart," *Experimental Physiology*, vol. 96, no. 3, pp. 325–337, 2011.

[32] K. A. Salem, M. A. Qureshi, V. Sydorenko et al., "Effects of exercise training on excitation-contraction coupling and related mRNA expression in hearts of Goto-Kakizaki type 2 diabetic rats," *Molecular and Cellular Biochemistry*, vol. 380, no. 1-2, pp. 83–96, 2013.

[33] L. Al Kury, V. Sydorenko, M. M. A. Smail et al., "Voltage dependence of the Ca2+ transient in endocardial and epicardial myocytes from the left ventricle of Goto-Kakizaki type 2 diabetic rats," *Molecular and Cellular Biochemistry*, vol. 446, no. 1-2, pp. 25–33, 2018.

[34] D. Baddeley, I. D. Jayasinghe, L. Lam, S. Rossberger, M. B. Cannell, and C. Soeller, "Optical single-channel resolution imaging of the ryanodine receptor distribution in rat cardiac myocytes," *Proceedings of the National Academy of Sciences of the United States of America*, vol. 106, no. 52, pp. 22275–22280, 2009.

[35] H. Cheng, M. R. Lederer, W. J. Lederer, and M. B. Cannell, "Calcium sparks and [Ca2+]i waves in cardiac myocytes," *American Journal of Physiology-Cell Physiology*, vol. 270, no. 1, pp. C148–C159, 1996.

[36] Y. Hou, I. Jayasinghe, D. J. Crossman, D. Baddeley, and C. Soeller, "Nanoscale analysis of ryanodine receptor clusters in dyadic couplings of rat cardiac myocytes," *Journal of Molecular and Cellular Cardiology*, vol. 80, pp. 45–55, 2015.

[37] I. Györke, N. Hester, L. R. Jones, and S. Györke, "The role of calsequestrin, triadin, and junctin in conferring cardiac ryanodine receptor responsiveness to luminal calcium," *Biophysical Journal*, vol. 86, no. 4, pp. 2121–2128, 2004.

[38] S. Györke and D. Terentyev, "Modulation of ryanodine receptor by luminal calcium and accessory proteins in health

and cardiac disease," *Cardiovascular Research*, vol. 77, no. 2, pp. 245–255, 2008.

[39] D. M. Bers, "Macromolecular complexes regulating cardiac ryanodine receptor function," *Journal of Molecular and Cellular Cardiology*, vol. 37, no. 2, pp. 417–429, 2004.

[40] L. A. Gonano and P. P. Jones, "FK506-binding proteins 12 and 12.6 (FKBPs) as regulators of cardiac ryanodine receptors: insights from new functional and structural knowledge," *Channels*, vol. 11, no. 5, pp. 415–425, 2017.

[41] E. Niggli, N. D. Ullrich, D. Gutierrez, S. Kyrychenko, E. Poláková, and N. Shirokova, "Posttranslational modifications of cardiac ryanodine receptors: Ca(2+) signaling and EC-coupling," *Biochimica et Biophysica Acta*, vol. 1833, no. 4, pp. 866–875, 2013.

[42] D. Terentyev and S. Hamilton, "Regulation of sarcoplasmic reticulum Ca2+ release by serine-threonine phosphatases in the heart," *Journal of Molecular and Cellular Cardiology*, vol. 101, pp. 156–164, 2016.

[43] J. Hain, H. Onoue, M. Mayrleitner, S. Fleischer, and H. Schindler, "Phosphorylation modulates the function of the calcium release channel of sarcoplasmic reticulum from cardiac muscle," *The Journal of Biological Chemistry*, vol. 270, no. 5, pp. 2074–2081, 1995.

[44] K. R. Eager, L. D. Roden, and A. F. Dulhunty, "Actions of sulfhydryl reagents on single ryanodine receptor Ca(2+)-release channels from sheep myocardium," *American Journal of Physiology–Cell Physiology*, vol. 272, no. 6, pp. C1908–C1918, 1997.

[45] L. Xu, J. P. Eu, G. Meissner, and J. S. Stamler, "Activation of the cardiac calcium release channel (ryanodine receptor) by poly-S-nitrosylation," *Science*, vol. 279, no. 5348, pp. 234–237, 1998.

[46] C. H. Shao, C. Tian, S. Ouyang et al., "Carbonylation induces heterogeneity in cardiac ryanodine receptor function in diabetes mellitus," *Molecular Pharmacology*, vol. 82, no. 3, pp. 383–399, 2012.

[47] L. S. Song, E. A. Sobie, S. McCulle, W. J. Lederer, C. W. Balke, and H. Cheng, "Orphaned ryanodine receptors in the failing heart," *Proceedings of the National Academy of Sciences of the United States of America*, vol. 103, no. 11, pp. 4305–4310, 2006.

[48] Z. Yu, G. F. Tibbits, and J. H. McNeill, "Cellular functions of diabetic cardiomyocytes: contractility, rapid-cooling contracture, and ryanodine binding," *American Journal of Physiology-Heart and Circulatory Physiology*, vol. 266, no. 5, pp. H2082–H2089, 1994.

[49] S.-M. Zhao, Y. L. Wang, C. Y. Guo, J. L. Chen, and Y. Q. Wu, "Progressive decay of Ca2+ homeostasis in the development of diabetic cardiomyopathy," *Cardiovascular Diabetology*, vol. 13, no. 1, pp. 75–75, 2014.

[50] G. E. Gilca, G. Stefanescu, O. Badulescu, D. M. Tanase, I. Bararu, and M. Ciocoiu, "Diabetic cardiomyopathy: current approach and potential diagnostic and therapeutic targets," *Journal Diabetes Research*, vol. 2017, article 1310265, 7 pages, 2017.

[51] C.-H. Shao, X. H. T. Wehrens, T. A. Wyatt et al., "Exercise training during diabetes attenuates cardiac ryanodine receptor dysregulation," *Journal of Applied Physiology*, vol. 106, no. 4, pp. 1280–1292, 2009.

[52] N. Yaras, M. Ugur, S. Ozdemir et al., "Effects of diabetes on ryanodine receptor Ca release channel (RyR2) and Ca2+ homeostasis in rat heart," *Diabetes*, vol. 54, no. 11, pp. 3082–3088, 2005.

[53] E. Tuncay, E. N. Okatan, A. Toy, and B. Turan, "Enhancement of cellular antioxidant-defence preserves diastolic dysfunction via regulation of both diastolic Zn2+ and Ca2+ and prevention of RyR2-leak in hyperglycemic cardiomyocytes," *Oxidative Medicine and Cellular Longevity*, vol. 2014, Article ID 290381, 15 pages, 2014.

[54] C. H. Shao, G. J. Rozanski, K. P. Patel, and K. R. Bidasee, "Dyssynchronous (non-uniform) Ca2+ release in myocytes from streptozotocin-induced diabetic rats," *Journal of Molecular and Cellular Cardiology*, vol. 42, no. 1, pp. 234–246, 2007.

[55] X. H. Wehrens, S. E. Lehnart, S. R. Reiken, and A. R. Marks, "Ca2+/calmodulin-dependent protein kinase II phosphorylation regulates the cardiac ryanodine receptor," *Circulation Research*, vol. 94, no. 6, pp. e61–e70, 2004.

[56] D. R. Witcher, R. J. Kovacs, H. Schulman, D. C. Cefali, and L. R. Jones, "Unique phosphorylation site on the cardiac ryanodine receptor regulates calcium channel activity," *The Journal of Biological Chemistry*, vol. 266, no. 17, pp. 11144–11152, 1991.

[57] S. Huke and D. M. Bers, "Ryanodine receptor phosphorylation at serine 2030, 2808 and 2814 in rat cardiomyocytes," *Biochemical and Biophysical Research Communications*, vol. 376, no. 1, pp. 80–85, 2008.

[58] S. O. Marx, S. Reiken, Y. Hisamatsu et al., "PKA phosphorylation dissociates FKBP12.6 from the calcium release channel (ryanodine receptor): defective regulation in failing hearts," *Cell*, vol. 101, no. 4, pp. 365–376, 2000.

[59] T. Netticadan, R. M. Temsah, A. Kent, V. Elimban, and N. S. Dhalla, "Depressed levels of Ca2+-cycling proteins may underlie sarcoplasmic reticulum dysfunction in the diabetic heart," *Diabetes*, vol. 50, no. 9, pp. 2133–2138, 2001.

[60] C. Tian, C. Hong Shao, C. J. Moore et al., "Gain of function of cardiac ryanodine receptor in a rat model of type 1 diabetes," *Cardiovascular Research*, vol. 91, no. 2, pp. 300–309, 2011.

[61] U. D. Dincer, A. Araiza, J. D. Knudson, C. H. Shao, K. R. Bidasee, and J. D. Tune, "Dysfunction of cardiac ryanodine receptors in the metabolic syndrome," *Journal of Molecular and Cellular Cardiology*, vol. 41, no. 1, pp. 108–114, 2006.

[62] E. N. Okatan, A. T. Durak, and B. Turan, "Electrophysiological basis of metabolic-syndrome-induced cardiac dysfunction," *Canadian Journal of Physiology and Pharmacology*, vol. 94, no. 10, pp. 1064–1073, 2016.

[63] E. M. Gaber, P. Jayaprakash, M. A. Qureshi et al., "Effects of a sucrose-enriched diet on the pattern of gene expression, contraction and Ca2+transport in Goto-Kakizaki type 2 diabetic rat heart," *Experimental Physiology*, vol. 99, no. 6, pp. 881–893, 2014.

[64] H. Reuter, S. Grönke, C. Adam et al., "Sarcoplasmic Ca2+ release is prolonged in nonfailing myocardium of diabetic patients," *Molecular and Cellular Biochemistry*, vol. 308, no. 1-2, pp. 141–149, 2008.

[65] L. C. Joseph, P. Subramanyam, C. Radlicz et al., "Mitochondrial oxidative stress during cardiac lipid overload causes intracellular calcium leak and arrhythmia," *Heart Rhythm*, vol. 13, no. 8, pp. 1699–1706, 2016.

[66] Y. Xie, Z. J. Gu, M. X. Wu et al., "Disruption of calcium homeostasis by cardiac-specific over-expression of PPAR-γ in mice: a role in ventricular arrhythmia," *Life Sciences*, vol. 167, pp. 12–21, 2016.

[67] T. Oda, Y. Yang, H. Uchinoumi et al., "Oxidation of ryanodine receptor (RyR) and calmodulin enhance Ca release and pathologically alter, RyR structure and calmodulin affinity," *Journal of Molecular and Cellular Cardiology*, vol. 85, pp. 240–248, 2015.

[68] D. R. Gonzalez, F. Beigi, A. V. Treuer, and J. M. Hare, "Deficient ryanodine receptor S-nitrosylation increases sarcoplasmic reticulum calcium leak and arrhythmogenesis in cardiomyocytes," *Proceedings of the National Academy of Sciences of the United States of America*, vol. 104, no. 51, pp. 20612–20617, 2007.

[69] G. Sánchez, F. Araneda, J. Peña et al., "High-fat-diet-induced obesity produces spontaneous ventricular arrhythmias and increases the activity of ryanodine receptors in mice," *International Journal of Molecular Sciences*, vol. 19, no. 2, p. 533, 2018.

[70] M. Periasamy and A. Kalyanasundaram, "SERCA pump isoforms: their role in calcium transport and disease," *Muscle & Nerve*, vol. 35, no. 4, pp. 430–442, 2007.

[71] K. F. Frank, B. Bölck, E. Erdmann, and R. H. Schwinger, "Sarcoplasmic reticulum Ca2+-ATPase modulates cardiac contraction and relaxation," *Cardiovascular Research*, vol. 57, no. 1, pp. 20–27, 2003.

[72] T. Toyofuku, K. Curotto Kurzydlowski, N. Narayanan, and D. MacLennan, "Identification of Ser38 as the site in cardiac sarcoplasmic reticulum Ca(2+)-ATPase that is phosphorylated by Ca2+/calmodulin-dependent protein kinase," *The Journal of Biological Chemistry*, vol. 269, no. 42, pp. 26492–26496, 1994.

[73] P. K. Ganguly, G. N. Pierce, K. S. Dhalla, and N. S. Dhalla, "Defective sarcoplasmic reticular calcium transport in diabetic cardiomyopathy," *The American Journal of Physiology*, vol. 244, no. 6, pp. E528–E535, 1983.

[74] H. W. Kim, Y. S. Cho, H. R. Lee, S. Y. Park, and Y. H. Kim, "Diabetic alterations in cardiac sarcoplasmic reticulum Ca2+-ATPase and phospholamban protein expression," *Life Sciences*, vol. 70, no. 4, pp. 367–379, 2001.

[75] K. R. Bidasee, Y. Zhang, C. H. Shao et al., "Diabetes increases formation of advanced glycation end products on Sarco(endo)plasmic reticulum Ca2+-ATPase," *Diabetes*, vol. 53, no. 2, pp. 463–473, 2004.

[76] G. D. Lopaschuk, S. Katz, and J. H. McNeill, "The effect of alloxan- and streptozotocin-induced diabetes on calcium transport in rat cardiac sarcoplasmic reticulum. The possible involvement of long chain acylcarnitines," *Canadian Journal of Physiology and Pharmacology*, vol. 61, no. 5, pp. 439–448, 1983.

[77] S. N. Allo, T. M. Lincoln, G. L. Wilson, F. J. Green, A. M. Watanabe, and S. W. Schaffer, "Non-insulin-dependent diabetes-induced defects in cardiac cellular calcium regulation," *American Journal of Physiology-Cell Physiology*, vol. 260, no. 6, pp. C1165–C1171, 1991.

[78] E. Okabe, M. L. Hess, M. Oyama, and H. Ito, "Characterization of free radical-mediated damage of canine cardiac sarcoplasmic reticulum," *Archives of Biochemistry and Biophysics*, vol. 225, no. 1, pp. 164–177, 1983.

[79] K. Y. Xu, J. L. Zweier, and L. C. Becker, "Hydroxyl radical inhibits sarcoplasmic reticulum Ca(2+)-ATPase function by direct attack on the ATP binding site," *Circulation Research*, vol. 80, no. 1, pp. 76–81, 1997.

[80] J. Ying, V. Sharov, S. Xu et al., "Cysteine-674 oxidation and degradation of sarcoplasmic reticulum Ca(2+) ATPase in diabetic pig aorta," *Free Radical Biology & Medicine*, vol. 45, no. 6, pp. 756–762, 2008.

[81] L. E. Wold, K. Dutta, M. M. Mason et al., "Impaired SERCA function contributes to cardiomyocyte dysfunction in insulin resistant rats," *Journal of Molecular and Cellular Cardiology*, vol. 39, no. 2, pp. 297–307, 2005.

[82] M. E. Young, P. H. Guthrie, P. Razeghi et al., "Impaired long-chain fatty acid oxidation and contractile dysfunction in the obese Zucker rat heart," *Diabetes*, vol. 51, no. 8, pp. 2587–2595, 2002.

[83] S. Fredersdorf, C. Thumann, W. H. Zimmermann et al., "Increased myocardial SERCA expression in early type 2 diabetes mellitus is insulin dependent: in vivo and in vitro data," *Cardiovascular Diabetology*, vol. 11, no. 1, pp. 57–57, 2012.

[84] A. Herchuelz and N. Pachera, "The Na + /Ca 2+ exchanger and the plasma membrane Ca 2+ -ATPase in β-cell function and diabetes," *Neuroscience Letters*, vol. 663, pp. 72–78, 2018.

[85] M. J. Shattock, M. Ottolia, D. M. Bers et al., "Na+/Ca2+ exchange and Na+/K+-ATPase in the heart," *The Journal of Physiology*, vol. 593, no. 6, pp. 1361–1382, 2015.

[86] M. J. Riedel, I. Baczkó, G. J. Searle et al., "Metabolic regulation of sodium-calcium exchange by intracellular acyl CoAs," *The EMBO Journal*, vol. 25, no. 19, pp. 4605–4614, 2006.

[87] M. Ottolia, N. Torres, J. H. B. Bridge, K. D. Philipson, and J. I. Goldhaber, "Na/Ca exchange and contraction of the heart," *Journal of Molecular and Cellular Cardiology*, vol. 61, pp. 28–33, 2013.

[88] M. Reppel, B. Fleischmann, H. Reuter, P. Sasse, H. Schunkert, and J. Hescheler, "Regulation of the Na+/Ca2+ exchanger (NCX) in the murine embryonic heart," *Cardiovascular Research*, vol. 75, no. 1, pp. 99–108, 2007.

[89] S. Wagner, T. Seidler, E. Picht et al., "Na(+)-Ca(2+) exchanger overexpression predisposes to reactive oxygen species-induced injury," *Cardiovascular Research*, vol. 60, no. 2, pp. 404–412, 2003.

[90] Y. Hattori, N. Matsuda, J. Kimura et al., "Diminished function and expression of the cardiac Na+-Ca2+ exchanger in diabetic rats: implication in Ca2+ overload," *The Journal of Physiology*, vol. 527, no. 1, pp. 85–94, 2000.

[91] A. Q. Sheikh, J. R. Hurley, W. Huang et al., "Diabetes alters intracellular calcium transients in cardiac endothelial cells," *PLoS One*, vol. 7, no. 5, article e36840, 2012.

[92] T. I. Lee, Y. C. Chen, Y. H. Kao, F. C. Hsiao, Y. K. Lin, and Y. J. Chen, "Rosiglitazone induces arrhythmogenesis in diabetic hypertensive rats with calcium handling alteration," *International Journal of Cardiology*, vol. 165, no. 2, pp. 299–307, 2013.

[93] L. Zhang, M. L. Ward, A. R. J. Phillips et al., "Protection of the heart by treatment with a divalent-copper-selective chelator reveals a novel mechanism underlying cardiomyopathy in diabetic rats," *Cardiovascular Diabetology*, vol. 12, no. 1, p. 123, 2013.

[94] L. Golfman, I. M. C. Dixon, N. Takeda, A. Lukas, K. Dakshinamurti, and N. S. Dhalla, "Cardiac sarcolemmal Na(+)-Ca2+ exchange and Na(+)-K+ ATPase activities and gene expression in alloxan-induced diabetes in rats," *Molecular and Cellular Biochemistry*, vol. 188, no. 1/2, pp. 91–101, 1998.

[95] L. T. Al Kury, V. Sydorenko, M. M. A. Smail et al., "Calcium Signaling in Endocardial and Epicardial Ventricular Myocytes from Streptozotocin-Induced Diabetic Rat," *Journal of Diabetes Investigation*, 2020.

[96] T. J. LaRocca, F. Fabris, J. Chen et al., "Na+/Ca2+exchanger-1 protects against systolic failure in the Akitains2model of diabetic cardiomyopathy via a CXCR4/NF-κB pathway," *American Journal of Physiology. Heart and Circulatory Physiology*, vol. 303, no. 3, pp. H353–H367, 2012.

[97] E. Ricci, S. Smallwood, C. Chouabe et al., "Electrophysiological characterization of left ventricular myocytes from obese Sprague-Dawley rat," *Obesity (Silver Spring)*, vol. 14, no. 5, pp. 778–786, 2006.

[98] R. Ashrafi, P. Modi, A. Y. Oo et al., "Arrhythmogenic gene remodelling in elderly patients with type 2 diabetes with aortic stenosis and normal left ventricular ejection fraction," *Experimental Physiology*, vol. 102, no. 11, pp. 1424–1434, 2017.

[99] Z. Hegab, S. Gibbons, L. Neyses, and M. A. Mamas, "Role of advanced glycation end products in cardiovascular disease," *World Journal of Cardiology*, vol. 4, no. 4, pp. 90–102, 2012.

[100] Z. Hegab, T. M. A. Mohamed, N. Stafford, M. Mamas, E. J. Cartwright, and D. Oceandy, "Advanced glycation end products reduce the calcium transient in cardiomyocytes by increasing production of reactive oxygen species and nitric oxide," *FEBS Open Bio*, vol. 7, no. 11, pp. 1672–1685, 2017.

[101] D. Yan, X. Luo, Y. Li et al., "Effects of advanced glycation end products on calcium handling in cardiomyocytes," *Cardiology*, vol. 129, no. 2, pp. 75–83, 2014.

[102] M. Poteser, C. Romanin, W. Schreibmayer, B. Mayer, and K. Groschner, "S-nitrosation controls gating and conductance of the α1 subunit of class C L-type Ca2+Channels," *The Journal of Biological Chemistry*, vol. 276, no. 18, pp. 14797–14803, 2001.

[103] K. R. Bidasee, K. Nallani, H. R. Besch Jr., and U. D. Dincer, "Streptozotocin-induced diabetes increases disulfide bond formation on cardiac ryanodine receptor (RyR2)," *The Journal of Pharmacology and Experimental Therapeutics*, vol. 305, no. 3, pp. 989–998, 2003.

[104] M. Ruiz-Meana, M. Minguet, D. Bou-Teen et al., "Ryanodine receptor glycation favors mitochondrial damage in the senescent heart," *Circulation*, vol. 139, no. 7, pp. 949–964, 2019.

[105] Y. Hu, D. Belke, J. Suarez et al., "Adenovirus-mediated overexpression of O-GlcNAcase improves contractile function in the diabetic heart," *Circulation Research*, vol. 96, no. 9, pp. 1006–1013, 2005.

[106] G. Antoons, R. Willems, and K. R. Sipido, "Alternative strategies in arrhythmia therapy: evaluation of Na/Ca exchange as an anti-arrhythmic target," *Pharmacology & Therapeutics*, vol. 134, no. 1, pp. 26–42, 2012.

[107] J. Zhang, Q. Zhou, C. D. Smith et al., "Non-β-blocking R-carvedilol enantiomer suppresses Ca2+ waves and stress-induced ventricular tachyarrhythmia without lowering heart rate or blood pressure," *The Biochemical Journal*, vol. 470, no. 2, pp. 233–242, 2015.

[108] D. J. Hunt, P. P. Jones, R. Wang et al., "K201 (JTV519) suppresses spontaneous Ca2+ release and [3H]ryanodine binding to RyR2 irrespective of FKBP12.6 association," *The Biochemical Journal*, vol. 404, no. 3, pp. 431–438, 2007.

[109] H. Uchinoumi, Y. Yang, T. Oda et al., "CaMKII-dependent phosphorylation of RyR2 promotes targetable pathological RyR2 conformational shift," *Journal of Molecular and Cellular Cardiology*, vol. 98, pp. 62–72, 2016.

[110] G. Santulli, G. Pagano, C. Sardu et al., "Calcium release channel RyR2 regulates insulin release and glucose homeostasis," *The Journal of Clinical Investigation*, vol. 125, no. 5, pp. 1968–1978, 2015.

[111] C. Tang, K. Koulajian, I. Schuiki et al., "Glucose-induced beta cell dysfunction in vivo in rats: link between oxidative stress and endoplasmic reticulum stress," *Diabetologia*, vol. 55, no. 5, pp. 1366–1379, 2012.

[112] J. E. Kontaraki, F. I. Parthenakis, E. G. Nyktari, A. P. Patrianakos, and P. E. Vardas, "Myocardial gene expression alterations in peripheral blood mononuclear cells of patients with idiopathic dilated cardiomyopathy," *European Journal of Heart Failure*, vol. 12, no. 6, pp. 541–548, 2010.

[113] C. Sardu, G. Santulli, G. Guerra et al., "Modulation of SERCA in patients with persistent atrial fibrillation treated by epicardial thoracoscopic ablation: the CAMAF study," *Journal of Clinical Medicine*, vol. 9, no. 2, p. 544, 2020.

Hindawi
Journal of Diabetes Research
Volume 2020, Article ID 6976153, 9 pages
https://doi.org/10.1155/2020/6976153

Research Article

Type 2 Diabetes Mellitus and Chronic Heart Failure with Midrange and Preserved Ejection Fraction: A Focus on Serum Biomarkers of Fibrosis

D. A. Lebedev, E. A. Lyasnikova, E. Yu Vasilyeva, A. Yu Babenko, and E. V. Shlyakhto

Almazov National Medical Research Centre, Saint-Petersburg, Russia

Correspondence should be addressed to D. A. Lebedev; doctorlebedev11@gmail.com

Received 22 July 2020; Revised 12 October 2020; Accepted 28 October 2020; Published 9 November 2020

Academic Editor: Gaetano Santulli

As myocardial fibrosis might be an important contributor to the association of diabetes mellitus with left ventricular (LV) dysfunction and chronic heart failure (HF), we investigated the profile of some proinflammatory, profibrotic biomarkers in patients with type 2 diabetes mellitus (T2DM) at various stages of the cardiovascular disease continuum from absence of clinic since and symptoms to HF with preserved (HFpEF) and midrange ejection fraction (HFmrEF). *Material and Methods*. Sixty-two patients with T2DM (age 60 [55; 61]), 20 patients without clinical manifestations of HF and 2 groups with clinical manifestations of stable HF, 29 patients with HFpEF, and 13 patients with HFmrEF, were included in the study. The control group consisted of 13 healthy subjects and normal BMI. All patients underwent transthoracic echocardiography, laboratory assessment of N-terminal fragment of the brain natriuretic peptide (Nt-proBNP), highly sensitive C-reactive protein (hsCRP), soluble suppression of tumorigenesis-2 (sST2), galectin-3, C-terminal propeptide of procollagen type I (PICP), N-terminal propeptide of procollagen type III (PIIINP), matrix metalloproteinase-9 (MMP-9), and tissue inhibitor of matrix proteinase-1 (TIMP-1). *Results*. Patients with HFmrEF had higher values of LV volumetric parameters, indexed parameters of LV myocardial mass (LVMM), and higher concentrations of Nt-proBNP (all $p < 0.05$). The concentrations of galectin-3 were greater in patients with HFpEF and HFmrEF compared to patients without HF ($p = 0.01$ and $p = 0.03$, respectively). PICP and PICP/PIIINP ratio were greater in patients with HFmrEF compared to patients with HFpEF ($p = 0.043$ and $p = 0.033$, respectively). In patients with T2DM and HF, a relationship was found between galectin-3 and LVMM/body surface area ($r = -0.58$, $p = 0.001$), PIIINP, TIMP-1, and LV end-diastolic volume ($r = -0.68$ and $p = 0.042$ and $r = 0.38$ and $p = 0.02$, respectively). *Conclusion*. The dynamics at various stages of the cardiovascular disease continuum in the serum fibrosis markers may reflect an increase in fibrotic and decrease in antifibrotic processes already at the preclinical stage of HF. At the same time, the changes found in the circulating procollagen levels may indicate a shift in balance towards type I collagen synthesis in HFmrEF compared with HFpEF.

1. Introduction

Chronic heart failure (HF) and type 2 diabetes mellitus (T2DM) are important problems of most national health systems. Patients with T2DM have a high risk of developing HF, and in a quarter of HF patients with reduced (HFrEF), midrange (HFmrEF), and preserved ejection fraction (EF) (HFpEF) already had T2DM, which significantly worse the prognosis of the disease, increasing mortality by 30-50%. [1, 2].

Taking into account the clinical phenotypic heterogeneity of HFpEF, its pathogenetic mechanisms have not been fully determined. At the same time, the basic characteristics, pathophysiology, and approaches to the treatment of patients with HFmrEF are being actively studied. The pathophysiology of cardiovascular diseases, including HF, in T2DM is multifactorial. T2DM is one of the most significant noncardiac diseases in which a proinflammatory and profibrotic state leads to the development of interstitial myocardial

fibrosis, increase in stiffness of myocardium, and a deterioration in elasticity. Also, insulin resistance promotes development of vascular stiffness and hypertension, dyslipidemia, and increased systemic inflammation. Elevated glucose levels lead to increased formation of advanced glycation end-products and accumulation of reactive oxygen species [3]. In combination with visceral obesity, T2DM with a high frequency causes diastolic dysfunction and HF [4]. Hyperglycemia inevitably deteriorates profibrotic processes associated with oxidative, hemodynamic, and metabolic stress in HF [3]. Diabetic cardiomyopathy is usually associated with arterial hypertension (AH) and ischemic heart disease (IHD), forming the so-called "mixed" clinical phenotype of HF, which may be present with both HFpEF and HFmrEF [5]. For specification of pathogenesis of different phenotypes of HF, research of different circulating biomarkers and their diagnostic and prognostic values seem perspective.

Much attention is paid to markers of myocardial stress, such as the N-terminal fragment of brain natriuretic peptide (Nt-proBNP) and markers of inflammation; the most available and studied from which is the highly sensitive C-reactive protein (hsCRP). However, markers associated with profibrotic processes are of particular interest too. Such markers include sST2 (stimulating factor growth expression gene 2, soluble form, also known as IL1RL1, and suppression of tumorigenicity 2), galectin-3, type I procollagen C-terminal propeptide (PICP) and type III procollagen N-terminal propeptide (PIIINP), matrix metalloproteinases (MMP), and their tissue inhibitors (TIMP) [6]. The role of each of these biomarkers is rather specific, and identification of their role in patients with T2DM is complicated by a row of factors. Firstly, T2DM usually occurs in patients with visceral obesity, which is characterized by chronic inflammation and oxidative stress. Thus, it is rather difficult to separate the effects of obesity on biomarker levels from the effects of T2DM itself. Secondly, most of the biomarkers circulating in the blood in HF can be influenced by various factors, including body mass index (BMI) and glycemic levels. Comparison of the serum biomarker levels in patients with similar BMI and similar glycemic control without HF and with HFpEF and HFmrEF will clarify these issues. It should be noted that the relationship between diabetes-related fibrosis and phenotype of HF has not been systematically studied. In addition, little has been studied about difference in patients with T2DM and HFpEF or HFmrEF. In this study, we evaluate fibrosis biomarkers in patients with T2DM and HFpEF or HFmrEF and compare their clinical characteristics and structural and functional parameters of myocardial remodeling.

2. Materials and Methods

All procedures were carried out in accordance with the Declaration of Helsinki. The Ethical Committee of the Almazov National Medical Research Centre approved the study (№020419). All patients provided written informed consent. Sixty-two patients with T2DM were included in the study: 20 patients without clinical signs and symptoms of HF (group 1) and 2 groups with clinical manifestations of stable HF: 29 patients with HFpEF (group 2) and 13 patients with HFmrEF (group 3). There was also a control group, which consisted of 13 healthy subjects comparable in age and sex with the studied cohorts, with normal BSA (22-25 kg/m^2) and heart function. The inclusion criteria in the study were age 40 to 75 years, T2DM, glycated hemoglobin (HbA1c) 7.0-11.0%, and stable hypoglycemic therapy for at least 12 weeks prior to study. In addition, for patients with HF, inclusion criteria were the presence of stable HF (II functional class (NYHA)), HFpEF or HFmrEF, and optimal drug therapy for HF for at least 3 months. The exclusion criteria were valvular heart disease, cardiomyopathy, rheumatological diseases, significant cardiovascular events, including acute myocardial infarction (MI) or major heart surgery, percutaneous coronary intervention (PCI), valvuloplasty within 12 months, and hospitalization due to decompensation of HF within 3 months prior to enrollment in the study; planned intervention on the coronary arteries, HFrEF, III-IV functional class (NYHA), and glomerular filtration rate (GFR) according to Chronic Kidney Disease Epidemiology Collaboration Formula (CKD − EPI) < 60 ml /min/1.73 m^2; obesity of the III degree; severe bronchial asthma or chronic obstructive pulmonary disease; and secondary arterial hypertension, blood pressure (BP) > 180 /110 mmHg, and severe liver disease. The diagnosis of HFpEF and HFmrEF was made according to the recommendations of the European Society of Cardiology 2016 [7]. Laboratory tests were performed, including HbA1c, lipids, and blood creatinine with calculation of GFR, ECG, and echocardiography (VIVID 9 GE, USA) according to a standard protocol by one blinded operator. The left ventricular myocardium mass (LVM) was additionally indexed to the height (in meters). Using height-based indexing (LVM/height in $m^{2.7}$) in individuals with BMI ≥30 kg/m^2 is preferred in order to avoid underestimation of the prevalence of LV hypertrophy in obese patient [8, 9]. LV hypertrophy was defined using gender-specific criteria with LVM corrected for BSA, height, and height raised to the allometric power of 2.7 according to ASE/EACVI-2015 recommendations on the use of echocardiography in adult hypertension [10]. Intraoperator variability for the assessment of volumetric echocardiographic parameters in our research centre was less than 4%. Longitudinal systolic myocardial deformation was assessed by 2D speckle tracking echocardiography. The automated functional imaging (AFI) software was used for the analysis. The maximum longitudinal strain (GLS) of left ventricle (LV) was calculated by averaging the peak systolic values of 18 segments obtained from 6 segments of three apical views (four-chamber, two-chamber, and long axis of LV). The panel of studied biomarkers included Nt-proBNP, hsCRP, sST2, galectin-3, PICP, PIIINP, MMP-9, and TIMP-1. The serum samples were frozen at -80°C until analysis. The serum hsCRP level was determined on an automatic biochemical analyzer "Cobas Integra 400+" by the immunoturbidimetric method. Serum Nt-proBNP concentration was assessed by electrochemiluminescence method using the Elecsys test system (Roche Diagnostic). Serum levels of galectin-3 (R&D system), MMP-9 and TIMP1 (R&D system), sST2 (Clinical diagnostics, Presage ST2 kit), and PICP and PIIINP (USCN Life Science) were assessed by enzyme immunoassay. Additionally, the ratios of

MMP-9/TIMP1 and PICP/PIIINP were calculated for each patient. Echocardiography and blood sampling for biomarkers were performed on the background of sinus rhythm in all patients.

2.1. Statistical Analysis. Statistical analysis was performed using the SPSS statistical software (version 21.0, IBM Corp, USA). Continuous variables were presented as medians with 25th to 75th interquartile ranges, and categorical variables were presented as percentages. Continuous variables were compared by Kruskal-Wallis tests followed by Mann–Whitney U test when appropriate. Correlations were analysed using Spearman's rank correlation tests. Categorical variables were compared by chi-squared test. Statistical significance was defined as p value < 0.05.

3. Results

Table 1 shows the main characteristics of the groups. The studied groups had comparable clinical and demographic characteristics. The median age in all groups was about 60 years; the proportion of men was more than 50%. AH was observed in all patients of the studied groups. The duration of AH and the level of office BP did not differ between the groups. Overweight or obesity was diagnosed in all patients. There were no significant differences in BMI and T2DM duration, low-density lipoproteins (LDL), and triglycerides (TG) levels between the groups. HbA1c concentrations in the group without HF, in the group with HFpEF, and in the group with HFmrEF were 8.3%, 8.5%, and 8.8%, respectively ($p > 0.05$). There were no significant gender differences, duration of HF and T2DM, the presence of concomitant diseases, and drug therapy in groups 2 and 3. More than 40% of patients between groups 2 and 3 underwent myocardial revascularization. The incidence of paroxysmal atrial fibrillation among patients with HF varied slightly (15-17%). An endocrinologist and a heart failure specialist consulted all patients with HF. Patients in groups 2 and 3 received the recommended therapy for HF: 77-90% angiotensin-converting enzyme inhibitors (ACEi) or angiotensin receptor antagonists (ARA), 77-90% beta-blockers, 55-61% mineralocorticoid receptor antagonists (MRA), and 100% diuretics. Combined antihyperglycemic therapy in all groups was represented by metformin, sulfonylureas, and/or dipeptidyl peptidase-4 inhibitors (DPP-4).

3.1. Echocardiographic Parameters. Echocardiography data are presented in Table 2. Patients with HFmrEF had significantly lower LV EF and lower values of GLS LV compared to patients with HFpEF and patients without HF (p 1.2 < 0.05). There was an increase in the left atrial volume index (LA volume index) in patients with HF. This increase was combined with grade 1 diastolic dysfunction in 30% of HF patients. In most cases, patients of all groups had concentric LV myocardial hypertrophy, characterized by an increase in the indexed values of LVM and relative wall thickness (RWT) of the LV. Patients with HFmrEF had significantly higher values of LV end-diastolic volume (EDV) and LV volume index compared to patients with HFpEF and patients without HF (all $p < 0.05$). The indexed parameters of LV MM increased in patients with HF, and their highest values were observed in patients with HFmrEF.

3.2. Molecular Biomarkers. Data on the concentrations of biomarkers are presented in Table 3. Lower (50% lower) threshold serum concentrations of Nt-proBNP were used in patients with clinical manifestations of HF, echocardiographic criteria, and BMI $> 30\,kg/m^2$, taking into account the high incidence of obesity in the study sample [8]. Higher Nt-proBNP concentrations were observed in the group of HFmrEF ($p < 0.05$). The sST-2 concentrations did not significantly differ between the investigated groups and the control group. The concentrations of galectin-3, PICP, PIIINP, and the PICP/PIIINP ratio were significantly higher in all investigated groups compared with the control group (all $p < 0.05$). The concentrations of galectin-3 were greater in patients with HFpEF and HFmrEF compared to patient without HF ($p = 0.01$ and $p = 0.03$, respectively). There was a negative correlation between galectin-3 and high-density lipoprotein (HDL) ($r = -0.542$; $p = 0.004$), which confirmed the participation of this biomarker in the process of atherogenesis. Higher PICP concentrations and the PICP/PIIINP ratio were observed in the group of HFmrEF and in the group without HF compared to the control group. PICP and PICP/PIIINP ratio were greater in patients with HFmrEF compared to patients with HFpEF ($p = 0.043$ and $p = 0.033$, respectively). There was a decrease in the serum concentration of MMP-9 in the groups with HF compared to the control group, although did not quite achieve the threshold for statistical significance. At the same time, the TIMP-1 levels between the studied groups did not significantly differ. The MMP-9/TIMP-1 ratio was significantly lower in all investigated groups compared to the control group (all $p < 0.05$). Furthermore, the decrease in the MMP-9/TIMP-1 ratio was more pronounced in patients with HF. There were no differences in the concentrations of hsCRP, galectin-3, PIIINP, MMP-9, TIMP-1, and the MMP-9/TIMP-1 ratio between patients with HFpEF and HFmrEF. There were no correlations between circulating biomarkers and gender, age, HbA1c, BMI, and drug therapy. There were positive associations between Nt-proBNP concentrations and LA volume index ($r = 0.44$; $p = 0.003$), galectin-3, and values of left ventricular myocardial mass/body surface area (LVM/BSA) ($r = -0.58$, $p = 0.001$), PIIINP and LV EDV ($r = 0.38$; $p = 0.02$), and negative association between TIMP-1 concentrations and LV EDV ($r = -0.68$; $p = 0.042$) in groups with HF.

4. Discussion

The list of potential mechanisms contributing to the development of HF in T2DM patients continues to expand each decade. The main processes include oxidative stress, inflammation, impaired sensitivity to insulin, metabolic abnormalities, such as calcium exchange in the myocardium, dysfunction of mitochondria and endothelium, neurohumoral activation, and death of cardiomyocytes. It is not the full list of the difficult processes mediated by hyperglycemia, leading to hypertrophy, excess diffuse extracellular matrix formation,

Table 1: Demographic and clinical characteristics of the patients.

Parameters	Group 1 without HF ($n = 20$) Me (25, 75)	Group 2 HFpEF ($n = 29$) Me (25, 75)	Group 3 HFmrEF ($n = 13$) Me (25, 75)	p for groups 1, 2, and 3
Age, years	57 (52, 60)	61 (57, 66)	59 (54, 62)	0.44
Gender, male, n (%)	13 (65)	15 (51.7)	7 (53.9)	0.74
Duration of CHF, years	—	9 (6, 13)	8 (5, 11)	0.68
CAD, n (%)	—	20 (68.9)	11 (84.6)	0.71
MI, n (%)	—	15 (51.7)	7 (63.6)	0.85
CABG/PCI, n (%)	—	14 (48.2)	7 (63.6)	0.22
Stable angina II, n (%)	—	11 (37.9)	6 (46.1)	0.62
Duration of hypertension, years	14 (9, 18)	18 (13, 22)	16 (11; 19)	0.19
SBP, mmHg	130 (115, 140)	140 (110, 155)	130 (110, 145)	0.76
DBP, mmHg	85 (75, 90)	80 (65, 90)	75 (60, 85)	0.62
Heart rate, b/min	77 (68, 90)	70 (62, 78)	68 (63, 74)	0.29
Atrial fibrillation, paroxysmal form, n (%)	—	5 (17.2)	2 (15,3)	0.31
Duration of diabetes, years	10 (6, 13)	12 (9, 16)	13 (5, 17)	0.14
BMI, kg/m^2	32.8 (30.2, 34.9)	32.3 (28.7, 36.8)	34.7 (31.7, 37.8)	0.38
Overweight, n (%)	3 (15)	7 (24.1)	2 (15.4)	0.67
Obesity I degree, n (%)	12 (60)	17 (58.6)	7 (53.8)	0.9
Obesity II degree, n (%)	5 (25)	5 (17.3)	4 (30.8)	0.59
Smoking, n (%)	10 (50)	13 (44.8)	6 (46.1)	0.76
Hemoglobin, g/l	144 (128, 157)	140 (125, 159)	138 (120, 151)	0.53
HbA_{1c}, %	8.3 (7.7, 9.3)	8.5 (7.9, 9.7)	8.8 (8.4, 9.9)	0.49
GFR, ml/min/1.73 m2,	98 (82, 109)	93 (74, 105)	86 (68, 96)	0.52
LDL, mmol/l	2.7 (2.0, 3.7)	2.1 (1.3, 3.3)	1.9 (1.1, 2.8)	0.65
HDL, mmol/l	1.15 (0.87, 1.28)	1.12 (0.91, 1.35)	0.96 (0.82, 1.33)	0.63
Triglycerides, mmol/l	2.4 (1.8, 3.2)	2.2 (1.7, 2.9)	2.6 (2.1, 3.3)	0.19
ACEi/ARA, n (%)	16 (80)	26 (89.6)	10 (76.9)	0.26
Beta-blockers, n (%)	—	22 (75.8)	11 (84.6)	0.56
MRA, n (%)	—	16 (55.1)	8 (61.5)	0.46
Loop diuretics, n (%)	—	19 (65.5)	10 (76.9)	0.28
Thiazide/thiazide-like diuretics, n (%)	6 (30)	13 (34.5)	5 (23.1)	0.57
Statins (%)	14 (70)	20 (68.9)	10 (76.9)	0.86
Therapy for DM				
Metformin	19 (95)	29 (100)	13 (100)	—
DPPi-4	14 (70)	18 (62.1)	8 (61.5)	0.82
Sulfonylurea	6 (30)	11 (37.9)	5 (38.5)	

CHF: chronic heart failure; CAD: coronary artery disease; MI: myocardial infarction; CABG: coronary artery bypass grafting; PCI: percutaneous coronary intervention; SBP: systolic blood pressure; DBP: diastolic blood pressure; BMI: body mass index; GFR: glomerular filtration rate; ACEi: angiotensin-converting-enzyme inhibitors; ARA: angiotensin receptor antagonists; MRA: mineralocorticoid receptor antagonists; DPPi-4: dipeptidil peptidase-4 inhibitors.

and cardiac steatosis. Cardiac remodeling and impaired microvascular coronary perfusion contribute to the development of diastolic dysfunction [3, 4, 11, 12]. High glucose level stimulates fibroblast proliferation and activates transcription and secretion of extracellular matrix proteins. Hyperglycemia also contributes to increased activity of local renin-angiotensin-aldosterone system (RAAS) in the heart. This increased activity may promote profibrotic processes due to increase in the TGF-β expression and reactive oxygen species formation [13].

Most patients with T2DM and HF have comorbidities such as obesity, AH, and accelerated atherosclerosis, which determining the complex clinical phenotype of HF, mainly with LV EF > 40%. The presented study included patients with T2DM, HF with midrange, and preserved LV EF, who have additional cardiometabolic risk factors for HF (increased BMI and AH), and in more than half of the cases, the presence of IHD. It is well known that insulin resistance, metabolic syndrome, and T2DM are associated with an increase in

Table 2: Echocardiographic parameters of patients, Me (25, 75).

Parameters	Group 1 without HF ($n = 20$) Me [25; 75]	Group 2 HFpEF ($n = 29$) Me (25, 75)	Group 3 HFmrEF ($n = 13$) Me (25, 75)	p value (1 vs. 2 vs. 3)	(1 vs. 2)	(1 vs. 3)	(2 vs. 3)
EF (Simpson), %	61 (59, 65)	61 (57, 62)	46 (41, 48)	<0.001	0.12	<0.001	<0.001
LA dimension, mm	43 (40, 47)	41 (38, 47)	44 (40, 50)	0.29	0.34	0.22	0.21
LA volume index, ml/m^2	33.5 (30.0, 38.7)	42.0 (37.1, 46.4)	48.3 (38.0, 59.0)	<0.001	0.003	<0.001	0.23
E/e'avg	7 (8, 9)	11 (9, 13)	11 (9, 14)	0.006	0.009	0.005	0.4
PAP, mmHg	26 (19, 30)	24 (18-29)	26 (20-31)	0.57	0.37	0.61	0.18
LV dimension, mm	49 (46, 53)	47 (45, 51)	50 (46, 52)	0.4	0.49	0.43	0.13
EDV, ml	111 (94.7, 126.7)	117 (102, 135)	167 (125, 220)	0.025	0.21	0.005	0.007
LV volume index, ml/m^2	50 (45, 63)	59 (49, 68)	66 (59, 74)	0.08	0.13	0.03	0.037
ESV, ml	46 (34, 53)	45 (39, 61)	89 (61, 134)	0.007	0.35	0.001	0.002
IVS, mm	10 (9, 11)	11 (10, 13)	11.5 (11, 13)	0.24	0.56	0.39	0.85
PW, mm	11 (10, 12)	11 (10, 13)	11 (9, 12)	0.51	0.43	0.53	0.41
RWT	0.44 (0.41, 0.46)	0.53 (0.49, 0.57)	0.52 (0.5, 0.55)	0.009	0.007	0.01	0.77
LVMM, g	197 (177, 244)	252 (207, 335)	271 (228, 401)	0.01	0.07	0.034	0.28
LVM/BSA, g/m^2	105 (91, 119)	118 (94, 142)	155 (97, 196)	0.023	0.27	0.02	0.17
LVM/height, g/m	116 (109, 131)	177 (156.0, 192.8)	205.7 (160.1, 220.6)	0.002	0.02	0.001	0.043
LVM/height, g/m$^{2.7}$	49 (42, 56)	52.5 (46.6, 75.1)	69.2 (52.6, 89.3)	0.04	0.15	0.01	0.08
GLS avg, %	-19 (-17, -20)	-19(-17, -20)	-16.5(-14, -19.0)	0.016	0.91	0.041	0.041

EF: ejection fraction; LV: left ventricle; ESV: end-systolic volume of the left ventricle; EDV: end-diastolic volume of the left ventricle; LVM: left ventricular myocardial mass; LA: left atrium; IVS: interventricular septum; PW: posterior wall of left ventricle; RWT: relative wall thickness of the left ventricle; BSA: body surface area.

myocardial mass and LV RWT [10] and predispose to the development of concentric LV hypertrophy. Therefore, we included patients with similar BMI and glycemic control. In our study, patients with T2DM and HFmrEF were characterized by increased values of EDV, indexed parameters of LVM, and higher values of Nt-proBNP compared with patients with HFpEF. This observation is consistent with the data of other authors, who conducted a comparative study of echocardiographic parameters in patients with HFpEF and HFmrEF [14]. Similar patterns of echocardiographic changes and Nt-proBNP concentrations were presented in other earlier studies; some authors consider HFmrEF as the initial stage of HFrEF [15]. An increase in LA size is an indicator of a long-term raising in LV filling pressure, and LA volume and function are predictors of an increase in brain natriuretic peptides in patients with HF [14, 16]. We did not find any correlations between the parameters of diastolic dysfunction and the level of Nt-proBNP; however, a strong positive association with the marker of myocardial stress and the LA volume index confirms the association of the LA parameters with neurohormonal activation of the heart in T2DM patients with HFmrEF or HFpEF. Various aspects associated with Nt-proBNP from diagnostics to B-type natriuretic peptide-guided therapy in different populations of patients with HF are actively studied [17–20].

Comparative studies of molecular biomarkers show that patients with HFmrEF have an intermediate biomarker profile associated with myocardial stress, inflammation, and fibrosis [21–23]. Despite the high incidence of T2DM in patients with HFpEF and HFmrEF in these studies, the data on the effect of glycemic status on the molecular biomarkers in these patients are lacking. In our study, we analyzed the wide range of biomarkers in patients with T2DM, multiple cardiometabolic risk factors, and stable HF with LV EF > 40%.

sST2 is a member of the interleukin-1 receptor family and a marker of inflammation and myocardial stress. An increase in the concentrations of sST2 is observed in various cardiovascular diseases, visceral obesity, and T2DM [24]. The significantly lower variability for sST2 in comparison with Nt-proBNP makes it promising for assessing the prognosis of the survival of patients with HF. sST2 is considered as a new marker of cardiovascular events and adverse clinical outcomes, primarily associated with HF and IHD [19]. In our study, serum sST2 in the group with HFpEF did not differ from group with HFmrEF, which is consistent with Song et al. [25]. The lack of differences in serum sST2 concentrations between the control group and study groups can be explained by both the inclusion of patients with mild HF, receiving optimal drug therapy for HF, and the probably low sensitivity of this marker in patients with visceral obesity and T2DM. Despite the prognostic value of sST2 in patients with HFmrEF, its predictive value in patients with concomitant T2DM is doubtful [22–25].

Galectin-3 is a mediator of cell adhesion, inflammation, and extracellular matrix formation both in the myocardium and in the vascular wall [6, 26]. In the studied cohort of patients with T2DM, irrespective of the existence of HF, the increase of galectin-3 was revealed compared to the control group. This observation confirms the intensity of inflammation and fibrosis in patients with T2DM and additional multiple etiological factors of HF, such as AH and obesity, even at the preclinical stage of HF. According to our data, higher

Table 3: Circulating biomarkers in patients and in the control group.

Parameters	Control group ($n = 13$) Me (25, 75)	Group 1 without HF ($n = 20$) Me (25, 75)	Group 2 HFpEF ($n = 29$) Me (25, 75)	Group 3 HFmrEF ($n = 13$) Me (25, 75)	p for gr. 1, 2, and 3	p for gr. 1 vs. 2	p for gr. 1 vs. 3	p for gr. 2 vs. 3
Nt-proBNP pg/ml	—	52.4 (14.5, 104.3)	133.6 (78.5, 198.5)	162.5 (134.6, 216.7)	0.005	0.005	0.003	0.03
sST-2, ng/ml	18.3 (15.6, 21.2)	19.2 (16.2, 26.3)	19.9 (12.9, 40.7)	19.6 (13.8, 37.1)	0.97	0.89	0.77	0.28
Galectin-3, ng/ml	5.7^{+} (4.9, 6.3)	8.6 (7.2, 10.8)	11.7 (8.1, 13.4)	10.4 (7.9, 14.0)	0.03	0.01	0.03	0.84
PICP, ng/ml	15.0^{+} (10.0, 34.0)	127.4 (113.3, 170.2)	46.8 (22.6, 98.6)	106.4 (85.4, 140.4)	0.005	0.006	0.09	0.043
PIIINP, ng/ml	1.27^{+} (0.67, 3.18)	3.38 (2.85, 3.61)	3.29 (1.96, 4.59)	3.46 (2.24, 4.97)	0.58	0.68	0.49	0.38
PICP/PIIINP	7.4^{+} (3.7, 8.4)	35.3 (30.1, 44.4)	18.4 (14.6, 25.3)	31.5 (25.8, 40.1)	0.07	0.017	0.35	0.033
MMP-9, ng/ml	540.0 (363.0, 669.0)	412.5 (289.5, 687.7)	277.0# (98.5, 403.5)	257.0 # (152.0, 483.5)	0.12	0.26	0.11	0.51
TIMP-1, ng/ml	149.0 (133.0, 170.0)	208 (172, 241)	178.5 (119.5, 210.7)	154 (114.7, 203.5)	0.16	0.21	0.05	0.81
MMP-9/TIMP-1	3.6^{+} (2.3, 5.2)	1.6 (1.2, 2.8)	1.1 (0.6, 3.6)	0.8 (0.42, 3.1)	0.31	0.44	0.39	0.5
hsCRP, mg/l	—	2.1 (0.8, 4.9)	2.5 (1.7, 5.9)	3.3 (2.0, 7.3)	0.41	0.29	0.31	0.61

$^{+}p < 0.05$ (between control group and investigated groups); #$p < 0.03$ (between control group and groups 2 and 3).

serum concentrations of this biomarker and a positive association with LVM in patients with HF confirm the role of galectin-3 in the pathogenesis of HF. However, we did not identify significant differences in galectin-3 concentrations between group with HFpEF and group with HFmrEF. Our data is consistent with another study of patients with HFmrEF and HFpEF; one-third of whom had T2DM and more severe HF [21]. An increase in serum galectin-3 is considered an adaptive response to inflammation and impaired glucose metabolism. However, the data on the predictive value of galectin-3 in relation to other traditional biomarkers in T2DM patients with HF remain ambiguous [24, 27, 28].

According to histological studies, interstitial and perivascular fibrosis in T2DM is associated with an increase in type I collagen and type III collagen, regardless of coronary atherosclerosis and AH [29, 30]. In addition to reactive fibrosis, magnetic resonance imaging often visualizes areas of fibrosis due to asymptomatic coronary events in T2DM patients without MI [31]. These changes contribute to the further remodeling of the myocardium and the progression of HF. The predominant type of the collagen in the extracellular matrix determines by etiological factor of HF. In addition, quantitative and qualitative changes of fibrotic processes are dynamic, presenting different phenotypes of interstitial fibrosis over time, including chronic hyperglycemia [32]. An association between diabetes and an increase in the collagen composition were observed only in patients with HFrEF, according to results of endomyocardial biopsies in patients with T2DM complicated by HFpEF and HFrEF (LV EF < 45%) in the absence of coronary atherosclerosis [29, 33]. Relevant circulating markers of fibrosis include PICP and PIIINP as biomarkers of types I and III collagen formation, respectively [34]. In a number of studies of patients with HF, endomyocardial biopsies have been shown a correlation between the serum PICP concentrations and the total collagen volume in patient with AH, as well as between the PIIINP concentration and the volume of type III collagen in patients with more significant myocardial remodeling in IHD and dilated cardiomyopathy [35–38]. However, there are some controversial issues with these circulating biomarkers in patients with HF [34]. It should be taken into account that in vitro secretion of PICP and PIIINP by fibroblasts is influenced by level of glycemia, AH, and obesity, which complicates their evaluation in patients with T2DM and HF [39–41]. There is a negative association of PIIINP with parameters of subclinical diastolic dysfunction in patients with T2DM in one study [42], while other authors showed a similar association in relation to PICP [43]. There are currently few studies of the described serum markers in HFmrEF, mainly in the meta-analysis of randomized clinical trials in patients with LV EF > 40% [44]. In our study, we identified an increase in the concentrations of PICP and PIIINP in patients with T2DM, regardless of the presence of HF. The PICP levels and the PICIP/PIIINP ratio were significantly higher in the group with HFmrEF compared with the group with HFpEF. PICP/PIIINP ratio was shifted towards the marker of harder collagen in patients with HFmrEF compared to healthy individuals and patients with HFpEF. Furthermore, PIIINP concentration was associated with an increase in LV EDV in all patients with T2DM and HF. The obtained data confirm that a delicate balance between the synthesis and degradation of two types of collagen can determine the structural and functional changes in the myocardium in HF patients with impaired glycemic status. Similar patterns of changes in PICP and PIIINP were observed in the group without HF, which confirms the difficulties discussed above in interpreting the changes of circulating procollagen markers in patients with multiple cardiometabolic risk factors and other possible factors affecting the serum concentrations of these biomarkers. Taking into account the ambiguous data on the diagnostic significance of PICP and PIIINP depending on the etiology of HF, concomitant diseases affecting collagen metabolism, the obtained results of our research require further investigation [34].

Matrix metalloproteinases and their inhibitors play an important role in the exchange of the extracellular matrix, determining the collagen degradation processes. It has been shown that changes in the level of MMP-9, as well as TIMP-1, associated with nonspecific inflammation, and the balance between MMP-9 and TIMP-1 depend on the etiological cause and stage of the cardiovascular disease continuum [26, 34, 45]. Despite numerous evidences of an imbalance in the MMP-9 in T2DM, information about changes in the MMP-9 and TIMP-1 system is contradictory. As in the study by Lewandowski et al., we recorded a decrease in the serum concentration of MMP-9 in patients with T2DM compared with the control group, without reaching the threshold of significance [45]. Low levels of MMP-9 in the studied cohort of patients can be promoted by the drug effects of inhibitors of the renin-angiotensin-aldosterone system, statins, or antihyperglycemic therapy [46–48]. Interestingly, the level of MMP-9 decreased to the greater extent in patients with HF, although not significantly. At the same time, MMP-9/TIMP-1 ratio significantly decreased in all groups of patients compared to the control group, especially in patients with more severe structural and functional heart remodeling. It can indicate the predominance of fibrotic processes in this group of patients. Negative association of TIMP-1 and LV EDV in patients with HF in our study confirms this assumption. The role of matrix metalloproteinases and their tissue inhibitors in the pathophysiology and prognosis in different HF phenotypes is not fully defined and continues to be studied. However, the MMP-9 expression is determined by the nature of the pathological process and the stage of HF [45].

5. Conclusion

There is a dynamic balance between the serum concentrations of biomarkers reflecting pro- and antifibrotic processes in patients with T2DM having additional risk factors of HF without and with clinical manifestations of HF in real clinical practice. The dynamics and direction of changes at various stages of the cardiovascular disease continuum in the serum fibrosis markers, MMP-9 and TIMP-1 systems, may reflect an increase in fibrotic and decrease in antifibrotic processes

already at the preclinical stage of HF. At the same time, the changes found in the PICP and PIIINP system may indicate a shift in balance towards type I collagen synthesis in HFmrEF compared with HFpEF.

Further prospective studies on large samples using a multibiomarker panel, methods of multivariate statistics in patients with T2DM, and various HF phenotypes are needed.

6. Research Limitations

Our study has several limitations. A small sample size as well as the presence of possible confounding factors, including obesity phenotype and other factors not considered in the study, can influence the concentrations of the studied biomarkers of fibrosis. MMP-9 and TIMP-1 were measured in the serum, which can overestimate the concentrations of these biomarkers compared with the levels in plasma samples [43]. The protocol did not include patients with severe HF (III-IV functional class NYHA) and with HFrEF; however, it may be of scientific interest for a more complete understanding of the clinical phenotype of HFmrEF in patients with T2DM.

Data Availability

Research data can be available after contact by e-mail doctorlebedev11@gmail.com with corresponding author.

Conflicts of Interest

The authors declare that they have no conflicts of interest.

Authors' Contributions

We confirm that all the authors participated in the preparation of the manuscript.

Acknowledgments

This research was conducted with the support of the Russian Scientific Fund (grant number 17-7530052).

References

[1] F. Cosentino, P. J. Grant, V. Aboyans et al., "2019 ESC Guidelines on diabetes, pre-diabetes, and cardiovascular diseases developed in collaboration with the EASD," *European Heart Journal*, vol. 41, no. 2, pp. 255–323, 2020.

[2] I. Johansson, U. Dahlström, M. Edner, P. Näsman, L. Rydén, and A. Norhammar, "Type 2 diabetes and heart failure: characteristics and prognosis in preserved, mid-range and reduced ventricular function," *Diabetes & Vascular Disease Research*, vol. 15, no. 6, pp. 494–503, 2018.

[3] T. Miki, S. Yuda, H. Kouzu, and T. Miura, "Diabetic cardiomyopathy: pathophysiology and clinical features," *Heart Failure Reviews*, vol. 18, no. 2, pp. 149–166, 2013.

[4] W. J. Paulus and C. Tschöpe, "A novel paradigm for heart failure with preserved ejection fraction: comorbidities drive myocardial dysfunction and remodeling through coronary microvascular endothelial inflammation," *Journal of the American College of Cardiology*, vol. 62, no. 4, pp. 263–271, 2013.

[5] F. T. Ageev and A. G. Ovchinnikov, "Heart failure with mid-range ejection fraction: are there clinical reasons in introduction of this new group as a distinct entity?," *Kardiologiia*, vol. 58, no. 12S, pp. 4–10, 2018.

[6] M. Sarhene, Y. Wang, J. Wei et al., "Biomarkers in heart failure: the past, current and future," *Heart Failure Reviews*, vol. 24, no. 6, pp. 867–903, 2019.

[7] P. Ponikowski, A. A. Voors, S. D. Anker et al., "2016 ESC Guidelines for the diagnosis and treatment of acute and chronic heart failure: the task force for the diagnosis and treatment of acute and chronic heart failure of the European Society of Cardiology (ESC). Developed with the special contribution of the Heart Failure Association (HFA) of the ESC," *European Heart Journal*, vol. 37, no. 27, pp. 2129–2200, 2016.

[8] B. Williams, G. Mancia, W. Spiering et al., "2018 ESC/ESH Guidelines for the management of arterial hypertension," *European Heart Journal*, vol. 39, no. 33, pp. 3021–3104, 2018.

[9] M. Singh, A. Sethi, A. K. Mishra, N. K. Subrayappa, D. D. Stapleton, and P. A. Pellikka, "Echocardiographic imaging challenges in obesity: guideline recommendations and limitations of adjusting to body size," *Journal of the American Heart Association*, vol. 9, no. 2, p. e014609, 2020.

[10] T. H. Marwick, T. C. Gillebert, G. Aurigemma et al., "Recommendations on the use of echocardiography in adult hypertension: a report from the European Association of Cardiovascular Imaging (EACVI) and the American Society of Echocardiography (ASE)," *Journal of the American Society of Echocardiography*, vol. 28, no. 7, pp. 727–754, 2015.

[11] H. C. Kenny and E. D. Abel, "Heart failure in type 2 diabetes mellitus," *Circulation Research*, vol. 124, no. 1, pp. 121–141, 2019.

[12] J. M. McGavock, I. Lingvay, I. Zib et al., "Cardiac steatosis in diabetes mellitus: a 1H-magnetic resonance spectroscopy study," *Circulation*, vol. 116, no. 10, pp. 1170–1175, 2007.

[13] G. Jia, M. A. Hill, and J. R. Sowers, "Diabetic Cardiomyopathy: An Update of Mechanisms Contributing to This Clinical Entity," *Circulation Research*, vol. 122, no. 4, pp. 624–638, 2018.

[14] L. al Saikhan, A. D. Hughes, W. S. Chung, M. Alsharqi, and P. Nihoyannopoulos, "Left atrial function in heart failure with mid-range ejection fraction differs from that of heart failure with preserved ejection fraction: a 2D speckle-tracking echocardiographic study," *European Heart Journal Cardiovascular Imaging*, vol. 20, no. 3, pp. 279–290, 2019.

[15] C. S. P. Lam and S. D. Solomon, "The middle child in heart failure: heart failure with mid-range ejection fraction (40-50%)," *European Journal of Heart Failure Supplements*, vol. 16, no. 10, pp. 1049–1055, 2014.

[16] M. Baba, K. Yoshida, and M. Ieda, "Clinical applications of natriuretic peptides in heart failure and atrial fibrillation," *International Journal of Molecular Sciences*, vol. 20, no. 11, p. 2824, 2019.

[17] G. Gallo, F. Bianchi, M. Cotugno, M. Volpe, and S. Rubattu, "Natriuretic peptides, cognitive impairment and dementia: an intriguing pathogenic link with implications in hypertension," *Journal of Clinical Medicine*, vol. 9, no. 7, p. 2265, 2020.

[18] D. Hakuno, T. Fukae, M. Takahashi et al., "Combinations of cardiac and non-cardiac predictors for prognoses in patients with acute heart failure," *European Heart Journal - Quality of Care and Clinical Outcomes*, vol. qcz059, pp. 1–14, 2019.

[19] K. Ejiri, T. Miyoshi, H. Kihara et al., "Effect of luseogliflozin on heart failure with preserved ejection fraction in patients with

diabetes mellitus," *Journal of the American Heart Association*, vol. 9, no. 16, article e015103, 2020.

[20] M. Pufulete, R. Maishman, L. Dabner et al., "B-type natriuretic peptide-guided therapy for heart failure (HF): a systematic review and meta-analysis of individual participant data (IPD) and aggregate data," *Systematic Reviews*, vol. 7, no. 1, p. 112, 2018.

[21] P. Moliner, J. Lupón, J. Barallat et al., "Bio-profiling and bio-prognostication of chronic heart failure with mid-range ejection fraction," *International Journal of Cardiology*, vol. 257, pp. 188–192, 2018.

[22] J. Tromp, M. A. F. Khan, R. J. Mentz et al., "Biomarker profiles of acute heart failure patients with a mid-range ejection fraction," *JACC: Heart Failure*, vol. 5, no. 7, pp. 507–517, 2017.

[23] O. Chioncel, M. Lainscak, P. M. Seferovic et al., "Epidemiology and one-year outcomes in patients with chronic heart failure and preserved, mid-range and reduced ejection fraction: an analysis of the ESC Heart Failure Long-Term Registry," *European Journal of Heart Failure Supplements*, vol. 19, no. 12, pp. 1574–1585, 2017.

[24] A. E. Berezin, "Prognostication of clinical outcomes in diabetes mellitus: emerging role of cardiac biomarkers," *Diabetes and Metabolic Syndrome: Clinical Research and Reviews*, vol. 13, no. 2, pp. 995–1003, 2019.

[25] Y. Song, F. Li, Y. Xu et al., "Prognostic value of sST2 in patients with heart failure with reduced, mid-range and preserved ejection fraction," *International Journal of Cardiology*, vol. 304, pp. 95–100, 2020.

[26] N. Ibrahim and J. Januzzi, "Established and emerging roles of biomarkers in heart failure," *Circulation Research*, vol. 123, no. 5, pp. 614–629, 2018.

[27] R. A. de Boer, D. J. van Veldhuisen, R. T. Gansevoort et al., "The fibrosis marker galectin-3 and outcome in the general population," *Journal of Internal Medicine*, vol. 272, no. 1, pp. 55–64, 2012.

[28] N. Alonso, J. Lupón, J. Barallat et al., "Impact of diabetes on the predictive value of heart failure biomarkers," *Cardiovascular Diabetology*, vol. 15, no. 1, p. 151, 2016.

[29] I. Russo and N. G. Frangogiannis, "Diabetes-associated cardiac fibrosis: cellular effectors, molecular mechanisms and therapeutic opportunities," *Journal of Molecular and Cellular Cardiology*, vol. 90, pp. 84–93, 2016.

[30] T. J. Regan, M. M. Lyons, S. S. Ahmed et al., "Evidence for cardiomyopathy in familial diabetes mellitus," *The Journal of Clinical Investigation*, vol. 60, no. 4, pp. 885–899, 1977.

[31] R. Y. Kwong, H. Sattar, H. Wu et al., "Incidence and prognostic implication of unrecognized myocardial scar characterized by cardiac magnetic resonance in diabetic patients without clinical evidence of myocardial infarction," *Circulation*, vol. 118, no. 10, pp. 1011–1020, 2008.

[32] A. González, E. B. Schelbert, J. Díez, and J. Butler, "Myocardial interstitial fibrosis in heart failure: biological and translational perspectives," *Journal of the American College of Cardiology*, vol. 71, no. 15, pp. 1696–1706, 2018.

[33] L. van Heerebeek, N. Hamdani, M. L. Handoko et al., "Diastolic stiffness of the failing diabetic heart: importance of fibrosis, advanced glycation end products, and myocyte resting tension," *Circulation*, vol. 117, no. 1, pp. 43–51, 2008.

[34] B. López, A. González, S. Ravassa et al., "Circulating biomarkers of myocardial fibrosis," *Journal of the American College of Cardiology*, vol. 65, no. 22, pp. 2449–2456, 2015.

[35] B. López, R. Querejeta, A. González, M. Larman, and J. Díez, "Collagen cross-linking but not collagen amount associates with elevated filling pressures in hypertensive patients with stage C heart failure: potential role of lysyl oxidase," *Hypertension*, vol. 60, no. 3, pp. 677–683, 2012.

[36] R. Querejeta, B. López, A. González et al., "Increased collagen type I synthesis in patients with heart failure of hypertensive origin: relation to myocardial fibrosis," *Circulation*, vol. 110, no. 10, pp. 1263–1268, 2004.

[37] B. López, R. Querejeta, A. González, E. Sánchez, M. Larman, and J. Díez, "Effects of loop diuretics on myocardial fibrosis and collagen type I turnover in chronic heart failure," *Journal of the American College of Cardiology*, vol. 43, no. 11, pp. 2028–2035, 2004.

[38] G. Klappacher, P. Franzen, D. Haab et al., "Measuring extracellular matrix turnover in the serum of patients with idiopathic or ischemic dilated cardiomyopathy and impact on diagnosis and prognosis," *The American Journal of Cardiology*, vol. 75, no. 14, pp. 913–918, 1995.

[39] S. P. Levick and A. Widiapradja, "The diabetic cardiac fibroblast: mechanisms underlying phenotype and function," *International Journal of Molecular Sciences*, vol. 21, no. 3, p. 970, 2020.

[40] Y. Benazzoug, C. Borchiellini, J. Labat-Robert, L. Robert, and P. Kern, "Effect of high-glucose concentrations on the expression of collagens and fibronectin by fibroblasts in culture," *Experimental Gerontology*, vol. 33, no. 5, pp. 445–455, 1998.

[41] W. Kosmala, M. Przewlocka-Kosmala, H. Szczepanik-Osadnik, A. Mysiak, and T. H. Marwick, "Fibrosis and cardiac function in obesity: a randomised controlled trial of aldosterone blockade," *Heart*, vol. 99, no. 5, pp. 320–326, 2013.

[42] C. Jellis, J. Wright, D. Kennedy et al., "Association of imaging markers of myocardial fibrosis with metabolic and functional disturbances in early diabetic cardiomyopathy," *Circulation. Cardiovascular Imaging*, vol. 4, no. 6, pp. 693–702, 2011.

[43] S. H. Ihm, H. J. Youn, D. I. Shin et al., "Serum carboxy-terminal propeptide of type I procollagen (PIP) is a marker of diastolic dysfunction in patients with early type 2 diabetes mellitus," *International Journal of Cardiology*, vol. 122, no. 3, pp. e36–e38, 2007.

[44] Y. Xiang, W. Shi, Z. Li et al., "Efficacy and safety of spironolactone in the heart failure with mid-range ejection fraction and heart failure with preserved ejection fraction: a meta-analysis of randomized clinical trials," *Medicine (Baltimore)*, vol. 98, no. 13, article e14967, 2019.

[45] T. Morishita, H. Uzui, Y. Mitsuke et al., "Association between matrix metalloproteinase-9 and worsening heart failure events in patients with chronic heart failure," *ESC Heart Failure*, vol. 4, no. 3, pp. 321–330, 2017.

[46] K. C. Lewandowski, E. Banach, M. Bieńkiewicz, and A. Lewiński, "Matrix metalloproteinases in type 2 diabetes and non-diabetic controls: effects of short-term and chronic hyperglycaemia," *Archives of Medical Science*, vol. 2, no. 2, pp. 294–303, 2011.

[47] W. D. Li, N. P. Li, D. D. Song, J. J. Rong, A. M. Qian, and X. Q. Li, "Metformin inhibits endothelial progenitor cell migration by decreasing matrix metalloproteinases, MMP-2 and MMP-9, via the AMPK/mTOR/autophagy pathway," *International Journal of Molecular Medicine*, vol. 39, no. 5, pp. 1262–1268, 2017.

[48] C. S. Ceron and M. R. Luizon, "Plasma matrix metalloproteinases in coronary artery disease patients," *European Journal of Clinical Investigation*, vol. 46, no. 1, pp. 104-105, 2016.

Hindawi
Journal of Diabetes Research
Volume 2020, Article ID 5316769, 8 pages
https://doi.org/10.1155/2020/5316769

Research Article

Combination of Composite Autonomic Symptom Score 31 and Heart Rate Variability for Diagnosis of Cardiovascular Autonomic Neuropathy in People with Type 2 Diabetes

Zhiyin Zhang,[1,2] Yujin Ma,[1,2] Liujun Fu,[1,2] Liping Li,[1,2] Jie Liu,[1,2] Huifang Peng,[1,2] and Hongwei Jiang[1,2]

[1]*Department of Endocrinology and Metabolism, The First Affiliated Hospital, and College of Clinical Medicine of Henan University of Science and Technology, Luoyang, China*
[2]*Clinical Medicine Research Center of Endocrine and Metabolic Diseases of Luoyang, Luoyang, China*

Correspondence should be addressed to Hongwei Jiang; jianghw@haust.edu.cn

Received 13 May 2020; Accepted 29 July 2020; Published 31 October 2020

Guest Editor: Celestino Sardu

Objective. Cardiovascular autonomic neuropathy (CAN) is a common but severe problem of diabetes, which a timely diagnosis may have important clinical implications. This study was carried out to investigate the diagnostic performance of Composite Autonomic Symptom Score 31 (COMPASS 31) combined with heart rate variability (HRV) for cardiovascular autonomic neuropathy in type 2 diabetes. *Methods*. A total of 103 hospitalized subjects with type 2 diabetes were recruited in the study. All cases received clinical data collection, laboratory examination, and related complication examinations. Cardiovascular autonomic function was assessed using CARTs, COMPASS 31, and HRV analyses. A score of at least 2 based on CARTs was defined as CAN. *Results*. Of the 103 subjects with type 2 diabetes, 41.8% were diagnosed with confirmed CAN. Participants with CAN had considerably higher COMPASS 31 scores. The CAN group showed a significant decrease in all HRV indices. COMPASS 31 scores and HRV indices were closely correlated with CARTs ($P < 0.05$). Receiver operating characteristics (ROC) curve results showed that COMPASS 31 score identified CAN with an AUC value of 0.816, while the AUC values of HRV indices were 0.648 to 0.919, among which SDNN and LF had the best diagnostic value, with the AUC values of 0.919 and 0.865, respectively. When combining COMPASS 31 score with SDNN and LF, the AUC value increased to 0.958, with a sensitivity of 90.7% and a specificity of 86.7%. *Conclusions*. The combination of COMPASS 31 and HRV could improve the diagnostic performance of CAN in type 2 diabetes, which might be conducive to the diagnosis of CAN.

1. Introduction

Diabetic autonomic neuropathy (DAN) is one of the most common chronic complications of diabetes, which may affect cardiovascular, gastrointestinal, urogenital, and sudomotor function [1]. Among the various forms of DAN, cardiovascular autonomic neuropathy (CAN) is the most severe and studied form. CAN is defined as the impairment of autonomic control of the cardiovascular system in the setting of diabetes after exclusion of other causes [2]. Screening for CAN has been recommended at the diagnosis of type 2 diabetes even if there are no symptoms, particularly in people with a history of poor glycemic control, increased cardiovascular risk, and presence of macrovascular or microvascular complications [2].

In type 2 diabetes, the prevalence of CAN varies widely from 15.5 to 73% [3–5]. The major clinical manifestations of CAN include resting tachycardia, orthostatic hypotension, and exercise intolerance.

CAN is an independent risk factor for any cardiovascular events in people with diabetes, such as arrhythmia and painless myocardial ischemia [6, 7]. At present, cardiovascular reflex tests (CARTs) are regarded as the gold standard in the diagnosis of CAN. However, this method is cumbersome and requires the active cooperation of people, which limits the widespread application in clinical practice. Given that

strengthening multifactor intervention can delay the occurrence and development of CAN, a simple and effective tool for CAN is needed to assist with early detection and management of CAN, which is of great significance for improving the prognosis and quality of life in people with diabetes [8].

Composite Autonomic Symptom Score 31 (COMPASS 31) is a comprehensive questionnaire-based scale proposed by Sletten et al. [9] in 2012 to assess the autonomic symptoms across multiple domains. It is proven to be a refined, internally consistent, and quantitative assessment tool of autonomic symptoms. COMPASS 31 has been utilized to evaluate autonomic dysfunction in people with systemic sclerosis, parkinsonism, fibromyalgia, and small-fiber polyneuropathy [10–12]. Moreover, COMPASS 31 was validated in a cohort of people with CAN [13]. A recent study that assessed the diagnostic performance of COMPASS 31 and electrochemical skin conductance found that the combination of the tests can provide a better diagnostic performance for CAN [14].

Heart rate variability (HRV) analysis is widely used in detecting CAN, which can quantitatively assess the tension of sympathetic and parasympathetic nerve and the balance of the two through the measurement and analysis from electrocardiography recordings. It is recommended by the Toronto Consensus Panel on Diabetic Neuropathy and the American Diabetes Association [2, 15] and has been used as the evaluation indicator of CAN in some major clinical trials [16, 17]. Several studies have shown that HRV analysis may be more sensitive and accurate than traditional CARTs in the early detection of CAN [18, 19].

At present, there has been no study on the diagnostic value of COMPASS 31 score combined with HRV analysis in people with type 2 diabetes. Therefore, this study is aimed at using both methods to evaluate the diagnostic performance for CAN in type 2 diabetes, and we hypothesized that the combination of COMPASS 31 score and certain indices of HRV could contribute to the diagnosis of CAN.

2. Materials and Methods

2.1. Study Subjects. This was a cross-sectional study. From October 2018 to September 2019, participants with type 2 diabetes, aged 18–75 years, were recruited, who were admitted to the Department of Endocrinology of the First Affiliated Hospital of Henan University of Science and Technology. The exclusion criteria were as follows: (1) type 1 diabetes or other types of diabetes; (2) severe cardiovascular diseases, such as myocardial infarction, heart failure, or arrhythmia; (3) acute complications, such as diabetic ketoacidosis (DKA), and a hyperosmolar hyperglycemic state (HHS); (4) acute stroke, severe infection, recent surgery; (5) severe anemia, thyroid disease, and severe liver or kidney dysfunction; (6) mental illness or neurosis; (7) taking drugs that affect heart rate within a month; (8) pregnant or lactating women; and (9) proliferative diabetic retinopathy.

In total, 112 participants were screened for CAN. Among them, 9 participants were excluded: 6 participants did not receive all the examinations and the other 3 participants did not have their CARTs data analyzed. Finally, a total of 103 participant observations were available for the analyses. The study was approved by the Ethics Committee of The First Affiliated Hospital of Henan University of Science and Technology and was performed in accordance with the Declaration of Helsinki. All subjects provided written informed consent to participate.

2.2. Methods

2.2.1. Collection of Clinical Data. Complete clinical history and anthropometric data were measured. The data included gender, age, duration of diabetes, smoking history, drinking history, hypertension, and family history of diabetes. Body mass index (BMI), waist-hip ratio (WHR), resting heart rate, and blood pressure were measured.

All biochemical measures were analyzed from venous blood samples (following a minimum of an 8-hour fast) except for urinary albumin and creatinine which were measured from urine samples. Biochemical indicators included glycated hemoglobin (HbA1c), fasting blood glucose (FBG), triglyceride (TG), total cholesterol (TC), high-density lipoprotein cholesterol (HDL-c), and low-density lipoprotein cholesterol (LDL-c). HbA1c was measured by high-performance liquid chromatography. FBG, TG, TC, HDL-c, and LDL-c were detected by the Siemens ADVIA 2400 automatic biochemical analyzer. Urinary albumin and creatinine levels were measured on a random urine sample by an enzyme immunoassay to evaluate renal function using the urinary albumin-to-creatinine ratio (UACR).

Distal symmetric polyneuropathy (DSPN) was confirmed by nerve conduction studies (NCS), and the exclusion of neuropathy by other causes [1]. For each subject, NCS were assessed with an electromyography (EMG) apparatus (Haishen NDI-097, Shanghai, China) by a professional physician in the electromyography room. NCS were performed on median, ulnar, peroneal, and tibial nerves for motor conduction velocity, and median, ulnar, and sural nerves for sensory conduction velocity. Slowness in the motor or sensory conduction velocity on two or more nerves less than the normal limit (mean − 2 SD) were identified as DSPN [20]. Diabetic nephropathy (DN) was defined as the presence of albuminuria (≥30 mg/g of UACR). Based on the Early Treatment Diabetic Retinopathy Study (ETDRS) retinopathy severity scale [21], diabetic retinopathy (DR) was evaluated and graded by an experienced ophthalmologist as no apparent retinopathy, nonproliferative diabetic retinopathy, and proliferative diabetic retinopathy through an optical fundus camera (Canon CR-2, Tokyo, Japan).

2.2.2. Cardiovascular Reflex Tests (CARTs). Standardized cardiovascular reflex tests were performed by the recording of a continuous electrocardiogram as previously described [22], which included tests of heart rate responses, such as heart rate responses to deep breathing, to Valsalva maneuver, and to lying to standing (30 : 15 ratio). The three tests explore mainly on the parasympathetic function, but the nervous pathways and reflex mechanisms involved are not identical: Valsalva maneuver and 30 : 15 ratio involves both sympathetic and parasympathetic arms [23, 24]. Data were

obtained by a 12-lead electrocardiography using MedEx ECG-2000 network system (MedEx, Beijing, China). Another test was the blood pressure responses to lying to standing (postural BP change) which assessed sympathetic function. It was measured using an electronic sphygmomanometer (Omron HEM-7136, Kyoto, Japan). Subjects were asked to have a rest at least 20 minutes before the tests and avoid intake of caffeine, smoking, alcohol, and food at least 2 h before testing. There were 5-minute intervals between each test, and all tests were performed by the same physician. Each of the four tests described above was scored as 0 for normal, 0.5 for borderline, and 1 for abnormal, for a total score of 4. Age-related normal reference values were used to define abnormality. The participants with a score of at least 2 was defined as CAN group and those less than 2 as non-CAN group [2, 22].

2.2.3. Composite Autonomic Symptom Score 31 (COMPASS 31). All subjects were requested to complete COMPASS 31 questionnaire independently according to the actual situation. All questionnaires were administered by the same physician. COMPASS 31 comprises 6 domains with 31 items (orthostatic intolerance 4 items, vasomotor 3 items, secretomotor 4 items, gastrointestinal 12 items, bladder 3 items, and pupillomotor 5 items) and provides the minimal weighted total score equals 0 and the maximum weighted total score equals 100. The higher the score, the more severe the autonomic neuropathy [9].

2.2.4. Heart Rate Variability (HRV) Analysis. For the HRV analysis, the ECG data were monitored continuously by 24-hour Holter recordings with BENEWARE Smart Ambulatory Electrocardiogram Analysis System (Zhejiang, China). And the completed data were analyzed by an experienced physician. Time domain analysis and frequency domain analysis were obtained. The selected time domain indices were the standard deviation (SD) of the NN intervals (SDNN), the percentage of adjacent NN intervals with a difference greater than 50 ms (PNN50), and the root mean square differences of successive NN intervals (RMSSD). For the frequency domain analysis, low-frequency (LF) and high-frequency (HF) powers were assessed, as well as the LF/HF ratio [25].

2.3. Statistical Analysis. Statistical analyses were performed using SPSS software (version 24.0, Chicago, IL) and MedCalc software (version 15.2.2, Ostend, Belgium). The Kolmogorov-Smirnov test was used to determine whether continuous variables followed a normal distribution. Normally distributed continuous variables were expressed as means ± standard deviation (SD), whereas variables with skewed continuous distribution were expressed as median (interquartile range). Differences in continuous variables between groups were assessed by t-test and Mann-Whitney U test. Categorical variables were expressed as number (percentage), and a chi-square test was used to compare different groups. Associations between variables were assessed using Spearman's rank correlation. We conducted receiver operating characteristic (ROC) analyses to evaluate the diagnostic performance of COMPASS 31 score and HRV indices, while the combination of them was evaluated by established multivariable-adjusted logistic regression mode. Kappa test was also used to analyze the consistency between each variable and gold standard.

3. Results

3.1. Participant Characteristics. The characteristics of 103 participants with type 2 diabetes are presented in Table 1. The participants consisted of 37 female (35.9%) and 66 male (64.1%), a mean age of 54 ± 9 years, and a median diabetes duration of 8(3, 15) years. A total of 43 participants (41.8%) were diagnosed with CAN. Participants with CAN were older with a longer duration of diabetes, increased resting heart rate, and elevated UACR ($P < 0.05$). In addition, the rates of DSPN, DN, and DR were also significantly higher among those with CAN.

3.2. Cardiovascular Autonomic Nervous Function. As demonstrated in Table 2, abnormal CARTs including deep breathing, lying to standing (30 : 15 ratio), the Valsalva maneuver, and postural BP change were shown in 65 subjects (63.1%), 14 subjects (13.6%), 37 subjects (35.9%), and 6 subjects (5.8%), respectively. The COMPASS 31 scores differed significantly between participants with and without CAN ($P < 0.001$). Furthermore, we compared domain scores, participants with CAN had significantly higher scores for orthostatic intolerance score ($P < 0.001$), vasomotor score ($P = 0.01$), gastrointestinal score ($P < 0.001$), bladder score ($P = 0.001$) (see Table S1). For HRV analysis, all indices in participants with CAN were significantly lower than those without CAN.

3.3. Association of COMPASS 31 Score, HRV Indices, and CARTs. A significant positive association was found between COMPASS 31 score and CARTs score ($r_s = 0.547$, $P < 0.001$), while each HRV index was significantly inversely related to CARTs score ($r_s = -0.284 \sim -0.722$, $P < 0.01$). Among these indices of HRV, SDNN ($r_s = -0.722$, $P < 0.001$) and LF ($r = -0.637$, $P < 0.001$) had the strongest correlation with CARTs score. In addition, the COMPASS 31 score was negatively correlated with SDNN, LF and LF/HF ($r_s = -0.222 \sim -0.397$, $P < 0.05$) (Table 3).

3.4. Diagnostic Performance of COMPASS 31 and HRV Indices for CAN. We explored the diagnostic value of COMPASS 31 score and HRV indices for CAN by using CARTs as the gold standard (Table 4, Figure 1). COMPASS 31 score showed a fair diagnostic value with the AUC of 0.816, and the cutoff was 19.5 with sensitivity of 67.4% and specificity of 83.3%. When considering the diagnostic performance of HRV indices, the AUC values of HRV indices for diagnosing CAN were 0.648 to 0.919, among which SDNN and LF had significantly higher diagnostic value than other indices ($P < 0.05$), with the AUC value of 0.919 and 0.865, respectively. However, there was no significant difference of diagnostic value between these two indices. The optimal cutoff of SDNN for diagnosing CAN was 95 ms, with sensitivity of 79.1% and specificity of 91.7%, while of LF was deemed to

Table 1: Clinical characteristics of the study population.

Variable	Overall ($n = 103$)	Non-CAN ($n = 60$)	CAN ($n = 43$)	P value
Female, n(%)	37(35.9)	18(30.0)	19(44.2)	0.139
Age (years)	54 ± 9	51 ± 9	58 ± 8	<0.001***
Duration of diabetes (years)	8(3, 15)	5(2, 10)	15(6, 18)	<0.001***
Smoking history, n(%)	24(23.3)	12(20.0)	12(27.9)	0.349
Drinking history, n(%)	23(22.3)	15(25.0)	8(18.6)	0.442
Hypertension, n(%)	49(47.6)	31(51.7)	18(41.9)	0.326
Family history of diabetes, n(%)	45(43.7)	27(45.0)	18(41.9)	0.751
Body mass index (kg/m^2)	24.6 ± 2.9	24.5 ± 2.7	24.5 ± 3.2	0.947
Waist-hip ratio	0.95 ± 0.06	0.94 ± 0.06	0.95 ± 0.06	0.556
Resting heart rate (bpm)	73 ± 11	70 ± 10	76 ± 13	0.013*
Blood pressure (mmHg)				
Systolic BP	127 ± 15	126 ± 15	128 ± 16	0.508
Diastolic BP	81 ± 10	81 ± 10	80 ± 9	0.404
Microvascular complications, n(%)				
DSPN	67(65.0)	32(53.3)	35(81.4)	0.003**
Diabetic nephropathy	43(41.7)	19(31.7)	24(55.8)	0.014*
Diabetic retinopathy	31(30.1)	9(15.0)	22(51.2)	<0.001***
Laboratory variables				
Fasting blood glucose (mmol/L)	9.8 ± 3.3	9.7 ± 3.6	9.9 ± 3.0	0.764
HbA1c (%)	9.6 ± 2.7	9.6 ± 2.9	9.7 ± 2.5	0.864
Total cholesterol (mmol/L)	4.76 ± 1.06	4.81 ± 1.10	4.69 ± 1.02	0.579
Triglyceride (mmol/L)	2.17 ± 1.50	2.38 ± 1.61	1.88 ± 1.30	0.095
LDL-c (mmol/L)	2.82 ± 0.92	2.88 ± 0.86	2.74 ± 1.00	0.425
HDL-c (mmol/L)	1.23 ± 0.29	1.22 ± 0.28	1.24 ± 0.31	0.644
UACR (mg/g)	18.0(7.8, 81.9)	13.4(6.7, 54.7)	44.5(10.4, 152.4)	0.006**

Data are means ± SD, median (IQR), or n (%). CAN: cardiovascular autonomic neuropathy; BP: blood pressure; DSPN: distal symmetric polyneuropathy; HbA1c: glycated hemoglobin; LDL-c: low-density lipoprotein cholesterol; HDL-c: high-density lipoprotein cholesterol; UACR: urinary albumin-to-creatinine ratio. *$P < 0.01$ (non-CAN group vs. CAN group); **$P < 0.01$ (non-CAN group vs. CAN group); ***$P < 0.001$ (non-CAN group vs. CAN group).

be 131.4 ms^2 for CAN (sensitivity of 65.1%, specificity of 96.7%). The diagnosis model incorporating COMPASS 31 score, SDNN, and LF was further analyzed. The AUC value for the combined model could be increased to 0.958, with sensitivity of 90.7%, specificity of 86.7%, and the Kappa value increased to 0.75.

4. Discussion

Dysfunction of the autonomic nervous system in CAN cause impaired cardiovascular regulation, resulting in an increased risk of cardiovascular death in patients with type 2 diabetes mellitus. Autonomic dysfunction plays an important role in the occurrence of arrhythmic events as ventricular arrhythmias and atrial fibrillation [26, 27]. Indeed, a method that is easy and noninvasive for diagnosis of CAN is necessary, for the timely treatment and a reduced risk of cardiovascular events. In the present study, we first explored the diagnostic performance of the combination of COMPASS 31 score and HRV indices for CAN in type 2 diabetes. Our data observed that a combination of COMPASS 31 score, SDNN, and LF showed a greater diagnostic ability than using COMPASS 31 score or HRV indices alone, while with a high sensitivity and specificity. For the diagnosis of CAN, autonomic function test is particularly important, and the evaluation of autonomic symptoms cannot be ignored as well. Therefore, a combination of both may provide a better diagnostic method for CAN in clinical practice.

Autonomic symptoms should be assessed in people with diabetes as recommended by current guidelines [15]. We evaluated autonomic symptoms in participants with type 2 diabetes by using COMPASS 31; the data showed that COMPASS 31 score differed significantly between participants with CAN and without CAN. Each subscale score was also higher than participants without CAN, in particular for orthostatic intolerance, vasomotor, gastrointestinal, and bladder symptoms. This finding confirms the observation in the previous studies [28, 29] that CAN may be closely related to autonomic dysfunction of other organs. Therefore,

Table 2: The indicators of cardiovascular autonomic nervous function.

Variables	Non-CAN ($n = 60$)	CAN ($n = 43$)	P value
CARTs			
Deep breathing, n (% abnormal)	23(38.3)	42(97.7)	<0.001
30 : 15 ratio, n (% abnormal)	0(0)	14(32.6)	<0.001
Valsalva maneuver, n (% abnormal)	5(8.3)	32(74.4)	<0.001
Postural BP change, n (% abnormal)	0(0)	6(14.0)	<0.001
CARTs score	1.0(0.5, 1.5)	2.0(2.0, 3.0)	<0.001
COMPASS 31 score	12.9 ± 6.9	23.7 ± 9.8	<0.001
HRV indices			
SDNN (ms)	126.5 ± 21.6	82.8 ± 22.3	<0.001
PNN50 (%)	4.3(2.2, 9.0)	1.4(0.3, 3.7)	<0.001
RMSSD (ms)	25.5(20.0, 37.3)	19.0(13.0, 37.0)	0.010
LF (ms^2)	386.1(227.7, 545.9)	108.7(37.0, 196.1)	<0.001
HF (ms^2)	239.0(125.0, 378.5)	104.6(42.0, 170.0)	<0.001
LF/HF ratio	1.49(1.07, 2.68)	0.94(0.62, 1.63)	0.001

Data are means ± SD, median (interquartile range), or n (%). CAN: cardiovascular autonomic neuropathy; CARTs: cardiovascular autonomic reflex tests; 30 : 15 ratio: lying to standing; COMPASS 31: Composite Autonomic Symptom Score 31; HRV: heart rate variability; SDNN: the standard deviation of the NN intervals; PNN50: the percentage of adjacent NN intervals with a difference greater than 50 ms; RMSSD: the root mean square differences of successive NN intervals; LF: low-frequency power; HF: high-frequency power.

Table 3: Correlation between COMPASS 31 score, HRV indices, and CARTs.

Variables	CARTs score		COMPASS 31 score	
	r_s	P value	r_s	P value
COMPASS 31 score	0.547	<0.001	/	/
HRV indices				
SDNN (ms)	−0.722	<0.001	−0.397	<0.001
PNN50 (%)	−0.449	<0.001	−0.175	0.078
RMSSD (ms)	−0.284	0.004	−0.120	0.227
LF (ms^2)	−0.637	<0.001	−0.306	0.002
HF (ms^2)	−0.456	<0.001	−0.149	0.134
LF/HF ratio	−0.350	<0.001	−0.222	0.024

CARTs: cardiovascular autonomic reflex tests; COMPASS 31: Composite Autonomic Symptom Score 31; HRV: heart rate variability; SDNN: the standard deviation of the NN intervals; PNN50: the percentage of adjacent NN intervals with a difference greater than 50 ms; RMSSD: the root mean square differences of successive NN intervals; LF: low-frequency power; HF: high-frequency power.

participants with other types of autonomic symptoms should be alert to the occurrence of CAN in clinic. We also found that COMPASS 31 score increased with the decrease of HRV indices, and a similar finding was obtained in a study of people with fibromyalgia [10]. In addition, the diagnostic performance of COMPASS 31 seemed to be better than that observed in similar studies [13, 30], and the cutoff was higher as well. We speculated that there be difference of the sample size, study subjects, and racial differences between studies, leading to different results. Nevertheless, what we have in common is that COMPASS 31 could be an effective tool for CAN.

HRV analysis is considered to be a widely used and readily available diagnostic method. It includes time domain and frequency domain analysis. Among the time domain indices, SDNN mainly reflects the change of overall HRV, while RMSSD and PNN50 represent the parasympathetic activity. LF and HF assess the sympathetic and parasympathetic functions, respectively, as frequency domain indices, and LF/HF ratio can be used to evaluate the interaction of both [17, 31]. Compared with subjects without CAN, we found that those with CAN had significantly reduced overall HRV, including the loss of parasympathetic and sympathetic, with mainly decreased parasympathetic. It indicated that parasympathetic impairment may precede the sympathetic dysfunction. Actually, the association between type 2 diabetes mellitus and autonomic dysfunction is not well established and still under investigation. A prospective multicenter study has shown that the existing link between autonomic dysfunction and the increase and recurrence of vaso vagal syncope events in type 2 diabetes mellitus might be the result of the excess in parasympathetic tone in contrast to sympathetic heart innervations [32]. Furthermore, a good correlation has been shown between HRV indices and CARTs. It is worth reminding that SDNN and LF have the best consistency with CARTs, which showed the highest diagnostic values. A study by Viggiano et al. [33], which observed that autonomic dysfunction could be detected by LF in participants with type 2 diabetes without obvious symptoms. SDNN, as an important indicator of HRV analysis, reflects the total tension of autonomic activity, with good repeatability and stability, which has been often used as a predictor of the prognosis in cardiovascular event [34]. Hence, SDNN and LF seem to be used as the important indicators for assessing CAN clinically. In the current study, the obtained cutoff values of HRV indices were lower than the values proposed

Table 4: Comparison of diagnostic value among COMPASS 31 score and HRV indices.

Variables	Cutoff	Sensitivity (%)	Specificity (%)	PPV (%)	NPV (%)	AUC	Youden's index	Kappa value
COMPASS 31 score	>19.5	67.4	83.3	74.4	78.1	0.816	0.51	0.52
HRV indices								
SDNN (ms)	≤95	79.1	91.7	87.2	85.9	0.919	0.71	0.72
PNN50 (%)	≤1.4	58.1	86.7	75.8	74.3	0.746	0.45	0.46
RMSSD (ms)	≤16	44.2	88.3	73.1	68.8	0.648	0.33	0.34
LF (ms^2)	≤131.4	65.1	96.7	93.3	79.5	0.865	0.62	0.65
HF (ms^2)	≤183.5	83.7	61.7	61.0	84.1	0.747	0.45	0.43
LF/HF ratio	≤0.86	48.8	88.3	75.0	70.7	0.699	0.37	0.39
Combined model	/	90.7	86.7	83.0	92.9	0.958	0.77	0.75

Combined model: the combination of COMPASS 31 score, SDNN, and LF. COMPASS 31: Composite Autonomic Symptom Score 31; HRV: heart rate variability; SDNN: the standard deviation of the NN intervals; PNN50: the percentage of adjacent NN intervals with a difference greater than 50 ms; RMSSD: the root mean square differences of successive NN intervals; LF: low-frequency power; HF: high-frequency power.

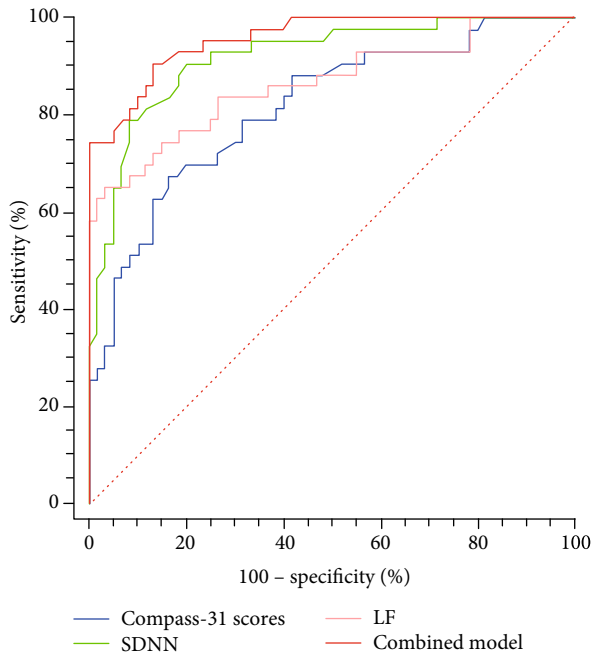

Figure 1: ROC curves comparing the ability of different variables and the combined model in distinguishing between participants with and without CAN. Combined model: the combination of COMPASS 31 score, SDNN, and LF.

in a study conducted in 1996 [25], while its interpretation and application need to be further confirmed by multicenter and large-scale studies.

Some limitations of the present study deserved to be noted. First, this is a single -center and cross-sectional study, resulting in a relatively small sample size, a limited scope of inclusion, and no relevant analysis by the severity of CAN. Second, the study subjects are all in-patients, leading to these results not being applicable to the out-patient population. Third, control subjects were not set in this study, because the primary aim was to evaluate the diagnostic capacity of COMPASS 31 and HRV indices for CAN. A large multicenter and longitudinal sample study still requires to be further confirmed.

5. Conclusions

In the present study, we found that COMPASS 31 and HRV indices were in good agreement with conventional CARTs, and the selected HRV indices SDNN and LF might be used as the important reference indicators. The combination of COMPASS 31 and HRV analysis is conducive to the diagnosis of CAN, providing certain reference for clinical practice. The limited scope of inclusion of this study requires further validation in the out-patient population with diabetes.

Data Availability

The raw data used to support the conclusions of this manuscript are available from the corresponding author, without undue reservation, to any qualified researcher.

Conflicts of Interest

The authors declare that there are no potential conflicts of interest relevant to this article.

Acknowledgments

The authors thank Jianfei Qiu for statistical consultation and helpful suggestions. This work was supported by Project of Clinical Medicine Research Center of Endocrine and Metabolic Disease of Luoyang (1801001A).

Supplementary Materials

Supplementary Table S1: comparison of the COMPASS 31 domain scores. *(Supplementary Materials)*

References

[1] S. Tesfaye, A. J. M. Boulton, P. J. Dyck et al., "Diabetic neuropathies: update on definitions, diagnostic criteria, estimation of severity, and treatments," *Diabetes Care*, vol. 33, no. 10, pp. 2285–2293, 2010.

[2] V. Spallone, D. Ziegler, R. Freeman et al., "Cardiovascular autonomic neuropathy in diabetes: clinical impact,

assessment, diagnosis, and management," *Diabetes/Metabolism Research and Reviews*, vol. 27, no. 7, pp. 639–653, 2011.

[3] P. A. Low, L. M. Benrud-Larson, D. M. Sletten et al., "Autonomic symptoms and diabetic neuropathy: a population-based study," *Diabetes Care*, vol. 27, no. 12, pp. 2942–2947, 2004.

[4] J.-S. Yun, J.-H. Kim, K.-H. Song et al., "Cardiovascular autonomic dysfunction predicts severe hypoglycemia in patients with type 2 diabetes: a 10-year follow-up study," *Diabetes Care*, vol. 37, no. 1, pp. 235–241, 2014.

[5] A. Bissinger, "Cardiac autonomic neuropathy: why should cardiologists care about that?," *Journal Diabetes Research*, vol. 2017, article 5374176, 9 pages, 2017.

[6] L. H. Young, F. J. T. Wackers, D. A. Chyun et al., "cardiac outcomes after screening for asymptomatic coronary artery disease in patients with type 2 diabetes," *Journal of the American Medical Association*, vol. 301, no. 15, pp. 1547–1555, 2009.

[7] R. Pop-Busui, G. W. Evans, H. C. Gerstein et al., "Effects of cardiac autonomic dysfunction on mortality risk in the action to control cardiovascular risk in diabetes (ACCORD) trial," *Diabetes Care*, vol. 33, no. 7, pp. 1578–1584, 2010.

[8] P. Gaede, P. Vedel, N. Larsen, G. V. Jensen, H. H. Parving, and O. Pedersen, "Multifactorial intervention and cardiovascular disease in patients with type 2 diabetes," *The New England Journal of Medicine*, vol. 348, no. 5, pp. 383–393, 2003.

[9] D. M. Sletten, G. A. Suarez, P. A. Low, J. Mandrekar, and W. Singer, "COMPASS 31: a refined and abbreviated composite autonomic symptom score," *Mayo Clinic Proceedings*, vol. 87, no. 12, pp. 1196–1201, 2012.

[10] J. H. Kang, J. K. Kim, S. H. Hong, C. H. Lee, and B. Y. Choi, "Heart rate variability for quantification of autonomic dysfunction in fibromyalgia," *Annals of Rehabilitation Medicine*, vol. 40, no. 2, pp. 301–309, 2016.

[11] Y. Kim, J. M. Seok, J. Park et al., "The composite autonomic symptom scale 31 is a useful screening tool for patients with parkinsonism," *PLoS One*, vol. 12, no. 7, article e0180744, 2017.

[12] B. L. Adler, J. W. Russell, L. K. Hummers, and Z. H. McMahan, "Symptoms of autonomic dysfunction in systemic sclerosis assessed by the COMPASS-31 questionnaire," *The Journal of Rheumatology*, vol. 45, no. 8, pp. 1145–1152, 2018.

[13] C. Greco, F. Di Gennaro, C. D'Amato et al., "Validation of the composite autonomic symptom score 31 (COMPASS 31) for the assessment of symptoms of autonomic neuropathy in people with diabetes," *Diabetic Medicine*, vol. 34, no. 6, pp. 834–838, 2017.

[14] C. D'Amato, C. Greco, G. Lombardo et al., "The diagnostic usefulness of the combined COMPASS 31 questionnaire and electrochemical skin conductance for diabetic cardiovascular autonomic neuropathy and diabetic polyneuropathy," *Journal of the Peripheral Nervous System*, vol. 25, no. 1, pp. 44–53, 2020.

[15] R. Pop-Busui, A. J. M. Boulton, E. L. Feldman et al., "Diabetic neuropathy: a position statement by the American Diabetes Association," *Diabetes Care*, vol. 40, no. 1, pp. 136–154, 2016.

[16] R. Pop-Busui, P. A. Low, B. H. Waberski et al., "Effects of prior intensive insulin therapy on cardiac autonomic nervous system function in type 1 diabetes mellitus: the diabetes control and complications trial/epidemiology of diabetes interventions and complications study (DCCT/EDIC)," *Circulation*, vol. 119, no. 22, pp. 2886–2893, 2009.

[17] A. S. Shah, L. El Ghormli, M. E. Vajravelu et al., "Heart rate variability and cardiac autonomic dysfunction: prevalence, risk factors, and relationship to arterial stiffness in the treatment options for type 2 diabetes in adolescents and youth (TODAY) study," *Diabetes Care*, vol. 42, no. 11, pp. 2143–2150, 2019.

[18] D. J. Ewing, J. M. Neilson, C. M. Shapiro, J. A. Stewart, and W. Reid, "Twenty four hour heart rate variability: effects of posture, sleep, and time of day in healthy controls and comparison with bedside tests of autonomic function in diabetic patients," *British Heart Journal*, vol. 65, no. 5, pp. 239–244, 1991.

[19] A. I. Vinik and D. Ziegler, "Diabetic cardiovascular autonomic neuropathy," *Circulation*, vol. 115, no. 3, pp. 387–397, 2007.

[20] J. D. England, G. S. Gronseth, G. Franklin et al., "Distal symmetric polyneuropathy: a definition for clinical research: report of the American Academy of Neurology, the American Association of Electrodiagnostic Medicine, and the American Academy of Physical Medicine and Rehabilitation," *Neurology*, vol. 64, no. 2, pp. 199–207, 2005.

[21] C. P. Wilkinson, F. L. Ferris, R. E. Klein et al., "Proposed international clinical diabetic retinopathy and diabetic macular edema disease severity scales," *Ophthalmology*, vol. 110, no. 9, pp. 1677–1682, 2003.

[22] D. J. Ewing, C. N. Martyn, R. J. Young, and B. F. Clarke, "The value of cardiovascular autonomic function tests: 10 years experience in diabetes," *Diabetes Care*, vol. 8, no. 5, pp. 491–498, 1985.

[23] M. J. Hilz and M. Dütsch, "Quantitative studies of autonomic function," *Muscle & Nerve*, vol. 33, no. 1, pp. 6–20, 2006.

[24] V. Spallone, F. Bellavere, L. Scionti et al., "Recommendations for the use of cardiovascular tests in diagnosing diabetic autonomic neuropathy," *Nutrition, Metabolism, and Cardiovascular Diseases*, vol. 21, no. 1, pp. 69–78, 2011.

[25] A. J. Camm, M. Malik, J. T. Bigger, G. Breithardt, S. Cerutti, and R. J. Cohen, "Heart rate variability: standards of measurement, physiological interpretation and clinical use. Task force of the European Society of Cardiology and the North American Society of Pacing and Electrophysiology," *Circulation*, vol. 93, pp. 1043–1065, 1996.

[26] M. R. Rizzo, F. C. Sasso, R. Marfella et al., "Autonomic dysfunction is associated with brief episodes of atrial fibrillation in type 2 diabetes," *Journal of Diabetes and its Complications*, vol. 29, no. 1, pp. 88–92, 2015.

[27] C. Sardu, G. Carreras, S. Katsanos et al., "Metabolic syndrome is associated with a poor outcome in patients affected by outflow tract premature ventricular contractions treated by catheter ablation," *BMC Cardiovascular Disorders*, vol. 14, no. 1, p. 176, 2014.

[28] M. Buysschaert, M. Moulart, J. L. Urbain et al., "Impaired gastric emptying in diabetic patients with cardiac autonomic neuropathy," *Diabetes Care*, vol. 10, no. 4, pp. 448–452, 1987.

[29] R. Pop-Busui, J. Hotaling, B. H. Braffett et al., "Cardiovascular autonomic neuropathy, erectile dysfunction and lower urinary tract symptoms in men with type 1 diabetes: findings from the DCCT/EDIC," *The Journal of Urology*, vol. 193, no. 6, pp. 2045–2051, 2015.

[30] R. Singh, M. Arbaz, N. K. Rai, and R. Joshi, "Diagnostic accuracy of composite autonomic symptom scale 31 (COMPASS-31) in early detection of autonomic dysfunction in type 2 diabetes mellitus," *Diabetes, Metabolic Syndrome and Obesity: Targets and Therapy*, vol. 12, pp. 1735–1742, 2019.

[31] R. Pop-Busui, "Cardiac autonomic neuropathy in diabetes: a clinical perspective," *Diabetes Care*, vol. 33, no. 2, pp. 434–441, 2010.

[32] C. Sardu, P. Paolisso, M. Santamaria et al., "Cardiac syncope recurrence in type 2 diabetes mellitus patients vs. normoglycemics patients: the CARVAS study," *Diabetes Research and Clinical Practice*, vol. 151, pp. 152–162, 2019.

[33] A. Viggiano, C. Vicidomini, M. Monda et al., "Fast and low-cost analysis of heart rate variability reveals vegetative alterations in noncomplicated diabetic patients," *Journal of Diabetes and its Complications*, vol. 23, no. 2, pp. 119–123, 2009.

[34] E. Buccelletti, E. Gilardi, E. Scaini et al., "Heart rate variability and myocardial infarction: systematic literature review and metanalysis," *European Review for Medical and Pharmacological Sciences*, vol. 13, no. 4, pp. 299–307, 2009.

Hindawi
Journal of Diabetes Research
Volume 2020, Article ID 7489795, 17 pages
https://doi.org/10.1155/2020/7489795

Review Article

Association of Glycemic Indices (Hyperglycemia, Glucose Variability, and Hypoglycemia) with Oxidative Stress and Diabetic Complications

Eleftheria Papachristoforou,[1] **Vaia Lambadiari**,[2] **Eirini Maratou**,[2] **and Konstantinos Makrilakis**[1]

[1]*First Department of Propaedeutic Internal Medicine, National and Kapodistrian University of Athens Medical School, Laiko General Hospital, Athens, Greece*
[2]*Second Department of Internal Medicine, Research Unit and Diabetes Centre, National and Kapodistrian University of Athens Medical School, Attikon Hospital, Athens, Greece*

Correspondence should be addressed to Konstantinos Makrilakis; kmakrila@med.uoa.gr

Received 1 May 2020; Revised 16 September 2020; Accepted 23 September 2020; Published 16 October 2020

Academic Editor: Celestino Sardu

Oxidative stress (OS) is defined as a disturbance in the prooxidant-antioxidant balance of the cell, in favor of the former, which results in the antioxidant capacity of the cell to be overpowered. Excess reactive oxygen species (ROS) production is very harmful to cell constituents, especially proteins, lipids, and DNA, thus causing damage to the cell. Oxidative stress has been associated with a variety of pathologic conditions, including diabetes mellitus (DM), cancer, atherosclerosis, neurodegenerative diseases, rheumatoid arthritis, ischemia/reperfusion injury, obstructive sleep apnea, and accelerated aging. Regarding DM specifically, previous experimental and clinical studies have pointed to the fact that oxidative stress probably plays a major role in the pathogenesis and development of diabetic complications. It is postulated that hyperglycemia induces free radicals and impairs endogenous antioxidant defense systems through several different mechanisms. In particular, hyperglycemia promotes the creation of advanced glycation end-products (AGEs), the activation of protein kinase C (PKC), and the hyperactivity of hexosamine and sorbitol pathways, leading to the development of insulin resistance, impaired insulin secretion, and endothelial dysfunction, by inducing excessive ROS production and OS. Furthermore, glucose variability has been associated with OS as well, and recent evidence suggests that also hypoglycemia may be playing an important role in favoring diabetic vascular complications through OS, inflammation, prothrombotic events, and endothelial dysfunction. The association of these diabetic parameters (i.e., hyperglycemia, glucose variability, and hypoglycemia) with oxidative stress will be reviewed here.

1. Introduction

Oxidative stress (OS) is defined as a disturbance in the prooxidant-antioxidant balance of the cell, in favor of the former, so that the antioxidant capacity of the cell is overcome [1, 2], potentially leading to tissue injury [3]. It occurs due to an increased generation and/or reduced elimination of reactive species by the antioxidant defense system.

Reactive species are generally defined as chemical species containing unpaired electrons that subsequently increase the chemical reactivity of an atom or molecule [4]. In that way, they render the other molecules unstable and have the potential of damaging them, by initiating a chain of reduction-oxidation (redox) reactions [5].

Reactive species usually stem from the elements oxygen, nitrogen, sulfur, or halogen, which give rise to reactive oxygen species (ROS), reactive nitrogen species (RNS), reactive sulfur species, or reactive halogen species, respectively. The main obstacles in the proper and sound perception of the effects of ROS/RNS are the lack of a proper and universally accepted definition. These terms are vague, and since there are many ROS/RNS which are different in chemistry (some

ROS/RNS are free radicals, but others are not; some free radicals are reactive, but others are not), or they can interconvert to one another [6], it is essential to explicitly specify the ROS used to properly interpret and discuss the role and effects of ROS in oxidative stress [2]. The most important reactive species formed in the human body are the oxygen derivatives. It is ironic that oxygen, an element indispensable for life, has detrimental effects on the human body under certain conditions [7]. Most of the potentially harmful effects of oxygen are due to the development and activity of these reactive oxygen species. They include the superoxide anion radical (O_2-), the hydroxyl free radical (OH·), hydrogen dioxide ($HO_2\cdot$), hydrogen peroxide (H_2O_2), hypochlorous acid (HOCl), singlet oxygen ($^1O_2$), and various lipid peroxides. Also, transition metals such as iron and copper, nitric oxide (NO), and peroxynitrite ($ONOO^-$) serve as free radicals [8, 9].

The human body continuously makes ROS during ordinary substantive metabolic processes. Mitochondria are the predominant source of ROS owing to the electron transport chain (ETC), but peroxisomes and the endoplasmic reticulum (ER) also contribute [10]. Actually, ROS may, under certain circumstances (low levels), have beneficial effects on the body, as they are used by the immune system as a way to assault and kill various pathogens [11]. In that way, they are considered to function in a beneficial way, modulating and maintaining key target functions by redox reactions, which is the essence of physiological oxidative stress, also called "oxidative eustress" [2, 12]. ROS are mainly produced during oxidative phosphorylation as a result of electron leak from the electron transport chain (ETC) located in the mitochondrial inner membrane [13] and are involved with the detoxification of xenobiotics by cytochrome P-450, with the elimination of microorganisms and cancer cells by macrophages and cytotoxic lymphocytes and with the manufacture of oxygenases (e.g., COX (cyclo-oxygenase) and LOX (lipooxygenase)) for the generation of prostaglandins and leukotrienes, which have many regulatory tasks. On the other hand, higher concentrations of ROS production lead to "adaptive stress" responses by the cell (via master switches, such as Nrf2/Keap1 (nuclear factor erythroid 2-related factor 2/Kelch-like ECH-associated protein 1) or NF-κB (nuclear factor-kappa B)). Furthermore, in the event of an excessive load of oxidative stress production, called "oxidative distress," it can lead to oxidative damage of the cells and provoke metabolic failure, compromising cell viability by inactivating enzymes of glycolysis, the Krebs cycle, and the ETC [12, 14, 15].

ROS can be composed by environmental and endogenous sources. Environmental sources include cigarette smoke, pollutants (such as ozone and nitrogen dioxide), ultraviolet light, ionizing radiation, and xenobiotics [7, 16]. Major endogenous sources include the NOX family of NADPH oxidases, complexes I and III of the mitochondrial ETC, the cytochrome P450-containing monooxygenase system, nitric oxide synthases (NOS), xanthine oxidoreductase, and myeloperoxidases [15]. In particular, NADPH oxidases are transmembrane proteins that transfer electrons from cytoplasmic NADPH across a biological membrane to molecular oxygen (O_2) at the outer side of the membrane. NOX oxidases can function as electron transport chains, which transfer electrons first from NADPH(H+) to FAD leading to the formation of NADP+ and FADH2. Further, one electron is transferred to ferric ion (Fe^{3+}) of the heme to produce ferrous ion (Fe^{2+}). Afterwards, the electron is transferred across the cell membrane to molecular oxygen for its incomplete one electron reduction with the formation of superoxide anion radical. Other important endogenous sources of superoxide anion radical are enzymatic complexes of the mitochondrial ETC, in which more than 11 electron leakage sites have been found. The ETC is located in the inner mitochondrial membrane and composed of five enzymatic complexes (I-V). These complexes provide electron transportation from NADH(H+) or FADH2, which are formed in reactions of oxidation of various substrates in both mitochondrial matrix and the cytoplasm, to the final electron acceptor, molecular oxygen. The transportation of high-energy electrons along the respiratory chain is accompanied by release of their energy that is further transformed into the transmembrane electrochemical potential ($\Delta\mu$H) utilized for ATP biosynthesis in the process of oxidative phosphorylation. However, another process that may take place during the ETC functioning is incomplete one electron reduction of O_2, which leads to formation of superoxide anion radical [17]. The produced superoxide anion radical can be released into either the mitochondrial matrix or the intermembrane space, depending on the site of its formation. Activities of the abovementioned ROS-producing enzymes can also be stimulated by arachidonic acid metabolites, such as prostaglandins, thromboxanes, and leukotrienes, produced by cyclooxygenases (COXs) and lipoxygenases (LOXs). In addition to NADPH oxidases and ETC complexes I and III, superoxide anion radical can be formed in the reactions catalyzed by xanthine oxidoreductase (XOR), in which hypoxanthine is irreversibly converted into xanthine, and further into uric acid in the final two reactions of purine catabolic pathway [18]. Superoxide anion radical can also be generated by enzymes containing transition metal ions as cofactors and heme as a coenzyme, i.e., metalloenzymes and hemoproteins, respectively [19]. ROS-producing hemoproteins include cytochrome P450- (CYP-) containing monooxygenase systems. Nitric oxide synthases (NOS) are heme-containing enzymes represented by three major isoforms (endothelial, neuronal, and inducible NOS) and generate NO (a primary type of RNS) in the cells, in the reaction of L-arginine conversion to L-citrulline. In addition to NO, all NOS isoforms can form superoxide anion radical as well [20]. Finally, myeloperoxidases (MPO), enzymes that catalyze the oxidation of substrates by hydrogen peroxide, can contribute to the formation of RNS (NO, nitrite ion, etc.), which contribute to their antibacterial activity [21].

ROS can assault various macromolecules in the body leading to damage of cells and homeostatic perturbations. Their targets include, among others, lipids, nucleic acids, and proteins [22]. Lipid peroxidation can lead to changes in membrane permeability and elasticity, as well as detrimental effects on membrane-bound proteins. Oxidation of nuclear or mitochondrial DNA can result in strand breaks, aberrant cross-linking, and DNA adducts (covalent bonding of DNA

elements to chemical mutagens/carcinogens). Proteins (including crucial enzymes) may sustain oxidative damage at a variety of weak sites and be rendered biologically inert at high ROS concentrations [23], but, as stated above describing oxidative eustress, through the regulatory functions of low ROS concentrations, proteins may undergo oxidative modification of redox-sensitive residues, and this can cause changes in their activity and underlie alterations in their regulatory functions with no damage in structures and functions of the proteins and the cells [15].

Because of the likelihood of significant harm as a result of the ROS strike, various antioxidant defense systems have evolved to shield body tissues [3]. An antioxidant is a molecule competent of decelerating or preventing the oxidation of other molecules [24]. The body has several mechanisms to offset oxidative stress by producing antioxidants, either naturally created in the body (endogenous antioxidants) [25] or externally supplied through foods (exogenous antioxidants) [26]. Antioxidants preclude ROS-induced tissue injury by hindering the creation of radicals, scavenging them, or by promoting their decay. They cease the oxidative chain reactions by eliminating ROS intermediates and restraining other oxidation reactions by being oxidized themselves. The antioxidants include enzymes to decay peroxides, proteins to sequester transition metals, and a variety of compounds to "scavenge" ROS [27].

The endogenous antioxidant defense system consists of enzymatic and nonenzymatic antioxidants. Enzymatic antioxidants incorporate superoxide dismutase (SOD), catalase (CAT), glutathione peroxidase (GPx), and glutathione reductase (GSR) [28]. The nonenzymatic antioxidants are also partitioned into metabolic antioxidants and nutrient antioxidants. Metabolic antioxidants, belonging to endogenous antioxidants, are produced by metabolism in the body, such as lipoic acid, glutathione (GSH), L-arginine, coenzyme-Q10, melatonin, uric acid, bilirubin, metal-chelating proteins, and transferrin [29]. On the other hand, nutrient antioxidants, belonging to exogenous antioxidants, are compounds that cannot be created in the body and must be provided through foods or supplements, such as vitamin E, vitamin C, carotenoids, lycopene, trace metals (selenium, manganese, zinc), flavonoids, omega-3, and omega-6 fatty acids.

In particular, examining the most important food-borne antioxidants, vitamin E is the collective name for a set of eight related tocopherols and tocotrienols (alpha-, beta-, gamma-, and delta-tocopherol and alpha-, beta-, gamma-, and delta-tocotrienol), which are fat-soluble vitamins with antioxidant properties [30]. Of these, α-tocopherol has been most studied as it has the highest bioavailability, with the body preferentially absorbing and metabolizing this form. Its dietary sources are vegetable oils (corn, safflower, soybean, and sunflower), wheat germ oil, whole grains, nuts, cereals, fruits, eggs, poultry, meat, etc. It has been claimed that the α-tocopherol form is the most important lipid-soluble antioxidant and that it protects membranes from oxidation by reacting with lipid radicals produced in the lipid peroxidation chain reaction. This removes the free radical intermediates and prevents the propagation reaction from continuing. Vitamin C, also known as ascorbic acid, is a water-soluble vitamin that is essential for collagen, carnitine, and neurotransmitters' biosynthesis. It is believed to have antioxidant, antiatherogenic, anticarcinogenic, and immune-modulator effects. It works synergistically with vitamin E to quench ROS and also regenerates the reduced form of vitamin E. Natural sources of vitamin C are acid fruits (orange, lemon, grapefruit, pineapple, strawberry, etc.), green vegetables, tomatoes, etc. [31]. Carotenoids are a family of pigmented compounds that are present as microcomponents in fruits and vegetables and are responsible for their yellow, orange, and red colors. They are thought to be responsible for the beneficial properties of fruits and vegetables in preventing human diseases including cardiovascular diseases and cancer. They are important dietary sources of vitamin A and are thought to possess antioxidant activities as well [32]. Lycopene is a member of the carotenoid family of phytochemicals. It is a lipid-soluble antioxidant that is synthesized by many plants and microorganisms, but not by animals and humans and is responsible for the red color of many fruits and vegetables, such as the tomatoes. It is one of the most potent antioxidants and has been suggested to protect critical biomolecules including lipids, low-density lipoproteins (LDL), proteins, and DNA. Several studies have indicated that lycopene is an effective antioxidant and free radical scavenger [33]. Finally, flavonoids are polyphenolic compounds, present in most plants, with beneficial effects on human health, mainly due to their potent antioxidant activity [33]. Every plant contains a unique combination of flavonoids, which is why different herbs, all rich in these substances, have very different effects on the body. The main natural sources of flavonoids include green tea, grapes (red wine), apple, cocoa (chocolate), ginkgo biloba, soybean, curcuma, berries, onion, and broccoli.

In summary, oxidative stress results from the metabolic reactions that use chiefly oxygen in the body and characterizes a disruption in the balanced state of prooxidant/antioxidant reactions in living organisms, in favor of the prooxidant effects. ROS are well-acknowledged for playing a dual role as both injurious (oxidative distress) and advantageous (oxidative eustress) species. ROS and RNS are typically created by firmly controlled enzymes, and their overproduction results in a harmful process (oxidative distress) that can be a central mediator of injury to cell constituents, including lipids and membranes, proteins, and DNA. Because of this, oxidative stress is postulated to be involved in many human diseases, such as diabetes mellitus (DM), cancer, arthritis, inflammation, and coronary heart disease, as well as in the aging process. In contrast, positive effects of ROS/RNS arise at low/moderate concentrations and entail physiological adaptive roles in cellular responses to injurious stimuli (oxidative eustress), for example, in defense versus infectious agents, in the function of several cellular signaling pathways, and in the induction of a mitogenic response. The "two-faced" character of ROS is clearly substantiated [23].

The dysglycemia of diabetes mellitus can be portrayed as the glycemic triumvirate with its 3 main components: the persistent chronic (ambient) hyperglycemia, glucose variability, and hypoglycemic incidents [34]. The individual contributions of these glycemic disorders to the total risk of

diabetic complications and the mode of their actions remain a topic of discussion. This review will examine the available evidence for the association between diabetes mellitus and oxidative stress, and especially the individual contribution of the three glycemic indices (hyperglycemia, glucose variability, and hypoglycemia) on the maintenance of "redox homeostasis" in people with diabetes and their involvement in the pathogenesis of diabetic complications.

2. Diabetes and Oxidative Stress

The prevalence of DM is rising and is achieving epidemic proportions. Recent data made available by the International Diabetes Federation (IDF) indicate that 463 million people were diagnosed with diabetes worldwide in 2019, and it is estimated that this number will increase to 700 million by 2045, the preponderance of who will be diagnosed with type 2 diabetes (T2D) [35]. Since DM is associated with augmented risk of micro- and macrovascular complications (such as retinopathy, neuropathy, and nephropathy, as well as cardiovascular disease (involving heart, cerebrovascular and peripheral arteries)), the projected increased incidence will result in higher medical care costs [36], reduced quality of life [37], and increased mortality [38].

Increased OS has been thought to be one of the key sources of the hyperglycemia-induced triggers of diabetic complications [39, 40]. On the other hand, OS has been alluded to the pathogenesis of diabetes per se [41], by leading to insulin resistance, dyslipidemia, β-cell dysfunction, and impaired glucose tolerance [42, 43]. As a matter of fact, even at the prediabetic state, visceral fat and superficial adipose tissue overexpress different cytokines (such as tumor necrosis factor-α (TNF-α) and interleukin 6 (IL-6)) and downregulate sirtuins (antiapoptotic proteins) that leads to increased inflammation and oxidative stress, which is associated to downregulation of mitochondrial biogenesis [44]. This may affect the cardiovascular functions in patients with diabetes vs. normo-glycemic individuals, leading to an altered myocardial performance and to the development of heart damage [45, 46]. Furthermore, it has been shown that prediabetes increases inflammatory burden in pericoronary adipose tissue as well, which also contributes to the increased CVD risk of these persons [47].

In diabetes, OS seems largely to be triggered by both a higher production of free radical species as well as a sharp decline in antioxidant defenses [48, 49]. The possible causes of OS might be the auto-oxidation of glucose [50, 51], swings in redox balances, decreased tissue concentrations of low molecular weight antioxidants (such as diminished GSH and vitamin E) [52], and impaired activities of antioxidant defense enzymes (such as SOD and CAT) [53]. This increase in ROS generation and the decrease in the activity of antioxidant defense systems due to hyperglycemia are thought to be largely responsible for the occurrence of diabetic complications [54, 55]. All three diabetic indices mentioned above (hyperglycemia, glucose variability, and hypoglycemia) [34] have been thought to play a role in the development of OS.

2.1. Hyperglycemia and Oxidative Stress. Hyperglycemia operates via several mechanisms to cause increased OS in DM and lead to vascular complications. Four core hypotheses have been proposed for the link between hyperglycemia-induced OS and complications [40]: "increased polyol (sorbitol) pathway flux, increased advanced glycation end-product (AGE) formation, activation of protein kinase C (PKC) isoforms, and increased hexosamine pathway flux". They all seem to be involved in a vicious circle of a single hyperglycemia-induced process of ROS (superoxide) overproduction by the mitochondrial electron-transport chain and activation of these pathways. It has been also shown that endoplasmic reticulum (ER) stress plays an important role in oxidative stress, as it is also a source of ROS [56]. The tight interconnection between both organelles through mitochondrial-associated membranes (MAMs) means that the ROS generated in mitochondria promote ER stress as well. A brief description of these four mechanisms and their association with OS will follow.

2.1.1. Increased Polyol (Sorbitol) Pathway Flux. The polyol pathway (or sorbitol-aldose reductase pathway) is a two-step process that converts glucose to fructose [57]. In this pathway, glucose is reduced to sorbitol, which is afterward oxidized to fructose. Aldose reductase (AR) is the first enzyme involved. It has a low affinity (high Km) for glucose, and at the normal glucose concentrations found in people without diabetes, metabolism of glucose by this pathway is negligible. But in a hyperglycemic setting (as occurs in uncontrolled diabetes), hexokinase (HK), the rate-limiting enzyme of the common glycolytic pathway (Figure 1), gets saturated and the surplus of glucose enters the polyol pathway, where AR reduces it to sorbitol (Figure 2). This reaction oxidizes NADPH (nicotinamide adenine dinucleotide phosphate) to $NADP^+$. Sorbitol dehydrogenase (SDH) can then oxidize sorbitol to fructose, which produces NADH (nicotinamide adenine dinucleotide) from its oxidized form NAD^+ [58]. Hexokinase can restore the molecule to the glycolysis pathway by phosphorylating fructose to form fructose-6-phosphate. However, in uncontrolled diabetes with high blood glucose—more than the glycolysis pathway can cope with—the reaction is altered towards the creation of sorbitol [59].

Many mechanisms have been proposed to explain the potentially harmful effects of hyperglycemia-induced increases in polyol pathway flux. These include sorbitol-induced osmotic stress, decreased Na^+/K^+-ATPase activity, increase in cytosolic $NADH/NAD^+$, and decrease in cytosolic NADPH [40]. It seems that the latter is the most important [58]. NADPH, which is required for the preservation of the antioxidant reduced glutathione (GSH), is oxidized to $NADP^+$ by the reduction of glucose to sorbitol in the AR pathway [60], and thus, the availability of intracellular NADPH is decreased. NADPH (a cofactor of NADPH-oxidases, the major ROS-generating system) is critically important, as it provides the reducing power that fuels the protein-based antioxidant systems and recycles oxidized glutathione. Furthermore, the antagonism between AR and glutathione reductase (GSR) for the NADPH cofactor further diminishes intracellular GSH [61]. GSH diminution regulates levels of

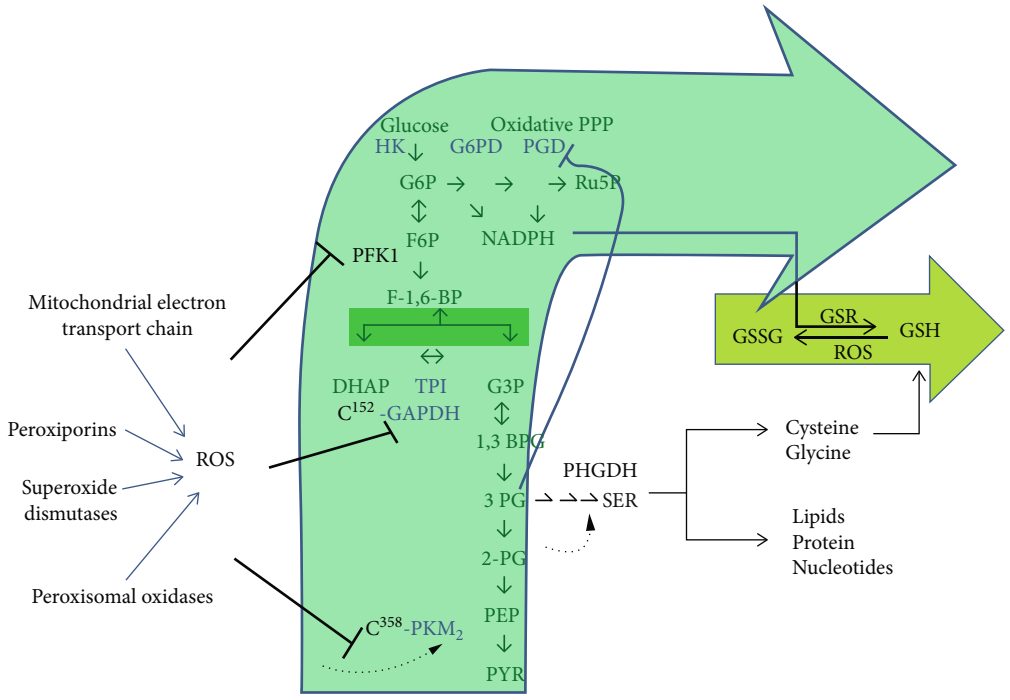

Figure 1: Reactive oxygen species- (ROS-) mediated inhibition of glycolysis reroutes flux into the oxidative arm of the pentose phosphate pathway. The enzymes inhibited by ROS are shown. ROS inhibits phosphofructokinase 1 (PFK1) and inactivates glyceraldehyde 3-phosphate dehydrogenase (GAPDH) and the pyruvate kinase isoform PKM2 by directly targeting cysteine residues. Thus, this glycolytic inhibition promotes flux into the oxidative pentose phosphate pathway (PPP) to produce NADPH and fuel cellular antioxidant systems (for example NADPH is consumed by glutathione reductase (GSR) to recycle oxidized glutathione (GSSG)). PKM2 inhibition is unique in that it allows for a diversion of flux into the serine synthesis pathway. Serine not only contributes to the synthesis of macromolecules but is also a precursor for glutathione (GSH). Serine synthesis is activated by a buildup of 2-phosphoglycerate (2PG), which prevents 3-phosphoglycerate- (3PG-) induced inhibition of the oxidative pentose phosphate arm. PPP: pentose phosphate pathway; HK: hexokinase; G6PD: glucose-6 phosphate dehydrogenase; PGD: phosphogluconate dehydrogenase; G6P: glucose-6-phosphate; Ru5P: ribulose-5-phosphate; F6P: fructose-6-phosphate; NADPH: nicotinamide adenine dinucleotide phosphate; PFK1: phosphofructokinase 1; F1,6 BP: fructose 1,6 bisphosphate; DHAP: dihydroxyacetone phosphate, TPI: tirose phosphate isomerase; G3P: glyceraldehyde-3-Phosphate; GAPDH: glyceraldehyde-3 phosphate dehydrogenase; 1,3 BPG: 1,3-bisphosphoglycerate; 3 PG: 3-phosphoglycerate; 2-PG: 2-phosphoglycerate; PEP: phosphoenolpyruvate; PYR: pyruvate; PKM2: pyruvate kinase isoform M2; PHGDH: 3-phosphoglycerate dehydrogenase; ROS: reactive oxygen species; GSSG: glutathione disulfide (oxidized glutathione); GSR: glutathione reductase; GSH: glutathione (reduced glutathione); SER: serine.

cellular ROS production and accrual. Also, an increased ratio of NADH/NAD^+ is connected with accelerated oxidation of sorbitol to fructose by NADH-dependent SDH [40]. The produced fructose can become phosphorylated to fructose-3-phosphate, which in turn can be broken down to 3-deoxyglucose and 3-deoxyglucosone. These two compounds are strong glycating agents that can glycate proteins and can result in the production of advanced glycation end-products (AGEs) [62], which, as mentioned below, are major pathogenic mediators of almost all diabetic complications. The NADH molecules are eventually transported to the mitochondria and oxidized by the respiratory chain reaction that results in the production of superoxide and other ROS, thus inciting oxidative damage to tissues [63, 64]. However, it has not been conclusively determined that activation of the polyol pathway in humans damages the vasculature [59].

2.1.2. Increased Formation of Advanced Glycation End-Products. Advanced glycation end-products (AGEs) are proteins or lipids that become glycated as a result of exposure to sugars [65]. AGEs are formed through the Maillard reaction, which is the nonenzymatic reaction between the free amino groups of proteins and carbonyl groups of reducing sugars or other carbonyl compounds [66]. During this reaction, glucose (or other reducing sugars such as fructose, galactose, and xylulose) reacts with a free amino group of biological amines to develop an unstable compound, the Schiff base. This subsequently undergoes a rearrangement to a more stable product, the Amadori product [67], from which, in a later stage of glycation, irreversible compounds (the AGEs) are formed [68]. AGEs are produced not only from glucose but also from the dicarbonyl compounds produced from the autoxidation and the degradation products of glucose, such as glyoxal, methylglyoxal, and 3-deoxyglucosone, or α-hydroxy aldehydes such as glyceraldehyde and glycolaldehyde [69, 70]. In the case of chronic hyperglycemia, AGEs are actively produced and accumulate in the circulating blood and various tissues, contributing to vascular complications in diabetes [71].

Glycation of proteins results in interference with their standard functions by perturbing molecular conformation, modifying enzymatic activity, and interfering with receptor

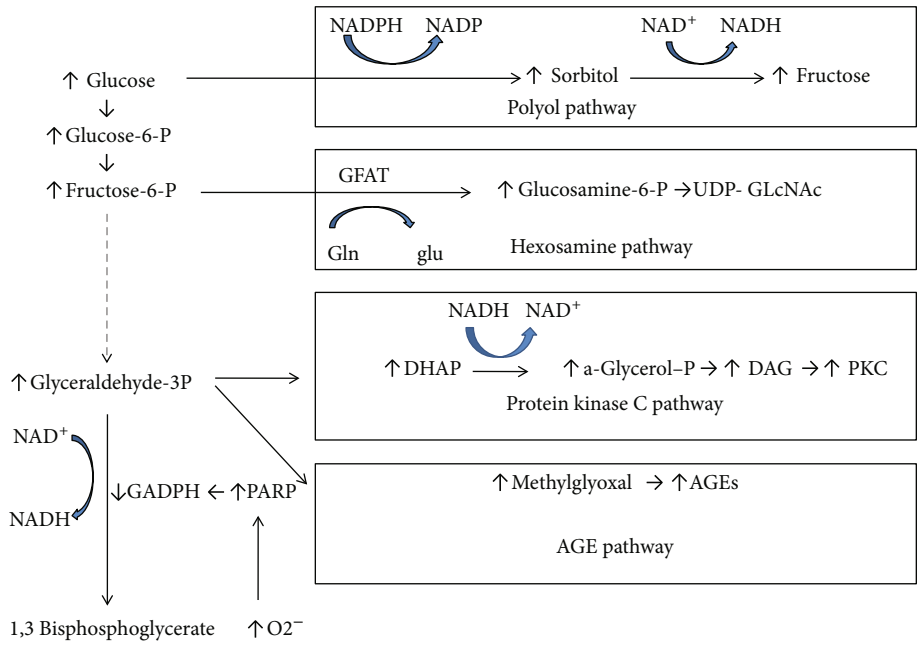

Figure 2: Mitochondrial overproduction of superoxide during hyperglycemic conditions activates four major pathways of hyperglycemic damage by inhibiting GAPDH. NADPH: nicotinamide adenine dinucleotide phosphate; NADH: nicotinamide adenine dinucleotide; GAPDH: glyceraldehyde-3 phosphate dehydrogenase; PARP: poly-ADP-ribose polymerase; GFAT: glutamine:fructose-6-phosphate amidotransferase; UDP-GlcNAc: UDP-N-acetylglucosamine; DAG: diacylglycerol; AGE: advanced glycation end-product.

functioning [72]. AGEs form intra- and extracellular cross-linking with proteins and some other endogenous vital molecules, including lipids and nucleic acids, play a significant role in the occurrence of diabetic complications.

AGEs interrelate with plasma membrane-localized receptors (RAGEs) to modify intracellular signaling, gene expression, the liberation of proinflammatory molecules, and free radicals [73, 74]. RAGE has three splice variants of full-length RAGE, an N-terminal variant that does not contain an AGE-binding domain, a soluble receptor for advanced glycation end-product (sRAGE), and a C-terminal splice variant that does not include transmembrane and effector domains [75].

AGEs accelerate the expression of RAGEs, and they play an important role in the development of diabetic vascular complications through various mechanisms [58, 70]. By altering the function of modified intracellular proteins or of extracellular matrix components (which interact abnormally with other matrix components and with matrix receptors (integrins) that are expressed on the cells' surface) or by promoting the attachment of AGE-modified plasma proteins to AGE receptors on cells such as macrophages, vascular endothelial cells (ECs), and vascular smooth muscle cells, it stimulates the production of ROS. These, in turn, activate the pleiotropic transcription factor, nuclear factor-kappa B (NF-κB), and increase expression of cell adhesion molecules, such as vascular cell adhesion molecule-1 (VCAM-1) in the vascular endothelial cells [76], causing numerous pathological changes in gene expression and giving rise to the pathogenesis of diabetic complications [77]. Furthermore, AGEs advance the production of the vascular endothelial growth factor (VEGF), leading to a rise in blood vessel permeability and the stimulation of neovascularization [78]. Also, circulating AGEs appear to react directly with lipoproteins, especially low-density lipoproteins (LDL), inducing structural alterations and damaging the mechanisms of LDL receptor-mediated particle removal at tissue level [79]. In patients with diabetes, RAGE expression is accelerated in atherosclerotic lesions in proportion to aggravation of blood sugar regulation [80, 81]. It has also been shown that the serum levels of the soluble form of RAGE (sRAGE) were significantly higher in type 2 DM patients compared to nondiabetic subjects and were positively associated with the presence of coronary artery disease [82]. AGEs are known to promote not only platelet aggregation but also the blood coagulation cascade through tissue factor production. The thrombotic tendency induced by AGEs is considered the cause of acute coronary syndromes, such as unstable angina or acute myocardial infarction through atheroma rupture and subsequent thrombogenesis in the coronary artery [68].

2.1.3. Activation of Protein Kinase C (PKC) Isoforms. The PKC family is comprised of at least 11 isoforms, 9 of which are triggered by the lipid second messenger diacylglycerol (DAG) [83], which is enhanced by intracellular hyperglycemia [84]. Furthermore, oxidants, such as H_2O_2 [85], and mitochondrial superoxide induced by elevated glucose levels [86] can also trigger PKC in a distinct manner to DAG. Activation of PKC has several pathogenic results, by affecting the expression of endothelial nitric oxide synthase (e-NOS), endothelin-1 (ET-1), vascular endothelial growth factor (VEGF), transforming growth factor-β (TGF-β), and plasminogen activator inhibitor-1 (PAI-1), all of which play a role in vascular disorders. Also, it has been associated with

activation of NF-κB (which connects hyperglycemia-induced oxidative stress to inflammation [87]) and NAD(P)H oxidase [40]. In that way, PKC has been associated with vascular modifications such as increases in permeability, contractility, extracellular matrix synthesis, cell growth and apoptosis, angiogenesis, leukocyte adhesion, and cytokine activation and inhibition. These perturbations in vascular cell homeostasis caused by different PKC isoforms (PKC-α, -β1/2, and PKC-δ) are linked to the development of pathologies affecting large vessel (atherosclerosis, cardiomyopathy) and small vessel (retinopathy, nephropathy, and neuropathy) complications in DM [88, 89].

2.1.4. Increased Hexosamine Pathway Flux. The hexosamine biosynthesis pathway (HBP) is a relatively insignificant limb of glycolysis, usually accounting for only 2–5% of the total glucose metabolism. Under hyperglycemic conditions, however, it can instigate posttranslational protein alterations by glycosylation and synthesis of glycolipids, proteoglycans, and glycosylphosphatidylinositol anchors [90]. In this pathway (Figure 2), fructose-6-phosphate is converted to glucosamine-6-phosphate, catalyzed by the first and rate-limiting enzyme, glutamine:fructose-6-phosphate amidotransferase (GFAT). The chief end-product is UDP-N-acetylglucosamine (UDP-GlcNAc) [91], which grants substrates for reactions such as proteoglycan synthesis and the formation of O-linked glycoproteins. Overalteration by this glucosamine frequently gives rise to pathologic transformations in gene expression [59, 92] and has been associated with some of the metabolic consequences of persistent hyperglycemia to promote the complications of diabetes [93, 94]. The reversible O-GlcNAc alteration of proteins by increased HBP activity could cause insulin resistance and the complications of diabetes [95]. Of particular relevance to diabetic vascular complications is the inhibition of endothelial nitric oxide synthase (e-NOS) activity in arterial endothelial cells by O-GlcNAcylation [96].

2.1.5. A Common Mechanism of the Major Pathways' Activation. All these major pathways implicated in the pathogenesis of diabetic complications are activated by a single upstream incident, overproduction of reactive oxygen species (superoxide) [97], caused by the hyperglycemic intracellular setting (Figure 2) [40, 58, 59]. Specifically, in cells with high intracellular glucose concentration, there is more glucose-derived pyruvate being oxidized in the tricarboxylic acid (TCA) cycle, escalating the flux of electron donors (NADH and FADH2) into the electron transport chain. As a result, the voltage gradient across the mitochondrial membrane raises until a critical threshold is achieved. At this point, electron transfer inside the mitochondrial electron transport chain causes the leak of one electron to be transferred to molecular oxygen, thereby generating superoxide. Hyperglycemia also diminishes the activity of the key glycolytic enzyme glyceraldehyde-3 phosphate dehydrogenase (GAPDH) [98], and afterward, the level of all the glycolytic intermediates that are upstream of GAPDH increases (Figure 2). Augmented levels of the upstream glycolytic metabolite glyceraldehyde-3-phosphate activate the AGE formation pathway (because the chief intracellular AGE precursor methylglyoxal is formed from glyceraldehyde-3 phosphate) and also the classic PKC pathway (since the activator of PKC, diacylglycerol, is also formed from glyceraldehyde-3 phosphate). Further upstream, amounts of the glycolytic metabolite fructose-6 phosphate increase, which enhances flux through the hexosamine pathway. Finally, inhibition of GAPDH boosts up intracellular amounts of glucose, which enhances flux through the polyol pathway. The hindering mechanisms act through the poly-ADP-ribose polymerase (PARP) pathway, which alters GAPDH through polymers of ADP-ribose. Hyperglycemia provokes overproduction of ROS [99] and DNA single-strand cracks [100], both of which can stimulate PARP [101], thereby resulting in an alteration of GAPDH and a decrease of its activity [102] (Figure 2).

At the same time, metabolism has also evolved to respond to such ROS stresses in an adaptive manner. Frequently, the mechanism revolves around thiol-based switches that allow the cell to rewire metabolism in a way that promotes an antioxidant response independent of transcriptional or signaling pathways. Cells tune glycolytic metabolism to cope with oxidative damage by diverting glycolytic flux into NADPH-generating processes (Figure 1). The oxidative pentose phosphate pathway (ox-PPP), which produces ribose-5-phosphate, a precursor for nucleotide synthesis, is traditionally considered the predominant producer of cellular NADPH and is thus critical for antioxidant defense [103, 104]. Figure 1 depicts the sites whereupon ROS-mediated inhibition of glycolysis reroutes flux into the oxidative arm of the pentose phosphate pathway, to produce more NADPH and maintain cellular reducing power.

In summary, in today's environment, an overabundance of calories through food intake, combined with an inactive way of life in people with DM, results in high glucose (and fatty acid) accrual within the muscle, adipose tissue, and pancreatic cells [105], which provokes generation of ROS. ROS can act as signaling molecules, but when their production is exacerbated, they induce mitochondrial dysfunction and a decrease in ATP production. This stimulates PARP, lowers GAPDH activity, plays a significant role in increasing flux of the polyol pathway, stimulates PKC, raises intracellular production of AGEs, and overexcites the hexosamine pathway. This mechanism provides a refined link between hyperglycemia-induced oxidative stress and diabetic complications.

Given this pivotal role of hyperglycemia and oxidative stress on the development of diabetic complications, it is reasonable to assume that therapeutic strategies targeting these biological mechanisms could be pivotal to manage diabetes and prevent its serious complications. Thus, antidiabetic therapeutic agents, both pharmacologic and nonpharmacologic (e.g., diet and exercise), with combined hypoglycemic and antioxidant capacities, are thought to be better suited for preventing complications. In fact, all major classes of hypoglycemic agents have been investigated not only for their glucose-lowering but also for their antioxidant capacities as well [106].

In particular, metformin, the first-line antidiabetic medication in most persons with type 2 DM, which is an activator of AMP-activated protein kinase (AMPK) and suppresses

hepatic glucose synthesis, improves insulin sensitivity by enhancing insulin-stimulated peripheral glucose uptake. Emerging evidence suggests that metformin boasts both direct and indirect antioxidant and anti-inflammatory properties, which may be contributing to its CVD protective effects [107]. Several mechanisms that explain metformin's beneficial actions have been proposed, including NF-κB inhibition, NO production increment, and inhibition of AGEs formation. The antioxidative effect of metformin may be related to the reduction of diacylglycerol (DAG) levels, inhibition of PKC translocation to the cellular membrane, and suppression of the NADPH oxidase activity, leading to reduced ROS production [108]. In obese mice fed with a high-fat diet, treatment with metformin improved endothelial function by reducing endoplasmic reticulum stress and superoxide production and by increasing NO bioavailability [109]. Metformin has also been shown to directly inhibit ROS production from complex I (NADH: ubiquinone oxidoreductase) of the mitochondrial ETC [110] and to increase the AMP/ATP ratio. A recent study demonstrated that metformin treatment ameliorated high glucose-induced beta cell dysfunction by decreasing intracellular ROS production [111]. Even in prediabetic persons treated with metformin therapy, it was shown that their abdominal fat tissue presented higher sirtuin-6 (SIRT-6) expression and lower NF-κB, PPAR-γ, and SREBP-1 expression levels, compared to a prediabetic control group [112]. Of note, it is known that SIRT6 activity is negatively regulated through reactive nitrogen species-mediated tyrosine nitration during oxidative stress [113], and at baseline, obese prediabetic patients show higher values of inflammatory and oxidative stress markers, and lower values of SIRT6 tissue protein expression than normoglycemic subjects, with a beneficial effect exerted by metformin therapy [112].

Thiazolidinediones (TZDs), including rosiglitazone and pioglitazone, are a class of drugs known to improve insulin sensitivity in peripheral tissues by binding to and activating the peroxisome proliferator-activated receptor gamma (PPARg). This receptor is involved in the regulation of expression of insulin-sensitive genes, which are crucial to glucose and lipid metabolism. Apart from the hypoglycemic effects, TZDs have shown an ability to modulate inflammatory, oxidative, and vascular functions. In *in vitro* and *in vivo* studies, pioglitazone protects against oxidative stress, reduces blood pressure, and decreases vascular cell adhesion molecule-1 (VCAM-1) expression on endothelial cells through modulation of NF-κB activity via a PPARa-dependent mechanism [114]. It is postulated that these hypoglycemic and antioxidant effects, together with the anti-inflammatory effects of pioglitazone, have contributed to the beneficial cardiovascular effects seen in the PROACTIVE (Prospective Pioglitazone Clinical Trial in Macrovascular Events) trial [115].

Regarding insulin and sulphonylureas, in patients with type 2 DM, insulin treatment only partially improved oxidative stress parameters, as evidenced by the elevated levels of thiobarbituric acid reactive substances and reduced erythrocyte GSH [116]. Treatment with gliclazide for 12 weeks, on the other hand, ameliorated oxidative stress better than did glibenclamide [117]. Since gliclazide is one of the few hypoglycemic agents with an antioxidant effect [118], this may have contributed to the delayed progression of diabetic nephropathy in the ADVANCE trial [119], although it produced no significant effect on the development or progression of retinopathy or macrovascular complications in that study.

The incretin-based therapies, which include DPP-IV inhibitors [120] and GLP-1 receptor (GLP-1R) agonists [121], are a new class of antidiabetic medications, which aim to ameliorate the "incretin defect" present in people with diabetes [122]. Over the last years, extrapancreatic protective effects, behind glucose-insulin control, have been suggested in distinct vascular conditions [123–125]. In addition to regulating glucose and metabolic control, GLP-1 has a potential beneficial effect on multiple pathways involved in atherogenesis. Although the mechanisms of vascular effect are still unclear, it seems that the protective action of GLP-1 may be related to an improvement in endothelial dysfunction through its anti-inflammatory and antioxidant effects [126]. Even in patients with diabetes and nonobstructive CHD, it has been shown that after a non-ST-elevation myocardial infarction, people previously treated with incretins had beneficial effects on all-cause mortality, cardiac death, and readmission for acute coronary syndrome, compared to people not previously treated with incretins [127]. Liraglutide exerts marked antioxidant and anti-inflammatory effects on vascular ECs by increasing NO production, with inhibition of PKC-a, NADPH oxidase, NF-κB, and JNK signaling, while also leading to the overexpression of superoxide dismutase (SOD) and catalase protective antioxidant enzymes [128]. Furthermore, it has been reported that liraglutide protects against atherogenesis by the reduction of Ox-LDL-induced mitochondrial ROS in human aortic vascular smooth muscle cells [129]. Regarding DPP-IV inhibitors, studies have demonstrated antioxidant and anti-inflammatory effects in animal models of diabetic nephropathy and diabetic retinopathy [130–132]. Clinical studies have failed though to show any benefit of this class of medications on CVD protection in people with DM at increased CVD risk [120].

Finally, the sodium-glucose cotransporter-2 (SGLT-2) inhibitors are the latest class of antidiabetic substances introduced in our therapeutic armamentarium for glycemic control. They work by inhibiting the absorption of glucose from the proximal tubule of the kidney, hence causing glucosuria, and have shown extremely favorable effects regarding cardiac and renal protection in persons with DM [133]. Recently, a few studies indicated that SGLT-2 inhibitors may exert their CVD and renal protection via anti-inflammatory and antioxidative effects [134]. Dapagliflozin was found to attenuate the formation of atherosclerotic lesions, increase the stability of lesions, reduce the production of IL-1b by macrophage infiltration, and decrease mitochondrial ROS generation in mice. These effects may be associated with an inhibitory effect on the NLRP3 inflammasome in diabetic atherosclerosis, which provides further evidence for its benefits in diabetic patients [135]. Moreover, also in diabetic rats, empagliflozin was shown to improve hyperglycemia, reduce urinary excretion levels of tubular injury markers, decrease expression levels of oxidative stress biomarkers (AGEs and

RAGE), and reduce inflammatory and fibrotic markers in the kidney, including MCP-1, ICAM-1, PAI-1, and TGF-β [134]. These data suggest that a blockade of SGLT-2 by empagliflozin might protect proximal tubular cells from glucotoxicity in diabetic nephropathy, partly via suppression of the AGE-RAGE-mediated oxidative stress generation. These effects may have contributed to the beneficial effects seen with these agents in clinical trials of CVD and renal protection [136].

2.2. Glycemic Variability and Oxidative Stress. The assessment of glycemia by determining HbA1c reflects the average blood glucose levels over around the previous 2-3 months but does not afford any information about the actual fluctuations of glucose [137]. Because of this, individuals with similar HbA1c values may actually have had wide variations in their blood glucose levels over that period. It has been proposed that repeated or large glucose swings may contribute to diabetes-related complications, unrelated to HbA1c degree [138]. Postprandial escalations in blood glucose, together with hypoglycemic events, are blamed for higher cardiovascular events in DM [139], and postprandial plasma glucose has been associated in some studies more strongly to cardiovascular disease than fasting plasma glucose [140]. Glycemic variability (GV), i.e., oscillations in blood glucose levels over time, can represent the existence of excess glycemic excursions and, consequently, the risk of both of these events (hyperglycemic spikes and hypoglycemic episodes) [141, 142] and has been associated with the presence and severity of CVD in persons with diabetes [143].

Glycemic variability is currently defined in many different ways, either as short-term (within-day and between-day variability) [142] or long-term GV, usually based on sequential determinations of HbA1c, fasting blood glucose or other degrees of glycemia over a longer period (months or years) [144]. In the past, short-term glycemic variability was computed from self-monitoring of blood glucose with fingersticks during a few days, but this method has been largely replaced over the past few years by continuous glucose monitoring (CGM), performed with the use of special devices [145] that measure the interstitial glucose levels continuously over several days [146]. These methods address many of the limitations inherent in HbA1c and self-monitoring of blood glucose [147]. The best and most accurate way to evaluate GV is still debated though [148], and the clinical relationship between GV and diabetes complications is actually difficult to ascertain because different studies are very heterogeneous regarding their design and the ways they use to assess GV.

Several studies (albeit not all [149–151]) have shown a positive relationship between glycemic variability and diabetes complications, both macrovascular and microvascular [152], as well as total and CVD mortality in both types of diabetes [144, 153, 154]. These data are in line with evidence that glycemic variability adversely affects plaque stability [155], is related to subclinical coronary atherosclerosis [156], and prolongs corrected QT interval duration [157], being also associated with the development of cardiac autonomic neuropathy [158–160].

Oxidative stress has been incriminated as the underlying mechanism for these effects of GV [161, 162] by the stimulation of superoxide production together with NADPH oxidase [163]. Interestingly, intermittently increased glucose levels have been shown to produce more oxidative stress than constantly elevated levels, since markers of inflammation, a well-recognized sign of oxidative stress, have been observed to increase in response to sporadically elevated glucose levels. In a study contrasting the consequences of inconsistent vs. constant glycemic conditions on cultured human kidney cells, it was noted that production of the inflammatory cytokines, transforming growth factor-β (TGF-β), and insulin-like growth factor-binding protein-3 (IGFBP-3) increased to a larger degree when exposed to erratic glucose concentrations compared with constant hyperglycemic states [164].

In other experimental studies, erratically high blood glucose rather than constant high blood glucose exposure was again shown to have harmful consequences [161, 165, 166]. In *in vivo* and *in vitro* studies, GV was associated with greater ROS production and vascular damage, compared to chronic hyperglycemia [162]. Intermittent high glucose levels (5 and 20 mmol/L (90 and 360 mg/dL) every 24 hours) induced ROS generation, which led to increased cellular apoptosis in human umbilical vein endothelial cells, compared with a constant high glucose setting (20 mmol/L (360 mg/dL)) [161, 165, 167]. *In vivo*, Horvath et al. investigated the effect of GV on oxidative stress and endothelial function in streptozotocin- (STZ-) induced diabetic rats [166]. Diabetic rats treated with intermediate long-acting insulin (insulin glargine) to accomplish stable normalization of blood glucose levels or long-acting insulin (ultralente insulin) once every other day, to generate "glycemic fluctuations" for 14 days, showed differing results of ROS production. Nitrotyrosine levels and endothelial dysfunction were elevated in diabetic rats with "glycemic swings" compared to rats with stable normalization of blood glucose.

Studies in humans have also substantiated these results. The effect of GV on oxidative stress and endothelial function in healthy controls and patients with T2D was examined with a euinsulinemic hyperglycemic clamp, to compare three different glycemic profiles over 24 hours: (1) 10 mmol/L (180 mg/dL) persistently, (2) 15 mmol/L (270 mg/dL) persistently, and (3) 5 and 15 mmol/L (90 and 270 mg/dL) every 6 hours ("glycemic swings") [168]. It was found that GV produced greater endothelial dysfunction and oxidative stress, assessed by plasma 3-nitrotyrosine and 24-hour urinary excretion rate of 8-iso-PGF2a compared with persistent, either 10 or 15 mmol/L (180 or 270 mg/dL), glucose. These changes were overturned by concurrent infusion of vitamin C, suggesting that oxidative stress was the cause of endothelial dysfunction.

The association between GV and oxidative stress has also been investigated using CGM. A strong positive correlation between mean amplitude of glycemic excursions (MAGE, a marker of GV assessed by CGM) and a marker of oxidative stress (24-hour urinary excretion rate of 8-iso-PGF2a) was found in 21 patients with T2D [169]. A significant association between GV and the 24-hour urinary excretion rate of PGF2a in 26 T2D patients treated with diet and/or metformin has also been reported [170]. Furthermore, evidence exists that hyperglycemia after recovery from hypoglycemia

leads to deterioration of endothelial function and rising oxidative stress and inflammation both in healthy control individuals and patients with type 1 diabetes (T1D), but not when recovery from hypoglycemia is followed by normoglycemia [171].

However, as mentioned earlier, some studies have shown conflicting results. Siegelaar et al. reported no significant correlation between GV and 24-hour urinary excretion of PGF2a in patients with T2D, well-controlled with oral antidiabetic medications [150]. In another study, Wentholt et al. explored the association between GV, assessed by CGM, and oxidative stress, assessed by 24-hour urinary excretion of 8-iso-PGF2a, in 25 patients with T1D [172]. Although higher levels of 8-iso-PGF2a were detected in patients with T1D compared with healthy subjects, no significant association was found between GV and oxidative stress in these patients. Differences in medications and patients' characteristics and also the dissimilar methods used to determine oxidative stress (ELISA vs. tandem mass spectrometry for 8-iso-PGF2a measurement) may explain the inconsistent results among these studies.

2.3. Hypoglycemia and Oxidative Stress. The maintenance of normoglycemia during treatment of diabetes while also trying to avoid hypoglycemia is a major challenge for patients and treating physicians. It has also been shown that excessive short-term glycemic variability, especially in the presence of target HbA1c levels, can contribute to the risk of hypoglycemia in both types of diabetes [173, 174].

There is evidence that hypoglycemia may unfavorably influence cardiovascular risk in patients with diabetes [175], and this is one possible explanation for the lack of CVD prevention in trials of intensive glycemic control. The ACCORD study [176], for example, showed that struggling to attain a very ambitiously low glycemic goal (HbA1c < 6% (42 mmol/-mol)) with intensive therapy resulted in a greater incidence of hypoglycemia, although this increase was not proven to be causally related to the augmented risk of cardiac death observed in the study [177].

Hypoglycemia produces a surge of physiologic effects that may involve generation of oxidative stress and cardiac arrhythmias, contribute to sudden cardiac death, and bring about ischemic cerebral damage [178], portraying several likely mechanisms through which acute and chronic incidents of hypoglycemia may increase CVD risk [179, 180].

Hypoglycemia stimulates the sympathoadrenal system, causing a prolific discharge of catecholamines that exercise overwhelming hemodynamic and hemorheological effects [181]. The fact that hypoglycemia results in platelet hyperaggregability [182] and augmentation in several factors involved in the coagulation cascade has been known for over two decades. Activated partial thromboplastin time is abridged; fibrinogen and factor VIII increase and platelet numbers descend in association with hypoglycemia. These effects have the aptitude to compromise endothelial function, blood flow, and tissue perfusion, endangering intravascular coagulation, and thrombosis [183]. The proinflammatory effects of hypoglycemia in humans with or without diabetes were lately examined by *ex vivo* stimulations of peripheral blood mononuclear cells (PBMCs) and monocytes obtained during hyperinsulinemic-euglycemic-hypoglycemic clamps in eleven healthy controls, ten patients with T1D and normal awareness of hypoglycemia (NAH), and ten patients with T1D and impaired awareness of hypoglycemia (IAH). Hypoglycemia increased leukocyte counts in healthy controls and patients with NAH, but not in patients with IAH. Leukocytosis was robustly associated with the adrenaline response to hypoglycemia. The production of proinflammatory cytokines from stimulated polymorphonuclear cells and monocytes was larger after hypoglycemia compared to euglycemia, although it was less prominent in patients with IAH [184].

Furthermore, several studies have shown an association between hypoglycemia and ROS production. In experimental cell cultures, complete glucose deprivation stimulated the creation of mitochondrial ROS and AMP-kinase in cultured human umbilical vein endothelial cells (HUVECs) [185]. Moreover, insulin-induced recurrent hypoglycemia (two episodes/day for two weeks) in STZ-induced diabetic rats led to an increase in malondialdehyde (MDA) levels (product of the oxidation of n-6 unsaturated fatty acids) and a reduction in aconitase activity, which is an indicator of oxidative stress in brain mitochondria [186].

Insulin-induced hypoglycemia in nondiabetic male subjects was associated with increased proinflammatory cytokines (TNF-α, IL-1β, IL-6, and IL-8), indicators of lipid peroxidation and ROS production [187]. The increases in inflammation markers and oxidative stress in this study were very striking, maybe because the method of induction of hypoglycemia was by a bolus intravenous injection, which led to a swift descend of blood glucose concentrations, resulting in a quick release of catecholamines and the stimulation of the inflammatory response.

Two other studies have corroborated that hypoglycemia produces an upsurge in proinflammatory mediators and platelet activation. Wright et al. [183] and Gogitidze Joy et al. [188] both used a hypoglycemic clamp, during which blood glucose levels were retained at 2.5 and 2.9 mmol/L (45 and 52.2 mg/dL), respectively. The former maintained hypoglycemia for 60 min while the latter maintained it for 120 min. The extended duration of hypoglycemia in the study by Gogitidze Joy et al. resulted in a more remarkable rise in proinflammatory mediators, even though blood glucose levels were not as low as in the study by Wright et al. In another study, Ceriello et al. used 2-hour hyperglycemic and hypoglycemic clamps, with or without the concurrent infusion of GLP-1, and quantified markers of oxidative stress (plasma nitrotyrosine and plasma 8-iso-PGF2a) and markers of inflammation (soluble intercellular adhesion molecule-1 (sICAM-1) and IL-6) [189]. It was established that hypoglycemia significantly increased both markers of oxidative stress and inflammation. The same results were found after 2 hours of hyperglycemia. The concurrent infusion of GLP-1 or vitamin C significantly attenuated these effects. Vitamin C was actually more effective, implying a causal role of oxidative stress in favoring the manifestation of endothelial dysfunction and inflammation during hypoglycemia since an antioxidant agent was beneficial in attenuating the detrimental hypoglycemia-induced effects. When GLP-1 and vitamin C

were infused concurrently, the harmful effect of hypoglycemia was almost entirely offset.

3. Conclusions

The overproduction of reactive oxygen species (ROS) is very harmful to the cell. Many studies are linking oxidative stress with a lot of pathological conditions, including diabetes as well as other human diseases. It has been reported that oxidative stress is implicated in the pathogenesis of diabetes per se, but also plays a major role in the occurrence and evolution of diabetic complications in both types of diabetes.

All three glycemic indices (hyperglycemia, glycemic variability, and hypoglycemia) have been associated with ROS production. Various mechanisms associated with hyperglycemia, such as the production of AGEs, the activation of PKC, the accumulation of sorbitol, and the hyperactivity of the hexosamine pathway, lead to reactive oxygen species overproduction and a decrease in the endogenous antioxidant defense systems. Several other studies have pointed that glycemic variability (GV) compared to chronic hyperglycemia is associated with greater ROS production, leading to vascular damage, most likely acting through the same mechanisms as hyperglycemia, but also with the possible additional effects of hypoglycemia. Recent evidence suggests that hypoglycemia is implicated in the production of oxidative stress, inflammation, hypercoagulability, and endothelial dysfunction, all of which favor diabetic vascular disorders. However, the exact mechanism by which oxidative stress is associated with hypoglycemia and the precise mechanism by which oxidative stress specifically contributes to the development of diabetic complications are partly unknown and need to be elucidated in future studies.

Conflicts of Interest

The authors declare no conflict of interest.

References

[1] K. Maiese, "New insights for oxidative stress and diabetes mellitus," *Oxidative Medicine and Cellular Longevity*, vol. 2015, Article ID 875961, 17 pages, 2015.

[2] E. Niki, "Oxidative stress and antioxidants: distress or eustress?," *Archives of Biochemistry and Biophysics*, vol. 595, pp. 19–24, 2016.

[3] D. J. Betteridge, "What is oxidative stress?," *Metabolism: clinical and experimental*, vol. 49, no. 2, pp. 3–8, 2000.

[4] J. P. Kehrer and L.-O. Klotz, "Free radicals and related reactive species as mediators of tissue injury and disease: implications for health," *Critical Reviews in Toxicology*, vol. 45, no. 9, pp. 765–798, 2015.

[5] W. Dröge, "Free radicals in the physiological control of cell function," *Physiological Reviews*, vol. 82, no. 1, pp. 47–95, 2002.

[6] A. Daiber, F. di Lisa, M. Oelze et al., "Crosstalk of mitochondria with NADPH oxidase via reactive oxygen and nitrogen species signalling and its role for vascular function," *British Journal of Pharmacology*, vol. 174, no. 12, pp. 1670–1689, 2017.

[7] V. Lobo, A. Patil, A. Phatak, and N. Chandra, "Free radicals, antioxidants and functional foods: impact on human health," *Pharmacognosy Reviews*, vol. 4, no. 8, pp. 118–126, 2010.

[8] P. Pacher, J. S. Beckman, and L. Liaudet, "Nitric oxide and peroxynitrite in health and disease," *Physiological Reviews*, vol. 87, no. 1, pp. 315–424, 2007.

[9] J.-M. Lü, P. H. Lin, Q. Yao, and C. Chen, "Chemical and molecular mechanisms of antioxidants: experimental approaches and model systems," *Journal of Cellular and Molecular Medicine*, vol. 14, no. 4, pp. 840–860, 2010.

[10] E. Mullarky and L. C. Cantley, "Diverting glycolysis to combat oxidative stress," in *Innovative Medicine*, pp. 3–23, Springer, Japan, 2015.

[11] A. W. Segal, "How neutrophils kill microbes," *Annual Review of Immunology*, vol. 23, no. 1, pp. 197–223, 2005.

[12] H. Sies, "Hydrogen peroxide as a central redox signaling molecule in physiological oxidative stress: oxidative eustress," *Redox Biology*, vol. 11, pp. 613–619, 2017.

[13] M. D. Brand, "Mitochondrial generation of superoxide and hydrogen peroxide as the source of mitochondrial redox signaling," *Free Radical Biology and Medicine*, vol. 100, pp. 14–31, 2016.

[14] K. Aschbacher, A. O'Donovan, O. M. Wolkowitz, F. S. Dhabhar, Y. Su, and E. Epel, "Good stress, bad stress and oxidative stress: insights from anticipatory cortisol reactivity," *Psychoneuroendocrinology*, vol. 38, no. 9, pp. 1698–1708, 2013.

[15] N. T. Moldogazieva, I. M. Mokhosoev, T. I. Mel'nikova, S. P. Zavadskiy, A. N. Kuz'menko, and A. A. Terentiev, "Dual character of reactive oxygen, nitrogen, and halogen species: endogenous sources, interconversions and neutralization," *Biochemistry (Moscow)*, vol. 85, Supplement 1, pp. 56–78, 2020.

[16] T. Liu, A. Stern, L. J. Roberts, and J. D. Morrow, "The isoprostanes: novel prostaglandin-like products of the free radical-catalyzed peroxidation of arachidonic acid," *Journal of Biomedical Science*, vol. 6, no. 4, pp. 226–235, 1999.

[17] M. P. Murphy, "How mitochondria produce reactive oxygen species," *Biochemical Journal*, vol. 417, no. 1, pp. 1–13, 2009.

[18] D. A. Kostić, D. S. Dimitrijević, G. S. Stojanović, I. R. Palić, A. S. Đorđević, and J. D. Ickovski, "Xanthine oxidase: isolation, assays of activity, and inhibition," *Journal of Chemistry*, vol. 2015, Article ID 294858, 8 pages, 2015.

[19] F. J. Gonzalez, "Role of cytochromes P450 in chemical toxicity and oxidative stress: studies with CYP2E1," *Mutation Research - Fundamental and Molecular Mechanisms of Mutagenesis*, vol. 569, no. 1–2, pp. 101–110, 2005.

[20] S. Luo, H. Lei, H. Qin, and Y. Xia, "Molecular mechanisms of endothelial NO synthase uncoupling," *Current Pharmaceutical Design*, vol. 20, no. 22, pp. 3548–3553, 2014.

[21] W. M. Nauseef, "Myeloperoxidase in human neutrophil host defence," *Cellular Microbiology*, vol. 16, no. 8, pp. 1146–1155, 2014.

[22] I. S. Young and J. V. Woodside, "Antioxidants in health and disease," *Journal of Clinical Pathology*, vol. 54, no. 3, pp. 176–186, 2001.

[23] M. Valko, D. Leibfritz, J. Moncol, M. T. D. Cronin, M. Mazur, and J. Telser, "Free radicals and antioxidants in normal physiological functions and human disease," *The International Journal of Biochemistry & Cell Biology*, vol. 39, no. 1, pp. 44–84, 2007.

[24] B. Halliwell and J. M. C. Gutteridge, "The definition and measurement of antioxidants in biological systems," *Free Radical Biology & Medicine*, vol. 18, no. 1, pp. 125-126, 1995.

[25] B. Halliwell, "Biochemistry of oxidative stress," *Biochemical Society Transactions*, vol. 35, no. 5, pp. 1147–1150, 2007.

[26] D. Giugliano, "Dietary antioxidants for cardiovascular prevention," *Nutrition, metabolism, and cardiovascular diseases: NMCD*, vol. 10, no. 1, pp. 38–44, 2000.

[27] K. H. Cheeseman and T. F. Slater, "An introduction to free radical biochemistry," *British Medical Bulletin*, vol. 49, no. 3, pp. 481–493, 1993.

[28] J. K. Willcox, S. L. Ash, and G. L. Catignani, "Antioxidants and prevention of chronic disease," *Critical Reviews in Food Science and Nutrition*, vol. 44, no. 4, pp. 275–295, 2004.

[29] Z. Hracsko, H. Orvos, Z. Novak, A. Pal, and I. S. Varga, "Evaluation of oxidative stress markers in neonates with intrauterine growth retardation," *Redox report*, vol. 13, no. 1, pp. 11–16, 2013.

[30] E. Herrera and C. Barbas, "Vitamin E: action, metabolism and perspectives," *Journal of Physiology and Biochemistry*, vol. 57, no. 1, pp. 43–56, 2001.

[31] S. J. Padayatty, A. Katz, Y. Wang et al., "Vitamin C as an antioxidant: evaluation of its role in disease prevention," *Journal of the American College of Nutrition*, vol. 22, no. 1, pp. 18–35, 2003.

[32] E. J. Johnson, "The role of carotenoids in human health," *Nutrition in clinical care*, vol. 5, no. 2, pp. 56–65, 2002.

[33] N. J. Miller, J. Sampson, L. P. Candeias, P. M. Bramley, and C. A. Rice-Evans, "Antioxidant activities of carotenes and xanthophylls," *FEBS Letters*, vol. 384, no. 3, pp. 240–242, 1996.

[34] L. Monnier, C. Colette, and D. Owens, "The glycemic triumvirate and diabetic complications: is the whole greater than the sum of its component parts?," *Diabetes Research and Clinical Practice*, vol. 95, no. 3, pp. 303–311, 2012.

[35] P. Saeedi, I. Petersohn, P. Salpea et al., "Global and regional diabetes prevalence estimates for 2019 and projections for 2030 and 2045: results from the International Diabetes Federation Diabetes Atlas, 9th edition," *Diabetes Research and Clinical Practice*, vol. 157, article 107843, 2019.

[36] C. Bommer, V. Sagalova, E. Heesemann et al., "Global economic burden of diabetes in adults: projections from 2015 to 2030," *Diabetes Care*, vol. 41, no. 5, pp. 963–970, 2018.

[37] K. Makrilakis, S. Liatis, A. Tsiakou et al., "Comparison of health-related quality of Life (HRQOL) among patients with pre-diabetes, diabetes and normal glucose tolerance, using the 15D-HRQOL questionnaire in Greece: the DEPLAN study," *BMC Endocrine Disorders*, vol. 18, no. 1, p. 32, 2018.

[38] American Diabetes Association, "4. Comprehensive medical evaluation and assessment of Comorbidities:Standards of medical care in diabetes-2020," *Diabetes care*, vol. 43, Supplement 1, pp. S37–S47, 2019.

[39] M. Brownlee and A. Cerami, "The biochemistry of the complications of diabetes mellitus," *Annual Review of Biochemistry*, vol. 50, no. 1, pp. 385–432, 1981.

[40] M. Brownlee, "Biochemistry and molecular cell biology of diabetic complications," *Nature*, vol. 414, no. 6865, pp. 813–820, 2001.

[41] A. Ceriello and E. Motz, "Is oxidative stress the pathogenic mechanism underlying insulin resistance, diabetes, and cardiovascular disease? The common soil hypothesis revisited," *Arteriosclerosis, Thrombosis, and Vascular Biology*, vol. 24, no. 5, pp. 816–823, 2004.

[42] J. L. Evans, B. A. Maddux, and I. D. Goldfine, "The molecular basis for oxidative stress-induced insulin resistance," *Antioxidants & Redox Signaling*, vol. 7, no. 7–8, pp. 1040–1052, 2005.

[43] S. Tangvarasittichai, "Oxidative stress, insulin resistance, dyslipidemia and type 2 diabetes mellitus," *World Journal of Diabetes*, vol. 6, no. 3, pp. 456–480, 2015.

[44] C. Sardu, G. Pieretti, N. D'Onofrio et al., "Inflammatory cytokines and SIRT1 levels in subcutaneous abdominal fat: relationship with cardiac performance in overweight prediabetics patients," *Frontiers in Physiology*, vol. 9, 2018.

[45] E. Rappou, S. Jukarainen, R. Rinnankoski-Tuikka et al., "Weight loss is associated with increased NAD+/SIRT1 expression but reduced PARP activity in white adipose tissue," *Journal of Clinical Endocrinology and Metabolism*, vol. 101, no. 3, pp. 1263–1273, 2016.

[46] Y. Huang, X. Cai, W. Mai, M. Li, and Y. Hu, "Association between prediabetes and risk of cardiovascular disease and all cause mortality: systematic review and meta-analysis," *BMJ*, vol. 355, article i5953, 2016.

[47] C. Sardu, N. D'Onofrio, M. Torella et al., "Pericoronary fat inflammation and Major Adverse Cardiac Events (MACE) in prediabetic patients with acute myocardial infarction: effects of metformin," *Cardiovascular Diabetology*, vol. 18, no. 1, 2019.

[48] D. Giugliano, A. Ceriello, and G. Paolisso, "Oxidative stress and diabetic vascular complications," *Diabetes Care*, vol. 19, no. 3, pp. 257–267, 1996.

[49] S. M. Son, "Role of vascular reactive oxygen species in development of vascular abnormalities in diabetes," *Diabetes Research and Clinical Practice*, vol. 77, no. 3, pp. S65–S70, 2007.

[50] S. P. Wolff and R. T. Dean, "Glucose autoxidation and protein modification. The potential role of 'autoxidative glycosylation' in diabetes," *Biochemical Journal*, vol. 245, no. 1, pp. 243–250, 1987.

[51] J. V. Hunt, R. T. Dean, and S. P. Wolff, "Hydroxyl radical production and autoxidative glycosylation. Glucose autoxidation as the cause of protein damage in the experimental glycation model of diabetes mellitus and ageing," *Biochemical Journal*, vol. 256, no. 1, pp. 205–212, 1988.

[52] P. Martín-Gallán, A. Carrascosa, M. Gussinyé, and C. Domínguez, "Biomarkers of diabetes-associated oxidative stress and antioxidant status in young diabetic patients with or without subclinical complications," *Free Radical Biology and Medicine*, vol. 34, no. 12, pp. 1563–1574, 2003.

[53] K. Haskins, B. Bradley, K. Powers et al., "Oxidative stress in type 1 diabetes," *Annals of the New York Academy of Sciences*, vol. 1005, no. 1, pp. 43–54, 2003.

[54] G. Marra, P. Cotroneo, D. Pitocco et al., "Early increase of oxidative stress and reduced antioxidant defenses in patients with uncomplicated type 1 diabetes: a case for gender difference," *Diabetes Care*, vol. 25, no. 2, pp. 370–375, 2002.

[55] D. M. Niedowicz and D. L. Daleke, "The role of oxidative stress in diabetic complications," *Cell Biochemistry and Biophysics*, vol. 43, no. 2, pp. 289–330, 2005.

[56] E. Burgos-Morón, Z. Abad-Jiménez, A. M. de Marañón et al., "Relationship between oxidative stress, ER stress, and

inflammation in type 2 diabetes: the battle continues," *Journal of Clinical Medicine*, vol. 8, no. 9, 2019.

[57] D. Bonnefont-Rousselot, "Glucose and reactive oxygen species," *Current Opinion in Clinical Nutrition and Metabolic Care*, vol. 5, no. 5, pp. 561–568, 2002.

[58] F. Giacco and M. Brownlee, "Oxidative stress and diabetic complications," *Circulation Research*, vol. 107, no. 9, pp. 1058–1070, 2010.

[59] M. Brownlee, "The pathobiology of diabetic Complications: A Unifying Mechanism," *Diabetes*, vol. 54, no. 6, pp. 1615–1625, 2005.

[60] R. G. Tilton, K. Chang, J. R. Nyengaard, M. Van den Enden, Y. Ido, and J. R. Williamson, "Inhibition of sorbitol dehydrogenase. Effects on vascular and neural dysfunction in streptozocin-induced diabetic rats," *Diabetes*, vol. 44, no. 2, pp. 234–242, 1995.

[61] E. Ciuchi, P. Odetti, and R. Prando, "Relationship between glutathione and sorbitol concentrations in erythrocytes from diabetic patients," *Metabolism: clinical and experimental*, vol. 45, no. 5, pp. 611–613, 1996.

[62] B. S. Szwergold, F. Kappler, and T. R. Brown, "Identification of fructose 3-phosphate in the lens of diabetic rats," *Science*, vol. 247, no. 4941, pp. 451–454, 1990.

[63] A. Ceriello, P. Dello Russo, P. Amstad, and P. Cerutti, "High glucose induces antioxidant enzymes in human endothelial cells in culture; evidence linking hyperglycemia and oxidative stress," *Diabetes*, vol. 45, no. 4, pp. 471–477, 1996.

[64] P. C. Chikezie, O. A. Ojiako, and A. C. Ogbuji, "Oxidative stress in diabetes mellitus," *Integrative Obesity and Diabetes*, vol. 1, no. 3, pp. 71–79, 2015.

[65] A. W. Stitt, A. J. Jenkins, and M. E. Cooper, "Advanced glycation end products and diabetic complications," *Expert Opinion on Investigational Drugs*, vol. 11, no. 9, pp. 1205–1223, 2005.

[66] C. Helou, D. Marier, P. Jacolot et al., "Microorganisms and Maillard reaction products: a review of the literature and recent findings," *Amino Acids*, vol. 46, no. 2, pp. 267–277, 2014.

[67] D. Aronson and E. J. Rayfield, "How hyperglycemia promotes atherosclerosis: molecular mechanisms," *Cardiovascular Diabetology*, vol. 1, no. 1, 2002.

[68] V. P. Singh, A. Bali, N. Singh, and A. S. Jaggi, "Advanced glycation end products and diabetic complications," *Korean Journal of Physiology and Pharmacology*, vol. 18, no. 1, pp. 1–14, 2014.

[69] N. Ahmed, P. J. Thornalley, J. Dawczynski et al., "Methylglyoxal-derived hydroimidazolone advanced glycation endproducts of human lens proteins," *Investigative Ophthalmology and Visual Science*, vol. 44, no. 12, pp. 5287–5292, 2003.

[70] S. Y. Rhee and Y. S. Kim, "The role of advanced glycation end products in diabetic vascular complications," *Diabetes and Metabolism Journal*, vol. 42, no. 3, pp. 188–195, 2018.

[71] S. Yamagishi and T. Imaizumi, "Diabetic vascular complications: pathophysiology, biochemical basis and potential therapeutic strategy," *Current Pharmaceutical Design*, vol. 11, no. 18, pp. 2279–2299, 2005.

[72] C.-L. Hsieh, M. H. Yang, C. C. Chyau et al., "Kinetic analysis on the sensitivity of glucose- or glyoxal-induced LDL glycation to the inhibitory effect of Psidium guajava extract in a physiomimic system," *Bio Systems*, vol. 88, no. 1–2, pp. 92–100, 2007.

[73] H. Yonekura, Y. Yamamoto, S. Sakurai, T. Watanabe, and H. Yamamoto, "Roles of the receptor for advanced glycation endproducts in diabetes-induced vascular injury," *Journal of Pharmacological Sciences*, vol. 97, no. 3, pp. 305–311, 2005.

[74] M. B. Manigrasso, J. Juranek, R. Ramasamy, and A. M. Schmidt, "Unlocking the biology of RAGE in diabetic microvascular complications," *Trends in Endocrinology and Metabolism*, vol. 25, no. 1, pp. 15–22, 2014.

[75] H. Yonekura, Y. Yamamoto, S. Sakurai et al., "Novel splice variants of the receptor for advanced glycation endproducts expressed in human vascular endothelial cells and pericytes, and their putative roles in diabetes-induced vascular injury," *Biochemical Journal*, vol. 370, no. 3, pp. 1097–1109, 2003.

[76] A. M. Schmidt, O. Hori, J. X. Chen et al., "Advanced glycation endproducts interacting with their endothelial receptor induce expression of vascular cell adhesion molecule-1 (VCAM-1) in cultured human endothelial cells and in mice. A potential mechanism for the accelerated vasculopathy of diabetes," *The Journal of Clinical Investigation*, vol. 96, no. 3, pp. 1395–1403, 1995.

[77] D. Han, Y. Yamamoto, S. Munesue et al., "Induction of receptor for advanced glycation end products by insufficient leptin action triggers pancreatic β-cell failure in type 2 diabetes," *Genes to Cells*, vol. 18, no. 4, pp. 302–314, 2013.

[78] M. Lu, M. Kuroki, S. Amano et al., "Advanced glycation end products increase retinal vascular endothelial growth factor expression," *Journal of Clinical Investigation*, vol. 101, no. 6, pp. 1219–1224, 1998.

[79] R. Bucala, Z. Makita, G. Vega et al., "Modification of low density lipoprotein by advanced glycation end products contributes to the dyslipidemia of diabetes and renal insufficiency," *Proceedings of the National Academy of Sciences*, vol. 91, no. 20, pp. 9441–9445, 1994.

[80] A. M. Schmidt and D. Stern, "Atherosclerosis and diabetes: the RAGE connection," *Current atherosclerosis reports*, vol. 2, no. 5, pp. 430–436, 2000.

[81] T. Wendt, L. Bucciarelli, W. Qu et al., "Receptor for advanced glycation endproducts (RAGE) and vascular inflammation: insights into the pathogenesis of macrovascular complications in diabetes," *Current atherosclerosis reports*, vol. 4, no. 3, pp. 228–237, 2002.

[82] K. Nakamura, S. I. Yamagishi, H. Adachi et al., "Elevation of soluble form of receptor for advanced glycation end products (sRAGE) in diabetic subjects with coronary artery disease," *Diabetes/Metabolism Research and Reviews*, vol. 23, no. 5, pp. 368–371, 2007.

[83] S. F. Steinberg, "Structural basis of protein kinase C isoform function," *Physiological Reviews*, vol. 88, no. 4, pp. 1341–1378, 2008.

[84] P. Xia, T. Inoguchi, T. S. Kern, R. L. Engerman, P. J. Oates, and G. L. King, "Characterization of the mechanism for the chronic activation of diacylglycerol-protein kinase C pathway in diabetes and hypergalactosemia," *Diabetes*, vol. 43, no. 9, pp. 1122–1129, 1994.

[85] H. Konishi, M. Tanaka, Y. Takemura et al., "Activation of protein kinase C by tyrosine phosphorylation in response to H2O2," *Proceedings of the National Academy of Sciences*, vol. 94, no. 21, pp. 11233–11237, 1997.

[86] T. Nishikawa, D. Edelstein, X. L. du et al., "Normalizing mitochondrial superoxide production blocks three pathways of

hyperglycaemic damage," *Nature*, vol. 404, no. 6779, pp. 787–790, 2000.

[87] H. Ha, M. R. Yu, Y. J. Choi, M. Kitamura, and H. B. Lee, "Role of High Glucose-Induced Nuclear Factor-κB Activation in Monocyte Chemoattractant Protein-1 Expression by Mesangial Cells," *Journal of the American Society of Nephrology*, vol. 13, no. 4, pp. 894–902, 2002.

[88] N. Dasevcimen and G. King, "The role of protein kinase C activation and the vascular complications of diabetes," *Pharmacological Research*, vol. 55, no. 6, pp. 498–510, 2007.

[89] P. Geraldes and G. L. King, "Activation of protein kinase C isoforms and its impact on diabetic complications," *Circulation Research*, vol. 106, no. 8, pp. 1319–1331, 2010.

[90] L. Wells, K. Vosseller, and G. W. Hart, "Glycosylation of nucleocytoplasmic proteins: signal transduction and O-GlcNAc," *Science*, vol. 291, no. 5512, pp. 2376–2378, 2001.

[91] M. G. Buse, "Hexosamines, insulin resistance, and the complications of diabetes: current status," *American Journal of Physiology Endocrinology and Metabolism*, vol. 290, no. 1, pp. E1–E8, 2006.

[92] X.-L. Du, D. Edelstein, L. Rossetti et al., "Hyperglycemia-induced mitochondrial superoxide overproduction activates the hexosamine pathway and induces plasminogen activator inhibitor-1 expression by increasing Sp1 glycosylation," *Proceedings of the National Academy of Sciences of the United States of America*, vol. 97, no. 22, pp. 12222–12226, 2000.

[93] V. Kolm-Litty, U. Sauer, A. Nerlich, R. Lehmann, and E. D. Schleicher, "High glucose-induced transforming growth factor beta1 production is mediated by the hexosamine pathway in porcine glomerular mesangial cells," *Journal of Clinical Investigation*, vol. 101, no. 1, pp. 160–169, 1998.

[94] L. R. James, D. Tang, A. Ingram et al., "Flux through the hexosamine pathway is a determinant of nuclear factor kappaB- dependent promoter activation," *Diabetes*, vol. 51, no. 4, pp. 1146–1156, 2002.

[95] R. J. Copeland, J. W. Bullen, and G. W. Hart, "Cross-talk between GlcNAcylation and phosphorylation: roles in insulin resistance and glucose toxicity," *American Journal of Physiology - Endocrinology and Metabolism*, vol. 295, no. 1, pp. E17–E28, 2008.

[96] B. Musicki, M. F. Kramer, R. E. Becker, and A. L. Burnett, "Inactivation of phosphorylated endothelial nitric oxide synthase (Ser-1177) by O-GlcNAc in diabetes-associated erectile dysfunction," *Proceedings of the National Academy of Sciences of the United States of America*, vol. 102, no. 33, pp. 11870–11875, 2005.

[97] D. C. Wallace, "Diseases of the mitochondrial DNA," *Annual Review of Biochemistry*, vol. 61, no. 1, pp. 1175–1212, 1992.

[98] X. Du, T. Matsumura, D. Edelstein et al., "Inhibition of GAPDH activity by poly(ADP-ribose) polymerase activates three major pathways of hyperglycemic damage in endothelial cells," *Journal of Clinical Investigation*, vol. 112, no. 7, pp. 1049–1057, 2003.

[99] C. S. Sultan, A. Saackel, A. Stank et al., "Impact of carbonylation on glutathione peroxidase-1 activity in human hyperglycemic endothelial cells," *Redox Biology*, vol. 16, pp. 113–122, 2018.

[100] Y. Mikhed, A. Daiber, and S. Steven, "Mitochondrial oxidative stress, mitochondrial DNA damage and their role in age-related vascular dysfunction," *International Journal of Molecular Sciences*, vol. 16, no. 7, pp. 15918–15953, 2015.

[101] E. M. Zakaria, H. M. El-Bassossy, N. N. El-Maraghy, A. F. Ahmed, and A. A. Ali, "PARP-1 inhibition alleviates diabetic cardiac complications in experimental animals," *European Journal of Pharmacology*, vol. 791, pp. 444–454, 2016.

[102] W. D. Qin, G. L. Liu, J. Wang et al., "Poly(ADP-ribose) polymerase 1 inhibition protects cardiomyocytes from inflammation and apoptosis in diabetic cardiomyopathy," *Oncotarget*, vol. 7, no. 24, pp. 35618–35631, 2016.

[103] D. Holten, D. Procsal, and H. L. Chang, "Regulation of pentose phosphate pathway dehydrogenases by NADP+ NADPH ratios," *Biochemical and Biophysical Research Communications*, vol. 68, no. 2, pp. 436–441, 1976.

[104] R. C. Stanton, "Glucose-6-phosphate dehydrogenase, NADPH, and cell survival," *IUBMB Life*, vol. 64, no. 5, pp. 362–369, 2012.

[105] E. Wright, J. L. Scism-Bacon, and L. C. Glass, "Oxidative stress in type 2 diabetes: the role of fasting and postprandial glycaemia," *International Journal of Clinical Practice*, vol. 60, no. 3, pp. 308–314, 2006.

[106] J. S. Teodoro, S. Nunes, A. P. Rolo, F. Reis, and C. M. Palmeira, "Therapeutic options targeting oxidative stress, mitochondrial dysfunction and inflammation to hinder the progression of vascular complications of diabetes," *Frontiers in Physiology*, vol. 9, 2019.

[107] S. J. Griffin, J. K. Leaver, and G. J. Irving, "Impact of metformin on cardiovascular disease: a meta-analysis of randomised trials among people with type 2 diabetes," *Diabetologia*, vol. 60, no. 9, pp. 1620–1629, 2017.

[108] B. Batchuluun, T. Inoguchi, N. Sonoda et al., "Metformin and liraglutide ameliorate high glucose-induced oxidative stress via inhibition of PKC-NAD(P)H oxidase pathway in human aortic endothelial cells," *Atherosclerosis*, vol. 232, no. 1, pp. 156–164, 2014.

[109] W. S. Cheang, X. Y. Tian, W. T. Wong et al., "Metformin protects endothelial function in diet-induced obese mice by inhibition of endoplasmic reticulum stress through 5′ adenosine monophosphate-activated protein kinase-peroxisome proliferator-activated receptor δ pathway," *Arteriosclerosis, Thrombosis, and Vascular Biology*, vol. 34, no. 4, pp. 830–836, 2014.

[110] M. R. Owen, E. Doran, and A. P. Halestrap, "Evidence that metformin exerts its anti-diabetic effects through inhibition of complex 1 of the mitochondrial respiratory chain," *Biochemical Journal*, vol. 348, no. 3, pp. 607–614, 2000.

[111] J. S. Moon, U. Karunakaran, S. Elumalai et al., "Metformin prevents glucotoxicity by alleviating oxidative and ER stress–induced CD36 expression in pancreatic beta cells," *Journal of Diabetes and its Complications*, vol. 31, no. 1, pp. 21–30, 2017.

[112] N. D'Onofrio, G. Pieretti, F. Ciccarelli et al., "Abdominal fat SIRT6 expression and its relationship with inflammatory and metabolic pathways in pre-diabetic overweight patients," *International Journal of Molecular Sciences*, vol. 20, no. 5, 2019.

[113] S. Hu, H. Liu, Y. Ha et al., "Posttranslational modification of Sirt6 activity by peroxynitrite," *Free Radical Biology and Medicine*, vol. 79, pp. 176–185, 2015.

[114] M. Hamblin, L. Chang, H. Zhang, K. Yang, J. Zhang, and Y. E. Chen, "Vascular smooth muscle cell peroxisome proliferator-activated receptor-γ mediates pioglitazone-reduced vascular lesion formation," *Arteriosclerosis, Thrombosis, and Vascular Biology*, vol. 31, no. 2, pp. 352–359, 2011.

[115] E. Erdmann, J. Dormandy, R. Wilcox, M. Massi-Benedetti, and B. Charbonnel, "PROactive 07: pioglitazone in the treatment of type 2 diabetes: results of the PROactive study," *Vascular Health and Risk Management*, vol. 3, no. 4, pp. 355–370, 2007.

[116] I. Seghrouchni, J. Drai, E. Bannier et al., "Oxidative stress parameters in type I, type II and insulin-treated type 2 diabetes mellitus; insulin treatment efficiency," *Clinica Chimica Acta*, vol. 321, no. 1–2, pp. 89–96, 2002.

[117] D. Fava, M. Cassone-Faldetta, O. Laurenti, O. De Luca, A. Ghiselli, and G. De Mattia, "Gliclazide improves antioxidant status and nitric oxide-mediated vasodilation in type 2 diabetes," *Diabetic Medicine*, vol. 19, no. 9, pp. 752–757, 2002.

[118] N. A. Scott, P. E. Jennings, J. Brown, and J. J. F. Belch, "Gliclazide: a general free radical scavenger," *European Journal of Pharmacology: Molecular Pharmacology*, vol. 208, no. 2, pp. 175–177, 1991.

[119] ADVANCE Collaborative Group, "Intensive blood glucose control and vascular outcomes in patients with type 2 diabetes," *The New England Journal of Medicine*, vol. 358, no. 24, pp. 2560–2572, 2008.

[120] K. Makrilakis, "The role of dpp-4 inhibitors in the treatment algorithm of type 2 diabetes mellitus: When to select, what to expect," *International Journal of Environmental Research and Public Health*, vol. 16, no. 15, p. 2720, 2019.

[121] V. Bistola, V. Lambadiari, G. Dimitriadis et al., "Possible mechanisms of direct cardiovascular impact of GLP-1 agonists and DPP4 inhibitors," *Heart Failure Reviews*, vol. 23, no. 3, pp. 377–388, 2018.

[122] B. Gallwitz, "New therapeutic strategies for the treatment of type 2 diabetes mellitus based on incretins," *The Review of Diabetic Studies*, vol. 2, no. 2, 2005.

[123] S. P. Marso, S. C. Bain, A. Consoli et al., "Semaglutide and cardiovascular outcomes in patients with type 2 diabetes," *New England Journal of Medicine*, vol. 375, no. 19, pp. 1834–1844, 2016.

[124] S. P. Marso, G. H. Daniels, K. Brown-Frandsen et al., "Liraglutide and cardiovascular outcomes in type 2 diabetes," *New England Journal of Medicine*, vol. 375, no. 4, pp. 311–322, 2016.

[125] H. C. Gerstein, H. M. Colhoun, G. R. Dagenais et al., "Dulaglutide and cardiovascular outcomes in type 2 diabetes (REWIND): a double-blind, randomised placebo-controlled trial," *The Lancet*, vol. 394, no. 10193, pp. 121–130, 2019.

[126] T. Nyström, M. K. Gutniak, Q. Zhang et al., "Effects of glucagon-like peptide-1 on endothelial function in type 2 diabetes patients with stable coronary artery disease," *American Journal of Physiology - Endocrinology and Metabolism*, vol. 287, no. 6, pp. E1209–E1215, 2004.

[127] R. Marfella, C. Sardu, P. Calabrò et al., "Non-ST-elevation myocardial infarction outcomes in patients with type 2 diabetes with non-obstructive coronary artery stenosis: effects of incretin treatment," *Diabetes, Obesity and Metabolism*, vol. 20, no. 3, pp. 723–729, 2018.

[128] A. Shiraki, J. I. Oyama, H. Komoda et al., "The glucagon-like peptide 1 analog liraglutide reduces TNF-α-induced oxidative stress and inflammation in endothelial cells," *Atherosclerosis*, vol. 221, no. 2, pp. 375–382, 2012.

[129] Y. Dai, F. Mercanti, D. Dai et al., "LOX-1, a bridge between GLP-1R and mitochondrial ROS generation in human vascular smooth muscle cells," *Biochemical and Biophysical Research Communications*, vol. 437, no. 1, pp. 62–66, 2013.

[130] L. Ferreira, E. Teixeira-de-Lemos, F. Pinto et al., "Effects of sitagliptin treatment on dysmetabolism, inflammation, and oxidative stress in an animal model of type 2 diabetes (ZDF rat)," *Mediators of Inflammation*, vol. 2010, Article ID 592760, 11 pages, 2010.

[131] C. Mega, E. Teixeira-De-Lemos, R. Fernandes, and F. Reis, "Renoprotective effects of the dipeptidyl peptidase-4 inhibitor sitagliptin: a review in type 2 diabetes," *Journal of Diabetes Research*, vol. 2017, Article ID 5164292, 14 pages, 2017.

[132] A. Gonçalves, E. Leal, A. Paiva et al., "Protective effects of the dipeptidyl peptidase IV inhibitor sitagliptin in the blood-retinal barrier in a type 2 diabetes animal model," *Diabetes, Obesity and Metabolism*, vol. 14, no. 5, pp. 454–463, 2012.

[133] A. Tentolouris, P. Vlachakis, E. Tzeravini, I. Eleftheriadou, and N. Tentolouris, "SGLT2 inhibitors: a review of their antidiabetic and cardioprotective effects," *International Journal of Environmental Research and Public Health*, vol. 16, no. 16, p. 2965, 2019.

[134] A. Ojima, T. Matsui, Y. Nishino, N. Nakamura, and S. Yamagishi, "Empagliflozin, an inhibitor of sodium-glucose cotransporter 2 exerts anti-inflammatory and antifibrotic effects on experimental diabetic nephropathy partly by suppressing AGEs-receptor axis," *Hormone and Metabolic Research*, vol. 47, no. 9, pp. 686–692, 2015.

[135] W. Leng, X. Ouyang, X. Lei et al., "The SGLT-2 inhibitor dapagliflozin has a therapeutic effect on atherosclerosis in diabetic ApoE-/- mice," *Mediators of Inflammation*, vol. 2016, Article ID 6305735, 13 pages, 2016.

[136] M. R. Cowie and M. Fisher, "SGLT2 inhibitors: mechanisms of cardiovascular benefit beyond glycaemic control," *Nature Reviews Cardiology*, 2020.

[137] R. W. Beck, C. G. Connor, D. M. Mullen, D. M. Wesley, and R. M. Bergenstal, "The fallacy of average: how using HbA1c alone to assess glycemic control can be misleading," *Diabetes Care*, vol. 40, no. 8, pp. 994–999, 2017.

[138] A. Ceriello and M. A. Ihnat, "'Glycaemic variability': a new therapeutic challenge in diabetes and the critical care setting," *Diabetic Medicine*, vol. 27, no. 8, pp. 862–867, 2010.

[139] I. B. Hirsch, "Glycemic variability and diabetes complications: does it matter? Of course it does!," *Diabetes Care*, vol. 38, no. 8, pp. 1610–1614, 2015.

[140] the DECODA Study Group and T. Nakagami, "Hyperglycaemia and mortality from all causes and from cardiovascular disease in five populations of Asian origin," *Diabetologia*, vol. 47, no. 3, pp. 385–394, 2004.

[141] S. Suh and J. H. Kim, "Glycemic variability: how do we measure it and why is it important?,," *Diabetes and Metabolism Journal*, vol. 39, no. 4, pp. 273–282, 2015.

[142] A. Ceriello, L. Monnier, and D. Owens, "Glycaemic variability in diabetes: clinical and therapeutic implications," *The Lancet Diabetes and Endocrinology*, vol. 7, no. 3, pp. 221–230, 2019.

[143] G. Su, S. Mi, H. Tao et al., "Association of glycemic variability and the presence and severity of coronary artery disease in patients with type 2 diabetes," *Cardiovascular Diabetology*, vol. 10, no. 1, 2011.

[144] C. Gorst, C. S. Kwok, S. Aslam et al., "Long-term glycemic variability and risk of adverse outcomes: a systematic review

and meta-analysis," *Diabetes Care*, vol. 38, no. 12, pp. 2354–2369, 2015.

[145] G. McGarraugh, "The chemistry of commercial continuous glucose monitors," *Diabetes technology & therapeutics*, vol. 11, no. S1, Supplement 1, pp. S-17–S-24, 2009.

[146] D. Rodbard, "New and improved methods to characterize glycemic variability using continuous glucose monitoring," *Diabetes Technology & Therapeutics*, vol. 11, no. 9, pp. 551–565, 2009.

[147] T. Danne, R. Nimri, T. Battelino et al., "International consensus on use of continuous glucose monitoring," *Diabetes Care*, vol. 40, no. 12, pp. 1631–1640, 2017.

[148] J. H. DeVries, "Glucose variability: where it is important and how to measure it," *Diabetes*, vol. 62, no. 5, pp. 1405–1408, 2013.

[149] E. S. Kilpatrick, A. S. Rigby, and S. L. Atkin, "Effect of glucose variability on the long-term risk of microvascular complications in type 1 diabetes," *Diabetes Care*, vol. 32, no. 10, pp. 1901–1903, 2009.

[150] S. E. Siegelaar, T. Barwari, W. Kulik, J. B. Hoekstra, and J. H. DeVries, "No relevant relationship between glucose variability and oxidative stress in well-regulated type 2 diabetes patients," *Journal of Diabetes Science and Technology*, vol. 5, no. 1, pp. 86–92, 2011.

[151] J. M. Lachin, I. Bebu, R. M. Bergenstal et al., "Association of glycemic variability in type 1 diabetes with progression of microvascular outcomes in the diabetes control and complications trial," *Diabetes Care*, vol. 40, no. 6, pp. 777–783, 2017.

[152] S. Frontoni, P. Di Bartolo, A. Avogaro, E. Bosi, G. Paolisso, and A. Ceriello, "Glucose variability: an emerging target for the treatment of diabetes mellitus," *Diabetes Research and Clinical Practice*, vol. 102, no. 2, pp. 86–95, 2013.

[153] C. L. Lee, W. H. H. Sheu, I. T. Lee et al., "Trajectories of fasting plasma glucose variability and mortality in type 2 diabetes," *Diabetes & Metabolism*, vol. 44, no. 2, pp. 121–128, 2018.

[154] S. S. Wightman, C. A. R. Sainsbury, and G. C. Jones, "Visit-to-visit HbA1c variability and systolic blood pressure (SBP) variability are significantly and additively associated with mortality in individuals with type 1 diabetes: an observational study," *Diabetes, Obesity and Metabolism*, vol. 20, no. 4, pp. 1014–1017, 2018.

[155] M. Gohbara, K. Hibi, T. Mitsuhashi et al., "Glycemic variability on continuous glucose monitoring system correlates with non-culprit vessel coronary plaque vulnerability in patients with first-episode acute coronary syndrome - optical coherence tomography study," *Circulation Journal*, vol. 80, no. 1, pp. 202–210, 2016.

[156] H. K. Yang, B. Kang, S. H. Lee et al., "Association between hemoglobin A1c variability and subclinical coronary atherosclerosis in subjects with type 2 diabetes," *Journal of Diabetes and its Complications*, vol. 29, no. 6, pp. 776–782, 2015.

[157] J.-B. Su, X. H. Yang, X. L. Zhang et al., "The association of long-term glycaemic variability versus sustained chronic hyperglycaemia with heart rate-corrected QT interval in patients with type 2 diabetes," *PloS one*, vol. 12, no. 8, article e0183055, 2017.

[158] S. Kalopita, S. Liatis, P. Thomakos et al., "Relationship between autonomic nervous system function and continuous interstitial glucose measurement in patients with type 2 diabetes," *Journal of Diabetes Research*, vol. 2014, Article ID 835392, 6 pages, 2014.

[159] J. Fleischer, S. Lebech Cichosz, P. Hoeyem et al., "Glycemic variability is associated with reduced cardiac autonomic modulation in women with type 2 diabetes," *Diabetes Care*, vol. 38, no. 4, pp. 682–688, 2015.

[160] J. E. Jun, S. M. Jin, J. Baek et al., "The association between glycemic variability and diabetic cardiovascular autonomic neuropathy in patients with type 2 diabetes," *Cardiovascular Diabetology*, vol. 14, no. 1, 2015.

[161] L. Quagliaro, L. Piconi, R. Assaloni, L. Martinelli, E. Motz, and A. Ceriello, "Intermittent high glucose enhances apoptosis related to oxidative stress in human umbilical vein endothelial cells: the role of protein kinase C and NAD(P)H-oxidase activation," *Diabetes*, vol. 52, no. 11, pp. 2795–2804, 2003.

[162] Y. Saisho, "Glycemic variability and oxidative stress: a link between diabetes and cardiovascular disease?," *International Journal of Molecular Sciences*, vol. 15, no. 10, pp. 18381–18406, 2014.

[163] M. Maeda, T. Hayashi, N. Mizuno, Y. Hattori, and M. Kuzuya, "Intermittent high glucose implements stress-induced senescence in human vascular endothelial cells: role of superoxide production by NADPH oxidase," *PLoS ONE*, vol. 10, no. 4, article e0123169, 2015.

[164] S. C. Jones, H. J. Saunders, W. Qi, and C. A. Pollock, "Intermittent high glucose enhances cell growth and collagen synthesis in cultured human tubulointerstitial cells," *Diabetologia*, vol. 42, no. 9, pp. 1113–1119, 1999.

[165] L. Piconi, L. Quagliaro, R. Assaloni et al., "Constant and intermittent high glucose enhances endothelial cell apoptosis through mitochondrial superoxide overproduction," *Diabetes/Metabolism Research and Reviews*, vol. 22, no. 3, pp. 198–203, 2006.

[166] E. M. Horváth, R. Benkő, L. Kiss et al., "Rapid 'glycaemic swings' induce nitrosative stress, activate poly(ADP-ribose) polymerase and impair endothelial function in a rat model of diabetes mellitus," *Diabetologia*, vol. 52, no. 5, pp. 952–961, 2009.

[167] A. Risso, F. Mercuri, L. Quagliaro, G. Damante, and A. Ceriello, "Intermittent high glucose enhances apoptosis in human umbilical vein endothelial cells in culture," *American Journal of Physiology-Endocrinology and Metabolism*, vol. 281, no. 5, pp. E924–E930, 2001.

[168] A. Ceriello, K. Esposito, L. Piconi et al., "Oscillating glucose is more deleterious to endothelial function and oxidative stress than mean glucose in normal and type 2 diabetic patients," *Diabetes*, vol. 57, no. 5, pp. 1349–1354, 2008.

[169] L. Monnier, E. Mas, C. Ginet et al., "Activation of oxidative stress by acute glucose fluctuations compared with sustained chronic hyperglycemia in patients with type 2 diabetes," *JAMA*, vol. 295, no. 14, pp. 1681–1687, 2006.

[170] A. Di Flaviani, F. Picconi, P. Di Stefano et al., "Impact of glycemic and blood pressure variability on surrogate measures of cardiovascular outcomes in type 2 diabetic patients," *Diabetes Care*, vol. 34, no. 7, pp. 1605–1609, 2011.

[171] A. Ceriello, A. Novials, E. Ortega et al., "Evidence that hyperglycemia after recovery from hypoglycemia worsens endothelial function and increases oxidative stress and inflammation in healthy control subjects and subjects with type 1 diabetes," *Diabetes*, vol. 61, no. 11, pp. 2993–2997, 2012.

[172] I. M. E. Wentholt, W. Kulik, R. P. J. Michels, J. B. L. Hoekstra, and J. H. DeVries, "Glucose fluctuations and activation of

oxidative stress in patients with type 1 diabetes," *Diabetologia*, vol. 51, no. 1, pp. 183–190, 2007.

[173] E. S. Kilpatrick, A. S. Rigby, K. Goode, and S. L. Atkin, "Relating mean blood glucose and glucose variability to the risk of multiple episodes of hypoglycaemia in type 1 diabetes," *Diabetologia*, vol. 50, no. 12, pp. 2553–2561, 2007.

[174] L. Monnier, A. Wojtusciszyn, C. Colette, and D. Owens, "The contribution of glucose variability to asymptomatic hypoglycemia in persons with type 2 diabetes," *Diabetes Technology & Therapeutics*, vol. 13, no. 8, pp. 813–818, 2011.

[175] K. Khunti, M. Davies, A. Majeed, B. L. Thorsted, M. L. Wolden, and S. K. Paul, "Hypoglycemia and risk of cardiovascular disease and all-cause mortality in insulin-treated people with type 1 and type 2 diabetes: a cohort study," *Diabetes Care*, vol. 38, no. 2, pp. 316–322, 2015.

[176] Action to Control Cardiovascular Risk in Diabetes Study Group, H. C. Gerstein, M. E. Miller et al., "Effects of intensive glucose lowering in type 2 diabetes," *The New England Journal of Medicine*, vol. 358, no. 24, pp. 2545–2559, 2008.

[177] E. R. Seaquist, M. E. Miller, D. E. Bonds et al., "The impact of frequent and unrecognized hypoglycemia on mortality in the ACCORD study," *Diabetes Care*, vol. 35, no. 2, pp. 409–414, 2012.

[178] P. Singh, A. Jain, and G. Kaur, "Impact of hypoglycemia and diabetes on CNS: correlation of mitochondrial oxidative stress with DNA damage," *Molecular and Cellular Biochemistry*, vol. 260, no. 1, pp. 153–159, 2004.

[179] J. K. Snell-Bergeon and R. P. Wadwa, "Hypoglycemia, diabetes, and cardiovascular disease," *Diabetes technology & therapeutics*, vol. 14, no. S1, Supplement 1, pp. S-51–S-58, 2012.

[180] S. A. Amiel, P. Aschner, B. Childs et al., "Hypoglycaemia, cardiovascular disease, and mortality in diabetes: epidemiology, pathogenesis, and management," *The Lancet Diabetes and Endocrinology*, vol. 7, no. 5, pp. 385–396, 2019.

[181] K. Makrilakis, C. Stathi, I. Vlahodimitris et al., "Hypoglycaemia causes both daytime and nighttime QTc interval prolongation in patients with type 2 diabetes receiving insulin treatment," *Diabetes and Metabolism*, vol. 44, no. 2, pp. 175–177, 2018.

[182] R. A. Hutton, D. Mikhailidis, K. M. Dormandy, and J. Ginsburg, "Platelet aggregation studies during transient hypoglycaemia: a potential method for evaluating platelet function," *Journal of Clinical Pathology*, vol. 32, no. 5, pp. 434–438, 1979.

[183] R. J. Wright, D. E. Newby, D. Stirling, C. A. Ludlam, I. A. Macdonald, and B. M. Frier, "Effects of acute insulin-induced hypoglycemia on indices of inflammation: putative mechanism for aggravating vascular disease in diabetes," *Diabetes Care*, vol. 33, no. 7, pp. 1591–1597, 2010.

[184] J. M. Ratter, H. M. M. Rooijackers, C. J. Tack et al., "Proinflammatory effects of hypoglycemia in humans with or without diabetes," *Diabetes*, vol. 66, no. 4, pp. 1052–1061, 2017.

[185] Z. Dagher, N. Ruderman, K. Tornheim, and Y. Ido, "Acute regulation of fatty acid oxidation and AMP-activated protein kinase in human umbilical vein endothelial cells," *Circulation Research*, vol. 88, no. 12, pp. 1276–1282, 2001.

[186] S. Cardoso, R. X. Santos, S. C. Correia et al., "Insulin-induced recurrent hypoglycemia exacerbates diabetic brain mitochondrial dysfunction and oxidative imbalance," *Neurobiology of Disease*, vol. 49, pp. 1–12, 2013.

[187] L. Razavi Nematollahi, A. E. Kitabchi, F. B. Stentz et al., "Proinflammatory cytokines in response to insulin-induced hypoglycemic stress in healthy subjects," *Metabolism*, vol. 58, no. 4, pp. 443–448, 2009.

[188] N. Gogitidze Joy, M. S. Hedrington, V. J. Briscoe, D. B. Tate, A. C. Ertl, and S. N. Davis, "Effects of acute hypoglycemia on inflammatory and pro-atherothrombotic biomarkers in individuals with type 1 diabetes and healthy individuals," *Diabetes Care*, vol. 33, no. 7, pp. 1529–1535, 2010.

[189] A. Ceriello, A. Novials, E. Ortega et al., "Glucagon-like peptide 1 reduces endothelial dysfunction, inflammation, and oxidative stress induced by both hyperglycemia and hypoglycemia in type 1 diabetes," *Diabetes Care*, vol. 36, no. 8, pp. 2346–2350, 2013.

Hindawi
Journal of Diabetes Research
Volume 2020, Article ID 3854630, 12 pages
https://doi.org/10.1155/2020/3854630

Research Article

Association of Maternal Diabetes Mellitus and Polymorphisms of the *NKX2.5* Gene in Children with Congenital Heart Disease: A Single Centre-Based Case-Control Study

Mingyi Zhao[1], **Jingyi Diao**[2], **Peng Huang**[3], **Jinqi Li**[2], **Yihuan Li**[2], **Yang Yang**[1], **Liu Luo**[2], **Senmao Zhang**[2], **Letao Chen**[2], **Tingting Wang**[2], **Ping Zhu**[4] and **Jiabi Qin**[2,4,5]

[1]*Department of Pediatrics, The Third Xiangya Hospital, Central South University, Changsha, Hunan, China*
[2]*Department of Epidemiology and Health Statistics, Xiangya School of Public Health, Central South University, Changsha, Hunan, China*
[3]*Department of Cardiothoracic Surgery, Hunan Children's Hospital, Changsha, Hunan, China*
[4]*Guangdong Cardiovascular Institute, Guangdong Provincial People's Hospital, Guangdong Academy of Medical Sciences, Guangzhou, Guangdong, China*
[5]*National Health Commission Key Laboratory for Birth Defect Research and Prevention, Changsha, Hunan, China*

Correspondence should be addressed to Ping Zhu; tanganqier@163.com and Jiabi Qin; qinjiabi123@163.com

Received 23 May 2020; Revised 19 July 2020; Accepted 4 August 2020; Published 26 September 2020

Guest Editor: Gaetano Santulli

Background. Congenital heart disease (CHD) is one of the most common birth defects among newborns, accounting for a large proportion of infant mortality worldwide. However, the mechanisms remain largely undefinable. This study aimed to investigate the association of CHD in offspring of mothers with diabetes mellitus (DM) and single nucleotide polymorphisms (SNPs) of *NKX2.5*. *Methods and Results*. A case-control study of 620 mothers of CHD patients and 620 mothers of healthy children admitted to Hunan Children's Hospital from November 2017 to December 2019 was conducted. We collected the mothers' information by questionnaire and detected children's *NKX2.5* variants with a MassARRAY system. The interaction coefficient (γ) was used to quantify the estimated gene-environment interactions. Univariate and multivariate analyses both showed that the infants had a higher risk of CHD if their mothers had a history of DM, including gestational DM (GDM) during this pregnancy (adjusted odds ratio [aOR = 4.98]), GDM in previous pregnancies (aOR = 4.30), and pregestational DM (PGDM) in the 3 months before this pregnancy (aOR = 6.78). Polymorphisms of the *NKX2.5* gene at rs11802669 (C/C vs. T/T: aOR = 4.97; C/T vs. T/T: aOR = 2.15) and rs2277923 (T/T vs. C/C, aOR = 1.74; T/C vs. C/C, aOR = 1.61) were significantly associated with the risk of CHD in offspring. In addition, significant interactions between maternal DM and *NKX2.5* genetic variants at rs11802669 (aOR = 8.12) and rs2277923 (aOR = 17.72) affecting the development of CHD were found. *Conclusions*. These results suggest that maternal DM, *NKX2.5* genetic variants, and their interactions are significantly associated with the risk of CHD in offspring.

1. Introduction

Congenital heart disease (CHD) is one of the most common birth defects among newborns, accounting for a large proportion of infant mortality worldwide. As a rough estimate, approximately 8 infants in every 1000 are born with CHD [1]. The pathogenesis of CHD, however, is very complicated and different from other congenital diseases, and its exact causes are largely undefinable [2].

Approximately 2% of CHD can be attributed to known environmental factors, of which maternal diabetes mellitus (DM) is a well-accepted risk factor [3]. Gestational diabetes mellitus (GDM) poses significant risks of immediate and long-term health for the mother and foetus, affecting 3%-

25% of pregnancies worldwide [4]. Studies have demonstrated that glycaemic control during pregnancy has a clear link to foetal malformations, and maternal DM appears to induce offspring malformation before the seventh week of gestation [5]. One hypothesis is that the abnormal glucose levels in maternal DM disrupt the expression of regulatory genes in the embryo, resulting in embryotoxic apoptotic cellular changes [6].

Over 40 genes have been implicated in the development of CHD [7]. Examples of CHD-causing mutations are those in *NKX2.5*, a transcriptional regulator during early embryonic heart development [8, 9]. Experiments have shown that *NKX2.5* is essential for the formation and maturation of the heart as well as the conduction system. Its absence in mice results in embryonic lethality and arrested heart development [10]. In addition, more than 40 mutations of *NKX2.5* have been found in CHD cases, which may reduce the transcriptional activity of *NKX2.5* and affect cardiac development [11]. Several animal experiments have shown that *NKX2.5* may be involved in the pathogenesis of embryonic congenital heart disease caused by gestational diabetes and that in a rat model, the expression of *NKX2.5* decreased during heart development in foetuses of mothers with gestational diabetes [12–14].

Accordingly, we conducted a case-control study including 620 mothers of CHD patients and 620 mothers of healthy children, collecting mothers' information by questionnaire and detecting children's *NKX2.5* variants with a MassARRAY system, to study the association of maternal DM, *NKX2.5* variants and their interaction with CHD in offspring to provide a new direction for the prevention of CHD.

2. Methods

2.1. Recruitment of Study Participants. We conducted a case-control study to investigate the role of maternal DM and *NKX2.5* SNPs in the aetiology of CHD in offspring. Recruitment was conducted by the Hunan Children's Hospital from November 2017 to December 2019. Children with CHD and their parents who were seen in this hospital were identified as the case group. All CHD patients were diagnosed using ultrasonography, and their diagnosis was confirmed by surgery. Children without any congenital malformation after a medical examination and their parents were identified as the control group. The study participants were recruited at 2 clinics from this hospital. The case group was recruited from the Department of Cardiothoracic Surgery, which provides diagnosis, treatment, surgery, and management for CHD, and the control group was recruited from the Department of Child Healthcare after health counselling or a medical examination. The controls were selected from the same hospital during the same study period as the cases. This study was approved by the ethics committee of the Xiangya School of Public Health of Central South University, and written informed consent was obtained from all mothers. This study was registered in the Chinese Clinical Trial Registry Center (registration number: ChiCTR1800016635).

2.2. Inclusion Criteria. In this study, the exposures of interest were maternal DM and children's genetic variants of the *NKX2.5* gene. DM was identified based on the following International Classification of Diseases and Related Health Problems, Tenth Revision (ICD-10) code: O24.4. Three types of maternal DM were included: gestational DM (GDM) during this pregnancy, GDM in previous pregnancies, and pregestational DM (PGDM) in the 3 months before this pregnancy. The outcomes of interest were CHD in the offspring, including seven subtypes: atrial septal defect (ASD), ventricular septal defect (VSD), atrioventricular septal defect (AVSD), patent ductus arteriosus (PDA), aortopulmonary septal defect (APSD), tetralogy of Fallot (TOF), and complete transposition of the great arteries (CTOGA). All CHD patients were diagnosed using ultrasonography, and their diagnosis was confirmed by surgery.

To reduce recall bias, mothers with children under 1 year old were recruited and asked to complete the same questionnaire in the same way by professionally trained investigators who were not informed in advance of the classification of the cases and controls. Additionally, this study was aimed at mothers of Han Chinese descent with singleton pregnancies. Eligible mothers needed to be able to complete the questionnaire and provide informed consent and blood samples. Nonsyndromic CHDs were of interest, and patients with other organ malformations or known abnormalities were excluded. Children without any congenital malformation after a medical examination served as the controls.

2.3. Information Collection. A standardized questionnaire was used to assess the history of maternal DM, including GDM during this pregnancy, GDM in previous pregnancies, and PGDM in the 3 months before this pregnancy. In addition, we consulted the Maternal and Child Health Manual and maternal medical records to further confirm the corresponding information on maternal DM history. In China, each pregnant woman is provided with a Maternal and Child Health Manual in which to record their basic demographic characteristics, behavioural habits, illnesses, and the results of various medical examinations during pregnancy. Another major exposure of interest in this study was the SNPs of the *NKX2.5* gene at rs6882776, rs118026695, rs2277923, and rs703752, which are described below.

When evaluating the association of maternal DM and *NKX2.5* SNPs with the risk of CHD in offspring, some other confounding factors needed to be considered. Therefore, we collected the following information about the mothers: (1) demographic characteristics, (2) abnormal pregnancy history, (3) family history, (4) personal medical history, (5) lifestyle and habits, (6) history of exposure to environmental hazardous substances, and (7) medical history during this pregnancy.

2.4. NKX2.5 SNP Sequencing. The genetic loci rs6882776, rs118026695, rs2277923, and rs703752 of the *NKX2.5* gene, which have been widely studied previously, were selected as candidate loci for this study [15–17]. Three to five millilitres of peripheral venous blood from the children was used for genotyping. Blood samples were collected in EDTA-treated

Table 1: Baseline characteristics comparison between control group and case group.

Variables	Control group ($n = 620$)	Case group ($n = 620$)	Univariable analysis
Demographic characteristics			
Maternal age at this pregnancy (years)	28.5 ± 4.7	28.0 ± 5.4	
≤24	124 (20.0%)	176 (28.4%)	$\chi^2 = 13.755$; $P = 0.003$
25-29	261 (42.1%)	235 (37.9%)	
30-34	152 (24.5%)	122 (19.7%)	
≥35	83 (13.4%)	87 (14.0%)	
Education level			
Less than primary or primary	7 (1.1%)	87 (14.0%)	
Junior high school	117 (18.9%)	263 (42.4%)	$Z = 14.342$; $P \leq 0.001$
Senior middle school	217 (35.0%)	167 (26.9%)	
College or above	279 (45.0%)	103 (16.6%)	
Body mass index before this pregnancy			
<18.5	156 (25.8%)	112 (18.3%)	$Z = 1.625$; $P = 0.104$
18.5-23.99	340 (56.3%)	404 (65.9%)	
≥24	108 (17.9%)	97 (15.8%)	
Family's annual income in the past 1 year (RMB)			
≤50,000	179 (28.9%)	494 (79.7%)	$Z = 17.785$; $P \leq 0.001$
60,000-100,000	267 (43.1%)	92 (14.8%)	
110,000-150,000	57 (9.2%)	12 (1.9%)	
≥160,000	117 (18.9%)	22 (3.5%)	
Residence location			
Rural areas	342 (55.2%)	444 (71.6%)	$\chi^2 = 36.153$; $P \leq 0.001$
Urban areas	278 (44.8%)	176 (28.4%)	
Abnormal pregnancy history			
Spontaneous abortion			
No	560 (90.3%)	545 (87.9%)	$\chi^2 = 1.870$; $P = 0.171$
Yes	60 (9.7%)	75 (12.1%)	
Induced abortion or labor			
No	428 (69.0%)	363 (58.5%)	$\chi^2 = 14.751$; $P \leq 0.001$
Yes	192 (31.0%)	257 (41.5%)	
Fetal death or stillbirth			
No	618 (99.7%)	584 (94.2%)	$\chi^2 = 31.383$; $P \leq 0.001$
Yes	2 (0.3%)	36 (5.8%)	
Premature delivery			
No	614 (99.0%)	603 (97.3%)	$\chi^2 = 5.360$; $P = 0.021$
Yes	6 (1.0%)	17 (2.7%)	
Low birth weight			
No	617 (99.5%)	603 (97.3%)	$\chi^2 = 9.961$; $P = 0.002$
Yes	3 (0.5%)	17 (2.7%)	
Neonatal death			
No	620 (100.0%)	603 (97.3%)	$\chi^2 = 17.236$; $P \leq 0.001$
Yes	0 (0.0%)	17 (2.7%)	
Embryo damage			
No	610 (98.4%)	604 (97.4%)	$\chi^2 = 1.414$; $P = 0.234$
Yes	10 (1.6%)	16 (2.6%)	
Hypertension of pregnancy			
No	611 (98.5%)	577 (93.1%)	$\chi^2 = 23.204$; $P \leq 0.001$

Table 1: Continued.

Variables	Control group ($n = 620$)	Case group ($n = 620$)	Univariable analysis
Yes	9 (1.5%)	43 (6.9%)	
Placenta previa			
No	615 (99.2%)	613 (98.9%)	$\chi^2 = 0.337$; $P = 0.562$
Yes	5 (0.8%)	7 (1.1%)	
Placental abruption			
No	620 (100.0%)	620 (100.0%)	
Yes	0 (0.0%)	0 (0.0%)	
Premature rupture of membranes			
No	620 (100.0%)	615 (99.2%)	$P = 0.062$ (Fisher's exact test)
Yes	0 (0.0%)	0.8%	
Anemia during pregnancy			
No	598 (96.5%)	554 (89.4%)	$\chi^2 = 23.681$; $P \leq 0.001$
Yes	22 (3.5%)	66 (10.6%)	
Family history			
Consanguineous marriages			
No	617 (99.5%)	599 (96.6%)	$\chi^2 = 13.766$; $P \leq 0.001$
Yes	3 (0.5%)	21 (3.4%)	
Congenital malformations			
No	615 (99.2%)	584 (94.2%)	$\chi^2 = 24.241$; $P \leq 0.001$
Yes	5 (0.8%)	36 (5.8%)	
Personal medical history			
Personal history of congenital malformations			
No	617 (99.5%)	611 (98.5%)	$\chi^2 = 3.029$; $P = 0.082$
Yes	3 (0.5%)	9 (1.5%)	
Cold history in the 3 months before this pregnancy			
No	548 (88.4%)	499 (80.5%)	$\chi^2 = 14.734$; $P \leq 0.001$
Yes	72 (11.6%)	121 (19.5%)	
Fever history in the 3 months before this pregnancy			
No	608 (98.1%)	569 (91.8%)	$\chi^2 = 25.435$; $P \leq 0.001$
Yes	12 (1.9%)	51 (8.2%)	
Cold history during this pregnancy			
No	488 (78.7%)	413 (66.6%)	$\chi^2 = 22.836$; $P \leq 0.001$
Yes	132 (21.3%)	207 (33.4%)	
Fever history during this pregnancy			
No	601 (96.9%)	561 (90.5%)	$\chi^2 = 21.890$; $P \leq 0.001$
Yes	19 (3.1%)	59 (9.5%)	
Lifestyle and habit			
History of active smoking in the 3 months before this pregnancy			
No	607 (97.9%)	584 (94.2%)	$\chi^2 = 11.240$; $P = 0.001$
Yes	13 (2.1%)	36 (5.8%)	
History of passive smoking in the 3 months before this pregnancy			
No	393 (63.4%)	293 (47.3%)	$\chi^2 = 32.628$; $P \leq 0.001$
Yes	227 (36.6%)	327 (52.7%)	
Drinking history in the 3 months before this pregnancy			
No	577 (93.1%)	539 (86.9%)	$\chi^2 = 12.939$; $P \leq 0.001$
Yes	43 (6.9%)	81 (13.1%)	
History of drinking tea in the 3 months before this pregnancy			

Table 1: Continued.

Variables	Control group ($n = 620$)	Case group ($n = 620$)	Univariable analysis
No	503 (81.1%)	542 (87.4%)	$\chi^2 = 9.256$; $P = 0.002$
Yes	117 (18.9%)	78 (12.6%)	
History of drinking coffee in the 3 months before this pregnancy			
No	592 (95.5%)	565 (91.1%)	$\chi^2 = 9.413$; $P = 0.002$
Yes	28 (4.5%)	55 (8.9%)	
History of chewing betel nut in the 3 months before this pregnancy			
No	608 (98.4%)	593 (95.6%)	$\chi^2 = 7.995$; $P = 0.005$
Yes	10 (1.6%)	27 (4.4%)	
Frequency of cosmetics use in the 3 months before this pregnancy			
Never	360 (58.1%)	293 (47.3%)	$Z = 4.993$; $P \leq 0.001$
Sometime	174 (28.1%)	150 (24.2%)	
Often	40 (6.5%)	105 (16.9%)	
Every day	46 (7.4%)	72 (11.6%)	
Did you keep pets in the 3 months before this pregnancy?			
No	573 (92.4%)	537 (86.6%)	$\chi^2 = 11.137$; $P = 0.001$
Yes	47 (7.6%)	83 (13.4%)	
Did you often dye or perm your hair in the 3 months before this pregnancy?			
No	584 (94.2%)	547 (88.2%)	$\chi^2 = 13.770$; $P \leq 0.001$
Yes	36 (5.8%)	73 (11.8%)	
Exposure history to environmental hazardous substance			
Was there a factory near place of residence that discharges environmentally harmful substances?			
No	574 (92.6%)	503 (81.1%)	$\chi^2 = 35.607$; $P \leq 0.001$
Yes	46 (7.4%)	117 (18.9%)	
Was there a traffic road or a noisy factory near where you live (noise exposure)?			
No	506 (81.6%)	446 (71.9%)	$\chi^2 = 16.282$; $P \leq 0.001$
Yes	114 (18.4%)	174 (28.1%)	
Was your house newly renovated in the 3 months before this pregnancy?			
No	567 (91.5%)	572 (92.3%)	$\chi^2 = 0.269$; $P = 0.604$
Yes	53 (8.5%)	48 (7.7%)	
Medicine history in this pregnancy			
Folate			
Yes	577 (93.1%)	526 (84.8%)	$\chi^2 = 21.344$; $P \leq 0.001$
No	43 (6.9%)	94 (15.2%)	
Macrolide antibiotics			
No	603 (97.3%)	569 (91.8%)	$\chi^2 = 17.986$; $P \leq 0.001$
Yes	17 (2.7%)	51 (8.2%)	
Antidepressants			
No	586 (94.5%)	551 (88.9%)	$\chi^2 = 12.971$; $P \leq 0.001$
Yes	34 (5.5%)	69 (11.1%)	
Fetal-prevention drugs			
No	539 (86.9%)	487 (78.5%)	$\chi^2 = 15.271$; $P \leq 0.001$
Yes	81 (13.1%)	133 (21.5%)	

(ethylenediamine tetraacetic acid) anticoagulant tubes and then immediately centrifuged into plasma and white blood cells. White blood cells were separated and stored at -80°C until genotyping was performed. DNA was extracted from blood cells by the QIAamp DNA Mini Kit (Qiagen, Valencia, CA, USA) according to the manufacturer's standard protocol and dissolved in sterile TBE (Tris-borate-EDTA) buffer. The concentration and purity of the DNA solution were detected

Table 2: Univariate analysis of maternal DM and offspring CHD.

Maternal DM	Control group ($n = 620$)	Case group ($n = 620$)	Univariable analysis	Unadjusted OR (95% CI)
GDM during this pregnancy				
No	592 (95.5%)	552 (89.0%)	$\chi^2 = 18.065$; $P \leq 0.001$	1
Yes	28 (4.5%)	68 (11.0%)		2.61 (1.65-4.11)*
GDM during previous pregnancy experience				
No	595 (96.0%)	550 (88.7%)	$\chi^2 = 23.084$; $P \leq 0.001$	1
Yes	25 (4.0%)	70 (11.3%)		3.03 (1.89-4.85)*
PGDM in the 3 months before this pregnancy				
No	603 (97.3%)	557 (89.8%)	$\chi^2 = 28.274$; $P \leq 0.001$	1
Yes	17 (2.7%)	63 (10.2%)		4.01 (2.32-6.94)*

DM: diabetes mellitus; CHD: congenital heart disease; GDM: gestational diabetes mellitus; PGDM: pregestational diabetes mellitus; OR: odds ratio; CI: confidence interval. *Statistically significant ($a = 0.05$).

Table 3: Multivariate analysis of maternal DM and offspring CHD.

Maternal DM	B	S.E	Wals	P value	Adjusted OR (95% CI)*
GDM during this pregnancy (yes vs. no)	1.609	0.340	22.326	0.001	4.98 (2.56-9.74)
GDM in previous pregnancy experiences (yes vs. no)	1.458	0.334	19.117	0.001	4.30 (2.24-8.27)
PGDM in the 3 months before this pregnancy (yes vs. no)	1.914	0.385	24.676	0.001	6.78 (3.19-14.43)

DM: diabetes mellitus; CHD: congenital heart disease; GDM: gestational diabetes mellitus; PGDM: pregestational diabetes mellitus; OR: odds ratio; CI: confidence interval. *Adjusted for factors with statistical differences in Table 1.

by ultraviolet spectrophotometry to ensure that the DNA was eligible as a template for polymerase chain reaction (PCR).

Primer designs, amplification conditions, and expected product sizes for *NKX2.5* have been described by previous studies [15–17]. The polymorphisms of the *NKX2.5* gene at rs6882776, rs118026695, rs2277923, and rs703752 were tested using a matrix-assisted laser desorption and ionization time-of-flight mass spectrometry MassARRAY system (Agena iPLEXassay, San Diego, CA, USA). The error rate for genotyping was less than 5%. The experimenters who performed the genotyping were not informed in advance of the status of the control or case groups. Each sample was retyped and double-checked to ensure the reliability of the experiments.

For rs6882776, three genotypes, including the homozygous wild-type G/G, the heterozygous variant T/A, and the homozygous variant A/A, were identified. For rs118026695, three genotypes were identified: the homozygous wild-type T/T, the heterozygous variant C/T, and the homozygous variant C/C. For rs2277923, three genotypes were identified: the homozygous wild-type T/T, the heterozygous variant T/C, and the homozygous variant C/C. For rs703752, three genotypes were identified: the homozygous wild-type C/C, the heterozygous variant C/A, and the homozygous variant A/A.

2.5. Statistical Analysis. Means and standard deviations were reported for normally distributed continuous variables. For continuous variables that did not seem normally distributed and categorical variables, quartiles (%) were reported. In the univariate analysis, the Pearson chi-squared test or Fisher's exact test was used to compare categorical variable data; the Wilcoxon rank sum test was used for nonnormally distributed continuous variables.

NKX2.5 SNPs were analysed for deviations from Hardy-Weinberg equilibrium (HWE). The correlation analysis for CHD and maternal DM or *NKX2.5* SNPs was performed by univariate and multivariate logistic regression analysis, and odds ratios (ORs) and their 95% confidence intervals (CIs) were used to assess the level of association. The ORs were adjusted (aORs) using the factors with P values less than 0.05 in Table 1. We used logistic regression and controlled for potential confounding factors to examine the main effects and interactive effects of the gene-environment interaction of the *NKX2.5* gene and maternal DM on the risk of CHD in offspring.

In the logistic regression model, the confounding factors, maternal DM, and *NKX2.5* SNPs were set as independent variables (covariates), and the effects were expressed as ORs with 95% CIs. Offspring diagnostic results were set as dependent variables (binary outcomes). Models of the gene-environment interactions and their implications referred to the method described by Wallace [17]. The interaction coefficient (γ) was calculated as a function of the regression coefficient (β) from the logistic regression analysis (e.g., $\gamma 1 = \beta e * g/\beta e$ and $\gamma 2 = \beta e * g/\beta g$ for gene-environment interaction) and was used to evaluate the interaction [18]. When all γ values were greater than 1, there was a positive interaction; when all γ values were less than 1, there was a negative interaction; and when the γ values were equal to 1, there was no interaction.

In this study, we examined the risk of total CHD instead of the risk of specific subtypes due to the limited sample size.

Table 4: Univariate analysis of *NKX2.5* gene polymorphism and CHD.

SNP of *NKX2.5* gene	Control group ($n = 620$)	Case group ($n = 620$)	Univariate analysis	Unadjusted OR (95% CI)
Genotype at rs6882776				**0.98 (0.83-1.16)**
A/A	216 (34.8%)	209 (33.7%)		1
G/A	308 (49.7%)	328 (52.9%)	$\chi^2 = 1.688$; $P = 0.430$	1.10 (0.86-1.41)
G/G	96 (15.5%)	83 (13.4%)		0.89 (0.63-1.27)
Recessive model at rs6882776				
A/A	216 (34.8%)	209 (33.7%)	$\chi^2 = 0.175$; $P = 0.675$	1
G/A+G/G	404 (65.2%)	411 (66.3%)		1.05 (0.83-1.33)
Dominant model at rs6882776				
A/A+ G/A	524 (84.5%)	537 (86.6%)	$\chi^2 = 1.103$; $P = 0.294$	1
G/G	96 (15.5%)	83 (13.4%)		0.84 (0.61-1.16)
Allele at rs6882776				
A	740 (59.7%)	746 (60.2%)	$\chi^2 = 0.060$; $P = 0.806$	1
G	500 (40.3%)	494 (39.8%)		0.98 (0.84-1.15)
Genotype at rs118026695				**1.83 (1.42-2.36)***
T/T	510 (82.3%)	443 (71.5%)		1
C/T	107 (17.3%)	164 (26.5%)	$\chi^2 = 22.949$; $P \leq 0.001$	1.77 (1.34-2.32)*
C/C	3 (0.5%)	13 (2.1%)		4.99 (1.41-17.62)*
Recessive model at rs118026695				
T/T	510 (82.3%)	443 (71.5%)	$\chi^2 = 20.352$; $P \leq 0.001$	1
C/T+C/C	110 (17.7%)	177 (28.5%)		1.85 (1.41-2.43)*
Dominant model at rs118026695				
T/T+C/T	617 (99.5%)	607 (97.9%)	$\chi^2 = 6.332$; $P = 0.012$	1
C/C	3 (0.5%)	13 (2.1%)		4.41 (1.25-15.53)*
Allele at rs118026695				
T	1127 (90.9%)	1050 (84.7%)	$\chi^2 = 22.291$; $P \leq 0.001$	1
C	113 (9.1%)	190 (15.3%)		1.81 (1.41-2.31)*
Genotype at rs2277923				**1.38 (1.17-1.62)***
C/C	291 (46.9%)	217 (35.0%)		1
T/C	254 (41.0%)	310 (50.0%)	$\chi^2 = 18.268$; $P \leq 0.001$	1.64 (1.29-2.08)*
T/T	75 (12.1%)	93 (15.0%)		1.66 (1.17-2.36)*
Recessive model at rs2277923				
C/C	291 (46.9%)	217 (35.0%)	$\chi^2 = 18.260$; $P \leq 0.001$	1
T/C+T/T	329 (53.1%)	403 (65.0%)		1.64 (1.31-2.06)*
Dominant model at rs2277923				
C/C+T/C	545 (87.9%)	527 (85.0%)	$\chi^2 = 2.231$; $P = 0.135$	1
T/T	75 (12.1%)	93 (15.0%)		1.28 (0.93-1.78)
Allele at rs2277923				
C	836 (67.4%)	744 (60.0%)	$\chi^2 = 14.761$; $P \leq 0.001$	1
T	404 (32.6%)	496 (40.0%)		1.38 (1.17-1.63)*
Genotype at rs703752				**1.66 (1.20-2.29)***
A/A	7 (1.1%)	2 (0.3%)	$P = 0.009$ (Fisher's exact test)	1
C/A	86 (13.9%)	57 (9.2%)		2.32 (0.47-11.57)
C/C	527 (85.0%)	561 (90.5%)		3.73 (0.77-18.02)
Recessive model at rs703752				
A/A+C/A	93 (15.0%)	59 (9.5%)	$\chi^2 = 8.668$; $P = 0.003$	1
C/C	527 (85.0%)	561 (90.5%)		1.68 (1.19-2.38)*

Table 4: Continued.

SNP of *NKX2.5* gene	Control group ($n = 620$)	Case group ($n = 620$)	Univariate analysis	Unadjusted OR (95% CI)
Dominant model at rs703752				
A/A	7 (1.1%)	2 (0.3%)	$P = 0.178$ (Fisher's exact test)	1
C/A+C/C	613 (98.9%)	618 (99.7%)		3.53 (0.73-17.05)
Allele at rs703752				
A	100 (8.1%)	61 (4.9%)	$\chi^2 = 10.103$; $P = 0.001$	1
C	1140 (91.9%)	1179 (95.1%)		1.70 (1.22-2.36)*

OR: odds ratio; CI: confidence interval. *Statistically significant ($a = 0.05$).

All data were analysed using SPSS (IBM SPSS Statistics for Macintosh, Version 26.0, Armonk, NY: IBM Corp). $P < 0.05$ was considered statistically significant.

3. Results

3.1. Comparison of Baseline Characteristics. We analysed seven aspects of the 1240 questionnaires (620 control groups and 620 case groups) (Table 1). The pregnancy age ($P = 0.003$), educational level ($P \leq 0.001$), and family annual income ($P \leq 0.001$) of women in the case group were significantly lower than those in the control group. However, there was no significant difference in BMI ($P = 0.104$). Moreover, the incidences of history of abnormal pregnancy (except for spontaneous abortion, embryo damage, and placenta previa), familial congenital malformations, personal medical history (except for history of congenital malformation), history of exposure to environmental hazardous substances (except for house renovation), and medication history during this pregnancy (except for folic acid) were significantly higher in the case group than in the control group. There were also significant differences in lifestyle between the two groups. The factors with P values less than 0.05 were included in the follow-up multivariate analysis.

3.2. Maternal DM Increases the Risk of Offspring CHD. During this pregnancy, 10.2% of women had PGDM, and 11.0% had GDM in the case group, both of which were significantly higher than the respective percentages of women in the control group ($P < 0.001$) (Table 2). There were also more women with GDM during previous pregnancies in the case group ($P \leq 0.001$). The unadjusted ORs for these three types of maternal DM were 2.61, 3.03, and 4.01, respectively, which demonstrated that if the mother had a history of DM, there was a higher risk for their offspring to develop CHD. Next, the relationship between maternal DM and offspring CHD was analysed by multivariate analysis (Table 3). Maternal DM was classified into 3 types, including GDM during this pregnancy, GDM in previous pregnancies, and PGDM in the 3 months before this pregnancy, and the risk factors in Table 1, such as age, educational level, and medical history, were adjusted in the analysis of these three types. There was a significant correlation between maternal DM and offspring CHD ($P \leq 0.001$), and maternal DM increased the risk of offspring CHD (aOR = 4.98, 4.30, 6.78, respectively).

3.3. NKX2.5 Variation Increases the Risk of CHD in Offspring. Univariate analysis showed that there were associations between CHD and the genotype or allele frequencies of any polymorphism of rs118026695, rs2277923, and rs703752 in *NKX2.5* (Table 4). Next, we performed multivariate analysis (Table 5). The homozygous genotypes with a larger number of control groups were used as the control genotype. The confounding factors in Table 1 were adjusted in the analysis. Mutations of rs118026695 and rs2277923 were demonstrated to be associated with CHD.

T/T, C/T, and C/C genotypes were detected at rs118026695, and their frequency distributions were significantly different between the control and case groups ($P \leq 0.001$). The logistic regression analysis revealed that C/T ($P \leq 0.001$, aOR = 2.15, 95% CI) and C/C ($P = 0.023$, aOR = 4.97, 95% CI) were positively correlated with CHD. The frequency distribution of 2 alleles (C, T) also showed a significant difference between the control and case groups ($P \leq 0.001$), and the logistic regression analysis showed that the C allele was positively correlated with CHD ($P \leq 0.001$, OR = 1.81, 95% CI).

C/C, T/C, and T/T genotypes were detected at rs2277923, and their frequency distributions were significantly different between the control and case groups ($P \leq 0.001$). The logistic regression analysis revealed that T/C ($P = 0.004$, aOR = 1.61, 95% CI) and T/T ($P = 0.021$, aOR = 1.74, 95% CI) were positively correlated with CHD. The frequency distribution of 2 alleles (C, T) also showed a significant difference between the control and case groups ($P \leq 0.001$), and the logistic regression analysis showed that the T allele was positively correlated with CHD ($P \leq 0.001$, OR = 1.38, 95% CI).

3.4. Analysis of the Interaction of Maternal DM and NKX2.5 in the Development of CHD in Offspring. Based on the above results, three types of maternal DM and the *NKX2.5* SNPs at rs11802669 and rs2277923 were chosen to undergo further analysis (Table 6). We analysed their interaction and found that the interactions between maternal GDM during this pregnancy and C/T at rs11802669 ($P = 0.008$, aOR = 8.12, 95% CI) or T/C at rs2277923 ($P \leq 0.001$, aOR = 17.72, 95% CI) increased the risk of CHD in offspring.

4. Discussion

Cardiac development is a complicated process involving the dual roles of genes and the environment. A classic example

Table 5: Multivariate analysis of *NKX2.5* gene polymorphism and CHD.

NKX2.5 gene	B	S.E	Wals	*P* value	Adjusted OR (95% CI)*
Genotype at rs6882776 (control genotype = A/A)					
G/A	0.082	0.169	0.238	0.626	1.09 (0.78-1.51)
G/G	0.018	0.239	0.006	0.940	1.02 (0.64-1.63)
Additive model	0.026	0.114	0.050	0.822	1.03 (0.82-1.28)
Recessive model	0.068	0.161	0.179	0.673	1.07 (0.78-1.47)
Dominant model	-0.031	0.217	0.020	0.886	0.97 (0.63-1.48)
Genotype at rs118026695 (control genotype = T/T)					
C/T	0.766	0.196	15.297	0.001	2.15 (1.47-3.16)
C/C	1.603	0.707	5.147	0.023	4.97 (1.24-19.86)
Additive model	0.774	0.175	19.521	0.001	2.17 (1.54-3.06)
Recessive model	0.821	0.191	18.546	0.001	2.27 (1.56-3.30)
Dominant model	1.450	0.704	4.241	0.039	4.26 (1.07-16.95)
Genotype at rs2277923 (control genotype = C/C)					
T/C	0.477	0.167	8.127	0.004	1.61 (1.16-2.24)
T/T	0.555	0.240	5.352	0.021	1.74 (1.09-2.79)
Additive model	0.328	0.113	8.478	0.004	1.39 (1.11-1.73)
Recessive model	0.496	0.158	9.840	0.002	1.64 (1.20-2.24)
Dominant model	0.302	0.222	1.842	0.175	1.35 (0.88-2.09)
Genotype at rs703752 (control genotype = A/A)					
C/A	0.467	0.970	0.232	0.630	1.60 (0.24-10.68)
C/C	0.893	0.947	0.889	0.346	2.44 (0.38-15.63)
Additive model	0.430	0.212	4.098	0.043	1.54 (1.01-2.33)
Recessive model	0.452	0.229	3.908	0.048	1.57 (1.00-2.46)
Dominant model	0.847	0.946	0.802	0.371	2.33 (0.37-14.90)

OR: odds ratio; CI: confidence interval; SNP: single-nucleotide polymorphism; CHD: congenital heart disease. *Adjusted for factors with statistical differences in Table 1.

of a perturbed maternal environment that is closely associated with CHD is maternal GDM [19]. GDM, with its hyperglycaemic milieu during the first trimester, is related to diabetic embryopathy, affecting the heart, great vessels, and neural tube [20]. GDM during the latter half of pregnancy is related to foetal macrosomia, cardiomyopathy, and an increased incidence of perinatal complications and mortality [21]. Maternal DM was found to be a risk factor for offspring CHD in this study, which suggests the role of glucose in the causal pathway. Studies have indicated that the offspring of women with DM have similar risks for most types of CHD, and the increased risk of CHDs for them exceeded the increased risk of noncardiac diseases associated with maternal DM, which might be due to the impacts of maternal DM on general cardiac development very early in embryogenesis [22, 23]. This is consistent with our results and implies that some degree of glycaemic control before and during pregnancy is necessary. In addition, obesity has been associated with a small increase in the risk of CHD [24]. Our study, however, did not support this conclusion. There was no significant difference in BMI between the control and case groups, which indicated that there were other vital factors impacting offspring CHD, especially for the women who developed DM during this pregnancy.

Many studies show that the occurrence and development of CHD might be associated with changes in transcription factors in offspring. Over the years, family-based studies have identified mutations in transcription factor genes controlling heart development, including NKX2.5, GATA4, and TBX5 [25]. These mutations are often observed in patients with CHD but are rarely found in patients without CHD [26]. In our study, *NKX2.5* was proven to be associated with the incidence of CHD, and mutations at rs118026695 and rs2277923 were demonstrated to increase the risk of CHD in the univariate and multivariate analyses.

NKX2.5 is a member of the NK-2 family of homeodomain-containing transcription factors, which are highly conserved in many organisms [27]. It is a transcriptional regulator during early embryonic heart development and essential for the formation and maturation of the heart as well as the conduction system. Experiments indicate that the absence of *NKX2.5* in mice results in embryonic lethality and arrested heart development [10]. In addition, more than 40 mutations of *NKX2.5* have been found in CHD cases, and the 63A>G (rs2277923) polymorphism was one of the most intensively investigated sites [28]. Several studies have found that this polymorphism is significantly associated with CHD risk [11] and that this mutation is capable of changing mRNA structure and stability instead of the amino acid sequence of the encoded protein [29]. Moreover, the transcriptional activity of *NKX2.5* is also related to CHD. Ouyang et al. revealed that the 63A>G mutation significantly reduced the transcriptional activity of *NKX2.5* by 20%, which might account for its association with CHD [11]. Some opposite results, however, were also found in CHD studies in which the SNPs of *NKX2.5* at rs2277923 were not associated with the incidence of CHD in China [30]. The difference in results might be due to the choice of region, race, and CHD subtypes. Thus, further studies with large sample sizes are required to clarify this association.

The incidence of CHD is a result of both genetic and environmental factors. Their interactions are profoundly heterogeneous but may operate on common pathways. Nina et al. thought that glucose itself might exert a teratogenic effect via a signalling pathway regulating insulin sensitivity, which is also a key mediator of embryogenesis and early development [22]. Experimental studies found that

Table 6: Interaction analysis of Maternal DM and *NKX2.5* on CHD in offspring.

Maternal DM	Genotype	β	*P* value	Adjusted OR (95% CI)*
GDM during this pregnancy	rs118026695			
No	T/T			1
No	C/T	0.804(β_{g1})	0.001	2.23 (1.50-3.33)
No	C/C	21.324(β_{g2})	0.998	1.823E9
Yes	T/T	1.987(β_{e1})	0.001	7.29 (3.29-16.17)
Yes	C/T	2.094(β_{e1}*$_{g1}$)	0.008	8.12 (1.71-38.51)
Yes	C/C	0.430(β_{e1}*$_{g2}$)	0.620	1.54 (0.28-8.40)
GDM in previous pregnancy experiences	rs118026695			
No	T/T			1
No	C/T	0.861(β_{g1})	0.001	2.37 (1.59-3.52)
No	C/C	1.496(β_{g2})	0.046	4.46 (1.03-19.44)
Yes	T/T	1.603(β_{e1})	0.001	4.97 (2.44-10.11)
Yes	C/T	1.681(β_{e1}*$_{g1}$)	0.074	5.37 (0.85-33.87)
Yes	C/C	21.345(β_{e1}*$_{g2}$)	0.999	1.862E9
PGDM in the 3 months before this pregnancy	rs118026695			
No	T/T			1
No	C/T	0.826(β_{g1})	0.001	2.29 (1.54-3.40)
No	C/C	1.753(β_{g2})	0.013	5.77 (1.45-23.05)
Yes	T/T	1.971(β_{e1})	0.001	7.18 (3.27-15.74)
Yes	C/T	20.740(β_{e1}*$_{g1}$)	0.998	1.017E9
Yes	C/C			
GDM during this pregnancy	rs2277923			
No	C/C			1
No	T/C	0.472(β_{g1})	0.007	1.60 (1.14-2.26)
No	T/T	0.703(β_{g2})	0.006	2.02 (1.22-3.34)
Yes	C/C	1.984(β_{e1})	0.001	7.27 (2.37-22.33)
Yes	T/C	2.875(βe1*g1)	0.001	17.72 (5.79-54.24)
Yes	T/T	0.338(β_{e1}*$_{g2}$)	0.628	1.40 (0.36-5.50)
GDM in previous pregnancy experiences	rs2277923			
No	C/C			1
No	T/C	0.628(β_{g1})	0.001	1.88 (1.33-2.65)
No	T/T	0.715(β_{g2})	0.004	2.05 (1.25-3.34)
Yes	C/C	3.255(β_{e1})	0.001	25.92 (7.20-93.26)
Yes	T/C	1.225(β_{e1}*$_{g1}$)	0.005	3.41 (1.44-80.07)
Yes	T/T	0.867(β_{e1}*$_{g2}$)	0.317	2.38 (0.44-12.99)
PGDM in the 3 months before this pregnancy	rs2277923			
No	C/C			1
No	T/C	0.579(β_{g1})	0.001	1.79 (1.27-2.52)
No	T/T	0.644(β_{g2})	0.009	1.90 (1.17-3.09)
Yes	C/C	3.592(β_{e1})	0.001	36.30 (7.62-172.98)
Yes	T/C	1.421(β_{e1}*$_{g1}$)	0.002	4.14 (1.67-10.27)
Yes	T/T	21.312(β_{e1}*$_{g2}$)	0.999	1.802E9

DM: diabetes mellitus; CHD: congenital heart disease; GDM: gestational diabetes mellitus; PGDM: pregestational diabetes mellitus; OR: odds ratio; CI: confidence interval. *Adjusted for factors with statistical differences in Table 1.

hyperglycaemia in early pregnancy affected regulatory gene expression in the embryo for genes, such as Bmp4, Msx1, and Pax3, leading to cardiac neural crest cell death and an increased risk of CHD [31]. Whether the expression of *NKX2.5*, an important transcriptional regulator in early cardiac development, is affected by hyperglycaemia is worthy of further experimental investigation. In addition, *NKX2.5* is expressed in the first heart field (FHF) and the second heart field (SHF), the two distinct sources of cardiac progenitor cells contributing to different parts of the heart [32]. In mice,

NKX2.5 repression of Bmp2/Smad1 signalling regulated SHF proliferation and outflow tract morphology [33]. In the cardiac fields of *NKX2.5* mutants, failed SHF proliferation and OFT truncation were also found [34]. Similarly, hyperglycaemia was found to take part in the development of SHF, and the association with maternal diabetes mellitus was much stronger for anterior second heart field defects than for posterior second heart field defects when grouping the outflow tract malformations and the inflow tract malformations [19]. Based on the above, the interaction of maternal DM and *NKX2.5* genetic variants deserves further exploration. To the best of our knowledge, this is the first study to explore the association of the interaction of maternal DM and *NKX2.5* genetic variants with the risk of CHD in offspring.

Finally, we acknowledge important limitations in our study. This is a retrospective study, and recall bias is inevitable, even though we took measures to reduce it in sample selection and information collection. In addition, this study was aimed at Han Chinese individuals and was restricted geographically, so different ethnic populations and large sample sizes are required to confirm our results. Finally, the outcome of interest in this study was total CHD instead of specific CHD subtypes, which might contribute to the inaccuracy of the results.

5. Conclusion

In this study, we investigated the risk factors associated with CHD. We demonstrated that maternal DM, *NKX2.5* variants, and their interaction were significantly associated with CHD in offspring. With the aim of preventing CHD, there is a need for women to control their glycaemic index during pregnancy and to screen for *NKX2.5* mutations in their children if necessary.

Data Availability

The data used to support the findings of this study are included within the article.

Conflicts of Interest

The authors declare no conflict of interest, financial or otherwise.

Acknowledgments

The authors would like to thank the editors and reviewers for their suggestions and all colleagues working in Maternal and Child Health Promotion and Birth Defect Prevention Group. This study was funded by the National Natural Science Foundation Program of China (Grant No. 81803313, 81974019, 81970248), Natural Science Foundation Program of Hunan Province (Grant No. 2018JJ2551), Hunan Provincial Key Research and Development Program (Grant No. 2018SK2062 and 2018SK2063), National Key Research and Development Program of China (2018YFA0108700, 2017YFA0105602), The key program of Guangzhou science research plan (805212639211), and The Special Project of Dengfeng Program of Guangdong Provincial People's Hospital (DFJH201812; KJ012019119).

References

[1] R. H. Anderson, "Has the congenitally malformed heart changed its face? Journey from understanding morphology to surgical cure in congenital heart disease," *Circulation Research*, vol. 120, no. 6, pp. 901–903, 2017.

[2] K. J. Jenkins, A. Correa, J. A. Feinstein et al., "Noninherited risk factors and congenital cardiovascular defects: current knowledge: a scientific statement from the american heart association council on cardiovascular disease in the young: endorsed by the american academy of pediatrics," *Circulation*, vol. 115, no. 23, pp. 2995–3014, 2007.

[3] T. van der Bom, A. C. Zomer, A. H. Zwinderman, F. J. Meijboom, B. J. Bouma, and B. J. Mulder, "The changing epidemiology of congenital heart disease," *Nature Reviews Cardiology*, vol. 8, no. 1, pp. 50–60, 2011.

[4] H. Melchior, D. Kurch-Bek, and M. Mund, "The prevalence of gestational diabetes," *Deutsches Aerzteblatt Online*, vol. 114, no. 24, pp. 412–418, 2017.

[5] J. G. Ray, T. E. O'Brien, and W. S. Chan, "Preconception care and the risk of congenital anomalies in the offspring of women with diabetes mellitus: a meta-analysis," *QJM*, vol. 94, no. 8, pp. 435–444, 2001.

[6] M. Basu and V. Garg, "Maternal hyperglycemia and fetal cardiac development: clinical impact and underlying mechanisms," *Birth Defects Research*, vol. 110, no. 20, pp. 1504–1516, 2018.

[7] M. W. Wessels and P. J. Willems, "Genetic factors in non-syndromic congenital heart malformations," *Clinical Genetics*, vol. 78, no. 2, pp. 103–123, 2010.

[8] S. M. Reamon-Buettner and J. Borlak, "NKX2-5: an update on this hypermutable homeodomain protein and its role in human congenital heart disease (chd)," *Human Mutation*, vol. 31, no. 11, pp. 1185–1194, 2010.

[9] J. J. Schott, D. W. Benson, C. T. Basson et al., "Congenital heart disease caused by mutations in the transcription factor NKX2-5," *Science*, vol. 281, no. 5373, pp. 108–111, 1998.

[10] R. Terada, S. Warren, J. T. Lu, K. R. Chien, A. Wessels, and H. Kasahara, "Ablation of Nkx2-5 at mid-embryonic stage results in premature lethality and cardiac malformation," *Cardiovascular Research*, vol. 91, no. 2, pp. 289–299, 2011.

[11] P. Ouyang, E. Saarel, Y. Bai et al., "A de novo mutation in *NKX2.5* associated with atrial septal defects, ventricular noncompaction, syncope and sudden *death*," *international journal of clinical chemistry*, vol. 412, no. 1-2, pp. 170–175, 2011.

[12] F. Sun and G. Liu, "Study on the expression of GATA4 and Nkx 2.5 genes in the heart development of fetal rats with gestational diabetes," in *Proceedings of the Second Neonology Conference of Guangdong Medical Association*, pp. 102–104, 2013.

[13] W. Li, J. Ren, X. Huang, F. Sun, and G. Liu, "Expression and significance of Nkx 2.5 in the heart development of gestational diabetic offspring," in *Proceedings of the Third National Conference of Neonatal Physicians of the Chinese Medical Doctor Association*, vol. 96, 2013.

[14] W. Li, G. Liu, S. Han, L. Song, and R. Qiang, "Expression and significance of Nkx 2. 5 in fetal murine heart development during gestational diabetes," *Journal of Guangzhou Medical University*, vol. 3, pp. 18–22, 2015.

[15] Y. Cao, J. Wang, C. Wei et al., "Genetic variations of NKX2-5 in sporadic atrial septal defect and ventricular septal defect in Chinese Yunnan population," *Gene*, vol. 575, no. 1, pp. 29–33, 2016.

[16] S. Pang, J. Shan, Y. Qiao et al., "Genetic and functional analysis of the NKX2-5 gene promoter in patients with ventricular septal defects," *Pediatric Cardiology*, vol. 33, no. 8, pp. 1355–1361, 2012.

[17] M. den Hoed, M. Eijgelsheim, T. Esko et al., "Identification of heart rate-associated loci and their effects on cardiac conduction and rhythm disorders," *Nature genetics*, vol. 45, no. 6, pp. 621–631, 2013.

[18] H. M. Wallace, "A model of gene-gene and gene-environment interactions and its implications for targeting environmental interventions by genotype," *Theoretical Biology and Medical Modelling*, vol. 3, no. 1, p. 35, 2006.

[19] S. Liu, K. S. Joseph, S. Lisonkova et al., "Association between maternal chronic conditions and congenital heart defects: a population-based cohort study," *Circulation*, vol. 128, no. 6, pp. 583–589, 2013.

[20] Z. Zhao and E. A. Reece, "New concepts in diabetic embryopathy," *Clinics in Laboratory Medicine*, vol. 33, no. 2, pp. 207–233, 2013.

[21] K. Kc, S. Shakya, and H. Zhang, "Gestational diabetes mellitus and macrosomia: a literature review," *Annals of Nutrition and Metabolism*, vol. 66, no. 2, pp. 14–20, 2015.

[22] N. Oyen, L. J. Diaz, E. Leirgul et al., "Prepregnancy diabetes and offspring risk of congenital heart disease: a nationwide cohort study," *Circulation*, vol. 133, no. 23, pp. 2243–2253, 2016.

[23] R. M. Simeone, O. J. Devine, J. A. Marcinkevage et al., "Diabetes and congenital heart defects: a systematic review, meta-analysis, and modeling project," *American Journal of Preventive Medicine*, vol. 48, no. 2, pp. 195–204, 2015.

[24] K. J. Stothard, P. W. G. Tennant, R. Bell, and J. Rankin, "Maternal overweight and obesity and the risk of congenital anomalies: a systematic review and meta-analysis," *Journal of the American Medical Association*, vol. 301, no. 6, pp. 636–650, 2009.

[25] B. G. Bruneau, "The developmental genetics of congenital heart disease," *Nature*, vol. 451, no. 7181, pp. 943–948, 2008.

[26] M. G. Posch, A. Perrot, K. Schmitt et al., "Mutations in gata 4, nkx 2.5, creld 1, and bmp 4 are infrequently found in patients with congenital cardiac septal defects," *American journal of medical genetics. Part A*, vol. 146a, no. 2, pp. 251–253, 2008.

[27] G. Ranganayakulu, D. A. Elliott, R. P. Harvey, and E. N. Olson, "Divergent roles for nk-2 class homeobox genes in cardiogenesis in flies and mice," *Development (Cambridge, England)*, vol. 125, pp. 3037–3048, 1998.

[28] B. Stallmeyer, H. Fenge, U. Nowak-Gottl, and E. Schulze-Bahr, "Mutational spectrum in the cardiac transcription factor gene nkx 2.5 (csx) associated with congenital heart disease," *Clinical genetics*, vol. 78, no. 6, pp. 533–540, 2010.

[29] Z. E. Sauna and C. Kimchi-Sarfaty, "Understanding the contribution of synonymous mutations to human disease," *Nature Reviews Genetics*, vol. 12, no. 10, pp. 683–691, 2011.

[30] W. Zhang, X. Li, A. Shen, W. Jiao, X. Guan, and Z. Li, "Screening NXK2.5 mutation in a sample of 230 Han Chinese children with congenital heart diseases," *Genetic Testing and Molecular Biomarkers*, vol. 13, no. 2, pp. 159–162, 2009.

[31] S. D. Kumar, S. T. Dheen, and S. S. Tay, "Maternal diabetes induces congenital heart defects in mice by altering the expression of genes involved in cardiovascular development," *Cardiovascular Diabetology*, vol. 6, no. 1, p. 34, 2007.

[32] M. Buckingham, S. Meilhac, and S. Zaffran, "Building the mammalian heart from two sources of myocardial cells," *Nature Reviews Genetics*, vol. 6, no. 11, pp. 826–835, 2005.

[33] O. W. Prall, M. K. Menon, M. J. Solloway et al., "An Nkx2-5/Bmp2/Smad1 negative feedback loop controls heart progenitor specification and proliferation," *Cell*, vol. 128, no. 5, pp. 947–959, 2007.

[34] B. Zhou, A. Gise, Q. Ma, J. Rivera-Feliciano, and W. T. Pu, "Nkx2-5- and Isl1-expressing cardiac progenitors contribute to proepicardium," *Biochemical and Biophysical Research Communications*, vol. 375, no. 3, pp. 450–453, 2008.

Hindawi
Journal of Diabetes Research
Volume 2020, Article ID 3069867, 9 pages
https://doi.org/10.1155/2020/3069867

Review Article

Prevalence of Cardiovascular Disease in Patients with Type 2 Diabetes Mellitus in Iran: A Systematic Review and Meta-Analysis

Mohsen Kazeminia,[1] Nader Salari,[2] and Masoud Mohammadi[1]

[1]*Department of Nursing, School of Nursing and Midwifery, Kermanshah University of Medical Sciences, Kermanshah, Iran*
[2]*Department of Biostatistics, School of Health, Kermanshah University of Medical Sciences, Kermanshah, Iran*

Correspondence should be addressed to Masoud Mohammadi; masoud.mohammadi1989@yahoo.com

Received 16 June 2020; Accepted 31 July 2020; Published 26 September 2020

Guest Editor: Markus Wallner

Background. Type 2 diabetes mellitus (DM) is the most common type of DM and accounts for 90% of the cases. One of the most important complications of type 2 DM is cardiovascular complications, which are the most common cause of mortality in patients with DM. Various studies have reported different incidence rates of cardiovascular disease in patients with type 2 DM. However, no comprehensive review of previous studies has been done. This study is aimed at determining the prevalence of cardiovascular disease in patients with type 2 diabetes mellitus in Iran with a systematic review and meta-analysis. *Methods*. In this review, studies were first extracted searching domestic and international databases including SID, MagIran, IranMedex, IranDoc, Cochrane, Embase, ScienceDirect, Scopus, PubMed, and Web of Science (ISI), published between 2001 and September 2019. The random effects model was adopted for the analysis, and heterogeneity of the extracted studies was investigated with the I^2 index. The data collected from the extracted studies were analyzed using a comprehensive meta-analysis (Version 2) software. *Results*. The prevalence of cardiovascular disease in patients with type 2 DM in Iran in 17 studies with a sample size of 9656 was 37.4% (95% CI: 31.4-43.8). Based on meta-regression, there was a significant difference on the effect of year of conducting the study and sample size with the prevalence of cardiovascular disease in patients with type 2 DM in Iran ($p \leq 0.001$). *Conclusion*. The results of this study indicated that there was a high prevalence rate of cardiovascular disease in patients with type 2 DM in Iran. Therefore, appropriate strategies should be taken to improve this situation and trace and supervise it at all levels, providing feedback to hospitals.

1. Background

Type 2 diabetes mellitus (DM) is the most common type of DM and accounts for 90% of the cases. The prevalence of type 2 DM is steadily increasing [1], and its incidence in children has increased approximately tenfold [2]. It is estimated that there are currently 1.5 million patients with DM in Iran [3]. In 1997, the DM prevalence rate was about 125 million, and a recent World Health Organization (WHO) estimate shows that by 2025, the number of individuals with DM in the world will increase to 300 million [4]. Although the incidence rate of type 1 and type 2 DM is increasing worldwide, it is expected that the type 2 DM will increase more rapidly due to lifestyle changes leading to decreased physical activity and increased prevalence of obesity [5, 6].

Epidemiological studies have indicated that DM has a variable distribution in Iran. In a study conducted in Isfahan on subjects aged 35 years and older, the prevalence of DM was 7-8%, and this rate was 13.6% in Bushehr and 14.52% among individuals over 30 years in urban areas of Yazd province [7]. Type 2 DM is a familial disease, and there are convincing arguments in support of this claim. Genetic factors play an important role in the development of this disease. However, many of the underlying genes for DM are still

unknown, but it is known to be polygenic and multifactorial. Various genetic loci are involved in the susceptibility of developing this disease. Environmental factors (such as nutrition and physical activity) also influence its phenotypic expression [5, 8].

The incidence of type 2 DM in identical twins is between 70% and 90%, and if one of them suffers from DM, the risk of the other twin developing diabetes is 50%. People with one parent with type 2 DM are at higher risk for developing DM; and obese individuals with type 2 diabetic parents are more likely to develop type 2 DM compared to those with parents without type 2 DM. In addition to the family history, other factors such as obesity, age, ethnicity, gestational DM, hypertension, and hyperlipidemia have been all involved in DM [9, 10].

Hypertension can be an early symptom of insulin resistance due to central obesity. A secondary hypothesis is that hypertension is a marker of endothelial dysfunction, which itself is a risk factor for insulin resistance, type 2 DM, and cardiovascular diseases (CVDs) [11]. Cardiovascular disease (CVD) is the name for the group of disorders of the heart and blood vessels and includes hypertension, coronary heart disease, stroke, peripheral vascular disease, heart failure, rheumatic heart disease, congenital heart disease, and cardiomyopathies. CVDs are the number one cause of death globally and more people die annually from CVDs than from any other cause, an estimated 17.3 million people died from CVDs in 2008, representing 30% of all global deaths [10–13].

Hypertension can be observed in 70% of patients with DM, and the risk of developing DM is 2 times higher in individuals with hypertension [12].

DM, especially the type 2, is often associated with lipid metabolism disorders. Increased plasma fatty acid levels play an essential role in increasing the insulin resistance. Additionally, plasma fatty acids cause dyslipidemia in DM by increasing low-density lipoprotein (LDL) and decreasing high-density lipoprotein (HDL). This androgenic function of lipoprotein (increased triglyceride, increased LDL, and decreased HDL) causes atherosclerosis and increased risk of CVDs, which is the most common cause of death in type 2 DM [13].

The incidence of coronary artery diseases (CADs) in individuals with type 2 DM is 2- to 4-fold higher than those without DM. The risk of myocardial infarction (MI) in patients with DM with no previous history of infarction appears to be as high as that of the individuals without DM with a history of MI [14]. The most common form of dyslipidemia in patients with type 2 DM is the elevated triglyceride levels and decreased HDL cholesterol [15].

The mean LDL cholesterol concentration in patients with type 2 DM is not significantly different from that in the individuals without DM. However, there may be qualitative changes in LDL cholesterol. In particular, patients with DM have smaller and denser LDL particles which make them more easily glycosylated and susceptible to oxidation and subsequently increase their risk of cardiovascular events [15–18].

According to a study conducted by Soltani and Fardin [19] in 2005, in the city of Isfahan located in north of Iran, 20.8% of patients with DM had ischemic heart disease [19]. In another relevant study by Abbasian et al. [20], 38% of patients with DM suffered from hypertension.

Given the effect of different factors on the prevalence of CVDs in patients with type 2 DM and lack of general/reliable statistics in this regard in Iran, we performed a comprehensive review of the literature published on patients in this geographical region and analyzed the results of these studies to assess the prevalence of CVDs in patients with type 2 DM in Iran.

This study is aimed at determining the prevalence of cardiovascular disease in patients with type 2 diabetes mellitus in Iran with a systematic review and meta-analysis. The findings of this study can be used to develop more precise planning to reduce CVDs in patients with type 2 DM.

2. Methods

In this systematic review and meta-analysis study, the prevalence rate of CVDs was evaluated in patients with type 2 DM in Iran without a time limit based on the studies published between 2001 and September 2019. To this end, the studies published in the Iranian databases including SID, MagIran, IranMedex, and IranDoc as well as the international databases Cochrane, Embase, ScienceDirect, Scopus, PubMed, and Web of Science (ISI) were searched with Persian keywords and their English equivalents including Prevalence, Complications, Cardiovascular, Diabetes, and Iran.

The observational (noninterventional) studies and all available full-text articles were included in this review. For more information, the references of the reviewed studies were also examined for access to other studies.

2.1. Selection of Studies. Initially, all studies referring to the prevalence of CVDs in patients with type 2 DM in Iran were collected and accepted by researchers (MK and MM) based on the inclusion and exclusion criteria. The exclusion criteria included unrelated cases, case reports, interventional studies, duplication of studies, unclear methodology, and inaccessibility of the full text of the study. In order to reduce bias, the studies were searched independently by two researchers (MK and MM), and in case of the lack of agreement on a study, it was judged by the third researcher (NS) or supervisor. A total of 24 studies entered into the third stage, i.e., the qualitative evaluation stage.

2.2. Qualitative Evaluation of Studies. The quality of the studies was evaluated based on the selected and related items of the 22-item STROBE checklist. Accordingly, the maximum quality score of 32 was considered, and papers with a score of less than 18 were considered to have low quality, and thus, they were excluded from the study [18]. In the present study, 17 high-quality and medium-quality studies were entered into the systematic meta-analysis review, and seven studies with a poor quality were excluded.

2.3. Data Extraction. All studies finally entered into the meta-analysis process were prepared for data extraction using a preprepared checklist. The checklist included the study title,

the first author's name, year of the data collection, study location, sample size, prevalence of CVDs, and mean age.

2.4. Statistical Analysis. Since the prevalence rate had a binomial distribution, the prevalence variance was calculated using the binomial distribution variance formula and a weighted mean was applied to combine the prevalence rate of the different studies. In order to evaluate the heterogeneity of the selected studies, the I^2 index test was used. In addition, the metaregression analysis was employed to investigate the relationship between the incidences of CVDs in patients with type 2 DM, the year of performing the study, and the sample size. In order to investigate publication bias, the Begg and Mazumdar test was used with a significance level 0.1 and its corresponding funnel plot. Furthermore, the sensitivity analysis was performed to evaluate the effect of each of the studies on the final result. The data was analyzed using the comprehensive meta-analysis implemented in "Version 2" software.

3. Results

The probability of bias in the results by the funnel diagram and Begg and Mazumdar test at the significant level of 0.1 indicated that there is no bias in the present study ($p = 0.174$) (Figure 1).

Based on PRISMA 2009, the studies published in the Iranian databases including SID, MagIran, IranMedex, and IranDoc and Cochrane, Embase, ScienceDirect, Scopus, PubMed, and Web of Science (ISI) were searched with Persian keywords and their English equivalents including Prevalence, Complications, Cardiovascular, Diabetes, and Iran between 2001 and September 2019. A total of 1077 articles were obtained. Subsequently, based on primary studies, after deleting 62 repetitive articles, there were 1015 articles with initial conditions to enter the study. Eventually, 17 articles were included in the meta-analysis process after secondary study with deletion of 991 unrelated articles and 7 articles which abstracts and full texts were unavailable and their quality was low (Figure 2).

The search terms were as follows: (((((Cardiovascular Diseases [Title/Abstract]) OR CARDIOVASC DIS [Title/-Abstract]) OR CVD [Title/Abstract] AND Blood glucose [Title/Abstract]) OR Hyperglycemia [Title/Abstract]) AND Diabetes [Title/Abstract]) OR Non-insulin dependent diabetes [Title/Abstract]) AND Nephropathy) OR Diabetic Nephropathies))))).

Based on the results of the heterogeneity of the studies ($I^2 = 96.8$) and due to the heterogeneity of the selected studies, the random effects model was conducted to combine the studies and the joint prevalence estimation. The total sample size was 9656 individuals with the mean age of subjects in each study presented in Table 1. The lowest and the highest sample sizes were related to Soltani et al. (2011) and Janghorbani et al. (2005) with 70 and 3202 subjects, respectively; and the highest and lowest prevalence of CVDs in patients with type 2 DM in Iran were, respectively, related to the studies by Soltani and Fardin Far [19] and Abbasian et al. [20] (Table 1). According to the meta-analysis, the prevalence of CVDs in patients with type 2 DM in Iran was estimated to be 37.4% (95% CI: 31.4-43.8%) (Figure 3).

The sensitivity analysis was performed in accordance with Figure 4 to ensure the stability of the study results; after removing each study, results did not change (Figure 4).

The relationship between the year of conducting the study ($p \leq 0.001$) and the sample size ($p \leq 0.001$) with the prevalence of cardiovascular disease in patients with type 2 DM in Iran was investigated using the metaregression. Significant differences were observed between cardiovascular disease and the two above cases. The prevalence of cardiovascular disease in patients with type 2 DM in Iran was increased with the increase in the year of conducting the study and decreased with the increase in the sample size (Figures 5 and 6).

With increasing age of participants in the study, the prevalence of cardiovascular disease in patients with type 2 DM in Iran increases, which is statistically significant ($p \leq 0.001$) (Figure 7).

4. Discussion

The aim of this study was to determine the prevalence of cardiovascular disease in patients with type 2 DM in Iran. DM is one of the most common diseases worldwide. The American Diabetes Association (ADA) reported that in 2007, $174 billion was spent treating patients with DM, of which $58 billion was spent to mitigate the damages due to the long-term complications of this disease [34]. This disease has an increasing trend and has been predicted to rise from 285 million in 2010 to 439 million in 2030 [36].

In the present study, the prevalence of cardiovascular disease in patients with type 2 DM in Iran was 37.4%. In the study performed by Liu et al. in China, the prevalence of CVDs in patients with type 2 DM was 30.1% [37]. In addition, in a study conducted by Shi et al. on morbidity associated with chronic complications of DM in China, CVDs were the most common chronic complication of type 2 DM [38]. The rate of cardiovascular disease in patients with type 2 DM was 26% in South Korea [39]. The results of a study in Denmark in 2010 reported a complication rate of 32 to 40% [40]. Patients with DM undergo periodic evaluation of renal and ocular complications; however, there is no specific plan to assess the related cardiovascular programs. Given the high prevalence of cardiovascular disease in patients with DM and lack of a clear plan for evaluating these complications, it is recommended that CVDs should be prevented by taking preventive measures such as regular exercise and developing cardiovascular periodic evaluation programs.

The long life and quality of life of patients with DM depend on the progression and severity of chronic complications, especially CVDs [41, 42]. The high prevalence of complications in these patients is a serious issue as these complications are not reversible and could cause damage to the organs and result in serious health problems for the patients. This could also incapacitate the patients and consequently incur heavy medical cost burden on the patients and society.

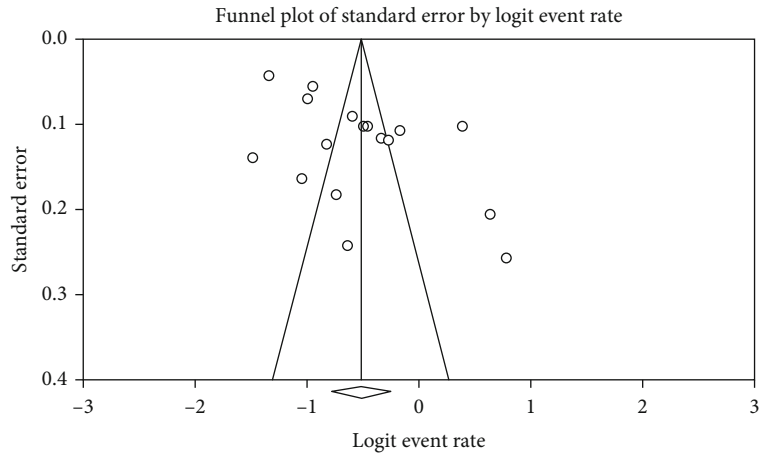

Figure 1: Funnel plot of results of the prevalence of cardiovascular disease in patients with type 2 diabetes mellitus (DM).

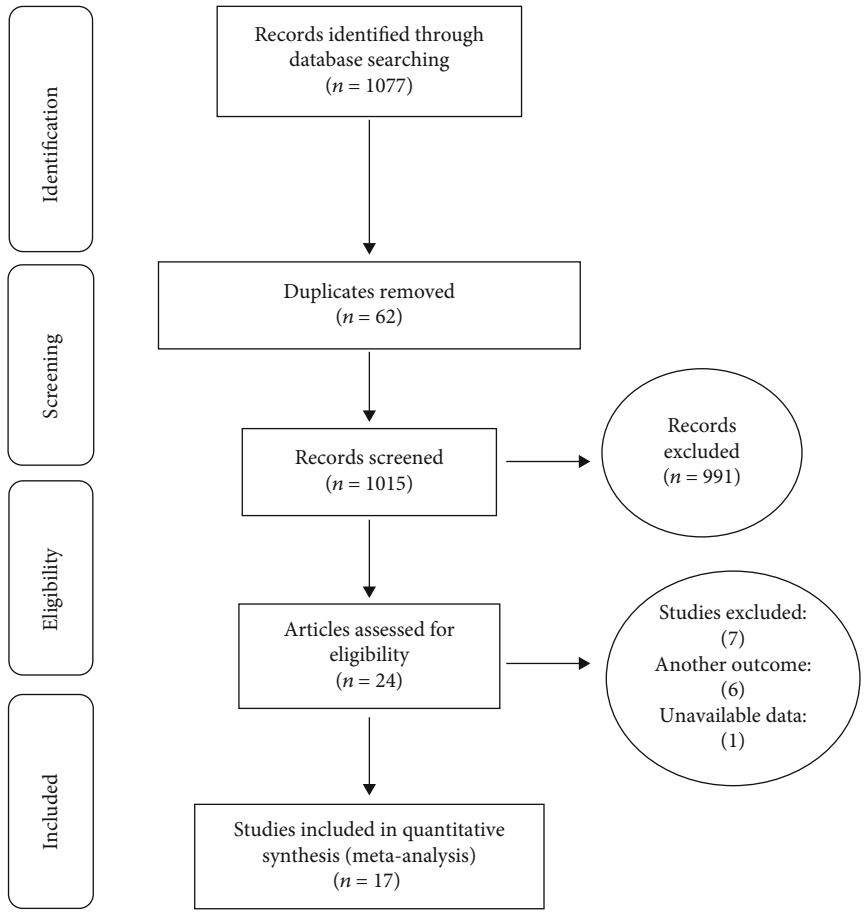

Figure 2: Flow diagram of study selection.

Grobbee showed that CVDs and hypertension are common problems in patients with DM; besides, obesity is one of the predisposing factors for CVDs [43]. In a report by the WHO published in 2010, obesity and overweight have been identified as the most important contributors to the rising trend of type 2 DM [44]. Moreover, numerous other studies have also suggested obesity to be the most important risk factor for type 2 DM [45–47]. Therefore, it seems that by the continuous control of the blood lipids and preventive measures to stop its increasing rate, the prevalence of type 2 DM and hence its chronic complications, especially cardiovascular disease, can be reduced in society. Adequate training on obesity and on reducing its complications is needed to be provided.

Table 1: Characteristics of included studies in the prevalence of cardiovascular disease in patients with type 2 diabetes.

Author [reference]	Year of the data collection	Mean age (years)	City	Sample size	Prevalence (%)	Quality
Janghorbani and Amini [21]	2005	48.3	Isfahan	3202	20.8	High
Abbasian et al. [22]	2006	49.6	Shahroud	400	38.0	High
Abbasian and Delorian [20]	2007	50.2	Shahroud	340	18.5	High
Janghorbani et al. [23]	2006	50.6	Isfahan	1566	28.0	High
Sarshar and Chamanzari [24]	2002	52	Gonabad	136	32.4	High
Hosseini et al. [25]	2014	53.9	Tehran	305	30.5	High
Taherkhani and Safi [26]	2014	54.09	Tehran	104	65.4	High
Kashi et al. [27]	2015	54.4	Sari	1021	27.0	High
Khatoni et al. [28]	2011	58.25	Qasr-e Shirin	286	43.4	High
Kaviani et al. [29]	2013	58.6	Khorramabad	299	41.8	High
Ranjbar et al. [30]	2004	—	Shiraz	392	59.7	Medium
Heshmati et al. [31]	2013	—	Fereydunkenar	400	38.8	High
Ajam et al. [32]	2005	—	Gonabad	347	26.0	Medium
Alfti Far et al. [33]	2017	—	Hamadan	89	45.8	High
Niroumand et al. [34]	2016	—	Northeast of Iran	75	34.7	High
Soltani and Fardin Far [19]	2011	—	Birjand	70	68.6	Medium
Cheraghi et al. [35]	2010	—	Shadegan	521	35.7	Medium

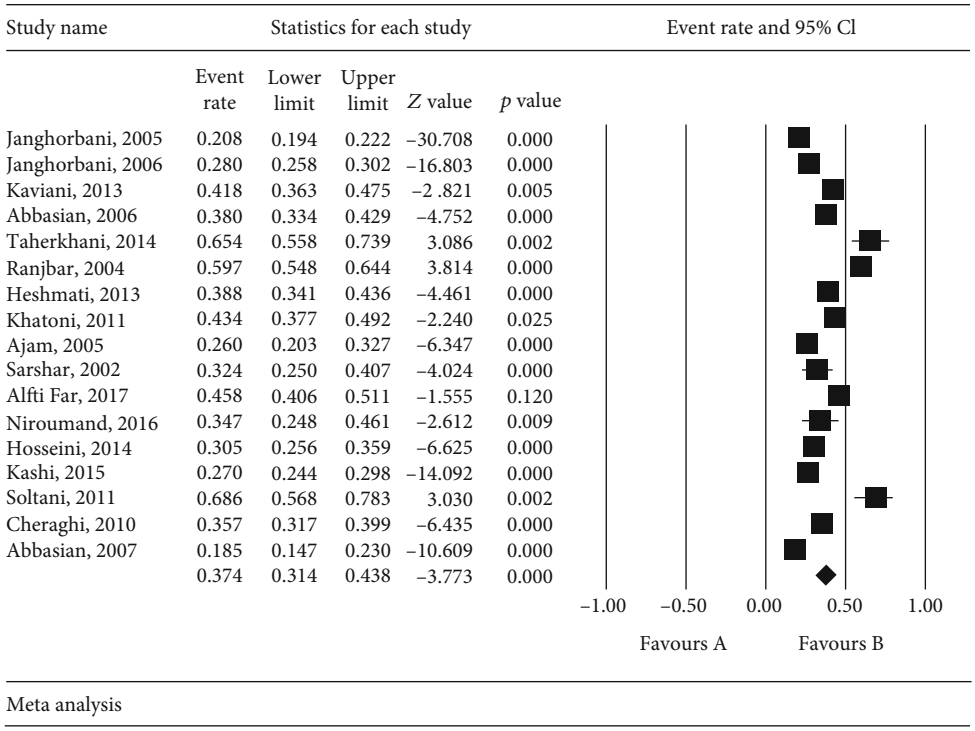

Figure 3: Prevalence of cardiovascular disease in patients with type 2 diabetes mellitus (DM) and 95% confidence interval in Iran. The middle point of each line shows the prevalence of cardiovascular disease in each study, and the rhombic figure shows the prevalence of cardiovascular disease in patients with type 2 DM in Iran for the whole studies.

The incidence of DM and obesity has rapidly increased in the last century, and the morbidity and mortality resulting from these two epidemics have caused enormous health problems for human societies [48–51]. Type 2 DM, which is the most common type of DM, could be developed due to the presence of an inherited background as well as environmental factors as the most affecting factors [52]. In many cases, the lack of a healthy nutrition and immobility would first cause prediabetes and then diabetes emerges [53].

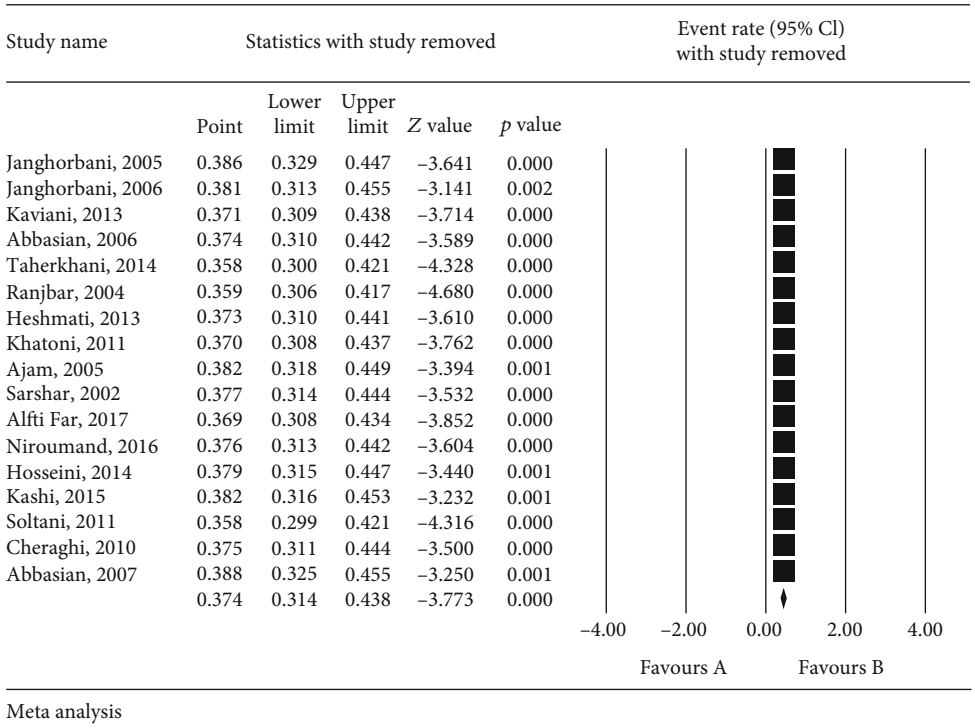

Figure 4: Sensitivity analysis results.

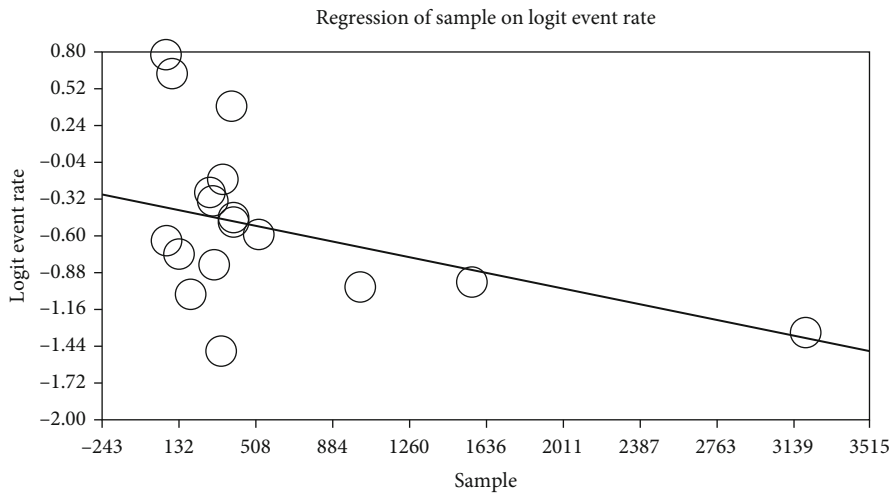

Figure 5: Metaregression of the relationship between the sample size and prevalence of cardiovascular disease in patients with type 2 diabetes mellitus (DM) in Iran.

According to a systematic review and meta-analysis reported in Ray et al., out of 1497 cases of nonlethal myocardial infarction, 2318 cases of cardiovascular diseases, 1127 cases of stroke, and 2892 deaths, it was found that glycemic control resulted in a 17% decrease in the incidence of nonlethal MI and a 15% decrease in CADs, but with no significant effect on stroke and mortality among patients [54]. Nutrition, physical activity, glycemic control, and training of patients are the basis of DM treatment for all diabetic patients. Medical treatment should be accompanied by nutritional therapy and physical activity, in addition to considering weight loss and healthy lifestyle when choosing a suitable treatment [55, 56].

The findings in this study indicated that there is a high incidence of cardiovascular disease in patients with type 2 DM in the population under study. As a result, interventions must be performed in lifestyle changes as well as regular control of blood pressure, cholesterol, and blood glucose in patients to prevent the disease and reduce DM-related complications. Since cardiovascular diseases in patients with DM are primarily preventable and can be controlled and treated in case of developing the complication, patients with

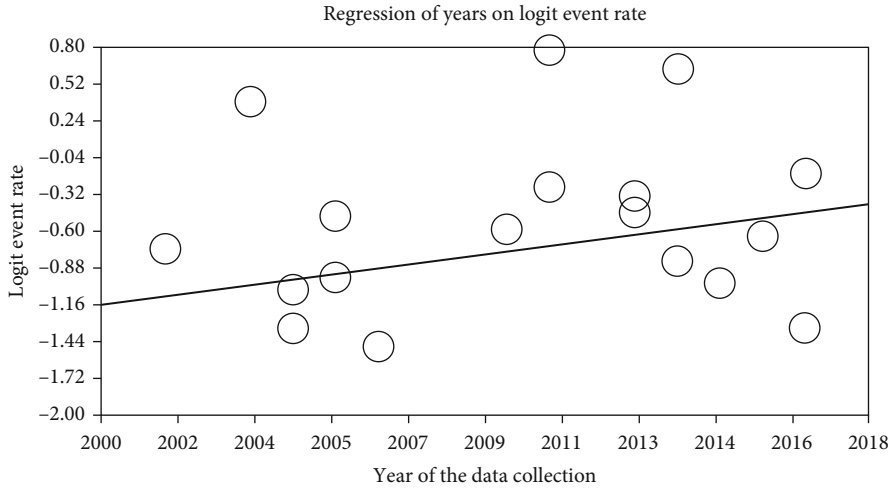

Figure 6: Metaregression of the relationship between the year of study and prevalence of cardiovascular disease in patients with type 2 diabetes mellitus (DM) in Iran.

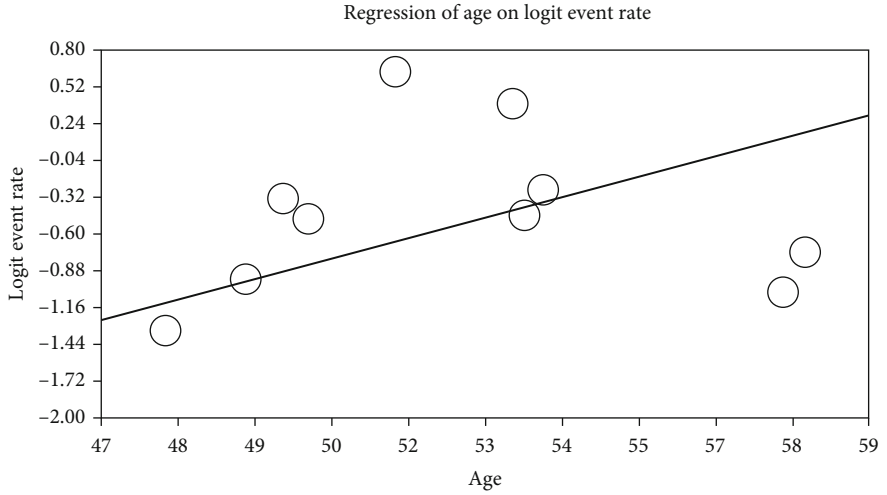

Figure 7: Metaregression of the relationship between the age of participants in the study and prevalence of cardiovascular disease in patients with type 2 diabetes mellitus (DM) in Iran.

DM need thus to be fully trained about this disease and learn the ways to prevent it. Moreover, the complications can be controlled and treated with early and timely diagnosis.

Given the high prevalence of cardiovascular disease in patients with type 2 DM in Iran, it is suggested that physicians pay more attention to the symptoms of this disease and that media training should be carried out with the aim to raise the awareness of individuals to reduce the delay in diagnosis. Studies are also recommended to be carried out on the prevalence of cardiovascular disease in patients with type 2 DM in other parts of the world to find out the worldwide rate.

5. Conclusion

The results of this review revealed that there is a high prevalence rate of cardiovascular disease in patients with type 2 DM in Iran. Therefore, appropriate strategies should be taken to improve this situation and trace and supervise it at all levels, providing feedback to hospitals.

Abbreviations

DM: Diabetes mellitus
CVDs: Cardiovascular diseases
WHO: World Health Organization
HDL: High-density lipoprotein
LDL: Low-density lipoprotein
STROBE: Strengthening the reporting of observational studies in epidemiology for cross-sectional study
PRISMA: Preferred reporting items for systematic reviews and meta-analysis.

Disclosure

The Deputy for Research and Technology, Kermanshah University of Medical Sciences, had no role in the design of the

study; collection, analysis, and interpretation of the data; and writing of the manuscript.

Conflicts of Interest

The authors declare that they have no conflict of interest.

Authors' Contributions

MK and NS contributed to the design; MM contributed to the statistical analysis and participated in most of the study steps. AA prepared the manuscript. MK and NS assisted in designing the study and helped in the interpretation of the study. All authors have read and approved the final manuscript.

Acknowledgments

This study was extracted from the research project no. 3008993 approved by the Student Research Committee of Kermanshah University of Medical Sciences, Kermanshah, Iran. The researchers of this study would like to appreciate the respected authorities of the university for funding the financial costs of the study. This study was supported by the Student Research Committee of Kermanshah University of Medical Sciences, Deputy for Research and Technology, Kermanshah University of Medical Sciences (IR) (3009523).

References

[1] J. P. Boyle, A. A. Honeycutt, K. M. V. Narayan et al., "Projection of diabetes burden through 2050:Impactofchanging demography and disease prevalence in the U.S," *Diabetes Care*, vol. 24, no. 11, pp. 1936–1940, 2001.

[2] M. Lean, L. McCombie, and J. McSorely, "Trends in type 2 diabetes," *BMJ*, vol. 366, p. l5407, 2019.

[3] F. Larijani, F. Zahedi, and S. Aghakhani, "Epidemiology of diabetes mellitus in Iran," *Shiraz E-Medical Journal*, vol. 4, p. 4, 2003.

[4] American Diabetes Association, "Prevention or delay of type 2 diabetes: standards of medical care in diabetes-2018," *Diabetes Care*, vol. 41, Suppl 1, pp. S51–S54, 2017.

[5] A. Powers, "Diabetes mellitus," *Harrison's principles of internal medicine*, E. Braunwald, A. S. Fauci, and D. L. Kasper, Eds., 2109–2137, 2001.

[6] H. King, R. E. Aubert, and W. H. Herman, "Global burden of diabetes, 1995–2025: prevalence, numerical estimates, and projections," *Diabetes Care*, vol. 21, no. 9, pp. 1414–1431, 1998.

[7] M. Afkhami-Ardekani, S. Vahidi, A. Vahidi, and M. H. Ahmadia, "Epidemiological survery of NIDDM in persons over 30 years old in Yazd province," *Journal of Shaheed Sadoughi University of Medical Sciences*, vol. 9, no. 1, pp. 22–31, 2001.

[8] J. C. Levy, A. Aetiology, and G. Hitman, *Type 2 diabetes prediction and prevention*, vol. 1, pp. 3–17, 1999.

[9] J. V. Bjørnholt, G. Erikssen, K. Liestøl, J. Jervell, E. Thaulow, and J. Erikssen, "Type 2 diabetes and maternal family history: an impact beyond slow glucose removal rate and fasting hyperglycemia in low-risk individuals? Results from 22.5 years of follow-up of healthy nondiabetic men," *Diabetes Care*, vol. 23, no. 9, pp. 1255–1259, 2000.

[10] P. H. Bennett, "Epidemiology of diabetes mellitus," in *Diabetes Mellitus: A Fundamental and Clinical Text*, D. LeRoith, S. I. Talor, and J. M. Olefsky, Eds., Lippincott William& Wilkins, 3rd edition, 2004.

[11] J. Tooke and K. Goh, "Vascular function in Type 2 diabetes mellitus and pre-diabetes: the case for intrinsic endotheliopathy," *Diabetic Medicine*, vol. 16, no. 9, pp. 710–715, 1999.

[12] S. Hill Golden, N.-Y. J. Wang, M. A. Klag, L. L. Meoni, and F. Brancati, "Blood pressure in young adulthood and the risk of type 2 diabetes in middle age," *Diabetes Care*, vol. 26, no. 4, pp. 1110–1115, 2003.

[13] A. Steinmetz, "Treatment of diabetic Dyslipoproteinemia," *Experimental and clinical endocrinology & diabetes*, vol. 111, no. 5, pp. 239–245, 2003.

[14] M. Evans, N. Khan, and A. Rees, "Diabetic dyslipidaemia and coronary heart disease: new perspectives," *Current Opinion in Lipidology*, vol. 10, no. 5, pp. 387–392, 1999.

[15] American Diabetes Association, "Dyslipidemia management in adults with diabetes," *Diabetes Care*, vol. 27, suppl 1, pp. s68–s71, 2004.

[16] S. Agashe and S. Petak, "Cardiac Autonomic Neuropathy in Diabetes Mellitus," *Methodist Debakey Cardiovasc J*, vol. 14, no. 4, pp. 251–256, 2018.

[17] A. Lejay, F. Fang, R. John et al., "Ischemia reperfusion injury, ischemic conditioning and diabetes mellitus," *J Mol Cell Cardiol*, vol. 91, pp. 11–22, 2016.

[18] J. P. Vandenbroucke, E. von Elm, D. G. Altman et al., "Strengthening the reporting of observational studies in epidemiology (STROBE)," *Epidemiology*, vol. 18, no. 6, pp. 805–835, 2007.

[19] M. Soltani and F. S. Fardin, *Relative frequency of diabetes complications in diabetic patients admitted to internal ward of Birjand Imam Reza and Vali Asr Hospital from October 2000 to October 2001, Birjand University of Medical Sciences. Numbe 2*, pp. 1–12, 2011.

[20] M. Abbasian and Z. M. Delorian, "Prevalence of diabetes complications in patients referred to Shahroud Diabetes Clinic," *Journal of Knowledge and Health*, vol. Numbe 4, pp. 17–21, 2007.

[21] M. Janghorbani and M. Amini, "Hypertension in type 2 diabetes mellitus in Isfahan, Iran: incidence and risk factors," *Diabetes research and clinical practice*, vol. 70, no. 1, pp. 71–80, 2005.

[22] M. Abbasian, M. Delorian Zadeh, S. Hosein Zadeh, and P. Norozi, *Prevalence of diabetes complications in patients referred to Shahroud Diabetes Clinic, 9th Iranian Congress of Nutrition*, 2006.

[23] M. Janghorbani, M. Amini, and A. Tavassoli, "Coronary heart disease in type 2 diabetes melittus in Isfahan, Iran," *Acta cardiologica*, vol. 61, no. 1, pp. 13–20, 2006.

[24] N. Sarshar and H. Chamanzari, "Diabetes complications in patients referred to Diabetes Clinic of Gonabad," *Journal of Gonabad University of Medical Science*, vol. 2, pp. 62–69, 2002.

[25] M. S. Hosseini, Z. Rostami, A. Saadat, S. M. Saadatmand, and E. Naeimi, "Anemia and microvascular complications in patients with type 2 diabetes mellitus," *Nephro-urology monthly*, vol. 6, no. 4, article e19976, 2014.

[26] M. Taherkhani and M. Safi, "Prevalence of microvascular complications and coronary artery disease in patients with type 2 diabetes," *Journal of Research in Medical School, Shahid Beheshti University of Medical Sciences*, vol. Numbe 3, pp. 167–172, 2014.

[27] Z. Kashi, A. Bahar, O. Akha et al., "Ischemic heart disease and related factors in patients with diabetes mellitus type II," *Journal of Mazandaran University of Medical Sciences*, vol. 25, no. 129, pp. 9–16, 2015.

[28] A. R. Khatoni, A. R. Abdi, E. Hosseini, T. Fatahpor, and H. Faizi, "Risk factors and complications of type 2 diabetes in Qasr Shirin Diabetes Center in the year 2010," *Journal of Vulnerable Groups Nursing, Boshehr University of Medical Sciences*, vol. Numbe 2, pp. 1–14, 2011.

[29] M. Kaviani, M. Abdolahian, V. Almaci, K. Anbari, and A. Jefferiesteh, *Frequency of chronic complications of type 1 diabetes in patients candidate for insulin use due to hyperglycemia, Lorestan University of Medical Sciences. the period 15, Numbe 4*, pp. 14–19, 2013.

[30] H. Ranjbar Gh, M. Soeid, H. Rajaei, and A. S. Sadegh, "The incidence of chronic complications of diabetes in patients referred to clinics affiliated to Shiraz University of Medical Sciences during a 12 year period," *Iranian Journal of Diabetes and Lipid*, vol. Numbe 2, pp. 127–134, 2004.

[31] H. Heshmati, N. Behnam Por, F. Khorasani, and Z. Moghadam, "Prevalence of chronic diabetes complications and some related factors in type 2 diabetic patients referred to Diabetes Center of Fereidoonker," *Journal of Neyshabour School of Medical Sciences*, vol. Numbe 1, pp. 36–43, 2013.

[32] M. Ajam, T. Raihani, A. A. Mirsani, and S. H. Nazemi, *Evaluation of chronic physical complications of diabetic patients referred to Gonabad Hospital, Gonabad University of Medical Sciences. the period 11, Numbe 4*, pp. 61–65, 2005.

[33] M. Alfti Far, M. Karami, P. Shokri, and S. M. Hosseini, "Prevalence of diabetes mellitus complications and associated risk factors in patients referred to Hamadan diabetes center," *Scientific Journal of Hamadan Nursing & Midwifery Faculty*, vol. - Numbe 2, pp. 69–74, 2017.

[34] S. Niroumand, M. Dadgarmoghaddam, B. Eghbali et al., "Cardiovascular disease risk factors profile in individuals with diabetes compared with non-diabetic subjects in north-east of Iran," *Iranian Red Crescent Medical Journal*, vol. 18, no. 8, article e29382, 2016.

[35] Z. Cheraghi, N. Amori, A. Dosti, and A. Bitaraf, *Prevalence of type 2 diabetes complications in diabetic patients covered by diabetes unit of Shadegan Health Center in 2009, Journal of Knowledge and Health, Special Issue of the 6th Iranian Epidemiology Congress. the period 5*, pp. 154-155, 2010.

[36] K. Ogurtsova, J. D. da Rocha Fernandes, Y. Huang et al., "IDF Diabetes Atlas: Global estimates for the prevalence of diabetes for 2015 and 2040," *Diabetes Research and Clinical Practice*, vol. 128, pp. 40–50, 2017.

[37] Z. Liu, C. Fu, W. Wang, and B. Xu, "Prevalence of chronic complications of type 2 diabetes mellitus in outpatients-a cross-sectional hospital based survey in urban China," *Health and Quality of Life Outcomes*, vol. 8, no. 1, p. 62, 2010.

[38] W. Shi, X. Li, and J. Li, "The morbidity of chronic diabetic complication with logistic regression analysis of related potential risk factors," *Zhonghua liu xing bing xue za zhi= Zhonghua liuxingbingxue zazhi*, vol. 25, no. 1, pp. 60–64, 2004.

[39] S.-S. Moon, Y.-K. Choi, H.-A. Seo et al., "Relationship between cardiovascular autonomic neuropathy and coronary artery calcification in patients with type 2 diabetes," *Endocrine Journal*, vol. 57, no. 5, pp. 445–454, 2010.

[40] M. K. Poulsen, J. E. Henriksen, J. Dahl et al., "Left ventricular diastolic function in type 2 diabetes mellitus: prevalence and association with myocardial and vascular disease," *Circulation: Cardiovascular Imaging*, vol. 3, no. 1, pp. 24–31, 2010.

[41] A. S. Krolewski, E. J. Kosinski, J. H. Warram et al., "Magnitude and determinants of coronary artery disease in juvenile-onset, insulin-dependent diabetes mellitus," *The American Journal of Cardiology*, vol. 59, no. 8, pp. 750–755, 1987.

[42] A. R. Delavari, A. R. Mahdavi Hezavei, A. Norozi Nezhad, and S. H. Yarahmadi, *National Program of Diabetes Prevention and Control*, Seda, Tehran, 1st edition, 2003.

[43] D. E. Grobbee, "How to ADVANCE prevention of cardiovascular complications in type 2 diabetes," *Metabolism*, vol. 52, 8 Suppl 1, pp. 24–28, 2003.

[44] A. Rodríguez, H. Delgado-Cohen, J. Reviriego, and M. Serrano-Ríos, "Risk factors associated with metabolic syndrome in type 2 diabetes mellitus patients according to World Health Organization, Third Report National Cholesterol Education Program, and International Diabetes Federation definitions," *Diabetes, metabolic syndrome and obesity: targets and therapy*, vol. 4, p. 1, 2011.

[45] H. Sanada, H. Yokokawa, M. Yoneda et al., "High body mass index is an important risk factor for the development of type 2 diabetes," *Internal Medicine*, vol. 51, no. 14, pp. 1821–1826, 2012.

[46] F. Hadaegh, A. Zabetian, H. Harati, and F. Azizi, "The prospective association of general and central obesity variables with incident type 2 diabetes in adults, Tehran lipid and glucose study," *Diabetes Research and Clinical Practice*, vol. 76, no. 3, pp. 449–454, 2007.

[47] R. Kawahara, T. Amemiya, M. Yoshino, T. Komori, N. Shibata, and Y. Hirata, "Adverse effects of obesity on lipid and lipoprotein levels in the patients with non-insulin dependent diabetes in the young," *Diabetes Research and Clinical Practice*, vol. 10, pp. S225–S230, 1990.

[48] R. J. Anderson, K. E. Freedland, R. E. Clouse, and P. J. Lustman, "The prevalence of comorbid depression in adults with diabetes: a meta-analysis," *Diabetes Care*, vol. 24, no. 6, pp. 1069–1078, 2001.

[49] M. De Groot, R. Anderson, K. E. Freedland, R. E. Clouse, and P. J. Lustman, "Association of depression and diabetes complications: a meta-analysis," *Psychosomatic Medicine*, vol. 63, no. 4, pp. 619–630, 2001.

[50] I. Eren, Ö. Erdi, and M. Şahin, "The effect of depression on quality of life of patients with type II diabetes mellitus," *Depression and Anxiety*, vol. 25, no. 2, pp. 98–106, 2008.

[51] World Health Organization DiabtesAugust 2011, http://www.who.int/mediacentre/factsheets/fs312/en.

[52] K. G. M. M. Alberti, P. Zimmet, and J. Shaw, "International Diabetes Federation: a consensus on type 2 diabetes prevention," *Diabetic Medicine*, vol. 24, no. 5, pp. 451–463, 2007.

[53] International Diabetes Federation, *IDF Diabetes Atlas*, International Diabetes federation, Brussels, Blegium, 6th edition, 2012, http://www.idf.org/diabetesatlas.

[54] K. K. Ray, S. R. K. Seshasai, S. Wijesuriya et al., "Effect of intensive control of glucose on cardiovascular outcomes and death in patients with diabetes mellitus: a meta-analysis of randomised controlled trials," *The Lancet*, vol. 373, no. 9677, pp. 1765–1772, 2009.

[55] Joslin Diabetes Center, *Clinical guideline for pharamacological of type 2 diabetes*, Jolin Diabetes Center, Boston (MA), 2007.

[56] American Diabetes Association, "Economic costs of diabetes in the U.S. in 2012," *Diabetes Care*, vol. 36, no. 4, pp. 1033–1046, 2013.

Hindawi
Journal of Diabetes Research
Volume 2020, Article ID 3634974, 19 pages
https://doi.org/10.1155/2020/3634974

Research Article

Protective Role of Tangshen Formula on the Progression of Renal Damage in *db/db* Mice by TRPC6/Talin1 Pathway in Podocytes

Qian Wang,[1,2] Xuefei Tian,[3] Wei'e Zhou,[2] Yan Wang,[4] Hailing Zhao,[2] Jialin Li,[1,2] Xuefeng Zhou,[1,2] Haojun Zhang,[2] Tingting Zhao,[2] and Ping Li[2]

[1]*Beijing University of Chinese Medicine, Beijing 100029, China*
[2]*Beijing Key Laboratory for Immune-Mediated Inflammatory Diseases, Institute of Clinical Medical Sciences, China-Japan Friendship Hospital, Beijing 100029, China*
[3]*Section of Nephrology, Department of Internal Medicine, Yale University School of Medicine, New Haven, CT 06510, USA*
[4]*Beijing Key Laboratory of Diabetes Research and Care, Center for Endocrine Metabolism and Immune Diseases, Lu He Hospital, Capital Medical University, Beijing 101149, China*

Correspondence should be addressed to Tingting Zhao; ttfrfr@163.com and Ping Li; lp8675@163.com

Received 16 February 2020; Revised 11 August 2020; Accepted 29 August 2020; Published 17 September 2020

Academic Editor: Claudio De Lucia

Tangshen Formula (TSF) is a Chinese Medicine formula that has been reported to alleviate proteinuria and protect renal function in humans and animals with diabetic kidney disease (DKD). However, little is known about its mechanism in improving proteinuria. The dysregulation of podocyte cell-matrix adhesion has been demonstrated to play an important role in the pathogenesis and progression of proteinuric kidney diseases including DKD. In the present study, the underlying protective mechanism of TSF on podocytes was investigated using the murine model of type 2 DKD *db*/*db* mice *in vivo* and advanced glycation end products (AGEs)-stimulated primary mice podocytes *in vitro*. Results revealed that TSF treatment could significantly mitigate reduction of podocyte numbers and foot process effacement, reduce proteinuria, and protect renal function in *db*/*db* mice. There was a significant increase in expression of transient receptor potential canonical channel 6 (TRPC6) and a decrease in expression of talin1 in podocytes of *db*/*db* mice. The results of AGEs-stimulated primary mice podocytes showed increased cell migration and actin-cytoskeleton rearrangement. Moreover, primary mice podocytes stimulated by AGEs displayed an increase in TRPC6-dependent Ca^{2+} influx, a loss of talin1, and translocation of nuclear factor of activated T cell (NFATC) 2. These dysregulations in mice primary podocytes stimulated by AGEs could be significantly attenuated after TSF treatment. 1-Oleoyl-2-acetyl-*sn*-glycerol (OAG), a TRPC6 agonist, blocked the protective role of TSF on podocyte cell-matrix adherence. In conclusion, TSF could protect podocytes from injury and reduce proteinuria in DKD, which may be mediated by the regulation of the TRPC6/Talin1 pathway in podocytes.

1. Introduction

Diabetic kidney disease (DKD) is one of the most common and severe complications of diabetes mellitus and is characterized by proteinuria and renal function impairment. DKD is the major cause of end-stage renal disease (ESRD) worldwide [1]. Accumulating evidence suggests that podocyte injury is a typical manifestation and a core event in the progression of DKD [2]. Podocytes are important components for glomerular filtration barrier integrity and maintenance of size selectivity in protein filtration. Changes in podocyte number and/or structure of foot processes have been demonstrated to be the main cause leading to glomerular proteinuria [3]. Under physiologic conditions, the podocyte actin backbone is well organized to maintain their normal morphology and function. Numerous studies on podocytes have shown that actin-cytoskeletal disorganization and related protein damage induced by multiple pathogenic factors lead to podocyte injury [4, 5]. Cell-matrix adhesion core structure complexes, including integrins/talins/actin, are crucial for maintaining the podocyte actin cytoskeleton. These adhesion complexes allow podocytes to attach tightly to the glomerular

basement membrane (GBM) to preserve the integrity of the glomerular filtration barrier. Any deficit in the structural components can disturb podocyte adhesion and lead to the disorganization of the actin cytoskeleton [6].

As a cell-matrix adhesion core structure complex, talin1 impairment can lead to integrin dysfunction, which is associated with a variety of pathologies, including thrombosis, stroke, and cancer metastasis [7]. Tian and colleagues [8] demonstrated that mice lacking talin1 specifically in podocytes displayed severe proteinuria, decreased podocyte adhesion, significant actin-cytoskeletal disorganization, foot process effacement, and progressive renal failure. Transient receptor potential canonical channel 6 (TRPC6) is a nonselective Ca^{2+} channel protein, which has been reported to be closely related to the cleavage of talin1 [9]. Mutation of the *TRPC6* gene in podocytes was first reported by Winn et al. in patients with focal segmental glomerulosclerosis (FSGS), suggesting the potential importance of TRPC6-mediated Ca^{2+} dynamics for podocyte function [10]. More and more studies have shown that aberrant changes in TRPC6 in podocytes lead to proteinuria development and progression of DKD, the mechanism by which may involve the rearrangement of the podocyte actin-cytoskeleton [11, 12]. TRPC6-dependent Ca^{2+} accumulation has been reported to lead to podocyte injury characterizing FSGS through reduced talin1 expression [13]. Furthermore, knockdown of *TRPC6* also results in decreased cleavage of talin1 [9]. However, it is unclear how the podocyte TRPC6/Talin1 signaling pathway affects the development and progression of DKD; thus, this mechanism needs to be investigated.

Tangshen Formula (TSF) is a Chinese Medicine formula that is effective in treating DKD and is based on the empirical evidence of Chinese physicians [14]. TSF is comprised of seven herbs: astragalus root, burning bush twig, rehmannia root, bitter orange fruit, cornus fruit, rhubarb root and rhizome, and notoginseng root and rhizome. Patients with stage III-IV DKD who were treated with one component of TSF, astragalus root injection, experienced improved renal function and decreased proteinuria excretion compared with those in a control group [15]. A decoction made from another TSF component, rehmannia root, was found *in vitro* to dramatically suppress the production of AGEs induced by inflammation [16]. Through liquid chromatography-mass spectrometry (LC-MS), we have successfully detected 40 compounds in TSF and 12 compounds in the serum of TSF-treated mice (supplementary Tables S1 and S2). Six compounds, including loganin, neohesperidin, naringenin, calycosin-7-O-β-D-glucoside, naringenine-7-rhamnosidoglucoside, and aloe-emodin, were selected to describe the quality of TSF by comparing the high-performance liquid chromatography (HPLC) fingerprints of 10 sample batches [17, 18]. The results confirmed that these six compounds exhibit renal protective effects [19–26]. Our preliminary multicenter clinical trial [14] and various animal models of DKD [27–29] showed that TSF has significant effects in reducing proteinuria and protecting renal function. However, little is known about its potential mechanism in improving proteinuria and its effects on podocytes. In the present study, we found that TSF mitigated podocyte number loss and foot process effacement reduced proteinuria, and protected renal function in *db*/*db* mice, a classic genetic model of type 2 diabetes that has clinical and histologic features of DKD resembling changes in humans [30]. Our results further showed that TSF might alleviate proteinuria mediated by the regulation of the TRPC6/Talin1 pathway in podocytes, following enhancement of the podocyte-matrix adhesion ability.

2. Materials and Methods

2.1. Herbal Formulation and Reagents. TSF (Lot number180408) was prepared and standardized by the Beijing Institute of Clinical Pharmacy, Beijing, China. TSF is composed of seven herbs: astragalus root (*Astragalus membranaceus* (Fisch) Bge.), burning bush twig (*Euonymus alatus* (Thunb.) Siebold.), rehmannia root (*Rehmannia glutinosa* (Gaertn.) Li-bosch.), bitter orange fruit (*Citrus aurantium* L.), cornus fruit (*Cornus officinalis* Sieb & Zucc.), rhubarb root and rhizome (*Rheum palmatum* L.), and notoginseng root and rhizome (*Panax Notoginseng* (Burk.) F. H. Chen) in the ratio of 10 : 5 : 4 : 3.4 : 3 : 2 : 1 (*w*/*w*). TSF was prepared as described in the *Chinese Pharmacopeia*, 2015. Six components, including loganin, neohesperidin, naringenin, calycosin-7-O-β-D-glucoside, naringenine-7-rhamnosidoglucoside, and aloe-emodin, were identified in the chemical fingerprint of TSF for quality control as previously described [18]. Irbesartan (J20171089) was purchased from Sanofi Pharmaceutical (Hangzhou, ZJ, China). For the animal experiments, both TSF (0.36 g/mL) and irbesartan (2.25 mg/mL) were dissolved in 0.5% carboxymethylcellulose sodium (CMC-Na).

Antibodies used in this study were as follows: TRPC6 (ab62461) (the specificity of the anti-TRPC6 antibody has been tested by MPC5 cells and *Trpc6* siRNA in Figure S1), WT1 (ab89901), AGE-BSA (ab51995), fibronectin antibody (ab2413), collagen type I (ab34710), and collagen type IV (ab6586), all purchased from Abcam (Cambridge, MA, USA). siRNA against TRPC6 was purchased from Shanghai Generay Biotech (Shanghai, China). Nephrin antibody (GP-N2) was obtained from Progen (Heidelberg, Germany). Talin1 antibody (14168-1-AP), NFATC2 (nuclear factor of activated T cell) antibody (22023-1-AP), NFATC3 antibody (18222-1-AP), integrin β1 antibody (26918-1-AP), and GAPDH antibody (60004-1-Ig) were purchased from Proteintech (Wuhan, HB, China). Paxillin antibody (sc-365379) was purchased from Santa Cruz Biotechnology (Dallas, TX, USA). N-2-hydroxyethylpiperazine-N-2-ethane sulfonic acid (HEPES) (15630080), RPMI 1640 medium (no phenol red) (11835030), penicillin-streptomycin (15140122), sodium pyruvate (11360070), sodium bicarbonate (25080094), fetal bovine serum (FBS) (10099141), Alexa Fluor 488 Phalloidin (A12379), Alexa Fluor 594 goat anti-guinea pig secondary antibody (A11076), Alexa Fluor 594 goat anti-rabbit secondary antibody (A11012), and Alexa Fluor 488 goat anti-rabbit secondary antibody (A11008) were purchased from Thermo Fisher Scientific (Waltham, MA, USA). 1-Oleoyl-2-acetyl-sn-glycerol (OAG) (O6754), Hanks' balanced salt solution (HBSS) (H6648), and collagen type I solution from rat tail (C3867) were purchased from Sigma-Aldrich

(St. Louis, MO, USA). Collagenase A (11088793001) and DNase (04716728001) were purchased from Roche (Mannheim, Germany). CMC-Na (C8621) was purchased from Solarbio (Beijing, China). ELISA Quantitation Set kit (E101) was obtained from Bethyl Laboratories (Montgomery, TX, USA). Fluo-4-AM (S1060), ionomycin (S1672), EDTA (ST066), and MTT Cell Proliferation and Cytotoxicity Assay Kit (C0009) were purchased from Beyotime Biotechnology (Shanghai, China). SAR7334 (HY-15699) was purchased from MedChemExpress (Shanghai, China).

2.2. Assay of the Compounds in TSF and in the Mouse Serum Treated with TSF Determined by UHPLC-MS/MS. The 1 g of dried TSF compound prescription power was extracted with methanol-water (25 mL, 75 : 25, *v*/*v*) using an FS30 ultrasonic sonicator (Fisher Scientific, Pittsburg, PA, USA) at 40 kHz and 100 W for 30 minutes at room temperature. A 10 μg of the extract was injected onto the analytical column for analysis. For the preparation of mouse serum sample treated with TSF, the 8-week-old male C57BL/6J mouse was gavaged with TSF at the dosage of 2.4 g/kg body weight, the serum sample was collected after 24 hours administration. The 150 μL of mouse serum sample was mixed with 400 μL methanol, following by centrifuging at 14480 g for 10 minutes at 4°C. The supernatant was evaporated to dryness by Centrivap Concentrator (LABCONCO, USA), then 400 μL methanol was added. After centrifuging at 14480 g for 20 minutes at 4°C, supernatant was collected for analysis.

The prepared samples were analyzed using the ultrahigh performance liquid chromatography-tandem mass spectrometry (UHPLC-MS/MS). Briefly, UHPLC-MS/MS analysis was performed using Q Exactive Plus High Resolution Mass Spectrometer (THERMO, USA) equipped with Ultimate 3000 (DIONEX, THERMO, USA), and Acquity™ UPLC BEH C18 column (2.1 × 100 mm, 1.7 μm) (Waters, USA). The optimized chromatographic conditions were achieved at a flow rate of 0.3 mL/min with a mobile phase consisting of acetonitrile (mobile phase A) and 0.1% formic acid solution (mobile phase B). The diode array detector (DAD) was set at 280, 254 nm for real-time monitoring of the peak intensity and full spectra (190-650 nm). The following conditions were applied for MS: capillary temperature 320°C, spray voltage 3.5 kV for ESI+analysis; and capillary temperature 320°C, spray voltage -3.5 kV for ESI-analysis. The mass scan range was set to 100-1500. The resolution of the Orbitrap was set to 70000. The resolution of dd-MS2 was set to 17500; CE was set to 20 : 40 : 60. The peak picking and alignment were processed using Sieve software (V1.2, Thermo Fisher Scientific, USA) applying a mass width of 0.02 Da and a retention time width of 0.5 minutes.

2.3. Animals and Experimental Design. Eight-week-old male C57BLKS/J^{Lepr}*db*/*db* mice ($n = 18$) weighing 42.68 ± 0.66 g and *db*/*m* mice ($n = 6$) weighing 23.97 ± 0.49 g were purchased from the Peking University Laboratory Animal Center (Beijing, China). Since the misty (*m*) gene has a greater effect on the metabolism of mice, *m*/*m* mice are 8% shorter and weigh 15% less than controls and have less inguinal adipose mass and complete loss of brown fat [31]. Therefore, the *db*/*m* mice are usually used as the control group in *db*/*db* mice studies [32]. All mice were maintained inhouse under the following specific pathogen-free conditions: 22 ± 2°C controlled temperature, 65-75% relative humidity, a regular 12-hour light/dark cycle, and received standard laboratory chow and water *ad libitum*. After 2 weeks of acclimation, the *db*/*m* mice were used as controls (designated *db*/*m*). *db*/*db* mice were randomly assigned into three groups ($n = 6$, per group): *db*/*db* mice (designated *db*/*db*), *db*/*db* mice treated with TSF (3.6 g/kg/day) (designated *db*/*db* + TSF), and *db*/*db* mice treated with irbesartan (22.5 mg/kg/day) (designated *db*/*db* + Irbesartan). The *db*/*m* and *db*/*db* groups were each given equal volume of 0.5% CMC-Na, gavage administration. All drugs were administered once daily by gastric gavage. Dose of TSF was adjusted based on our previous studies and standard conversion formulas [14, 33]. Body weight was recorded weekly during the study period. Urine was collected at the beginning of treatment and the 12th week. The mice were sacrificed after 12 weeks of treatment. After overnight fasting, the serum and tissue samples were collected rapidly for further analysis. All experimental animal procedures were in accord with the National Institutes of Health *Guide for the Care and Use of Laboratory Animals* (2011 edition). The protocol was approved by the Ethics Committee of the China-Japan Friendship Institute of Clinical Medical Sciences (Approval no.13005).

2.4. Biochemistry Measurements. Mouse urine samples were collected using metabolic cages (Fengshi Inc., Suzhou, JS, China) [27]. Urine albumin was quantified in duplicates using the Mouse Albumin ELISA Kit according to the manufacturer's protocol (Bethyl Laboratories). Urine creatinine was measured in duplicate for each sample using an automatic analyzer (Abbott Diagnostics, Abbott Park, IL, USA).

2.5. Histologic Assessment of Glomerular Injury. Kidney tissues were fixed in 10% formalin, embedded in paraffin sections (2-3 μm), and stained with periodic acid-Schiff (PAS) and periodic acid-silver methenamine (PASM). Kidney ultrastructure was detected by transmission electron microscopy (TEM) (JEOL-100CXII, JEOL, Tokyo, Japan). Kidney tissues (1 mm^3) were fixed with 2.5% glutaraldehyde at 4°C for 24 hours and embedded in epoxy resin. Ultrathin sections were sliced and stained with uranyl acetate and lead citrate. Twenty glomerular cross-sections (with the vascular pole and the urinary pole on the same plane) per sample were randomly selected under a 400x light microscope (Olympus, Tokyo, Japan), and the areas of each glomerulus and mesangial matrix were measured using Image-Pro Plus 6.0 software (Media Cybernetics, Warrendale, PA, USA) by two pathologists in a double-blinded manner. Thirty glomerular capillaries per sample were randomly selected (magnification 12000x) to measure GBM thickness, podocyte foot process width, and the number of foot processes per micron in a double-blinded manner [34, 35].

2.6. Immunohistochemistry and Immunofluorescence. Paraffin-embedded mice kidney sections were deparaffinized with xylene following hydration with ethanol. Antigen retrieval

was induced by microwave following washing with 1× phosphate buffer saline (PBS) as previously described [8]. Sections were incubated overnight at 4°C with anti-fibronectin antibody (1 : 500), anti-collagen type I antibody (1 : 1000), anti-collagen type IV antibody (1 : 400), anti-nephrin antibody (1 : 2000), and anti-WT1 antibody (1 : 1000). Subsequently, the sections were incubated with secondary antibodies and counterstained with hematoxylin for the nuclei. Images were captured under the light microscope and then measured by Image-Pro Plus 6.0 software. For immunofluorescence, paraffin-embedded kidney sections were incubated in blocking buffer (5% BSA in 1× PBS) for 1 hour at room temperature and stained with antibodies in the following concentration: anti-nephrin antibody (1 : 100) and secondary antibody Alexa Fluor 594 goat anti-guinea (1 : 200). Costaining was with the following antibodies: anti-TRPC6 antibody (1 : 100), anti-talin1 antibody (1 : 100), anti-WT1 antibody (1 : 100), and secondary antibody Alexa Fluor 488 goat anti-rabbit (1 : 200). For cell immunofluorescence, primary mice podocytes on collagen type I-coated coverslips were washed with 1× PBS and fixed with 4% paraformaldehyde for 15 minutes. The cells were permeated with 0.5% Triton X-100 for 20 minutes at room temperature. The cells were blocked with 5% BSA in 1× PBS for 1 hour and stained with antibodies in the following concentration: anti-TRPC6 antibody (1 : 100), anti-WT1 antibody (1 : 100), anti-Talin1 antibody (1 : 50), anti-paxillin antibody (1 : 100), anti-NFATC2 antibody (1 : 100), anti-NFATC3 antibody (1 : 100), and secondary antibody Alexa Fluor 488 goat anti-rabbit (1 : 300). The resulting images were obtained by a fluorescent inverted microscope (Olympus).

2.7. Isolation of Primary Mice Podocytes. The protocol for primary mice podocytes culture isolated from newborn mice was performed as previously described [8]. The freshly removed kidneys from the C57BL/6J newborn mice (Beijing HFK Bioscience, Beijing, China) were minced into very small pieces in a 10 cm dish. After digestion for 30-45 minutes in a collagenase solution (5 mg/mL collagenase A and 1 : 10 DNase) at 37°C and 5% CO_2 incubation, the resulting suspension was filtered with a 70 μm BD Falcon cell strainer (Corning Life Sciences, Corning, NY, USA). The filtered solution (glomerular cells) was then plated onto the 10 cm culture dish coated with collagen type I to total 1640 RPMI medium with 10% FBS, 1% penicillin-streptomycin, 10 mM HEPES, 0.075% sodium bicarbonate, and 1 mM sodium pyruvate. The primary mice podocytes were harvested by separating the glomerular cells with 0.25% trypsin (Invitrogen) and then sieving through a 40 μm BD Falcon cell strainer. Cells were cultured in a humidified incubator with 5% CO_2 at 37°C and used at passages 1 or 2 for all experiments. The purity of the primary mice podocytes was 95% as determined by immunofluorescence staining with the WT-1 antibody, a specific marker of podocytes [36].

2.8. Cell Treatments. To investigate the role of AGEs, the primary mice podocytes were exposed to AGE-BSA for 24 hours sequentially at 60, 80, 100, and 120 μg/mL. Equal amounts of BSA were added to the control cells. After successfully producing the podocyte injury model induced by AGEs, the cells were treated with a series of concentrations (250, 500, and 750 μg/mL) of TSF for 24 hours with AGE-BSA (100 μg/mL). The cells cultured with BSA (100 μg/mL) served as controls. SAR7334 (0.1 μmol/L) was used as a TRPC6 inhibitor while OAG (100 μmol/L) as a TRPC6 agonist.

2.9. Determination of Cell Viability. The effect of TSF on cell viability was determined using the 3-(4,5-dimethylthiazol-2-yl)-2,5-diphenyltetrazolium bromide (MTT) assay. After being starved with 1640 RPMI medium without FBS overnight, the primary mice podocytes (2×10^3 cells/well) growing in 96-well plates were incubated with BSA (100 μg/mL) and TSF (0, 100, 250, 500, 750, and 1000 μg/mL) for 24 hours. Each well was incubated with 10 μL MTT solution (5 mg/mL) for 4 hours in a cell culture incubator. Subsequently, 100 μL formazan lysate was added to each well and measured at 570 nm with a microplate reader (Thermo Fisher Scientific). Cell viability was calculated as a percentage according to the manufacturer's instructions.

2.10. Wound Healing Assay. The primary mice podocytes (1×10^6 cells/well) were incubated in 6-well plates and were starved for 24 hours. Once the cells reached 100% confluence, an artificial linear wound (scratch) was introduced using a sterile 200 μL pipette tip. Cells were allowed to heal for 24 hours. The percentage of wound closure was calculated as $[(\text{Area } T_{24\,\text{hours}} - \text{Area } T_0)/\text{Area } T_0]$ using the ImageJ software 1.8.0 (National Institutes of Health, Bethesda, MD, USA) [37].

2.11. Quantitative Analysis of Changes in the Actin Cytoarchitecture of Primary Mice Podocytes. Changes in actin cytoarchitecture of primary mice podocytes were analyzed as previously described [8]. The multiplicity of different phalloidin staining patterns was grouped into four major classes and used for scoring as follows: Type A: more than 90% of cell area filled with thick cables; Type B: at least two thick cables running under the nucleus and the rest of the cell filled with fine cables; Type C: no thick cables, but some fine cables present; Type D: no cables visible in the central area of the cell. All slides were scored in a double-blinded manner; thirty cells in each slide were analyzed in three separate experiments.

2.12. Intracellular Ca^{2+} Determination. Intracellular Ca^{2+} concentration was determined using the Ca^{2+} fluorescent probe Fluo-4-AM. Primary mice podocytes in each group were washed three times with HBSS (no calcium, no magnesium, no phenol red) and incubated with Fluo-4-AM (5 μmol/L in RPMI 1640 medium) at 37°C for 45 minutes. Podocytes were trypsinized with 0.25% trypsin-EDTA, followed by centrifugation at 200 × g for 5 minutes. Intracellular Ca^{2+} level was measured and calculated using the FACScan flow cytometer (BD Biosciences, San Jose, CA, USA) [38]. Then, the cells were incubated with 5 μmol/L ionomycin in a zero Ca^{2+} bath (0 mmol/L Ca^{2+}, 5 mmol/L EDTA) and 5 μmol/L ionomycin in saturating Ca^{2+} solution (5 mmol/L $CaCl_2$), to measure minimal and maximal responses to Ca^{2+} [39].

2.13. Western Blot Analysis. Protein samples of kidney tissue and cells were extracted in RIPA lysis buffer (EpiZyme, Shanghai, China) at 4°C. Concentrations of protein were determined using BCA assay. Equal amounts of total protein were denatured for 10 minutes at 95°C. The protein lysates (25 μg) were separated in 10% or 12% polyacrylamide gels (EpiZyme) and transferred onto 0.45 μm polyvinylidene fluoride (PVDF) membranes (Millipore Sigma, Darmstadt, Germany). After blocking with 5% BSA in 1× PBS, membranes were incubated with antibodies overnight at 4°C in the following concentrations: anti-nephrin antibody (1 : 500), anti-WT1 antibody (1 : 500), and anti-talin1 antibody (1 : 500). Blots were detected using enhanced chemiluminescence (Amersham Pharmacia Biotech, Buckinghamshire, UK) with the ChemiDoc XRS system (Bio-Rad, Hercules, CA, USA). Finally, the protein bands were quantified using the ImageJ software.

2.14. Statistical Analysis. All data were presented as the mean ± SEM. Numbers for each experiment are displayed in the Methods or the figure legends. Statistical difference between two groups was evaluated by a 2-tailed *t*-test. Multiple-group comparisons were evaluated using one-way ANOVA followed by Dunnett's multiple-comparisons tests. Statistical analysis was performed by the GraphPad Prism 6.0 software (San Diego, CA, USA). A *P* value less than 0.05 was considered statistically significant.

3. Results

3.1. TSF Reduced Proteinuria and Attenuated Renal Injury in db/db Mice. During the 12-week intervention with TSF or irbesartan, there were no obvious side effects observed in the *db/db* mice. The body weights between the mice of *db/db* group and the mice of *db/db* + TSF group were similar at the age of 10 weeks. TSF treatment significantly reduced the body weights of *db/db* mice compared with the *db/db* mice without treatment starting from age of 19 weeks till the end of the study. However, there were no significant changes in the body weights of *db/db* mice treated with irbesartan observed (Figure 1(a)). There were no changes in the kidney weights either TSF-treatment or irbesartan-treatment in the *db/db* mice compared to vehicle-treatment control *db/db* mice (Figure 1(b)).

Renal damage in *db/db* mice was assessed by the urine albumin-to-creatinine ratio (ACR) assay and serum creatinine levels. Compared with mice of 10 weeks of age, ACR in *db/db* mice was significantly decreased after 12 weeks of TSF treatment (Figure 1(c)). Moreover, TSF significantly reduced serum creatinine levels in *db/db* mice (Figure 1(d)). Irbesartan-treated *db/db* mice also showed significant improvement in ACR and serum creatinine. The typical pathologic damage changes in *db/db* mice, including glomerular hypertrophy, mesangial expansion, thickened GBM, and abnormal deposition of fibronectin, collagen type IV, and collagen type I, were relieved by TSF or irbesartan treatment (Figures 1(e), 1(f), and S2). Therefore, TSF could effectively alleviate proteinuria and renal injury in *db/db* mice, which is consistent with our previously reported results [29, 40].

3.2. TSF Improved Podocyte Injury, Reduced Expression of TRPC6 and Enhanced Expression of talin1 in db/db Mice Podocytes. To investigate the ultrastructural changes in the podocytes, transmission electron microscopy was performed. The results showed that there were a severe foot process effacement and an increased GBM thickness in the *db/db* mice, which was strikingly improved by either TSF or irbesartan treatment at a similar effect (Figure 2(a)). Consistent with the PASM results (Figure 1(e)), the thickened GBM in *db/db* mice under the electron microscopy also showed significant relief after TSF treatment. We further studied the expression of WT1 and nephrin, two specific podocyte markers, on kidney tissue of *db/db* mice. Our results showed that there was a significant decrease in WT1 expression, and no significant change in nephrin either in protein expression or localization (Figures 2(b) and 2(c)). Given the presenting characteristics of early DKD in *db/db* mice, it was speculated that partial foot process effacement of *db/db* mice had not seriously affected the structure of the slit diaphragm (SD) of podocytes and the related protein nephrin.

Considering reduction of WT1 represented decrease in podocyte numbers, we examined the podocyte-associated protein talin1, which is a crucial part of the podocyte-matrix adhesion structure. Results showed that there was a significant loss in talin1 protein in *db/db* mice and that TSF could prevent its loss (Figure 3(a)). Since talin1 expresses ubiquitously, we observed the change in talin1 in podocytes by costaining with nephrin. We found that talin1 loss was mainly concentrated in podocytes in *db/db* mice (Figure 3(b)). Verheijden et al. [13] reported that loss of talin1 is closely related to the abnormal expression of TRPC6. Based on this, we attempted to determine the potential changes in the expression of TRPC6 on podocytes by costaining with nephrin. Our results showed there was increased TRPC6 expression in *db/db* mice podocytes, which could be mitigated by TSF treatment (Figure 3(c)). This suggested that podocyte injury in *db/db* mice could be attributed to the loss of podocyte-specific talin1 protein, which may be associated with the increase in TRPC6 expression. Thus, TSF had a significant protective effect on podocyte talin1 in *db/db* mice.

3.3. TSF Alleviated Cell Migration and Actin-Cytoskeletal Disorganization in AGEs-Stimulated Primary Mice Podocytes. To further understand the role of talin1 and TRPC6 in podocytes and the mechanism of TSF, we continued our investigation by culturing primary mice podocytes *in vitro*. AGEs are involved in the pathogenesis of DKD and are closely related to the extent of podocyte injury [41, 42]. In combination with the AGEs deposition found in the kidney tissue of *db/db* mice, we used AGEs to establish a primary mice podocyte injury model *in vitro*. Loss of podocyte talin1 results in a reduction in cell adhesion, an increase in cell migration, and actin-cytoskeletal disorganization [8]. TRPC6-dependent Ca^{2+} accumulation has been found to cause podocyte injury through the loss of talin1 in human and experimental FSGS [13]. Therefore, we hypothesize that the lack of talin1 in type 2 DKD model *db/db* mice may also occur following TRPC6 activation, and TSF may have a certain degree of therapeutic effect through this mechanism. Cells lacking talin1 have

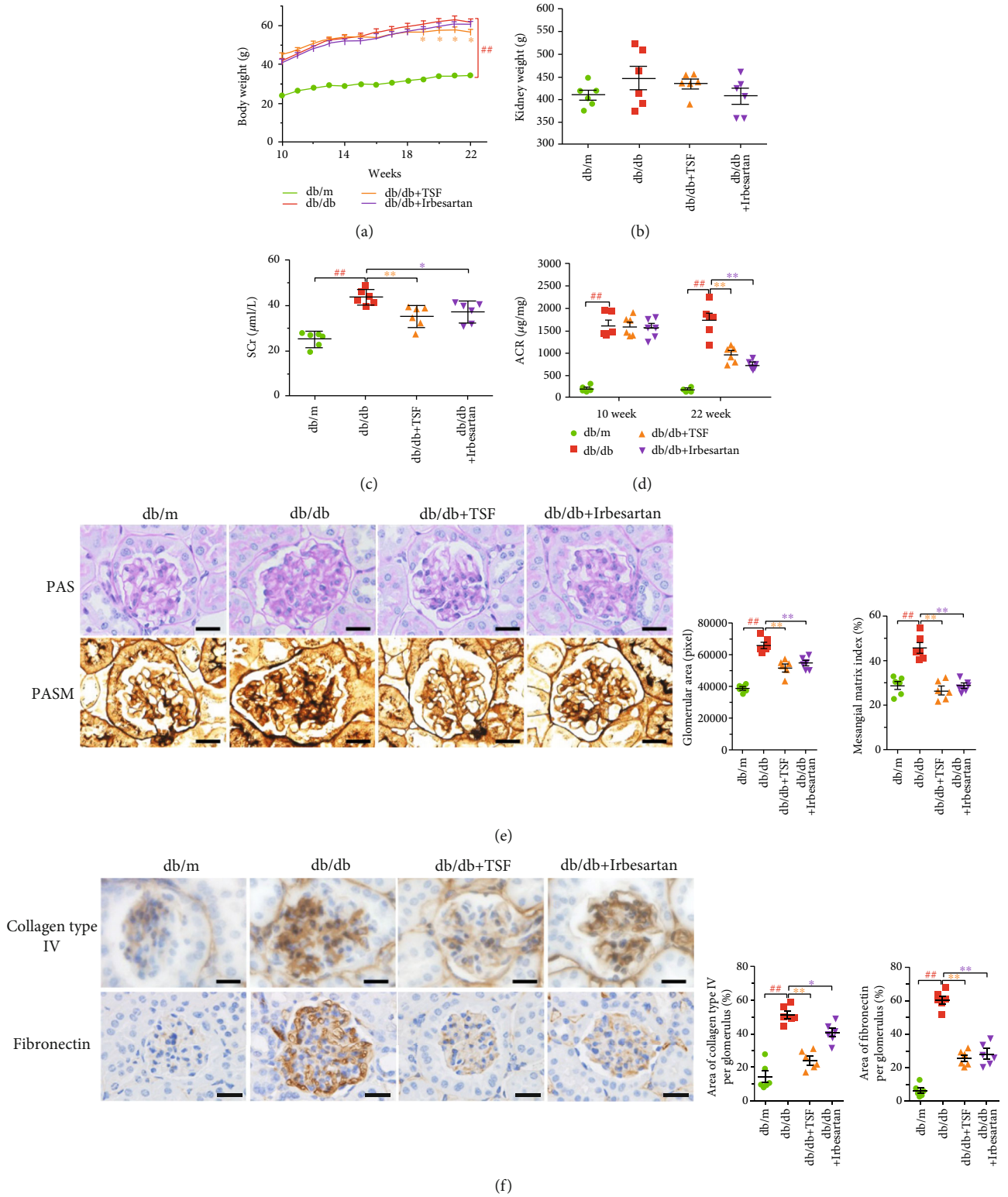

FIGURE 1: TSF reduced proteinuria and alleviated renal injury in *db/db* mice. (a) Body weight was recorded each week ($n = 6$). (b) Kidney weight of mice in each group at 22 weeks of age ($n = 6$). (c) Urinary albumin to creatinine ratio (ACR) ($n = 6$). (d) Serum creatinine in each group ($n = 6$). (e) Representative PAS staining (scale bars, 20 μm) and quantitative analysis of glomerular hypertrophy and mesangial expansion ($n = 6$); representative PASM staining (scale bars, 20 μm). (f) Representative immunohistochemical staining and quantitative analysis of collagen type IV and fibronectin (scale bars, 20 μm) (20 glomeruli were randomly evaluated per section) ($n = 6$). The data were expressed as the mean ± SEM. $^{\#}P < 0.05$, $^{\#\#}P < 0.01$ vs. *db/m* group; $^{*}P < 0.05$, $^{**}P < 0.01$ vs. *db/db* group. Statistically analyzed via a one-way ANOVA with Dunnett's correction.

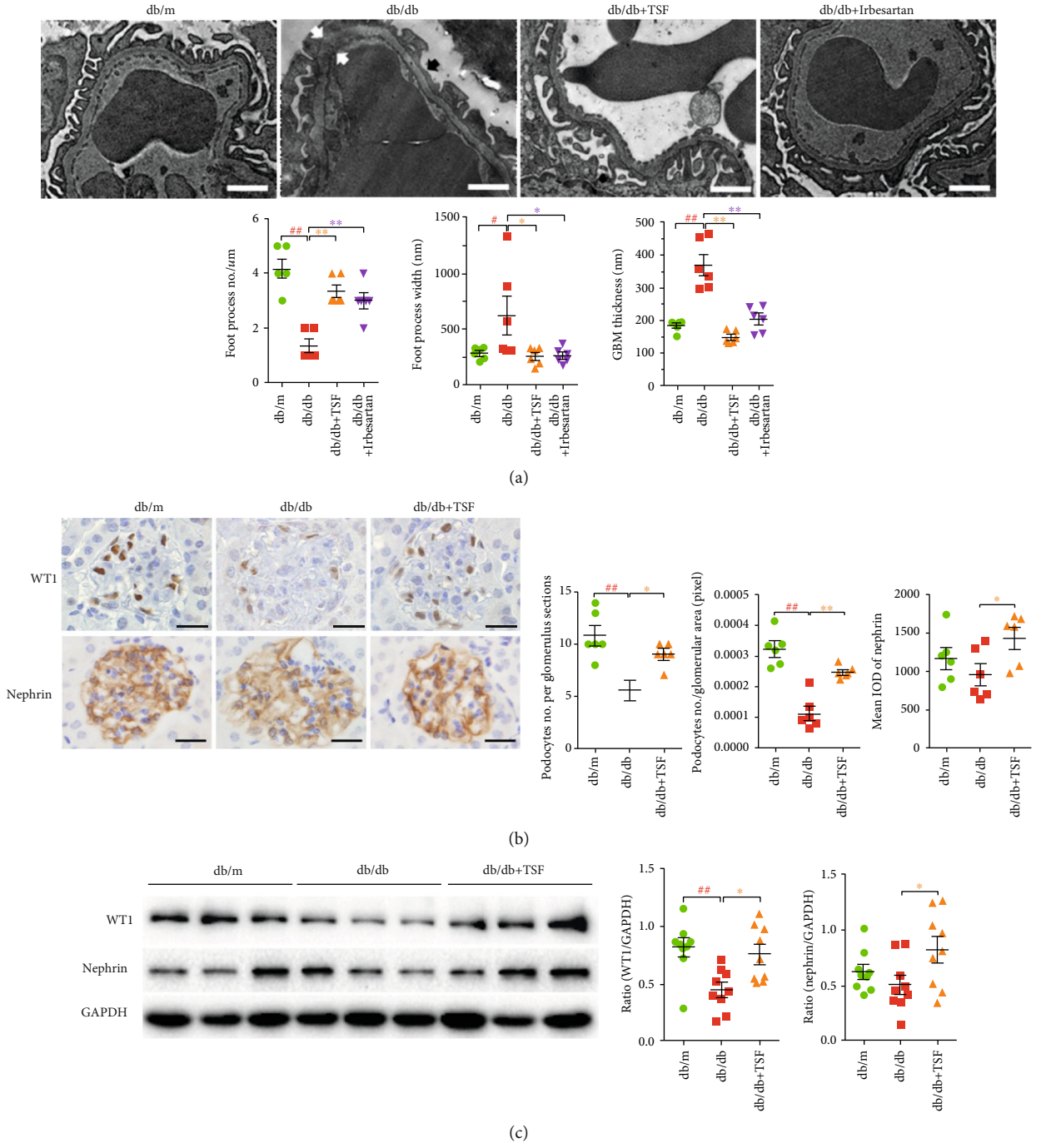

Figure 2: TSF reduced foot process effacement, prevented WT1 from loss in *db/db* mice. (a) Representative transmission electron micrographs (scale bars, 1 μm) illustrate foot process effacement (black arrow) and GBM thickness (white arrow); the number and width of foot process and GBM thickness were subsequently calculated ($n = 6$). (b) Representative immunohistochemical staining and quantitative analysis of WT1 and nephrin (scale bars, 20 μm) (20 glomeruli were randomly evaluated per section, $n = 6$). (c) Immunoblotting for WT1 and nephrin; quantification of the gels is shown on the right ($n = 3$ experiments). The data were expressed as the mean ± SEM. $^{\#}P < 0.05$, $^{\#\#}P < 0.01$ vs. *db/m* group; $^{*}P < 0.05$, $^{**}P < 0.01$ vs. *db/db* group. Statistically analyzed via a one-way ANOVA with Dunnett's correction.

impaired abilities on reduced cell adhesion, spreading, and migration [43]. Moreover, the changes in different phalloidin staining patterns in podocytes have been shown to be associated with podocyte migration ability [44]. We observed their migration ability through the wound healing assay after starving for 24 hours. Given that podocytes are terminally differentiated epithelial cells lacking the proliferative ability and our results, the effects of podocyte proliferation on the wound healing assay are less likely especially under the same experimental conditions. The most obvious migration

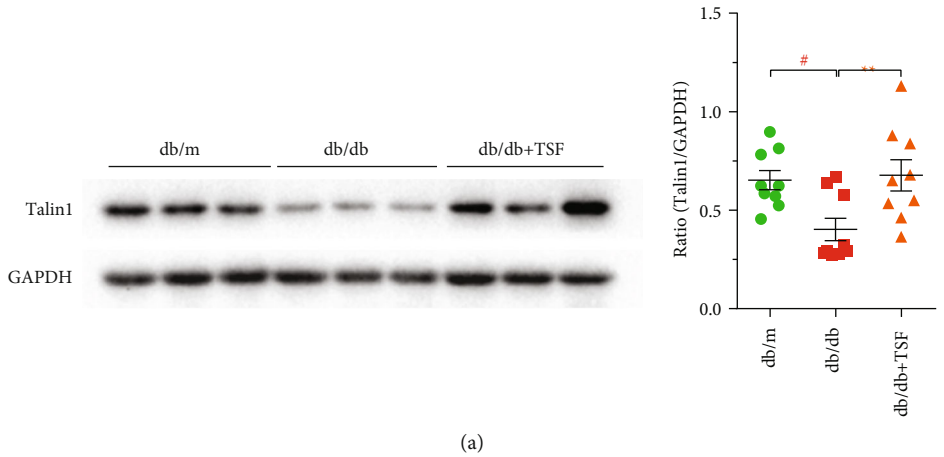

(a)

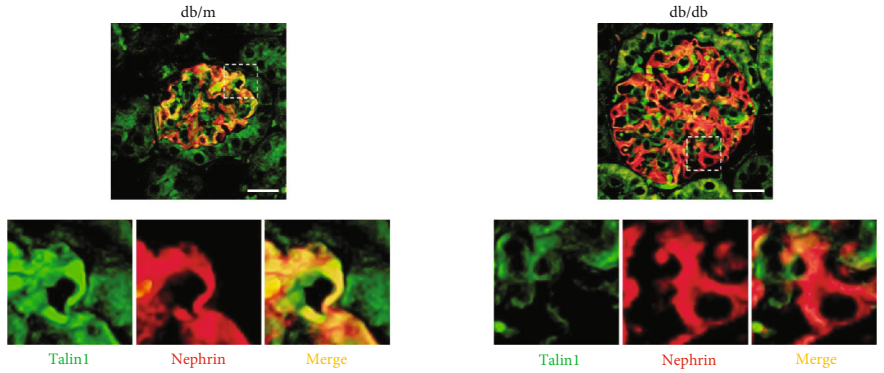

(b)

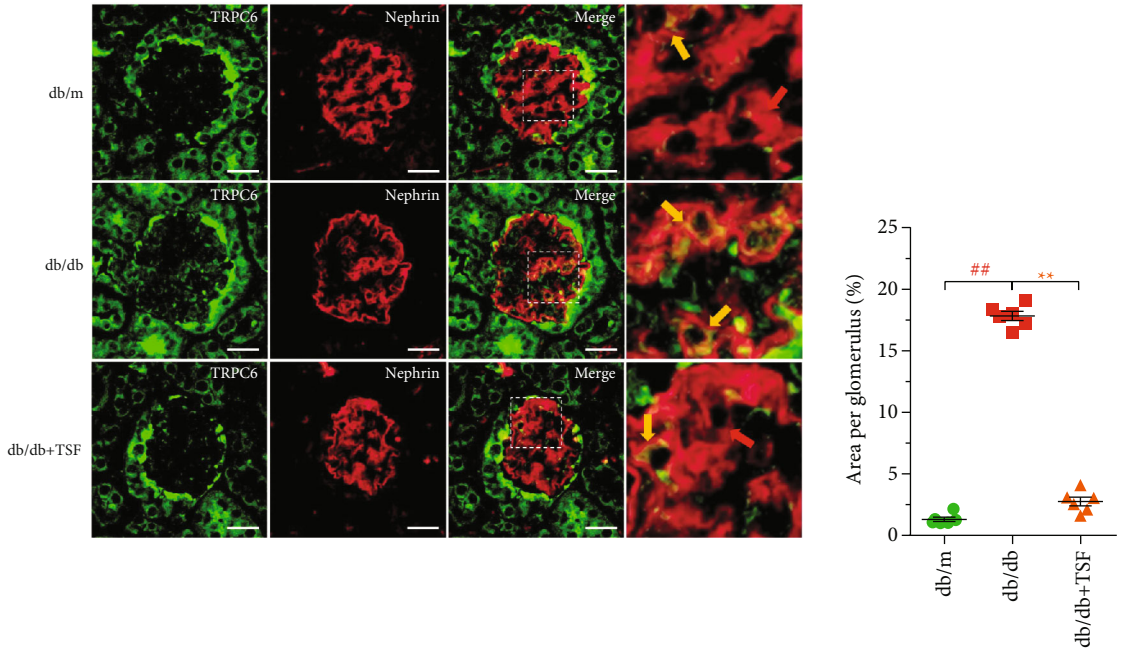

(c)

Figure 3: TSF protects podocyte-associated protein talin1 in *db*/*db* mice, which may involve increased expression of TRPC6 in podocytes. (a) Immunoblotting and quantitative analysis of talin1 ($n = 3$ experiments). (b) Immunofluorescence costaining (scale bars, 25 μm) of nephrin (red) and talin1 (green) showed that talin1 had a specific deletion in podocytes. (c) Immunofluorescence costaining (scale bars, 25 μm) of nephrin (red; red arrow) and TRPC6 (green) showed that increased expression of podocyte TRPC6 in *db*/*db* mice (yellow arrow) compared to *db*/*m* mice and *db*/*db* + TSF mice ($n = 6$). Fluorescent images were collected and assessed using a high-content screening system. The data were expressed as the mean ± SEM. $^{\#}P < 0.05$, $^{\#\#}P < 0.01$ vs. *db*/*m* group; $^{*}P < 0.05$, $^{**}P < 0.01$ vs. *db*/*db* group. Statistically analyzed via a one-way ANOVA with Dunnett's correction.

occurred in primary mice podocytes after AGEs stimulation at a dose of 100 μg/mL for 24 hours (Figures 4(a) and 4(b)). The cytotoxicity of TSF on primary mice podocytes was analyzed using MTT at a concentration range of 100 μg/mL to 1000 μg/mL. Results showed that TSF treatment at a concentration of up to 750 μg/mL had no effect on the cells (Figure 4(c)). MTT results revealed that TSF treatment with AGEs (100 μg/mL) at a concentration of up to 750 μg/mL had no effect on primary mice podocytes (Figure 4(d)). TSF mitigated podocyte migration induced by AGEs in a dose-dependent manner (250, 500, and 750 μg/mL) (Figures 4(e) and 4(f)).

Based on this, we observed podocyte morphology as related to migration. Compared with the control group, podocytes in the AGEs-stimulated group appeared to have the more obvious formation of lamellipodia and filopodia (Figures 5(a) and 5(b)), which are associated with increased cell motility and actin rearrangement.

Immunofluorescence labeling of the podocyte nucleus with WT1 and F-actin with phalloidin showed that AGEs caused actin-cytoskeletal disorganization in cultured primary mice podocytes. The AGEs-stimulated primary mice podocytes had fewer cells with types A (>90% of cell area filled with thick cables) and B (at least two thick cables running under the nucleus and rest of cell area filled with fine cables) staining patterns and more cells in type C (no thick cables, but some cables present), and type D (no cables visible in the central area of the cell) pattern when compared with control podocytes, and these effects were decreased by TSF (500 μg/mL) (Figures 5(c) and 5(d)). In short, TSF inhibited cell migration and attenuated actin-cytoskeletal disorganization in primary mice podocytes stimulated by AGEs.

3.4. TSF Alleviated Podocyte Injury by Improving Cell-Matrix Adhesion Ability through Regulation of TRPC6/Talin1 Pathway. We explored the relationship between AGEs and TRPC6 by calculating the relative concentration of Ca^{2+} in AGEs-stimulated primary mice podocytes using Ca^{2+}-sensitive dye fluo-4-AM. Results showed that compared with the BSA group, the BSA+TSF group had no effect on podocyte intracellular Ca^{2+} concentration. However, there was a significant increase in Ca^{2+} level in AGEs-treated podocytes compared with the control group, while in the groups that were pretreated with TSF and SAR7334 (0.1 μmol/L), a potent and specific cell-membrane permeable inhibitor of TRPC6 [45], there was a significant decrease in Ca^{2+} level compared with AGEs-treated podocytes (Figure 6(a)). Also, there was a decrease in talin1 in AGEs-stimulated primary mice podocytes, accompanied by an increase in the expression of TRPC6 (Figures 6(b) and 6(c)). The loss of talin1 has been shown to affect the expression of some focal adhesions; thus, we initially evaluated the expression of integrin β1 and paxillin, two kinds of intracellular anchor proteins in cell-matrix adhesion that can bind directly to actin. The results showed a decrease in integrin β1 and paxillin in AGEs-treated podocytes (Figures 6(c) and 6(d)). TSF protected talin1, integrin β1, and paxillin from loss and reduced expression of TRPC6, and all phenomena could be attenuated by OAG (100 μmol/L), agonist of TRPC6. These results showed that TSF could improve cell-matrix adhesion ability and reduce TRPC6-dependent Ca^{2+} accumulation in AGEs-stimulated primary mice podocytes. We also observed that the protective effect of TSF on podocyte actin fibers was inhibited by OAG (Figures 7(a) and 7(b)). This indicates that TRPC6 plays an important role in maintaining the stability of the podocyte actin-cytoskeleton and that TSF could alleviate TRPC6-dependent Ca^{2+} accumulation mediated actin-cytoskeletal disorganization and increase the cell-matrix adhesion ability in podocytes.

The downstream signaling pathway cascade of TRPC6 involves a Ca^{2+}-dependent Calpain/Calcineurin signal transduction, which usually activates NFATCs. NFATC family members (NFATC1 through NFATC4) can be dephosphorylated by Calpain/Calcineurin signaling, resulting in their translocation to the nucleus to exert their function. The important transcriptional target of NFATCs is TRPC6 itself, which results in a harmful feedforward loop. In our study, we initially observed the expression of NFATC2 and 3 in AGEs-stimulated primary mice podocytes. Immunofluorescence morphology results revealed that AGEs-stimulated podocytes increased the percentage of NFATC2 translocated to the nucleus rather than NFATC3, and translocation could be reduced by TSF, while OAG attenuated its efficacy (Figures 8(a) and 8(b)). Therefore, we initially concluded that TSF reduced TRPC6-dependent Ca^{2+} accumulation, loss of talin1, and NFATC 2 nuclear translocation in primary mice podocytes stimulated by AGEs.

4. Discussion

In this study, a decreasing trend in the podocyte marker protein nephrin in *db*/*db* mice was observed; although, there was no significant difference in protein expression and localization compared with *db*/*m* control mice. The reduction in podocyte WT1 protein was more significant. Excluding some hereditary kidney diseases, foot process effacement is thought to help damaged podocytes attach to GBM by actin-cytoskeleton rearrangement, covering the exposed GBM due to partial podocyte exfoliation; it is an adaptive and reversible reaction to injury stimuli [46]. If the actin-cytoskeleton is repaired, early podocyte damage can be recovered to allow the foot process to branch again into their interdigitating pattern [2]. Thus, we hypothesized that partial foot process effacement of *db*/*db* mice in this study had not seriously affected the structure of the SD of podocytes and the related protein nephrin. The decrease in WT1-positive cells in glomeruli suggests a partial loss of podocytes, which allows us to focus on the cell-matrix adhesion structure.

The decrease of podocyte number is the strongest predictor of DKD progression. Podocyte apoptosis and detachment are the possible reasons for the loss of podocyte. Because the former is rarely observed in *in vivo* studies, podocyte loss can be attributed to detachment caused by podocyte adhesion failure [47, 48]. Podocytes adhere to the GBM by combining the actin cytoskeleton with the heterodimeric transmembrane integrin adhesion receptors. There are 18 kinds of α subunits and 8 kinds of β subunits, which can form 24 integrins in different combinations. Since the integrin cytoplasmic

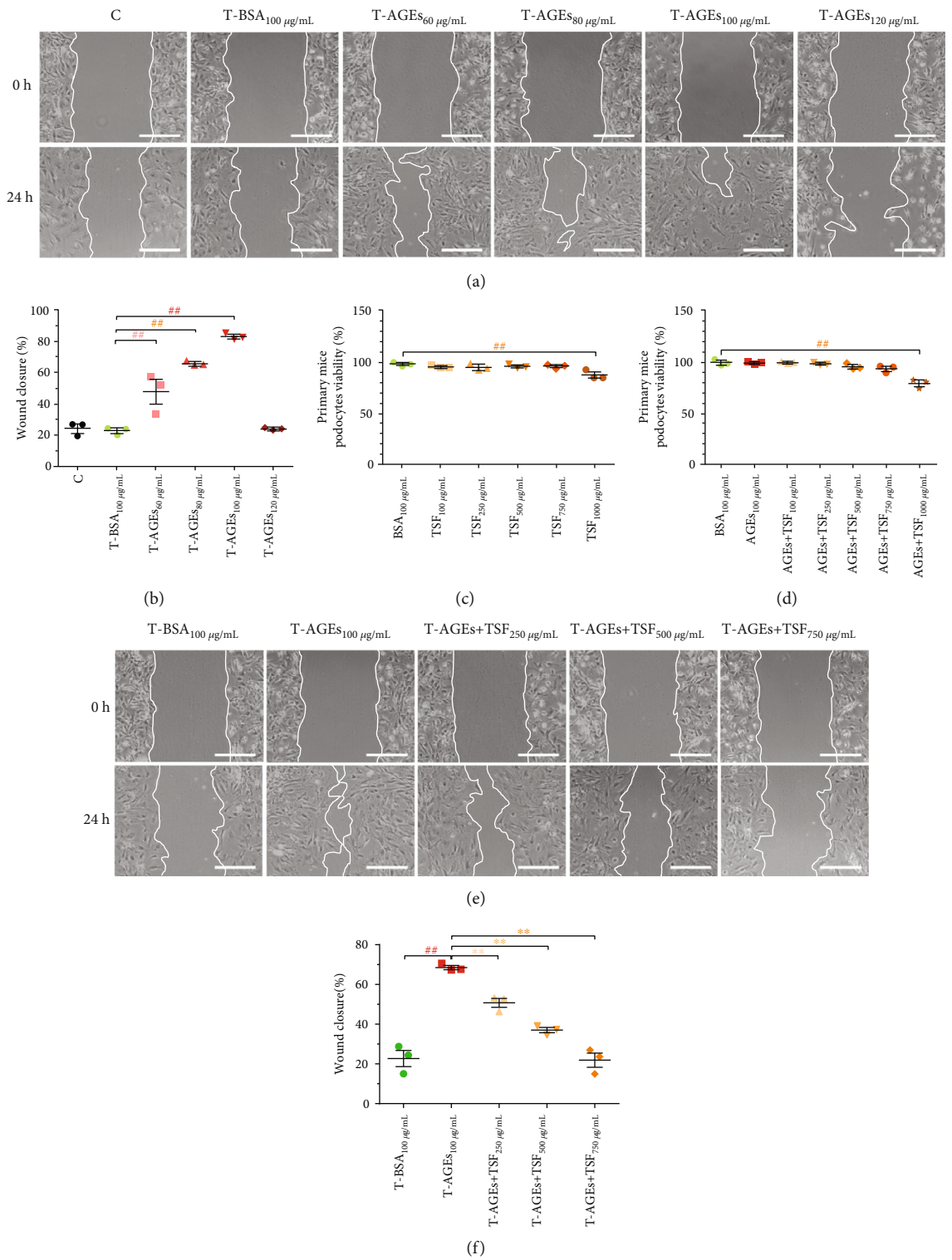

FIGURE 4: TSF attenuated the increased cell migration in AGEs-stimulated primary mice podocytes. (a, b) Wound healing assay and quantitative analysis using different doses of AGEs for 24 hours to observe the effect on primary mice podocytes (scale bars, 100 μm) ($n = 3$ experiments). (c, d) Viability of primary mice podocytes was determined with MTT assay ($n = 3$ experiments). (e, f) Wound healing assay and quantitative analysis using different doses of TSF for 24 hours (scale bars, 100 μm) ($n = 3$ experiments). The data were expressed as the mean ± SEM of three independent experiments performed in triplicate. $^{\#}P < 0.05$, $^{\#\#}P < 0.01$ vs. BSA group; $^{*}P < 0.05$, $^{**}P < 0.01$ vs. AGEs group. Statistically analyzed via a one-way ANOVA with Dunnett's correction.

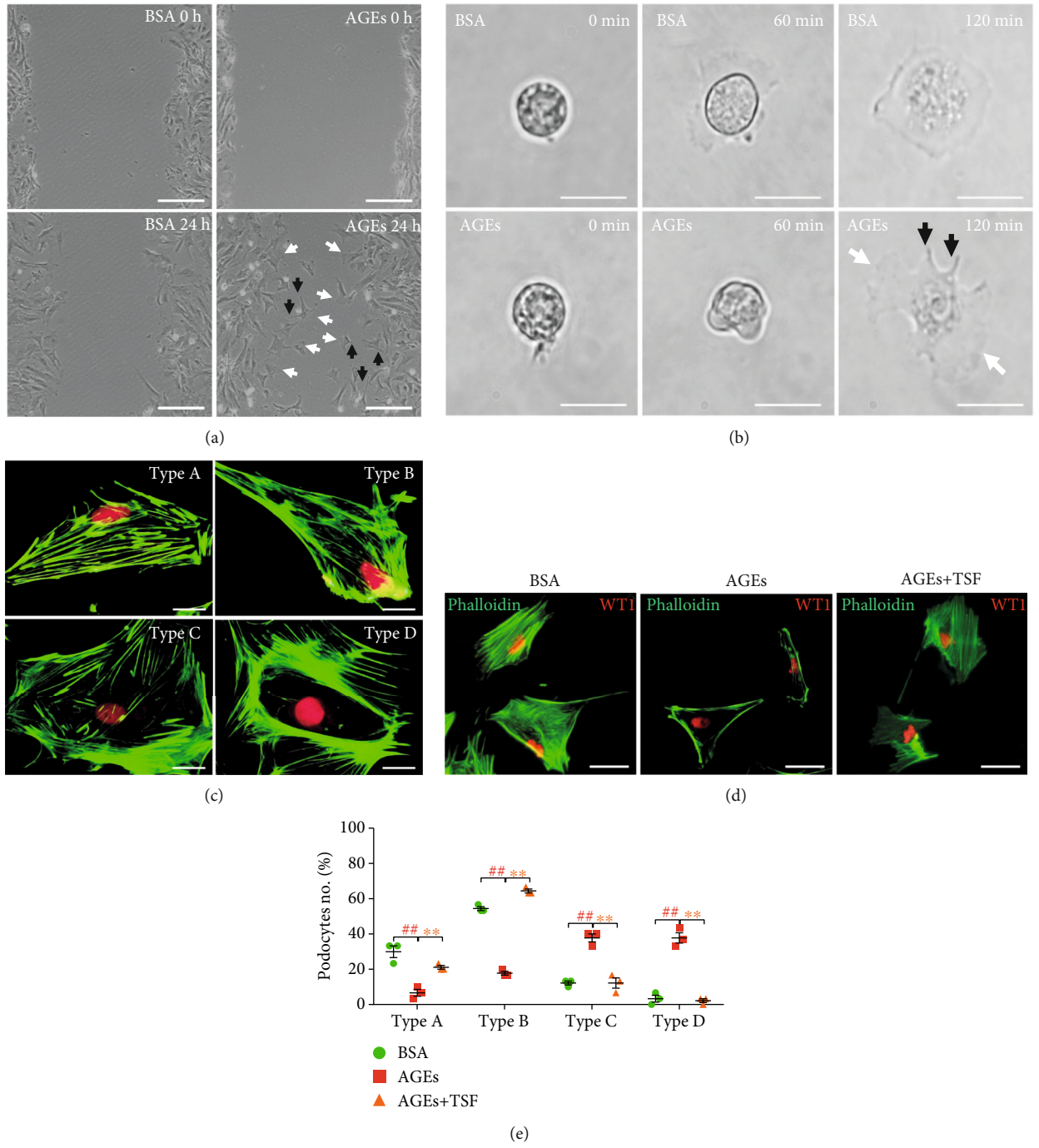

Figure 5: TSF inhibited actin-cytoskeletal disorganization in AGEs-stimulated primary mice podocytes. (a) Morphology of primary mice podocytes in wound healing assay (scale bars, 100 μm). (b) Time-lapse images of primary mice podocytes (scale bars, 50 μm). Lamellipodia are marked with white arrows and filopodia with black arrows. (c) Representative images of different types of phalloidin staining patterns observed in isolated control podocytes (scale bars, 25 μm). (d) Representative immunofluorescence stained with phalloidin and WT1 showed actin-cytoskeletal disorganization in AGEs-stimulated primary mice podocytes which could be relieved by TSF (scale bars, 50 μm). (e) Quantitative analysis of the percentage of four types of phalloidin staining patterns in (d) by a blinded observer (30 cells evaluated per experiment, $n = 3$ experiments). The data were expressed as the mean ± SEM of three independent experiments performed in triplicate. $^{\#}P < 0.05$, $^{\#\#}P < 0.01$ vs. BSA group; $^{*}P < 0.05$, $^{**}P < 0.01$ vs. AGEs group. Statistically analyzed via a one-way ANOVA with Dunnett's correction.

domain lacks actin-binding sites and catalytic activity, it is necessary to interact with cytoskeletal, adaptor and signaling molecules to form focal adhesion [49]. More than 200 components have been found at focal adhesions [50], including different receptor classes, linker molecules, GTPases, kinases, and phosphatases, collectively known as the adhesome. Focal

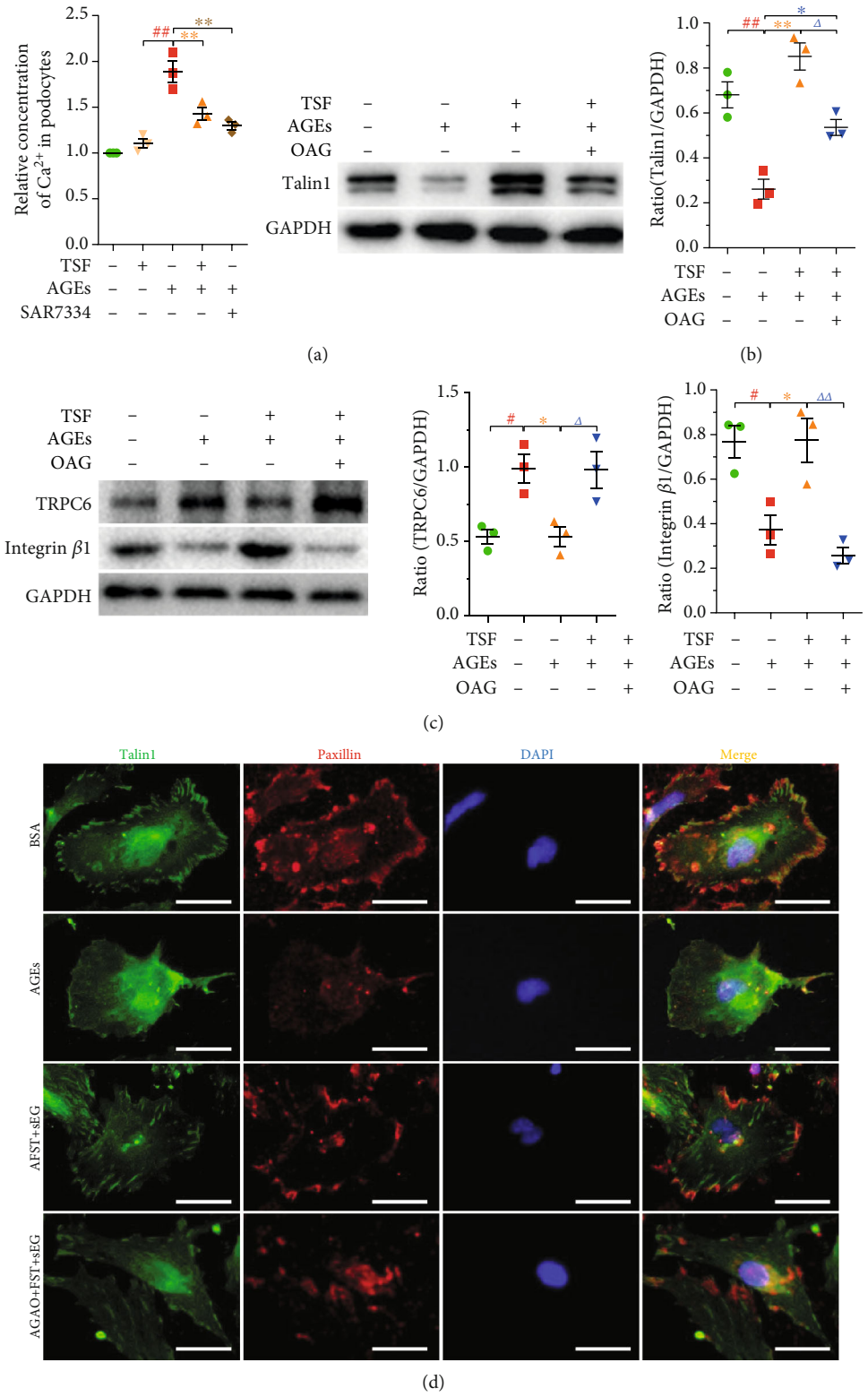

FIGURE 6: TSF improved TRPC6-dependent Ca^{2+} accumulation-mediated reduction of focal adhesions in AGEs-stimulated primary mice podocytes. (a) Effects of TSF or SAR7334 on intracellular Ca^{2+} level of AGEs-induced primary mice podocyte injury ($n = 3$ experiments). (b) Immunoblotting and quantitative analysis of talin1 ($n = 3$ experiments). (c) Immunoblotting and quantitative analysis of TRPC6 and integrin $\beta 1$ ($n = 3$ experiments). (d) Representative immunofluorescence stained with talin1 (green) and paxillin (red) (scale bars, 50 μm). The data were expressed as the mean ± SEM of three independent experiments performed in triplicate. $^{\#}P < 0.05$, $^{\#\#}P < 0.01$ vs. BSA group; $^{*}P < 0.05$, $^{**}P < 0.01$ vs. AGEs group; $^{\Delta}P < 0.05$, $^{\Delta\Delta}P < 0.01$ vs. AGEs + TSF group. Statistically analyzed via a one-way ANOVA with Dunnett's correction.

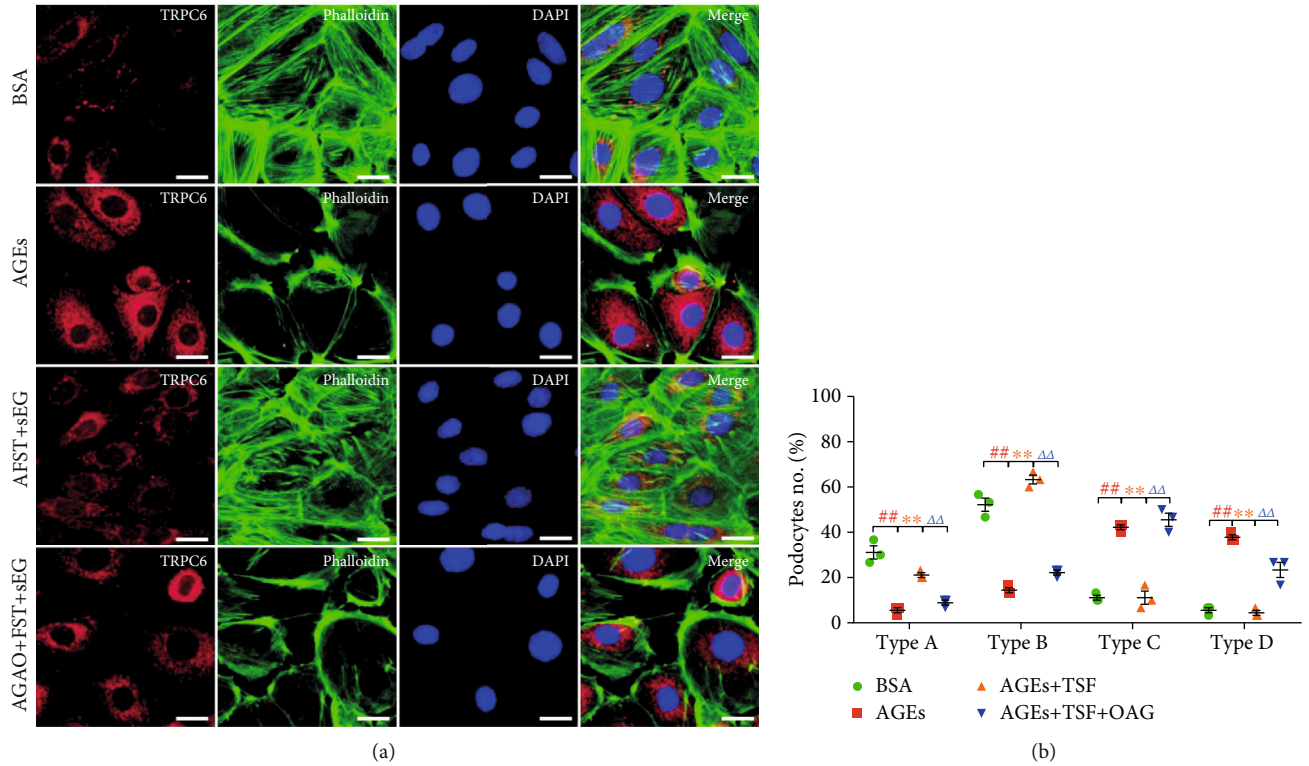

(a) (b)

Figure 7: TSF alleviated TRPC6-dependent Ca^{2+} accumulation-mediated actin-cytoskeletal disorganization in AGEs-stimulated primary mice podocytes. (a) Representative immunofluorescence stained with phalloidin and TRPC6 (scale bars, 25 μm). (b) Quantitative analysis of the percentage of four types of phalloidin staining patterns in (a) by an observer blinded to the group (30 cells evaluated per experiment, $n = 3$ experiments). The data were expressed as the mean ± SEM of three independent experiments performed in triplicate. $^{\#}P < 0.05$, $^{\#\#}P < 0.01$ vs. BSA group; $^{*}P < 0.05$, $^{**}P < 0.01$ vs. AGEs group; $^{\Delta}P < 0.05$, $^{\Delta\Delta}P<0.01$ vs. AGEs + TSF group. Statistically analyzed via a one-way ANOVA with Dunnett's correction.

adhesion provides a physical connection for podocytes to adhere to the GBM and regulates intracellular and extracellular signal transduction and actin network remodeling, thus controlling cell functions and morphologies [51]. Integrin activation is essential for the initiation of focal adhesions [52]. Talin is a large, 270 kDa protein with 18 domains and binds to at least 11 different focal adhesion components [53]. Compared with other focal adhesion proteins, talin has a special role as it binds to the cytoplasmic domain of the β integrin subunit, thereby activating the entire integrin that is capable of high-affinity interactions with extracellular matrix ligands [54]. At the same time, the active talin engaged with integrin can span the entire structure of focal adhesion, not only can mediate the signal transmission from the inside out but also to act as a mechanical sensor, which is essential for regulating the maturity and stability of focal adhesion [55, 56]. Studies have shown that the absence of β1 or α3 integrin in podocytes can lead to severe proteinuria [57, 58], and abnormal loss of talin1 affects the activation of β1 integrin, adhesion complex dynamics, and adhesion ability [8]. To ascertain the importance of proteins regulating focal adhesion in podocyte, we interrogated the Nephroseq v5 transcriptomic database. We observed that there was a striking negative correlation between the glomerular *TLN1* (talin1) expression with the body weight in *db*/*db* mice (Figure S4). Our results showed that TSF could significantly improve the body weight of *db*/*db* mice, while the irbesartan treatment did not exhibit the effect on the body weight of *db*/*db* mice. Furthermore, we observed that the glomerular *TLN1* expression negatively correlated with an increase of serum creatinine in the chronic kidney disease (CKD) cohort (Figure S4), our previous work demonstrated that TSF could significantly improve the serum creatinine level in the DKD patients [14]. These findings provided the impetus to further examine the importance of glomerular talin1 in the pathogenesis of DKD.

Talin1 has a strong positive correlation with the severity of proteinuria, reduction in cell adhesion, and podocyte actin-cytoskeletal disorganization [8]. To the best of our knowledge, our research is the first to explore the role of podocyte talin1 in DKD. We initially found that there was a significant loss in podocyte talin1 in *db*/*db* mice and AGEs-stimulated primary mice podocyte, which could be restored by TSF treatment. Meanwhile, increased cell migration and actin-cytoskeleton rearrangement caused by reduced talin1 were also seen in AGEs-induced primary mice podocytes. Talin1 in podocytes appears to be an important factor in the pathogenesis of DKD. As the key adhesion protein of the cell-matrix adhesion complexes, talins bind and activate integrins, coupling them to the actin cytoskeleton [59]. The two isoforms of talins in vertebrates are talin1 and talin2. Talin1 is closely linked to cell adhesion [60] and early

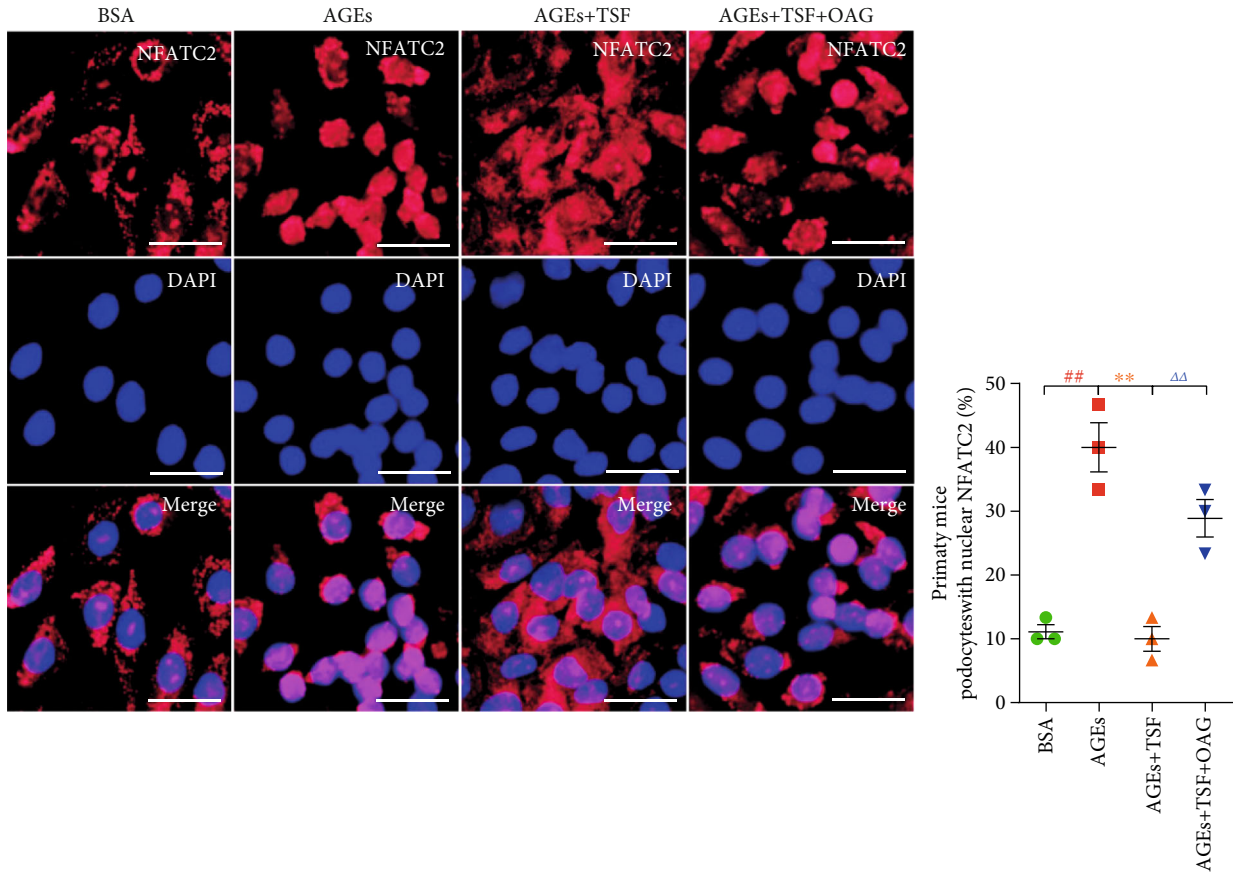

(a)

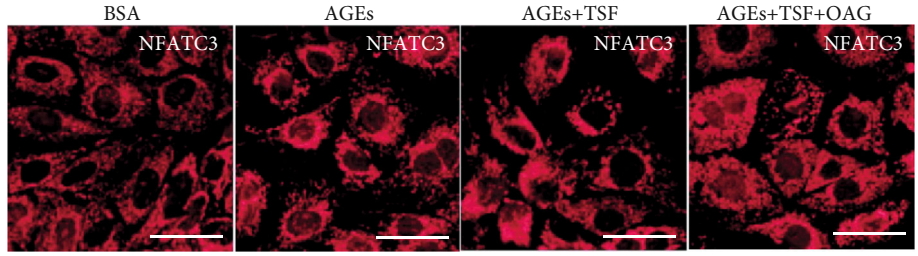

(b)

Figure 8: TSF alleviated NFATC2 nuclear translocation in AGEs-stimulated primary mice podocytes. (a) Representative immunofluorescence staining and quantitative analysis of NFATC2 (scale bars, 50 μm; 30 cells evaluated per experiment, $n = 3$ experiments). Nuclei were stained with DAPI. (b) Immunofluorescence staining for NFATC3 (scale bars, 50 μm). The data were expressed as the mean ± SEM. $^{\#}P < 0.05$, $^{\#\#}P < 0.01$ vs. BSA group; $^{*}P < 0.05$, $^{**}P < 0.01$ vs. AGEs group; $^{\Delta}P < 0.05$, $^{\Delta\Delta}P < 0.01$ vs. AGEs + TSF group. Statistically analyzed via a one-way ANOVA with Dunnett's correction.

embryonic development [61]. Talin1 function most likely predominates in normal podocyte physiology based on the evidence that podocyte-specific deletion of talin1 leads to severe podocyte injury and progressive proteinuria, while ablation of podocyte talin2 in mice lacking talin1 does not significantly change its phenotype [8].

AGEs are the nonenzymatic glycation of proteins caused by the long-term high glucose levels. AGEs have been demonstrated to be closely related to the development and progression of DKD, and can be involved in podocyte injury, endothelial cell damage, and renal fibrosis, and ultimately lead to impaired renal function [41, 42]. AGEs have been extensively used to explore the mechanism of podocyte injury in DKD. The enhancement of podocyte migration ability has been implicated as an injury phenotype. In renal pathology induced by adriamycin or unilateral ureteral ligation, dynamic podocyte movement can be observed [62]. Pan and colleagues [63] showed that SRGAP2a expression in podocytes of DKD patients and *db*/*db* mice was significantly reduced compared to normal controls. Overexpression of SRGAP2a could reverse previously abnormal actin cytoskeletal rearrangement, inhibit podocyte migration, and alleviate foot process effacement by inhibiting over-activated Rho A and Cdc42. In this study, we found that AGEs caused

an abnormal increase in podocyte migration. We also observed increased formation of lamellipodia and filopodia, suggesting that rearrangement of the actin cytoskeleton in podocytes could be induced by AGEs. These findings are consistent with previously published reports [64–67]. The decreased expressions of talin1, integrin β1, and paxillin in primary mice podocytes after treatment with AGEs suggested that AGEs could cause the impairment in the cell-matrix adhesion ability of podocytes. TSF had a significant effect on the improvement of expressions of talin1, integrin β1, and paxillin in podocytes damaged by AGE stimulation. TSF also inhibited the migration phenotype of podocytes and alleviated the disorder of actin cytoskeleton. These effects of TSF are beneficial to the maintenance of the glomerular filtration barrier by improving the adhesion ability of podocytes.

Podocyte hypertrophy, foot process effacement, and the loss of podocytes in DKD are closely related to the abnormal expression of TRPC6 in podocytes, but little is known about its mechanism [68]. Cleavage of talin1 has been shown to be associated with TRPC6-dependent Ca^{2+} accumulation in podocyte injury [13]. Also, knockdown of *TRPC6* also led to decreased cleavage of talin1 [9]. This suggests that TRPC6-dependent Ca^{2+} accumulation is involved in the cleavage of talin1. Chen and colleagues [69] demonstrated that AGEs could induce an increase in $[Ca^{2+}]_i$ through influx of extracellular Ca^{2+} in podocytes. However, little is known about the relationship between AGEs and TRPC6 in this pathophysiologic process. In the current study, we found increased TRPC6 expression in both *db*/*db* mice and AGEs-stimulated primary mice podocytes. The intracellular Ca^{2+} level of podocytes regulated by TRPC6 plays a key role in maintaining the stability of the actin-cytoskeleton structure and podocyte injury [70]. Although the mechanism for TRPC6 activation remains unclear, abnormal changes in angiotensin II and reactive oxygen species (ROS) in the DKD setting can stimulate overexpression of TRPC6 in podocytes. This causes a large amount of Ca^{2+} influx into podocytes, resulting in foot process effacement, podocyte loss, and other damage, which eventually leads to proteinuria development. Our results showed that there was a significant increase in Ca^{2+} level in AGEs-treated podocytes compared with the control, and this increase was attenuated by TSF and the TRPC6 inhibitor SAR7334. This indicated that increased intracellular Ca^{2+} accumulation induced by TRPC6 is involved in podocyte injury caused by AGEs, and that TSF could reduce TRPC6-mediated Ca^{2+} accumulation.

Decrease in talin1 protein, increase in cell migration, and disorganization of F-actin in podocytes were also observed with the activation of TRPC6. The F-actin pattern determined by phalloidin staining transformed from more than 90% of cell area filled with thick cables or at least two thick cables running under the nucleus into no thick cables or no cables visible in the central area of the cell after the podocytes were stimulated by AGEs. These pattern changes are similar to the results reported in other studies, that TRPC6 KO podocytes display less motility, more adhesiveness and more actin stress fibers. These changes are alleviated after the reexpression of wtTRPC6 [9]. However, previous studies also showed the role of TRPC6 in regulating Rho A activation, stress fiber contraction, and motility [71, 72]. This difference may be attributed to the difference in *TRPC6* knockout level caused by siRNA technology used in previous studies, where some preservation of expression is seen. Our *in vitro* cell culture results showed that TSF could inhibit the increase in TRPC6 expression, decrease in talin1, and disorganization of actin-cytoskeleton. This effect could also be attenuated by the TRPC6 agonist OAG. These results suggest that TSF protects talin1 by inhibiting TRPC6 activation. Although much progress has been made in the development of TRPC6 agonists, either OAG, GSK1702934A [73], piperazine derivatives [74], or pyrazolopyrimidines [75], subtype selectivity is still lacking within the TRPC3/6/7 group of ion channels. Thus, further studies and more convincing evidence are needed to elucidate the protective effect of TSF on talin1 by inhibiting TRPC6 activation in podocytes.

Additionally, we observed an increase in NFATC2 entry into nuclei in AGEs-stimulated primary mice podocytes, but not NFATC3. The NFATC family (including NFATC1 through NFATC4) is usually located in the cytoplasm as a potential form of hyperphosphorylation [76] and is mainly regulated by serine/threonine phosphatase calcineurin. Upon activation, NFATCs can undergo dephosphorylation into the nucleus to perform their functions. The important transcriptional target of NFATCs is TRPC6 itself, which results in a harmful feedforward loop [77]. NFATCs are expressed in a variety of cell types, including podocytes. It has been shown that NFATC2 podocyte-specific overexpression leads to proteinuria and glomerular sclerosis [78]. Further studies [79, 80] have also found a significant increase in NFATC2 activation in podocytes of *db*/*db* mice and could be inhibited by the NFAT inhibitor peptide (11R-VIVIT). High glucose-induced mice podocytes also activate NFATC2 in a time- and dose-dependent manner and is prevented by *Nfatc2* gene knockdown. In our study, AGEs-stimulated primary mice podocytes increased intracellular Ca^{2+} concentration, leading to subsequent nuclear accumulation of NFATC2. We only explored the occurrences in NFATC2 and 3, as abundant literature on these two proteins provided the foundation for our investigation. Given our findings, we believe that TRPC6-dependent Ca^{2+} accumulation is involved in DKD podocyte injury, and the protective effect of TSF on podocytes may be through inhibition of TRPC6 activation and protection of talin1 from loss. However, TSF is a complex Chinese Medicine compound with multiple active ingredients. It is indeed difficult to accurately explain the protective effect of TSF on DKD with one mechanism. Therefore, it is important to explore all the possible biochemical interactions of TSF in podocytes and to clarify how the compounds interact with podocytes. This will be the focus of our further research.

5. Conclusion

In conclusion, the present study demonstrated that TSF could alleviate podocyte injury and reduce proteinuria induced by DKD, the mechanism of which might be mediated by the regulation of TRPC6/Talin1 pathway in

podocytes, following an improvement in the podocyte-matrix adherence. These findings may be beneficial to our understanding of the role of TSF in protecting podocytes and further enrich our knowledge of the mechanism of podocyte injury in DKD.

Data Availability

The data used to support the findings of this study are available from the corresponding authors upon request.

Ethical Approval

The animal study was reviewed and approved by the Ethics Committee of the China-Japan Friendship Institute of Clinical Medical Sciences, Beijing, China.

Conflicts of Interest

The authors have no conflicts of interest to declare.

Authors' Contributions

TZ and PL designed the experiments. HJZ and WZ performed the herbal preparation. QW, YW, and HLZ conducted the experiments. JL and XZ analyzed the data. QW and XT wrote the manuscript. All authors read and approved the manuscript.

Acknowledgments

We are very grateful to Dr. Shuta Ishibe's laboratory at the Yale School of Medicine for kindly providing us the protocol of primary mice podocytes culture. Thanks to Professor Qionglin Liang and Researcher Zixing Shao of Tsinghua University for their help in screening the effective ingredients of TSF. This work was funded by the following sources: National Natural Science Foundation of China grants 81620108031 (Dr. Ping Li) and 81973627 (Dr. Tingting Zhao). The authors thank Nissi S. Wang, MSc, for the content editing of the manuscript.

Supplementary Materials

Table S1: compounds detected in TSF. Table S2: compounds detected in the serum of TSF treated mice. Figure S1: immunoblotting of TRPC6 and talin1 in MPC5 cells treated with scramble siRNA or *Trpc6* siRNA. Figure S2: immunohistochemical staining and quantitative analysis of collagen type I. Figure S3: the effect of irbesartan in combination with AGEs in wound healing assay. Figure S4: glomerular *TLN1* expression in *db*/*db* mice and CKD patients. *(Supplementary Materials)*

References

[1] R. Z. Alicic, M. T. Rooney, and K. R. Tuttle, "Diabetic kidney disease: challenges, progress, and possibilities," *Clinical Journal of the American Society of Nephrology: CJASN*, vol. 12, no. 12, pp. 2032–2045, 2017.

[2] A. Greka and P. Mundel, "Cell biology and pathology of podocytes," *Annual Review of Physiology*, vol. 74, no. 1, pp. 299–323, 2012.

[3] W. H. Fissell and J. H. Miner, "What is the glomerular ultrafiltration barrier?," *Journal of Cell Biology*, vol. 29, no. 9, pp. 2262–2264, 2018.

[4] C. Faul, K. Asanuma, E. Yanagida-Asanuma, K. Kim, and P. Mundel, "Actin up: regulation of podocyte structure and function by components of the actin cytoskeleton," *Trends in Cell Biology*, vol. 17, no. 9, pp. 428–437, 2007.

[5] Y. Maezawa and K. Yokote, "Human glomerular transcriptome of diabetic kidneys: can the podocyte cytoskeleton be a therapeutic target?," *Journal of Diabetes Investigation*, vol. 10, no. 2, pp. 224–226, 2019.

[6] C. Schell and T. B. Huber, "The evolving complexity of the podocyte cytoskeleton," *Journal of the American Society of Nephrology: JASN*, vol. 28, no. 11, pp. 3166–3174, 2017.

[7] D. Cox, M. Brennan, and N. Moran, "Integrins as therapeutic targets: lessons and opportunities," *Nature Reviews Drug Discovery*, vol. 9, no. 10, pp. 804–820, 2010.

[8] X. Tian, J. J. Kim, S. M. Monkley et al., "Podocyte-associated talin 1 is critical for glomerular filtration barrier maintenance," *The Journal of Clinical Investigation*, vol. 124, no. 3, pp. 1098–1113, 2014.

[9] L. K. Farmer, R. Rollason, D. J. Whitcomb et al., "TRPC6 binds to and activates calpain, independent of its channel activity, and regulates podocyte cytoskeleton, cell adhesion, and motility," *Journal of the American Society of Nephrology: JASN*, vol. 30, no. 10, pp. 1910–1924, 2019.

[10] M. P. Winn, P. J. Conlon, K. L. Lynn et al., "A mutation in the TRPC6 cation channel causes familial focal segmental glomerulosclerosis," *Science*, vol. 308, no. 5729, pp. 1801–1804, 2005.

[11] D. Rogacka, I. Audzeyenka, P. Rachubik et al., "Insulin increases filtration barrier permeability via TRPC6-dependent activation of PKGIα signaling pathways," *Biochimica et Biophysica Acta (BBA) - Molecular Basis of Disease*, vol. 1863, no. 6, pp. 1312–1325, 2017.

[12] J. S. Kang, S. J. Lee, J. H. Lee et al., "Angiotensin II-mediated MYH9 downregulation causes structural and functional podocyte injury in diabetic kidney disease," *Scientific Reports*, vol. 9, no. 1, p. 7679, 2019.

[13] K. A. T. Verheijden, R. Sonneveld, M. Bakker-van Bebber, J. F. M. Wetzels, J. van der Vlag, and T. Nijenhuis, "The calcium-dependent protease calpain-1 links TRPC6 activity to podocyte injury," *Journal of the American Society of Nephrology: JASN*, vol. 29, no. 8, pp. 2099–2109, 2018.

[14] P. Li, Y. Chen, J. Liu et al., "Efficacy and safety of tangshen formula on patients with type 2 diabetic kidney disease: a multicenter double-blinded randomized placebo-controlled trial," *PLoS One*, vol. 10, no. 5, article e0126027, 2015.

[15] M. Li, W. Wang, J. Xue, Y. Gu, and S. Lin, "Meta-analysis of the clinical value of Astragalus membranaceus in diabetic nephropathy," *Journal of Ethnopharmacology*, vol. 133, no. 2, pp. 412–419, 2011.

[16] G. H. Baek, Y. S. Jang, S. I. Jeong et al., "Rehmannia glutinosa suppresses inflammatory responses elicited by advanced glycation end products," *Inflammation*, vol. 35, no. 4, pp. 1232–1241, 2012.

[17] T. Zhao, H. Zhang, X. Yin et al., "Tangshen formula modulates gut Microbiota and reduces gut-derived toxins in diabetic

nephropathy rats," *Biomedicine & Pharmacotherapy*, vol. 129, p. 110325, 2020.

[18] Q. Kong, H. Zhang, T. Zhao et al., "Tangshen formula attenuates hepatic steatosis by inhibiting hepatic lipogenesis and augmenting fatty acid oxidation in db/db mice," *International Journal of Molecular Medicine*, vol. 38, no. 6, pp. 1715–1726, 2016.

[19] K. Liu, H. Xu, G. Lv et al., "Loganin attenuates diabetic nephropathy in C57BL/6J mice with diabetes induced by streptozotocin and fed with diets containing high level of advanced glycation end products," *Life Sciences*, vol. 123, pp. 78–85, 2015.

[20] W. L. Jiang, S. P. Zhang, J. Hou, and H. B. Zhu, "Effect of loganin on experimental diabetic nephropathy," *Phytomedicine*, vol. 19, no. 3-4, pp. 217–222, 2012.

[21] D. Tang, B. He, Z. G. Zheng et al., "Inhibitory effects of two major isoflavonoids in Radix Astragali on high glucose-induced mesangial cells proliferation and AGEs-induced endothelial cells apoptosis," *Planta Medica*, vol. 77, no. 7, pp. 729–732, 2011.

[22] M. J. Oza and Y. A. Kulkarni, "Formononetin attenuates kidney damage in type 2 diabetic rats," *Life Sciences*, vol. 219, pp. 109–121, 2019.

[23] J. Zhang, S. Yang, H. Li, F. Chen, and J. Shi, "Naringin ameliorates diabetic nephropathy by inhibiting NADPH oxidase 4," *European Journal of Pharmacology*, vol. 804, pp. 1–6, 2017.

[24] S. Jia, Y. Hu, W. Zhang et al., "Hypoglycemic and hypolipidemic effects of neohesperidin derived from Citrus aurantium L. in diabetic KK-A (y) mice," *Food & Function*, vol. 6, no. 3, pp. 878–886, 2015.

[25] Q. Zhang, L. Liu, W. Lin et al., "Rhein reverses Klotho repression via promoter demethylation and protects against kidney and bone injuries in mice with chronic kidney disease," *Kidney International*, vol. 91, no. 1, pp. 144–156, 2017.

[26] S. Duan, Y. Wu, C. Zhao et al., "The wnt/β-catenin signaling pathway participates in rhein ameliorating kidney injury in DN mice," *Molecular and Cellular Biochemistry*, vol. 411, no. 1-2, pp. 73–82, 2016.

[27] H. Zhang, P. Li, F. J. Burczynski et al., "Attenuation of diabetic nephropathy in Otsuka long-evans Tokushima fatty (OLETF) rats with a combination of Chinese herbs (tangshen formula)," *Evidence-based Complementary and Alternative Medicine: Ecam*, vol. 2011, article 613737, 8 pages, 2011.

[28] T. Zhao, S. F. Sun, H. J. Zhang et al., "Therapeutic Effects of Tangshen Formula on Diabetic Nephropathy in Rats," *PLoS One*, vol. 11, no. 1, article e0147693, 2016.

[29] H. Zhao, X. Li, T. Zhao et al., "Tangshen formula attenuates diabetic renal injuries by upregulating autophagy via inhibition of PLZF expression," *PLoS One*, vol. 12, no. 2, article e0171475, 2017.

[30] K. Sharma, P. McCue, and S. R. Dunn, "Diabetic kidney disease in the db/db mouse," *American Journal of Physiology. Renal Physiology*, vol. 284, no. 6, pp. F1138–F1144, 2003.

[31] G. E. Truett, R. J. Tempelman, J. A. Walker, and J. K. Wilson, "Misty (m) affects growth traits," *American Journal of Physiology*, vol. 275, no. 1, pp. R29–R32, 1998.

[32] H. Zhang, H. M. Zhang, L. P. Wu et al., "Impaired mitochondrial complex III and melatonin responsive reactive oxygen species generation in kidney mitochondria of db/db mice," *Journal of Pineal Research*, vol. 51, no. 3, pp. 338–344, 2011.

[33] S. Reagan-Shaw, M. Nihal, and N. Ahmad, "Dose translation from animal to human studies revisited," *The FASEB Journal*, vol. 22, no. 3, pp. 659–661, 2007.

[34] H. Cheng, H. Wang, X. Fan, P. Paueksakon, and R. C. Harris, "Improvement of endothelial nitric oxide synthase activity retards the progression of diabetic nephropathy in db/db mice," *Kidney International*, vol. 82, no. 11, pp. 1176–1183, 2012.

[35] S. Majumder, M. J. Hadden, K. Thieme et al., "Dysregulated expression but redundant function of the long non-coding RNA HOTAIR in diabetic kidney disease," *Diabetologia*, vol. 62, no. 11, pp. 2129–2142, 2019.

[36] K. Soda, D. M. Balkin, S. M. Ferguson et al., "Role of dynamin, synaptojanin, and endophilin in podocyte foot processes," *The Journal of Clinical Investigation*, vol. 122, no. 12, pp. 4401–4411, 2012.

[37] H. Ma, A. Togawa, K. Soda et al., "Inhibition of podocyte FAK protects against proteinuria and foot process effacement," *Journal of the American Society of Nephrology: JASN*, vol. 21, no. 7, pp. 1145–1156, 2010.

[38] G. Grynkiewicz, M. Poenie, and R. Y. Tsien, "A new generation of Ca^{2+} indicators with greatly improved fluorescence properties," *Journal of Biological Chemistry*, vol. 260, no. 6, pp. 3440–3450, 1985.

[39] J. Wu, C. Zheng, X. Wang et al., "MicroRNA-30 family members regulate calcium/calcineurin signaling in podocytes," *Journal of Clinical Investigation*, vol. 125, no. 11, pp. 4091–4106, 2015.

[40] P. Liu, L. Peng, H. Zhang et al., "Tangshen formula attenuates diabetic nephropathy by promoting ABCA1-mediated renal cholesterol efflux in db/db mice," *Frontiers in Physiology*, vol. 9, p. 343, 2018.

[41] T. Wendt, N. Tanji, J. Guo et al., "Glucose, glycation, and RAGE: implications for amplification of cellular dysfunction in diabetic nephropathy," *Journal of the American Society of Nephrology: JASN*, vol. 14, no. 5, pp. 1383–1395, 2003.

[42] X. Zhao, Y. Chen, X. Tan et al., "Advanced glycation end-products suppress autophagic flux in podocytes by activating mammalian target of rapamycin and inhibiting nuclear translocation of transcription factor EB," *Journal of Pathology*, vol. 245, no. 2, pp. 235–248, 2018.

[43] X. Zhang, G. Jiang, Y. Cai, S. J. Monkley, D. R. Critchley, and M. P. Sheetz, "Talin depletion reveals independence of initial cell spreading from integrin activation and traction," *Nature Cell Biology*, vol. 10, no. 9, pp. 1062–1068, 2008.

[44] H. Zhou, X. Tian, A. Tufro, G. Moeckel, S. Ishibe, and J. Goodwin, "Loss of the podocyte glucocorticoid receptor exacerbates proteinuria after injury," *Scientific Reports*, vol. 7, no. 1, p. 9833, 2017.

[45] T. Maier, M. Follmann, G. Hessler et al., "Discovery and pharmacological characterization of a novel potent inhibitor of diacylglycerol-sensitive TRPC cation channels," *British Journal of Pharmacology*, vol. 172, no. 14, pp. 3650–3660, 2015.

[46] W. Kriz, I. Shirato, M. Nagata, M. LeHir, and K. V. Lemley, "The podocyte's response to stress: the enigma of foot process effacement," *American Journal of Physiology Renal Physiology*, vol. 304, no. 4, pp. F333–F347, 2013.

[47] R. Lennon, M. J. Randles, and M. J. Humphries, "The importance of podocyte adhesion for a healthy glomerulus," *Frontiers in Endocrinology*, vol. 5, no. 14, p. 160, 2014.

[48] W. Kriz and K. V. Lemley, "A potential role for mechanical forces in the detachment of podocytes and the progression of CKD," *Journal of the American Society of Nephrology: JASN*, vol. 26, no. 2, pp. 258–269, 2015.

[49] H. B. Schiller, C. C. Friedel, C. Boulegue, and R. Fässler, "Quantitative proteomics of the integrin adhesome show a myosin II-dependent recruitment of LIM domain proteins," *EMBO Reports*, vol. 12, no. 3, pp. 259–266, 2011.

[50] S. E. Winograd-Katz, R. Fässler, B. Geiger, and K. R. Legate, "The integrin adhesome: from genes and proteins to human disease," *Nature Reviews Molecular Cell Biology*, vol. 15, no. 4, pp. 273–288, 2014.

[51] R. O. Hynes, "Integrins: bidirectional, allosteric signaling machines," *Cell*, vol. 110, no. 6, pp. 673–687, 2002.

[52] B. Geiger, J. P. Spatz, and A. D. Bershadsky, "Environmental sensing through focal adhesions," *Nature Reviews Molecular Cell Biology*, vol. 10, no. 1, pp. 21–33, 2009.

[53] B. T. Goult, J. Yan, and M. A. Schwartz, "Talin as a mechanosensitive signaling hub," *Journal of Cell Biology*, vol. 217, no. 11, pp. 3776–3784, 2018.

[54] K. L. Wegener, A. W. Partridge, J. Han et al., "Structural basis of integrin activation by talin," *Cell*, vol. 128, no. 1, pp. 171–182, 2007.

[55] D. S. Harburger and D. A. Calderwood, "Integrin signalling at a glance," *Journal of Cell Science*, vol. 122, no. 2, pp. 159–163, 2008.

[56] A. Kumar, M. Ouyang, K. Van den Dries et al., "Talin tension sensor reveals novel features of focal adhesion force transmission and mechanosensitivity," *Journal of Cell Biology*, vol. 213, no. 3, pp. 371–383, 2016.

[57] A. Pozzi, G. Jarad, G. W. Moeckel et al., "Beta 1 integrin expression by podocytes is required to maintain glomerular structural integrity," *Developmental Biology*, vol. 316, no. 2, pp. 288–301, 2008.

[58] N. Sachs, M. Kreft, M. A. van den Bergh Weerman et al., "Kidney failure in mice lacking the tetraspanin CD151," *Journal of Cell Biology*, vol. 175, no. 1, pp. 33–39, 2006.

[59] R. E. Gough and B. T. Goult, "The tale of two talins - two isoforms to fine-tune integrin signalling," *FEBS Letters*, vol. 592, no. 12, pp. 2108–2125, 2018.

[60] A. M. Manso, H. Okada, F. M. Sakamotoet al. et al., "Loss of mouse cardiomyocyte talin-1 and talin-2 leads to β-1 integrin reduction, costameric instability, and dilated cardiomyopathy," *Proceedings of the National Academy of Sciences of the United States of America*, vol. 114, no. 30, pp. E6250–E6259, 2017.

[61] S. J. Monkley, X. H. Zhou, S. J. Kinston et al., "Disruption of the talin gene arrests mouse development at the gastrulation stage," *Developmental Dynamics: an Official Publication of the American Association of Anatomists*, vol. 219, no. 4, pp. 560–574, 2000.

[62] M. J. Hackl, J. L. Burford, K. Villanueva et al., "Tracking the fate of glomerular epithelial cells in vivo using serial multiphoton imaging in new mouse models with fluorescent lineage tags," *Nature Medicine*, vol. 19, no. 12, pp. 1661–1666, 2013.

[63] Y. Pan, S. Jiang, Q. Hou et al., "Dissection of glomerular transcriptional profile in patients with diabetic nephropathy: SRGAP2a protects podocyte structure and function," *Diabetes*, vol. 67, no. 4, pp. 717–730, 2018.

[64] H. L. Kuo, C. C. Huang, T. Y. Lin, and C. Y. Lin, "IL-17 and CD40 ligand synergistically stimulate the chronicity of diabetic nephropathy," *Nephrology, Dialysis, Transplantation*, vol. 33, no. 2, pp. 248–256, 2018.

[65] Y. Chen, J. Chen, M. Jiang et al., "Loganin and catalpol exert cooperative ameliorating effects on podocyte apoptosis upon diabetic nephropathy by targeting AGEs-RAGE signaling," *Life Sciences*, vol. 252, p. 117653, 2020.

[66] Q. Wang, Z. Shen, G. Qi, Y. Zhao, H. Zhang, and R. Wang, "Thymol alleviates AGEs-induced podocyte injury by a pleiotropic effect via NF-κB-mediated by RhoA/ROCK signalling pathway," *Cell Adhesion & Migration*, vol. 14, no. 1, pp. 42–56, 2020.

[67] C. Cheng, Z. Zheng, C. Shi, X. Liu, Z. Ye, and T. Lou, "Advanced glycation end-products reduce podocyte adhesion by activating the renin-angiotensin system and increasing integrin-linked kinase," *Experimental and Therapeutic Medicine*, vol. 6, no. 6, pp. 1494–1498, 2013.

[68] A. Staruschenko, D. Spires, and O. Palygin, "Role of TRPC6 in Progression of Diabetic Kidney Disease," *Current Hypertension Reports*, vol. 21, no. 7, p. 48, 2019.

[69] Y. Chen, C. P. Liu, K. F. Xu et al., "Effect of taurine-conjugated ursodeoxycholic acid on endoplasmic reticulum stress and apoptosis induced by advanced glycation end products in cultured mouse podocytes," *American Journal of Nephrology*, vol. 28, no. 6, pp. 1014–1022, 2008.

[70] D. V. Ilatovskaya and A. Staruschenko, "TRPC6 channel as an emerging determinant of the podocyte injury susceptibility in kidney diseases," *American Journal of Physiology. Renal Physiology*, vol. 309, no. 5, pp. F393–F397, 2015.

[71] D. Tian, S. M. P. Jacobo, D. Billing et al., "Antagonistic regulation of actin dynamics and cell motility by TRPC5 and TRPC6 channels," *Science Signaling*, vol. 3, no. 145, article ra77, 2010.

[72] S. Park, S. Lee, E. J. Park et al., "TGFβ1 induces stress fiber formation through upregulation of TRPC6 in vascular smooth muscle cells," *Biochemical and Biophysical Research Communications*, vol. 483, no. 1, pp. 129–134, 2017.

[73] X. Xu, I. Lozinskaya, M. Costell et al., "Characterization of small molecule TRPC3 and TRPC6 agonist and antagonists," *Biophysical Journal*, vol. 104, no. 2, p. 454a, 2013.

[74] S. Sawamura, M. Hatano, Y. Takada et al., "Screening of transient receptor potential canonical channel activators identifies novel neurotrophic piperazine compounds," *Molecular Pharmacology*, vol. 89, no. 3, pp. 348–363, 2016.

[75] C. Qu, M. Ding, Y. Zhu et al., "Pyrazolopyrimidines as potent stimulators for transient receptor potential canonical 3/6/7 channels," *Journal of Medicinal Chemistry*, vol. 60, no. 11, pp. 4680–4692, 2017.

[76] A. Rao, C. Luo, and P. G. Hogan, "Transcription factors of the NFAT family: regulation and function," *Annual Review of Immunology*, vol. 15, no. 1, pp. 707–747, 1997.

[77] T. Nijenhuis, A. J. Sloan, J. G. J. Hoenderop et al., "Angiotensin II contributes to podocyte injury by increasing TRPC6 expression via an NFAT-mediated positive feedback signaling pathway," *American Journal of Physiology*, vol. 179, no. 4, pp. 1719–1732, 2011.

[78] Y. Wang, G. Jarad, P. Tripathi et al., "Activation of NFAT signaling in podocytes causes glomerulosclerosis," *Journal of the American Society of Nephrology: JASN*, vol. 21, no. 10, pp. 1657–1666, 2010.

[79] L. Zhang, R. Li, W. Shi et al., "NFAT2 inhibitor ameliorates diabetic nephropathy and podocyte injury in db/db mice," *British Journal of Pharmacology*, vol. 170, no. 2, pp. 426–439, 2013.

[80] R. Li, L. Zhang, W. Shi et al., "NFAT2 mediates high glucose-induced glomerular podocyte apoptosis through increased Bax expression," *Experimental Cell Research*, vol. 319, no. 7, pp. 992–1000, 2013.

Hindawi
Journal of Diabetes Research
Volume 2020, Article ID 4085757, 12 pages
https://doi.org/10.1155/2020/4085757

Research Article

The Alteration of Carnitine Metabolism in Second Trimester in GDM and a Nomogram for Predicting Macrosomia

Man Sun,[1] Baihui Zhao,[1] Sainan He,[1] Ruopeng Weng,[1] Binqiao Wang,[1] Yunping Ding,[1] Xinwen Huang,[2] and Qiong Luo[1]

[1]*Department of Obstetrics, Women's Hospital, School of Medicine, Zhejiang University, China*
[2]*Department of Genetic and Metabolic Diseases, The Children's Hospital, School of Medicine, Zhejiang University, No.1, Xueshi Road, Shangchen District, Hangzhou, China*

Correspondence should be addressed to Qiong Luo; luoq@zju.edu.cn

Received 7 May 2020; Revised 20 June 2020; Accepted 13 July 2020; Published 11 August 2020

Guest Editor: Markus Wallner

Objective. The metabolism of three major nutrients (sugar, lipid, and protein) will change during pregnancy, especially in the second trimester. The present study is aimed at evaluating carnitine alteration in fatty acid metabolism in the second trimester of pregnancy and the correlation between carnitine and GDM. *Methods*. 450 pregnant women were recruited in the present prospective study. Metabolic profiling of 31 carnitines was detected by LC-MS/MS in these women. Correlation between carnitine metabolism and maternal and neonatal complication with GDM was analyzed. *Results*. We found the levels of 7 carnitines increased in age > 35, BMI ≥ 30, weight gain > 20 kg, and ART pregnant groups, but the level of free carnitine (C0) decreased. Nine carnitines were specific metabolites of GDM. Prepregnancy BMI, weight gain, and carnitines (C0, C3, and C16) were independent risk factors associated with GDM and related macrosomia. C0 was negatively correlated with FBG, LDL, TG, and TC. A nomogram was developed for predicting macrosomia in GDM based on carnitine-related metabolic variables. *Conclusion*. The carnitine metabolism in the second trimester is abnormal in GDM women. The dysfunction of carnitine metabolism is closely related to the abnormality of blood lipid and glucose in GDM. Carnitine metabolism abnormality could predict macrosomia complicated with GDM.

1. Introduction

Pregnancy is a complex process accompanied by substantial changes in sugar, protein, and lipid metabolism [1]. Maternal lipid and protein metabolism of the second trimester is an anabolic state combined with accelerating maternal fat stores and increasing protein synthesis [2]. Dyslipidemia is associated with maternal metabolic disorder (GDM, hyperlipemia, and hypertension) and adverse neonate outcomes (macrosomia, fetal growth restriction) [3]. Fatty acid oxidation decreases in obesity during pregnancy and has linked to GDM development [4].

GDM is a common metabolic disorder during pregnancy and occurs in approximately 10–15% of pregnancies globally [5]. Pregnant women with GDM are more prone to hypertension and metabolic syndrome. The risks to the fetus include macrosomia, respiratory distress syndrome, childhood obesity, and type 2 diabetes mellitus (T2DM) in adults [6]. GDM is associated with profound changes in metabolism. Free carnitine (C0) has a critical role in energy metabolism of transporting long-chain fatty acid from the cytosol into the mitochondria, which results in C0 transforming into acylcarnitine (AC) [7, 8]. Carnitine deficiency is defined as a serum C0 level < 20 μmol/L [9]. C0 deficiency might impair lipid metabolism resulting in GDM [10]. Evaluated circulating AC (such as C3 and C5) is associated with GDM and induces pancreatic β-cell dysfunction [11]. A previous study proposed that C0 and AC decreased in pregnancy in the first trimester compared with nonpregnancy [12]. However, studies of metabolic profiling of carnitine in the second trimester

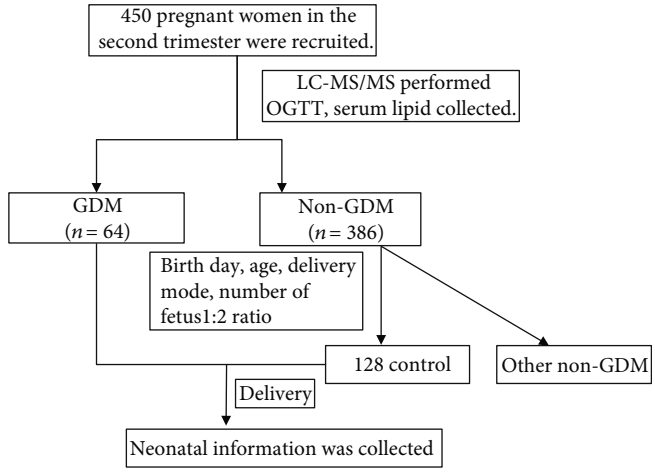

Figure 1: Study workflow of the present prospective study.

among diverse pregnant women are rare. Herein, we provide a study of the metabolism of carnitine to investigate the potential risk factors in GDM.

In the present study, a LC–MS/MS-based metabolomics approach was used to quantify the maternal plasma level of AC in order to identify the correlation between nonglucose metabolism abnormalities and pregnancy metabolic diseases during the second trimester. We analyzed metabolic alteration in the second trimester and detected the independent risk factors of GDM. Moreover, we established a prognostic nomogram of incorporating AC for predicting GDM macrosomia.

2. Method

2.1. Subject. This study was a prospective study. Between June 2017 and April 2018, 450 pregnant women in the second trimester were recruited in this study at Women's Hospital, School of Medicine, Zhejiang University, in Hangzhou. The study design has been approved by the Ethics Committee of the hospital. All participants were of Chinese Han ethnicity. We obtain maternal characteristic information as follows: gravidity, parity, age, height, prepregnancy BMI, weight gain during pregnancy, use of assisted reproductive technique (ART), and method of pregnancy termination. The following information of the offspring was collected: termination of pregnancy weeks, sex, birth length, actual birth weight, head circumference, abdomen circumference, and abdomen minus head circumference (data from fetal growth measurement ultrasound before labor).

GDM was defined according to the Chinese Current Care Guidelines for GDM as one or more pathological glucose values in a standard oral glucose tolerance test (OGTT) [13]. The diagnostic thresholds were fasting plasma glucose: 5.1 mmol/L, 1 h 10.0 mmol/L, and 2 h 8.5 mmol/L [14]. According to the guideline, 64 GDM cases were diagnosed. The control group was composed of 128 randomly sampled women without GDM from residual pregnant women participating in this study matched by birthday, age, delivery mode, and number of fetuses with 2 : 1 ratio. The 2 : 1 design can eliminate the interference of many factors (such as age, height, and gestational week at delivery) in the study, and a double sample has good statistical performance. The common definition of macrosomia is birth weight over 4000 g [15]. Biochemical status of the GDM and control groups was also collected and analyzed.

2.2. Metabolic Profiling Detection by LC-MS/MS. We used the method of LC-MS/MS to investigate the level of 31 plasma carnitines of pregnant women in the second trimester. We also obtain their neonate blood plasma sample. Blood samples were taken via venipuncture, using 4 mL Vacutainer Tubes containing K2-EDTA as anticoagulant centrifuged at 2500 g for 15 min; then, samples of plasma were stored at –20°C and detected monthly. For plasma analysis, plasma was pipetted into a 2.0 mL 96-deep-well plate. To this, internal standard solution was added, and the plate was vortex mixed for 1 min. Proteins were precipitated by adding 0.3 M zinc sulfate in methanol (1 : 5 *v*/*v*), and the plate was vortexed again for 1 min. Water was added, and the plate was sealed and centrifuged. Following centrifugation, supernatant was injected for analysis [16]. Furthermore, sample preparation used in tandem mass spectrometry (4000 QTrap™; AB Sciex, Darmstadt, Germany) test the concentration. The method used in the present study was essentially a modification of the procedure described elsewhere [17]. AA and AC were quantified using appropriate isotope-labelled standards. LC separation was performed on an Acquity UPLC HSS T3 column (2.1 ∗ 100 mm, 100 Å, 1.8 lm particle size; Waters Corporation, MA) using water with 0.1% formic acid, 5 mM ammonium acetate, and 0.015% heptafluorobutyric acid as solvent A and methanol with 0.1% formic acid and 5 mM detected with a Xevo-G2-QTOF MS (Waters Corporation) operating in a positive mode. Raw data was processed using Targetlynx as described previously. Accuracy of quantification was below 6% for all quantified metabolites except glutamic acid (13.9%). Quantitative data was obtained using MetIDQTM Software [18].

Table 1: The maternal plasma levels of acylcarnitine (AC) at the second trimester in 450 pregnant women according to clinical characteristic. Values are presented as the mean ± SD; $^*P < 0.05$ is considered statistically significant.

	Age			*P* value	Prepregnancy BMI				*P* value	Weight gain (kg)				*P* value	ART		*P* value
	<25	25-35	>35		<18.5	18.5-24.9	25.0-29.9	≥30		<12.5	12.5-15	15-20	>20		No	Yes	
n	12	247	191		9	253	153	35		97	147	150	56		376	74	
C0	23.26 ± 3.86	20.34 ± 3.81	16.18 ± 7.55	0.035*	24.15 ± 3.8	20.63 ± 5.49	16.43 ± 4.76	15.52 ± 3.13	0.038*	22.85 ± 3.8	19.83 ± 5.45	16.63 ± 4.62	15.28 ± 3.14	0.016*	23.71 ± 5.54	16.25 ± 7.43	0.002*
C2	2.08 ± 0.54	2.43 ± 0.76	2.61 ± 0.92	0.043*	1.84 ± 0.49	2.25 ± 0.82	2.48 ± 0.78	2.61 ± 0.67	0.017*	2.34 ± 0.42	2.49 ± 0.56	2.48 ± 0.28	2.39 ± 0.67	0.640	2.51 ± 0.90	2.79 ± 0.82	0.016*
C3	0.52 ± 0.14	0.56 ± 0.17	0.58 ± 0.20	0.042*	0.42 ± 0.14	0.45 ± 0.19	0.48 ± 0.18	0.55 ± 0.17	0.015*	0.48 ± 0.14	0.55 ± 0.19	0.58 ± 0.19	0.65 ± 0.17	0.035*	0.57 ± 0.23	0.68 ± 0.15	0.042*
C4DC+C5OH	0.13 ± 0.03	0.14 ± 0.05	0.16 ± 0.02	0.014*	0.14 ± 0.03	0.14 ± 0.06	0.14 ± 0.04	0.14 ± 0.04	0.290	0.14 ± 0.03	0.14 ± 0.06	0.14 ± 0.02	0.14 ± 0.04	0.490	0.14 ± 0.06	0.14 ± 0.06	0.185
C5	0.05 ± 0.02	0.04 ± 0.01	0.04 ± 0.01	0.524	0.03 ± 0.01	0.04 ± 0.02	0.05 ± 0.01	0.06 ± 0.01	0.027*	0.02 ± 0.01	0.03 ± 0.02	0.04 ± 0.01	0.06 ± 0.01	0.038*	0.03 ± 0.01	0.05 ± 0.01	0.035*
C16	0.43 ± 0.13	0.44 ± 0.17	0.45 ± 0.18	0.019*	0.44 ± 0.13	0.47 ± 0.19	0.54 ± 0.18	0.68 ± 0.28	0.026*	0.42 ± 0.15	0.44 ± 0.19	0.45 ± 0.18	0.47 ± 0.25	0.029*	0.47 ± 0.28	0.48 ± 0.17	0.338
C18	0.26 ± 0.08	0.27 ± 0.11	0.30 ± 0.10	0.032*	0.30 ± 0.09	0.28 ± 0.13	0.28 ± 0.10	0.29 ± 0.17	0.510	0.31 ± 0.09	0.31 ± 0.13	0.29 ± 0.11	0.30 ± 0.17	0.560	0.28 ± 0.13	0.27 ± 0.11	0.483
C18:1	0.48 ± 0.13	0.49 ± 0.16	0.54 ± 0.24	0.017*	0.32 ± 0.12	0.38 ± 0.23	0.46 ± 0.19	0.52 ± 0.17	0.019*	0.32 ± 0.18	0.41 ± 0.26	0.48 ± 0.16	0.55 ± 0.16	0.045*	0.57 ± 0.21	0.57 ± 0.27	0.467

2.3. Statistical Analysis. Data distributed normally were expressed as means ± standard deviation. The statistical method used for testing difference between two groups was Student's*t*-test. One-way ANOVA was used in more than two groups. For correlation analysis, the Spearman correlation coefficient was calculated in the level of AA and AC between the mothers in the second trimester and their neonates. In PLS-DA, metabolomics data were log-transformed to ensure a normally distributed data set; R^2 (goodness of fitness) and Q^2 (goodness of prediction) were assessed in the PLS-DA models. Multivariate logistic regression analysis was used to determine the association of GDM and macrosomia with prepregnancy BMI, weight gain, and ACs. Odds ratios (ORs) and 95% confidence intervals (CIs) were reported per standard deviation. All statistical analysis was performed using IBM SPSS 23.0 edition, SIMCA 14.0, and R vision 3.6.0. A significance level of 0.05 was used for all statistical tests.

3. Results

The study setup is illustrated in Figure 1. We identified the metabolic alternation in 450 pregnant women of the second trimester. We also investigated the metabolic risk factors in GDM and established a prognostic nomogram based on AC risk factors for predicting macrosomia.

3.1. Maternal Plasma AC Levels of the Second Trimester in 450 Pregnant Women. The baseline characteristics of 450 study participants divided into different categories according to natural conditions of pregnant women such as gravidity, parity, age, height, prepregnancy BMI, weight gain, ART, and method of pregnancy termination. The statistically significant results are shown in Table 1 and Figure 2. In the age subgroup, there was a trend that the level of AC (C2, C3, C4DC+C5OH, C16, C18, and C18:1) was higher in the age > 35 group, whereas the level of C0 in the age > 35 group was lower. In prepregnancy BMI ≥ 25.0 and 30 subgroups, several ACs (C2, C3, C5, C16, and C18:1) were higher, whereas the level of C0 was lower. In the weight gain group, C3, C5, C16, and C18:1 were higher in the weight gain ≥ 20 kg group than the other groups, while C0 was lower. In the ART group, C2, C3, and C5 were higher while C0 was lower. There was no statistical difference in gravity, parity, height, and method of pregnancy termination subgroups (data not shown).

Additionally, we investigated the maternal level AC in second trimester pregnancy under the different neonate subgroups (termination of pregnancy weeks, sex, birth length, birth weight, head circumference, abdomen circumference, and abdomen minus head circumference). The results are shown in Table 2 and Figure 3. In the birth weight > 4000 g group, we found that ACs (C2, C3, C5, C16, and C18:1) were higher; these metabolites increased with birth weight, while C0 was lower. In the abdomen circumference > 35 cm group, several ACs (C2, C3, C5, and C16) were higher; C0 was lower. In the abdomen minus circumference subgroup, the metabolite characteristics have a similar trend with the abdomen circumference > 35 cm subgroup.

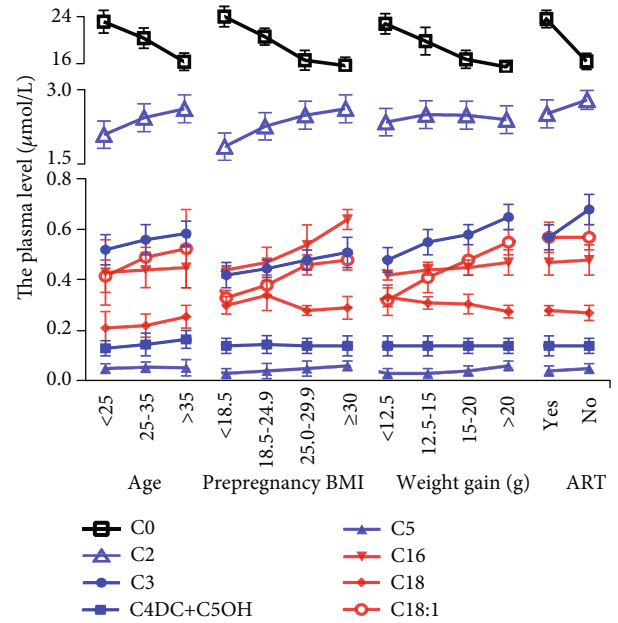

Figure 2: The maternal plasma levels of acylcarnitine (AC) at the second trimester in 450 pregnant women according to clinical characteristic. The AC level was higher in the age > 35 group, in prepregnancy BMI ≥ 25.0 and 30, in the weight gain group, and in the ART group, while C0 was decreased. Values are presented as the mean ± SEM.

3.2. Specific AC Distribution in GDM. We examined the serum metabolite in 64 GDM patients and 128 matched patients without GDM. Our study used the PLS-DA model ($R^2 = 0.527$, $Q^2 = 0.464$) to analyze differences between two groups. The PLS-DA scatterplot showed a clear class separation with GDM at the left and the control group at the right (Figure 4(a)). Furthermore, we used variable importance in projection (VIP) to estimate the contribution of every AC to class separation (GDM vs. control). A VIP value > 1.0 was considered with a high contribution to class separation. The VIP analysis (Figure 4(b)) showed that C0 (VIP = 1.87) plays the main role in class separation.

3.3. Clinical Characteristics and AC Plasma Level of GDM. Table 3 shows the characteristics of GDM patients and control. The prepregnancy BMI, weight gain, ART, and the serum levels of C2, C3, C4DC+C5OH, C6DC, C8, C16, C18, and C18:1 were higher, while those of C0 was lower in the GDM group.

3.4. Multiple Logistic Regression Analysis of the Association between GDM and Other Factors. We selected significant factors from univariate analysis to enter multiple logistic regression analysis to examine whether acting independently. Prepregnancy BMI (OR = 1.15, 95%CI = 1.06-1.78), weight gain (OR = 1.18, 95%CI = 1.03-1.64), C0 (OR = 0.70, 95% CI = 0.60-0.83), C3 (OR = 1.03, 95%CI = 1.02-2.08), C16 (OR = 1.30, 95%CI = 1.12-3.28), and C18 (OR = 1.27, 95% CI = 1.00-3.01) were statistically associated with GDM.

Table 2: The maternal plasma levels of acylcarnitine (AC) at the second trimester in 450 pregnant women according to different neonate subgroups. Values are presented as the mean ± SD; $^*P < 0.05$ is considered statistically significant.

	Birth weight (g)				*P* value	Abdomen circumference (cm)			*P* value	Abdomen-head circumference (cm)			*P* value
	<2800	2800-3500	3500-4000 g	>4000 g		<32	32-35	>35		<2	2-5	5	
C0	23.38 ± 5.23	21.37 ± 4.77	18.52 ± 3.13	16.40 ± 4.74	0.026*	23.15 ± 3.80	20.22 ± 5.18	16.11 ± 4.04	0.018*	23.19 ± 5.16	21.08 ± 4.06	16.61 ± 3.14	0.014*
C2	2.30 ± 0.82	2.42 ± 0.78	2.49 ± 0.67	2.56 ± 0.78	0.023*	1.84 ± 0.49	2.55 ± 0.82	2.73 ± 0.76	0.023*	2.20 ± 0.82	2.47 ± 0.76	2.57 ± 0.66	0.033*
C3	0.46 ± 0.18	0.51 ± 0.16	0.53 ± 0.17	0.56 ± 0.18	0.014*	0.52 ± 0.14	0.54 ± 0.16	0.57 ± 0.18	0.024*	0.44 ± 0.164	0.51 ± 0.18	0.55 ± 0.17	0.013*
C5	0.02 ± 0.01	0.03 ± 0.02	0.04 ± 0.01	0.05 ± 0.01	0.037*	0.05 ± 0.02	0.04 ± 0.01	0.06 ± 0.01	0.025*	0.04 ± 0.02	0.05 ± 0.01	0.06 ± 0.01	0.026*
C16	0.42 ± 0.12	0.44 ± 0.18	0.47 ± 0.20	0.44 ± 0.16	0.027*	0.42 ± 0.10	0.43 ± 0.12	0.47 ± 0.17	0.026*	0.41 ± 0.12	0.44 ± 0.18	0.48 ± 0.20	0.015*
C18:1	0.48 ± 0.15	0.50 ± 0.17	0.52 ± 0.17	0.55 ± 0.14	0.017*	0.48 ± 0.12	0.49 ± 0.15	0.52 ± 0.16	0.207	0.48 ± 0.15	0.49 ± 0.16	0.49 ± 0.18	0.123

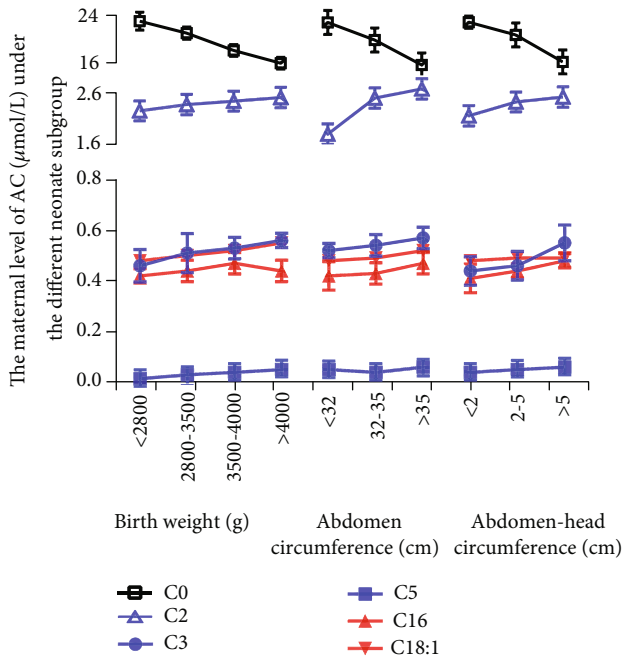

FIGURE 3: The maternal plasma levels of acylcarnitine (AC) at the second trimester in 450 pregnant women according to different neonate subgroups. The AC level was higher in the birth weight > 4000 g group, in the abdomen circumference > 35 cm group, and in the abdomen minus circumference > 5 subgroup. Values are presented as the mean ± SEM.

These factors can work as independent risk factors involve in the process of GDM (Table 4).

3.5. Association of C0 Deficiency and Blood Glucose and Lipid in GDM and Control. When divided into two groups according to the C0 level (<20 μmol/L or ≥20 μmol/L), we found that 81.25% of GDM women of the second trimester pregnancy are in C0 deficiency status. In GDM women, FBG, TG, TC, LDL, and homocysteine (HCY) were significantly higher in the C0 < 20 μmol/L group. Similar results were also seen in the control group of C0 < 20 μmol/L (Table 5). In GDM and control groups, C0 was negatively correlated with FBG, LDL, TG, TC, and HCY and positively correlated with HDL. There were no significant correlations between C0 and OGTT-1 h and OGTT-2 h (Figure 5).

3.6. Cluster Correlation Heat Map. The heat map depicting the internal correlations between metabolites revealed the predominant clusters of intercorrelated metabolites: C2, C4, C6, and C8 (Figure 6). The four metabolites included in the final model showed strongly internal correlations. There were no strong intercorrelations in others.

3.7. Clinical Characteristics and AC Plasma Level and a Nomogram of Prediction of Macrosomia. Here, we investigated the clinical characteristics and AC metabolite between GDM with macrosomia and GDM without macrosomia (Table 6). We found that prepregnancy weight, BMI, weight gain, C0, C2, C3, C16, and C18 were higher in GDM with macrosomia ($P < 0.05$). In the multiple logistic regression analysis, we found that prepregnancy BMI, weight gain, C0, C3, and C16 were also evaluated (Table 7, $P < 0.05$). These factors are independent risk factors involved in the process of GDM-induced macrosomia. The nomogram of predicting GDM-induced macrosomia had incorporated these significant variables. Among these metabolites, C0 deficiency showed the highest OR (OR = 0.75, 95%CI = 0.50-0.87). Vertical lines should be drawn from the correct location from each independent risk factor. "Total points" which could be obtained by adding all points of the axis to the bottom axes made the conversion into a macrosomia probability. The accuracy of the model was well assessed by the AUC equal to 0.78 (Figure 7).

4. Discussion

In the present study, we have identified metabolic alteration in the second trimester of pregnancy by LC-MS/MS. We found that 9 carnitines including free carnitine (C0) were significantly related to GDM. Combined with clinical information, multivariable logistic regression had demonstrated that prepregnancy BMI, weight gain, C0, C3, C16, and C18 were independent metabolic risk factors associated with GDM. C0 played a vital role in GDM and GDM-complicated macrosomia. C0 deficiency was significantly related to GDM, and abnormal metabolism of blood glucose and lipid was accompanied by GDM. We also had developed a nomogram to predict probability of macrosomia with GDM based on C0-related metabolites. To our knowledge, this is the first study reporting carnitine alteration during the second trimester of pregnancy and abnormal metabolism of carnitine in GDM and macrosomia with GDM.

Carnitine metabolism is an important part of fatty acid metabolism. Several experimental works have indicated characteristics of carnitine-related metabolites during pregnancy [12, 19, 20]. Total carnitine consisted of C0 and AC. C0 is required for fatty acid transfer into the mitochondrial membrane; in this process, the ester carnitines are formed. Ester carnitine presented as AC releasing into plasma [21].

An interesting finding appears that there is a pronounced fall of the plasma content of C0, AC, and total carnitine during pregnancy [22]. In our study, we found that some carnitines (C0, C2, C3, C4DC+C5OH, C5, C16, C18, and C18:1) increased in the age > 35, BMI ≥ 30, and weight gain > 20 kg groups. However, C0 was decreased in these groups. These results were similar with the findings of a study by Fujiwara et al. which demonstrated that AC was accumulated in obesity of hepatocellular carcinoma [23]. The plasma AC accumulation suggested an incomplete long-chain fatty acid oxidation and altered tricarboxylic acid activity. Oxidative stress associated with AC accumulation is likely responsible for insulin resistance and diabetes. The study demonstrated that long-term AC accumulation was a feature of T2DM [24]. C0 may increase fatty acid β-oxidation and basal metabolic rates. Other studies had proved that the oxidation rate of fatty acids gradually decreased with age [25].

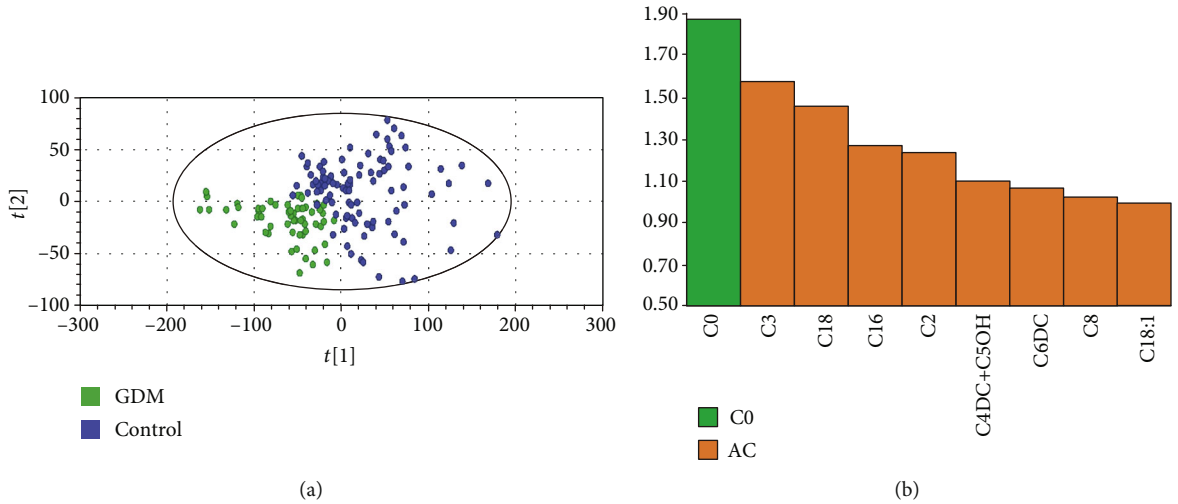

(a) (b)

Figure 4: Specific acylcarnitine (AC) distribution in GDM. (a) Partial least squares discrimination analysis (PLS-DA). Class separation is shown by loading plot. (b) Variable importance in prediction (VIP).

Table 3: Clinical characteristics and ACs of women with GDM and matched control women. Values are presented as the mean ± SD for continuous variables and percentage for dichotomous variables. Cases and controls were matched for birth day, age, delivery mode, and number of fetuses with a 2 : 1 ratio. *P value for Student's t-test (continuous variables) or chi-squared test (dichotomous variables).

	GDM	Control	P value
Total	64	128	
Maternal age (years)	34.32 ± 3.42	32.41 ± 3.65	0.28
Height (cm)	160.34 ± 5.45	161.23 ± 4.45	0.35
Prepregnancy weight (kg)	60.52 ± 4.53	64.45 ± 3.69	0.21
Prepregnancy BMI (kg/m^2)	23.82 ± 3.42	21.25 ± 2.32	0.03*
Weight gain (kg)	22.53 ± 4.37	17.23 ± 2.89	0.02*
Gestational week at delivery (weeks)	38.32 ± 0.67	39.45 ± 0.72	0.54
Nulliparous	76.40	80.20	0.64
ART	19.6	14.2	0.04
Smoker	7.1	8.0	0.35
Birth weight (g)	3847.23 ± 100.78	3304.56 ± 92.65	0.03*
C0 (μmol/L)	16.66 ± 3.37	24.12 ± 8.34	0.03*
C2	3.60 ± 0.77	3.06 ± 1.08	0.03*
C3	0.54 ± 0.16	0.63 ± 0.29	0.02*
C4DC+C5OH	0.13 ± 0.04	0.16 ± 0.07	0.01*
C6DC	0.06 ± 0.01	0.04 ± 0.01	0.03*
C8	0.07 ± 0.04	0.04 ± 0.02	0.04*
C16	0.84 ± 0.14	0.46 ± 0.20	0.04*
C18	0.47 ± 0.09	0.28 ± 0.14	0.02*
C18:1	0.78 ± 0.16	0.50 ± 0.24	0.04*

Table 4: Multiple logistic regression analysis of the association between GDM and other factors. OR: odds ratio; 95% CI: 95% confidence intervals.

	OR	95% CI	P value
Prepregnancy BMI (kg/m^2)	1.15	1.06-1.78	0.03*
Weight gain (kg)	1.18	1.03-1.64	0.03*
ART	1.24	1.00-1.39	0.73
C0 (μmol/L)	0.70	0.60-0.83	0.02*
C2	1.32	0.65-4.37	0.32
C3	1.03	1.02-2.08	0.01*
C4DC+C5OH	1.01	1.01-2.48	0.81
C6DC	1.93	1.20-3.72	0.93
C8	1.26	1.10-4.35	0.56
C16	1.30	1.12-3.28	0.03*
C18	1.27	1.00-3.01	0.04*
C18:1	1.17	1.13-2.76	0.17

GDM is defined as glucose intolerance dysfunction during pregnancy. The prevalence of GDM increased from 5% to 14% in USA [26]. The plasma carnitine concentrations show a strong correlation with the development of diabetes [27]. In our present study, C0 could be confirmed as the potential risk factor in GDM. A study by Batchuluun et al. stated that evaluated AC was associated with GDM through impairing insulin synthesis [28]. Our study also found that serum concentration of some AC significantly increased in the GDM group. A research by Hansen et al. reported that excess of AC in mitochondria might be harmful for metabolism dynamic balance due to aerobic glycolysis disturbance [29]. Previous studies suggested that accumulation of AC affected glucose and lipid metabolism in GDM [10, 28]. An interesting finding by Yau et al. reported that AC might impair mammalian insulin signal transduction through acting at mTOR phosphorylation [30].

Table 5: The association of C0 deficiencies and maternal lipid and glucose in GDM and non-GDM groups. Values are presented as the mean ± SD for continuous variables and percentage for dichotomous variables. *P value for Student's t-test.

	GDM		P value	Control		P value
	C0 < 20	C0 ≥ 20		C0 < 20	C0 ≥ 20	
n	52 (81.25%)	12 (128.75)		96 (75%)	32 (25%)	
FBG (mmol/L)	5.62 ± 0.82	5.19 ± 0.63	0.02*	5.03 ± 0.65	4.65 ± 0.32	0.03*
OGTT-1 h (mmol/L)	10.12 ± 0.29	10.14 ± 0.26	0.43	9.84 ± 0.44	9.43 ± 0.51	0.36
OGTT-2 h (mmol/L)	8.67 ± 0.45	8.59 ± 0.41	0.39	8.35 ± 0.26	7.92 ± 0.33	0.28
TG (mmol/L)	3.12 ± 0.32	1.64 ± 0.25	0.02*	3.02 ± 0.27	1.94 ± 0.21	0.02*
TC (mmol/L)	6.32 ± 0.45	4.43 ± 0.62	0.03*	5.18 ± 0.62	4.32 ± 0.32	0.03*
HDL (mmol/L)	1.78 ± 0.26	1.83 ± 0.31	0.39	1.71 ± 0.13	1.92 ± 0.28	0.04*
LDL (mmol/L)	4.89 ± 0.82	3.16 ± 0.76	0.02*	4.63 ± 0.21	3.04 ± 0.65	0.02*
HCY (μmol/L)	17.67 ± 1.02	12.31 ± 1.11	0.03*	15.32 ± 0.64	11.01 ± 0.82	0.03*

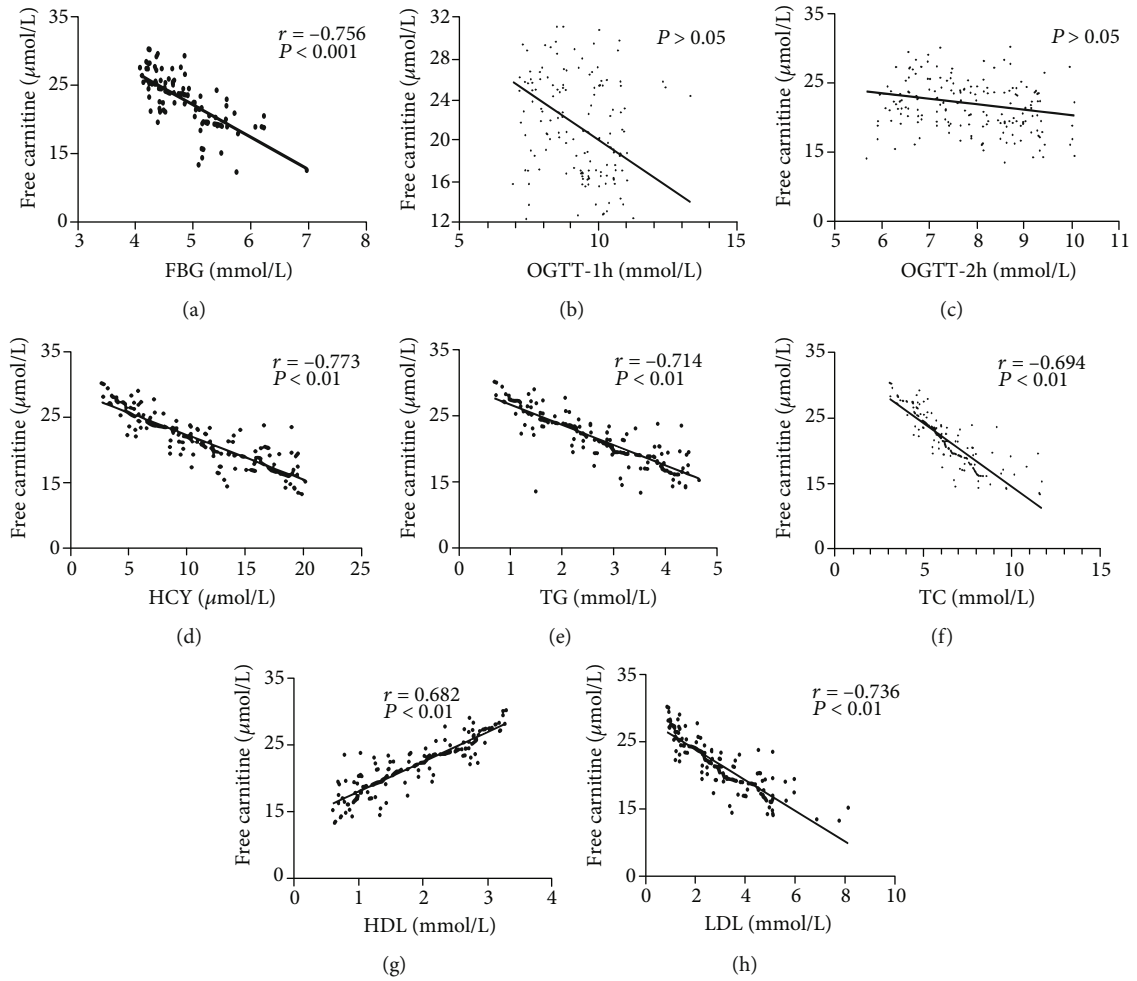

Figure 5: The relationship between C0 and blood glucose and lipid in GDM ($n = 64$) and non-GDM ($n = 128$) groups. The correlation between C0 and FBG (a), OGTT-1 h (b), OGTT-2 h (c), HCY (d), TG (e), TC (f), HDL (g), and LDL (h). r = Spearman's correlation coefficient.

Lack of C0 may elevate the lipid level and further results in GDM [31]. A meta-analysis by Asadi et al. showed a significant relationship between C0 and TG, TC, LDL, and HDL in adults with cardiovascular risk factors. The study indicated a significant effect of C0 supplement (1500 mg/d) on lowering serum levels of TG, TC, and LDL in atherosclerosis patients [32]. Our study reported that serum C0 concentration was negatively correlated with FBG, LDL, TG, TC, and HCY

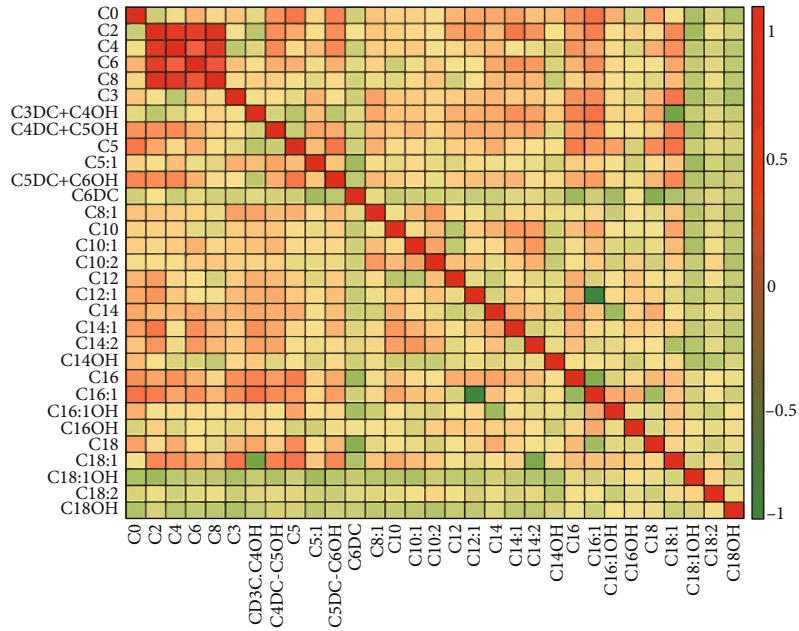

Figure 6: Correlation heat map of all targeted metabolites. In red is the cluster of strongly intercorrelated metabolites.

Table 6: Clinical characteristics and ACs of GDM with macrosomia and nonmacrosomia. Values are presented as the mean ± SD for continuous variables and percentage for dichotomous variables. $^*P$ value for Student's t-test (continuous variables) or chi-squared test (dichotomous variables).

	Macrosomia	Nonmacrosomia	P value
n	12	52	
Maternal age (years)	34.98 ± 4.68	32.23 ± 4.43	0.79
Height (cm)	159.46 ± 5.94	161.46 ± 5.95	0.33
Prepregnancy weight (kg)	56.25 ± 9.98	52.42 ± 7.84	0.04*
Prepregnancy BMI (kg/m^2)	24.55 ± 4.15	22.21 ± 3.02	0.03*
Weight gain (kg)	24.07 ± 4.11	18.42 ± 4.10	0.02*
Gestational week at delivery (weeks)	38.4 ± 0.78	39.6 ± 0.97	0.83
Nulliparous (%)	74.2	62.5	0.82
ART	19.6	14.2	0.55
Smoker	7.4	8.2	0.96
Birth weight (g)	4247.52 ± 100.78	3597.34 ± 98.65	0.02*
C0 (μmol/L)	10.68 ± 3.28	17.12 ± 5.66	0.03*
C2	3.64 ± 0.76	3.58 ± 1.25	0.03*
C3	0.43 ± 0.17	0.64 ± 0.26	0.02*
C4DC+C5OH	0.12 ± 0.04	0.14 ± 0.05	0.05
C6DC	0.06 ± 0.01	0.06 ± 0.01	0.77
C8	0.08 ± 0.04	0.07 ± 0.01	0.54
C16	0.86 ± 0.12	0.84 ± 0.20	0.03*
C18	0.50 ± 0.09	0.47 ± 0.13	0.04*
C18:1	0.52 ± 0.16	0.48 ± 0.24	0.55

Table 7: Multiple logistic regression analysis of factors associated with GDM macrosomia. OR: odds ratio; 95% CI: 95% confidence intervals.

	OR	95% CI	P value
Prepregnancy weight (kg)	1.28	0.76-1.98	0.64
Prepregnancy BMI (kg/m^2)	1.27	1.02-2.37	0.03*
Weight gain (kg)	1.24	1.46-3.45	0.04*
C0	0.75	0.50-0.87	0.02*
C2	1.15	1.02-3.37	0.68
C3	1.16	1.12-1.98	0.03*
C16	1.15	1.03-1.22	0.04*
C18	1.17	1.24-3.23	0.97

and positively correlated with HDL especially in the GDM group, which is consistent with previous researches [33]. In Nowak et al.'s study, C0 showed no association with insulin resistance during OGTT, and C10 and C12 decreased during OGTT with worse insulin resistance as well [34]. Our present study confirmed that C0 was significantly related to FBG but not 1 h and 2 h during OGTT. It is widely accepted that FBG represented the severity of GDM. Our results confirmed that C0 deficiency was significantly related to the abnormal metabolism of glucose and lipid in the second trimester of pregnancy with GDM.

Macrosomia is associated with an increased risk of neonatal morbidity and obesity in adult [35]. GDM is associated with an increasing risk of macrosomia [36]. Many studies have proved that carnitine deficiency is associated with lipid metabolism in GDM [37, 38]. So, we speculated that carnitine is involved in macrosomia with GDM. C0 supplement is effective in normalizing insulin sensitivity of GDM and controlling the synthesis of key glycolytic and gluconeogenic

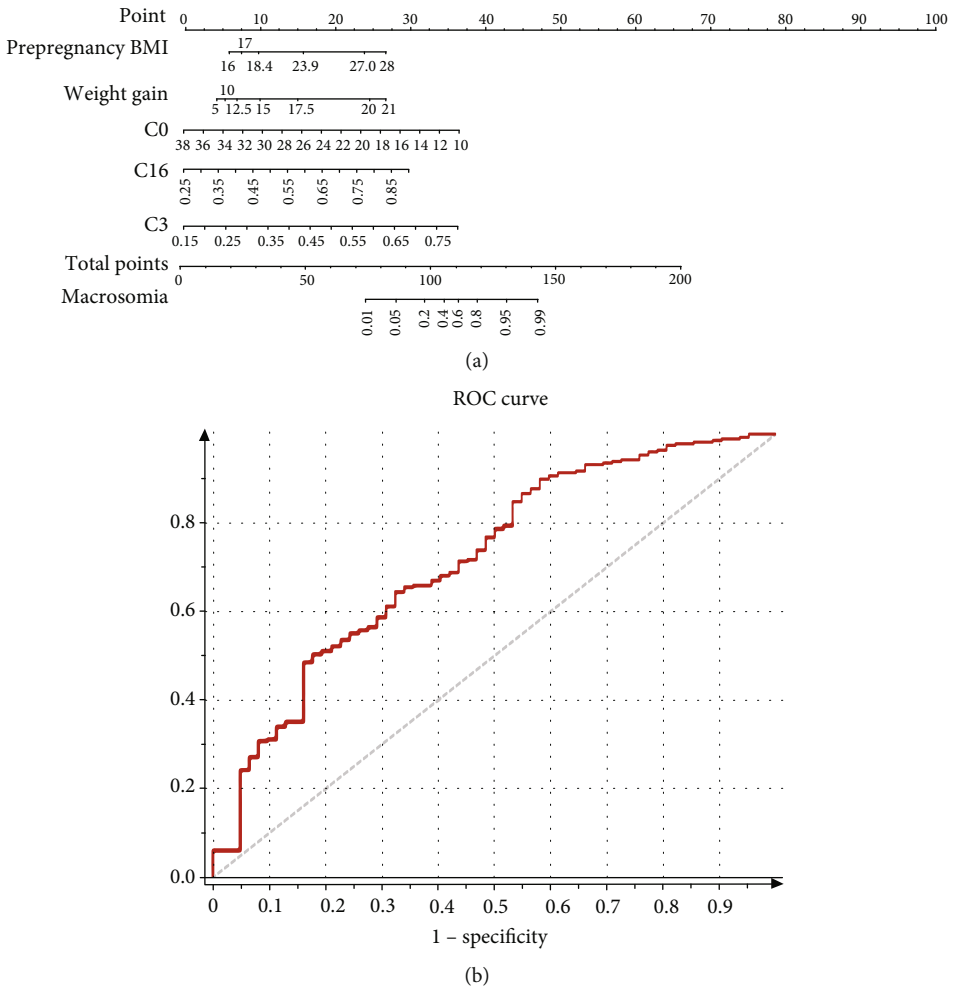

Figure 7: Predictive graphic nomogram for probability of GDM macrosomia and ROC curve. (a) Prepregnancy BMI, weight gain, C0, C3, and C16-based nomogram for predicting macrosomia, predictor points (points^ scale; top) correspond to each variable. Points for all these variables are added and translated into the probability of macrosomia in GDM. (b) Receiver operating characteristic (ROC) curves for validated models. AUC = 0.88.

enzymes. Macrosomia is regarded as a disorder of energy balance, which perturbs body weight homeostasis [39]. Antimacrosomia effect of C0 supplement might be mediated by the induction of lipolysis and fatty acid oxidation. Our study confirmed that C0 is a protective factor for macrosomia. However, C3 and C16 were risk factors for macrosomia with GDM. Therefore, the characteristics of carnitine metabolism had enabled us to discover reliable biomarkers and set up a nomogram model to predicting GDM-related macrosomia.

Our study has several limitations. We should expand the sample size and detect more metabolites to clarify the significance of nonglycometabolism during pregnancy. Also, the metabolites in the other trimesters such as the first trimester should be detected for predicting the occurrence of GDM by carnitine or other metabolites.

5. Conclusions

In conclusion, by analyzing the metabolic alteration in the second trimester, we found abnormal metabolism of carnitine including C0, C3, C16, and C18 which are independent risk factors of GDM. C0 deficiency during pregnancy is significantly obvious in GDM and closely related to the abnormality of blood lipid and glucose of GDM. Carnitine metabolism abnormality could predict macrosomia complicated with GDM. In all, the abnormality of fatty acid metabolism is of great significance in the pathogenesis and the maternal and neonatal complications of GDM.

Data Availability

The datasets used and analyzed during the current study are available from the corresponding author on reasonable request.

Conflicts of Interest

The authors declare no conflicts of interest.

Acknowledgments

The authors thank the staff at Women's Hospital, Zhejiang University, School of Medicine, for technical assistance and

facility support. This work was supported by the Natural Science Foundation of Zhejiang Province of China (Grant Nos. LQ20H040008 and LY20H040009) and Zhejiang Medical and Health Technology Project, No.2018244300.

References

[1] T. G. M. Vrijkotte, N. Krukziener, B. A. Hutten, K. C. Vollebregt, M. van Eijsden, and M. B. Twickler, "Maternal lipid profile during early pregnancy and pregnancy complications and outcomes: the ABCD study," *The Journal of Clinical Endocrinology & Metabolism*, vol. 97, no. 11, pp. 3917–3925, 2012.

[2] M. E. Bianco and J. L. Josefson, "Hyperglycemia during pregnancy and long-term offspring outcomes," *Current Diabetes Reports*, vol. 19, no. 12, 2019.

[3] S. Yamashita, D. Masuda, and Y. Matsuzawa, "Clinical applications of a novel selective PPARα modulator, pemafibrate, in dyslipidemia and metabolic diseases," *Journal of Atherosclerosis and Thrombosis*, vol. 26, no. 5, pp. 389–402, 2019.

[4] A. Taschereau-Charron, M. S. Da Silva, J.-F. Bilodeau, A.-S. Morisset, P. Julien, and I. Rudkowska, "Alterations of fatty acid profiles in gestational diabetes and influence of the diet," *Maturitas*, vol. 99, pp. 98–104, 2017.

[5] J. J. Chamberlain, K. Doyle-Delgado, L. Peterson, and N. Skolnik, "Diabetes technology: review of the 2019 American Diabetes Association standards of medical care in diabetes," *Annals of Internal Medicine*, vol. 171, no. 6, pp. 415–420, 2019.

[6] T. Geach, "A metabolomic signature to predict the transition from GDM to T2DM," *Nature Reviews Endocrinology*, vol. 12, no. 9, p. 498, 2016.

[7] J. Simcox, G. Geoghegan, J. A. Maschek et al., "Global analysis of plasma lipids identifies liver-derived acylcarnitines as a fuel source for brown fat thermogenesis," *Cell Metabolism*, vol. 26, no. 3, pp. 509–522.e6, 2017.

[8] A. Weiser, P. Giesbertz, H. Daniel, and B. Spanier, "Acylcarnitine profiles in plasma and tissues of hyperglycemic NZO mice correlate with metabolite changes of human diabetes," *Journal of Diabetes Research*, vol. 2018, Article ID 1864865, 9 pages, 2018.

[9] L. M. Tanner, K. Näntö-Salonen, M. S. Rashed et al., "Carnitine deficiency and L-carnitine supplementation in lysinuric protein intolerance," *Metabolism: clinical and experimental*, vol. 57, no. 4, pp. 549–554, 2008.

[10] K. I. Pappa, N. P. Anagnou, E. Salamalekis et al., "Gestational diabetes exhibits lack of carnitine deficiency despite relatively low carnitine levels and alterations in ketogenesis," *The Journal of Maternal-Fetal & Neonatal Medicine*, vol. 17, no. 1, pp. 63–68, 2005.

[11] W. L. Lowe, D. M. Scholtens, L. P. Lowe et al., "Association of gestational diabetes with maternal disorders of glucose metabolism and childhood adiposity," *JAMA*, vol. 320, no. 10, pp. 1005–1016, 2018.

[12] J. Nevalainen, M. Sairanen, H. Appelblom, M. Gissler, S. Timonen, and M. Ryynanen, "First-trimester maternal serum amino acids and acylcarnitines are significant predictors of gestational diabetes," *The Review of Diabetic Studies*, vol. 13, no. 4, pp. 236–245, 2016.

[13] C. Kim, K. M. Newton, and R. H. Knopp, "Gestational diabetes and the incidence of type 2 diabetes: a systematic review," *Diabetes Care*, vol. 25, no. 10, pp. 1862–1868, 2002.

[14] L. Bellamy, J. P. Casas, A. D. Hingorani, and D. Williams, "Type 2 diabetes mellitus after gestational diabetes: a systematic review and meta-analysis," *Lancet*, vol. 373, no. 9677, pp. 1773–1779, 2009.

[15] K. Kc, S. Shakya, and H. Zhang, "Gestational diabetes mellitus and macrosomia: a literature review," *Annals of Nutrition and Metabolism*, vol. 66, no. 2, pp. 14–20, 2015.

[16] M. Peng, L. Liu, M. Jiang et al., "Measurement of free carnitine and acylcarnitines in plasma by HILIC-ESI-MS/MS without derivatization," *Journal of Chromatography B*, vol. 932, pp. 12–18, 2013.

[17] J. Bene, K. Komlosi, V. Havasi et al., "Changes of plasma fasting carnitine ester profile in patients with ulcerative colitis," *World Journal of Gastroenterology*, vol. 12, no. 1, pp. 110–113, 2006.

[18] C. Jia, H. Xu, Y. Xu, Y. Xu, and Q. Shi, "Serum metabolomics analysis of patients with polycystic ovary syndrome by mass spectrometry," *Molecular Reproduction and Development*, vol. 86, no. 3, pp. 292–297, 2019.

[19] G. C. Talian, K. Komlosi, T. Decsi, B. Koletzko, and B. Melegh, "Determination of carnitine ester patterns during the second half of pregnancy, at delivery, and in neonatal cord blood by tandem mass spectrometry: complex and dynamic involvement of carnitine in the intermediary metabolism," *Pediatric Research*, vol. 62, no. 1, pp. 88–92, 2007.

[20] X. Mao, X. Chen, C. Chen, H. Zhang, and K. P. Law, "Metabolomics in gestational diabetes," *Clinica Chimica Acta*, vol. 475, pp. 116–127, 2017.

[21] S. E. Reuter and A. M. Evans, "Carnitine and acylcarnitines: pharmacokinetic, pharmacological and clinical aspects," *Clinical Pharmacokinetics*, vol. 51, no. 9, pp. 553–572, 2012.

[22] K. L. Lindsay, C. Hellmuth, O. Uhl et al., "Longitudinal metabolomic profiling of amino acids and lipids across healthy pregnancy," *PLoS One*, vol. 10, no. 12, p. e0145794, 2015.

[23] N. Fujiwara, H. Nakagawa, K. Enooku et al., "CPT2 downregulation adapts HCC to lipid-rich environment and promotes carcinogenesis via acylcarnitine accumulation in obesity," *Gut*, vol. 67, no. 8, pp. 1493–1504, 2018.

[24] J. Bene, K. Hadzsiev, and B. Melegh, "Role of carnitine and its derivatives in the development and management of type 2 diabetes," *Nutrition & Diabetes*, vol. 8, no. 1, p. 8, 2018.

[25] C. Nasca, B. Bigio, F. S. Lee et al., "Acetyl-l-carnitine deficiency in patients with major depressive disorder," *Proceedings of the National Academy of Sciences*, vol. 115, no. 34, pp. 8627–8632, 2018.

[26] W. L. Lowe, D. M. Scholtens, A. Kuang et al., "Hyperglycemia and adverse pregnancy outcome follow-up study (HAPO FUS): maternal gestational diabetes mellitus and childhood glucose metabolism," *Diabetes Care*, vol. 42, no. 3, pp. 372–380, 2019.

[27] X. Zhao, X. Gang, Y. Liu, C. Sun, Q. Han, and G. Wang, "Using metabolomic profiles as biomarkers for insulin resistance in childhood obesity: a systematic review," *Journal of Diabetes Research*, vol. 2016, Article ID 8160545, 12 pages, 2016.

[28] B. Batchuluun, D. Al Rijjal, K. J. Prentice et al., "Elevated medium-chain acylcarnitines are associated with gestational diabetes mellitus and early progression to type 2 diabetes and induce pancreatic β-cell dysfunction," *Diabetes*, vol. 67, no. 5, pp. 885–897, 2018.

[29] J. S. Hansen, X. Zhao, M. Irmler et al., "Type 2 diabetes alters metabolic and transcriptional signatures of glucose and amino

acid metabolism during exercise and recovery," *Diabetologia*, vol. 58, no. 8, pp. 1845–1854, 2015.

[30] W. W. Yau, B. K. Singh, R. Lesmana et al., "Thyroid hormone (T3) stimulates brown adipose tissue activation via mitochondrial biogenesis and MTOR-mediated mitophagy," *Autophagy*, vol. 15, no. 1, pp. 131–150, 2019.

[31] S. L. White, on behalf of the UPBEAT Consortium, D. Pasupathy et al., "Metabolic profiling of gestational diabetes in obese women during pregnancy," *Diabetologia*, vol. 60, no. 10, pp. 1903–1912, 2017.

[32] M. Asadi, M. Rahimlou, F. Shishehbor, and A. Mansoori, "The effect of l-carnitine supplementation on lipid profile and glycaemic control in adults with cardiovascular risk factors: a systematic review and meta-analysis of randomized controlled clinical trials," *Clinical nutrition*, vol. 39, no. 1, pp. 110–122, 2020.

[33] L. Katalinic, B. Krtalic, B. Jelakovic, and N. Basic-Jukic, "The unexpected effects of L-carnitine supplementation on lipid metabolism in hemodialysis patients," *Kidney & Blood Pressure Research*, vol. 43, no. 4, pp. 1113–1120, 2018.

[34] C. Nowak, S. Hetty, S. Salihovic et al., "Glucose challenge metabolomics implicates medium-chain acylcarnitines in insulin resistance," *Scientific Reports*, vol. 8, no. 1, pp. 8691–8691, 2018.

[35] A. Elhakeem, R. Cooper, D. Bann, D. Kuh, and R. Hardy, "Birth weight, school sports ability, and adulthood leisure-time physical activity," *Medicine and Science in Sports and Exercise*, vol. 49, no. 1, pp. 64–70, 2017.

[36] E. Herrera and H. Ortega-Senovilla, "Implications of lipids in neonatal body weight and fat mass in gestational diabetic mothers and non-diabetic controls," *Current Diabetes Reports*, vol. 18, no. 2, 2018.

[37] X. Huo, J. Li, Y.-F. Cao et al., "Trimethylamine N-oxide metabolites in early pregnancy and risk of gestational diabetes: a nested case-control study," *The Journal of Clinical Endocrinology and Metabolism*, vol. 104, no. 11, pp. 5529–5539, 2019.

[38] C. Roy, P. Y. Tremblay, E. Anassour-Laouan-Sidi et al., "Risk of gestational diabetes mellitus in relation to plasma concentrations of amino acids and acylcarnitines: a nested case-control study," *Diabetes Research and Clinical Practice*, vol. 140, pp. 183–190, 2018.

[39] J. Beta, N. Khan, A. Khalil, M. Fiolna, G. Ramadan, and R. Akolekar, "Maternal and neonatal complications of fetal macrosomia: systematic review and meta-analysis," *Ultrasound in Obstetrics & Gynecology*, vol. 54, no. 3, pp. 308–318, 2019.

Hindawi
Journal of Diabetes Research
Volume 2020, Article ID 7574245, 14 pages
https://doi.org/10.1155/2020/7574245

Research Article

Geranylgeranyl Transferase-I Knockout Inhibits Oxidative Injury of Vascular Smooth Muscle Cells and Attenuates Diabetes-Accelerated Atherosclerosis

Guo-Ping Chen,[1] **Jian Yang**,[2] **Guo-Feng Qian**,[1] **Wei-Wei Xu**,[1] **and Xiao-Qin Zhang**[3]

[1]*Department of Endocrinology, The First Affiliated Hospital, College of Medicine, Zhejiang University, Hangzhou, Zhejiang 310003, China*
[2]*Institute of Cardiology, The First Affiliated Hospital, College of Medicine, Zhejiang University, Hangzhou, Zhejiang 310003, China*
[3]*Department of Respirology, Zhejiang Provincial People's Hospital, People's Hospital of Hangzhou Medical College, Hangzhou, Zhejiang 310014, China*

Correspondence should be addressed to Xiao-Qin Zhang; zhangxiaoqin@hmc.edu.cn

Received 18 April 2020; Accepted 28 July 2020; Published 11 August 2020

Academic Editor: Claudio De Lucia

The proliferation of vascular smooth muscle cells (VSMCs) induced by oxidative injury is one of the main features in diabetes-accelerated atherosclerosis. Geranylgeranyl transferase-I (GGTase-I) is an essential enzyme mediating posttranslational modification, especially the geranylgeranylation of small GTPase, Rac1. Our previous studies found that GGTase-I played an important role in diabetes-accelerated atherosclerosis. However, its exact role is largely unclear. In this study, mouse conditional knockout of VSMC GGTase-I ($Pggt1b^{\Delta/\Delta}$ mice) was generated using the CRISPR/Cas9 system. The mouse model of diabetes-accelerated atherosclerosis was induced by streptozotocin injections and an atherogenic diet. We found that GGTase-I knockout attenuated diabetes-accelerated atherosclerosis in vivo and suppressed high-glucose-induced VSMC proliferation in vitro. Moreover, after a 16-week duration of diabetes, $Pggt1b^{\Delta/\Delta}$ mice exhibited lower α-smooth muscle actin (α-SMA) and nitrotyrosine level, Rac1 activity, p47phox and NOXO1 expression, and phospho-ERK1/2 and phosphor-JNK content than wild-type mice. Meanwhile, the same changes were found in $Pggt1b^{\Delta/\Delta}$ VSMCs cultured with high glucose (22.2 mM) in vitro. In conclusion, GGTase-I knockout efficiently blocked diabetes-accelerated atherosclerosis, and this protective effect must be related to the inhibition of VSMC proliferation. The potential mechanisms probably involved interfering Rac1 geranylgeranylation, inhibiting the assembly of NADPH oxidase cytosolic regulatory subunits, reducing oxidative injury, and decreasing ERK1/2 and JNK phosphorylation.

1. Introduction

Patients with diabetes exhibit an increased susceptibility to develop a wide range of atherosclerotic diseases by 2-4-fold, especially the stroke and myocardial infarction, which account for the majority of deaths and disability in diabetes patients [1–3]. Atherosclerosis occurs earlier and with greater severity in the population with diabetes [1–3] and is characterized pathologically by endothelial cell injury, proliferation and migration of vascular smooth muscle cells (VSMCs), and thickening of intima [4, 5]. However, the exact mechanisms responsible for this diabetes-accelerated atherosclerosis have remained elusive.

Geranylgeranyl transferase-I (GGTase-I) is one of the key enzymes mediating protein isoprenylation during the post-translational modification, especially the geranylgeranylation of small GTPase, Rac1 [6]. Previous studies on GGTase-I mainly focused on the regulation of cell growth and differentiation via the Rac1 pathway and have been proved to be closely related to the occurrence, invasion, and metastasis of various malignant tumors [7]. Moreover, in recent years, the research on GGTase1-I in vascular remodeling has been

gradually carried out and attracted attention [8, 9]. Zuckerbraun et al. found that GGTase-I inhibitor (GGTI-298) could alleviate carotid intimal thickening after balloon injury in SD rats [8]. Khan et al. reported that GGTase-I deficiency in mouse macrophages slowed down the progression of atherosclerosis [9]. But the exact role of GGTase-I in diabetes-accelerated atherosclerosis has not been involved, and further research is needed.

In recent years, our group has conducted several studies on GGTase-I and achieved some research results [10–12]. We found that in rats with abdominal aortic coarctation, the proximal aortic media (mainly VSMCs) proliferated and hypertrophied, accompanying with upregulated expression of GGTase-I [10]. It was also found that with the growth of age, VSMCs from aortic media of spontaneously hypertensive rats proliferated remarkably, the expression of GGTase-I increased, and the activity of reactive oxygen species (ROS) and NADPH oxidase (NOX) amplified gradually [11]. All these results suggest that GGTase-I plays an important role in the proliferation of VSMCs, at least in part via regulating the oxidative stress pathway. Furthermore, our latest study revealed that in diabetes-accelerated atherosclerosis, VSMCs proliferated and GGTase-I overexpressed simultaneously [12]. Then, we speculate that GGTase-I may participate in the process of diabetes-accelerated atherosclerosis by regulating the proliferation of VSMCs, but the proper mechanisms remain to be explored.

Therefore, the present study was designed to determine whether/how GGTase-I regulated oxidative stress, affecting the proliferation of VSMCs, thereby participating in the progress of diabetes-accelerated atherosclerosis.

2. Materials and Methods

2.1. Animal Models. All animal procedures conformed to the Guide for the Care and Use of Laboratory Animal published by the US National Institutes of Health (NIH Publication no. 85-23, revised 1996) and the guidelines of the Animal Care and Use Committee of Zhejiang University. Animals were maintained on a 12 h light-dark cycle and stable environmental temperature (23°C) in a pathogen-free environment with free access to chow and water. All chemicals and reagents were purchased from Sigma (St. Louis, MO, USA), unless otherwise stated.

To produce mice lacking GGTase-I in VSMCs, Pggt1b conditional knockout mice were generated using the CRISPR/Cas9 system in Shanghai Biomodel Organism Science & Technology Development Co. Briefly, Cas9 mRNA and guide RNA for Pggt1b third exon were obtained by transcription in vitro. Homologous recombinant vectors (donor vectors) were constructed by In-Fusion cloning, including 0.7 kb 5′ homology arm, 2.0 kb flox region, and 4.0 kb 3′ homology arm. Cas9 mRNA, guide RNA, and donor vectors were microinjected into the fertilized eggs of C57BL/6J mice. The resulting homologous recombinant mice were bred with C57BL/6J mice, and heterozygous offsprings were identified by genomic PCR. After backcrossed with C57BL/6J, heterozygous mice ($Pggt1b^{flox/+}$) were mated with SM22α-Cre transgenic mice to generate Pggt1b conditional knockout mice ($Pggt1b^{flox/flox}$Cre, and defined as $Pggt1b^{\Delta/\Delta}$). Littermate control $Pggt1b^{+/+}$Cre, $Pggt1b^{flox/+}$, $Pggt1b^{+/+}$, and $Pggt1b^{flox/-flox}$ were indistinguishable in phenotype and defined as wild type. Genetic deletion of Pggt1b was confirmed at the RNA and protein level by real-time PCR and western blotting, respectively, as previously described [12, 13].

The mouse model of diabetes-accelerated atherosclerosis was induced as previously described [12]. In brief, male eight-week $Pggt1b^{\Delta/\Delta}$ and wild-type mice were rendered diabetes by i.p. daily injection of streptozotocin (STZ, S0130, Sigma-Aldrich, St. Louis, MO, USA) at a dose of 40 mg/kg for 5 days; nondiabetic animals received the vehicle (citrate buffer; 0.05 mol/l, pH: 4.5). STZ-injected mice were also fed with an atherogenic diet (21% fat and 0.15% cholesterol, wt/wt), to accelerate the progression of atherosclerosis by adding hyperlipidemia to hyperglycemia. Two weeks after the fifth STZ injection, fasting blood glucose (FBG) levels were measured in venous blood drawn from the tail by using a CONTOUR glucose meter (Bayer, Mishawaka, IN, USA). Mice with FBG over 13.9 mM were considered diabetic. Accordingly, mice were divided into four groups: diabetic $Pggt1b^{\Delta/\Delta}$, nondiabetic $Pggt1b^{\Delta/\Delta}$, diabetic wild type, and nondiabetic wild type. After a 16-week duration of diabetes, animals were sacrificed by cervical dislocation, their blood samples were collected, and their organs were rapidly dissected. The animal work was completed in the Central Laboratory of the First Affiliated Hospital of Zhejiang University. All assessments were performed by two investigators in a blinded manner.

2.2. Glucose and Lipid Measurements. FBG levels were evaluated as described above. The levels of serum total cholesterol (TC), high-density lipoprotein cholesterol (HDL-C), low-density lipoprotein cholesterol (LDL-C), and triglyceride (TG) were measured by commercial enzymatic methods (test kits from Shanghai Rongsheng Biotech, Inc., Shanghai, China).

2.3. Morphometric Analysis of Aortic Lesions. Aortic lesions were evaluated by en face analysis of the whole aorta and by cross-sectional analysis as previously described [14, 15]. For the en face analysis, the whole aorta was dissected out, opened longitudinally from the heart to the iliac arteries, and stained with oil red O. The total aortic surface area and the lesion area were analyzed, and the ratio of lesion area to total surface was calculated. For cross-sectional analysis, the aorta was dissected, fixed in 10% neutral formalin, embedded in paraffin, and sequentially stained with hematoxylin and eosin. Lesion areas per section were counted by taking the average of 6 sections spaced 30 μm apart, beginning at the base of the aortic root. Media thickness at 10 different points of the thoracic aorta was measured and calculated. The morphometric analysis above was performed with Image-Pro Plus 6.0.

2.4. Immunohistochemical and Immunofluorescence Staining. Fresh-frozen aortic cryosections (10 μm thick) were stored at -20°C until ready for staining. Smooth muscle cells in lesions were analyzed immunohistochemically with an antibody

against α-smooth muscle actin (α-SMA, 1 : 2000, ab5694, Abcam). Lesion nitrotyrosine protein expression, a marker for oxidative stress in atheromatous lesions, was assessed by immunofluorescence staining with an antibody against nitrotyrosine (1 : 50, GTX41979, GeneTex Inc). The number of cells displaying specific staining was scored in a blinded manner.

2.5. Cell Culture and Treatments. VSMCs were isolated from thoracic aortic explants as previously described [13]. In brief, aortic explants from male eight-week-old Pggt1b$^{\Delta/\Delta}$ and wild-type mice were cultured in Dulbecco's modified Eagle's medium (DMEM; Gibco, Grand Island, NY, USA) supplemented with 10% fetal bovine serum (FBS; Gibco) and maintained at 37°C in a humidified atmosphere of 5% CO_2 and 95% air. After 2 weeks, cells migrating onto the tissue culture dish were collected by trypsinization and subcultured successively. The identity of the VSMCs was determined by the positive immunocytochemistry reactivity to smooth muscle-specific α-actin. To ensure the consistency of results, passages 5-12 of VSMCs were used for experiment. According to our previous report [12, 13], VSMC proliferation was induced by high glucose (22.2 mM) for 72 h, while the control cells were treated with normal glucose (5.6 mM). Mannitol was used as an osmotic control. VSMCs from wild-type mice were also cultured in the presence of selective GGTase-I inhibitor (GGTI-286, 10 μM) or Rac1 inhibitor (100 μM) for 24 h.

2.6. Cell Proliferation Assay. After above treatments, VSMC proliferation was measured by 3-[4,5-dimethylthiazol-2-yl]-2,5-diphenyltetrazolium bromide (MTT) assay as described previously [12, 13]. Cells were cultured in 96-well plates (5×10^3 cells/well). After synchronization for 24 h, different treatments as stated above were given. Then, the cells of 96 wells were incubated with 100 μl of 0.5 mg/ml MTT at 37°C for 4 h, washed with cold PBS, and lysed with 100 μl of DMSO. After the insoluble crystals were completely dissolved, the optical density of each well was immediately measured at 570 nm using an automatic microplate reader (Molecular Devices, Sunnyvale, CA, USA).

2.7. Measurement of ROS In Vitro. Hydrogen peroxide (H_2O_2) was measured in VSMCs using the Amplex Red Hydrogen Peroxide/Peroxidase Assay Kit following the manufacturer's instructions (A22188, Invitrogen Molecular Probes, Eugene, OR, USA). In short, cells seeded in 6-well plates received different treatments as stated above prior to protein harvest. 20 μl of whole-cell preparations, standards, and blank were assayed in triplicate in black 96-well plates after the addition of prewarmed (37°C) working solution containing 100 μM Amplex Red reagents and 0.2 U/ml horseradish peroxidase. Fluorescence intensity was measured in 30 min intervals at 37°C on the fluorescence microplate reader at 544 nm excitation/590 nm emission. Data from the 120 min time point are presented as nmol of H_2O_2 standardized to protein concentration.

Moreover, H_2O_2 in VSMCs was also detected by 6-carboxy-2′,7′-dichlorodihydrofluorescein diacetate (carboxy-H_2DCFDA, C2938, Invitrogen Molecular Probes, Eugene, OR, USA) fluorescence. Briefly, VSMCs were given different treatments as stated above. Then, cells were washed with PBS, trypsinized, and resuspended. 200 μl of the resuspension was added into a black 96-well microplate and placed into an incubator at 37°C for 24 h. On the day of the experiment, cells were washed with PBS; 100 μl prewarmed (37°C) loading buffer containing 10 μM carboxy-H_2DCFDA was added to each well and loaded for 40 min at 37°C. Each well was washed with PBS twice, and 100 μl of PBS was added and immediately read with the fluorescence microplate reader (495 nm/525 nm) every 5 min for 60 min.

2.8. Determination of Activation Status of Rac1. As described previously [13], Rac1 activation was determined from tissue or cell lysates using the Rac1 G-LISA Activation Assay Kit (BK128, Cytoskeleton, Denver, CO, USA) according to the manufacturer's instruction. The signal was measured at 490 nm with an automatic microplate reader. Results are expressed as fold increase in activity compared with the control group.

2.9. Western Blot Analysis. The membrane protein extractions from the aortic media (VSMCs were the only cell type in this layer) or cultured VSMCs were carried out by the Plasma Membrane Protein Isolation Kit (Abcam, UK) according to the manufacturer's instructions. Total proteins were also extracted, and western blot was performed as described in our previous reports [12, 13]. The expressions of NOX subunits and mitogen-activated protein kinase (MAPK) signaling pathway were detected using their specific antibodies: anti-NOX1 (1 : 2000, ab55831, Abcam, Cambridge, UK), anti-NOX2 (1 : 500, ab80508, Abcam, Cambridge, UK), anti-p47phox (1 : 1000, ab795, Abcam, Cambridge, UK), anti-NADPH oxidase organizer 1 (anti-NOXO1, 1 : 500, sc-390927, Santa Cruz Biotechnology Co., Ltd., Japan), anti-Rac1 (1 : 1000, sc-95, Santa Cruz Biotechnology Co.), anti-p38 (1 : 1000, ab31828, Abcam), anti-phospho-p38 (p-p38, 1 : 1000, ab47363, Abcam), anti-ERK1/2 (1 : 1000, ab17942, Abcam), anti-phospho-ERK1/2 (p-ERK1/2, 1 : 1000, 9101, Cell Signaling Technology, Inc., Danvers, MA, USA), anti-JNK (1 : 1000, ab179461, Abcam), and anti-phospho-JNK (p-JNK, 1 : 1000, ab124956, Abcam). To ensure equal protein loading, β-actin (1 : 5000, ab8226; Abcam) and Na^+/K^+-ATPase (1 : 100000, ab76020, Abcam) were used as loading controls for the cytoplasm and plasma membrane, respectively.

2.10. Statistical Analysis. Results were expressed as mean ± standard errors of mean (SEM). All analyses were performed with SPSS (version 13.0; SPSS, Inc., Chicago, IL, USA). A two-way ANOVA followed by the Bonferroni post hoc test was used to determine significant differences between groups. Differences were considered statistically significant at a value of $P < 0.05$.

3. Results

3.1. Generation and Validation of Conditional GGTase-I Knockout Mice. To produce mice lacking GGTase-I in VSMCs, Pggt1b conditional knockout mice were generated using the CRISPR/Cas9 system. The strategy for creating

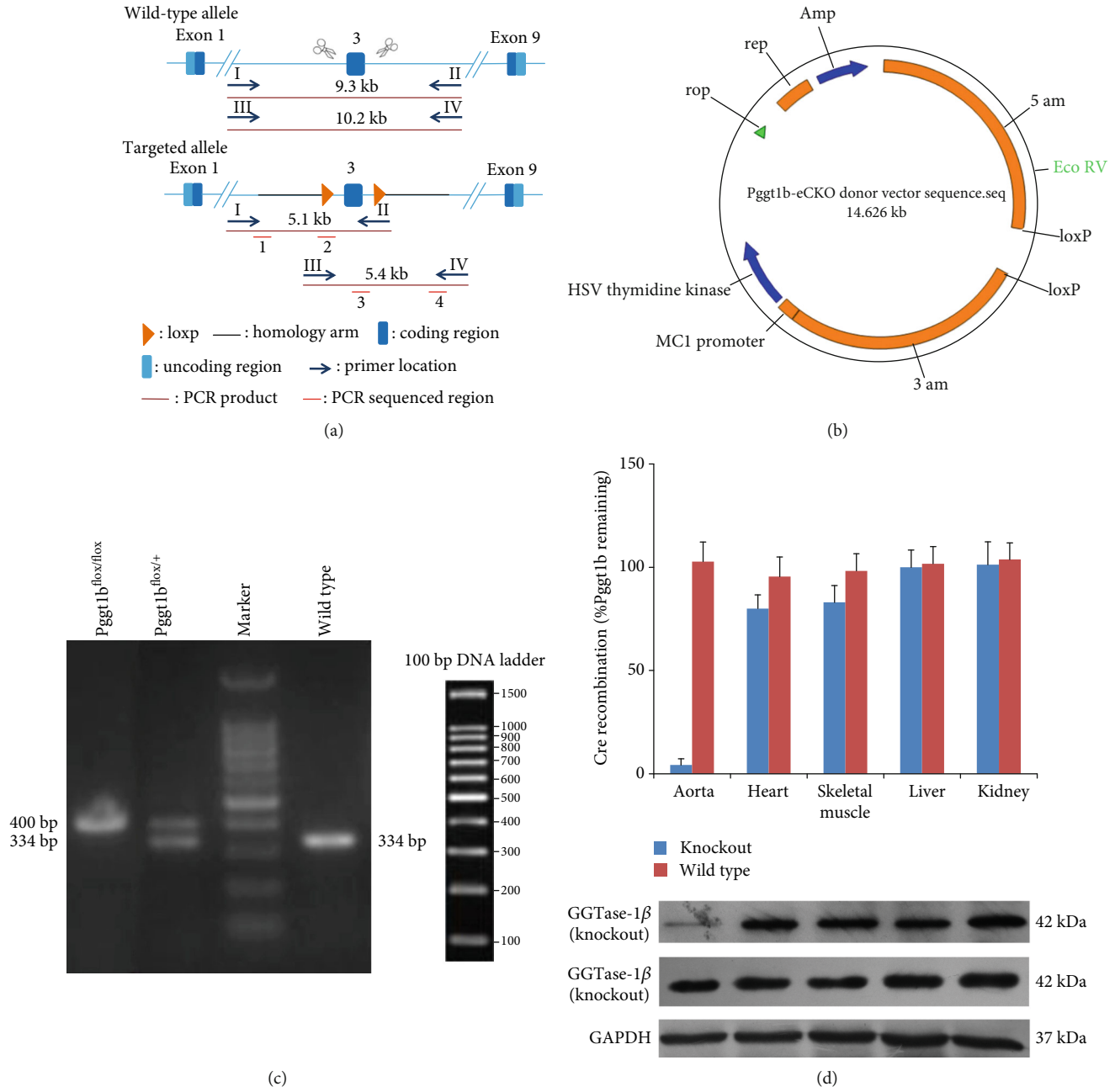

Figure 1: Generation and confirmation of the conditional knockout mice for the β subunit of GGTase-1. (a) The strategy for creating Pggt1b^{flox} mice. In homologous recombinant vectors (donor vectors), exon 3 of Pggt1b is flanked by loxP sites (arrowheads). The expression of Cre recombinase results in the excision of exon 3, creating a frameshift mutation and a null allele. The locations of primers for genotyping are indicated. (b) The plasmid map of homologous recombinant vectors (donor vectors). (c) Analysis of different genotypes by different sizes of PCR product fragments. Pggt1b$^{flox/flox}$: one band with 400 bp; Pggt1b$^{flox/+}$: two bands with 334 bp and 400 bp; wild type: one band with 334 bp. (d) GGTase-1 conditional knockout was confirmed by real-time PCR and western blot in different tissues from Pggt1b$^{\Delta/\Delta}$ mice.

Pggt1b^{flox} mice is illustrated in Figure 1(a). In the targeted allele (Pggt1b^{flox}), loxP sites flank exon 3, which is critical for enzymatic activity. Homologous recombinant vectors (donor vectors) were constructed by In-Fusion cloning and are shown in Figure 1(b). Pggt1b$^{flox/+}$ and Pggt1b$^{flox/flox}$ mice were healthy and fertile. After loxP locus insertion, different genotypes (Pggt1b$^{flox/+}$, Pggt1b$^{flox/flox}$, and wild type) could be distinguished by different sizes of PCR product fragments (Figure 1(c)). To test the conditional knockout of GGTase-I, we detected the RNA and protein expressions in different tissues using real-time PCR and western blotting. As expected, homozygous Pggt1b$^{\Delta/\Delta}$ mice eliminated GGTase-I expression in aortic lysates, but not in the heart, skeletal muscle, liver, or kidney (Figure 1(d)). In heterozygous knockout mice (Pggt1b$^{\Delta/+}$), GGTase-I expression in the aorta was reduced by approximately 40% (data not shown).

Table 1: Glucose and lipid analysis after a 16-week diabetic duration in Pggt1b$^{\Delta/\Delta}$ or wide-type mice.

Group	FBG (mM)	TC (mM)	HDL-C (mM)	LDL-C (mM)	TG (mM)
Wild type					
Nondiabetic	6.44 ± 0.75	1.88 ± 0.08	0.90 ± 0.06	0.47 ± 0.07	1.42 ± 0.07
Diabetic	21.86 ± 1.10**	2.56 ± 1.10**	0.84 ± 0.07	0.84 ± 0.07*	2.14 ± 0.07**
Pggt1b$^{\Delta/\Delta}$					
Nondiabetic	6.30 ± 0.61	1.86 ± 0.07	0.90 ± 0.09	0.43 ± 0.17	1.33 ± 0.06
Diabetic	23.34 ± 1.41**	2.55 ± 0.08**	0.93 ± 0.06	0.91 ± 0.09**	2.09 ± 0.09**

Data are expressed as mean ± SEM, $n = 5$ for each group. $^{*}P < 0.05$ and $^{**}P < 0.01$ versus strain-matched nondiabetic mice. FBG: fasting blood glucose; TC: total cholesterol; HDL-C: high-density lipoprotein cholesterol; LDL-C: low-density lipoprotein cholesterol; TG: triglyceride.

3.2. Glucose and Lipid Content. As shown in Table 1, both in Pggt1b$^{\Delta/\Delta}$ and wild-type mice, STZ and atherogenic diet caused extremely higher FBG than in strain-matched nondiabetic groups. FBG levels were similar between the diabetic wild-type and the diabetic Pggt1b$^{\Delta/\Delta}$ mice. Meanwhile, the contents of TC, LDL-C, and TG were also considerably greater in diabetic Pggt1b$^{\Delta/\Delta}$ and wild-type mice than in nondiabetic mice. There was no difference in TC, LDL-C, and TG levels between the diabetic wild-type and the diabetic Pggt1b$^{\Delta/\Delta}$ mice. However, STZ and atherogenic diet did not affect the levels of HDL-C either in Pggt1b$^{\Delta/\Delta}$ or in wild-type mice.

3.3. Knockout of VSMC GGTase-I Attenuates Diabetes-Accelerated Atherosclerosis. The morphometric data of atherosclerotic lesion are summarized in Figure 2. Analysis of en face aortas (Figures 2(a) and 2(b)) indicated that diabetic wild-type mice developed greater atherosclerotic lesions than nondiabetic wild type. Similarly, diabetic Pggt1b$^{\Delta/\Delta}$ mice have more lesion burden at the aorta than nondiabetic Pggt1b$^{\Delta/\Delta}$. However, the atherosclerotic lesions were remarkably attenuated in diabetic Pggt1b$^{\Delta/\Delta}$ mice than in diabetic wild type. Correlated with these findings, analysis of cross-sectional aortas (Figures 2(c) and 2(d)) also revealed that the lesion area and media thickness were notably less in diabetic Pggt1b$^{\Delta/\Delta}$ mice than in diabetic wild type.

3.4. Knockout of VSMC GGTase-I Reduces the Abundant Hypertrophy of VSMCs in the Atherosclerotic Lesions of Diabetic Mice. Next, to ascertain the hypertrophy of VSMCs in the atherosclerotic lesions, α-SMA was detected by immunohistochemical staining. As shown in Figure 3, in both diabetic wild-type and diabetic Pggt1b$^{\Delta/\Delta}$ mice, the α-SMA-positive area in the atherogenic lesions was remarkably increased than in strain-matched nondiabetic groups. However, the α-SMA-positive area in the lesions of diabetic Pggt1b$^{\Delta/\Delta}$ mice was diminished to 69.6% of that observed in diabetic wild-type mice (Figure 3(c)). In contrast, the extent of α-SMA immunoreactivity was similar in the nonplaque area of four groups (data not shown).

3.5. Knockout of VSMC GGTase-I Reduces the Excessive Oxidative Stress in the Aortic Wall from Diabetic Mice. Protein nitration, a marker for oxidative stress in the aortic wall, was assessed by immunofluorescence staining with an antibody against nitrotyrosine. As shown in Figure 3, the levels of nitrotyrosine were increased in aortic walls from two diabetic groups when compared with vessels from strain-matched nondiabetic groups. Lack of VSMC GGTase-I caused substantially lower nitrotyrosine levels in diabetic Pggt1b$^{\Delta/\Delta}$ aortas than in diabetic wild-type mice (Figures 3(b) and 3(d)).

3.6. Knockout of VSMC GGTase-I Inhibits the Proliferation of VSMCs Induced by High Glucose In Vitro. As expected, VSMCs from both Pggt1b$^{\Delta/\Delta}$ and wild-type aortas incubated with high glucose (22.2 mM) resulted in a remarkable increase of cell proliferation than normal glucose (5.6 mM) (Figure 4(a)). However, conditional knockout of VSMC GGTase-I caused a notable reduction of cell proliferation evoked by high glucose than in the wild-type high-glucose group. Similarly, in wild-type VSMCs, coincubation with a selective GGTase-I inhibitor (GGTI-286, 10 μM) or Rac1 inhibitor (100 μM) both reduced the high-glucose-induced VSMC proliferation ($P < 0.05$ and $P < 0.01$ versus the wild-type high-glucose group, respectively).

3.7. Knockout of VSMC GGTase-I Inhibits the Excessive ROS in VSMCs Induced by High Glucose In Vitro. ROS production (H_2O_2) in VSMCs was measured by Amplex Red and carboxy-H_2DCFDA chemiluminescence, respectively, and the results obtained by these two different approaches were almost consistent (Figures 4(b) and 4(c)). Both Pggt1b$^{\Delta/\Delta}$ and wild-type VSMCs cultured under high glucose (22.2 mM) showed greater ROS levels when compared to normal glucose (5.6 mM) treated strain-matched VSMCs, whereas the ROS level in Pggt1b$^{\Delta/\Delta}$ VSMCs treated with high glucose was dramatically decreased than in wild-type VSMCs treated with the same high glucose. Additionally, in wild-type VSMCs, coincubation with a selective GGTase-I inhibitor (GGTI-286, 10 μM) or Rac1 inhibitor (100 μM) both attenuated the high-glucose-evoked excessive ROS levels.

3.8. Knockout of VSMC GGTase-I Inhibits the Activation of Small GTPase, Rac1. The activation of small GTPase, Rac1, depends on its conversion from the GDP- to GTP-bound state and the membrane location via the process of protein geranylgeranylation by GGTase-I [6]. The levels of GTP-bound active form of Rac1 in aortas and cultured VSMCs were determined by G-LISA kits. In vivo, diabetic wild-type mice exhibited a remarkably higher Rac1 activity than nondiabetic wild-type, whereas a 16-week duration of diabetes had

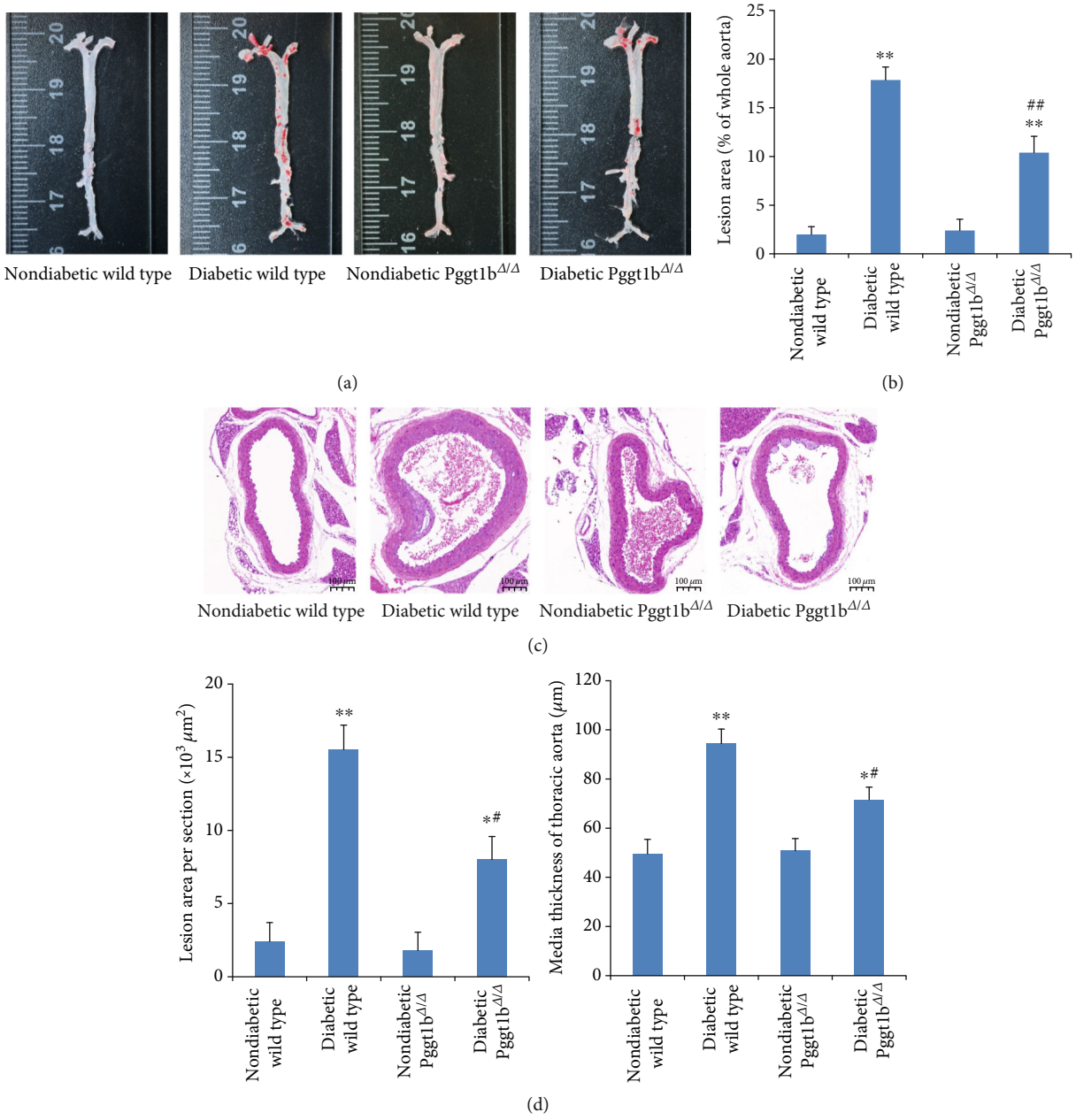

Figure 2: Conditional knockout of VSMC GGTase-I attenuates diabetes-accelerated atherosclerosis. (a) Representative images of en face oil red O staining of aortas. (b) Quantification of oil red O positive areas in en face aortas. (c) Representative hematoxylin and eosin staining (HE) of cross-sectional aortas. (d) Quantification of lesion areas and media thickness from HE staining cross-sectional aortas. Data are expressed as mean ± SEM, $n = 5$ for each group. $^{*}P < 0.05$ and $^{**}P < 0.01$ versus strain-matched nondiabetic mice. $^{\#}P < 0.05$ and $^{\#\#}P < 0.01$ versus diabetic wild-type mice.

no obvious effect on aortic Rac1 activity in Pggt1b$^{\Delta/\Delta}$ mice (Figure 5(a)). In other words, the Rac1 activity in diabetic Pggt1b$^{\Delta/\Delta}$ mice was much lower than in the diabetic wild-type aorta. In vitro, wild-type VSMCs treated with high glucose (22.2 mM) showed a significantly greater level of Rac1 activity ($P < 0.01$ vs. wild-type normal glucose VSMCs), while coincubation with a selective GGTase-I inhibitor (GGTI-286, 10 μM) or Rac1 inhibitor (100 μM) restrained this increase of Rac1 activity evoked by high glucose (Figure 5(b)). Similarly, Rac1 activity in Pggt1b$^{\Delta/\Delta}$ VSMCs treated with high glucose was much lower than wild-type VSMCs treated with the same high glucose (Figure 5(b)). However, either in vivo or in vitro, high glucose had no effect on the expression of total Rac1 in all groups mentioned above (data not shown).

3.9. Knockout of VSMC GGTase-I Suppresses the Membrane Localization of p47phox and NOXO1. NOX is the main source of ROS in the vasculature [16–19]. Of the various NOX isoforms, NOX1 and NOX2 are the most important ones in VSMC proliferation [16–19]. These enzymes consist of a membrane-bound NOX isoforms (NOX1 and NOX2)

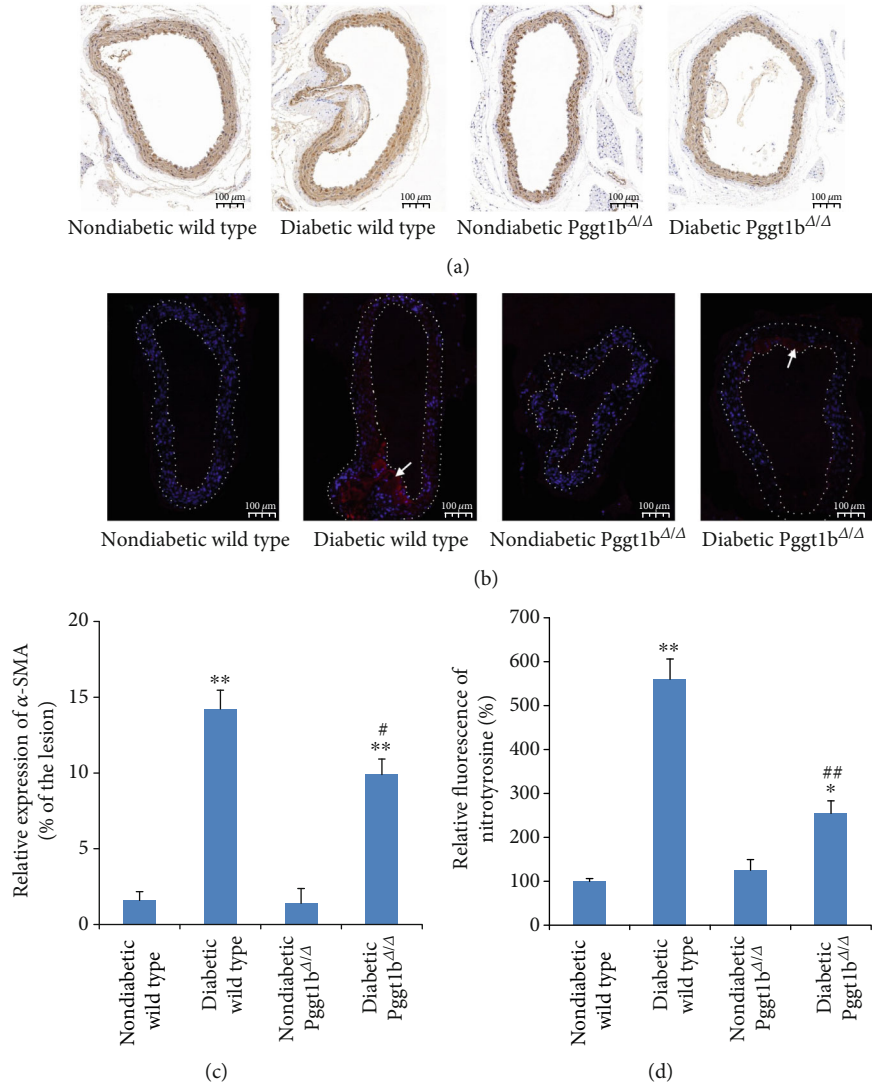

Figure 3: Conditional knockout of VSMC GGTase-I reduces the abundant hypertrophy and excessive oxidative stress of VSMCs in the atherosclerotic lesions of diabetic mice. (a) Representative immunohistochemical analysis of atherosclerotic lesions via staining with α-SMA. (b) The immunofluorescence expression of nitrotyrosine (FITC staining, red) was examined in the aortic walls. DAPI counterstaining (blue) indicates nuclear localization. The arrows show the areas with obvious FITC staining. (c) Quantification of the α-SMA-positive area in aortic lesions. (d) Relative fluorescence intensity of nitrotyrosine in aortic walls. Data are expressed as mean ± SEM, $n = 5$ for each group. $^{*}P < 0.05$ and $^{**}P < 0.01$ versus strain-matched nondiabetic mice. $^{\#}P < 0.05$ and $^{\#\#}P < 0.01$ versus diabetic wild-type mice.

and several cytosolic regulatory subunits. p47phox and NOXO1 are cytoplasmic subunit for NOX1 and NOX2, respectively [16–19]. The activation of NOX is initiated by translocation of the cytoplasmic components, involving p47phox, NOXO1, and Rac1, to the membrane [16–19]. In our study, hyperglycemia had no effect on the expressions of membrane-bound NOX isoforms (NOX1 and NOX2) in vivo or in vitro in all groups (data not shown). For cytosolic subunits (p47phox and NOXO1), the situation is quite different. In vivo data showed that the expression of p47phox and NOXO1 was significantly increased in both membrane and cytoplasmic fractions of aortas from diabetic wild-type mice, when compared to nondiabetic wild type (Figures 6(a)–6(d)). These upregulations of p47phox and NOXO1 also happened in aortas from diabetic Pggt1b$^{\Delta/\Delta}$ mice ($P < 0.01$ versus nondiabetic Pggt1b$^{\Delta/\Delta}$ mice), whereas these increases were greatly inhibited when compared to diabetic wild-type mice (Figures 6(a)–6(d)). In vitro, wild-type VSMCs treated with high glucose (22.2 mM) exhibited a much higher level of membrane p47phox and NOXO1 expression (both $P < 0.01$ vs. wild-type normal glucose VSMCs), while coincubation with a selective GGTase-I inhibitor (GGTI-286, 10 μM) or Rac1 inhibitor (100 μM) restrained this increase (Figures 6(e)–6(g)). Meanwhile, membrane p47phox and NOXO1 expression in Pggt1b$^{\Delta/\Delta}$ VSMCs under high glucose was dramatically lower than wild-type VSMCs treated with the same high glucose (Figures 6(e)–6(g)). However, in either wild-type or Pggt1b$^{\Delta/\Delta}$ VSMCs, cytoplasmic p47phox and NOXO1 expressions did not change in response to high glucose, GGTI-286, or Rac1 inhibitor (data not shown).

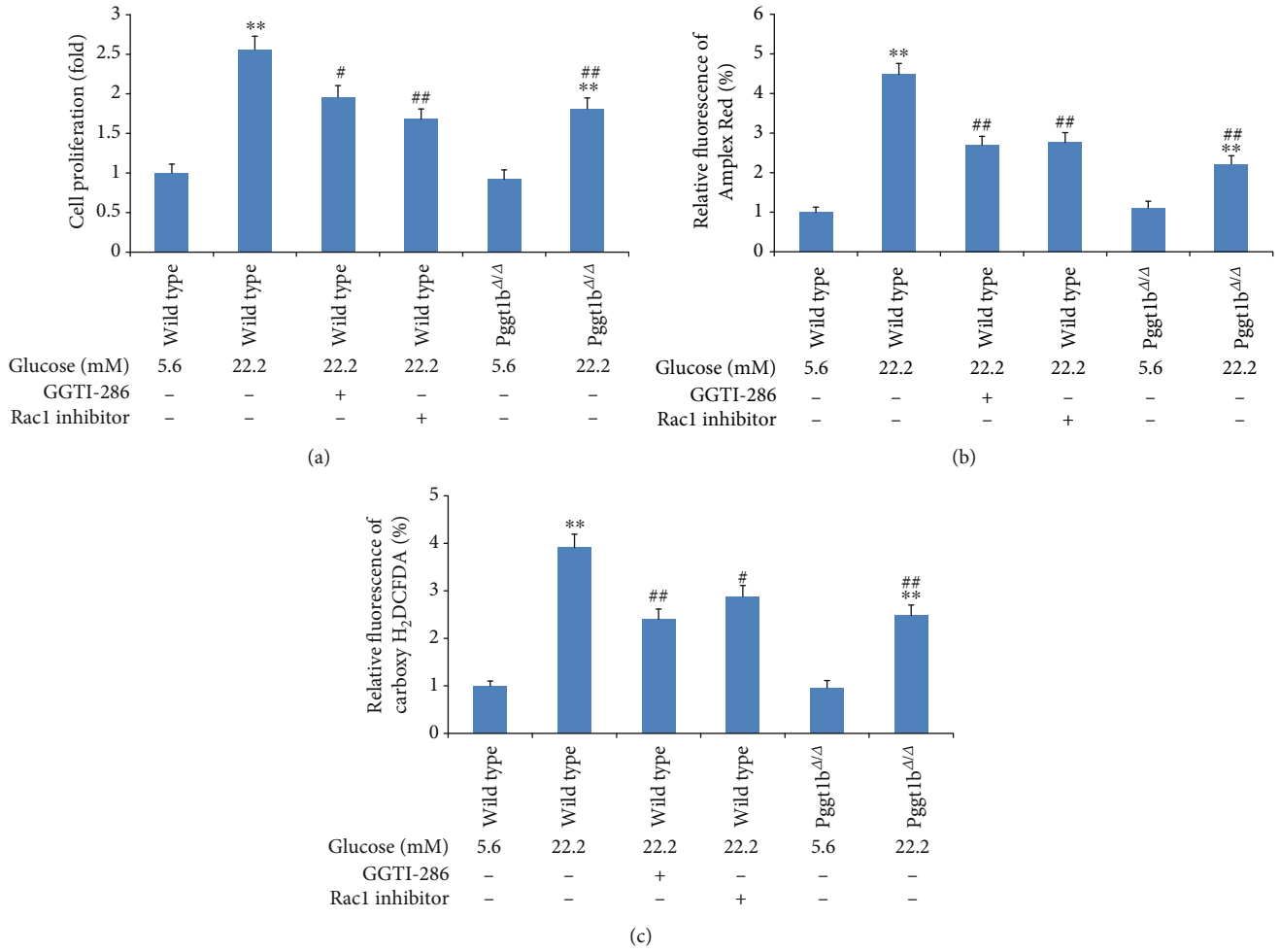

Figure 4: Effects of GGTase-I knockout on high glucose (22.2 mM) induced proliferation and ROS generation of VSMCs. VSMCs were isolated from wild-type and Pggt1b$^{\Delta/\Delta}$ mice and treated with normal glucose (5.6 mM) or high glucose (22.2 mM) for 72 h. VSMCs from wild-type mice were also cultured with a selective GGTase-I inhibitor (GGTI-286, 10 μM) or Rac1 inhibitor (100 μM) for 24 h. Cell proliferation was assessed by MTT incorporation assay (a). ROS production in VSMCs was measured by Amplex Red (b) and carboxy-H2DCFDA (c) chemiluminescence, respectively. Data are expressed as mean ± SEM, $n = 5$ for each group. $^{**}P < 0.01$ versus the strain-matched normal glucose group. $^{\#}P < 0.05$ and $^{\#\#}P < 0.01$ versus the wild-type high-glucose group.

3.10. Knockout of VSMC GGTase-I Attenuates the Phosphorylation of ERK1/2 and JNK. To investigate the effects of GGTase-I knockout on the MAPK signaling pathway, the phosphorylated protein levels of extracellular signal-regulated kinase (ERK1/2), c-Jun N-terminal kinase (JNK), and p38 MAPK were measured by western blot (Figure 7). The protein expressions of phospho-ERK1/2 and phospho-JNK were markedly increased in aortas from diabetic wild-type mice than nondiabetic wild type. However, these increases were eliminated in diabetic Pggt1b$^{\Delta/\Delta}$ mice when compared to diabetic wild-type mice (Figures 7(a) and 7(b)). Likewise, in wild-type VSMCs cultured in vitro, the expressions of phospho-ERK1/2 and phospho-JNK were notably increased by incubation with 22.2 mM glucose, and these effects were attenuated by pretreatment with a selective GGTase-I inhibitor (GGTI-286, 10 μM) or Rac1 inhibitor (100 μM) (Figures 7(d) and 7(e)). Then, in Pggt1b$^{\Delta/\Delta}$ VSMCs cultured with 22.2 mM glucose, phospho-ERK1/2 and phospho-JNK expressions were dramatically lower than in wild-type VSMCs treated with the same high glucose (Figures 7(d) and 7(e)). However, the expressions of total ERK1/2 and total JNK did not change among all groups mentioned above (Figures 7(a), 7(b), 7(d), and 7(e)). Besides, there was no difference of phospho-p38 and total p38 expressions among all groups mentioned above (Figures 7(c) and 7(f)), especially between diabetic wild-type and diabetic Pggt1b$^{\Delta/\Delta}$ mice in vivo, between wild-type and Pggt1b$^{\Delta/\Delta}$ VSMCs treated with high glucose in vitro.

4. Discussion

Our experiments provide strong evidence of a major pathophysiological role for GGTase-I in diabetes-accelerated atherosclerosis. We found that GGTase-I deficiency in VSMCs markedly reduced the lesion burden in an experimental mouse model of atherosclerosis secondary to hyperglycemia and hyperlipemia. Furthermore, in vivo and in vitro studies demonstrated that this protective effect must be related to

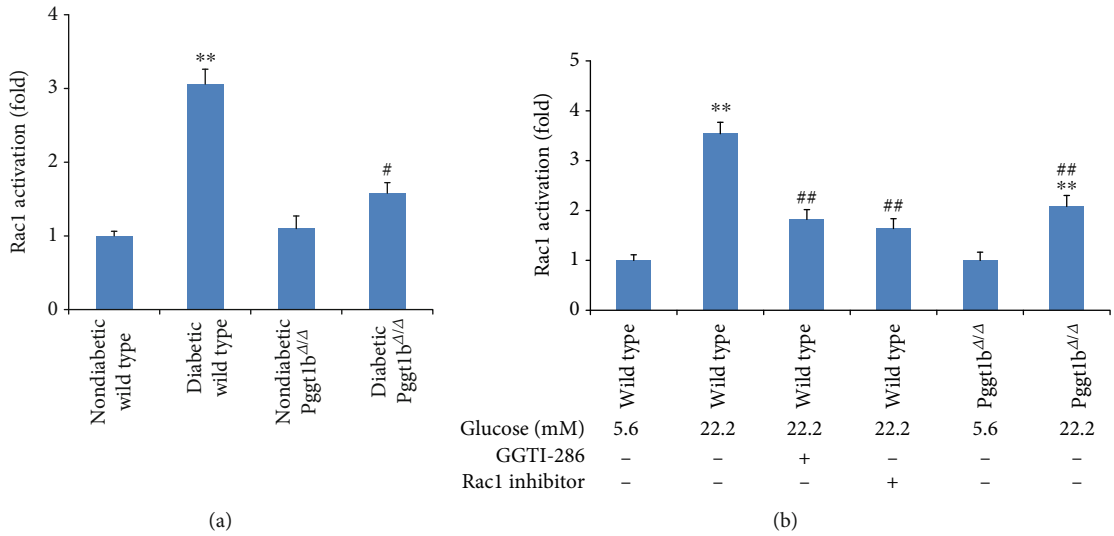

Figure 5: Conditional knockout of VSMC GGTase-I inhibits the activation of small GTPase, Rac1, both in vivo and in vitro. (a) Rac1 activities were determined in aortas from four groups. (b) VSMCs were isolated from wild-type and Pggt1b$^{\Delta/\Delta}$ mice and treated with normal glucose (5.6 mM) or high glucose (22.2 mM) for 72 h. VSMCs from wild-type mice were also cultured with selective GGTase-I inhibitor (GGTI-286, 10 μM) or Rac1 inhibitor (100 μM) for 24 h. Rac1 activities were measured by the Rac1 G-LISA Activation Assay Kit according to the manufacturer's instruction. Data are expressed as mean ± SEM, $n = 5$ for each group. $^{**}P < 0.01$ versus strain-matched nondiabetic mice (or strain-matched normal glucose VSMCs). $^{\#}P < 0.05$ and $^{\#\#}P < 0.01$ versus diabetic wild-type mice (or wild-type high-glucose VSMCs).

inhibition of VSMC proliferation, and potential mechanisms probably involved interfering Rac1, p47phox, and NOXO1 membrane localization, inhibiting ROS generation, and decreasing ERK1/2 and JNK phosphorylation.

Diabetes-accelerated atherosclerosis is a complex pathological process, which plays a pivotal role in the progression of cardio-, cerebro-, and peripheral vascular diseases, accounting for the major mortalities and disabilities of diabetic patients [5, 20–22]. How diabetes promotes the pathogenesis of atherosclerosis is not completely understood and probably has a multifactorial origin. It has been widely accepted that accelerated proliferation of VSMCs is the fundamental event in the development of atherosclerosis in diabetes [4, 23]. In our previous study, high glucose (22.2 mM) remarkably induced the VSMC proliferation and GGTase-I upregulation in vitro and in vivo [12]. Then, in our present experiments, Pggt1b$^{\Delta/\Delta}$ mice were induced diabetes by STZ and an atherogenic diet. As expected, diabetic Pggt1b$^{\Delta/\Delta}$ mice exhibited accelerated atherosclerotic lesions, but the lesion burden was remarkably reduced versus diabetic wild-type mice regardless of the similar levels of glucose and lipid. Additionally, genetic knockout of GGTase-I inhibited the proliferation of VSMCs in both atherosclerotic lesions and high-glucose cultured cells. All these findings excitingly suggested the important role of GGTase-I in VSMC proliferation during diabetes-accelerated atherosclerosis, but mechanisms involved were not clear.

Oxidative stress mediated by ROS plays a key role in the pathogenesis of diabetes-accelerated atherosclerosis. The probable mechanisms include endothelial cell dysfunction, monocyte/macrophage recruitment and activation, stimulation of inflammation, and VSMC migration and proliferation [24–26]. In our present study, GGTase-I deficiency in VSMCs caused a significant decrease of excessive oxidative stress in diabetic aortas. In vitro, excessive ROS production evoked by high glucose was also notably inhibited in cultured Pggt1b$^{\Delta/\Delta}$ VSMCs. Both results confirmed that genetic knockout of GGTase-I protected VSMCs from oxidative injury under diabetic state, and further exploration was needed.

NOX has been implicated as the main source of vascular ROS generation in response to high glucose [16–19]. Seven distinct isoforms of this enzyme have been identified, of which NOX1 and NOX2 are the most important ones in VSMC proliferation [16–19]. These enzymes consist of a membrane-bound heterodimer (NOX1 and NOX2) and several cytosolic regulatory subunits, involving NOXO1 for NOX1, p47phox for NOX2, and small GTP-binding protein Rac1 [27, 28]. The activation of NOX is initiated by translocation of the cytoplasmic components to the membrane [16–19]. As one of the important factors initiating NOX assembly, Rac1, its membrane localization and activation depends on the process of protein geranylgeranylation by GGTase-I [29–31]. In our experiments in vitro and in vivo, GGTase-I deficiency in VSMCs inhibited Rac1 activation stimulated by hyperglycemia but had no effect on the expression of total Rac1, proving in turn that knockout of GGTase-I only affected the activating process of small GTP-binding protein Rac1, possibly via inhibition of its geranylgeranylation. Moreover, we also found that lack of VSMC GGTase-I in vivo suppressed the upregulation of membrane p47phox and NOXO1 induced by hyperglycemia, and the situation was almost the same in the cytoplasm. But high glucose had no effect on the expressions of NOX1 and NOX2 in vivo or in vitro in all groups. Taken together, these results further supported the hypothesis that GGTase-I deficiency prevented Rac1 geranylgeranylation and inhibited the

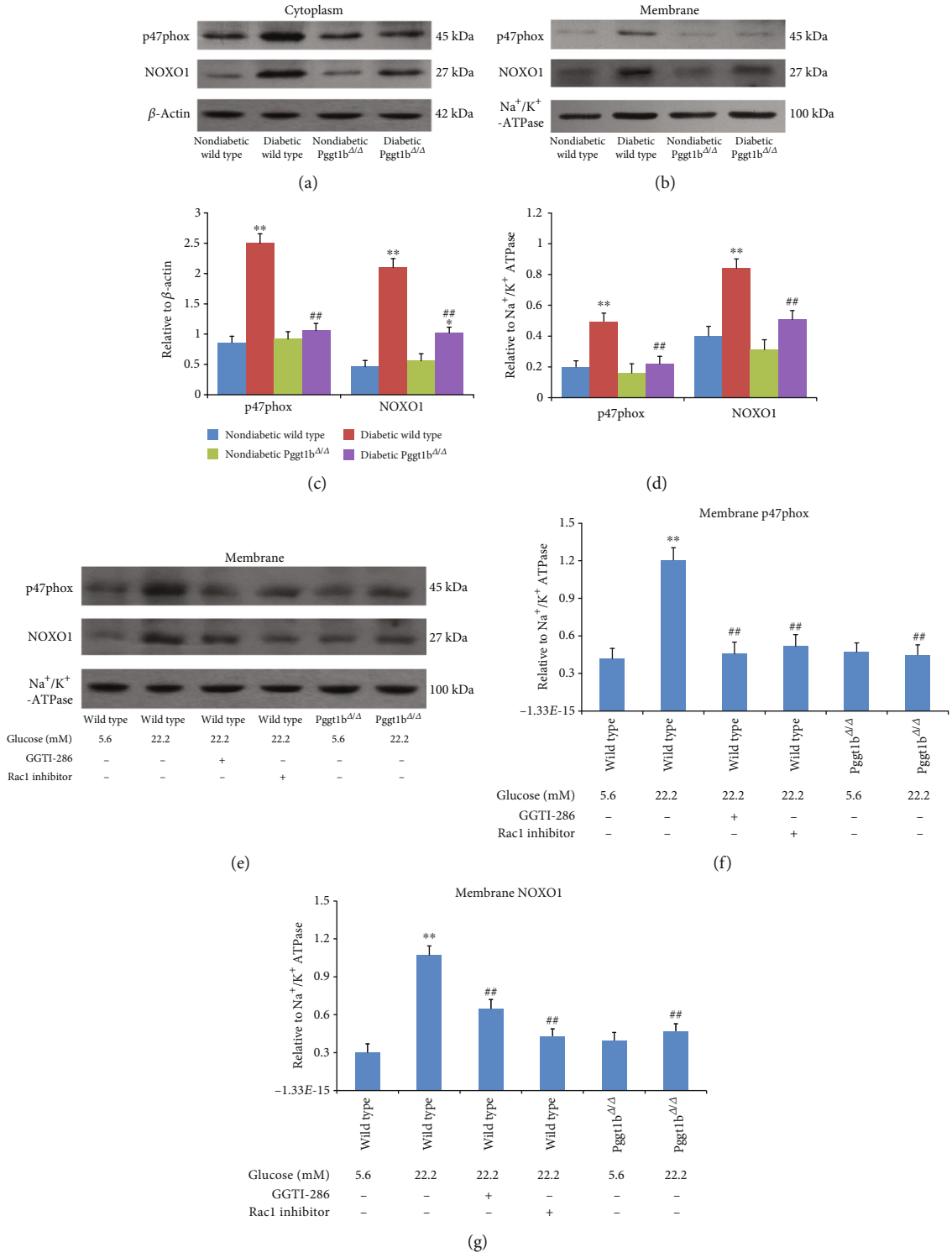

Figure 6: Effects of GGTase-I knockout on p47phox and NOXO1 in cytosolic and membrane fractions from cultured VSMCs in vitro and aortic tissue in vivo. The protein expressions were detected by western blot analysis. (a) Representative blots and (c) densitometric average in membrane fractions from aortic tissue in vivo. (b) Representative blots and (d) densitometric average in cytosolic fractions from aortic tissue in vivo. (e) Representative blots and (f, g) densitometric average in membrane fractions from cultured VSMCs in vitro. VSMCs were isolated from wild-type and Pggt1b$^{\Delta/\Delta}$ mice and treated with normal glucose (5.6 mM) or high glucose (22.2 mM) for 72 h. VSMCs from wild-type mice were also cultured with a selective GGTase-I inhibitor (GGTI-286, 10 μM) or Rac1 inhibitor (100 μM) for 24 h. β-Actin and Na^+/K^+-ATPase were used as loading controls for the cytoplasm and plasma membrane, respectively. Data are expressed as mean ± SEM, $n = 5$ for each group. $^*P < 0.01$ and $^{**}P < 0.01$ versus strain-matched nondiabetic mice (or strain-matched normal glucose VSMCs). $^{\#\#}P < 0.01$ versus diabetic wild-type mice (or wild-type high-glucose VSMCs).

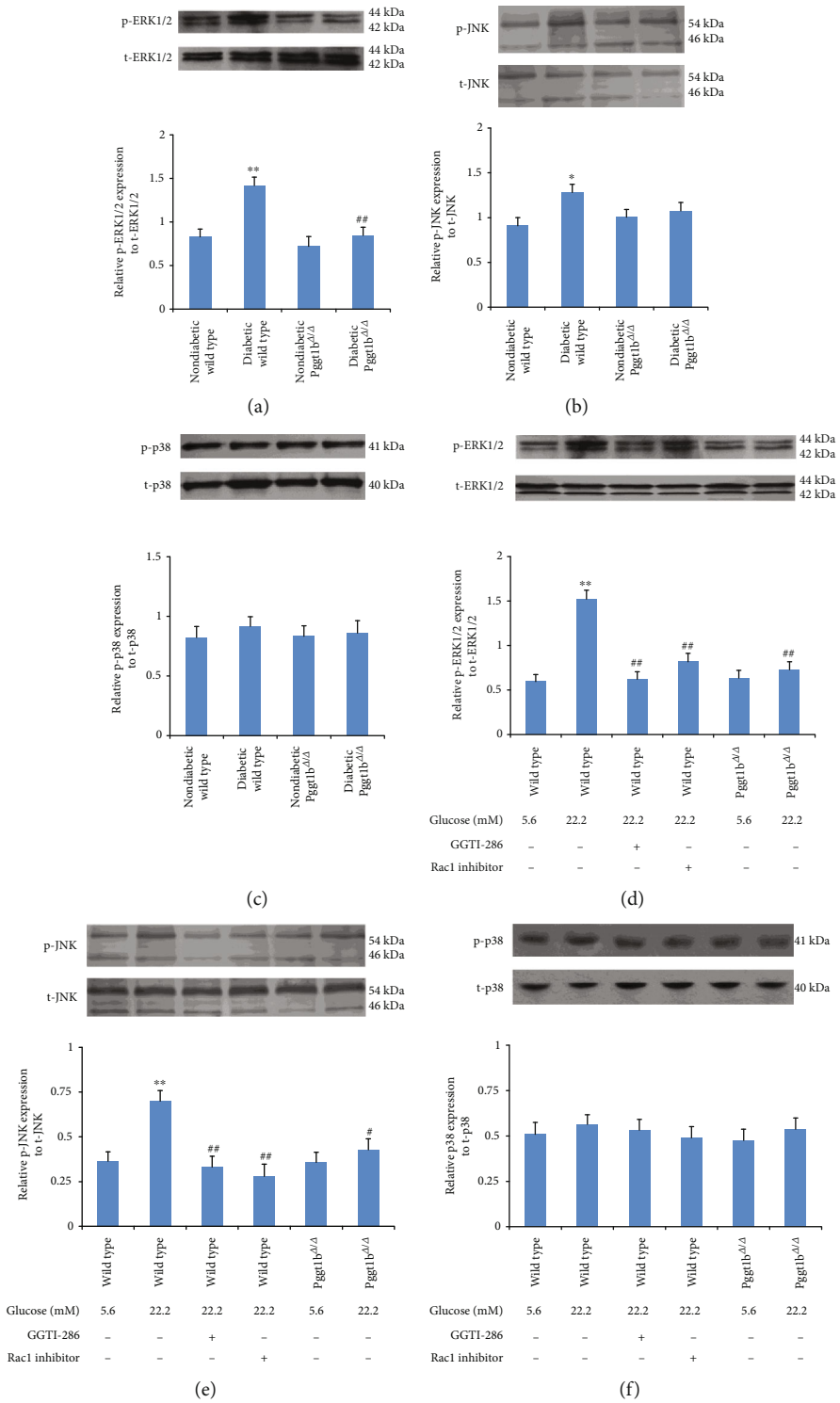

Figure 7: Effects of GGTase-I knockout on the phosphorylation of ERK1/2, JNK, and p38 in cultured VSMCs in vitro and aortic tissue in vivo. Western blot analysis of ERK1/2 (a), JNK (b), and p38 (c) phosphorylation and total protein expression in aortic tissue from four groups. Western blot of ERK1/2 (d), JNK (e), and p38 (f) phosphorylation and total protein expression in cultured VSMCs in vitro. VSMCs were isolated from wild-type and Pggt1b$^{\Delta/\Delta}$ mice and treated with normal glucose (5.6 mM) or high glucose (22.2 mM) for 72 h. VSMCs from wild-type mice were also cultured with a selective GGTase-I inhibitor (GGTI-286, 10 μM) or Rac1 inhibitor (100 μM) for 24 h. β-Actin was used as an internal control. Data expressed as mean ± SEM, $n = 5$ for each group. $^{*}P < 0.01$ and $^{**}P < 0.01$ versus strain-matched nondiabetic mice (or strain-matched normal glucose VSMCs). $^{\#}P < 0.05$ and $^{\#\#}P < 0.01$ versus diabetic wild-type mice (or wild-type high-glucose VSMCs).

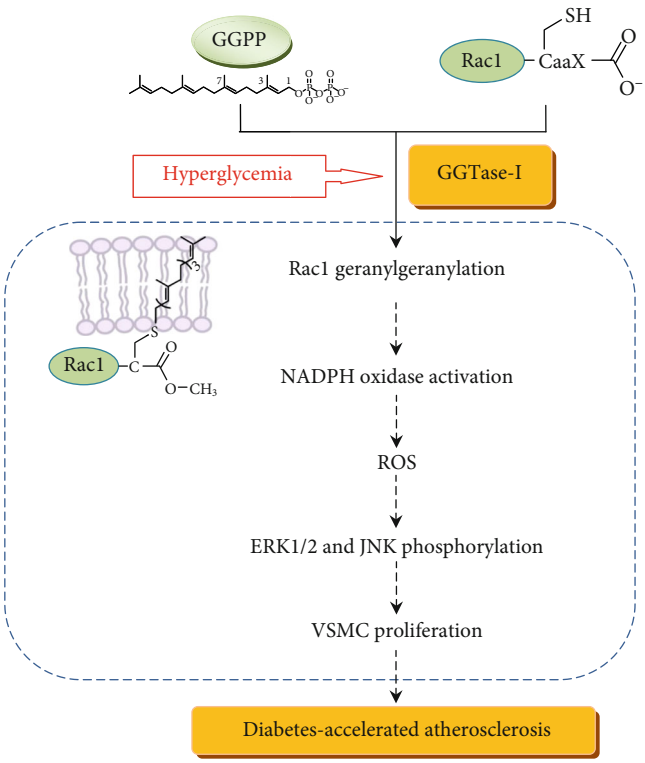

Figure 8: The role of GGTase-I in diabetes-accelerated atherosclerosis and the probable mechanisms are summarized. GGPP: geranylgeranyl pyrophosphate.

assembly of NOX1 and NOX2 cytosolic regulatory subunits, which subsequently led to the decrease of vascular ROS generation.

The signaling molecular by which GGTase-I deficiency exerts an antiatherosclerotic effect in diabetes remains unclear. MAPKs are serine-threonine kinases that mediate intracellular signaling responding to varieties of stimuli including ROS [32–34]. As is well known, the MAPK family is composed of ERK1/2, JNK, and p38. A growing body of evidence has demonstrated that ROS-ERK1/2 cascades participate in the regulation of VSMC proliferation in vitro and neointima formation in vivo [35–37]. Previous studies also showed that JNK, p38, and ERK1/2 phosphorylation acted a critical role in high-glucose-induced oxidative injury and VSMC proliferation [38, 39]. In our in vivo study, we found that lack of VSMC GGTase-I reduced the hyperphosphorylation of ERK1/2 and JNK stimulated by diabetes. In line with in vivo results, ERK1/2 and JNK phosphorylation was inhibited in high-glucose-treated VSMCs with GGTase-I knockdown. However, different from the previous experiments, the phosphorylation of p38 in our study was of no significant change. Therefore, based on these results, our presumption was that GGTase-I deficiency protected proliferative VSMCs from oxidative injury under diabetic state, probably via ERK1/2 and JNK pathways, but not p38.

Furthermore, in our study, VSMCs from wild-type mice were also cultured in the presence of a selective GGTase-I inhibitor or Rac1 inhibitor. Then, it was observed that both inhibitors notably restrained high-glucose-evoked upregulation of VSMC proliferation, ROS content, Rac1 activity, membrane p47phox and NOXO1 expression, and phospho-ERK1/2 and phospho-JNK level. These results are very consistent with the above data from Pggt1b$^{\Delta/\Delta}$ VSMCs stimulated by high glucose, indicating that the geranylgeranylation of Rac1 mediated by GGTase-I is probably responsible for the antiatherosclerotic effect in our study.

5. Conclusions

Our work provided the experimental evidences that GGTase-I knockdown efficiently blocked diabetes-accelerated atherosclerosis, and this protective effect must be related to inhibition of VSMC proliferation. The potential mechanisms probably involved interfering Rac1 geranylgeranylation, inhibiting p47phox and NOXO1 membrane localization, reducing ROS generation, and decreasing ERK1/2 and JNK phosphorylation (summarized in Figure 8). Although there are many essential differences between experimental and clinical studies, our study represents a potentially promising therapeutic strategy for the treatment of diabetic macrovascular disease in the future.

Data Availability

The data used to support the findings of this study are available from the corresponding author upon request.

Conflicts of Interest

The authors declare that there are no interests associated with the manuscript.

Acknowledgments

We thank Prof. Shen-Jiang Hu of Zhejiang University for his sincere assistance. We express our sincere gratitude to Prof. Iain C. Bruce (University of Hong Kong) for checking the English. This work was supported by the National Natural Science Foundation of China (grant number 81701365), the Natural Science Foundation of Zhejiang Province (grant number LQ13H070001), the Zhejiang Province Public Welfare Technology Application Research Project (grant number 2017C33124), and the Medical and Health Science Project of Zhejiang Province (grant numbers 2018KY363 and 2020KY023).

References

[1] J. L. Harding, M. E. Pavkov, D. J. Magliano, J. E. Shaw, and E. W. Gregg, "Global trends in diabetes complications: a review of current evidence," *Diabetologia*, vol. 62, no. 1, pp. 3–16, 2019.

[2] S. N. Bhupathiraju and F. B. Hu, "Epidemiology of obesity and diabetes and their cardiovascular complications," *Circulation Research*, vol. 118, no. 11, pp. 1723–1735, 2016.

[3] J. A. Beckman and M. A. Creager, "Vascular complications of diabetes," *Circulation Research*, vol. 118, no. 11, pp. 1771–1785, 2016.

[4] S. Park, H. J. Kang, J. H. Jeon, M. J. Kim, and I. K. Lee, "Recent advances in the pathogenesis of microvascular complications in diabetes," *Archives of Pharmacal Research*, vol. 42, no. 3, pp. 252–262, 2019.

[5] G. Rodriguez-Araujo and H. Nakagami, "Pathophysiology of cardiovascular disease in diabetes mellitus," *Cardiovascular Endocrinology & Metabolism*, vol. 7, no. 1, pp. 4–9, 2018.

[6] M. Wang and P. J. Casey, "Protein prenylation: unique fats make their mark on biology," *Nature Reviews. Molecular Cell Biology*, vol. 17, no. 2, pp. 110–122, 2016.

[7] N. Ullah, M. Mansha, and P. J. Casey, "Protein geranylgeranyltransferase type 1 as a target in cancer," *Current Cancer Drug Targets*, vol. 16, no. 7, pp. 563–571, 2016.

[8] B. S. Zuckerbraun, J. E. Barbato, A. Hamilton, S. Sebti, and E. Tzeng, "Inhibition of geranylgeranyltransferase I decreases generation of vascular reactive oxygen species and increases vascular nitric oxide production[1]," *The Journal of Surgical Research*, vol. 124, no. 2, pp. 256–263, 2005.

[9] O. M. Khan, M. K. Akula, K. Skalen et al., "Targeting GGTase-I activates RHOA, increases macrophage reverse cholesterol transport, and reduces atherosclerosis in mice," *Circulation*, vol. 127, no. 7, pp. 782–790, 2013.

[10] B. Chen, L.-Y. Zhong, J.-X. Yang et al., "Alteration of mevalonate pathway related enzyme expressions in pressure overload-induced cardiac hypertrophy and associated heart failure with preserved ejection fraction," *Cellular Physiology and Biochemistry*, vol. 32, no. 6, pp. 1761–1775, 2013.

[11] J. Han, D.-M. Jiang, C.-Q. Du, and S.-J. Hu, "Alteration of enzyme expressions in mevalonate pathway," *Circulation Journal*, vol. 75, no. 6, pp. 1409–1417, 2011.

[12] G. P. Chen, X. Q. Zhang, T. Wu, L. Li, J. Han, and C. Q. Du, "Alteration of Mevalonate Pathway in Proliferated Vascular Smooth Muscle from Diabetic Mice: Possible Role in High-Glucose-Induced Atherogenic Process," *Journal of Diabetes Research*, vol. 2015, Article ID 379287, 11 pages, 2015.

[13] G. P. Chen, X. Q. Zhang, T. Wu, J. Han, and D. Ye, "Inhibition of farnesyl pyrophosphate synthase attenuates high glucose-induced vascular smooth muscle cells proliferation," *Molecular Medicine Reports*, vol. 15, no. 5, pp. 3153–3160, 2017.

[14] Q. N. Dinh, S. Chrissobolis, H. Diep et al., "Advanced atherosclerosis is associated with inflammation, vascular dysfunction and oxidative stress, but not hypertension," *Pharmacological Research*, vol. 116, pp. 70–76, 2017.

[15] W. Liang, Q. Wang, H. Ma, W. Yan, and J. Yang, "Knockout of low molecular weight FGF2 attenuates atherosclerosis by reducing macrophage infiltration and oxidative stress in mice," *Cellular Physiology and Biochemistry*, vol. 45, no. 4, pp. 1434–1443, 2018.

[16] G. Salazar, "NADPH oxidases and mitochondria in vascular senescence," *International Journal of Molecular Sciences*, vol. 19, no. 5, p. E1327, 2018.

[17] A. B. Garcia-Redondo, A. Aguado, A. M. Briones, and M. Salaices, "NADPH oxidases and vascular remodeling in cardiovascular diseases," *Pharmacological Research*, vol. 114, pp. 110–120, 2016.

[18] Q.-A. Sun, N. Madamanchi, and M. Runge, "Oxidative stress, NADPH oxidases, and arteries," *Hämostaseologie*, vol. 36, no. 2, pp. 77–88, 2017.

[19] S. Gray and K. Jandeleit-Dahm, "The role of NADPH oxidase in vascular disease – hypertension, atherosclerosis & stroke," *Current Pharmaceutical Design*, vol. 21, no. 41, pp. 5933–5944, 2015.

[20] R. Vadivelu and R. Vijayvergiya, "Panvascular risk factor - diabetes," *Cor et Vasa*, vol. 60, no. 1, pp. e18–e29, 2018.

[21] S. L. Yang, L. Y. Zhu, R. Han, L. L. Sun, J. X. Li, and J. T. Dou, "Pathophysiology of peripheral arterial disease in diabetes mellitus," *Journal of Diabetes*, vol. 9, no. 2, pp. 133–140, 2017.

[22] E. L. MacDougal, W. H. Herman, J. J. Wing, L. B. Morgenstern, and L. D. Lisabeth, "Diabetes and ischaemic stroke outcome," *Diabetic Medicine*, vol. 35, no. 9, pp. 1249–1257, 2018.

[23] J. K. Beverly and M. J. Budoff, "Atherosclerosis: pathophysiology of insulin resistance, hyperglycemia, hyperlipidemia, and inflammation," *Journal of Diabetes*, vol. 12, no. 2, pp. 102–104, 2019.

[24] N. Goncharov, P. Avdonin, A. Nadeev, I. Zharkikh, and R. Jenkins, "Reactive oxygen species in pathogenesis of atherosclerosis," *Current Pharmaceutical Design*, vol. 21, no. 9, pp. 1134–1146, 2015.

[25] W. N. Nowak, J. Deng, X. Z. Ruan, and Q. Xu, "Reactive oxygen species generation and atherosclerosis," *Arteriosclerosis, Thrombosis, and Vascular Biology*, vol. 37, no. 5, pp. e41–e52, 2017.

[26] H. Kaneto, N. Katakami, M. Matsuhisa, and T. A. Matsuoka, "Role of reactive oxygen species in the progression of type 2 diabetes and atherosclerosis," *Mediators of Inflammation*, vol. 2010, Article ID 453892, 11 pages, 2010.

[27] H. Peshavariya, "NADPH oxidase-derived ROS signaling and therapeutic opportunities," *Current Pharmaceutical Design*, vol. 21, no. 41, pp. 5931-5932, 2015.

[28] K. Bedard and K. H. Krause, "The NOX family of ROS-generating NADPH oxidases: physiology and pathophysiology," *Physiological Reviews*, vol. 87, no. 1, pp. 245–313, 2007.

[29] J. Gao, K. Shao, X. Chen et al., "The involvement of post-translational modifications in cardiovascular pathologies: focus on SUMOylation, neddylation, succinylation, and prenylation," *Journal of Molecular and Cellular Cardiology*, vol. 138, pp. 49–58, 2020.

[30] C. C. Palsuledesai and M. D. Distefano, "Protein prenylation: enzymes, therapeutics, and biotechnology applications," *ACS Chemical Biology*, vol. 10, no. 1, pp. 51–62, 2014.

[31] J. Winkelblech, A. Fan, and S. M. Li, "Prenyltransferases as key enzymes in primary and secondary metabolism," *Applied Microbiology and Biotechnology*, vol. 99, no. 18, pp. 7379–7397, 2015.

[32] Y. Son, S. Kim, H. T. Chung, and H. O. Pae, "Reactive oxygen species in the activation of MAP kinases," *Methods in Enzymology*, vol. 528, pp. 27–48, 2013.

[33] Y. Son, Y.-K. Cheong, N.-H. Kim, H.-T. Chung, D. G. Kang, and H.-O. Pae, "Mitogen-activated protein kinases and reactive oxygen species: how can ROS activate MAPK pathways?," *Journal of Signal Transduction*, vol. 2011, Article ID 792639, 6 pages, 2011.

[34] Z. Lu, H. Zhou, S. Zhang et al., "Activation of reactive oxygen species-mediated mitogen-activated protein kinases pathway regulates both extrinsic and intrinsic apoptosis induced by arctigenin in Hep G2," *The Journal of Pharmacy and Pharmacology*, vol. 72, no. 1, pp. 29–43, 2019.

[35] H. Zhao, T. Han, X. Hong, and D. Sun, "Adipose differentiation-related protein knockdown inhibits vascular smooth muscle cell proliferation and migration and attenuates neointima formation," *Molecular Medicine Reports*, vol. 16, no. 3, pp. 3079–3086, 2017.

[36] T. H. Kim, D. G. Lee, Y. A. Kim, B. H. Lee, K. Y. Yi, and Y. S. Jung, "A novel urotensin II receptor antagonist, KR-36996 inhibits smooth muscle proliferation through ERK/ROS pathway," *Biomolecules & Therapeutics*, vol. 25, no. 3, pp. 308–314, 2017.

[37] M. He, Z. M. Xue, J. Li, and B. Q. Zhou, "Breviscapine inhibits high glucose-induced proliferation and migration of cultured vascular smooth muscle cells of rats via suppressing the ERK1/2 MAPK signaling pathway," *Acta Pharmacologica Sinica*, vol. 33, no. 5, pp. 606–614, 2012.

[38] Y. Liu, X. Li, S. Jiang, and Q. Ge, "Tetramethylpyrazine protects against high glucose-induced vascular smooth muscle cell injury through inhibiting the phosphorylation of JNK, p38MAPK, and ERK," *The Journal of International Medical Research*, vol. 46, no. 8, pp. 3318–3326, 2018.

[39] R. Guo, W. Li, B. Liu, S. Li, B. Zhang, and Y. Xu, "Resveratrol protects vascular smooth muscle cells against high glucose-induced oxidative stress and cell proliferation in vitro," *Medical Science Monitor Basic Research*, vol. 20, pp. 82–92, 2014.

Hindawi
Journal of Diabetes Research
Volume 2020, Article ID 6210865, 7 pages
https://doi.org/10.1155/2020/6210865

Research Article

Evaluation of Foveal and Parafoveal Microvascular Changes Using Optical Coherence Tomography Angiography in Type 2 Diabetes Patients without Clinical Diabetic Retinopathy in South Korea

Young Gun Park,[1] **Minhee Kim**,[2] **and Young Jung Roh**[2]

[1]*Department of Ophthalmology and Visual Science, Seoul St. Mary's Hospital, College of Medicine, The Catholic University of Korea, 222 Banpo-daero, Seochu-gu, Seoul 06591, Republic of Korea*
[2]*Department of Ophthalmology and Visual Science, Yeouido St. Mary's Hospital, College of Medicine, The Catholic University of Korea, 63-ro 10, Yeoungdeongpo-gu, Seoul 07345, Republic of Korea*

Correspondence should be addressed to Young Gun Park; cuteyg2000@catholic.ac.kr

Received 24 April 2020; Revised 3 June 2020; Accepted 25 June 2020; Published 7 August 2020

Guest Editor: Gaetano Santulli

The aim of this study was to investigate foveal and parafoveal microvascular changes in retinal vascular plexuses in patients with type 2 diabetes mellitus (DM) without clinical diabetic retinopathy (NDR) using optical coherence tomography angiography (OCTA) in South Korea. We included 64 patients in the NDR group and included 48 healthy control subjects for comparison. All subjects underwent ocular examination with visual acuity and wide-field fundus photos. Foveal and parafoveal vessel density and foveal avascular zone (FAZ) area (mm^2) in the superficial capillary plexus (SCP) and deep capillary plexus (DCP) were analyzed. Foveal vessel densities in both the SCP and DCP were decreased in the NDR group compared to the controls ($p = 0.034$ and 0.001, respectively). Vessel densities in the superior and inferior parafoveae in the DCP were decreased in the NDR group compared to the controls ($p = 0.006$ and 0.034, respectively). The FAZs of the SCP and DCP were significantly different between the NDR group and the controls ($p = 0.003$ and 0.001, respectively). The average vessel densities of the SCP and DCP were not correlated with HbA1c, serum creatinine, or the duration of DM in the NDR group. We demonstrated that OCTA can identify early-stage DR before the manifestation of clinically apparent retinopathy in diabetic eyes. Diabetic patients without clinical DR have microvascular alterations (foveal vessel density, parts of the parafovea, and enlarged FAZ) in the SCP and DCP. Our results suggest that OCTA might be a promising tool for early detection of eyes with DR.

1. Introduction

Diabetic retinopathy (DR) is one of several complications of diabetic mellitus (DM) and an important cause of blindness worldwide [1, 2]. Efforts in early detection and screening for DR could reduce the severity and possibility of blindness. It is difficult to reverse the damage from DR, and the risk of DR progression increases once retinal lesions become clinically visible [3]. Having a clearer understanding of the early changes in DR might provide novel and more effective preventive strategies. Thus, it is necessary to detect and monitor the subtle microvascular changes in patients with DM and subclinical DR.

The most common early clinically visible manifestations of DR include microaneurysm formation and intraretinal hemorrhage. At present, ophthalmoscopy and color fundus photography are still the gold standards for the diagnosis and staging of DR [4, 5]. However, microvascular damage is known to occur before findings of retinopathy become apparent on clinical examination or fundus photography. Although fluorescein angiography (FA) is an important modality in revealing capillary leakage and nonperfusion in patients with DM, it is rarely used and not suggested for eyes without visible retinopathy or mild DR.

Optical coherence tomography angiography (OCTA) is a novel and noninvasive angiographic technique without

intravenous dye injections. It can easily show vessel densities, vascular abnormalities in retinal blood flow, and the shape of the foveal avascular zone (FAZ) [6]. The microvascular dropout of the macula in early-stage DR has been reported in recent OCTA studies [7, 8]. Recently, advances in projection artifact removal allowed to accurately define not only the superficial plexus but also the deep retinal vascular layers. Some researchers reported microvascular changes in the SCP and DCP in patients with diabetes without retinopathy [9, 10]. However, there has not been much research in quantitative microvascular changes on the different vascular layers of the retina using OCTA in patients with preclinical DR. The aim of this study was to investigate retinal microvascular alterations of the foveal and parafoveal areas and compare these changes between diabetic eyes with no signs of DR and healthy normal controls using OCTA in South Korea.

2. Materials and Methods

2.1. Subjects. This study was a retrospective review of consecutive cases. Patients attending the Department of Ophthalmology of Seoul St. Mary's Hospital in Seoul, Korea, between January 2018 and January 2019 with a confirmed diagnosis of type 2 DM without clinical DR were included. The healthy control group included healthy patients attending medical checkups with no posterior segment abnormalities or systemic comorbidities. All procedures were conducted in accordance with the Declaration of Helsinki and its later amendments. The study was approved by the ethics committee of Seoul St. Mary's Hospital and the Catholic University of Korea. The need to obtain informed patient consent was waived due to the retrospective design of the study.

All patients and controls had their best-corrected visual acuity (BCVA) measured initially and then underwent standardized dilated fundus examinations, including measurements by swept-source OCT (SS-OCT) and OCTA imaging (DRI OCT Triton; Topcon, Tokyo, Japan). Subjects underwent fundus examinations and ultrawide-field fundus photography capable of capturing 200° of the retina (Optos California; Dunfermline, United Kingdom). After that, two experienced examiners (YGP and MHK) reviewed the fundus photographs and confirmed eyes with no diabetic retinopathy (NDR) [11]. In both patients and controls, the exclusion criteria were any other ocular disease that may affect ocular circulation (e.g., glaucoma, age-related macular degeneration, and refractive error > 5 diopters), intraocular surgery, or severe media opacity (e.g., lens opacity due to cataract or thick asteroid hyalosis).

2.2. Optical Coherence Tomography Angiography. OCTA was performed with a DRI OCT Triton (Topcon). This instrument has an A-scan rate of 70,000 scans/s with an 840 nm wavelength light source and a 45 nm bandwidth. Patients with low-quality images (signal strength index < 50) were excluded. OCTA images were evaluated using automatic segmentation. We analyzed the vascular density of the superficial and deep retinal vascular zone within 1 and 3 mm inner and outer circles using computer software. The extent of the FAZ was also manually measured on the OCTA images of each participant by two investigators (YGP and MHK) who were blinded to each other (Figure 1).

2.3. Statistical Analysis. Unpaired t-tests were used to compare groups, and Pearson's correlation coefficients were used for correlation analysis. $p < 0.05$ was considered statistically significant. All analyses were produced using commercial software (SPSS version 22.0; IBM, Armonk, NY).

3. Results and Discussion

Sixty-four NDR eyes and forty-eight age-matched control subjects were included. Baseline demographics were comparable between the two cohorts (Table 1). The mean age of patients with DM was 61.0 ± 9.34 years while that of the controls was 62.94 ± 11.2 years ($p = 0.729$). DM patients had an average HbA1c of 7.48 ± 1.28%, average serum creatinine of 0.92 ± 0.31 mg/dL, and e-GFR of 82.67 ± 21.72 mmol/L. The average duration of diabetes for DM patients was 7.85 ± 4.37 years (Table 1).

The foveal vascular densities of both the SCP and DCP were significantly lower in the NDR group than in the control group (13.81 ± 4.37% vs. 15.77 ± 3.45%, 11.53 ± 4.41% vs. 13.68 ± 3.59%; $p = 0.034$ and $p = 0.001$, respectively). The parafoveal vascular density in the SCP did not differ significantly between the two groups (superior/temporal/inferior/nasal; all $p > 0.05$). Although the average parafoveal vessel densities in both the SCP and DCP were decreased in eyes with DM, only the vessel densities of the superior and inferior parafoveal areas in the DCP were significantly decreased in the NDR group compared to those in the controls (superior/temporal/inferior/nasal: $p = 0.006$, $p = 0.395$, $p = 0.034$, and $p = 0.079$, respectively; Table 2).

The correlation between the average vessel density of the SCP, the DCP, and HbA1c was unremarkable ($p = 0.264$ and 0.19, respectively). The average vessel densities of the SCP and DCP were not correlated with serum creatinine ($p = 0.424$ and 0.395, respectively). No significant correlation was found between the duration of diabetes and vessel density in the SCP or DCP, either ($p = 0.648$ and 0.713, respectively).

Reduction of the DCP network in the superior and inferior parafoveae and foveae was identified in the NDR group. Only the foveal vascular density in the SCP was lower in the NDR group than in the control group. This suggests a relationship between disease progression and vascular changes.

The FAZs of the SCP and DCP were significantly enlarged in the NDR group when compared with those in the control group (0.34 ± 0.11 mm^2 vs. 0.31 ± 0.08 mm^2, $p = 0.003$; 0.55 ± 0.13 mm^2 vs. 0.43 ± 0.07 mm^2, $p = 0.001$, respectively; Table 2). In addition, microaneurysms were found in six diabetic eyes (9.38%) (Figure 2). We observed that the vessel densities of the SCP and DCP were not significantly associated with HbA1c, serum creatinine, e-GFR, or duration of diabetes. There was also no significant correlation between BCVA (logMAR), FAZs, and vascular density in the SCP or DCP in the NPR group.

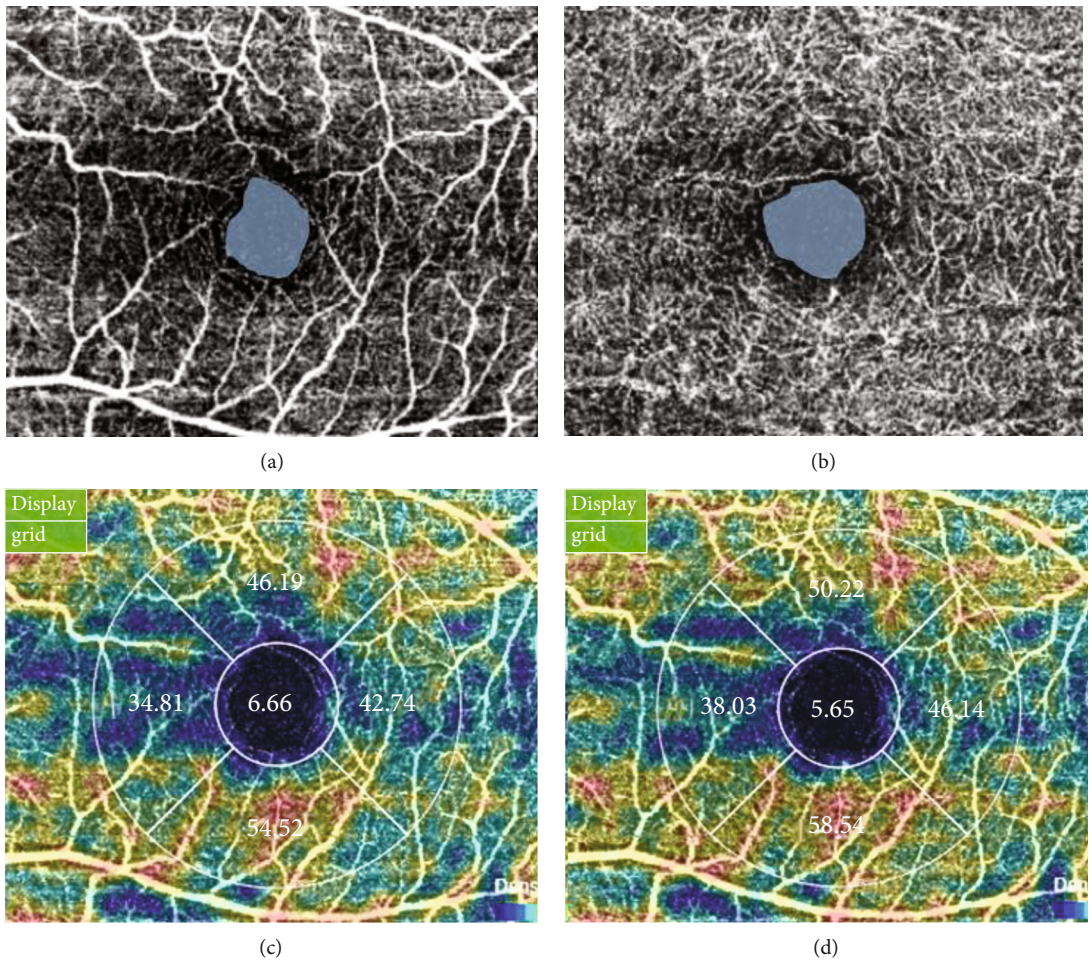

Figure 1: (a, b) Measurements of foveal avascular zone area and (c, d) results of vessel density measurements using optical coherence tomography angiography in a diabetic eye without clinical diabetic retinopathy (superficial capillary plexus, deep capillary plexus).

Table 1: Baseline characteristics.

	NDR group	Control group	p value
Patients	64	48	
Mean age (years)	61.0 ± 9.34	62.9 ± 11.2	0.73
Male : female	36 : 28	26 : 22	0.45
HbA1c (%)	7.48 ± 1.28	N/A	
DM duration (years)	7.85 ± 4.37	N/A	
Serum creatinine (mg/dL)	0.92 ± 0.31	N/A	
e-GFR (mmol/L)	82.67 ± 21.72	N/A	
BCVA (logMAR)	0.07 ± 0.08	0.07 ± 0.09	0.62
Signal strength index	64.71 ± 7.34	67.86 ± 6.32	0.15

NDR: patients with type 2 diabetes mellitus without clinical diabetic retinopathy; N/A: not applicable; e-GFR: estimated glomerular filtration rate.

4. Discussion

OCTA can selectively visualize specific retinal layers, which can be used to compare microvascular changes in patients without detectable clinical retinopathy [12, 13]. There is evidence that OCTA can identify subclinical microvascular alteration in various diseases. In particular, it could more accurately diagnose early-stage DR [14, 15]. Previous studies have reported changes in FAZs or macular vessel density in DR but with different results [16, 17].

Our study compared superficial and deep retinal vascular density and FAZs in type 2 DM patients with NDR and in control subjects by OCTA and assessed the correlation of earlier diabetic changes. As we obtained foveal and parafoveal vessel density within circles 1 and 3 mm in diameter, changes in foveal and parafoveal lesions could be separated and compared. We demonstrated that significant foveal vascular density changes occur in the SCP and DCP layers in NDR groups compared to healthy controls, and the changes in parafoveal vascular density only appeared in superior and inferior DCP lesions. There were no significant differences in the parafoveal vascular density of the SCP between groups.

These results may be due to small differences in vascular density in early-stage DM patients, which were not reflected over the whole macula. However, it implies that subtle microvascular changes have already started in diabetic retinas even in the absence of visible retinal lesions. In our study, there

Table 2: Foveal and parafoveal vascular densities of the superficial capillary plexus and deep capillary plexus evaluated by optical coherence tomography angiography.

	NDR group	Control group	p value
Superficial capillary plexus			
Fovea (%)	13.81 ± 4.37	15.77 ± 3.45	0.034*
Superior (%)	46.37 ± 5.17	48.82 ± 4.57	0.294
Temporal (%)	44.26 ± 4.75	45.68 ± 3.29	0.424
Inferior (%)	48.17 ± 6.74	47.38 ± 5.59	0.421
Nasal (%)	41.18 ± 4.34	43.27 ± 3.83	0.311
FAZ area (mm^2)	0.34 ± 0.11	0.31 ± 0.08	0.003*
Deep capillary plexus			
Fovea (%)	11.53 ± 4.41	13.68 ± 3.59	0.001*
Superior (%)	48.28 ± 6.58	51.92 ± 4.67	0.006*
Temporal (%)	47.35 ± 4.65	47.75 ± 3.97	0.395
Inferior (%)	47.36 ± 7.35	50.31 ± 6.39	0.034*
Nasal (%)	44.34 ± 4.51	46.52 ± 4.01	0.079
FAZ area (mm^2)	0.55 ± 0.13	0.43 ± 0.07	0.001*

NDR: patients with type 2 diabetes mellitus without clinical diabetic retinopathy; FAZ: foveal avascular zone.

was only a significant decrease in vessel density in the superior and inferior parafoveal areas in the DCP layer. Unfortunately, the reason why this part was vulnerable is not clear and more research will be needed.

Changes in FAZs have recently been reported after the introduction of OCTA, but previous studies have provided different conclusions about this in diabetic patients without DR [18]. Cao et al. found no significant difference in the FAZ of SCPs between two groups ($0.32 \pm 0.18\,mm^2$ vs. $0.35 \pm 0.09\,mm^2$) [19]. On the other hand, de Carlo et al. reported an enlarged FAZ in the SCPs of diabetic eyes compared to control eyes ($0.348\,mm^2$ vs. $0.288\,mm^2$, $p = 0.04$) [20]. Our study also showed significant differences in the FAZs of both the SCP and DCP layers between the NDR group and controls ($0.33 \pm 0.07\,mm^2$ vs. $0.26 \pm 0.07\,mm^2$, $0.51 \pm 0.13\,mm^2$ vs. $0.38 \pm 0.12\,mm^2$, respectively; all $p = 0.002$). FAZs can vary between individuals, and so direct comparison may be difficult [21, 22]. However, alterations of FAZs may be an important marker to identify early-stage DR, which might be one of the earliest signs of diabetic damage to retinal vasculature.

The pathogenesis of DR is not completely understood. Microvascular changes in the retina due to retinal ischemia may occur from damage to the endothelial cells and pericyte loss in the retinal capillaries as the disease progresses [23, 24]. Some researchers reported that the DCP might be more vulnerable to ischemia than the SCP due to anatomical differences [25, 26]. The DCP drains into the superficial venules through vertical anastomoses, whereas the SCP is organized with transverse capillaries directly connected to the retinal arterioles with higher perfusion pressure [27]. This might be helpful in explaining our results.

The most common early visible manifestations of DR are microaneurysms and intraretinal hemorrhage with fundus examinations. However, microvascular changes in the macula are not easily identifiable and can be easily missed. Previous studies have demonstrated subtle changes in diabetic eyes without clinical manifestations [28, 29]. Some researchers have showed changes in retinal blood circulation with fluorescence angiography in DM patients without DR [30, 31]. A number of OCTA-related studies are currently underway [28, 32–34].

OCTA is a method that allows for a detailed representation of retinal microvasculature through the segmentation of individual retinal vascular layers, and it has been widely applied in the identification of various retinopathies [35, 36]. In our study, patients with type 2 DM without NDR also showed prominent changes in foveal vessel density in the SCP and, to some extent, parafoveal vessel density in the DCP compared to healthy controls. Altered vessel density at the DCP may imply a preference for the retinal vascular system in the pathogenesis of DR, as retinal venules originate from the deep retinal vascular layers. Sambhav et al. showed progressive vessel density reduction in the deep vascular layer from 25.23% in mild DR to 11.16% in severe DR [37]. The earlier alteration in the deep vascular layer probably reflects retinal venular widening, damage to capillary endings, and microaneurysms. It may also influence the breakdown of the blood-retinal barrier and the progression of DR.

Recently, Zeng et al. reported that peripapillary retinal nerve fiber layer thickness and radial peripapillary capillary density were significantly lower in their NDR group compared to healthy controls [38]. This also demonstrated that subtle retinal microvascular changes have already started, which might be associated with early functional changes. In addition, Sousa et al. detected the retinal vascular responses, a vasodilatory response and a vasoconstriction response, with OCTA [39]. They suggested that OCTA could provide a new way of studying retinal vascular changes before clinically detectable disease. Further studies are needed to clarify this in NDR patients.

There were a few limitations of our study. First, this was a cross-sectional observational study. A longitudinal study should be performed to explain the relationship between the microvascular changes of parafoveal lesions and disease progression in early-stage DR. Secondly, the sample size was relatively small and not large enough to draw clear conclusions. Thirdly, precise fundus examinations such as fluorescence fundus angiography were not available in early-stage DM patients without clinical DR. Lastly, OCTA image artifacts can interfere with accurate assessment of the actual status of the retinal microvasculature; for example, projection artifacts might interrupt visualization of the deep layer.

5. Conclusions

Our results suggested that microvascular alterations detected by OCTA in early-stage DM patients without DR can provide appropriate diagnosis and proper managements for patients with a risk of further clinically apparent DR in South Korea. If we could detect microvascular changes in early-stage DR, we

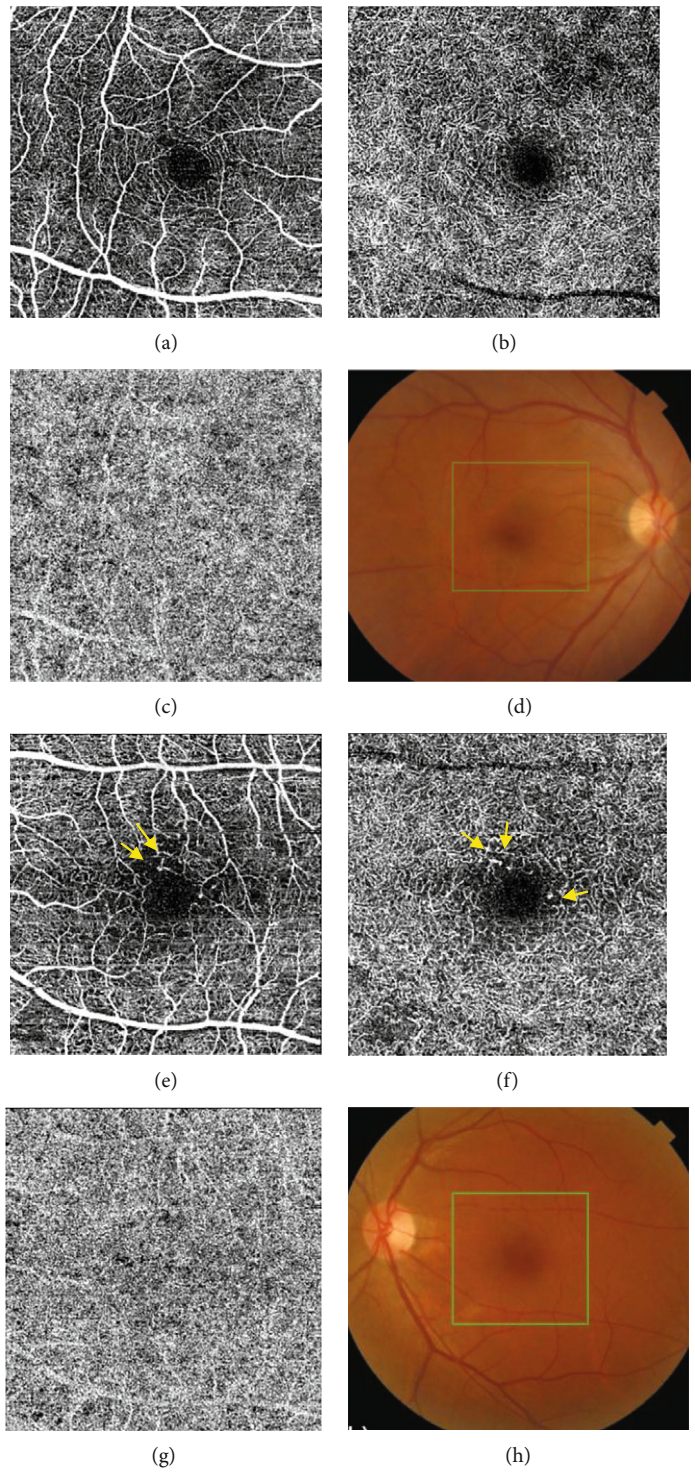

Figure 2: Optical coherence tomography angiography of a control eye (a–d) and a diabetic eye without clinical diabetic retinopathy (e–h) (superficial capillary plexus, deep capillary plexus, choriocapillary, and fundus photography from left to right). A few capillary nonperfusion areas with microaneurysm were observed in the diabetic eye (arrows).

could use a more cautious approach with regard to individual disease statuses. OCTA may be able to detect diabetic eyes at risk of developing retinopathy and to screen for diabetes quickly and noninvasively before a systemic diagnosis is made.

Data Availability

The data used to support the findings of this study are available from the corresponding author upon request.

Conflicts of Interest

The authors have no conflict of interest with regard to this manuscript.

Acknowledgments

The authors wish to acknowledge the financial support of the Catholic Medical Center Research Foundation made in the program year of 2019.

References

[1] G. L. Ong, L. G. Ripley, R. S. Newsom, and A. G. Casswell, "Assessment of colour vision as a screening test for sight threatening diabetic retinopathy before loss of vision," *The British Journal of Ophthalmology*, vol. 87, no. 6, pp. 747–752, 2003.

[2] R. Raman, A. Gupta, S. Krishna, V. Kulothungan, and T. Sharma, "Prevalence and risk factors for diabetic microvascular complications in newly diagnosed type II diabetes mellitus. Sankara Nethralaya Diabetic Retinopathy Epidemiology and Molecular Genetic Study (SN-DREAMS, report 27)," *Journal of Diabetes and its Complications*, vol. 26, no. 2, pp. 123–128, 2012.

[3] I. M. Stratton, E. M. Kohner, S. J. Aldington et al., "UKPDS 50: risk factors for incidence and progression of retinopathy in type II diabetes over 6 years from diagnosis," *Diabetologia*, vol. 44, no. 2, pp. 156–163, 2001.

[4] K. Tanaka, T. Kawai, Y. Saisho et al., "Relationship between stage of diabetic retinopathy and pulse wave velocity in Japanese patients with type 2 diabetes," *Journal Diabetes Research*, vol. 2013, article 193514, pp. 1–4, 2013.

[5] M. Kołodziej, A. Waszczykowska, I. Korzeniewska-Dyl et al., "The HD-OCT study may be useful in searching for markers of preclinical stage of diabetic retinopathy in patients with type 1 diabetes," *Diagnostics*, vol. 9, no. 3, p. 105, 2019.

[6] A. H. Kashani, C. L. Chen, J. K. Gahm et al., "Optical coherence tomography angiography: a comprehensive review of current methods and clinical applications," *Progress in Retinal and Eye Research*, vol. 60, pp. 66–100, 2017.

[7] Y. Kaizu, S. Nakao, H. Sekiryu et al., "Retinal flow density by optical coherence tomography angiography is useful for detection of nonperfused areas in diabetic retinopathy," *Graefe's Archive for Clinical and Experimental Ophthalmology*, vol. 256, no. 12, pp. 2275–2282, 2018.

[8] L. Lahme, E. Marchiori, G. Panuccio et al., "Changes in retinal flow density measured by optical coherence tomography angiography in patients with carotid artery stenosis after carotid endarterectomy," *Scientific Reports*, vol. 8, no. 1, article 17161, 2018.

[9] D. C. Sousa, I. Leal, S. Moreira et al., "Optical coherence tomography angiography study of the retinal vascular plexuses in type 1 diabetes without retinopathy," *Eye*, vol. 34, no. 2, pp. 307–311, 2020.

[10] A. Y. Alibhai, E. M. Moult, R. Shahzad et al., "Quantifying microvascular changes using OCT angiography in diabetic eyes without clinical evidence of retinopathy," *Ophthalmology Retina*, vol. 2, no. 5, pp. 418–427, 2018.

[11] Early Treatment Diabetic Retinopathy Study Research Group, "Early treatment diabetic retinopathy study design and baseline patient characteristics. ETDRS report number 7," *Ophthalmology*, vol. 98, 5 Supplement, pp. 741–756, 1991.

[12] J. I. Fernández-Vigo, B. Kudsieh, A. Macarro-Merino et al., "Reproducibility of macular and optic nerve head vessel density measurements by swept-source optical coherence tomography angiography," *European Journal of Ophthalmology*, vol. 30, no. 4, pp. 756–763, 2020.

[13] J. Fujimoto and E. Swanson, "The development, commercialization, and impact of optical coherence tomography," *Investigative Ophthalmology & Visual Science*, vol. 57, no. 9, pp. OCT1–OCT13, 2016.

[14] T. E. de Carlo, M. A. Bonini Filho, M. Adhi, and J. S. Duker, "Retinal and choroidal vasculature in birdshot chorioretinopathy analyzed using spectral domain optical coherence tomography angiography," *Retina*, vol. 35, no. 11, pp. 2392–2399, 2015.

[15] F. J. Freiberg, M. Pfau, J. Wons, M. A. Wirth, M. D. Becker, and S. Michels, "Optical coherence tomography angiography of the foveal avascular zone in diabetic retinopathy," *Graefe's Archive for Clinical and Experimental Ophthalmology*, vol. 254, no. 6, pp. 1051–1058, 2016.

[16] M. Ashraf, P. L. Nesper, L. M. Jampol, F. Yu, and A. A. Fawzi, "Statistical model of optical coherence tomography angiography parameters that correlate with severity of diabetic retinopathy," *Investigative Ophthalmology & Visual Science*, vol. 59, no. 10, pp. 4292–4298, 2018.

[17] K. Kim, E. S. Kim, and S. Y. Yu, "Optical coherence tomography angiography analysis of foveal microvascular changes and inner retinal layer thinning in patients with diabetes," *The British Journal of Ophthalmology*, vol. 102, no. 9, pp. 1226–1231, 2018.

[18] A. N. Kulikov, D. S. Maltsev, and M. A. Burnasheva, "Improved analysis of foveal avascular zone area with optical coherence tomography angiography," *Graefe's Archive for Clinical and Experimental Ophthalmology*, vol. 256, no. 12, pp. 2293–2299, 2018.

[19] D. Cao, D. Yang, Z. Huang et al., "Optical coherence tomography angiography discerns preclinical diabetic retinopathy in eyes of patients with type 2 diabetes without clinical diabetic retinopathy," *Acta Diabetologica*, vol. 55, no. 5, pp. 469–477, 2018.

[20] T. E. de Carlo, A. T. Chin, M. A. Bonini Filho et al., "Detection of microvascular changes in eyes of patients with diabetes but not clinical diabetic retinopathy using optical coherence tomography angiography," *Retina*, vol. 35, no. 11, pp. 2364–2370, 2015.

[21] F. Gómez-Ulla, P. Cutrin, P. Santos et al., "Age and gender influence on foveal avascular zone in healthy eyes," *Experimental Eye Research*, vol. 189, p. 107856, 2019.

[22] S. A. Somilleda-Ventura, D. M. Razo-Blanco-Hernandez, J. A. Reyes-Calderon, G. M. Ceballos-Reyes, and V. Lima-Gomez, "Circularity of the foveal avascular zone and its correlation with parafoveal vessel density, in subjects with and without diabetes," *Cirugia y Cirujanos*, vol. 87, no. 4, pp. 390–395, 2019.

[23] D. A. Antonetti, R. Klein, and T. W. Gardner, "Diabetic retinopathy," *The New England Journal of Medicine*, vol. 366, no. 13, pp. 1227–1239, 2012.

[24] I. Klaassen, C. J. Van Noorden, and R. O. Schlingemann, "Molecular basis of the inner blood-retinal barrier and its breakdown in diabetic macular edema and other pathological conditions," *Progress in Retinal and Eye Research*, vol. 34, pp. 19–48, 2013.

[25] S. Bonnin, V. Mané, A. Couturier et al., "New insight into the macular deep vascular plexus imaged by optical coherence tomography angiography," *Retina*, vol. 35, no. 11, pp. 2347–2352, 2015.

[26] F. Coscas, A. Glacet-Bernard, A. Miere et al., "Optical coherence tomography angiography in retinal vein occlusion: evaluation of superficial and deep capillary plexa," *American Journal of Ophthalmology*, vol. 161, pp. 160–171.e2, 2016.

[27] S. Yu, C. E. Pang, Y. Gong et al., "The spectrum of superficial and deep capillary ischemia in retinal artery occlusion," *American Journal of Ophthalmology*, vol. 159, no. 1, pp. 53–63.e2, 2015.

[28] G. Dimitrova, E. Chihara, H. Takahashi, H. Amano, and K. Okazaki, "Quantitative retinal optical coherence tomography angiography in patients with diabetes without diabetic retinopathy," *Investigative Ophthalmology & Visual Science*, vol. 58, no. 1, pp. 190–196, 2017.

[29] G. L. Trick, R. M. Burde, M. O. Gordon, J. V. Santiago, and C. Kilo, "The relationship between hue discrimination and contrast sensitivity deficits in patients with diabetes mellitus," *Ophthalmology*, vol. 95, no. 5, pp. 693–698, 1988.

[30] O. Arend, S. Wolf, F. Jung et al., "Retinal microcirculation in patients with diabetes mellitus: dynamic and morphological analysis of perifoveal capillary network," *The British Journal of Ophthalmology*, vol. 75, no. 9, pp. 514–518, 1991.

[31] X. X. Luo, J. G. Duan, P. Z. Liao et al., "Effect of qiming granule on retinal blood circulation of diabetic retinopathy: a multicenter clinical trial," *Chinese Journal of Integrative Medicine*, vol. 15, no. 5, pp. 384–388, 2009.

[32] F. Tang and C. Y. Cheung, "Quantitative retinal optical coherence tomography angiography in patients with diabetes without diabetic retinopathy," *Investigative Opthalmology & Visual Science*, vol. 58, no. 3, p. 1766, 2017.

[33] K. Y. Tey, K. Teo, A. C. S. Tan et al., "Optical coherence tomography angiography in diabetic retinopathy: a review of current applications," *Eye and Vision*, vol. 6, no. 1, p. 37, 2019.

[34] R. Forte, H. Haulani, and I. Jurgens, "Quantitative and qualitative analysis of the three capillary plexuses and choriocapillaris in patients with type 1 and type 2 diabetes mellitus without clinical signs of diabetic retinopathy: a prospective pilot study," *Retina*, vol. 40, no. 2, pp. 333–344, 2019.

[35] J. M. Simonett, F. Scarinci, F. Picconi et al., "Early microvascular retinal changes in optical coherence tomography angiography in patients with type 1 diabetes mellitus," *Acta Ophthalmologica*, vol. 95, no. 8, pp. e751–e755, 2017.

[36] A. Carnevali, R. Sacconi, E. Corbelli et al., "Optical coherence tomography angiography analysis of retinal vascular plexuses and choriocapillaris in patients with type 1 diabetes without diabetic retinopathy," *Acta Diabetologica*, vol. 54, no. 7, pp. 695–702, 2017.

[37] K. Sambhav, K. K. Abu-Amero, and K. V. Chalam, "Deep capillary macular perfusion indices obtained with OCT angiography correlate with degree of nonproliferative diabetic retinopathy," *European Journal of Ophthalmology*, vol. 27, no. 6, pp. 716–729, 2017.

[38] Y. Zeng, D. Cao, H. Yu et al., "Early retinal neurovascular impairment in patients with diabetes without clinically detectable retinopathy," *The British Journal of Ophthalmology*, vol. 103, no. 12, pp. 1747–1752, 2019.

[39] D. C. Sousa, I. Leal, S. Moreira et al., "A protocol to evaluate retinal vascular response using optical coherence tomography angiography," *Frontiers in Neuroscience*, vol. 13, p. 566, 2019.

Hindawi
Journal of Diabetes Research
Volume 2020, Article ID 2091341, 9 pages
https://doi.org/10.1155/2020/2091341

Research Article

Atherogenic Index of Plasma (AIP) a Tool to Assess Changes in Cardiovascular Disease Risk Post Laparoscopic Sleeve Gastrectomy

Eman Al Shawaf,[1] Ebaa Al-Ozairi,[2] Fahad Al-Asfar,[3] Anwar Mohammad,[1] Shaima Al-Beloushi,[4] Sriraman Devarajan,[5] Fahd Al-Mulla,[6] Jehad Abubaker,[1] and Hossein Arefanian[4]

[1]*Department of Biochemistry and Molecular Biology, Dasman Diabetes Institute, Kuwait*
[2]*Medical Division, Clinical Research Unit, Dasman Diabetes institute, Kuwait*
[3]*Departement of Surgery, Faculty of Medicine, Kuwait University, Kuwait*
[4]*Department of Immunology and Microbiology, Dasman Diabetes Institute, Kuwait*
[5]*National Dasman Diabetes Biobank, Dasman Diabetes Institute, Kuwait*
[6]*Research Division, Dasman Diabetes Institute, Kuwait*

Correspondence should be addressed to Jehad Abubaker; jehad.abubakr@dasmaninstitute.org and Hossein Arefanian; hossein.arefanian@dasmaninstitute.org

Received 21 April 2020; Revised 8 July 2020; Accepted 13 July 2020; Published 3 August 2020

Academic Editor: Claudio De Lucia

Predictive indices like the atherogenic index of plasma (AIP) have been developed to estimate the risk of cardiovascular disease (CVD). Metabolic surgery is the most effective treatment for a rapid improvement of morbid obesity and its comorbidities such as type 2 diabetes (T2D) and CVD. A decreased reoccurrence of CVD after metabolic surgery has been reported by several studies. However, studies utilizing predictive indices for CVD risk in CVD-free morbid-obese patients who undertook laparoscopic sleeve gastrectomy (LSG) are lacking. Here, we use AIP as a tool to evaluate the improvement in CVD risk post-LSG in morbid-obese people who had no history of CVD. *Method.* We compared baseline, 6- and 12-month post-LSG score of AIP, vascular age, circulating biochemical markers related to CVD in two groups of BMI and age-matched morbid-obese participants with and without T2D. *Results.* At baseline, people with T2D had significantly higher AIP both, with morbid obesity (0.23 ± 0.06, $p < 0.001$) and normal weight (0.022 ± 0.05, $p < 0.001$) compared to their BMI-matched without T2D group. People with morbid obesity had low AIP (-0.083 ± 0.06). Vascular age was significantly higher in people with morbid obesity and T2D (65.8 ± 3.7year, $p < 0.0001$) compared to morbid obesity (37.9 ± 2.6 year). After one year, AIP was significantly reduced compared to baseline score in people with morbid obesity with/without T2D, respectively (-0.135 ± 0.07, $p = 0.003$; and -0.36 ± 0.04, $p = 0.0002$). *Conclusion.* Our data illuminates AIP as a reliable predictive index for CVD risk in morbid-obese people who had no history of CVD. Moreover, AIP accurately distinguishes between morbid obesity with T2D and morbid obesity and showed a rapid and significant reduction in CVD risk after LSG in people who had no history of CVD. This is a ClinicalTrials.gov registered trial (Reference NCT03038373).

1. Introduction

Obesity is a global health burden that is associated with a number of abnormalities and comorbidities, most notably insulin resistance, dyslipidemia, hypertension [1], a higher risk of developing type 2 diabetes (T2D), and cardiovascular disease (CVD) [2]. The past years involved a rise in metabolic surgeries that emerged as a rapid and effective treatment option for people with severe obesity. These surgeries improved weight and resolved obesity-related comorbidities

through correcting various mechanisms/factors such as oxidative stress and inflammation [3–5].

Elevated levels of a proinflammatory molecule, such as c-reactive protein (CRP), contribute to a rise in oxidative stress and consequently lipid peroxidation. Oxidative stress is one of the factors contributing to vascular dysfunction, which is implicated in the pathogenesis of atherosclerosis, T2D, and hypercholesterolemia [6, 7]. Lipid peroxidation is a potential key event in pathological processes affecting the integrity of the vascular wall [8, 9]. In addition to this, dyslipidemia is another risk factor for premature atherosclerosis and an increased CVD risk. The significance of dyslipidemia is based on the triad of an increase in low-density lipoprotein (LDL) and triglycerides (TG) particles and a decrease in high-density lipoprotein (HDL) levels [10]. To assess patients' risk of developing CVD, various novel biomarkers have been identified [11]. The use of biomarkers in clinical investigation has a prognostic value, as it helps in an early identification of CVD at-risk patients [11–13]. Conventional risk factors for CVD helped in developing various risk prediction models, which had and continues to hold great importance. However, there is a considerable percentage of patients who do not show the traditional risk factors [11]. Additionally, quantitative measurement of LDL subpopulations was introduced as an effective way for CVD risk stratification, but the current analytical methodologies lack standardization and clear clinical relevance [14]. For which identifying novel biomarkers and developing new indices that are accurate, reliable and easy to quantify is required.

The atherogenic index of plasma (AIP) is a calculated index that strongly reflects the future risk of atherosclerosis and CVD and predicts atherogenicity [15–17]. AIP which is the logarithm of plasma TG to HDL ratio has shown a direct and independent association with arterial stiffness [17]. Considering the factors used to calculate AIP, this index reflects the opposing influence of TG and HDL on inflammation, oxidative stress, extracellular matrix formation, and the phenotypic changes affecting vascular smooth muscle [18, 19]. In this study, our aim was to assess the use of AIP in predicting CVD risk in morbid-obese people who had no history of CVD before and after laparoscopic sleeve gastrectomy (LSG). Furthermore, we used AIP to identify the time required for LSG to induce a significant change in the patients' CVD risk.

2. Materials and Methods

2.1. Study Population. The study included two main groups of people, individuals with morbid obesity who underwent LSG as a surgical intervention, and people with normal weight as control. The group with morbid obesity included people with T2D ($n = 17$, mean age 39 ± 2.5 years), and people without T2D ($n = 23$, mean age 32 ± 2.6 years). As described previously [20], from participants who underwent LSG, only 11 with T2D and 17 without T2D were followed up for one year after surgery (i.e., after 6 months and 1 year). The control groups included normal-weight participants that were not exposed to the surgical intervention. This included normal-weight people with T2D ($n = 19$) and normal-weight people without T2D ($n = 15$) who had no previous or current medical conditions. Exclusion criteria in this study were having a previous metabolic surgery, type 1 diabetes mellitus, T2D>5-years, insulin replacement therapy, CVD history, malignancy, and pregnancy. Power analysis for the study was calculated using G-Power software, version 3.1.9.6 [21, 22], to calculate the effective sample size required for our cross-sectional study. The total sample size requirement was calculated with a statistical power (1-β) of 0.09, α of 0.05, and an effective size of 0.80, whereby the minimum size was 34 participants in each group to test the hypothesis at $p < 0.05$. Recruitment process congregated 40 participants with morbid obesity and 34 participants with normal weight. Additionally, participants were classified depending on the presence/absence of T2D into 36 participants with T2D and 38 participants without T2D. This study was approved by the Scientific Advisory Board and Ethical Review Committee at Dasman Diabetes Institute (DDI). Both verbal and written consents were obtained from all participants. This is a ClinicalTrials.gov registered trial (Reference NCT03038373).

2.2. Anthropometric and Biochemical Measurements. As described [20], body measurements including weight, height, hip, and waist circumference were taken by a trained nurse. Blood pressure (BP) values are the average of three consecutive measurements. Body composition analysis was performed using the IOI 353 body composition Analyzer (Jawon Medical, Korea). The diagnostic criteria were based on ADA classification [23], according to which participants were classified as people with diabetes when having fasting plasma glucose ≥7.0 mmol/L, 2-hr postprandial plasma glucose ≥11.1 mmol/L, A1c ≥6.5%, or having a random blood glucose level ≥11.1 mmol/L in the presence of signs and symptoms of diabetes. Circulating biochemical parameters were quantified in peripheral venous blood samples collected from participants following an overnight fast, a minimum of 10 hours. Presurgery, baseline blood samples were collected from all participants. Follow-up visits involved a similar procedure of taking body composition and collecting fasting blood samples. Fasting insulin levels were determined using the Access Ultrasensitive Insulin Assay (Beckman Coulter, Brea, CA); c-peptide was determined by the DiaSorin LIAISON® analyzer. Fasting plasma glucose (FPG), serum total cholesterol (TC), LDL, HDL, TG, albumin, alanine aminotransferase (ALT), aspartate aminotransferase (AST), and high-sensitivity c-reactive protein (hsCRP) were measured by the Siemens Dimension RXL Max Integrated Chemistry analyzer (Diamond Diagnostics, Holliston, MA). A1c was measured using Variant™ (Bio-Rad, Hercules, CA). All clinical tests were performed by the clinical laboratory of Dasman Diabetes Institute as routine clinical diagnostic tests. In our research lab, plasma was collected from blood samples, aliquoted, and stored at -80°C for further analysis. Levels of oxidized low-density lipoprotein (oxLDL) were quantified through a commercial human ELISA kit (SEA527Hu; Wuhan USCN, China) following manufacturer's protocol with an intra-assay CV <10% and an interassay CV <12% (provided by the manufacturer).

Table 1: Clinical characteristics of study participants subjects at baseline.

Variable	Morbid obese			Normal weight		
	With T2D $N = 17$	Without T2D $N = 23$	p value	With T2D $N = 19$	Without T2D $N = 15$	p value
Age (year)	39.9 ± 2.4	31.5 ± 2.2		51.6 ± 2.1	39.9 ± 2.9	0.008*
Weight (kg)	121.0 ± 5.2	120.7 ± 4.8		67.4 ± 2.2	66.0 ± 3.0	
Height (cm)	166 ± 1.6	164.7 ± 2.2		166.2 ± 2.4	164.8 ± 2.2	
BMI (kg/m^2)	43.8 ± 1.5	44.6 ± 1.6		23.8 ± 0.2	23.5 ± 0.3	
Body fat (%)	42.8 ± 1.1	44.4 ± 1.0		28.6 ± 1.2	29.0 ± 1.0	
Abdominal circumference (cm)	128.6 ± 2.9	125.0 ± 2.9		96.0 ± 1.7	89.3 ± 2.0	
Waist/hip ratio	0.94 ± 0.02	0.87 ± 0.02		0.95 ± 0.01	0.8 ± 0.02	0.01*
SBP (mmHg)	127.9 ± 3.2	125.4 ± 2.6		125.7 ± 2.8	116.3 ± 4.6	
DBP (mmHg)	81.2 ± 2.2	76.5 ± 1.9		77.6 ± 2.4	71.3 ± 2.8	
Vascular age (year)	65.0 ± 3.0	37.0 ± 2.0	0.0001**	65.0 ± 3.0	38.0 ± 4.0	0.0001**
TC (mM)	4.8 ± 0.3	4.9 ± 0.1		4.4 ± 0.2	4.8 ± 0.2	
TG (mM)	1.54 (1.07-2.02)	0.92 (0.71-1.65)	0.01*	1.29 (0.91-1.73)	0.66(0.45-0.82)	0.001**
LDL (mM)	3.1 ± 0.2	3.1 ± 0.1		2.6 ± 0.2	2.9 ± 0.2	
HDL (mM)	0.9 ± 0.05	1.2 ± 0.1	0.003**	1.2 ± 0.05	1.6 ± 0.1	0.0008**
VLDL (mM)	0.7 ± 0.09	0.4 ± 0.05	0.025*	0.5 ± 0.045	0.3 ± 0.04	0.056
oxLDL (mg/mL)	1.7 ± 0.17	0.9 ± 0.09	0.007**	1.16 ± 0.23	1.18 ± 0.23	
AIP (log TG/HDL)	0.23 ± 0.06	−0.08 ± 0.06	0.0001**	0.02 ± 0.05	−0.39 ± 0.07	0.0006**
hsCRP (mg/dl)	1.4 ± 0.2	1.1 ± 0.1		0.27 ± 0.07	0.3 ± 0.07	
Insulin (pg/mL)	2092 ± 202	1210 ± 126	0.0004**	650 ± 112	350 ± 63	0.03*
c-peptide (pg/mL)	2407 ± 207	1824 ± 135	0.01*	1064 ± 118	875 ± 75	
FPG (mM)	10.7 ± 0.6	5.4 ± 0.08	0.0001**	10.0 ± 0.5	5.5 ± 0.1	0.0001**
A1c (%)	8.6 ± 0.3	5.8 ± 0.1	0.0001**	8.5 ± 0.4	5.5 ± 0.1	0.0001**
ALT (IU/L)	51 (39.5-67)	43 (35-56)		42 (38-54)	34 (32-39)	0.005**
AST (IU/L)	25 (19.5-36)	20 (16-30)		18 (16-22)	19 (16.75-20.5)	
Sex (women/men)	13 : 4	16 : 7		7 : 13	8 : 7	

Baseline data are presented as mean ± SEM, or median with interquartile. Based on the normality test, nonparametric comparison (Mann–Whitney test) or unpaired t-test (two-tailed) was applied to test significance between diabetic and nondiabetic subjects in both groups, p value ≤0.05 was considered significant (*), and p value <0.01 indicates highly significant values (**). SBP, DBP: Systolic and diastolic blood pressure; TC: total cholesterol; TG: triglycerides;ALT: alanine aminotransferase; AST: aspartate aminotransferase; hsCRP: high-sensitivity c-reactive protein; FPG: fasting plasma glucose; A1c: hemoglobin A1c.

2.3. Calculations. Body mass index, BMI (kg/m^2), was calculated as the body weight (in kilograms)/height (in square meters). Hip and waist circumference values were used to calculate the waist-hip ratio. AIP was calculated as the base 10 logarithm of the ratio of (TG/HDL) [15]. An AIP value <0.11 is associated with a low risk of CVD; AIP value from 0.11 to 0.24 indicates an intermediate CVD risk, while AIP ≥0.24 suggests an increased CVD risk [15, 16]. Framingham CVD risk equation was used to calculate an estimate of participants' vascular age [24]. In this mathematical model, various parameters are considered including age, sex, diabetes, systolic blood pressure, smoking, TC, and HDL levels.

2.4. Statistical Analysis. Statistical analysis was performed as previously described [20]. Briefly, normal distribution was tested using the Shapiro-Wilk normality test. Differences between the study groups at baseline were determined by a two-tailed unpaired t-test for normally distributed parameters. Data not following normal distribution was analyzed with nonparametric tests, Mann–Whitney U and Wilcoxon test, as appropriate to evaluate the difference between study groups at baseline. Analysis of variance (ANOVA) was used to compare pre- and postsurgery data and Bonferroni test for multiple comparisons to determine statistical significance. Data are presented as mean ± SEM, or median with interquartile range, with a p value ⊠0.05 indicating significance. Statistical analysis was performed using GraphPad Prism 6 software (GraphPad software, Inc., CA, USA) and SPSS version 25 (SPSS Inc., Chicago, IL, USA).

3. Results

Table 1 summarizes the anthropometric characteristics and metabolic variables of the study population at baseline.

Levels of hs-CRP were elevated in people with morbid obesity and T2D (1.3 ± 0.1 mM, $n = 17$) and without T2D (1.1 ± 0.1 mM, $n = 23$), reflecting a state of inflammation that suggests a possible moderate CVD risk in participants with morbid obesity, both with and without T2D. At baseline, lipid profile of people with morbid obesity and T2D was characterized by increased levels of TG (median: 1.54, 1.07-2.02, $n = 17$), and very-low-density lipoprotein (VLDL; 0.7 ± 0.08 mM, $n = 17$) and reduced HDL (0.9 ± 0.04 mM, $n = 17$) that was significantly different from people with morbid obesity (Table 1).

3.1. Diabetes Is a Critical Factor in Determining AIP and the Vascular Age of Patients. At baseline, the AIP showed that (1) people with T2D had elevated levels of AIP (i.e., both morbid obese and normal weight) compared to participants without T2D; (2) AIP was significantly higher in people with morbid obesity and T2D (0.23 ± 0.06 log TG/HDL, $n = 17$, $p < 0.001$) compared to BMI-matched people (-0.083 ± 0.06 log TG/HDL, $n = 23$), and normal-weight participants with T2D (0.02 ± 0.05 log TG/HDL, $n = 19$, $p < 0.001$) compared to control (-0.39 ± 0.07 log TG/HDL, $n = 15$); (3) normal-weight participants with T2D had lower AIP score (0.022 ± 0.05 log TG/HDL, $n = 19$), indicating a lower CVD risk compared to participants with morbid obesity and T2D. This suggests T2D as an essential factor for higher AIP score; however, T2D combined with obesity would exacerbate the condition leading to a significant increase in AIP score and consequently elevated CVD risk (Figure 1(a)). Quantification of plasma oxLDL showed that people with morbid obesity and T2D had the highest levels of oxLDL (1.7 ± 0.17 mg/mL, $n = 17$, $p < 0.01$) compared to other groups (Table 1).

There was a significant increase in the estimated vascular age in comparison to the actual age at baseline (Table 1). The comparison between the actual age and the calculated vascular age showed participants with morbid obesity and T2D to have the highest mean difference 26 ± 2.5 years (95% CI: 20.6–31.28, $p < 0.001$). People with normal weight and T2D showed the second-highest difference between vascular age and their actual age, with a mean difference 14 ± 3, (95% CI: 8.27–21.06, $p < 0.01$). Finally, people with morbid obesity had the lowest mean difference 6 ± 1.5 years (95% CI: 3.11–9.75, $p < 0.001$). There was no significant difference between the actual age and the vascular age in people with normal weight (Figure 1(b)).

3.2. LSG Reduces the Risk of CVD and Improves Vascular Age of Patients. Post-LSG participants displayed a rapid improvement in various clinical parameters. LSG ameliorated FPG, A1C, c-peptide, insulin resistance (iHOMA-IR), and β-cell activity (iHOMA2% β), indicating T2D remission (previously reported [20]). There was a gradual decline in weight loss post-LSG that was reflected by BMI, excess weight loss (%EWL), and body fat (%BF) in people with morbid obesity, with and without T2D, which was significant after one year of LSG [20]. Lipid metabolism improved significantly post-LSG, and VLDL levels dropped significantly after 6 months (0.48 ± 0.07 mM, $n = 10$, $p < 0.05$) and 1 year (0.39 ± 0.06 mM, $n = 10$, $p < 0.01$) of surgery in people with morbid obesity and T2D. There was no significant difference between levels of oxLDL at baseline and 1-year post-LSG, in people with morbid obesity (i.e., with and without T2D) (Table 2).

In general, there was a gradual decline in AIP score post-LSG (Figure 2). People with morbid obesity and T2D showed a significant reduction in AIP score after 6 months of LSG (-0.03 ± 0.07 log TG/HDL, $n = 11$, $p < 0.05$), and AIP was further reduced after 1 year (-0.13 ± 0.09 log TG/HDL, $n = 11$, $p < 0.01$). AIP in people with morbid obesity significantly changed after 1 year of surgery (-0.36 ± 0.04 log TG/HDL, $n = 17$, $p < 0.01$). Furthermore, we report a prominent decline in the calculated vascular age in both study groups after 1 year of LSG. The difference between the actual age and the calculated vascular age decreased by 23% in people with morbid obesity and T2D, and it dropped by 6.5% in people with obesity. Consequently, there was no significant statistical difference between the actual age and the calculated vascular age of participants 1 year after LSG (Table 2).

4. Discussion

Obesity on its own or when combined with T2D introduces a range of physiological and biochemical abnormalities that predispose to the development of CVD. Many studies have reported the relationship between obesity, inflammation, and CVD and its consequences on vascular structure and function, which leads to the development of atherosclerosis [25]. As such, an early detection of atherosclerosis at the subclinical period is important. In clinical settings, plasma lipoprotein profile is used as an indicator of cardiovascular risk; however, recent studies have reported the atherogenic index of plasma as a better marker of atherosclerosis and arterial stiffness [17, 26].

In the present study, we used AIP as a tool to evaluate the vascular health of participants concomitantly with the conventional biomarkers. The measurements were taken at baseline and subsequently after LSG, to ascertain the improvement in the vascular health of individuals with obesity and T2D. From our results, T2D was associated with elevated AIP, and AIP score exacerbated when T2D was combined with morbid obesity (Figure 1(a)). The AIP results corroborated with the vascular age data, whereby the greatest increase occurred in individuals with T2D and morbid obesity combined. Additionally, independent of obesity, T2D was associated with an increase in the vascular age (Figure 1(b)). Therefore, our data supports the use of AIP as a method to reflect vascular health and potential CVD risk.

Our baseline data showed that people with morbid obesity (i.e., with and without T2D) have a significant increase in inflammation compared to people with normal weight (Table 1). On the other hand, people with T2D showed an abnormal lipid profile, and this is independent of BMI. In our study, people with T2D, both with morbid obesity and normal weight, had a significant increase in TG and VLDL levels and a significant reduction in HDL levels compared to those without T2D (Table 1). In people with T2D, hypertriglyceridemia occurred secondary to having high

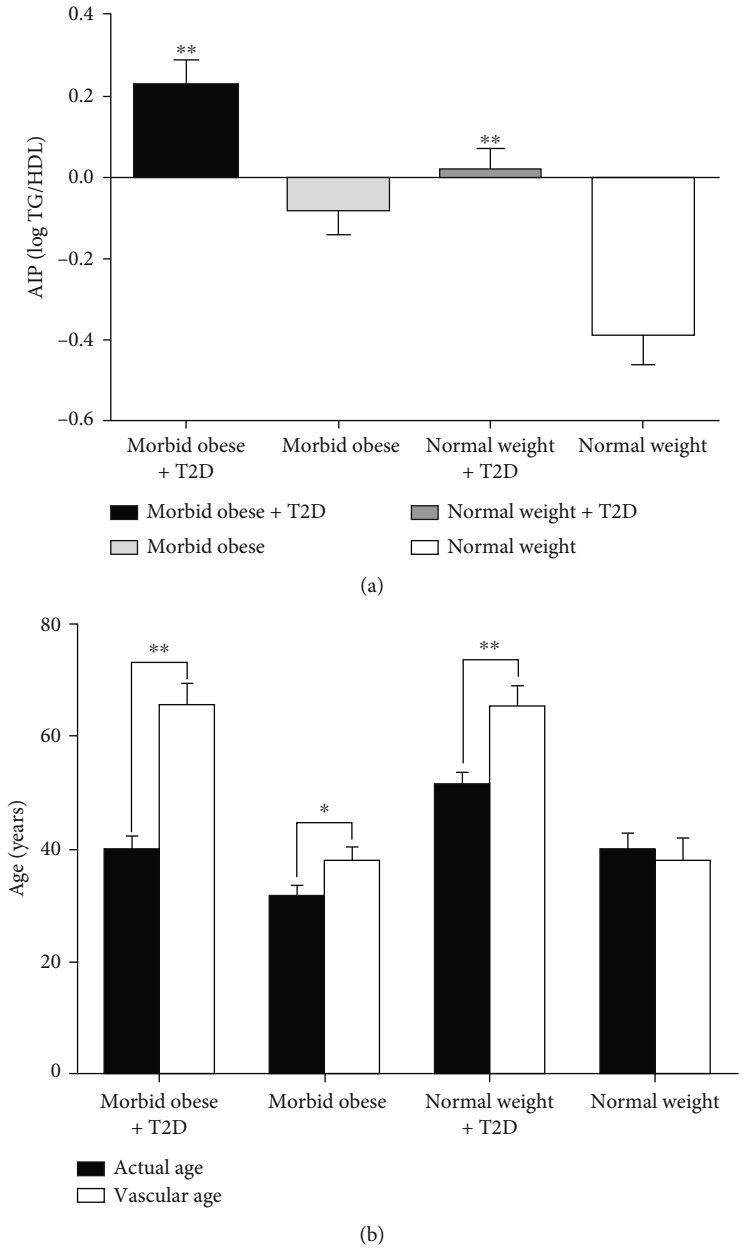

Figure 1: Baseline data calculation of (a) Atherogenic index of plasma (AIP) score in all study groups. Participants with morbid obesity and T2D ($n = 17$) show a significantly higher AIP (0.23 ± 0.06, $p < 0.0001$), compared to morbid obesity alone ($n = 23$, -0.083 ± 0.06). In participants with normal-weight and T2D ($n = 19$), the calculated AIP (0.022 ± 0.05) reflecting a lower CVD risk was compared to participants with morbid obesity and T2D. Black, light gray, dark gray, and white bars represent calculated baseline AIP of morbid obese + T2D, morbid obese, normal weight + T2D, and normal weight groups, respectively. (b) The estimated vascular age (Framingham score) has a significant rise in participants with T2D from both weight groups morbid obese (65.8 ± 3.7 year), and normal weight (65.6 ± 3.6 year, $p < 0.0001$) compared to their actual age. Participants with morbid obesity showed a significant difference between the vascular age (37.9 ± 2.6 year, $p < 0.001$) and chronological age. There was no significant difference between the vascular age and the actual age of people with normal weight. Black and white bars represent actual age and estimated vascular age, respectively, in each group. $^{*}p < 0.001$, and $^{**}p < 0.0001$.

levels of VLDL, small dense LDL (sdLDL), and low HDL levels [27, 28], which are known to hold atherogenic traits [29]. Henceforth, TG levels would serve as a predictive marker for atherosclerosis and potential CVD. Moreover, sdLDL particles were reported with a significant role in the development of arteriosclerosis and CVD [28]. Therefore, the importance of AIP as an index to detect premature atherosclerosis [30] came from its correlation with sdLDL particles [31], and its inverse correlation with LDL particle size [32].

Considering the importance of oxLDL molecules in systemic inflammation and oxidative stress [33], we quantified

Table 2: Clinical characteristics of the morbid-obese participants baseline, 6-month, and 1-year post-LSG.

Variable	Morbid obese with T2D			Morbid obese without T2D		
	Baseline ($n = 11$)	6 months ($n = 11$)	1 year ($n = 11$)	Baseline ($n = 17$)	6 months ($n = 17$)	1 year ($n = 17$)
BMI (kg/m^2)	41 ± 1	31** ± 0.75	31** ± 1	44 ± 1	31 ± 1	28 ± 1
EBL (%)	—	61** ± 4	59** ± 7	—	67** ± 3	83** ± 5
EWL (%)	—	62** ± 4	60** ± 6	—	66** ± 4	86** ± 6
Body fat (%)	45 ± 1	29** ± 2	27** ± 2	47 ± 1	32** ± 2	26** ± 2
VFA (cm^2)	200 ± 9	121* ± 6	113** ± 8	211 ± 6	120 ± 13	87** ± 8
SBP (mmHg)	127.9 ± 3.1	117.6 ± 4.5	111.1** ± 3.3	125.4 ± 2.6	120.5 ± 3.5	116.8 ± 3.4
DBP (mmHg)	81.1 ± 2.2	72.9* ± 2.7	68.2** ± 1.6	76.4 ± 1.9	72.1 ± 1.7	69.9 ± 2
Vascular age (year)	65 ± 3	55 ± 5	50* ± 5	37 ± 2	35 ± 3	34 ± 3
TC (mM)	5.02 ± 0.34	5.2 ± 0.53	5 ± 0.46	5 ± 0.1	4.7** ± 0.11	4.8 ± 0.14
TG (mM)	1.84 (1.09-2.8)	0.98** (0.7-1.4)	1.14** (0.6-1.2)	0.88 (0.7-1.7)	0.76* (0.6-1.01)	0.58** (0.44-1)
LDL (mM)	3.15 ± 0.2	3.8 ± 0.5	3.7 ± 0.4	3.1 ± 0.1	2.8 ± 0.1	2.9 ± 0.1
HDL (mM)	0.97 ± 0.07	1.2 ± 0.08	1.3** ± 0.12	1.3 ± 0.08	1.4 ± 0.08	1.5* ± 0.07
VLDL (mM)	0.8 ± 0.12	0.46* ± 0.07	0.37** ± 0.05	0.45 ± 0.05	0.33* ± 0.02	0.3** ± 0.03
oxLDL (mg/mL)	1.7 ± 0.17	1.58 ± 0.3	1.55 ± 0.3	0.9 ± 0.09	0.7 ± 0.06	0.8 ± 0.08
AIP (log TG/HDL)	0.27 ± 0.09	−0.03** ± 0.07	−0.13** ± 0.07	−0.11 ± 0.07	−0.26 ± 0.03	−0.36** ± 0.04
hsCRP (mg/dl)	1.24 ± 0.2	0.62 ± 0.2	0.39** ± 0.1	1.23 ± 0.1	0.47* ± 0.06	0.47* ± 0.07
Insulin (pg/mL)	2176 ± 273	608** ± 64	923** ± 186	1132 ± 147	308** ± 69	298** ± 45
c-peptide (pg/mL)	2328 ± 303	1164* ± 129	1156** ± 189	1804 ± 172	1063* ± 128	843** ± 92
FPG (mM)	10.6 ± 0.7	5.4** ± 0.2	5.4** ± 0.2	5.4 ± 0.1	4.8* ± 0.06	4.8** ± 0.1
A1c (%)	8.5 ± 0.5	6** ± 0.12	5.6** ± 0.1	5.7 ± 0.1	5.3* ± 0.09	5.4* ± 0.1
ALT (IU/L)	40 (37-53)	31 (28-34)	34 (29-38)	39 (32.5-53)	31 (27-34)	29 (27-39)
AST (IU/L)	23 (17-28)	15 (12-19)	18 (16-25)	18 (15.5-27)	18 (14.5-19)	13 (10-19)

Baseline, 6 months, and 1-year post-LSG data are presented as mean ± SEM, or median with interquartile. Analysis of variance (ANOVA) (unpaired analysis) with post hoc Bonferroni test for multiple comparisons was used to determine significant change post-LSG in diabetic and nondiabetic morbid-obese subjects, p value ≤0.05 was considered significant (*), and p value <0.01 indicates highly significant values (**). VFA: visceral fat area; %EWL: percent excess weight loss; %EBL: percent of excess BMI loss.

levels of circulating oxLDL. In our study, oxLDL was elevated in people with morbid obesity and T2D, in comparison to all other groups (Table 1). Elevated levels of circulating oxLDL have been associated with obesity, hyperglycemia, and hypertriglyceridemia [34]. Nonetheless, changes in oxLDL levels after LSG were not significant in comparison to baseline levels (Table 2). The absence of a significant change in LDL oxidation in our results might be due to other factors related to the study population. The study was limited to people who had been diagnosed with T2D <5 years and had no history of CVD. This might indicate that specific pathological conditions are required to exacerbate the presence of oxLDL at which it would serve as a marker of inflammation and atherosclerosis, which were not attained in our study population. On the other hand, the association between oxLDL and metabolic syndrome is established, where weight loss was found to reduce oxLDL [35, 36]. Thus, our oxLDL data must be interpreted with caution.

Baseline AIP was elevated in people with T2D compared to those without diabetes. Additionally, people with both obesity and T2D had the highest AIP score suggesting an intermediate risk of CVD, compared to people with a normal weight and T2D. In the absence of T2D, people with obesity and normal weight had low AIP values indicating a negligible adverse effect on vascular health (Figure 1(a)). This was emphasized in a recent report where having a combination of low HDL levels and high TG accompanied by reduced insulin sensitivity defined atherogenic dyslipidemia [37]. Additionally, we used Framingham's CVD Risk Predictive formula as a method to estimate the vascular age of participants [38, 39]. Our data showed a significant rise in the calculated vascular age of people with T2D and morbid obesity (Figure 1(b)), which accentuated the deleterious effects of T2D and dyslipidemia on vascular health. Independent of T2D, there was a significant difference between the actual age and the calculated vascular age of participants with morbid obesity; however, the difference was less prominent compared to the combined effect of T2D and obesity.

AIP is an independent risk factor of coronary artery disease, which has been associated with the lipoprotein particle size and was found to have an inverse correlation with LDL particle size [17]. AIP is reported to have a predictive potential for hypertension, diabetes, and vascular events [16, 31] as it reflects the health of the arteries through a number of

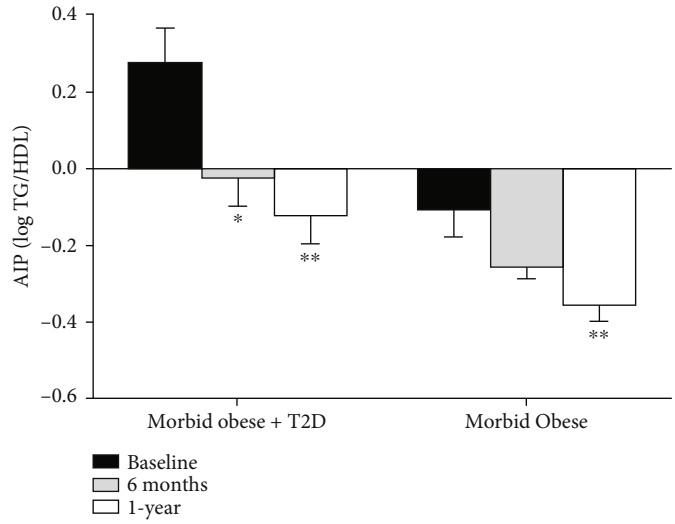

Figure 2: Improvement in AIP score post-LSG. There is a significant drop in AIP score in participants with morbid obesity and T2D, $n = 11$ after 6 months (-0.03 ± 0.07, $p < 0.01$) and after 1 year of LSG (-0.13 ± 0.07, $p < 0.01$) compared to their baseline levels. In people with morbid-obesity ($n = 17$), AIP decreased after 6 months of LSG (-0.26 ± 0.03), and the change was significant only after 1 year of LSG (-0.36 ± 0.04, $p < 0.001$) compared to the baseline levels. Black, gray, and white bars represent calculated AIP at baseline, 6-month, and 1-year post-LSG, respectively. $^{*}p < 0.01$, and $^{**}p < 0.001$.

processes involved in arterial stiffness such as inflammation, oxidative stress, extracellular matrix formation, and vascular smooth muscle phenotype change. Dobiasova et al. reported a significant correlation between AIP and the number of total large and medium-sized VLDL particles [16]. Additionally, AIP was significantly associated with the atherogenic apoB and the atheroprotective ApoAI molecules [16]. Considering the importance and efficacy of AIP in predicting and evaluating CVD risk [15–17, 31], we utilized it to evaluate the effect of LSG on patients' vascular health. Our data showed a significant improvement in AIP score post-LSG, which indicated an improvement in the vascular health of people with morbid obesity and T2D. The improved vascular health came secondary to an improved lipid metabolism, insulin sensitivity, and T2D remission after LSG. Therefore, an easily calculated index as AIP would be a valuable tool to monitor the efficacy of metabolic surgery on vascular health. It is noteworthy to highlight that our study participants were diagnosed with T2D for a relatively short time span (i.e., ≤5 years). This was a critical factor to limit and avoid the occurrence of nonreversible T2D complications, and consequently allow T2D remission.

Our study displayed several limitations, including the small sample size combined with the difference in men/women ratio, the lack of a detailed analysis of LDL population, and a relatively reduced follow-up rate in some post-LSG visits due to unexpected circumstances leading to participants unavailability. This is a major limitation for which our data should be interpreted with caution. A similar study on a larger scale that would consider including other parameters as a direct measurement of arterial stiffness (i.e., pulse wave velocity) would be expected to give a better understanding of the importance of AIP as a simple tool to evaluate the rapid improvement in vascular health after metabolic surgery procedures.

5. Conclusion

Our AIP data showed T2D as an important factor with a potential effect on vascular health. AIP score was worsened with the combined effect of T2D and morbid obesity. AIP as a reflection of vascular health, accurately made the distinction between the conditions, T2D, morbid obesity or T2D, and morbid obesity combined. Additionally, AIP showed the rapid improvement post-LSG indicating a quick reversion and restoration of cardiovascular health. Thus, AIP would be an alternative to complex and expensive methods that require measuring LDL subpopulations (e.g., using filtration chromatography) and determination of sdLDL concentration to evaluate biomarkers atherogenic potential in patients.

Abbreviations

AIP:	Atherogenic index of plasma
T2D:	Type 2 diabetes mellitus
CVD:	Cardiovascular disease
LSG:	Laparoscopic sleeve gastrectomy
BMI:	Body mass index
%EWL:	Percent excess weight loss
%EWL:	Percent of excess BMI loss
SBP, DBP:	Systolic and diastolic blood pressure
HDL:	High-density lipoprotein-cholesterol
LDL:	Low-density lipoprotein-cholesterol
VLDL:	Very low-density lipoprotein
oxLDL:	Oxidized low-density lipoprotein
TC:	Total cholesterol
TG:	Triglycerides
hsCRP:	High sensitivity c-reactive protein
FPG:	Fasting plasma glucose
A1c:	Hemoglobin A1c.

Data Availability

Data will only be shared upon request from the corresponding authors due to unpublished data and ethical restriction by the institute.

Conflicts of Interest

The authors declare that there are no Potential Conflicts of interest associated with this manuscript.

Authors' Contributions

EA and HA performed the study design, data collection, analysis and data interpretation, and laboratory investigation and wrote the manuscript. EO did the study design, patient follow-up, and reviewed the manuscript critically. FA performed LSG surgical intervention. AM involved in manuscript conception and critical revision of the manuscript. SA performed patient coordination, sample collection, and blood processing. SD conceived the data and statistical analysis. FM revised the manuscript critically. HA and JA did the data interpretation and critically revised manuscript.

Acknowledgments

We are grateful to Clinical Laboratory and the Tissue Bank Core Facility at DDI for their contribution in handling samples. Special thanks go to Mrs. Sabina Sabau, Etab Taghadom, Asma Alhubail, Hadeel Malallah, Surbhi Kumari, and Dr. Mira Bisso for their technical support. The corresponding authors had full access to all the data in the study and had final responsibility for the decision to submit for publication. This work was supported by the Kuwait Foundation for the Advancement of Science (KFAS) under project (RA 2011-014).

References

[1] S. M. Grundy, J. I. Cleeman, S. R. Daniels et al., "Diagnosis and management of the metabolic Syndrome," *Circulation*, vol. 112, no. 17, pp. 2735–2752, 2005.

[2] R. H. Eckel, S. M. Grundy, and P. Z. Zimmet, "The metabolic syndrome," *The Lancet*, vol. 365, no. 9468, pp. 1415–1428.

[3] E. João Cabrera, A. C. Valezi, V. D. A. Delfino, E. L. Lavado, and D. S. Barbosa, "Reduction in plasma levels of inflammatory and oxidative stress indicators after roux-en-Y gastric bypass," *Obesity Surgery*, vol. 20, no. 1, pp. 42–49, 2010.

[4] H. Uzun, D. Konukoglu, R. Gelisgen, K. Zengin, and M. Taskin, "Plasma protein carbonyl and thiol stress before and after laparoscopic gastric banding in morbidly obese patients," *Obesity Surgery*, vol. 17, no. 10, pp. 1367–1373, 2007.

[5] G. Kisakol, E. Guney, F. Bayraktar, C. Yilmaz, T. Kabalak, and D. Özmen, "Effect of surgical weight loss on free radical and antioxidant balance: a preliminary report," *Obesity Surgery*, vol. 12, no. 6, pp. 795–800, 2002.

[6] Z. Nedeljkovic, N. Gokce, and J. Loscalzo, "Mechanisms of oxidative stress and vascular dysfunction," *Postgraduate Medical Journal*, vol. 79, no. 930, pp. 195–200, 2003.

[7] K. Luc, A. Schramm-Luc, T. J. Guzik, and T. P. Mikolajczyk, "Oxidative stress and inflammatory markers in prediabetes and diabetes," *Journal of Physiology and Pharmacology*, vol. 70, no. 6, 2019.

[8] E. Esteve, W. Ricart, and J. M. Fernández-Real, "Dyslipidemia and inflammation: an evolutionary conserved mechanism," *Clinical Nutrition*, vol. 24, no. 1, pp. 16–31, 2005.

[9] A. Nègre-Salvayre, N. Augé, C. Camaré, T. Bacchetti, G. Ferretti, and R. Salvayre, "Dual signaling evoked by oxidized LDLs in vascular cells," *Free Radical Biology & Medicine*, vol. 106, pp. 118–133, 2017.

[10] F. H. Rached, M. J. Chapman, and A. Kontush, "An overview of the new frontiers in the treatment of atherogenic dyslipidemias," *Clinical Pharmacology and Therapeutics*, vol. 96, no. 1, pp. 57–63, 2014.

[11] J. Wang, G.-J. Tan, L.-N. Han, Y.-Y. Bai, M. He, and H.-B. Liu, "Novel biomarkers for cardiovascular risk prediction," *Journal of Geriatric Cardiology*, vol. 14, no. 2, pp. 135–150, 2017.

[12] A. F. G. Cicero, S. Gitto, F. Fogacci et al., "Fatty liver index is associated to pulse wave velocity in healthy subjects: data from the Brisighella Heart Study," *European Journal of Internal Medicine*, vol. 53, pp. 29–33, 2018.

[13] A. F. G. Cicero, F. Fogacci, G. Tocci et al., "Awareness of major cardiovascular risk factors and its relationship with markers of vascular aging: data from the Brisighella Heart Study," *Nutrition, Metabolism and Cardiovascular Diseases*, vol. 30, no. 6, pp. 907–914, 2020.

[14] P. Srisawasdi, S. Vanavanan, M. Rochanawutanon et al., "Heterogeneous properties of intermediate- and low-density lipoprotein subpopulations," *Clinical Biochemistry*, vol. 46, no. 15, pp. 1509–1515, 2013.

[15] M. Dobiasova and J. Frohlich, "The plasma parameter log (TG/HDL-C) as an atherogenic index: correlation with lipoprotein particle size and esterification rate inapob-lipoprotein-depleted plasma (FERHDL)," *Clinical Biochemistry*, vol. 34, no. 7, pp. 583–588, 2001.

[16] M. Dobiasova, J. Frohlich, M. Sedova, M. C. Cheung, and B. G. Brown, "Cholesterol esterification and atherogenic index of plasma correlate with lipoprotein size and findings on coronary angiography," *Journal of Lipid Research*, vol. 52, no. 3, pp. 566–571, 2011.

[17] M. K. Choudhary, A. Eraranta, J. Koskela et al., "Atherogenic index of plasma is related to arterial stiffness but not to blood pressure in normotensive and never-treated hypertensive subjects," *Blood Pressure*, vol. 28, no. 3, pp. 157–167, 2019.

[18] M. F. O'Rourke, J. A. Staessen, C. Vlachopoulos, D. Duprez, and G. E. Plante, "Clinical applications of arterial stiffness; definitions and reference values," *American Journal of Hypertension*, vol. 15, no. 5, pp. 426–444, 2002.

[19] A. R. Aroor, G. Jia, and J. R. Sowers, "Cellular mechanisms underlying obesity-induced arterial stiffness," *American Journal of Physiology. Regulatory, Integrative and Comparative Physiology*, vol. 314, no. 3, pp. R387–R398, 2018.

[20] E. Al-Shawaf, E. Al-Ozairi, F. Al-Asfar et al., "Biphasic changes in angiopoietin-like 8 level after laparoscopic sleeve gastrectomy and type 2 diabetes remission during a 1-year follow-up," *Surgery for Obesity and Related Diseases*, vol. 14, no. 9, pp. 1284–1294, 2018.

[21] F. Faul, E. Erdfelder, A. Buchner, and A.-G. Lang, "Statistical power analyses using G∗Power 3.1: tests for correlation and regression analyses," *Behavior Research Methods*, vol. 41, no. 4, pp. 1149–1160, 2009.

[22] F. Faul, E. Erdfelder, A.-G. Lang, and A. Buchner, "G*Power 3: a flexible statistical power analysis program for the social, behavioral, and biomedical sciences," *Behavior Research Methods*, vol. 39, no. 2, pp. 175–191, 2007.

[23] American Diabetes Association, "2. Classification and Diagnosis of Diabetes: *Standards of Medical Care in Diabetes—2019*," *Diabetes Care*, vol. 42, Supplement 1, pp. S13–S28, 2018.

[24] R. B. D'Agostino, R. S. Vasan, M. J. Pencina et al., "General cardiovascular risk profile for use in primary care: the Framingham Heart Study," *Circulation*, vol. 117, no. 6, pp. 743–753, 2008.

[25] B. Freestone, S. Krishnamoorthy, and G. Y. H. Lip, "Assessment of endothelial dysfunction," *Expert Review of Cardiovascular Therapy*, vol. 8, no. 4, pp. 557–571, 2014.

[26] A. Icli, E. Cure, A. U. Uslu et al., "The Relationship Between Atherogenic Index and Carotid Artery Atherosclerosis in Familial Mediterranean Fever," *Angiology*, vol. 68, no. 4, pp. 315–321, 2016.

[27] M. W. Freeman and G. A. Walford, "Chapter 41- Lipoprotein Metabolism and the Treatment of Lipid Disorders," in *In: Endocrinology: Adult and Pediatric (Seventh Edition)*, J. L. Jameson, L. J. Groot, D. M. Kretser, L. C. Giudice, A. B. Grossman, S. Melmed, J. T. Potts, and G. C. Weir, Eds., no. article e717pp. 715–736, W.B.Saunders, Philadelphia, 2016.

[28] R. M. Krauss, "Lipids and lipoproteins in patients with type 2 diabetes," *Diabetes Care*, vol. 27, no. 6, pp. 1496–1504, 2004.

[29] M. Cure, A. Tufekci, E. Cure et al., "Low-density lipoprotein subfraction, carotid artery intima-media thickness, nitric oxide, and tumor necrosis factor alpha are associated with newly diagnosed ischemic stroke," *Annals of Indian Academy of Neurology*, vol. 16, no. 4, pp. 498–503, 2013.

[30] G. Yildiz, A. Duman, H. Aydin et al., "Evaluation of association between atherogenic index of plasma and intima-media thickness of the carotid artery for subclinic atherosclerosis in patients on maintenance hemodialysis," *Hemodialysis International*, vol. 17, no. 3, pp. 397–405, 2013.

[31] A. Onat, G. Can, H. Kaya, and G. Hergenc, ""Atherogenic index of plasma" ($\log_{10}$ triglyceride/high- density lipoprotein –cholesterol) predicts high blood pressure, diabetes, and vascular events," *Journal of Clinical Lipidology*, vol. 4, no. 2, pp. 89–98, 2010.

[32] X.-W. Zhu, F.-Y. Deng, and S.-F. Lei, "Meta-analysis of Atherogenic index of plasma and other lipid parameters in relation to risk of type 2 diabetes mellitus," *Primary Care Diabetes*, vol. 9, no. 1, pp. 60–67, 2015.

[33] B. M. Wolfe, E. Kvach, and R. H. Eckel, "Treatment of obesity: weight loss and bariatric surgery," *Circulation Research*, vol. 118, no. 11, pp. 1844–1855, 2016.

[34] G. J. Blake, N. Rifai, J. E. Buring, and P. M. Ridker, "Blood pressure, C-reactive protein, and risk of future cardiovascular events," *Circulation*, vol. 108, no. 24, pp. 2993–2999, 2003.

[35] P. Holvoet, "Association between circulating oxidized low-density lipoprotein and incidence of the metabolic syndrome," *JAMA*, vol. 299, no. 19, pp. 2287–2293, 2008.

[36] T. Weinbrenner, H. Schroder, V. Escurriol et al., "Circulating oxidized LDL is associated with increased waist circumference independent of body mass index in men and women," *The American Journal of Clinical Nutrition*, vol. 83, no. 1, pp. 30–35, 2006, quiz 181-182.

[37] S. Kutkiene, Z. Petrulioniene, A. Laucevicius et al., "Cardiovascular risk profile of patients with atherogenic dyslipidemia in middle age Lithuanian population," *Lipids in Health and Disease*, vol. 17, no. 1, p. 208, 2018.

[38] A. B. Adolphe, X. Huang, and L. S. Cook, "Carotid intima-media thickness determined vascular age and the Framingham Risk Score," *Critical Pathways in Cardiology*, vol. 10, no. 4, pp. 173–179, 2011.

[39] L. Jahangiry, M. A. Farhangi, and F. Rezaei, "Framingham risk score for estimation of 10-years of cardiovascular diseases risk in patients with metabolic syndrome," *Journal of Health, Population and Nutrition*, vol. 36, no. 1, p. 36, 2017.

Hindawi
Journal of Diabetes Research
Volume 2020, Article ID 7504798, 15 pages
https://doi.org/10.1155/2020/7504798

Review Article

Research Progress on the Pathological Mechanisms of Podocytes in Diabetic Nephropathy

Lili Zhang,[1] **Zhige Wen**,[1] **Lin Han**,[1] **Yujiao Zheng**,[2] **Yu Wei**,[2] **Xinmiao Wang**,[1] **Qing Wang**,[2] **Xinyi Fang**,[2] **Linhua Zhao**,[1] **and Xiaolin Tong**[1]

[1]*Department of Endocrinology, Guang'anmen Hospital, China Academy of Chinese Medical Sciences, Beijing 100053, China*
[2]*Graduate College, Beijing University of Traditional Chinese Medicine, Beijing 100029, China*

Correspondence should be addressed to Linhua Zhao; melonzhao@163.com and Xiaolin Tong; tongxiaolin@vip.163.com

Received 2 March 2020; Revised 3 June 2020; Accepted 23 June 2020; Published 10 July 2020

Academic Editor: Claudio De Lucia

Diabetic nephropathy (DN) is not only an important microvascular complication of diabetes but also the main cause of end-stage renal disease. Studies have shown that the occurrence and development of DN are closely related to morphological and functional changes in podocytes. A series of morphological changes after podocyte injury in DN mainly include podocyte hypertrophy, podocyte epithelial-mesenchymal transdifferentiation, podocyte detachment, and podocyte apoptosis; functional changes mainly involve podocyte autophagy. More and more studies have shown that multiple signaling pathways play important roles in the progression of podocyte injury in DN. Here, we review research progress on the pathological mechanism of morphological and functional changes in podocytes associated with DN, to provide a new target for delaying the occurrence and development of this disorder.

1. Introduction

Diabetic nephropathy (DN) is a common microvascular complication in diabetes, with a prevalence rate of 30–40% in patients with type 1 or type 2 diabetes [1]; DN also accounts for 30–47% of end-stage renal disease (ESRD). It is the main cause of death in diabetic patients and the main cause of renal failure in ESRD [2]. DN accounts for 54% of new ESRD [3], and about 30% of chronic dialysis patients [4, 5]. With the developing economy, change in diet, and decreasing physical activity, the incidence of DN is increasing. DN is a progressive process. The early clinical manifestations are glomerular hyperfiltration and increased urinary albumin excretion rate. The pathological features are glomerular basement membrane thickening, mesangial dilatation, and tuberous sclerosis [6, 7]. With the development of DN, the number of damaged glomeruli increases and the glomerular filtration rate decreases significantly. The clinical manifestations are massive proteinuria, and glomerular and tubulointerstitial fibrosis [8, 9]. More and more studies have shown that the occurrence and development of DN are closely related to podocyte injury [10]. Podocytes are a unique and highly differentiated terminal glomerular epithelial cell and are attached to the outside of the glomerular basement membrane (GBM) to form a glomerular filtration barrier together with endothelial cells and the GBM. Podocytes are an indispensable part of the glomerular filtration barrier. The morphological changes in podocytes after injury in DN include podocyte hypertrophy, podocyte epithelial-mesenchymal transdifferentiation (EMT), podocyte detachment, and podocyte apoptosis [11]. The main functional changes involve podocyte autophagy. This article reviews research progress on the pathological mechanisms related to the morphological and functional changes of podocytes in DN.

2. Functional Changes of Podocytes

2.1. Autophagy. Autophagy was first proposed by Belgian scientist Christian de Duff in 1963, after Ashford and Porter discovered the phenomenon of "self-eating" in cells in 1962 [12]. Subsequent studies focused on the regulatory

mechanisms of autophagy and its effects on human health and disease. Autophagy is a highly conserved process of intracellular protein recycling, which involves transferring damaged proteins and organelles to lysosomes for degradation; autophagy serves to mediate the recycling of intracellular nutrients, the continuous renewal of organelles, and the maintenance of intracellular homeostasis [13]. According to the different types of degraded substrates, the function of autophagy in cells is mainly classified as selective or nonselective autophagy [14–16]; in a nutrient-deficient environment, the recycling of intracellular energy sources is termed nonselective autophagy [17], and the removal of cytotoxic proteins and damaged organelles under different emergency conditions is known as selective autophagy [18]. In addition, depending on the different ways in which intracellular substrates are transported to lysosomes, autophagy can be divided into three types: macroautophagy, microautophagy, and molecular chaperone-mediated autophagy [19]; macroautophagy is the most widely studied process at present [20] and is the focus of this review.

2.2. Podocyte Autophagy and DN. Autophagy is a defense mechanism that is essential for maintaining podocyte homeostasis [21]. One study found that under normal circumstances, podocytes maintain a high level of autophagy for a long time [22]. However, there is a downregulation of podocyte autophagy activity in DN [23]. Continuous high glucose (HG) in DN can inhibit the expression of autophagy-related proteins Beclin-1, Atgl2, and LC3-II, weaken podocyte autophagy, and prevent the timely removal of damaged proteins and cytotoxins produced by organelle accumulation, resulting in irreversible podocyte damage and dysfunction [24, 25]. Tagawa et al. [26] directly revealed the progress of podocyte autophagy in DN for the first time. Presently, it has been found that a variety of signal pathways are involved in the regulation of podocyte autophagy, among which DN is closely related to mammalian target of rapamycin (mTOR), AMP-activated protein kinase (AMPK), oxidative stress, NAD +-dependent histone deacetylase, silent information regulatory factor-1 (Sirt1) signal pathway, Atg12-ATG5 coupling system, and vascular endothelial growth factor (VEGF).

2.2.1. mTOR Signaling Pathway. mTOR is an evolutionarily highly conserved serine/threonine-protein kinase, which plays a key role in regulating cell growth and proliferation. It is very important to inhibit autophagy [27–31]. mTOR exists widely in eukaryotes. In mammals, it combines with different proteins to form two complexes with different structures and functions, mTORC1 and mTORC2. mTORC1 is sensitive to rapamycin and is mainly involved in the regulation of cell growth and development, proliferation, apoptosis, metabolism, autophagy, and so on. Studies have shown that the pathogenesis of DN is related to the activity of the mTORC1 pathway [22]. In a HG environment, mTORC1 was activated and protective autophagy was inhibited. The expression of mTORC1 was found to be upregulated in all patients with DN. MTORC1 was highly activated after knockout of a podocyte-specific upstream inhibitor of mTOR gene tuberous sclerosis complex 1 (TSC1), which inhibited autophagosomes by activating UNC-51-like kinase (ULK1) activity, resulting in podocyte damage [28, 32, 33]. In addition, rapamycin increases the number of LC3-expressing podocytes, promotes podocyte autophagy, and ameliorates renal injury in diabetic mice [34]. It is suggested that mTORC1 activity plays a key regulatory role in DN podocyte injury. Recently, Liu et al. [35] research confirmed that rapamycin inhibits mTOR activity, thereby regulating the pathological autophagic process. These studies suggest that mTOR activation in podocytes is the key reason for the occurrence and development of DN.

2.2.2. AMPK Signal Pathway. AMPK is a heterotrimeric protein composed of one catalytic subunit (α subunit) and two regulatory subunits (β and γ subunits) of a serine protein kinase [36]. It plays an important role in the cells and tissues of patients with DN and is also an important metabolic stress protein kinase. AMPK can be activated by an increase in Ca^{2+} concentration in the cytoplasm [37, 38] and by the stimulation of numerous hormones, adipokines, and cytokines. Additionally, a decrease in the ratio of intracellular AMP/ATP activates AMPK, as does nutrient starvation. Under HG conditions, the phosphorylation level of AMPK is decreased and its activity is inhibited. AMPK could inhibit mTORC1 activity and induce autophagy through TSC1/2-Rheb signaling pathways and/or phosphorus acidification of raptor-related regulatory protein [31]. Additionally, AMPK directly mediates the phosphorylation of Ulkl/2 and induction of autophagy [39]. Other studies have shown that resveratrol, an AMPK activator, can reduce the early renal injury of DN by restoring the activity of AMPK in streptozotocin-induced diabetic rats [40]. Jin et al. [41] have shown that berberine can reduce HG-induced mouse podocyte autophagy by enhancing the activity of AMPK.

2.2.3. Oxidative Stress. In 2001, Brownlee proposed that oxidative stress is commonly involved in the pathogenesis of diabetes and its complications [42]. Under HG conditions, cells produce a large number of advanced glycation end products (AGEs), which accumulate in the cells. In the process of AGE production, mitochondria release a large amount of reactive oxygen species (ROS), and excess ROS disturbs the balance of the oxidation and antioxidant systems, resulting in cell damage. Specifically, AGEs produced by cells stimulated by HG can upregulate the expression of the angiotensin II (AngII) receptor [43]. An in vitro podocyte experiment also showed that the expression of AngII increased under HG conditions [44]. Stimulated by AngII, podocytes increase ROS production and autophagy activation [45]. A study by Ma et al. [46] found that exposure to HG for 24 hours activated podocyte autophagy, through an upregulation of ROS production, and they also found that HG induced the generation of ROS by podocytes in a time-dependent manner. Wang et al. [47] found that the Rho/ROCK signal pathway may be activated, and Drp1 at serine 600, as a substrate of the Rho signal pathway, can initiate mitochondrial ROS under HG conditions. In addition, under the stimulation of HG, excess ROS can activate the intracellular AMPK signal pathway in the kidney [48].

Excess ROS can activate PKR-like kinase (PERK) to oxidize Atg4 protease by eIF2a phosphorylation, promote LC3 proteolysis, and prevent mTOR activation [49]. However, excess ROS will destroy the mitochondrial membrane, and the release of ROS into the cytoplasm may damage other organelles. As the function of autophagy targeting and degrading damaged organelles is selective, so the increase in ROS is limited [50]. Fang et al. [21] found that chronic exposure to HG conditions leads to autophagy insufficiency and subsequently causes lysosomal dysfunction and podocyte apoptosis, finally resulting in DN. Therefore, reduction of ROS generation is a potential therapeutic approach for preventing the development of DN.

2.2.4. Sirt1 Signal Pathway. Sirt1 is a highly conserved NAD +-dependent III histone deacetylase, which exists widely in embryos and human tissues. At present, autophagy mediated by Sirt1 has attracted much attention. Sirt1 plays an important role in cells by deacetylating autophagy-related gene (Atg) products, such as Atg5, Atg7, Atg8, and forkhead protein transcription factor 3a [51], activating autophagy body formation and promoting autophagy [52]. Among them, Sirt1 plays an important role in the regulation of autophagy through the deacetylation of transcription factor fork frame O3 (FoxO3). Sirt1 is closely related to the occurrence and development of DN. Under the condition of HG, the expression of Sirt1 is inhibited, which increases oxidative stress and triggers apoptosis. For example, studies in db/db mice and streptozotocin-induced mice have found that the expression of Sirt1 is significantly downregulated before the occurrence of proteinuria [53]. Studies have shown that in proximal tubule cells, Sirt1 decreases albuminuria in diabetes mellitus through maintaining nicotinamide mononucleotide concentrations around glomeruli and controlling podocyte function [53, 54]. The above research shows that Sirt1 has a regulatory effect on autophagy.

2.2.5. Atg12-Atg5 Conjugated System. Autophagy originates from the endoplasmic reticulum, and its formation includes initiation, nucleation, prolongation, and closure. Each step is strictly regulated by Atg coding products. The Atg12-Atg5 conjugated system is a class of Atg proteins closely related to podocyte autophagy. In vitro experiments showed that the autophagy activity of podocytes exposed to HG was significantly decreased, which was characterized by a significant decrease in the expression of autophagy-associated protein Atg12-Atg5 [22]. The activation of the Atg12-Atg5 conjugated system promotes the production of autophagosomes and activates podocyte autophagy. Studies have shown [55] that in a HG environment, the β-suppressor protein in the intracellular signal protein of G protein-coupled receptors inhibits podocyte autophagy by downregulating the Atg12-Atg5 conjugated system, which leads to the occurrence and development of DN.

2.2.6. VEGF. VEGF, synthesized by podocytes, is the promoter of angiogenesis and plays a key role in the maintenance of endothelial cell function [56], is the main pathogenic medium and important marker of DN, and participates in the occurrence and development of DN. In a HG environment, many factors activate transforming growth factor- (TGF-) β1. Through the binding of type I and type II receptors on the podocyte membrane, downstream Smad2 or Smad3 phosphorylation is induced, and the complex formed by binding with Smad4 and translocates to the nucleus, thus stimulating the secretion of VEGF [57]. The increase in VEGF is related to the increase of glomerular permeability [58]. In addition, VEGF, ROS, and AngII can stimulate TGF-β, which leads to renal hypertrophy, accumulation of mesangial extracellular matrix, and changes in podocyte morphology and function through Smad signal transduction. Studies have shown that HG increases VEGF levels by downregulating autophagy activity [32] Miaomiao et al. [59] found that diabetes caused podocyte foot process effacement and a significant upregulation of VEGF. In vitro, HG induced VEGF and reduced podocyte viability. After treatment with rapamycin in podocytes, an autophagy inducer, VEGF activation was significantly abrogated and podocyte injury was ameliorated. These studies show the vital role of autophagy in the regulation of VEGF, which serves as a protective mechanism against HG-induced podocyte injury (Figure 1).

3. Morphological Changes of Podocytes

Podocytes play an important role in the development of DN. A series of signal transduction pathways and changes in the renal microenvironment, involving related proteins and growth factors, lead to morphological cell damage and DN progression. Podocytes in DN are prone to a series of morphological changes after injury, including podocyte hypertrophy, podocyte EMT, podocyte detachment, and podocyte apoptosis [11].

3.1. Podocyte Hypertrophy

3.1.1. mTOR Signal Pathway. mTOR signaling mainly comprises mTOR complex 1(mTORC1) and mTOR complex 2 (mTORC2). Several studies have suggested that mTORC1 is closely associated with the activation of podocyte hypertrophy, which is induced by HG [32]. Research by Herbach et al. [60] indicates that podocyte hypertrophy is directly linked to hyperglycemia. Gödel et al. [61] found that tightly balanced mTOR activity in podocyte homeostasis is required and suggest that mTOR inhibition can protect podocytes and prevent progressive DN. Kim et al. [62] found that translationally controlled tumour protein (TCTP), a mediator of cell growth, was overexpressed in the glomeruli of diabetic mice and gave rise to podocyte hypertrophy. Studies showed that TCTP could activate the mTORC1 signaling pathway and promote high expression of cyclin-dependent kinase inhibitors (CKIs), which caused podocyte cycle arrest and hypertrophy. In contrast, overexpression of mTORC1 and CKIs could be inhibited by TCTP knockout, to make the podocyte bodies smaller. Additionally, in vitro experiments indicated that a TCTP inhibitor could downregulate the expression of CKIs, ameliorating podocyte hypertrophy caused by HG. In addition, Das et al. found that Akt2 causes TGF-β-induced

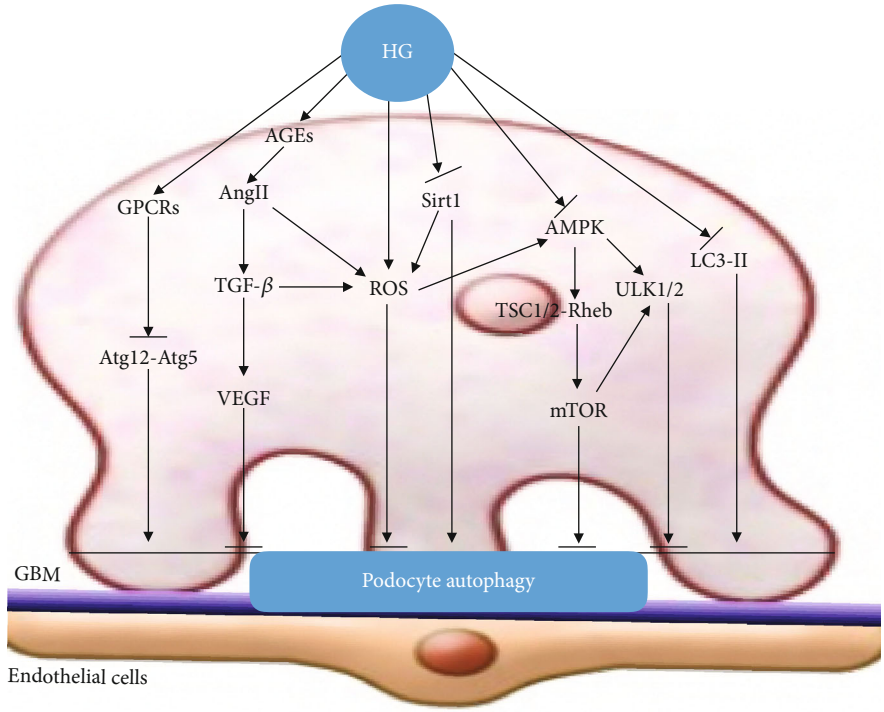

Figure 1: Podocyte autophagy. This figure illustrates the signal pathways of podocyte dysfunction in DN. HG inhibits podocyte autophagy by activating mTOR, ROS, and VEGF signaling pathways and inhibiting Sirt1, AMPK, LC3-II, and Atg12-Atg5 signaling pathways.

deptor downregulation facilitating mTOR to drive podocyte hypertrophy [63].

3.1.2. TGF-β Signal Pathway. TGF-β is a multifunctional cytokine that mediates multiple signal pathways leading to podocyte hypertrophy in the pathogenesis of DN. It has been shown that exposure of differentiated podocytes to hyperglycemic conditions in vitro results in the upregulation of TGF-β expression [64, 65]. HG also augments the response of the podocyte to ambient levels of TGF-β [64]. Das et al. [66] believe that the production of proteinuria in patients with DN is related to TGF-β1, which can induce podocyte apoptosis, and found that TGF-β1 can induce the increase of podocyte mitochondrial NADPH oxidase, inhibiting podocyte mitochondrial function. From this, it can be inferred that TGF-β overexpression can induce podocyte hypertrophy and cause shape deformity. A HG environment increases the phosphorylation of Akt2 in glomerular podocytes, and TGF-β increases the phosphorylation of Akt2 and upregulates mTOR by stimulating PI3 kinase. Importantly, inhibition of Akt2 blocked TGF-β-induced podocyte hypertrophy [63]. In addition, TGF-β possesses an activation effect on the ERK pathway [67], and ERK1/2 activation is related to glomerular podocyte hypertrophy [68].

3.1.3. AngII Signaling Pathway. HG induces the activation of the local renin-angiotensin system (RAS), which leads to an increase in AngII. AngII is an important mediator of DN and plays a key role in its occurrence and development [57, 69]. HG reportedly caused cultured podocytes to become hypertrophic in vitro, possibly through AngII [70]. Romero et al. [71] observed that PTHrP plays a key role in the mechanisms of HG-induced podocyte hypertrophy. In these studies, HG-induced podocyte hypertrophy was inhibited by the presence of a specific PTHrP neutralizing antibody. Moreover, PTHrP is able to upregulate the negative cell cycle regulatory protein p27Kip1, which plays a key role in diabetic cell hypertrophy by preventing activation of cyclin E activity and arresting the cell cycle later in G1 [71]. In addition, Rüster et al. reported that under HG conditions, AGEs induce podocyte cycle arrest and hypertrophy by stimulating the expression of p27Kip1 [72]. Romero et al. [71] found that the pharmacological blockade of PTH1R inhibited p27Kip1 upregulation induced by both HG and AngII. Taken together, these data suggest that PTHrP might mediate hypertrophic signaling, acting in an autocrine/intracrine fashion through the PTH1R receptor. Kim et al. [73] found that HG resulted in the activation of ERK1/2 and Akt/PKB and promoted podocyte hypertrophy, AngII can also increase ERK1/2 and Akt/PKB phosphorylation and cell hypertrophy in podocytes, and HG and AngII have a synergistic effect.

3.1.4. IL-6/JAK2/STAT3 Signaling Pathway. Interleukin-6 (IL-6) regulates cellular hypertrophy through the gp130/Janus kinase 2 (JAK2)/signal transducer and activator of transcription 3 (STAT3) pathway. Jo et al. [74] found that HG-stimulated podocytes produced and secreted IL-6, which activated the JAK2/STAT3 pathway via autocrine

or paracrine mechanisms and participated in the process of cellular hypertrophy in vitro. This effect was attenuated by the addition of IL6NAbs to podocytes cultured under HG conditions, directly demonstrating that IL-6 was the cause of HG-induced podocyte hypertrophy. IL-6 might play a prominent role in the local activation of JAK2/STAT3 in podocyte hypertrophy under HG conditions. Local activation of the IL-6/JAK2/STAT3 pathway in podocytes could activate p21Cip and p27Kip1 expression. High expression of p27Kip1 may eventually lead to podocyte hypertrophy (Figure 2).

3.2. Podocyte EMT

3.2.1. TGF-β Signaling Pathway. HG can increase the expression of TGF-β1. Numerous studies have shown that TGF-β1 is a master regulator governing the induction of EMT [75, 76]. Podocytes can be injured by hyperglycemia through the TGF-β/Smad classic pathway and multiple other pathways. Following the EMT process, the podocyte foot processes are effaced, which results in a loss of the slit diaphragm. The expression of nephrin, podocin, P-cadherin, and ZO-1 is downregulated, the actin cytoskeleton is rearranged, and the podocyte is no longer able to restrict urinary protein loss. This EMT process can finally cause podocyte-related DN. Activated TGF-β first integrates the TGF-β receptor type II (TbRII) and TGF-β receptor type I (TbRI) to form a ligand-receptor complex. This association results in the downstream phosphorylation and activation of Smad2 and Smad3. Phosphorylated Smad2/3 combines with Smad4 to form a Smad complex in the cytoplasmic domain, which gets translocated to the nucleus [77]. Then, activated TGF-β can lead to podocyte EMT. Stromal cell-derived factor-1α (SDF-1α), one of the substrates of DPP-4, can activate the protein kinase A pathway and subsequently inhibit its downstream effector, TGF-β1, which induces podocyte EMT. Chang et al. [78] found that SDF-1α plays an essential role in podocyte EMT inhibition.

3.2.2. ILK Signaling Pathway. The ILK signaling pathway is also an important signaling pathway that mediates podocyte EMT. ILK, which binds the cytoplasmic domain of β1 integrin [79], is a serine-threonine kinase [80] and plays an important role in transmembrane signal transduction via integrins. Activated ILK causes phosphorylation of the downstream molecules Akt and GSK-3β. Phosphorylated Akt and GSK-3β can inhibit the phosphorylation of β-catenin, rendering high cytoplasmic concentrations of β-catenin. The cytoplasmic β-catenin will be transferred to the nucleus and binds to related transcription factors, which will cause the expression of Snail protein. Snail protein is an important protein that mediates podocyte EMT. Blockade of ILK activity with a highly selective small-molecule inhibitor reduced Snail induction and preserved podocyte phenotypes following TGF-beta1 or adriamycin stimulation. Kang et al. [81] found that ILK expression was induced in mouse podocytes by various harmful stimuli known to cause proteinuria, including TGF-β1, and high ambient glucose. Podocyte ILK was also found to be upregulated in human proteinuric glomerular diseases. Chen et al. [82] found that emodin ameliorated HG-induced EMT and subsequent podocyte dysfunction through nephrin upregulation, as well as desmin and ILK inhibition in vitro and in vivo. This reflects ILK-mediated HG-induced podocyte EMT. A previous study found that ILK upregulation and nephrin downregulation disrupted the balance of the ternary complex [83], which might be responsible for EMT. These results show that the upregulation of ILK is a convergent pathway leading to podocyte EMT.

3.2.3. Wnt/β-Catenin Signaling Pathway. The Wnt/β-catenin signaling pathway is also closely related to podocyte EMT [84]. Wnt/β-catenin is a highly conserved signaling pathway, and β-catenin is its core molecule. Li and Siragy [85] showed that in a HG environment, podocyte Wnt/β-catenin signaling is activated, and HG significantly decreased mRNA and protein expression of nephrin and increased mRNA and protein expressions of Wnt3a, β-catenin, and Snail. Snail, one of the downstream target genes of the Wnt-β-catenin signaling pathway, is an important transcription factor inducing podocyte EMT. Studies by Dai et al. [86] observed that Wnt1 was upregulated and β-catenin was activated in podocytes of human DN. Ectopic expression of either Wnt1 or stabilized β-catenin in vitro induced the transcription factor Snail and suppressed nephrin expression. Since Snail is the main transcription factor of EMT, so this study reflects that Wnt/β-catenin may promote podocyte transdifferentiation and phenotypic change mainly by promoting Snail expression. Another study showed that Rac1/-PAK1 signaling contributed to HG-induced podocyte EMT via promoting β-catenin and Snail transcriptional activities [87]. In addition, miR-21 can upregulate the levels of TGF-β1 and P-Smad3 and reduce the level of Smad7 in the TGF-β1/Smads pathway by activating β-catenin, a key factor in the Wnt/β-catenin pathway, to promote podocyte dedifferentiation and podocyte EMT [88] (Figure 3).

3.3. Podocyte Detachment

3.3.1. α3β1 Integrin. Podocytes and the GBM are closely connected and prevent the excretion of proteinuria via sustaining the glomerular filtration barrier. Podocyte detachment is closely related to the expression of adhesion molecules. Podocytes are anchored to the GBM by many molecules. Among them, integrin α3β1 is an important receptor that could tightly connect the podocyte to the GBM [89]. In podocytes cultured in vitro, TGF-β1 and mechanical stretching significantly reduce the expression of α3β1 integrin, reduce the adhesion function of podocytes, and promote podocyte detachment and apoptosis [90]. Kriz and Lemley [91] found that podocyte detachment depends on specific downstream effects: hypertension, ultrafiltration, and excessive glomerular growth, especially increased shear stress through the fissure membrane, and that mechanical forces are a key factor in the progression of glomerular disease to renal failure. Dai et al. [92] found that angiopoietin-like3 (Angptl3) is involved in podocyte detachment and apoptosis caused by puromycin, resulting in a large loss of podocytes. However, knockdown of Angptl3 by siRNA markedly ameliorated these injuries.

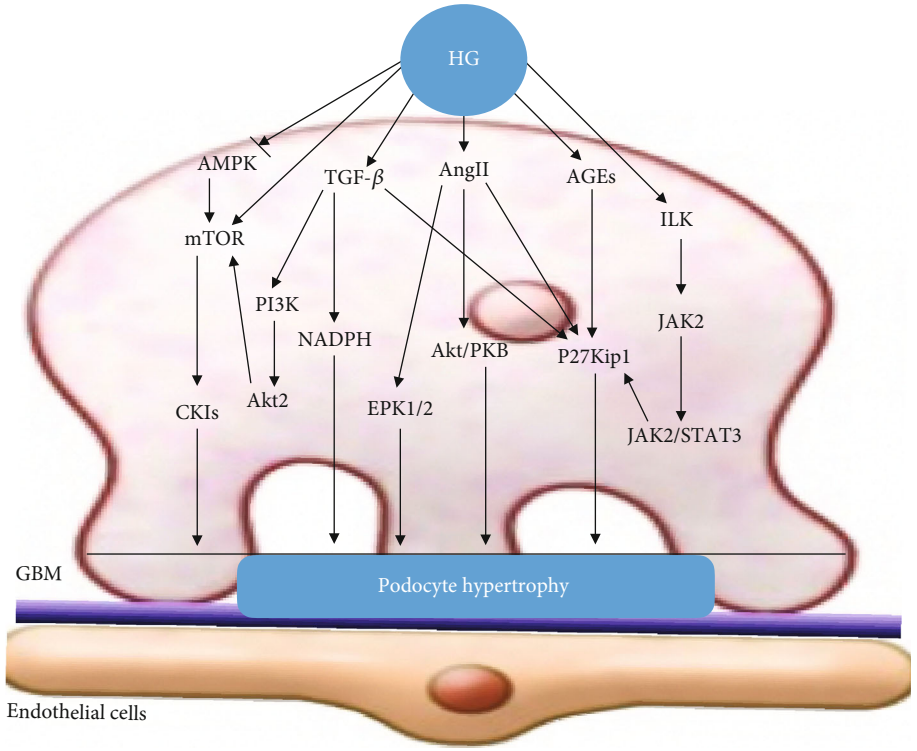

Figure 2: Podocyte hypertrophy. Elevated glucose upregulates TGF-β, mTOR, Ang II, AGEs, and integrin-linked kinase (ILK) pathways and activates the expression of p27Kip1, P38MAPK, Akt/PKB, and NADPH, which eventually leads to podocyte hypertrophy.

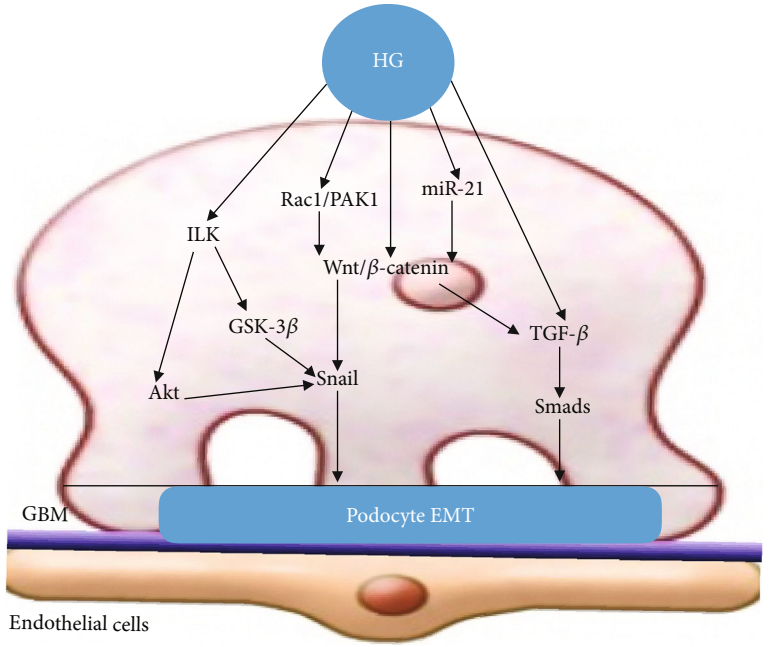

Figure 3: Podocyte EMT. HG activates the TGF-β, Notch, ILK, NF-κB, and Wnt/β-catenin signaling pathways, which promotes the expression of Snail and eventually induces podocyte EMT.

Observed effects were partially correlated with the altered $\alpha 3\beta 1$ integrin, ILK, and p53, rather than caspase-3. Chen et al. [93] found that the expression of $\alpha 3\beta 1$ integrin on podocytes was suppressed in both humans and rats with diabetes, possibly due to the effects of hyperglycemia, and the suppression became more severe with the duration of

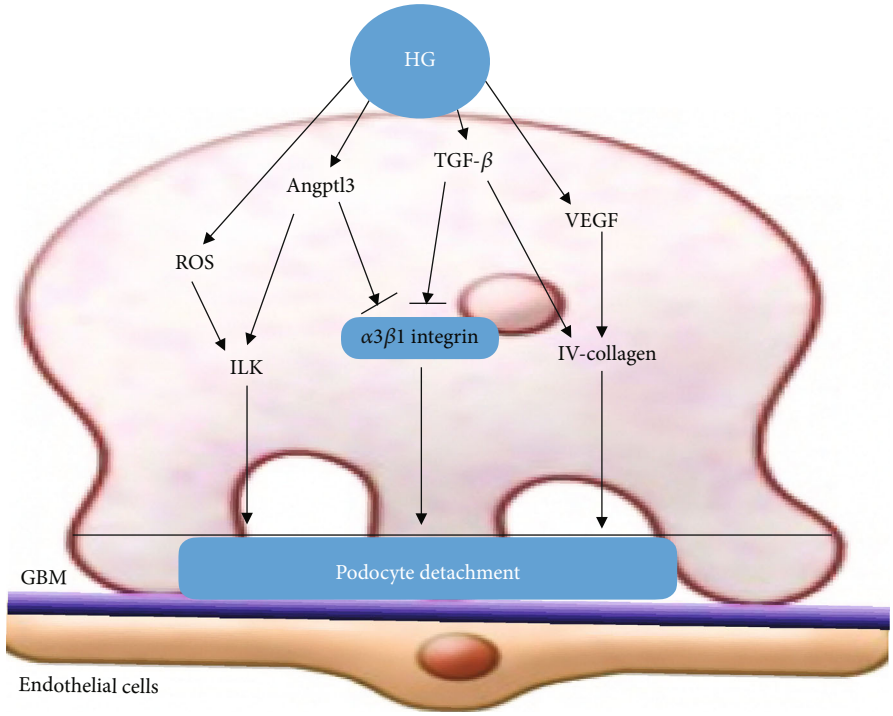

Figure 4: Podocyte detachment. HG can inhibit the expression of $\alpha 3\beta 1$ integrin through Angptl3, and TGF-β pathways, thus promoting podocyte isolation. In addition, HG promotes podocyte detachment by upregulating ROS and VEGF pathways.

diabetes. Susztak et al. [94] found that glucose-induced ROS production initiates podocyte depletion in vitro and in vivo. Further research showed that ROS can increase ILK expression in a dose-dependent manner, causing podocytes to detach [95]. Chen et al. [96] found that HG strongly inhibited the adhesion of podocytes to the BMC, which was accompanied by a reduction in $\alpha 3\beta 1$ integrin mRNA and protein expression, as well as an increase in ILK activity and expression. Teixeira et al. [97] found that when glomerular ILK activity increases, β-catenin moves from the cell membrane into the cell, thus changing the cell phenotype and promoting the detachment of podocytes from the GBM. In addition, the overexpression of the ILK anchor protein repeat sequence can inhibit the binding of PINCH-1 to ILK, preventing the formation of the ternary complex, reducing the adhesion between podocytes and the GBM, and promoting apoptosis and exfoliation of podocytes [98]. It has been found that AngII stimulates podocytes to produce collagen IV, through TGF-β and VEGF signaling pathways, which leads to the accumulation of ECM, thickening of the GBM, and detachment of podocytes [57]. In addition, AngII can lead to oxidative stress, which in turn mediates the production of ROS and decreases the expression of $\alpha 3\beta 1$ integrin.

3.3.2. TGF-β Signaling Pathway. In the kidneys, TGF-β1 has been reported to be a strong regulator of the expression of integrins [99]. TGF-β1 has been demonstrated to suppress the expression of α3-integrin in the glomeruli of nephrotic rats [100]. HG can upregulate the expression of TGF-β receptor II; increase the sensitivity of podocytes to TGF-β; promote the paracrine effect in podocytes, mesangial cells, and glomerular endothelial cells; promote the secretion of TGF-β; and promote podocyte exfoliation. Dessapt et al. [90] found that downregulation of $\alpha 3\beta 1$ integrin expression, by mechanical forces or TGF-β1, is sufficient to reduce podocyte adhesion (Figure 4).

3.4. Podocyte Apoptosis

3.4.1. TGF-β1 Signaling Pathway. In the HG state, the TGF-β1 pathway is active and participates in podocyte apoptosis by mediating Smads, mTOR, and other signaling pathways. Das et al. [66] found that TGF-β1 selectively upregulates the transcription of Nox4 mRNA by Smad2/3, resulting in an elevated mitochondrial Nox4 protein level, oxidative stress, mitochondrial dysfunction, and apoptosis in podocytes. TGF-β1 induces podocyte apoptosis through the Erk-mediated mTORC1/Nox4 axis [101]. A study by Das et al. [101] found that TGF-β1 increases the translation of Nox4 through the Smad-ERK1/2-mTORC1 axis. Activation of this pathway plays a crucial role in ROS generation and mitochondrial dysfunction, leading to podocyte apoptosis. Gremlin plays an important role in regulating podocyte apoptosis. Overexpression of gremlin aggravates podocyte apoptosis. Gremlin is a developmental gene and is associated with DN [102]. Li et al. [103] found that HG induces increased expression of gremlin, which activates the TGF-β/Smad2/3 signaling pathway and aggravates podocyte apoptosis. Wang et al. [104] found that apoptosis-related

proteins (Bcl-2 and Bax) are activated in the pathophysiology of DN. Overexpression of gremlin under HG conditions enhanced the expression of the TGF-β pathway, decreased the expression of the antiapoptotic gene Bcl-2, and increased the expression of the proapoptotic genes Bax and cleaved-caspase-3, causing podocyte apoptosis. TGF-β1 upregulated the expression of Cdk5 and p35 and Cdk5 kinase activity. HG increased the expression of Egr-1 via the TGF-β1-ERK1/2 pathway. Egr-1 is a member of a family of zinc-finger transactivators and is a known regulator of the p35 promoter. Inhibition of Cdk5 kinase activity alleviated podocyte apoptosis induced by HG or TGF-β1 [105]. Liu et al. [106] also found that HG stimulation increased the protein and mRNA expression of Cdk5 in a time-dependent manner in cultured mouse podocytes. The protein activator of Cdk5, p35, was also increased in a time-dependent manner by HG stimulation.

3.4.2. AngII Signaling Pathway. HG promotes AngII expression and increases podocyte apoptosis. Liu et al. [107] found that AngII can increase podocyte apoptosis. AngII induces the relocalization and reduction of CD2AP via AT1R, which would cause podocyte apoptosis by the suppression of CD2AP/PI3-K signaling [108]. Treatment with AngII suppressed the viability and promoted the apoptosis of podocytes in a dose- and time-dependent manner. AngII decreased phosphor-Akt, phospho-p65 NF-κB, nephrin, and podocin and increased caspase-9 expression, and podocyte apoptosis was promoted [109].

3.4.3. AMPK Signaling Pathway. HG induces apoptosis in podocytes, inhibits AMPK activation, inactivates tuberin, and activates mTOR. HG also increases the levels of Nox4, Nox1, and NADPH oxidase activity [110]. Eid et al. [110] provided evidence that podocyte apoptosis in diabetic conditions is mediated by activation of the mTOR pathway through inactivation of AMPK. Lin et al. [111] found that HG stimulation negatively affects the mitochondria and reduces the sesn2 and p-AMPK levels, thereby promoting podocyte apoptosis. Cai et al. [112] found that grape seed proanthocyanidin extract, a strong antioxidant, prevents HG-induced mitochondrial dysfunction and apoptosis in podocytes via the AMPK-Sirt1-PGC-1α (Sirt1 silent information regulator T1) pathway. This study reflects AMPK-mediated podocyte apoptosis. Eid et al. [113] found that inactivation of AMPK by HG upregulated the expression and phosphorylation of p53, and p53 acted downstream of Nox4. To investigate the mechanism of podocyte apoptosis in vivo, they used OVE26 mice, a model of type 1 diabetes. Glomeruli isolated from these mice showed decreased phosphorylation of AMPK and enhanced expression of Nox4 and p53. Their results uncover a novel function of AMPK that integrates metabolic input to Nox4 and provides new insight for the activation of p53 to induce podocyte apoptosis.

3.4.4. ROS Signaling Pathway. In DN, excessive ROS production induced by HG decreases the number of podocytes. Related studies have confirmed [114] that mitochondria are considered to be an important source of intracellular ROS and participate in the endogenous apoptosis pathway. Previous studies have demonstrated that ROS was increased in podocytes [115] and that HG-induced ROS increase promotes podocyte apoptosis in DN [94]. Further research found that ROS can activate the P38 MAPK pathway, which may be an important pathological mechanism of podocyte apoptosis induced by oxidative stress [116]. Susztak et al. [94] found that HG rapidly stimulated the generation of intracellular ROS through NADPH oxidase and mitochondrial pathways and led to the activation of proapoptotic p38 MAPK and caspase-3 and to the apoptosis of conditionally immortalized podocytes in vitro. Among the members of the NADPH oxidase family, Nox4 is the key enzyme in ROS production and podocyte apoptosis induced by oxidative stress in DN [117, 118]. Liu et al. found that [119] metadherin is a potent modulator of podocyte apoptosis and that it represents the target of miR-30s, facilitating podocyte apoptosis through the activation of a HG-induced p38 MAPK-dependent pathway. In addition, Wang et al. [120] indicated that inhibiting mitochondrial oxidative damage and the release of cytochrome C can eliminate ROS, thereby preventing the transmission of podocyte damage and apoptosis signals.

3.4.5. Endoplasmic Reticulum Stress (ERS) Signaling Pathway. Activated ERS plays an important role in podocyte apoptosis in HG environments. HG can initiate ERS through a variety of ways. AGE products are important in the pathogenesis of DN. AGEs can upregulate the expression of glucose-regulated protein 78 in podocytes, induce ERS, and eventually lead to podocyte apoptosis in a dose- and time-dependent manner [121]. Lei et al. [122] found that the activated mTOR by ERK1/2 results in energy consumption, which in turn leads to ERS signaling and triggers apoptosis in HG-treated podocytes. Cao et al. [123] found that ER stress inhibitors ursodeoxycholic acid (UDCA) or 4-phenylbutyrate (4-PBA) prevented hyperglycemia-induced or HG-induced apoptosis in podocytes in vivo and in vitro via the inhibition of caspase-3 and caspase-12 activation. In addition, Shen et al. [124] found that TUG1 was highly expressed in cells following treatment with HG, and PGC-1α and cleaved-caspase-3 levels were much lower, while CHOP levels were much higher. Furthermore, CHOP inhibited PGC-1α expression. TUG1 negatively regulated CHOP expression and positively regulated PGC-1α expression. Their study suggested that the long noncoding RNA (lncRNA) TUG1 influenced podocyte apoptosis via mediating the ERS-CHOP-PGC-1α signaling pathway in HG-induced DN.

3.4.6. Other Related Signaling Pathway. Under normal circumstances, proapoptotic and antiapoptotic signaling pathways coexist to maintain the body's homeostasis. The podocyte-associated proteins nephrin and podocin have antiapoptotic signal transduction properties. β-Arrestin 1/2 expression levels of podocytes were found to be upregulated in HG-induced podocytes, and β-arrestin 1/2 overexpression inhibited the expression of nephrin and

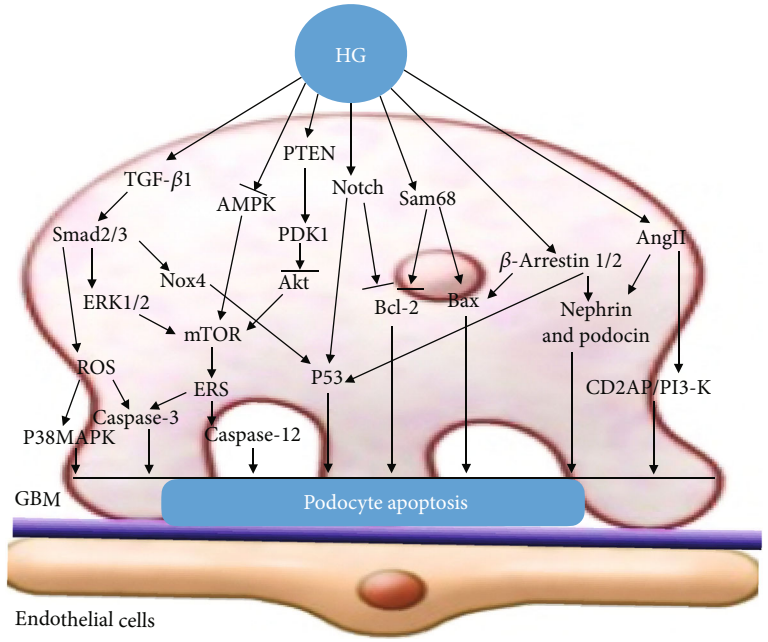

Figure 5: Podocyte apoptosis. HG can stimulate the upregulation of TGF-β, mTOR, Notch, AngII, Sam68, ROS, and ERS signal pathways, inhibit the activity of AMPK and expression of Bcl-2, and activate the apoptosis pathways of p53, Bax, caspase-3, P38MAPK, CD2AP/PI3-K, and caspase-12, to induce podocyte apoptosis.

podocin proteins. Upregulated β-arrestin 1/2 promoted podocyte apoptosis and the p53 pathway by increasing Bax, cleaved-caspase-3, and p-p53 levels in HG-induced podocytes [125]. High expression of PVT1 or low expression of FOXA1 can downregulate the expression of synaptophysin and podocyte protein, decrease the expression of Bcl-2, and increase the expression of Bax and cleaved-caspase-3, thus promoting podocyte apoptosis [126]. Chen et al. [127] found that Sam68 was upregulated in a time- and dose-dependent manner in in vitro HG-treated podocytes. Furthermore, HG increased Bax and decreased Bcl-2 protein expression in cultured podocytes, and this effect was blocked by Sam68 knockdown. Their results showed that Sam68 mediated HG-induced podocyte apoptosis, probably through the Bax/Bcl-2 signaling pathway. Gao et al. [128] found that HG upregulated the Notch pathway in podocytes, which was accompanied by the alteration of Bcl-2 and p53 pathways, subsequently leading to podocyte apoptosis. In addition, Wang et al. [120] found that SS-31 prevented oxidative stress and mitochondria-dependent apoptosis signaling by hypochlorite-modified albumin (HOCl-alb) in vivo and in vitro, as evidenced by the release of cytochrome c, the binding of apoptosis activated factor-1 (Apaf-1) and caspase-9, and the activation of caspases. These data suggest that SS-31 may prevent podocyte apoptosis, exerting renal protection in diabetes mellitus, probably through an apoptosis-related signaling pathway involving oxidative stress. A study by Feng et al. [129] found that mitochondrial pyruvate carrier 2 may mediate mitochondrial dysfunction in HG-treated podocytes, ultimately leading to cell apoptosis. High D-glucose (HDG) significantly increased PLK2 expression in mouse podocytes. Suppressing PLK2 attenuated HDG-induced apoptosis and inflammatory responses both in vitro and in vivo [130]. Bai et al. [131] found that VEGF-A inhibition ameliorates podocyte apoptosis by regulating activator protein 1 (AP-1) and Bcl-2 signaling. AP-1 is a direct target of VEGF-A and a novel component of podocyte apoptosis. Recent studies have found that HG can promote podocyte apoptosis through the PTEN-PDK1-Akt-mTOR pathway [132] (Figure 5).

4. Conclusion

Podocyte injury is a key factor in the occurrence and development of DN. Most studies have shown that the pathological mechanism of podocyte injury mainly includes four morphological changes: podocyte hypertrophy, podocyte EMT, podocyte detachment, and podocyte apoptosis, as well as functional changes in podocyte autophagy. There is a close relationship between the function and morphology of podocyte injury. For example, HG conditions activate mTOR signaling to inhibit podocyte autophagy and promote podocyte hypertrophy and podocyte EMT. Alternatively, HG conditions inhibit AMPK and generate ROS to inhibit podocyte autophagy and promote podocyte apoptosis (Figure 6). In the early lesions of DN, abnormal podocyte function is particularly prominent, including the downregulation of key structural molecular proteins in the podocyte fissure membrane, or protein binding disorders of adjacent structural molecules. With the deepening of research, more and more pathways concerning podocyte injury have been revealed. However, DN is a serious global

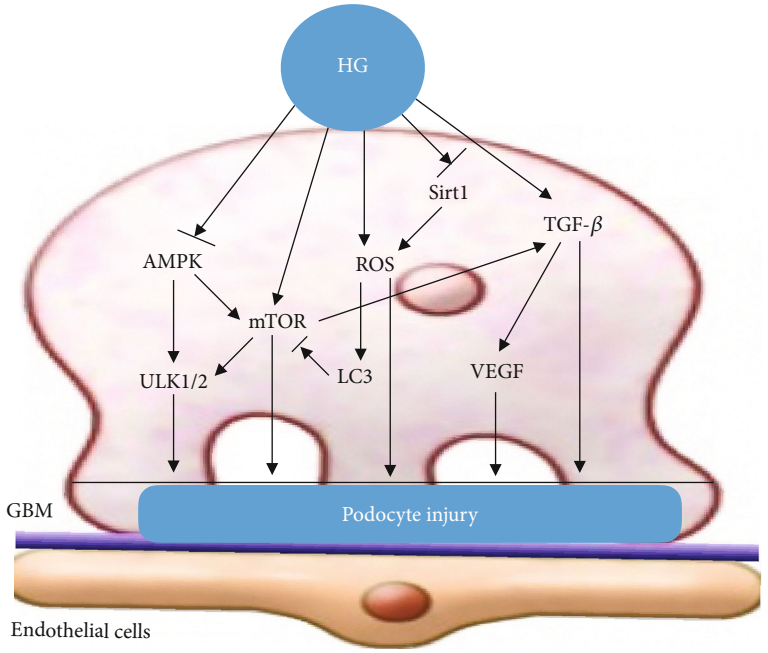

Figure 6: The function of podocyte injury is closely related to morphological changes. HG inhibits podocyte autophagy and promotes podocyte hypertrophy by activating the mTOR signaling pathway. HG inhibits podocyte autophagy and promotes podocyte apoptosis by inhibiting AMPK and activating ROS signaling.

health problem, and the potential pathological mechanisms of podocyte morphological and functional damage require further investigation.

Conflicts of Interest

The authors declare that there is no conflict of interest regarding the publication of this paper.

Authors' Contributions

Dr. Lili Zhang, Dr. Zhige Wen, Dr. Lin Han, and Dr. Yujiao Zheng contributed equally to this work.

Acknowledgments

This study was supported by the National Natural Science Foundation of China (grant number 81430097) and the Major Achievement Guidance Project of Traditional Chinese Medicine Science and Technology (grant number 44223).

References

[1] L. Gnudi, R. J. M. Coward, and D. A. Long, "Diabetic nephropathy: perspective on novel molecular mechanisms," *Trends in Endocrinology and Metabolism: TEM*, vol. 27, no. 11, pp. 820–830, 2016.

[2] D. Sharma, P. Bhattacharya, K. Kalia, and V. Tiwari, "Diabetic nephropathy: new insights into established therapeutic paradigms and novel molecular targets," *Diabetes Research and Clinical Practice*, vol. 128, pp. 91–108, 2017.

[3] UADRA, *United States Renal Data System, N.I.O.H. of ESRD*, National Institute of Diabetes, and Digestive and Kidney Diseases, Bethesda, MD, 2009.

[4] G. R. Reddy, K. Kotlyarevska, R. F. Ransom, and R. K. Menon, "The podocyte and diabetes mellitus:is the podocyte the key to the origins of diabetic nephropathy?," *Current opinion innephrology and hypertension*, vol. 17, no. 1, pp. 32–36, 2008.

[5] N. R. Burrows, J. Wang, L. S. Geiss et al., "Incidence of end-stage renal disease among persons with diabetes—United. States, 1990-2002," *MMWR. Morbidity and mortality weekly report*, vol. 54, no. 43, pp. 1097–1100, 2005.

[6] S. M. Mauer, M. W. Steffes, E. N. Ellis, D. E. Sutherland, D. M. Brown, and F. C. Goetz, "Structural-functional relationships in diabetic nephropathy," *The Journal of Clinical Investigation*, vol. 74, no. 4, pp. 1143–1155, 1984.

[7] K. Drummond and M. Mauer, "The early natural history of nephropathy in type 1 diabetes: II. Early renal structural changes in type 1 diabetes," *Diabetes*, vol. 51, no. 5, pp. 1580–1587, 2002.

[8] R. E. Gilbert and M. E. Cooper, "The tubulointerstitium in progressive diabetic kidney disease: more than an aftermath of glomerular injury?," *Kidney International*, vol. 56, no. 5, pp. 1627–1637, 1999.

[9] C. Ponchiardi, M. Mauer, and B. Najafian, "Temporal profile of diabetic nephropathy pathologic changes," *Current Diabetes Reports*, vol. 13, no. 4, pp. 592–599, 2013.

[10] X. An, L. Zhang, Y. Yuan et al., "Hyperoside pre-treatment prevents glomerular basement membrane damage in diabetic nephropathy by inhibiting podocyte heparanase expression," *Scientific Reports*, vol. 7, no. 1, p. 6413, 2017.

[11] Y. Maezawa, M. Takemoto, and K. Yokote, "Cell biology of diabetic nephropathy: roles of endothelial cells,

tubulointerstitial cells and podocytes," *Journal of Diabetes*, vol. 6, no. 1, pp. 3–15, 2015.

[12] N. Mizushima, T. Yoshimori, and B. Levine, "Methods in mammalian autophagy research," *Cell*, vol. 140, no. 3, pp. 313–326, 2010.

[13] M. W. Han, J. C. Lee, J. Y. Choi et al., "Autophagy inhibition can overcome radioresistance in breast cancer cells through suppression of TAK1 activation," *Anticancer Research*, vol. 34, no. 3, pp. 1449–1455, 2014.

[14] I. Beau, A. Esclatine, and P. Codogno, "Lost to translation: when autophagy targets mature ribosomes," *Trends in Cell Biology*, vol. 18, no. 7, pp. 311–314, 2008.

[15] C. Kraft, F. Reggiori, and M. Peter, "Selective types of autophagy in yeast," *Biochimica et Biophysica Acta*, vol. 1793, no. 9, pp. 1404–1412, 2009.

[16] A. van der Vaart, M. Mari, and F. Reggiori, "A picky eater: exploring the mechanisms of selective autophagy in human pathologies," *Traffic (Copenhagen, Denmark)*, vol. 9, no. 3, pp. 281–289, 2008.

[17] A. Kuma, M. Hatano, M. Matsui et al., "The role of autophagy during the early neonatal starvation period," *Nature*, vol. 432, no. 7020, pp. 1032–1036, 2004.

[18] G. Kroemer, G. Mariño, and B. Levine, "Autophagy and the integrated stress response," *Molecular Cell*, vol. 40, no. 2, pp. 280–293, 2010.

[19] N. Liu, Y. Shi, and S. Zhuang, "Autophagy in chronic kidney diseases," *Kidney diseases (Basel, Switzerland)*, vol. 2, no. 1, pp. 37–45, 2016.

[20] K. Liu, E. Zhao, G. Ilyas et al., "Impaired macrophage autophagy increases the immune response in obese mice by promoting proinflammatory macrophage polarization," *Autophagy*, vol. 11, no. 2, pp. 271–284, 2015.

[21] L. Fang, Y. Zhou, H. Cao et al., "Autophagy attenuates diabetic glomerular damage through protection of hyperglycemia-induced podocyte injury," *PLoS One*, vol. 8, no. 4, p. e60546, 2013.

[22] B. Hartleben, M. Gödel, C. Meyer-Schwesinger et al., "Autophagy influences glomerular disease susceptibility and maintains podocyte homeostasis in aging mice," *The Journal of Clinical Investigation*, vol. 120, no. 4, pp. 1084–1096, 2010.

[23] N. Liu, L. Xu, Y. Shi, and S. Zhuang, "Podocyte autophagy: a potential therapeutic target to prevent the progression of diabetic nephropathy," *Journal of Diabetes Research*, vol. 2017, Article ID 3560238, 6 pages, 2017.

[24] S. Kume, M. C. Thomas, and D. Koya, "Nutrient sensing, autophagy, and diabetic nephropathy," *Diabetes*, vol. 61, no. 1, pp. 23–29, 2011.

[25] O. Lenoir, M. Jasiek, C. Hénique et al., "Endothelial cell and podocyte autophagy synergistically protect from diabetes-induced glomerulosclerosis," *Autophagy*, vol. 11, no. 7, pp. 1130–1145, 2015.

[26] A. Tagawa, M. Yasuda, S. Kume et al., "Impaired podocyte autophagy exacerbates proteinuria in diabetic nephropathy," *Diabetes*, vol. 65, no. 3, pp. 755–767, 2016.

[27] P. Boya, F. Reggiori, and P. Codogno, "Emerging regulation and functions of autophagy," *Nature Cell Biology*, vol. 15, no. 7, pp. 713–720, 2013.

[28] N. Hosokawa, T. Hara, T. Kaizuka et al., "Nutrient-dependent mTORC1 association with the ULK1-Atg13-FIP200 complex required for autophagy," *Molecular Biology of the Cell*, vol. 20, no. 7, pp. 1981–1991, 2009.

[29] M. Høyer-Hansen and M. Jäättelä, "AMP-activated protein kinase: a universal regulator of autophagy?," *Autophagy*, vol. 3, no. 4, pp. 381–383, 2014.

[30] I. H. Lee, L. Cao, R. Mostoslavsky et al., "A role for the NAD-dependent deacetylase Sirt1 in the regulation of autophagy," *Proceedings of the National Academy of Sciences of the United States of America*, vol. 105, no. 9, pp. 3374–3379, 2008.

[31] J. Kim, M. Kundu, B. Viollet, and K. L. Guan, "AMPK and mTOR regulate autophagy through direct phosphorylation of Ulk1," *Nature Cell Biology*, vol. 13, no. 2, pp. 132–141, 2011.

[32] M. K. Lu, X. G. Gong, and K. L. Guan, "mTOR in podocyte function: is rapamycin good for diabetic nephropathy?," *Cell Cycle*, vol. 10, no. 20, pp. 3415-3416, 2014.

[33] K. Inoki, H. Mori, J. Wang et al., "mTORC1 activation in podocytes is a critical step in the development of diabetic nephropathy in mice," *The Journal of Clinical Investigation*, vol. 121, no. 6, pp. 2181–2196, 2011.

[34] T. Xiao, X. Guan, L. Nie et al., "Rapamycin promotes podocyte autophagy and ameliorates renal injury in diabetic mice," *Molecular and Cellular Biochemistry*, vol. 394, no. 1-2, pp. 145–154, 2014.

[35] L. Liu, L. Yang, B. Chang, J. Zhang, Y. Guo, and X. Yang, "The protective effects of rapamycin on cell autophagy in the renal tissues of rats with diabetic nephropathy via mTOR-S6K1-LC3II signaling pathway," *Renal Failure*, vol. 40, no. 1, pp. 492–497, 2018.

[36] Y. Kim and C. W. Park, "Adenosine monophosphate-activated protein kinase in diabetic nephropathy," *Kidney Research and Clinical Practice*, vol. 35, no. 2, pp. 69–77, 2016.

[37] B. B. Zhang, G. Zhou, and C. Li, "AMPK: An Emerging Drug Target for Diabetes and the Metabolic Syndrome," *Cell metabolism*, vol. 9, no. 5, pp. 407–416, 2009.

[38] M. J. Sanders, P. O. Grondin, B. D. Hegarty, M. A. Snowden, and D. Carling, "Investigating the mechanism for AMP activation of the AMP-activated protein kinase cascade," *Biochemical Journal*, vol. 403, no. 1, pp. 139–148, 2007.

[39] Y. Tanaka, S. Kume, M. Kitada et al., "Autophagy as a therapeutic target in diabetic nephropathy," *Experimental diabetes research*, vol. 2012, Article ID 628978, 12 pages, 2012.

[40] D. F. Ding, N. You, X. M. Wu et al., "Resveratrol attenuates renal hypertrophy in early-stage diabetes by activating AMPK," *American Journal of Nephrology*, vol. 31, no. 4, pp. 363–374, 2010.

[41] Y. Jin, S. Liu, Q. Ma, D. Xiao, and L. Chen, "Berberine enhances the AMPK activation and autophagy and mitigates high glucose-induced apoptosis of mouse podocytes," *European Journal of Pharmacology*, vol. 794, pp. 106–114, 2017.

[42] M. Brownlee, "Biochemistry and molecular cell biology of diabetic complications," *Nature*, vol. 414, no. 6865, pp. 813–820, 2001.

[43] A. Kumar Pasupulati, P. S. Chitra, and G. B. Reddy, "Advanced glycation end products mediated cellular and molecular events in the pathology of diabetic nephropathy," *Biomolecular Concepts*, vol. 7, no. 5-6, pp. 293–309, 2016.

[44] Z. C. Qin, Y. Qi, and R. S. Li, "Effect of Radix Astragali on VEGF secretion induced by AngII in human podocytes," *China Science and Technology of traditional Chinese Medicine*, vol. 17, no. 1, pp. 42-43, 2010.

[45] A. Yadav, S. Vallabu, S. Arora et al., "ANG II promotes autophagy in podocytes," *American Journal of Physiology. Cell Physiology*, vol. 299, no. 2, pp. C488–C496, 2010.

[46] T. Ma, J. Zhu, X. Chen, D. Zha, P. C. Singhal, and G. Ding, "High glucose induces autophagy in podocytes," *Experimental Cell Research*, vol. 319, no. 6, pp. 779–789, 2013.

[47] W. Wang, Y. Wang, J. Long et al., "Mitochondrial fission triggered by hyperglycemia is mediated by ROCK1 activation in podocytes and endothelial cells," *Cell Metabolism*, vol. 15, no. 2, pp. 186–200, 2012.

[48] H. B. Lee, M.-R. Yu, Y. Yang, Z. Jiang, and H. Ha, "Reactive oxygen species-regulated signaling pathways in diabetic nephropathy," *Journal of the American Society of Nephrology*, vol. 14, no. 90003, pp. 241S–2245, 2003.

[49] L. Liu, D. R. Wise, J. A. Diehl, and M. C. Simon, "Hypoxic reactive oxygen species regulate the integrated stress response and cell survival," *Journal of Biological Chemistry*, vol. 283, no. 45, pp. 31153–31162, 2008.

[50] M. B. Azad, Y. Chen, and S. B. Gibson, "Regulation of autophagy by reactive oxygen species (ROS): implications for cancer progression and treatment," *Antioxidants & Redox Signaling*, vol. 11, no. 4, pp. 777–790, 2009.

[51] R. Yacoub, K. Lee, and J. C. He, "The role of SIRT1 in diabetic kidney disease," *Frontiers in Endocrinology*, vol. 5, p. 166, 2014.

[52] R. Huang, Y. Xu, W. Wan et al., "Deacetylation of Nuclear LC3 Drives Autophagy Initiation under Starvation," *Molecular Cell*, vol. 57, no. 3, pp. 456–466, 2015.

[53] K. Hasegawa, S. Wakino, P. Simic et al., "Renal tubular Sirt1 attenuates diabetic albuminuria by epigenetically suppressing Claudin-1 overexpression in podocytes," *Nature Medicine*, vol. 19, no. 11, pp. 1496–1504, 2013.

[54] E. Bible, "Sirt1 attenuates diabetic albuminuria," *Nature Reviews Nephrology*, vol. 9, no. 12, p. 696, 2013.

[55] J. Liu, Q. X. Li, X. J. Wang et al., "_β_ -Arrestins promote podocyte injury by inhibition of autophagy in diabetic nephropathy," *Cell death & disease*, vol. 7, no. 4, p. e2183, 2016.

[56] H. Sugimoto, Y. Hamano, D. Charytan et al., "Neutralization of circulating vascular endothelial growth factor (VEGF) by anti-VEGF antibodies and soluble VEGF receptor 1 (sFlt-1) induces proteinuria," *The Journal of Biological Chemistry*, vol. 278, no. 15, pp. 12605–12608, 2003.

[57] S. Chen, J. S. Lee, M. C. Iglesias-de la Cruz et al., "Angiotensin II stimulates α3(IV) collagen production in mouse podocytes via TGF-β and VEGF signalling: implications for diabetic glomerulopathy," *Nephrology, Dialysis, Transplantation*, vol. 20, no. 7, pp. 1320–1328, 2005.

[58] P. L. Tharaux and T. B. Huber, "How many ways can a podocyte die?," *Seminars in Nephrology*, vol. 32, no. 4, pp. 394–404, 2012.

[59] W. Miaomiao, L. Chunhua, Z. Xiaochen, C. Xiaoniao, L. Hongli, and Y. Zhuo, "Autophagy is involved in regulating VEGF during high-glucose-induced podocyte injury," *Molecular BioSystems*, vol. 12, no. 7, pp. 2202–2212, 2016.

[60] N. Herbach, I. Schairer, A. Blutke et al., "Diabetic kidney lesions of GIPRdn transgenic mice: podocyte hypertrophy and thickening of the GBM precede glomerular hypertrophy and glomerulosclerosis," *American Journal of Physiology-Renal Physiology*, vol. 296, no. 4, pp. F819–F829, 2009.

[61] M. Gödel, B. Hartleben, N. Herbach et al., "Role of mTOR in podocyte function and diabetic nephropathy in humans and mice," *The Journal of Clinical Investigation*, vol. 121, no. 6, pp. 2197–2209, 2011.

[62] D. K. Kim, B. Y. Nam, J. J. Li et al., "Translationally controlled tumour protein is associated with podocyte hypertrophy in a mouse model of type 1 diabetes," *Diabetologia*, vol. 55, no. 4, pp. 1205–1217, 2012.

[63] F. Das, N. Ghosh-Choudhury, D. Y. Lee, Y. Gorin, B. S. Kasinath, and G. G. Choudhury, "Akt2 causes TGFβ-induced deptor downregulation facilitating mTOR to drive podocyte hypertrophy and matrix protein expression," *PLoS One*, vol. 13, no. 11, p. e0207285, 2018.

[64] M. C. I.-d. la Cruz, F. N. Ziyadeh, M. Isono et al., "Effects of high glucose and TGF-β1 on the expression of collagen IV and vascular endothelial growth factor in mouse podocytes," *Kidney International*, vol. 62, no. 3, pp. 901–913, 2002.

[65] T. Nakamura, M. Fukui, I. Ebihara et al., "mRNA expression of growth factors in glomeruli from diabetic rats," *Diabetes*, vol. 42, no. 3, pp. 450–456, 1993.

[66] R. Das, S. Xu, X. Quan et al., "Upregulation of mitochondrial Nox4 mediates TGF-β-induced apoptosis in cultured mouse podocytes," *American Journal of Physiology-Renal Physiology*, vol. 306, no. 2, pp. F155–F167, 2014.

[67] R. M. Wang, Z. B. Wang, Y. Wang et al., "Swiprosin-1 promotes mitochondria-dependent apoptosis of glomerular podocytes via P38 MAPK pathway in early-stage diabetic nephropathy," *Cellular Physiology and Biochemistry*, vol. 45, no. 3, pp. 899–916, 2018.

[68] V. Benedetti, A. M. Lavecchia, M. Locatelli et al., "Alteration of thyroid hormone signaling triggers the diabetes-induced pathological growth, remodeling, and dedifferentiation of podocytes," *JCI Insight*, vol. 4, no. 18, p. e130249, 2019.

[69] J. J. Li, S. J. Kwak, D. S. Jung et al., "Podocyte biology in diabetic nephropathy," *Kidney International*, vol. 72, no. 106, pp. S36–S42, 2007.

[70] N. H. Kim, "Podocyte hypertrophy in diabetic nephropathy," *Nephrology*, vol. 10, no. s2, pp. S14–S16, 2005.

[71] M. Romero, A. Ortega, A. Izquierdo, P. Lopez-Luna, and R. J. Bosch, "Parathyroid hormone-related protein induces hypertrophy in podocytes via TGF-β1 and p27Kip1: implications for diabetic nephropathy," *Nephrology Dialysis Transplantation*, vol. 25, no. 8, pp. 2447–2457, 2010.

[72] C. Ruster, T. Bondeva, S. Franke, M. Forster, and G. Wolf, "Advanced glycation end-products induce cell cycle arrest and hypertrophy in podocytes," *Nephrology Dialysis Transplantation*, vol. 23, no. 7, pp. 2179–2191, 2008.

[73] N. H. Kim, H. Rincon-Choles, B. Bhandari, G. G. Choudhury, H. E. Abboud, and Y. Gorin, "Redox dependence of glomerular epithelial cell hypertrophy in response to glucose," *American Journal of Physiology-Renal Physiology*, vol. 290, no. 3, pp. F741–F751, 2006.

[74] H. A. Jo, J.-Y. Kim, S. H. Yang et al., "The role of local IL6/JAK2/STAT3 signaling in high glucose-induced podocyte hypertrophy," *Kidney Research and Clinical Practice*, vol. 35, no. 4, pp. 212–218, 2016.

[75] M. Iwano, A. Kubo, T. Nishino et al., "Quantification of glomerular TGF-β1 mRNA in patients with diabetes mellitus," *Kidney International*, vol. 49, no. 4, pp. 1120–1126, 1996.

[76] T. Yamamoto, T. Nakamura, N. A. Noble, E. Ruoslahti, and W. A. Border, "Expression of transforming growth factor

beta is elevated in human and experimental diabetic nephropathy," *Proceedings of the National Academy of Sciences*, vol. 90, no. 5, pp. 1814–1818, 1993.

[77] U. Valcourt, M. Kowanetz, H. Niimi, C. H. Heldin, and A. Moustakas, "TGF-beta and the Smad signaling pathway support transcriptomic reprogramming during epithelial-mesenchymal cell transition," *Molecular Biology of the Cell*, vol. 16, no. 4, pp. 1987–2002, 2005.

[78] Y. P. Chang, B. Sun, Z. Han et al., "Saxagliptin attenuates albuminuria by inhibiting podocyte epithelial-to-mesenchymal transition via SDF-1α in diabetic nephropathy," *Frontiers in Pharmacology*, vol. 8, p. 780, 2017.

[79] G. E. Hannigan, C. Leung-Hagesteijn, L. Fitz-Gibbon et al., "Regulation of cell adhesion and anchorage-dependent growth by a new β1-integrin-linked protein kinase," *Nature*, vol. 379, no. 6560, pp. 91–96, 1996.

[80] M. Delcommenne, C. Tan, V. Gray, L. Rue, J. Woodgett, and S. Dedhar, "Phosphoinositide-3-OH kinase-dependent regulation of glycogen synthase kinase 3 and protein kinase B/AKT by the integrin-linked kinase," *Proceedings of the National Academy of Sciences*, vol. 95, no. 19, pp. 11211–11216, 1998.

[81] Y. S. Kang, Y. Li, C. Dai, L. P. Kiss, C. Wu, and Y. Liu, "Inhibition of integrin-linked kinase blocks podocyte epithelial-mesenchymal transition and ameliorates proteinuria," *Kidney International*, vol. 78, no. 4, pp. 363–373, 2010.

[82] T. Chen, L. Y. Zheng, W. Xiao, D. Gui, X. Wang, and N. Wang, "Emodin ameliorates high glucose induced-podocyte epithelial-mesenchymal transition in-vitro and in-vivo," *Cellular Physiology and Biochemistry*, vol. 35, no. 4, pp. 1425–1436, 2015.

[83] C. Dai, D. B. Stolz, S. I. Bastacky et al., "Essential role of integrin-linked kinase in podocyte biology: bridging the integrin and slit diaphragm signaling," *Journal of the American Society of Nephrology: JASN*, vol. 17, no. 8, pp. 2164–2175, 2006.

[84] X. Wu, Y. Gao, L. Xu et al., "Exosomes from high glucose-treated glomerular endothelial cells trigger the epithelial-mesenchymal transition and dysfunction of podocytes," *Scientific Reports*, vol. 7, no. 1, pp. 1–12, 2017.

[85] C. Li and H. M. Siragy, "High glucose induces podocyte injury via enhanced (pro) renin receptor-Wnt-β-catenin-snail signaling pathway," *PLoS One*, vol. 9, no. 2, p. e89233, 2014.

[86] C. Dai, D. B. Stolz, L. P. Kiss, S. P. Monga, L. B. Holzman, and Y. Liu, "Wnt/beta-catenin signaling promotes podocyte dysfunction and albuminuria," *Journal of the American Society of Nephrology: JASN*, vol. 20, no. 9, pp. 1997–2008, 2009.

[87] Z. Lv, M. Hu, J. Zhen, J. Lin, Q. Wang, and R. Wang, "Rac1/-PAK1 signaling promotes epithelial-mesenchymal transition of podocytes in vitro via triggering β-catenin transcriptional activity under high glucose conditions," *The international journal of biochemistry & cell biology*, vol. 45, no. 2, pp. 255–264, 2013.

[88] X. Wang, Y. Gao, N. Tian, D. Zou, Y. Shi, and N. Zhang, "Astragaloside IV improves renal function and fibrosis via inhibition of miR-21-induced podocyte dedifferentiation and mesangial cell activation in diabetic mice," *Drug Design, Development and Therapy*, vol. 12, pp. 2431–2442, 2018.

[89] S. Mathew, X. Chen, A. Pozzi, and R. Zent, "Integrins in renal development," *Pediatric Nephrology*, vol. 27, no. 6, pp. 891–900, 2012.

[90] C. Dessapt, M. O. Baradez, A. Hayward et al., "Mechanical forces and TGFβ1 reduce podocyte adhesion through $\alpha 3\beta 1$ integrin downregulation," *Nephrology Dialysis Transplantation*, vol. 24, no. 9, pp. 2645–2655, 2009.

[91] W. Kriz and K. V. Lemley, "A potential role for mechanical forces in the. Detachment of podocytes and the progression of CKD," *Journal of the American Society of Nephrology*, vol. 26, no. 2, pp. 258–269, 2015.

[92] R. Dai, Y. Lin, H. Liu et al., "A vital role for Angptl3 in the PAN-induced. podocyte loss by affecting detachment and apoptosis in vitro," *BMC Nephrology*, vol. 16, no. 1, p. 38, 2015.

[93] H. C. Chen, C. A. Chen, J. Y. Guh, J. M. Chang, S. J. Shin, and Y. H. Lai, "Altering expression of $\alpha 3\beta 1$ integrin on podocytes of human and rats with diabetes," *Life Sciences*, vol. 67, no. 19, pp. 2345–2353, 2000.

[94] K. Susztak, A. C. Raff, M. Schiffer, and E. P. Bottinger, "Glucose-induced reactive oxygen species cause apoptosis of podocytes and podocyte depletion at the onset of diabetic nephropathy," *Diabetes*, vol. 55, no. 1, pp. 225–233, 2005.

[95] M. F. Bek, M. Bayer, B. Müller et al., "Expression and function of C/EBP homology protein (GADD153) in podocytes," *The American Journal of Pathology*, vol. 168, no. 1, pp. 20–32, 2006.

[96] J. Chen, D. Gui, Y. Chen, L. Mou, Y. Liu, and J. Huang, "Astragaloside IV improves high glucose-induced podocyte adhesion dysfunction via $\alpha_3\beta_1$ integrin upregulation and integrin-linked kinase inhibition," *Biochemical pharmacology*, vol. 76, no. 6, pp. 796–804, 2008.

[97] V. D. P. C. Teixeira, S. M. Blattner, M. Li et al., "Functional consequences of integrin-linked kinase activation in podocyte damage," *Kidney International*, vol. 67, no. 2, pp. 514–523, 2005.

[98] Y. Yang, L. Guo, S. M. Blattner, P. Mundel, M. Kretzler, and C. Wu, "Formation and phosphorylation of the PINCH-1–integrin linked kinase–α-parvin complex are important for regulation of renal glomerular podocyte adhesion, architecture, and survival," *Journal of the American Society of Nephrology*, vol. 16, no. 7, pp. 1966–1976, 2005.

[99] K. Sharma and F. N. Ziyadeh, "The emerging role of transforming growth factor-beta in kidney diseases," *American Journal of Physiology-Renal Physiology*, vol. 266, no. 6, pp. F829–F842, 1994.

[100] S. Kagami, W. Border, E. Ruoslahti, and N. A. Noble, "Coordinated expression of beta 1 integrins and transforming growth factor-beta-induced matrix proteins in glomerulonephritis," *Laboratory Investigation*, vol. 69, no. 1, pp. 68–76, 1993.

[101] R. Das, S. Xu, T. T. Nguyen et al., "Transforming growth factor β1-induced apoptosis in podocytes via the extracellular signal-regulated kinase-mammalian target of rapamycin complex 1-NADPH oxidase 4 axis," *Journal of Biological Chemistry*, vol. 290, no. 52, pp. 30830–30842, 2015.

[102] D. W. P. Lappin, C. Hensey, R. McMahon, C. Godson, and H. R. Brady, "Gremlins, glomeruli and diabetic nephropathy," *Current Opinion in Nephrology and Hypertension*, vol. 9, no. 5, pp. 469–472, 2000.

[103] G. Li, Y. Li, S. Liu et al., "Gremlin aggravates hyperglycemia-induced podocyte injury by a TGFβ/smad dependent signaling pathway," *Journal of Cellular Biochemistry*, vol. 114, no. 9, pp. 2101–2113, 2013.

[104] X. B. Wang, H. Zhu, W. Song, and J. H. Su, "Gremlin regulates podocyte apoptosis via transforming growth factor-β (TGF-β) pathway in diabetic nephropathy," *Medical Science Monitor*, vol. 24, pp. 183–189, 2018.

[105] Y. Zhang, H. Li, J. Hao, Y. Zhou, and W. Liu, "High glucose increases Cdk5 activity in podocytes via transforming growth factor-β1 signaling pathway," *Experimental Cell Research*, vol. 326, no. 2, pp. 219–229, 2014.

[106] W. Liu, Y. Zhang, J. Hao et al., "Nestin protects mouse podocytes against high glucose-induced apoptosis by a Cdk5-dependent mechanism," *Journal of Cellular Biochemistry*, vol. 113, no. 10, pp. 3186–3196, 2012.

[107] Y. Liu, H. Hitomi, S. Diah et al., "Roles of Na+/H+ exchanger type 1 and intracellular pH in angiotensin II-induced reactive oxygen species generation and podocyte apoptosis," *Journal of Pharmacological Sciences*, vol. 122, no. 3, pp. 176–183, 2013.

[108] H. Y. Park, S. B. Seong, S. Y. Min, and T. S. Ha, "CD2-associated protein/phosphoinositide 3-kinase signaling has a preventive role in angiotensin II-induced podocyte apoptosis," *The International Journal of Biochemistry & Cell Biology*, vol. 79, pp. 370–381, 2016.

[109] J. Wang, D. Fu, S. Senouthai, and Y. You, "Critical roles of PI3K/Akt/NF-κB survival axis in angiotensin II-induced podocyte injury," *Molecular Medicine Reports*, vol. 20, no. 6, pp. 5134–5144, 2019.

[110] A. A. Eid, B. M. Ford, B. Bhandary et al., "Mammalian target of rapamycin regulates Nox4-mediated podocyte depletion in diabetic renal injury," *Diabetes*, vol. 62, no. 8, pp. 2935–2947, 2013.

[111] Q. Lin, Y. Ma, Z. Chen et al., "Sestrin-2 regulates podocyte mitochondrial dysfunction and apoptosis under high-glucose conditions via AMPK," *International Journal of Molecular Medicine*, vol. 45, no. 5, pp. 1361–1372, 2020.

[112] X. Cai, L. Bao, J. Ren, Y. Li, and Z. Zhang, "Grape seed procyanidin B2 protects podocytes from high glucose-induced mitochondrial dysfunction and apoptosis via the AMPK-SIRT1-PGC-1α axis in vitro," *Food & Function*, vol. 7, no. 2, pp. 805–815, 2016.

[113] A. A. Eid, B. M. Ford, K. Block et al., "AMP-activated protein kinase (AMPK) negatively regulates Nox4-dependent activation of p53 and epithelial cell apoptosis in diabetes," *Journal of Biological Chemistry*, vol. 285, no. 48, pp. 37503–37512, 2010.

[114] T. Zhang, Y. Chi, Y. Ren, C. du, Y. Shi, and Y. Li, "Resveratrol reduces oxidative stress and apoptosis in podocytes via Sir2-related enzymes, Sirtuins1. (SIRT1)/peroxisome proliferator-activated receptor γ co-activator 1α (PGC-1α) axis," *Medical Science Monitor*, vol. 25, no. 2, pp. 1220–1231, 2019.

[115] A. Piwkowska, D. Rogacka, I. Audzeyenka, M. Jankowski, and S. Angielski, "High glucose concentration affects the oxidant-antioxidant balance in cultured mouse podocytes," *Journal of Cellular Biochemistry*, vol. 112, no. 6, pp. 1661–1672, 2011.

[116] K. Gao, Y. Chi, W. Sun, M. Takeda, and J. Yao, "5'-AMP-activated protein kinase attenuates adriamycin-induced oxidative podocyte injury through thioredoxin-mediated suppression of the apoptosis signal-regulating kinase 1–p38 signaling pathway," *Molecular Pharmacology*, vol. 85, no. 3, pp. 460–471, 2014.

[117] A. A. Eid, Y. Gorin, B. M. Fagg et al., "Mechanisms of podocyte injury in diabetes: role of cytochrome P450 and NADPH oxidases," *Diabetes*, vol. 58, no. 5, pp. 1201–1211, 2009.

[118] J. Toyonaga, K. Tsuruya, H. Ikeda et al., "Spironolactone inhibits hyperglycemia-induced podocyte injury by attenuating ROS production," *Nephrology Dialysis Transplantation*, vol. 26, no. 8, pp. 2475–2484, 2011.

[119] W. T. Liu, F. F. Peng, H. Y. Li et al., "Metadherin facilitates podocyte apoptosis in diabetic nephropathy," *Cell Death & Disease*, vol. 7, no. 11, pp. e2477–e2477, 2016.

[120] X. Wang, D. Tang, Y. Zou et al., "A mitochondrial-targeted peptide ameliorated podocyte apoptosis through a HOCl-alb-enhanced and mitochondria-dependent signalling pathway in diabetic rats and in vitro," *Journal of Enzyme Inhibition and Medicinal Chemistry*, vol. 34, no. 1, pp. 394–404, 2019.

[121] Y. Chen, C. P. Liu, K. F. Xu et al., "Effect of taurine-conjugated ursodeoxycholic acid on endoplasmic reticulum stress and apoptosis induced by advanced glycation end products in cultured mouse podocytes," *American Journal of Nephrology*, vol. 28, no. 6, pp. 1014–1022, 2008.

[122] J. Lei, L. Zhao, Y. Zhang, Y. Wu, and Y. Liu, "High glucose-induced podocyte injury involves activation of mammalian target of rapamycin (mTOR)-induced endoplasmic reticulum (ER) stress," *Cellular Physiology and Biochemistry*, vol. 45, no. 6, pp. 2431–2443, 2018.

[123] A. L. Cao, L. Wang, X. Chen et al., "Ursodeoxycholic acid and 4-phenylbutyrate prevent endoplasmic reticulum stress-induced podocyte apoptosis in diabetic nephropathy," *Laboratory Investigation*, vol. 96, no. 6, pp. 610–622, 2016.

[124] H. Shen, Y. Ming, C. Xu, Y. Xu, S. Zhao, and Q. Zhang, "Deregulation of long noncoding RNA (TUG1) contributes to excessive podocytes apoptosis by activating endoplasmic reticulum stress in the development of diabetic nephropathy," *Journal of cellular Physiology*, vol. 234, no. 9, pp. 15123–15133, 2019.

[125] Y. Wang, H. Li, and S.-P. Song, "β-Arrestin 1/2 aggravates podocyte apoptosis of diabetic nephropathy via Wnt/β-catenin pathway," *Medical Science Monitor*, vol. 24, pp. 1724–1732, 2018.

[126] D. W. Liu, J. H. Zhang, F. X. Liu et al., "Silencing of long noncoding RNA PVT1 inhibits podocyte damage and apoptosis in diabetic nephropathy by upregulating FOXA1," *Experimental & Molecular Medicine*, vol. 51, no. 8, pp. 1–15, 2019.

[127] Y. Chen, L. Zhang, S. Liu et al., "Sam68 mediates high glucose-induced podocyte apoptosis through modulation of Bax/Bcl-2," *Molecular Medicine Reports*, vol. 20, no. 4, pp. 3728–3734, 2019.

[128] F. Gao, M. Yao, Y. Shi et al., "Notch pathway is involved in high glucose-induced apoptosis in podocytes via Bcl-2 and p53 pathways," *Journal of Cellular Biochemistry*, vol. 114, no. 5, pp. 1029–1038, 2013.

[129] J. Feng, Y. Ma, Z. Chen, J. Hu, Q. Yang, and G. Ding, "Mitochondrial pyruvate carrier 2 mediates mitochondrial dysfunction and apoptosis in high glucose-treated podocytes," *Life Sciences*, vol. 237, p. 116941, 2019.

[130] H.-h. Zou, P.-p. Yang, T.-l. Huang, X.-x. Zheng, and G.-s. Xu, "PLK2 plays an essential role in high D-glucose-induced apoptosis, ROS generation and inflammation in podocytes," *Scientific Reports*, vol. 7, no. 1, pp. 1–14, 2017.

[131] X. Bai, J. Geng, X. Li, F. Yang, and J. Tian, "VEGF-A inhibition ameliorates podocyte. Apoptosis via repression of activating protein 1 in diabetes," *American Journal of Nephrology*, vol. 40, no. 6, pp. 523–534, 2015.

[132] R. Xue, R. Zhai, L. Xie et al., "Xuesaitong protects podocytes from apoptosis in diabetic rats through modulating PTEN-PDK1-Akt-mTOR pathway," *Journal of diabetes research*, vol. 2020, Article ID 9309768, 12 pages, 2020.

Hindawi
Journal of Diabetes Research
Volume 2020, Article ID 8305460, 7 pages
https://doi.org/10.1155/2020/8305460

Review Article

Genetic and Biological Effects of ICAM-1 E469K Polymorphism in Diabetic Kidney Disease

Xiuli Zhang,[1] **Norhashimah Abu Seman**,[2] **Henrik Falhammar**,[3,4] **Kerstin Brismar**,[3] **and Harvest F. Gu**[5]

[1]*Department of Nephrology, The second People's Hospital, Shenzhen, The first Affiliated Hospital of Shenzhen University, Guangdong 518000, China*
[2]*Cardiovascular, Diabetes and Nutrition Research Center, Institute for Medical Research, Kuala Lumpur 50588, Malaysia*
[3]*Rolf Luft Research Center for Diabetes and Endocrinology, Department of Molecular Medicine and Surgery, Karolinska Institutet, Stockholm 17176, Sweden*
[4]*Department of Endocrinology, Metabolism and Diabetes, Karolinska University Hospital, Stockholm 17176, Sweden*
[5]*Center for Pathophysiology, School of Basic Medicine and Clinical Pharmacy, China Pharmaceutical University, Nanjing 210009, China*

Correspondence should be addressed to Xiuli Zhang; zhangxiuli54321@sina.com and Harvest F. Gu; feng.gu@cpu.edu.cn

Received 10 March 2020; Accepted 22 May 2020; Published 15 June 2020

Guest Editor: Markus Wallner

Diabetic kidney disease (DKD) is a complex disease, in which local inflammatory stress results from both metabolic and hemodynamic derangements. Intercellular adhesion molecule 1 (ICAM-1) is an acute-phase protein marker of inflammation. In the recent years, clinical observations have reported that increased serum/plasma ICAM-1 levels are positively correlated with albuminuria in the patients with type 1 (T1D) and type 2 diabetes (T2D). Genetic association studies have demonstrated that genetic polymorphisms, including SNP rs5498 (E469K, G/A), in the *ICAM1* gene is associated with DKD. rs5498 is a nonsynonymous SNP and caused by substitution between E (Glu) and K (Lys) for ICAM-1 protein. In this review, we first summarized the genetic effects of *ICAM1* E469K polymorphism in DKD and then demonstrated the possible changes of ICAM-1 protein crystal structures according to the genotypes of this polymorphism. Finally, we discussed the genetic effects of the *ICAM1* E469K polymorphism and the biological role of increased circulating ICAM-1 protein and its formation changes in DKD.

1. Introduction

Diabetes has become a global epidemic and a large proportion of diabetes patients develop microvascular complications. Diabetic kidney disease (DKD) is a prevalent microvascular complication and presents in approximately 25–40% of patients with long-standing diabetes [1, 2]. This complication is characterized with progressive proteinuria from microalbuminuria to persistent proteinuria and confers additional risk of cardiovascular disease and mortality. DKD is the leading global cause of end-stage renal disease, a condition which requires treatment with dialysis or kidney transplantation [2, 3]. The treatment costs of patients with DKD are increasing and impose a substantial burden on the healthcare system. However, as is the case with the majority of complex diseases, identifying causal genetic variants contributing to DKD has proven difficult. A better understanding of the heritable genetic factors underlying DKD by using not only genetic studies but also biological functional analysis may lead to the discovery of new biomarkers of disease susceptibility and novel therapeutic strategies.

Although the pathogenesis in DKD is multifactorial, local inflammatory stress results from both metabolic and hemodynamic derangements [4, 5]. Intercellular adhesion molecule 1 (ICAM-1, OMIM: 147840) is a 90 kD acute-phase protein marker of inflammation. It is an inducible surface glycoprotein expressed in leukocytes, endothelial, and other cell types that promotes adhesion in immunological and inflammatory

reactions [4–6]. To better understand the genetic and biological effects of ICAM-1 in DKD, we have performed the genetic studies of the ICAM1 gene in Swedish patients with type 1 diabetes (T1D) and also in Malays type 2 diabetes (T2D) with or without DKD [7, 8]. According to the genotypes of *ICAM1* genetic polymorphisms, we have analyzed the crystal structures of ICAM-1 protein by using the molecular graphics program PyMol [9–11]. In this article, we focused on the evaluation of the genetic effects of the *ICAM1* E469K polymorphism in DKD and also demonstrated the possible biological changes of ICAM-1 protein crystal structure according to the genotypes of this polymorphism. Based upon that, we summarized the genetic and biological effects of the *ICAM1* E469K polymorphism in DKD, which may provide useful information for better understanding the pathophysiology of the disease.

1.1. The ICAM1 Gene and Its E469K Polymorphism in DKD. The *ICAM1* gene locates to chromosome 19p13.2 in human. Genetic linkage analyses in T1D, T2D, and DKD have indicated that this chromosomal segment resides in a region linked to diabetes. Based upon a genome-wide scan study in 93 affected sib-pairs and 263 multiplex families from the UK, Mein et al. reported that a chromosomal region of 19p13 was linked to T1D [12]. Later on, this linkage with T1D in chromosome 19p13 was replicated by the study of 2658 affected sib-pairs in the USA [13]. The chromosomal region of 19p13 was also found to be linked with several lipid-related traits, including total cholesterol, triglycerides, and low-density lipoprotein in T2D according to the studies of Caucasian, African-American, and Hispanic families [14–16]. All these studies demonstrated that the loci in chromosome 19p13 might confer the susceptibility to diabetes and diabetic vascular complications. Interestingly, there are several genes, including *INSR* (Insulin receptor), RETN (Resistin), and *ICAM1*, located in this chromosomal region.

In 2006, we performed a genetic association study of the *ICAM1 g*ene in Swedish subjects with normal glucose tolerance (NGT), T1D with, or without DKD. Six single nucleotide polymorphisms (SNPs), including three Tag SNPs rs5498 (E469K A/G), rs1799969 (R241G, A/G), and rs281432 (C/G), in the *ICAM1* gene were selected for genotyping experiments based upon the information of their position and function in dbSNP. The SNP rs5498 is a nonsynonymous SNP and caused by substitution between GAG for E (Glu) and AAG for K (Lys) in the 469th codon of ICAM-1 protein (position 10285007 of chromosome 19, contig ID NT_011295.12, from the version of GRCCh38.p7). The *ICAM1* gene consists of 7 exons and the E469K polymorphism is located in the 6th one [6, 17]. There is high linkage disequilibrium (LD) in the gene region covering exons 5 and 6 but LD from promoter to intron 4 is low. The 7th exon has a large 3′-UTR. Genotyping experiments were conducted with a high-throughput SNP scoring technique called dynamic allele-specific hybridization (DASH) [18], which was the first genotyping protocol that we have used in our laboratory. Results showed that there was a significant association of SNP rs5498 (E469K) in the *ICAM1* gene between the subjects with NGT and T1D patients in Swedish population. Further analysis between T1D with and without DKD indicated that this polymorphism was associated with DKD. Interestingly, we found a high heterozygous index of this polymorphism presenting in this population [7]. About 10 years later, we replicated the genetic association study of the *ICAM1* gene in Malays T2D subjects with or without DKD, and the genotyping experiments were done by using TaqMan allelic discrimination. The high heterozygous index of ICAM1 E469K polymorphism was also found in Malays population [8]. With the extension of sample collection and follow-up study, our studied cohorts were enlarged. Thereby, we were able to further evaluate the genotyping data by using TaqMan allelic discrimination. Therefore, Figure 1 in this paper was modified from our previous publications [7, 8] and represented the genotype distribution of the *ICAM1* E469K polymorphism, respectively, in Swedish T1D (Figure 1(a)) and Malays T2D subjects with or without DKD (Figure 1(b)). As seen in the figure, the frequency of heterozygous E469K genotype was higher than the frequencies of both homozygous genotypes, i.e., E469 and 469K.

Once the high heterozygous index in genotyping distribution was seen, several questions had been taken into our consideration. First, was the high heterozygous index of the *ICAM1* K469E polymorphism caused by genotyping error? We replicated genotyping experiments for all Swedish subjects but using another technique named pyrosequencing [19], and the genotyping results were fully matched. Thereby, the possibility of a high heterozygous index caused by genotyping error was excluded. Second, was the high heterozygous index of the *ICAM1* K469E polymorphism induced by genomic duplicons in the *ICAM1* gene? Several reports of human genome analyses have demonstrated that segmental duplications (duplicons) with >90% similarity between two copies may comprise at least 5% of g.DNA in human [20–22]. If a SNP is involved into the region of duplicons, a high heterozygous index may be presented in the genotype distribution. We conducted sequencing analyses along the *ICAM1* gene in the studied subjects, and no duplicated sequence in the gene region was found. Third, did the high heterozygous index of the *ICAM1* E469K polymorphism present in other populations? According to the record in HapMap, the highest genotype frequency of the *ICAM1* E469K polymorphism in 226 European Caucasian individuals was heterozygous at 46.0% [23], which was similar with the genotyping data in Swedish population, while the heterozygous frequency of the *ICAM1* K469E polymorphism in Malays population was even higher (Figures 1(a) and 1(b)). Before we reported the high heterozygous index of *ICAM1* E469K polymorphism [7], there were several genetic association studies of *ICAM1* E469K polymorphism in Danish, Finnish, and Japanese T1D subjects [24–26]. However, the information concerning the genotype distribution of this SNP in Danish and Finnish population was unclear. By the personal communications, we found that the phenomenon of high heterozygous index of this SNP exists in all studied populations.

1.2. Circulating ICAM-1 and Its Formation Changes according to the E469K Polymorphism. DKD is a progressive disease, in

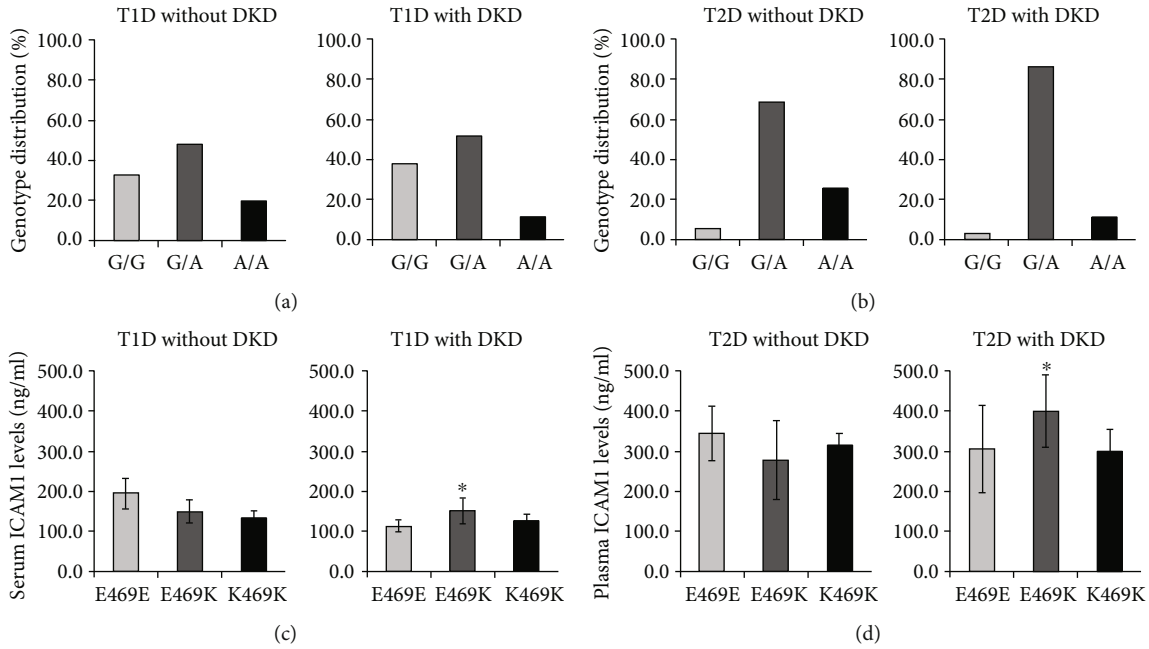

Figure 1: Genotype distribution of the *ICAM1* E469K polymorphism and circulating ICAM-1 levels in type 1 and type 2 diabetes with or without diabetic kidney disease. Genotype distribution patterns (top) showed a high frequency of heterozygous genotypes in type 1 diabetes (T1D) subjects with or without diabetic kidney disease (DKD) (Figure 1(a)) and type 2 diabetes (T2D) patients with or without DKD (Figure 1(b)). According to the genotypes, serum/plasma ICAM-1 levels were analyzed (bottom). In T1D subjects with DKD, the heterozygous *ICAM1* E469K carriers had higher circulating ICAM-1 levels than what in homozygous E469E and K469K carriers ($P < 0.05$, adjusted for age and sex) (Figure 1(c)). The similar finding was found in T2D patients with DKD ($P < 0.05$, adjusted for age and sex) (Figure 1(d)). Data were replicated and modified from Ma et al. 2006 and Abu Seman et al. 2013.

T1D and T2D patients as a result of increased urinary albumin excretion (UAE) rate and compromised renal function. The early phase of microalbuminuria could be reversed, while the reduction of renal function begins with proteinuria. Clinical observation has demonstrated that high circulating ICAM1 levels are associated with DKD, and all caused mortality and cardiovascular morbidity in T1D patients [27, 28]. Similarly, serum/plasma ICAM-1 levels were found to be correlated with albuminuria in T2D patients [29–31]. At the same time, experimental studies with diabetic animal models have supported these clinical observations and demonstrated that serum ICAM-1 levels in streptozotocin-induced rats were increased in parallel with the elevation of UAE [32]. Furthermore, ICAM-1 was found to be overexpressed in tubular epithelial cells of kidney in T2D db/db mice and in glomeruli of diabetic rats [33, 34].

ICAM-1 proteins act as ligands and the primary receptors for ICAM-1 are integrins for mediating cell–cell interactions and signal transduction. However, ICAM-1, unlike most integrin-binding proteins, does not contain an RGD (Arg-Gly-Asp) motif to promote integrin binding but is targeted to two integrins of the $\beta 2$ subunit family, i.e., leukocyte adhesion protein-1 (LFA-1) and Mac-1 (integrin, alpha M) [35, 36]. Thus, ICAM-1 has a role not only for T lymphocytes activation but also for leukocyte–endothelial cell interaction. Considering the presentation of high heterozygous index of *ICAM1* E469K polymorphism, we have for several years paid the attention for analysis of biochemical structure and functional changes of ICAM-1 protein according the genotypes of this polymorphism. We thus used the molecular graphics program PyMol to analyze the formation of ICAM-1 protein. ICAM-1 is composed of five immunoglobulin-like domains (D1-D5), a transmembrane domain with a Gly-X-X-Gly dimerization motif, and a cytoplasmic domain that binds ezrin-radixin-moesin family adaptors that link to the actin cytoskeleton [37–40]. D1 and D3 of ICAM-1 bind to the integrins LFA-1 and Mac-1, respectively. A substantial portion of ICAM-1 on the cell surface dimerizes by fusion of each of the two β-sheets in D4 into a super β-sheet (Yang et al. 2004). The structure of a domain 3-domain 5 (D3-D5) fragment of ICAM-1 has been revealed in both monomeric and dimeric forms (Figure 2(a)). The structure of a D1-D2 fragment of ICAM-1 reveals how the αI domain of integrin LFA-1 binds to D1 [41]. At the center of the interface, a Mg^{2+} ion held by the αI domain binds to an acidic residue, Glu-34, in an edge β-strand of D1 of ICAM-1. Crystal structures of ICAM-1 containing domains 3, 4, and 5 [42] (Protein Databank ID 1p53 and 2 oz4) were visualized. Residue numbering in these structures is according to the mature sequence after removal of a 27-residue signal peptide; numbering in Figures 2(a) and 2(b) follows the immature sequence consistent with the nomenclature used in genetics. The E469K polymorphism locates to domain 5 of ICAM-1. Furthermore, the E-469 sidechain in the D4-D5 crystal structure protrudes from a face of D5 that is rotated about 90° away from the dimer interface. In the K-469 polymorphism, the K sidechain will protrude in a similar direction. Sidechains in the vicinity of residue 469 are shown in Figure 2(b).

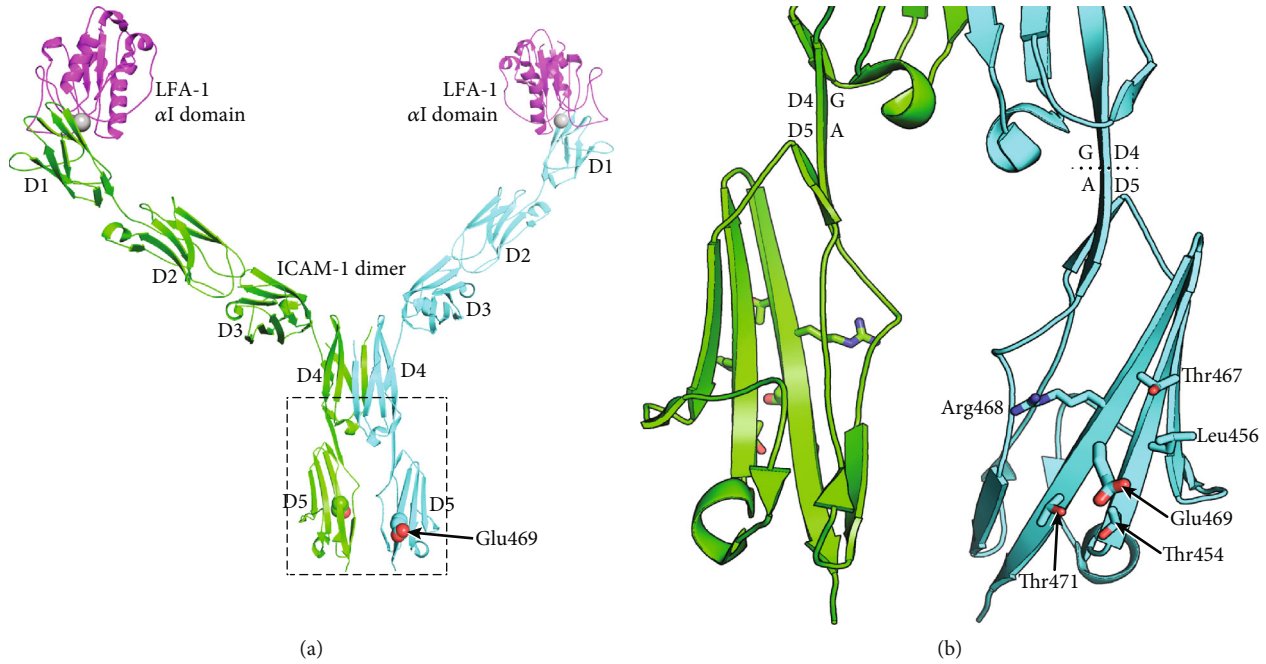

Figure 2: Structural context of the *ICAM1* E469K polymorphism. The structures are shown as ribbon cartoon diagrams. (a) Model of the dimeric ICAM-1 ectodomain bound to the αI domain of integrin LFA-1 reconstructed by combining two crystal structures. Glu-469 in domain 5 is shown with its sidechain atoms as spheres. The Mg^{2+} ion at the center of the LFA-1/ICAM-1 binding site is shown as a silver sphere. (b) Detailed view of the region boxed in (a). Sidechains of Glu-469 and nearby residues are shown in stick representation, and Glu-469 is emphasized with thicker stick. The boundary between the G β-strand in D4 that continues into the A β-strand in D5 is shown with a dotted line in the cyan ICAM-1 monomer.

1.3. Prediction of Genetic and Biological Effects of the E469K Polymorphism in DKD. Ours and other groups have found that the *ICAM1* E469K polymorphism represents a high heterozygous frequency in the genotype distribution of the studied populations [7, 8, 24–26]. This high heterozygous frequency in genotype distribution is unlikely an error due to genotyping limitation or genomic duplication. We have demonstrated that DKD subjects with heterozygous genotype have increased circulating ICAM-1 levels, indicating that the *ICAM1* E469K polymorphism heterozygous is most likely involved in the pathogenesis of DKD.

To understand whether the *ICAM1* E469K polymorphism heterozygous has a biochemical functional role in ICAM-1 protein, we have carried out a structural analysis. Figure 2 shows a model of the dimeric form of ICAM-1 bound to LFA-1 αI domains, constructed from separate crystal structures of LFA-1 αI complexed to D1-D2 and the D3-D5 dimer. The E469K (immature sequence numbering) polymorphism locates to D5 of ICAM-1. Glu-469 is well exposed to solvent in a central location in β-strand G in D5. β-strand G is present in one of the two β-sheets of D5, which contains from one edge to the other the A′, G, F, C, and C′ strands [40]. β-strand G is the last segment of D5 and is followed by a linker of 4 residues and the TM domain. Because of the dyad symmetry of the ICAM-1 dimer, its average orientation on the cell surface will be with the long axes of D4 and D5 normal to the membrane bilayer. This orientation of ICAM-1 dimers is shown in Figure 2; in this view, the membrane would locate horizontally and perpendicular to the plane of the page. The orientation between D4 and D5 is maintained by a continuous β-strand formed by β-strand G in D4 and A in D5. Thus, although in the ICAM-1 dimer the D4-D4 interface is extensive and the D5-D5 interface is small, the stable orientation between D4 and D5 provides confidence that the monomer-monomer interface at D5 of ICAM-1 dimers on cell surfaces. There are no significant interactions between any of the neighboring residues that would be perturbed by the polymorphism. The E469K polymorphism is therefore expected to have no effect on the equilibrium between monomeric and dimeric forms of ICAM-1 on the cell surface. The polymorphism also locates distal from the integrin-binding sites in D1 and D3 and might disrupt the protein biochemical function.

We speculate that it may affect the formation of higher-order assemblies of ICAM-1 on the cell surface. Interaction between cells bearing LFA-1 and ICAM-1 results in the clustering of ICAM-1 at sites of cell-cell adhesion. Clustering has been visualized both at immunological synapses and in "cups" that form around lymphocytes that are migrating through endothelial cells [39]. Clustering is likely to be enhanced by association of integrins with the actin cytoskeleton through adaptors such as talin and kindlin and association of ICAM-1 with the actin cytoskeleton through ezrin-radixin-moesin family members. "Strings" of ICAM-1 may form on the cell surface through dimerization of ICAM-1 both at the D4-D4 interface and a weaker D1-D1 interface [40]. We speculate that ICAM-1 strings laterally associate to form higher-order assemblies through an interface in which Glu-469 participates. Glu-469 protrudes from a relatively flat surface on D5 that bears three Thr residues of

modest hydrophobicity and the hydrophobic residue Leu-456 (Figure 2(b)) that make this face of D5 a candidate for an interface in higher-order lateral association of strings. Because Lys is opposite in charge from Glu, the polymorphism might disrupt such a lateral association. Glu-469 has no specific interactions such as hydrogen bonds with neighboring residues, so an effect on the stability of D5 or ICAM-1 of the polymorphism seems unlikely. We speculate that Glu-469 is involved in the formation of higher-order ICAM-1 assemblies on cell surfaces, an idea that requires further investigation. The question why DKD subjects heterozygous have increased circulating ICAM-1 levels still remains; although, we have demonstrated the *ICAM1* E469K polymorphism has the effects in structure and biochemical functional changes of ICAM-1. It may be necessary to purify the ICAM-1 protein from serum or plasma samples of DKD subjects heterozygous for further 3D protein structural and functional analyses.

There are several reports concerning the heterozygous carriers with increased phenotypes. Previously, Leiber et al. have demonstrated that the 50% of the heterozygous carriers of MEFV mutations have increased serum concentrations of neutrophil-derived protein S100A12 [43]. Recently, Taillandier et al. have reported that the Pro549Ala heterozygous carriers of COL1A2 have more serious phenotypes of hypophosphatasia, mainly due to the dominant-negative effects [44]. Zhu et al. have identified a novel heterozygous variant, which leads to the formation of a truncated COL4A4 protein in Alport Syndrome [45]. Moreover, Serra-Juhe et al. have showed that heterozygous rare variants in several candidate genes of the melanocortin pathway have strong effects in non-syndromic severe obesity [46]. Therefore, the genetic effects of heterozygous of *ICAM1* E469K and its related functional changes that we have been reported in the present study may not be the findings "by chance." Liu et al. have conducted a meta-analysis for *ICAM1* E469K polymorphism and DKD in several cohorts by using allelic, dominant, recessive, and additive models. The statistically significant heterogeneity (I^2 ranged from 62-95) across the studies is observed [47].

Evidence from experimental studies with animal models for diabetes has indicated that ICAM-1 is overexpressed not only in glomeruli diabetic rats (48) but also in tubular epithelial cells of kidney in T2D db/db mice (49). Figure 3 is a schematic diagram to implicate the possible cellular mechanism of ICAM-1 in the development of DKD. In a diabetic condition with hyperglycemia, the *ICAM1* DNA transcription in the nuclei and mRNA translation in plasma of endothelium cells are increased. Subsequently, the ICAM-1 protein expression on the surface of endothelium cells is upregulated. There are leukocyte adhesion protein-1 (LEA-1) in blood. ICAM-1 protein binding activity with LFA-1 is increased, while heterozygous of ICAM-1 E469K protein possibly more actively binds with LFA-1. Thereby, more and more lymphocytes from blood due to combining ICAM-1 and IFA-1 are transferred through endothelium cells in glomeruli and peritubular capillaries of the nephron in the kidney. Consequently, injure of kidney glomeruli and tubular has occurred, and the proteins are excreted to urine.

1.4. Summary and Perspective. Taking together the evidence from genetic studies and biochemical functional analyses,

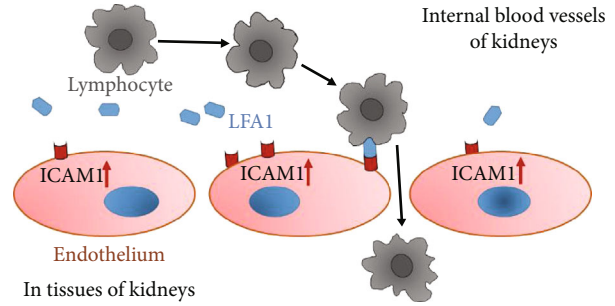

Figure 3: Possible cellular mechanism of ICAM1 in the development of diabetic kidney disease. This schematic diagram implicates that *ICAM1* DNA transcription in the nuclei and mRNA translation in plasma of endothelium cells is increased under a diabetic condition with hyperglycemia. Subsequently, the ICAM-1 protein expression on the surface of endothelium cells is upregulated. ICAM-1 protein binding activity with leukocyte adhesion protein-1 (LEA-1), which is from blood, is increased, while heterozygous of ICAM-1 E469K protein likely more actively binds with LFA-1. Thereby, more and more lymphocytes from blood due to combining ICAM-1 and IFA-1 are transferred through endothelium cells in glomeruli and peritubular capillaries of the nephron in the kidney. Consequently, injure of kidney glomeruli and tubular has occurred.

we propose that the heterozygous carriers of the *ICAM1* E469K polymorphism among the patients with DKD have increased circulating ICAM-1 protein, while the formation of ICAM-1 protein and related biological function are changed. ICAM-1 plays a pathophysiological role in the development of DKD as previously described [6]. Under a diabetic condition with hyperglycemia, the *ICAM1* gene transcription in the nuclei is increased and expression on the surface of endothelium cells is upregulated. ICAM-1 protein binding activity with leukocyte adhesion protein-1 (LFA-1) is increased and more lymphocytes from blood are transferred into cells of glomeruli and peritubular capillaries of the nephron in the kidney. Clinically, serum/plasma ICAM-1 levels are found to be increased and the proteins are released to urine, while injury in kidney glomeruli and tubular has occurred. Therefore, we suggest that heterozygosity of the *ICAM1* E469K polymorphism may confer an increased risk susceptibility in DKD.

Although the additional information concerning the genetic and biological effects of ICAM-1 in DKD in this article has been provided, there are still several questions remained. For instance, what are "the ICAM-1 protein molecular structure and biological function per see" in serum/plasma of DKD subjects with the ICAM1 E469K heterozygous genotype? How does ICAM-1 heterozygous protein bind with LFA-1 with higher activity and subsequently induces more lymphocytes transferred from blood into the cells of glomeruli and peritubular capillaries of the nephron in the kidneys? Further investigation to address these questions has been taken into our consideration.

Conflicts of Interest

The authors declare that they have no conflicts of interest.

Acknowledgments

The authors wish to thank Professor Timothy A. Springer from Harvard Medical School, USA, and Dr. Björn Anderstam from Karolinska University Hospital, Sweden, for their excellent guideline and valuable discussion in the crystal structure and plasma/serum levels of ICAM-1 protein.

References

[1] International Diabetes Federation, *Diabetes Atlas*, International Diabetes Federation, Brussels., 7th ed edition, 2015.

[2] A. Levin, M. Tonelli, J. Bonventre et al., "Global kidney health 2017 and beyond: a roadmap for closing gaps in care, research, and policy," *Lancet*, vol. 390, no. 10105, pp. 1888–1917, 2017.

[3] A. S. Krolewski, J. Skupien, P. Rossing, and J. H. Warram, "Fast renal decline to end-stage renal disease: an unrecognized feature of nephropathy in diabetes," *Kidney International*, vol. 91, no. 6, pp. 1300–1311, 2017.

[4] J. F. Navarro-González, C. Mora-Fernández, M. M. de Fuentes, and J. García-Pérez, "Inflammatory molecules and pathways in the pathogenesis of diabetic nephropathy," *Nature Reviews Nephrology*, vol. 7, no. 6, pp. 327–340, 2011.

[5] R. Pichler, M. Afkarian, B. P. Dieter, and K. R. Tuttle, "Immunity and inflammation in diabetic kidney disease: translating mechanisms to biomarkers and treatment targets," *American Journal of Physiology-Renal Physiology*, vol. 312, no. 4, pp. F716–F731, 2017.

[6] H. F. Gu, J. Ma, K. T. Gu, and K. Brismar, "Association of intercellular adhesion molecule 1 (ICAM1) with diabetes and diabetic nephropathy," *Frontiers in Endocrinology*, vol. 3, 2013.

[7] J. Ma, A. Möllsten, M. Prázny et al., "Genetic influences of the intercellular adhesion molecule 1 (ICAM-1) gene polymorphisms in development of Type 1 diabetes and diabetic nephropathy," *Diabetic Medicine*, vol. 23, no. 10, pp. 1093–1099, 2006.

[8] N. Abu Seman, B. Anderstam, W. N. Wan Mohamud, C. G. Östenson, K. Brismar, and H. F. Gu, "Genetic, epigenetic and protein analyses of intercellular adhesion molecule 1 in Malaysian subjects with type 2 diabetes and diabetic nephropathy," *Journal of Diabetes and its Complications*, vol. 29, no. 8, pp. 1234–1239, 2015.

[9] A. Arroyuelo, J. A. Vila, and O. A. Martin, "Azahar: a PyMOL plugin for construction, visualization and analysis of glycan molecules," *Journal of Computer-Aided Molecular Design*, vol. 30, no. 8, pp. 619–624, 2016.

[10] S. Yuan, H. C. S. Chan, S. Filipek, and H. Vogel, "PyMOL and Inkscape bridge the data and the data visualization," *Structure*, vol. 24, no. 12, pp. 2041-2042, 2016.

[11] Schrodingerhttps://www.schrodinger.com/pymol.

[12] C. A. Mein, L. Esposito, M. G. Dunn et al., "A search for type 1 diabetes susceptibility genes in families from the United Kingdom," *Nature Genetics*, vol. 19, no. 3, pp. 297–300, 1998.

[13] P. Concannon, W. M. Chen, C. Julier et al., "Genome-wide scan for linkage to type 1 diabetes in 2,496 multiplex families from the type 1 diabetes genetics consortium," *Diabetes*, vol. 58, no. 4, pp. 1018–1022, 2009.

[14] G. Imperatore, W. C. Knowler, D. J. Pettitt, S. Kobes, P. H. Bennett, and R. L. Hanson, "Segregation analysis of diabetic nephropathy in Pima Indians," *Diabetes*, vol. 49, no. 6, pp. 1049–1056, 2000.

[15] A. Malhotra, J. K. Wolford, and the American Diabetes Association GENNID Study Group, "Analysis of quantitative lipid traits in the genetics of NIDDM (GENNID) study," *Diabetes*, vol. 54, no. 10, pp. 3007–3014, 2005.

[16] A. A. Adeyemo, T. Johnson, J. Acheampong et al., "A genome wide quantitative trait linkage analysis for serum lipids in type 2 diabetes in an African population," *Atherosclerosis*, vol. 181, no. 2, pp. 389–397, 2005.

[17] https://www.ncbi.nlm.nih.gov/snp/rs5498/.

[18] W. M. Howell, M. Jobs, U. Gyllensten, and A. J. Brookes, "Dynamic allele-specific hybridization. A new method for scoring single nucleotide polymorphisms," *Nature Biotechnology*, vol. 17, no. 1, pp. 87-88, 1999.

[19] M. Ronaghi, M. Uhlén, and P. Nyrén, "A sequencing method based on real-time pyrophosphate," *Science*, vol. 281, no. 5375, pp. 363–365, 1998.

[20] J. C. Venter, M. D. Adams, E. W. Myers et al., "The sequence of the human genome," *Science*, vol. 291, no. 5507, pp. 1304–1351, 2001.

[21] D. Fredman, S. J. White, S. Potter, E. E. Eichler, J. T. D. Dunnen, and A. J. Brookes, "Complex SNP-related sequence variation in segmental genome duplications," *Nature Genetics*, vol. 36, no. 8, pp. 861–866, 2004.

[22] Z. Cheng, M. Ventura, X. She et al., "A genome-wide comparison of recent chimpanzee and human segmental duplications," *Nature*, vol. 437, no. 7055, pp. 88–93, 2005.

[23] https://www.ncbi.nlm.nih.gov/variation/news/ncbi_retiring_HapMap/.

[24] O. P. Kristiansen, R. L. Nolsøe, H. Holst et al., "The intercellular adhesion molecule-1 K469E polymorphism in type 1 diabetes," *Immunogenetics*, vol. 52, no. 1-2, pp. 107–111, 2000.

[25] S. Nejentsev, A. P. Laine, O. Simell, and J. Ilonen, "Intercellular adhesion molecule-1 (ICAM-1) K469E polymorphism: no association with type 1 diabetes among Finns," *Tissue Antigens*, vol. 55, no. 6, pp. 568–570, 2000.

[26] M. Nishimura, H. Obayashi, E. Maruya et al., "Association between type 1 diabetes age-at-onset and intercellular adhesion molecule-1 (ICAM-1) gene polymorphism," *Human Immunology*, vol. 61, no. 5, pp. 507–510, 2000.

[27] J. Lin, R. J. Glynn, N. Rifai et al., "Inflammation and progressive nephropathy in type 1 diabetes in the diabetes control and complications trial," *Diabetes Care*, vol. 31, no. 12, pp. 2338–2343, 2008.

[28] A. S. Astrup, L. Tarnow, L. Pietraszek et al., "Markers of endothelial dysfunction and inflammation in type 1 diabetic patients with or without diabetic nephropathy followed for 10 years: association with mortality and decline of glomerular filtration rate," *Diabetes Care*, vol. 31, no. 6, pp. 1170–1176, 2008.

[29] A. Becker, V. W. M. van Hinsbergh, A. Jager et al., "Why is soluble intercellular adhesion molecule-1 related to cardiovascular mortality?," *European Journal of Clinical Investigation*, vol. 32, no. 1, pp. 1–8, 2002.

[30] A. F. Rubio-Guerra, H. Vargas-Robles, G. V. Ayala, and B. A. Escalante-Acosta, "Correlation between circulating adhesion molecule levels and albuminuria in type 2 diabetic normotensive patients," *Medical Science Monitor*, vol. 13, no. 8, pp. -CR349–CR352, 2007.

[31] K. Sahakyan, B. E. K. Klein, K. E. Lee, M. Y. Tsai, and R. Klein, "Inflammatory and endothelial dysfunction markers and proteinuria in persons with type 1 diabetes mellitus," *European Journal of Endocrinology*, vol. 162, no. 6, pp. 1101–1105, 2010.

[32] Y. Qian, S. Li, S. Ye et al., "Renoprotective effect of rosiglitazone through the suppression of renal intercellular adhesion molecule-1 expression in streptozotocin-induced diabetic rats," *Journal of Endocrinological Investigation*, vol. 31, no. 12, pp. 1069–1074, 2008.

[33] T. Kosugi, T. Nakayama, M. Heinig et al., "Effect of lowering uric acid on renal disease in the type 2 diabetic db/db mice," *American Journal of Physiology-Renal Physiology*, vol. 297, no. 2, pp. F481–F488, 2009.

[34] N. Watanabe, K. Shikata, Y. Shikata et al., "Involvement of MAPKs in ICAM-1 expression in glomerular endothelial cells in diabetic nephropathy," *Acta Medica Okayama*, vol. 65, no. 4, pp. 247–257, 2011.

[35] A. van de Stolpe, N. Jacobs, W. J. Hage et al., "Fibrinogen binding to ICAM-1 on EA.hy 926 endothelial cells is dependent on an intact cytoskeleton," *Thrombosis and Haemostasis*, vol. 75, no. 1, pp. 182–189, 1996.

[36] C. A. Janeway Jr., "How the immune system works to protect the host from infection: a personal view," *Proceedings of the National Academy of Sciences of the United States of America*, vol. 98, no. 13, pp. 7461–7468, 2001.

[37] D. E. Staunton, M. L. Dustin, H. P. Erickson, and T. A. Springer, "The arrangement of the immunoglobulin-like domains of ICAM-1 and the binding sites for LFA-1 and rhinovirus," *Cell*, vol. 61, no. 2, pp. 243–254, 1990.

[38] P. L. Reilly, J. R. Woska, D. D. Jeanfavre, E. McNally, R. Rothlein, and B. J. Bormann, "The native structure of intercellular adhesion molecule-1 (ICAM-1) is a dimer. Correlation with binding to LFA-1," *Journal of Immunology*, vol. 155, no. 2, pp. 529–532, 1995.

[39] O. Barreiro, M:. Yáñez-Mó, J. M. Serrador et al., "Dynamic interaction of VCAM-1 and ICAM-1 with moesin and ezrin in a novel endothelial docking structure for adherent leukocytes," *The Journal of Cell Biology*, vol. 157, no. 7, pp. 1233–1245, 2002.

[40] Y. Yang, C. D. Jun, J. H. Liu et al., "Structural basis for dimerization of ICAM-1 on the cell surface," *Molecular Cell*, vol. 14, no. 2, pp. 269–276, 2004.

[41] M. Shimaoka, T. Xiao, J. H. Liu et al., "Structures of the alpha L I domain and its complex with ICAM-1 reveal a shape-shifting pathway for integrin regulation," *Cell*, vol. 112, no. 1, pp. 99–111, 2003.

[42] X. Chen, T. D. Kim, C. V. Carman, L. Z. Mi, G. Song, and T. A. Springer, "Structural plasticity in Ig superfamily domain 4 of ICAM-1 mediates cell surface dimerization," *Proceedings of the National Academy of Sciences of the United States of America*, vol. 104, no. 39, pp. 15358–15363, 2007.

[43] M. Lieber, T. Kallinich, P. Lohse et al., "Increased serum concentrations of neutrophil-derived protein S100A12 in heterozygous carriers of MEFV mutations," *Clinical and Experimental Rheumatology*, vol. 33, 6 Suppl 94, pp. S113–S116, 2015.

[44] A. Taillandier, C. Domingues, A. Dufour et al., "Genetic analysis of adults heterozygous for ALPL mutations," *Journal of Bone and Mineral Metabolism*, vol. 36, no. 6, pp. 723–733, 2018.

[45] F. Zhu, W. Li, Z. Li, H. Zhu, and J. Xiong, "Identification of a Novel COL4A4 Variant in Compound-Heterozygous State in a Patient with Alport Syndrome and Histological Findings Similar to Focal Segmental Glomerulosclerosis (FSGS)," *Frontiers in Genetics*, vol. 9, 2019.

[46] C. Serra-Juhé, G. Á. Martos-Moreno, F. Bou de Pieri et al., "Heterozygous rare genetic variants in non-syndromic early-onset obesity," *International Journal of Obesity*, vol. 44, no. 4, pp. 830–841, 2020.

[47] L. Liu, D. He, L. Fang, and X. Yan, "Association between E469K polymorphism in the ICAM1 gene and the risk of diabetic nephropathy: a meta-analysis," *Lipids in Health and Disease*, vol. 17, no. 1, p. 293, 2018.

Hindawi
Journal of Diabetes Research
Volume 2020, Article ID 3781214, 11 pages
https://doi.org/10.1155/2020/3781214

Research Article

The 7-Year Change in the Prevalence of Insulin Resistance, Inflammatory Biomarkers, and Their Determinants in an Urban South African Population

Saarah Fatoma Gadija Davids,[1,2] Tandi Edith Matsha,[2] Nasheeta Peer,[1,3] Rajiv Timothy Erasmus,[4] and Andre Pascal Kengne[1,3]

[1]*Department of Medicine, University of Cape Town, Cape Town, South Africa*
[2]*SAMRC/CPUT Cardiometabolic Health Research Unit, Department of Biomedical Sciences, Cape Peninsula University of Technology, Cape Town, South Africa*
[3]*Non-Communicable Diseases Research Unit, South African Medical Research Council, Cape Town, South Africa*
[4]*Department of Chemical Pathology, National Health Laboratory Service (NHLS) and Stellenbosch University, Cape Town, South Africa*

Correspondence should be addressed to Tandi Edith Matsha; matshat@cput.ac.za

Received 3 April 2020; Revised 29 April 2020; Accepted 12 May 2020; Published 22 May 2020

Guest Editor: Markus Wallner

Background. Insulin resistance (IR) and subclinical inflammation are involved in pathological pathways leading to the development of biological cardiovascular risk factors and subsequent cardiovascular events. Therefore, monitoring these processes can provide advanced information on the trajectory of cardiovascular risk profile of a population and inform prevention and control strategies. We investigated changes in IR and subclinical inflammation in a population from Cape Town, South Africa, between 2008/09 and 2014/16. *Methods*. In a total of 2503 ($n = 797$, 2008/09) and ($n = 1706$, 2014/16) participants, IR was calculated using five indices, i.e., insulin fasting, HOMA-IR, QUICKI, McAuley, and Matsuda while subclinical inflammation was measured using usCRP and gamma GT. Linear and logistic regression analyses and interaction tests were conducted. *Results*. The mean age of participants was 53.2 (2008/09) and 48.2 (2014/16), respectively. In females, IR prevalence significantly decreased between 2008/09 and 2014/2016 by all indices ($p \leq 0.021$), while subclinical inflammation prevalence increased from 54.7% (2008/09) to 57.1% (2014/16) based on usCRP and 29.6% to 33.4% based on gamma GT. In a multivariate analysis adjusted for the year of study, age, and gender, prominent factors associated with increased IR or subclinical inflammation were obesity levels measured using waist circumference, glycated haemoglobin, and fasting insulin levels. *Conclusions*. Over the 7-year period, subclinical inflammation increased and this was associated with IR and the metabolic syndrome components, both of which are strong predictors of CVDs. The decrease in IR over the year period reflects in part the much younger age in the second survey.

1. Introduction

Insulin resistance (IR) and subclinical inflammation are among the pathophysiological derangements involved in the development of cardiometabolic risk factors and related cardiometabolic diseases, the leading cause of death worldwide. Insulin is an anabolic hormone that plays a critical role in the maintenance of glucose homeostasis by promoting glucose transport into muscle and adipose tissue (AT) and inhibiting glucose output by the liver [1]. Resistance to these metabolic actions of insulin (IR) is a major determinant for the development of type 2 diabetes mellitus [2]. In addition, a cluster of other cardiovascular disorders such as dyslipidaemia, obesity, hypertension, and endothelial dysfunction (ED) is associated with IR and is known to interact with each other to promote the development of cardiovascular diseases (CVD) [3]. CVDs are associated with low-grade inflammation; this is demonstrated from increased levels of circulating

markers and mediators of inflammation, which in turn are linked to IR [4]. These proinflammatory proteins play a crucial role in the development of IR and subsequent CVDs by activating various inflammatory pathways. For instance, in obesity, macrophages secrete proinflammatory cytokines, tumour necrosis factor alpha (TNFα), and interleukin-6 (IL-6) that impairs insulin signalling [5]. TNFα reduces the expression of glucose transporter type 4 (GLUT4) which is an insulin-regulated glucose transporter and mainly located in adipocytes, skeletal, and cardiac muscles, resulting in increased circulating triglycerides [6]. IL-6 on the other hand regulates the production of C-reactive protein (CRP), a systemic inflammatory biomarker that has been strongly associated with cardiovascular mortality, hypertension, coronary heart disease, stroke, and diabetes [7].

These pathophysiological derangements involved in the occurrence of CVD develop in apparently healthy individuals in the population for some time, before CVDs and their risk factors occur. Therefore, monitoring pathophysiological biomarkers involved in the development of CVD at a population level can provide early information on the trajectory of CVD burden in the population, even before sizable changes are observed in the population level of CVD risk factors. Such preclinical information can assist in the planning of population-level interventions to timeously curb the rising trajectories. However, there has been a dearth of information on the prevalence and patterns of raised pathophysiological biomarkers linked to the development of CVD in the mixed-ancestry population of Cape Town. Therefore, the aim of this study is to investigate the temporal changes in the prevalence of IR, inflammatory biomarkers, and their determinants in the mixed ancestry population of Bellville South, Cape Town, between 2008/09 and 2014/16.

2. Materials and Methods

2.1. Study Population and Sampling Procedure. In the mixed ancestry population in Bellville South, Cape Town, two independent cross-sectional surveys were conducted in 2008/09 and 2014/16. Residents who were 18 years and older (2008/09) or 20 years and older (2014/16) were invited to participate in the survey by recruiters who visited each dwelling in the area. Individuals who were bed-ridden or pregnant and underweight and those who were under the age of 20 years in the 2008/2009 survey were excluded. Therefore, the number of participants was 946 in 2008/09 and 1989 in 2014/16. After excluding participants with missing data, who did not fulfil the age criteria, had known diabetes, or were underweight, the final sample size was 797 in 2008/09 and 1706 in 2014/16.

2.2. Data Collection. Eligible participants were assessed at a designated research site where trained personnel took informed consent, administered the World Health Organization (WHO) stepwise questionnaire [8], and conducted clinical and biochemical assessments. Anthropometric measurements were performed as per the WHO standardized techniques. Waist and hip circumferences were collected using a nonelastic tape measure while height was measured using a stadiometer to the nearest centimeter [8]. Blood pressure was measured three times in 3-minute intervals [8]. The lowest systolic blood pressure (SBP) and its corresponding diastolic blood pressure (DBP) and pulse readings were used. An oral glucose tolerance test (OGTT) was administered to individuals without known diabetes after an overnight fasting to diagnose type 2 diabetes [9]. Biochemical measurements were sent to an ISO 15189 accredited lab in Cape Town. The following were tested: plasma glucose, plasma insulin, high-density lipoprotein cholesterol (HDL-C), low-density lipoprotein cholesterol (LDL-C), total cholesterol (TC), triglycerides, ultrasensitive C-reactive protein (usCRP), and gamma-glutamyl transferase (gamma GT).

2.3. Assessment of Insulin Resistance and Subclinical Inflammation. IR was calculated using five indices: the 75th percentile of fasting insulin, the homeostatic model assessment of IR (HOMA-IR) [10], the 25th percentile QUICKI [11], McAuley index [12], and Matsuda index [13]. The 75th or 25th percentiles were derived from the first survey and the same cut-off points were applied to the two survey populations. Using percentiles specific to each of the sample would lead to differing cut-off points and no change in IR prevalence over time. Subclinical inflammation was assessed using two biomarkers with the following values defining subclinical inflammation: usCRP > 3 mg/L [14] and gamma GT $\geq$ 38 IU/L [15].

2.4. Calculations and Definitions. Body mass index (BMI) was calculated as weight [in kilograms (kg)] divided by height [in meters squared (m^2)]. For this study, BMI status was divided into three categories, as per the WHO [16]: normal weight (<25.0 kg/m^2), overweight (25.0 kg/m^2-29.9 kg/m^2), and obesity ($\geq$30.0 kg/m^2). The level of education was divided into two categories: $\leq$7 years of education (up to completion of primary school) and >7 years of education (secondary schooling and higher). Cotinine level of >10 ng/mL was defined as current smoker. Alcohol consumption was self-reported in the administered questionnaire [8]. Hypertension was defined as SBP $\geq$ 140 mmHg and/or DBP $\geq$ 90 mmHg or taking blood pressure lowering medication. The glucose tolerance status was determined using the recommended OGTT test. Prediabetes was defined as fasting plasma glucose between 6.1 and 6.9 mmol/L and/or a 2-hour glucose value between 7.8 mmol/L and 11.1 mmol/L [17]. Screened type 2 diabetes was defined as fasting plasma glucose $\geq$ 7.0 mmol/L and/or a 2-hour post-OGTT plasma glucose $\geq$ 11.1 mmol/L. Known type 2 diabetes was self-reported and/or on diabetes medication [17].

2.5. Statistical Analysis. Statistica v.13 (TIBCO Software Inc., 2017) and SPSS v.25 (IBM Corp., 2011) were used for the data analyses. Data was tested for normality using normality Q-Q plot. The results are reported as the median (25th and 75th percentiles), mean (standard deviation), and count (percentages). For comparison, the chi-square test, analysis of variance test (ANOVA), or Kruskal-Wallis test was used as appropriate. IR was based on the 75th percentile of fasting insulin (12.5 mIU/L) and HOMA IR (3.1) or the 25th

percentile of QUICKI (0.53), McAuley index (6.1), and Matsuda index (4.0). Crude prevalence of IR and inflammatory biomarkers was estimated in all participants as well as in participants only with normoglycemia and who were not taking lipid and/or blood pressure lowering medications. Linear regressions and logistic regression, adjusted for age, gender, and year of study, were used to determine the changes in IR indices, inflammatory biomarkers, and their respective determinants between the two cross-sectional studies. A p value < 0.05 was used to characterize statistically significant results.

3. Results

3.1. Characteristics. The population characteristics by year are presented in Table 1. In both surveys, i.e., 2008/09 and 2014/16, majority of participants were women. The average age in 2014/16 was younger compared to that in 2008/09 (48.2 ± 15.3 years vs. 53.2 ± 14.8 years, $p < 0.001$). Waist circumference (91.4 ± 17.1 cm vs. 96.3 ± 15.0 cm, $p < 0.001$) and hip circumference (103.8 ± 16.5 cm vs. 109.8 ± 14.7 cm, $p < 0.001$) were smaller in 2014/16 vs. 2008/09. The average BMI decreased between 2008/09 and 2014/16 ($p = 0.013$), as did both the prevalence of overweight (27.7% vs. 22.9%) and obesity (44.7% vs. 41.3%). However, blood pressure levels increased significantly between the two periods (Table 1) (both $p < 0.001$). Lipid profiles improved between the two periods: HDL-C increased from 1.2 (1.0, 1.5) mmol/L to 1.3 (1.1; 1.5) mmol/L and LDL-C decreased from 3.6 (3.0; 4.3) to 3.1 (2.5; 3.7) mmol/L (both $p < 0.001$). The abnormal glucose tolerance status significantly decreased between 2008/09 and 2014/16 for prediabetes (23.2% vs. 17.4%) and screen-detected diabetes (17.1% vs. 7.3%) (both $p < 0.001$). Current smokers significantly increased between 2008/09 (43.8%) and 2014/16 (52.9%) ($p < 0.001$), while alcohol use was similar between the periods ($p = 0.958$).

3.2. Markers of IR and Inflammation across the Two Time-Points. Markers of subclinical inflammation increased slightly between the periods; i.e., median usCRP increased from 3.6 mg/L in 2008/2009 to 3.9 mg/L in 2014/2016 ($p = 0.228$) and gamma GT from 27 IU/L to 28 IU/L ($p = 0.011$). The indices of IR were generally similar between the two periods (all $p \geq 0.05$) (Table 1).

3.3. Prevalence of Insulin Resistance and Subclinical Inflammation. In the overall study population including screen-detected diabetes, prediabetes, and normoglycemia, IR prevalence significantly decreased between 2008/09 and 2014/2016, fasting insulin from 24.8% in 2008/2009 to 16.9% in 2014/2016, HOMA-IR from 24.8% to15.4%, QUICKI from 23.6% to 13.3%, McAuley from 25.5% to 21.3%, and Matsuda from 25.5% to 18.8% ($p \leq 0.021$). A similar pattern was observed among women between the periods for all the IR indices ($p < 0.023$). Although the prevalence of IR also decreased in men, it was not significant ($p \geq 0.050$). In participants with normoglycemia, excluding those taking lipid lowering and/or hypertension medication, the decrease in IR was not significant with McAuley index, from 35.7% in 2008/2009 to 32.8% ($p = 0.157$) in the overall study population. A similar trend was observed in women; however, in men, significant decreases in the prevalence of IR were observed with QUICKI from 27.8% to 19.9% ($p = 0.034$) and Matsuda index from 26.7% to 18.2% ($p = 0.020$) (Table 2).

Subclinical inflammation prevalence increased slightly between 2008/09 and 2014/16, from 54.7% to 57.1% ($p = 0.264$) for usCRP and 29.6% to 33.4% ($p = 0.055$) for gamma GT. Both subclinical inflammatory biomarkers increased in women, but this was significant only for gamma GT (26.2% to 32.1%, $p = 0.009$). In contrast, there were no significant changes in these biomarkers in men between the periods, with both markers ($p \geq 0.368$), respectively. In the group with normoglycemia without lipid lowering and/or hypertension medication, the prevalence of subclinical inflammation as measured by gamma GT increased significantly in women, with $p = 0.030$ (Table 2).

3.4. Determinants of Levels of Markers of Insulin Resistance. From the two surveys, linear regression models for IR and subclinical inflammation, adjusted for year of study, gender, age, and smoking, were determined using log-transformed dependent variables. For IR, the QUICKI, McAuley, and Matsuda indices showed inverse values since their cut-off values are inverse. Using the HOMA-IR index, an increased level of IR was indicated in year of study and age, while men were inversely affected (Table 3). Furthermore, IR markers with the exception of the QUICKI index were positively associated with HbA1c, waist circumference, triglycerides, and gamma GT (all $p \leq 0.004$), while HDL-C, education level < 7 years, and those who reported current alcohol drinking status were negatively associated, with all $p \leq 0.018$ (Table 3). Similarly, in a logistic regression adjusted for year of study, age, and gender, the odds of IR in participants in 2014/16 were lower compared to those in 2008/09 (Table 4). Smokers and current drinkers had a lower odds ratio of IR, while usCRP and gamma GT were associated with higher odds of IR, using HOMA-IR (usCRP odds ratio (OR) 2.39, 95% CI 1.88; 3.04 and gamma GT OR: 1.93, 95% 1.54; 2.43) (all $p \leq 0.011$).

3.5. Determinants of Levels of Markers of Subclinical Inflammation. In a secondary analysis presented in Table 5, subclinical inflammation was significantly higher by usCRP in 2014/16 compared with 2008/09 [0.08% (0.04; 0.13), $p = 0.001$]. Additionally, waist circumference, hip circumference, 2-hour glucose, HbA1c, gamma GT, and education < 7 years increased with higher usCRP levels (all $p \leq 0.009$). Similar findings were observed in the associations with gamma GT with the addition of men gender, current drinkers, systolic blood pressure, fasting glucose, fasting insulin, HDL-C, triglycerides, and usCRP, also associated with subclinical inflammation ($p \leq 0.017$).

The logistic regression, adjusted for year of study, age, and gender, had shown an almost 1.5-fold higher odds of inflammation in 2014/16 compared to 2008/09 for both markers of inflammation. Insulin resistance, using McAuley and Matsuda indices, had demonstrated an almost 2-fold significantly greater odds of inflammation using usCRP or

Table 1: Characteristics of participants in 2008/09 and 2014/16.

Characteristics	2008/09 ($n = 797$) ($n = 797$) Median (25^{th}; 75^{th} percentiles)	2014/16 ($n = 1706$) ($n = 1706$) Median (25^{th}; 75^{th} percentiles)	p value
Gender			0.114
Women, n (%)	620 (77.8)	1278 (74.9)	
Men, n (%)	177 (22.2)	428 (25.1)	
Age, year*	53.2 ± 14.8	48.2 ± 15.3	<0.001
Level of education			
Education level ≤ 7 years, n (%)	271 (34.2)	559 (33.0)	0.553
Education level > 7 years, n (%)	522 (65.8)	1136 (67)	0.553
Alcohol use			
Current drinker, n (%)	563 (71.4)	1213 (71.5)	0.958
Nondrinker, n (%)	225 (28.6)	483 (28.5)	0.958
Cotinine (ng/mL)	10 (9; 311)	48.2 (10; 268)	<0.001
Tobacco use			
Nonsmoker, n (%)	447 (56.2)	779 (47.1)	<0.001
Smoker, n (%)	348 (43.8)	874 (52.9)	<0.001
Anthropometry			
Body mass index (kg/m^2)*	29.64 ± 7.24	28.83 ± 8.1	0.013
BMI status			
Normal (18.5 kg/m^2 to 25 kg/m^2), n (%)	218 (27.7)	603 (35.8)	<0.001
Overweight (25 kg/m^2 to 29.9 kg/m^2), n (%)	218 (27.7)	385 (22.9)	0.009
Obese (≥30 kg/m^2), n (%)	352 (44.7)	696 (41.3)	0.109
Waist circumference (cm)*	96.3 ± 15.0	91.4 ± 16.9	<0.001
Hip circumference (cm)*	109.8 ± 14.7	103.83 ± 16.5	<0.001
Waist-to-hip ratio*	0.9 ± 0.1	0.88 ± 0.09	0.504
Systolic blood pressure (mmHg)*	123 ± 19	126 ± 24	<0.001
Diastolic blood pressure (mmHg)*	75 ± 12	82 ± 14	<0.001
Fasting glucose (mmol/L)	5.6 (5.0;6.5)	5.0 (4.6;5.6)	<0.001
2 hr glucose (mmol/L)	6.8 (5.7;8.7)	6.1 (4.9; 7.6)	<0.001
HBA1c (mmol/mol)*	65 ± 10	63 ± 9	<0.001
HBA1c (%)*	5.9 ± 0.9	5.8 ± 0.8	<0.001
Fasting insulin (mIU/L)	6.6 (2.7; 12.5)	6.6 (4.2; 10.4)	0.414
2 hr insulin (mIU/L)	38.1 (19.5; 72.2)	38.8 (20.7; 71.9)	0.829
Normoglycemia, n (%)	474 (59.7)	1278 (75.3)	<0.001
Pre-diabetes, n (%)	184 (23.2)	296 (17.4)	<0.001
Screened-detected diabetes, n (%)	136 (17.1)	124 (7.3)	<0.001
HDL-C (mmol/L)	1.2 (1.0; 1.5)	1.3 (1.1; 1.5)	<0.001
LDL-C (mmol/L)	3.6 (3.0; 4.3)	3.1 (2.5; 3.7)	<0.001
Triglycerides (mmol/L)	1.2 (0.9; 1.7)	1.5 (0.8; 1.7)	0.620
Ultra-sensitive C-reactive protein (mg/L)	3.6 (0.9; 9.4)	3.9 (1.5; 8.6)	0.228
Gamma-glutamyl transferase (IU/L)	27 (19; 42)	28 (20; 45)	0.011
HOMA-IR	1.6 (0.6; 3.1)	1.4 (0.9; 2.4)	0.859
QUICKI	0.6 (0.5; 0.9)	0.7 (0.6; 0.8)	0.124
McAuley index	7.9 (6.1; 10.7)	7.9 (6.4; 9.4)	0.050
Matsuda index	7.9 (4.0; 17.8)	8.4 (4.8; 15.3)	0.685

*Mean ± SD; screen-detected diabetes: newly diagnosed diabetics; HDL-C: high-density lipoprotein cholesterol; LDL-C: low-density lipoprotein cholesterol; HOMA-IR: homeostatic model assessment of insulin resistance.

Table 2: Prevalence of IR and inflammation in all participants and in those with normoglycemia and not on lipid lowering and/or hypertension medication.

	Overall			Women			Men			Gender ∗ year of study
	2008/09 *n* (%)	2014/16 *n* (%)	*p* value	2008/09 *n* (%)	2014/16 *n* (%)	*p* value	2008/09 *n* (%)	2014/16 *n* (%)	*p* value	*p* interaction
Insulin resistance: all participants										
Fasting insulin	196 (24.8)	278 (16.9)	<0.001	174 (28.4)	231 (18.7)	<0.001	22 (12.5)	47 (11.4)	0.706	0.939
HOMA-IR	196 (24.8)	253 (15.4)	<0.001	170 (27.7)	205 (16.6)	<0.001	26 (14.8)	48 (11.7)	0.296	0.375
QUICKI	186 (23.6)	218 (13.3)	<0.001	158 (25.8)	176 (14.3)	<0.001	28 (15.9)	42 (10.2)	0.050	0.550
McAuley index	201 (25.5)	348 (21.3)	0.021	167 (27.2)	275 (22.4)	0.023	34 (19.5)	73 (18.0)	0.667	0.369
Matsuda index	200 (25.5)	299 (18.8)	<0.001	174 (28.6)	255 (21.5)	0.001	26 (14.8)	44 (10.9)	0.194	0.119
Insulin resistance: normoglycemia and not on lipid lowering and/or hypertension medication										
Fasting insulin	247 (31.3)	413 (25.1)	0.001	211 (34.4)	343 (27.8)	0.004	36 (20.5)	70 (17.0)	0.317	0.765
HOMA-IR	288 (36.5)	451 (27.4)	<0.001	248 (40.5)	377 (30.6)	<0.001	40 (22.7)	74 (18.0)	0.181	0.455
QUICKI	323 (40.9)	504 (30.6)	<0.001	274 (44.7)	422 (34.2)	<0.001	49 (27.8)	82 (19.9)	0.034	0.548
McAuley index	281 (35.7)	535 (32.8)	0.157	233 (38.0)	430 (35.1)	0.216	48 (27.6)	105 (25.9)	0.678	0.236
Matsuda index	310 (39.5)	542 (34.1)	0.009	263 (43.3)	469 (39.5)	0.123	47 (26.7)	73 (18.2)	0.020	0.170
Sub-clinical inflammation: all participants										
usCRP	436 (54.7)	967 (57.1)	0.264	351 (56.6)	772 (60.8)	0.079	85 (48.02)	195 (45.9)	0.631	0.092
Gamma GT	235 (29.6)	567 (33.4)	0.055	162 (26.2)	408 (32.1)	0.009	73 (42.2)	159 (37.3)	0.368	0.158
Sub-clinical inflammation: normoglycemia and not on lipid lowering and/or hypertension medication										
usCRP	160 (46.2)	480 (49.5)	0.3	124 (47.9)	356 (53.1)	0.157	36 (41.4)	124 (41.5)	0.625	0.217
Gamma GT	83 (24.1)	276 (28.4)	0.12	50 (19.4)	176 (26.2)	0.03	33 (37.9)	100 (33.3)	0.372	0.166

∗Interaction between men and women; HOMA-IR: homeostatic model assessment of insulin resistance; usCRP: ultrasensitive C-reactive protein; gamma GT: gamma-glutamyl transferase.

gamma GT. Additionally, age was significantly associated with inflammation using usCRP, while the lower level of education was associated with inflammation using gamma GT. Subclinical inflammation, using gamma GT, had shown greater odds in smokers (OR 1.26, 95% 1.03; 1.53) and current drinkers (OR 2.47, 95% CI 1.99; 3.06) (Table 6).

4. Discussion

Our study found a significant decrease in the overall prevalence of IR over time, which was mainly driven by a significant decrease in women. Using HOMA-IR for example, IR prevalence decreased significantly from 24.8% in 2008/09 to 15.4% in 2014/16 in the overall study population and from 27.7% to 16.6% in women but was not significantly different in men (2008/09: 14.8% to 2014/16: 11.7%). However, using the McAuley index, which is recommended for population-based studies, the decrease in IR prevalence was nonsignificant (35.7% to 32.8%, $p = 0.157$), particularly when only normoglycemic participants excluding those on lipid lowering and/or hypertension medication were analysed separately. Subclinical inflammation marginally increased with both usCRP and gamma GT, indicating increases from 2008/09 to 2014/16. In a multivariable analysis adjusted for the year of study, age, and gender, prominent factors associated with increased IR or subclinical inflammation were abdominal obesity, glycated haemoglobin, and fasting insulin levels.

IR and inflammation are unequivocally associated with the development of type 2 diabetes and CVDs; however, it has also been established that IR even in subjects without type 2 diabetes is connected to high mortality rates, mainly through coronary heart diseases [18]. Estimates from the international diabetes federation have shown that there is a major shift occurring worldwide with regard to type 2 diabetes and CVDs, with predictions of over 100% increases in Africa [19]. In our study, the prevalence of IR ranged from 24.8% to 15.4% using HOMA-IR cut-off of 3.1 between 2008/2009 and 2014/2016. Although our study findings suggest a decrease in IR between the two time periods, these results need to be interpreted with caution. First, the mean age of participants in these two cohorts was significantly different with 2014/2016 overrepresented by younger participants; second, when using the McAuley index, which is recommended for population-based studies, IR nonsignificantly decreased from 35.7% in 2008/2009 to 32.8% in 2014/2016; and lastly, subclinical inflammation increased between the two periods suggesting an increasing risk of CVD.

With regard to comparing the prevalence of IR in our study population with the literature, our findings are somewhat similar to a report from Denmark which reported a prevalence of 17% using a HOMA-IR cut-off of 2.5 [20]. However, our findings contrast with a South African study which reported a prevalence of 55.5% using a cut-off of 2.6 [21]. This varying prevalence could be related to the noncensus on the cut-off criteria for the definition of IR. According to the WHO [22], the $\geq 75^{th}$ percentile value is recommended for the definition of IR; however, various cut-offs are reported in the literature.

Table 3: Year of study-, gender-, age-, and smoking-adjusted linear regression models for determinants of insulin resistance in all participants.

	Model 1: log insulin fasting*				Model 2: log HOMA-IR*				Model 3: log QUICKI index*				Model 4: log McAuley index*				Model 5: log Matsuda index*			
	B	95% confidence interval		*p* value	B	95% confidence interval		*p* value	B	95% confidence interval		*p* value	B	95% confidence interval		*p* value	B	95% confidence interval		*p* value
		Lower	Upper			Lower	Upper			Lower	Upper			Lower	Upper			Lower	Upper	
Year of study (2014/16)	0.16	0.13	0.20	<0.001	0.06	0.03	0.10	<0.001	-0.39	-0.51	-0.26	<0.001	-0.05	-0.06	-0.04	<0.001	-0.09	-0.12	-0.06	<0.001
Gender (men)	-0.15	-0.19	-0.11	<0.001	-0.15	-0.18	-0.11	<0.001	0.18	0.04	0.32	0.012	0.04	0.03	0.05	<0.001	0.21	0.18	0.25	<0.001
Age	0.43	0.30	0.55	<0.001	0.40	0.28	0.51	<0.001	-0.39	-0.85	-0.05	0.085	-0.12	-0.16	-0.08	<0.001	-0.21	-0.33	-0.10	<0.001
Current smokers	-0.08	-0.12	-0.05	<0.001	-0.08	-0.11	-0.05	<0.001	0.09	-0.02	0.21	0.122	0.02	0.01	0.03	<0.001	0.12	0.09	0.15	<0.001
Education (<7 years)	-0.05	-0.09	-0.02	0.002	-0.04	-0.08	-0.01	0.007	0.01	-0.11	0.13	0.829	0.01	0.01	0.02	0.002	0.04	0.01	0.07	0.012
Current drinkers	-0.06	-0.10	-0.02	0.003	-0.05	-0.08	-0.01	0.007	0.03	-0.11	0.16	0.707	0.02	0.01	0.03	0.003	0.05	0.01	0.08	0.006
Waist circumference	0.85	0.65	1.04	<0.001	0.87	0.68	1.05	<0.001	-0.82	-1.50	-0.15	0.017	-0.24	-0.29	-0.18	<0.001	-0.87	-1.05	-0.70	<0.001
Hip circumference	-0.15	-0.34	0.05	0.142	-0.15	-0.33	0.03	0.107	0.58	-0.10	1.27	0.094	0.04	-0.01	0.09	0.142	0.22	0.05	0.40	0.014
Systolic blood pressure	0.01	-0.07	0.09	0.792	0.03	-0.04	0.10	0.369	0.00	-0.26	0.27	0.993	0.00	-0.02	0.02	0.792	-0.05	-0.12	0.02	0.142
HbA1c	2.95	0.92	5.02	0.004	8.67	6.66	10.72	<0.001	-9.78	-15.87	-3.25	0.004	-0.81	-1.36	-0.26	0.004	-8.19	-9.92	-6.41	<0.001
HDL-C*	-0.28	-0.51	-0.05	0.018	-0.29	-0.50	-0.07	0.010	0.06	-0.75	0.87	0.877	0.08	0.01	0.14	0.018	0.35	0.13	0.56	0.001
LDL-C*	0.29	-0.10	0.68	0.150	0.26	-0.11	0.62	0.172	-0.46	-1.84	0.91	0.509	-0.08	-0.19	0.03	0.150	-0.27	-0.62	0.09	0.148
Triglycerides*	0.31	0.19	0.43	<0.001	0.31	0.20	0.42	<0.001	-0.20	-0.62	0.22	0.342	-0.40	-0.43	-0.36	<0.001	-0.34	-0.45	-0.23	<0.001
usCRP*	-0.02	-0.05	0.02	0.323	-0.01	-0.04	0.02	0.505	0.07	-0.03	0.18	0.177	0.00	0.00	0.01	0.323	0.00	-0.03	0.03	0.945
Gamma GT*	0.10	0.04	0.15	<0.001	0.13	0.07	0.18	<0.001	-0.16	-0.36	0.03	0.098	-0.03	-0.04	-0.01	<0.001	-0.13	-0.19	-0.08	<0.001

*Log transformed; HOMA-IR: homeostatic model assessment of insulin resistance; HDL-C: high-density lipoprotein cholesterol; LDL-C: low-density lipoprotein cholesterol; usCRP: ultrasensitive C-reactive protein; gamma GT: gamma-glutamyl transferase.

Table 4: Age-, sex-, and year of study-adjusted odds ratios (with 95% confidence intervals) for the determinants of insulin resistance in all participants.

	Model 1: insulin fasting				Model 2: HOMA-IR				Model 3: QUICKI index				Model 4: McAuley index				Model 5: Matsuda index			
	Odds ratio	95% confidence interval		p value	Odds ratio	95% confidence interval		p value	Odds ratio	95% confidence interval		p value	Odds ratio	95% confidence interval		p value	Odds ratio	95% confidence interval		p value
		Lower	Upper			Lower	Upper			Lower	Upper			Lower	Upper			Lower	Upper	
Year of study																				
2008/09	1				1				1				1				1			
2014/16	0.57	0.46	0.71	<0.001	0.51	0.41	0.64	<0.001	0.45	0.36	0.57	<0.001	0.78	0.63	0.97	0.025	0.67	0.54	0.84	<0.001
Gender																				
Women	1				1				1				1				1			
Men	0.58	0.43	0.77	<0.001	0.67	0.50	0.89	0.006	0.72	0.54	0.97	0.031	0.83	0.64	1.06	0.137	0.53	0.4	0.71	<0.001
Age	0.99	0.98	1.00	0.002	0.99	0.99	1.00	0.106	0.99	0.98	1.00	0.031	1.00	1.00	1.01	0.538	1.00	0.99	1.01	0.548
Tobacco use																				
Nonsmoker	1				1				1				1				1			
Smoker	0.66	0.52	0.83	<0.001	0.64	0.50	0.80	<0.001	0.72	0.57	0.92	0.009	0.69	0.56	0.86	0.001	0.50	0.39	0.63	<0.001
Level of education																				
<7 years	1				1				1				1				1			
≥7 years	1.26	0.99	1.61	0.063	1.14	0.89	1.45	0.310	1.13	0.88	1.46	0.349	1.09	0.87	1.37	0.461	1.21	0.95	1.54	0.115
Alcohol use																				
Nondrinker	1				1				1				1				1			
Current drinker	0.66	0.5	0.88	0.004	0.7	0.52	0.92	0.011	0.66	0.49	0.88	0.005	0.74	0.57	0.95	0.02	0.62	0.47	0.83	0.001
BMI status																				
Normal	1				1				1				1				1			
Overweight	1.18	0.88	1.56	0.518	1.07	0.80	1.44	0.778	1.19	0.88	1.60	0.538	1.08	0.82	1.42	0.501	1.15	0.86	1.54	0.563
Obese	1.11	0.86	1.43	0.518	1.1	0.85	1.41	0.778	1.08	0.83	1.41	0.538	1.15	0.91	1.46	0.501	1.12	0.87	1.44	0.563
usCRP																				
No	1				1				1				1				1			
Yes	2.28	1.81	2.88	<0.001	2.39	1.88	3.04	<0.001	2.16	1.69	2.77	<0.001	2.05	1.65	2.55	<0.001	2.38	1.89	3.01	<0.001
Gamma GT																				
No	1				1				1				1				1			
Yes	1.75	1.4	2.19	<0.001	1.93	1.54	2.43	<0.001	2.08	1.65	2.64	<0.001	2.33	1.89	2.88	<0.001	2.23	1.78	2.79	<0.001

HOMA-IR: homeostatic model assessment of insulin resistance; usCRP: ultrasensitive C-reactive protein; gamma GT: gamma-glutamyl transferase.

Table 5: Year of study-, gender-, age-, and smoking-adjusted linear regression models for determinants of inflammation in all participants.

	Model 1: log usCRP				Model 2: log gamma GT			
	B	95% confidence interval		*p* value	*B*	95% confidence interval		*p* value
		Lower	Upper			Lower	Upper	
Year of study (2014/16)	0.08	0.04	0.13	0.001	0.03	0.00	0.06	0.033
Gender (men)	-0.04	-0.09	0.02	0.200	0.08	0.05	0.11	<0.001
Age	0.09	-0.08	0.26	0.316	-0.28	-0.37	-0.18	<0.001
Current smokers	0.10	0.05	0.14	<0.001	0.06	0.03	0.08	<0.001
Education (<7 years)	0.07	0.03	0.12	0.002	0.03	0.00	0.05	0.040
Current drinkers	-0.05	-0.10	0.00	0.040	0.11	0.08	0.14	<0.001
Waist circumference	0.75	0.49	1.01	<0.001	0.33	0.19	0.48	<0.001
Hip circumference	0.43	0.17	0.68	0.001	-0.29	-0.43	-0.14	<0.001
Systolic blood pressure	-0.04	-0.14	0.06	0.414	0.11	0.05	0.17	<0.001
Fasting glucose*	-0.36	-0.71	-0.01	0.043	0.24	0.04	0.43	0.017
2 hr glucose*	0.41	0.21	0.60	<0.001	0.30	0.19	0.40	<0.001
HbA1c	4.88	1.16	8.74	0.010	-1.97	-3.92	0.02	0.052
Fasting insulin*	-0.01	-0.07	0.06	0.872	0.05	0.02	0.09	0.004
2 hr insulin*	-0.03	-0.09	0.04	0.442	-0.01	-0.04	0.03	0.673
HDL-C*	-0.65	-0.86	-0.44	<0.001	0.59	0.47	0.70	<0.001
LDL-C*	-0.09	-0.25	0.08	0.296	-0.10	-0.19	-0.01	0.031
Triglycerides*	-0.13	-0.25	-0.02	0.022	0.30	0.24	0.36	<0.001
C-reactive protein*	—	—	—	—	0.08	0.06	0.10	<0.001
Gamma GT*	0.26	0.19	0.33	<0.001	—	—	—	—

*Log transformed; HDL-C: high-density lipoprotein cholesterol; LDL-C: low-density lipoprotein cholesterol; usCRP: ultrasensitive C-reactive protein; gamma GT: gamma-glutamyl transferase.

usCRP is a well-established inflammatory biomarker for predicting future risk of CVD events [22, 23]. Thus, the measurement of usCRP has been used in the identification of high-risk individuals who may benefit from therapeutic interventions [23]. Another biomarker that has attracted interest is gamma GT activity which is widely accepted for the diagnosis of liver and obstructive biliary diseases as well as excessive alcohol consumption. Evidence from epidemiological studies has shown that gamma GT activity is associated with type 2 diabetes, metabolic syndrome, atherosclerosis, and CVDs [24]. In a meta-analysis involving 67 905 individuals, gamma GT activity was significantly associated with the metabolic syndrome in individuals in the highest versus lowest thirds of baseline gamma GT activity [25]. Indeed, in our study, dyslipidaemia parameters (triglycerides, LDL-C, and HDL-C), glucose homeostasis (HbA1c, fasting glucose, and insulin), SBP, age, and gender (men) were associated with increased gamma GT levels. Similarly, other epidemiological studies have reported these findings [26, 27]. For example, a study of 1680 Han Chinese patients found that gamma GT was positively correlated with waist circumference, fasting plasma glucose, triglycerides, blood pressure levels, and the metabolic syndrome [27]. Several mechanisms underlying the association between gamma GT activity and the metabolic syndrome or its components have been suggested. One example is the association between gamma GT activity and IR whereby IR is viewed as a bridging mechanism linking gamma GT with CVD and coronary heart diseases [28]. Indeed, in our study, we have demonstrated that both usCRP and gamma GT had an almost 2.5-fold higher odds for IR.

The strength of this study is that the two surveys were conducted in the population from the same geographical area, using similar procedures. However, the study has the following limitations: (i) it consisted of only two cross-sectional surveys, which prevents reliable assessment of time trends; (ii) the second study was not a follow-up but rather another cross-sectional study assessing new participants from the area; (iii) there was a low proportion of men in both studies (24%), a common problem in SA research [29]; (iv) cotinine levels were used to distinguish smokers from nonsmokers; thus, past smokers and those using nicotine gum could not be identified objectively, which is important as previous studies reported that past smokers and those using nicotine gum had increased levels of IR and inflammatory biomarkers [30]; (v) although numerous IR surrogates were used, only the McAuley index is recommended for population-based studies.

5. Conclusion

Our findings have shown increases in subclinical inflammation over a 7-year period, and this was associated with IR and the metabolic syndrome components, both of which are strong predictors of CVDs. Given the estimated increases in the incidence of T2DM and CVD in South Africa and Africa

Table 6: Age-, sex-, and year of study-adjusted ORs (with 95% CIs) for the determinants of inflammation in all participants.

	Model 1: usCRP				Model 2: gamma GT			
	Odds ratio	95% confidence interval		*p* value	Odds ratio	95% confidence interval		*p* value
		Lower	Upper			Lower	Upper	
Year of study								
2008/09	1				1			
2014/16	1.23	1.02	1.49	0.029	1.32	1.07	1.61	0.008
Gender								
Female	1				1			
Male	0.64	0.52	0.78	<0.001	1.30	1.05	1.61	0.016
Age	1.01	1.00	1.01	0.021	1.00	1.00	1.01	0.239
Tobacco use								
Nonsmoker	1				1			
Smoker	1.03	0.86	1.24	0.722	1.26	1.03	1.53	0.024
Level of education								
<7 years	1				1			
≥7 years	0.83	0.68	1.01	0.056	0.76	0.62	0.94	0.011
Alcohol use								
Nondrinker	1				1			
Current drinker	0.82	0.67	1.01	0.062	2.47	1.99	3.06	<0.001
BMI status								
Normal	1				1			
Overweight	0.86	0.68	1.07	0.064	0.87	0.68	1.11	0.315
Obese	1.11	0.91	1.35	0.064	0.86	0.69	1.06	0.315
Insulin fasting								
No	1				1			
Yes	1.19	0.76	1.86	0.452	0.63	0.39	1.01	0.055
HOMA-IR								
No	1				1			
Yes	1.53	0.79	2.99	0.210	0.82	0.43	1.57	0.551
QUICKI index								
No	1				1			
Yes	0.71	0.40	1.28	0.258	1.58	0.90	2.74	0.101
McAuley index								
No	1				1			
Yes	1.40	1.05	1.87	0.022	2.12	1.59	2.84	<0.001
Matsuda index								
No	1				1			
Yes	1.76	1.25	2.47	0.001	1.78	1.27	2.50	0.001

HOMA-IR: homeostatic model assessment of insulin resistance; usCRP: ultrasensitive C-reactive protein; gamma GT: gamma-glutamyl transferase.

in general, monitoring of these biomarkers involved in the pathophysiological development of CVD is important. It can provide early information on the trajectory of the CVD burden in the population, even before substantial changes are observed in population levels of CVD risk factors.

Data Availability

The datasets generated and/or analysed during the current study are available from the principal investigator (TEM) on reasonable request.

Ethical Approval

The University of Cape Town Human Research Ethics Committee had granted ethical approval for this study (ref. no. 442/2016), while the Cape Peninsula University of Technology had granted ethical approval for the 2008/09 and 2014/16 studies (ref. nos. CPUT/HW-REC 2008/002 and CPUT/HW-REC 2015/H01, respectively). The Ward Councillors, representing the City of Cape Town and community management, had granted permission to conduct the surveys in the designated areas. The study was conducted according

to the Code of Ethics of the World Medical Association (Declaration of Helsinki).

Consent

Written informed consent was obtained from all participants.

Disclosure

Any opinions, findings, conclusions, or recommendations expressed in this article are those of the author(s), and the SAMRC and/or SANRF do not accept any liability in this regard.

Conflicts of Interest

The authors declare no conflict of interests.

Authors' Contributions

SFGD is responsible for the drafting of the article, statistical analysis, and interpretation of data. TEM is assigned to the conception and design of the study and analysis and interpretation of the data, revising it for intellectual content and final approval of the version to be published. NP is also assigned to the interpretation of data revising it for intellectual content and final approval of the version to be published. RTE participated in the conception, revising it for intellectual content and final approval of the version to be published. APK participated in the conception and design of the study analysis and interpretation of the data, revising it for intellectual content and final approval of the version to be published.

Acknowledgments

This research project was supported by a grant from the University Research Fund of the Cape Peninsula University of Technology and the South African Medical Research Council (SAMRC), with funds from National Treasury under its Economic Competitiveness and Support Package (MRC-RFA-UFSP-01-2013/VMH Study) and South African National Research Foundation (SANRF) (Grant no. 115450). We thank the Bellville South community and their community Health Forum for supporting the study.

References

[1] V. Ormazabal, S. Nair, O. Elfeky, C. Aguayo, C. Salomon, and F. A. Zuñiga, "Association between insulin resistance and the development of cardiovascular disease," *Cardiovascular Diabetology*, vol. 17, no. 1, p. 122, 2018.

[2] M. A. R. Lauterbach and F. T. Wunderlich, "Macrophage function in obesity-induced inflammation and insulin resistance," *Pflügers Archiv - European Journal of Physiology*, vol. 469, no. 3–4, pp. 385–396, 2017.

[3] S. I. Q. Syed Ikmal, H. Zaman Huri, S. R. Vethakkan, and W. A. Wan Ahmad, "Potential biomarkers of insulin resistance and atherosclerosis in type 2 diabetes mellitus patients with coronary artery disease," *International Journal of Endocrinology*, vol. 2013, Article ID 698567, 11 pages, 2013.

[4] B. B. Duncan, M. I. Schmidt, J. S. Pankow et al., "Low-grade systemic inflammation and the development of type 2 diabetes: the atherosclerosis risk in communities study," *Diabetes*, vol. 52, no. 7, pp. 1799–1805, 2003.

[5] G. S. Hotamisligil, "Inflammation and metabolic disorders," *Nature*, vol. 444, no. 7121, pp. 860–867, 2006.

[6] A. L. Olson, "Regulation of GLUT4 and insulin-dependent glucose flux," *ISRN Molecular Biology*, vol. 2012, Article ID 856987, 12 pages, 2012.

[7] J. Zacho, A. Tybjærg-Hansen, and B. G. Nordestgaard, "C-reactive protein and all-cause mortality-the Copenhagen City Heart Study," *European Heart Journal*, vol. 31, no. 13, pp. 1624–1632, 2010.

[8] World Health Organization, *WHO STEPS Surveillance Manual*, WHO, 2017.

[9] World Health Organization, *Guidelines for Definition, Diagnosis and Classification pf Diabetes Mellitus and its Complications*, WHO, 1999.

[10] D. R. Matthews, J. P. Hosker, A. S. Rudenski, B. A. Naylor, D. F. Treacher, and R. C. Turner, "Homeostasis model assessment: insulin resistance and ?-cell function from fasting plasma glucose and insulin concentrations in man," *Diabetologia*, vol. 28, no. 7, pp. 412–419, 1985.

[11] A. Katz, S. S. Nambi, K. Mather et al., "Quantitative insulin sensitivity check index: a simple, accurate method for assessing insulin sensitivity in humans," *The Journal of Clinical Endocrinology and Metabolism*, vol. 85, no. 7, pp. 2402–2410, 2000.

[12] K. A. McAuley, S. M. Williams, J. I. Mann et al., "Diagnosing insulin resistance in the general population," *Diabetes Care*, vol. 24, no. 3, pp. 460–464, 2001.

[13] M. Matsuda and R. A. DeFronzo, "Insulin sensitivity indices obtained from oral glucose tolerance testing: comparison with the euglycemic insulin clamp," *Diabetes Care*, vol. 22, no. 9, pp. 1462–1470, 1999.

[14] M. Koc, O. Karaarslan, G. Abali, and M. K. Batur, "Variation in high-sensitivity C-reactive protein levels over 24 hours in patients with stable coronary artery disease," *Texas Heart Institute Journal*, vol. 37, no. 1, pp. 42–48, 2010.

[15] K. D. Pagana and T. J. Pagana, *Mosby's Diagnostic and Laboratory Test Reference-E-Book*, Elsevier, 2012.

[16] World Health Organization, *Body Mass Index - BMI*, World Health Organization, 2019.

[17] World Health Organization, *Definition and Diagnosis of Diabetes Mellitus and Intermediate Hyperglycemia*, WHO, 2006.

[18] P. Lempiäinen, L. Mykkänen, K. Pyörälä, M. Laakso, and J. Kuusisto, "Insulin resistance syndrome predicts coronary heart disease events in elderly nondiabetic men," *Circulation*, vol. 100, no. 2, pp. 123–128, 1999.

[19] International Diabetes Federation, *IDF Diabetes Atlas Ninth*, IDF, Dunia, 2019.

[20] N. Friedrich, et al.B. Thuesen, T. Jorgensen et al., "The association between IGF-I and insulin resistance: a general population study in Danish adults," *Diabetes Care*, vol. 35, no. 4, pp. 768–773, 2012.

[21] D. R. Prakaschandra, T. M. Esterhuizen, A. A. Motala, P. Gathiram, and D. P. Naidoo, "High prevalence of cardiovascular risk factors in Durban South African Indians: the Phoenix Lifestyle Project," *South African Medical Journal*, vol. 106, no. 3, pp. 284–289, 2016.

[22] W. Koenig, "High-sensitivity C-reactive protein and atherosclerotic disease: from improved risk prediction to risk-

guided therapy," *International Journal of Cardiology*, vol. 168, no. 6, pp. 5126–5134, 2013.

[23] P. M. Ridker, "A test in context: high-sensitivity C-reactive protein," *Journal of the American College of Cardiology*, vol. 67, no. 6, pp. 712–723, 2016.

[24] K. G. M. M. Alberti and P. Z. Zimmet, "Definition, diagnosis and classification of diabetes mellitus and its complications. Part 1: diagnosis and classification of diabetes mellitus. Provisional report of a WHO Consultation," *Diabetic Medicine*, vol. 15, no. 7, pp. 539–553, 1998.

[25] S. K. Kunutsor, T. A. Apekey, and D. Seddoh, "Gamma glutamyltransferase and metabolic syndrome risk: a systematic review and dose-response meta-analysis," *International Journal of Clinical Practice*, vol. 69, no. 1, pp. 136–144, 2015.

[26] D. H. Lee, M. H. Ha, J. H. Kim et al., "Gamma-glutamyltransferase and diabetes—a 4 year follow-up study," *Diabetologia*, vol. 46, no. 3, pp. 359–364, 2003.

[27] C. F. Liu, W. N. Zhou, Z. Lu, X. T. Wang, and Z. H. Qiu, "The associations between liver enzymes and the risk of metabolic syndrome in the elderly," *Experimental Gerontology*, vol. 106, pp. 132–136, 2018.

[28] G. Ndrepepa, R. Colleran, and A. Kastrati, "Gamma-glutamyl transferase and the risk of atherosclerosis and coronary heart disease," *Clinica Chimica Acta*, vol. 476, pp. 130–138, 2018.

[29] N. Peer, K. Steyn, C. Lombard, N. Gwebushe, and N. Levitt, "A high burden of hypertension in the urban black population of Cape Town: the Cardiovascular Risk in Black South Africans (CRIBSA) Study," *PLoS One*, vol. 8, no. 11, article e78567, 2013.

[30] M. Śliwińska-Mossoń and H. Milnerowicz, "The impact of smoking on the development of diabetes and its complications," *Diabetes and Vascular Disease Research*, vol. 14, no. 4, pp. 265–276, 2017.